FINAL REPORT

Assessing White-nose Syndrome in the Context of Non-Stationary Conditions in an Advancing Continental Epidemic

SERDP Project RC-2633

FEBRUARY 2021

Dr. Sarah H. Olson
Wildlife Conservation Society

SERDP
DOD • EPA • DOE

REPORT DOCUMENTATION PAGE

Form Approved
OMB No. 0704-0188

1. REPORT DATE *(DD-MM-YYYY)* 19-02-2021	2. REPORT TYPE Final Report	3. DATES COVERED *(From - To)* July 2016 - February 2021

4. TITLE AND SUBTITLE	5a. CONTRACT NUMBER
Assessing White-nose Syndrome In The Context Of Non-Stationary Conditions In An Advancing Continental Epidemic	W912HQ-16-C-0015
	5b. GRANT NUMBER
	5c. PROGRAM ELEMENT NUMBER

6. AUTHOR(S)	5d. PROJECT NUMBER
Olson, Sarah H.; Crowley, Daniel; Dickson, Brett G.; Dzal, Yvonne A.; Fuller, Nathan W.; Haase, Catherine G.; Hayman, David T.S.; Hranac, Carter Reed; Kunkel, Emma L.; Lausen, Cori L.; McGuire, Liam P.; McClure, Meredith L.; Plowright, Raina K.; Silas, Kirk A.; Willis, Craig K.R.	RC-2633
	5e. TASK NUMBER
	5f. WORK UNIT NUMBER

7. PERFORMING ORGANIZATION NAME(S) AND ADDRESS(ES) Wildlife Conservation Society 2300 Southern Boulevard Bronx. NY 10460-1090	8. PERFORMING ORGANIZATION REPORT NUMBER RC-2633

9. SPONSORING / MONITORING AGENCY NAME(S) AND ADDRESS(ES) SERDP Program Office 4800 Mark Center Drive, Suite 17008 Alexandria, VA 22350-3600	10. SPONSOR/MONITOR'S ACRONYM(S) SERDP
	11. SPONSOR/MONITOR'S REPORT NUMBER(S) RC-2633

12. DISTRIBUTION / AVAILABILITY STATEMENT

13. SUPPLEMENTARY NOTES

14. ABSTRACT

Hibernating bat species across North America face a dangerous introduced environmental pathogen, Pseudogymnoascus destructans, which causes white-nose syndrome (WNS). WNS is an imminent extinction threat to susceptible bat species found on Department of Defense installations and neighboring lands. Our goal was to predict the impacts of WNS and fill the critical ecological, physiological, behavioral, and environmental knowledge gaps for western species before WNS arrived. To achieve this goal our objectives were to: (1) collect robust morphometric, bioenergetic, and hibernacula environmental data on up to five western North American bat species representing different hibernating behaviors and geographic settings at three to five sites each year; (2) examine the transferability of a mechanistic WNS bioenergetics survivorship model (based on host, pathogen, and environmental characteristics) developed for bat species affected by WNS in the East to a set of five representative bat species found in the West; (3) develop approaches that integrate the mechanistic WNS survivorship model with species distribution models to evaluate the presence of WNS with plausible scenarios of non-stationary conditions (e.g. climate change) and to explore the sensitivity of the integrated model to different parameters and data availability; and (4) disseminate knowledge and findings through scientific meetings and peer-reviewed literature..

15. SUBJECT TERMS

white-nose syndrome, WNS, non-stationary conditions, bat species

16. SECURITY CLASSIFICATION OF:			17. LIMITATION OF ABSTRACT	18. NUMBER OF PAGES	19a. NAME OF RESPONSIBLE PERSON Dr. Sarah Olson
a. REPORT U	b. ABSTRACT SAR	c. THIS PAGE U	U	324	19b. TELEPHONE NUMBER *(include area code)* (608)347-3828

Standard Form 298 (Rev. 8-98)
Prescribed by ANSI Std. Z39.18

Table of Contents

List of Tables

List of Figures

List of Acronyms

AIC   Akaike's Information Criterion
ANOVA   analysis of variance
AUC   area under the receiver operating characteristic curve
BRT   boosted-regression trees
CHILI   Continuous Heat-Insolation Load Index
CMIP5   Coupled Model Intercomparison Project 5
CR   cooling rate $^{\circ}$C h^{-1}
D_{cool} duration of cooling phase (h)
D_{warm} duration of warming phase(h)
DEM   digital elevation model
DMSP   Defense Meteorological Program
DSM   Digital Surface Model
dWVP   water vapor deficit (ΔkPa)
ECS   equilibrium climate sensitivity
EWL   evaporative water loss (mg H_2O h^{-1})
GAM   generalized additive models
GCM   global climate model
GLM   generalized linear models
IUCN   International Union for Conservation of Nature
JRC   Joint Research Center
MAST   mean annual surface temperature ($^{\circ}$C)
MRDS   Mineral Resources Data System
NCAR   National Center for Atmospheric Research
OLS   Operational Line-Scan System
TMR   torpid metabolic rate (ml O_2 h^{-1})
PRCC   partial rank correlation coefficients
Q_{10} the change in metabolic rate over a 10 $^{\circ}$C change in temperature
QMR   quantitative magnetic resonance
RCM   regional climate model
RegCM4   Regional Climate Model 4
RH   relative humidity (%)
RMR   mass-specific resting metabolic rate at T_a (ml O_2 g^{-1} h^{-1})
SDM   species distribution model
SE   standard error(s)
SPCC   squared semi-partial correlation coefficient
SRTM   Shuttle Radar Topography Mission
T_a ambient temperature ($^{\circ}$C)
T_b body temperature ($^{\circ}$C)
$T_{defended}$ temperature below which metabolic rate increases ($^{\circ}$C)
TPI   topographic position index
T_{sk} skin temperature of a bat ($^{\circ}$C)
USGS   United States Geological Survey
VCF   Vegetation Continuous Fields
WNS   white-nose syndrome

WR	warming rate (°C h^{-1})
WRF	Weather Research and Forecasting
WVP	water vapor pressure (kPa)

Model-associated and measured parameters

$area_{Pd}$	area (cm^2) of fungal growth calculated as a function of T_b (°C) and relative humidity (%) given equations from Hayman et al. 2016
BMR	mass-specific basal metabolic rate (ml O$_2$ g^{-1} h^{-1})
C_{eu}	thermal conductance of euthermic tissue (ml O$_2$ g^{-1} °C^{-1})
CEWL	cutaneous evaporative water loss (mg H$_2$O h^{-1})
C_t	thermal conductance of torpid tissue (ml O$_2$ g^{-1} °C^{-1})
E_{bout}	energy a bat expends during a torpor-arousal cycle (ml O$_2$ g^{-1} h^{-1})
E_{cool}	energetic cost of cooling (ml O$_2$ g^{-1})
E_{eu}	energetic cost of euthermia (ml O$_2$ g^{-1} h^{-1})
E_{tor}	energetic costs of torpor (ml O$_2$ g^{-1} h^{-1})
E_{warm}	energy required to warm from torpor to euthermia (ml O$_2$ g^{-1})
M_b	bat body mass (g)
REWL	respiratory evaporative water loss (mg H$_2$O h^{-1})
rEWL	area-specific rate of evaporative water loss from all tissue (mg H$_2$O h^{-1} ΔWVP^{-1} cm^{-2})
rEWL$_{body}$	area-specific rate of evaporative water loss from bodily tissue (mg H$_2$O h^{-1} ΔWVP^{-1} cm^{-2})
rEWL$_{wing}$	area-specific rate of evaporative water loss from wing tissue (mg H$_2$O h^{-1} ΔWVP^{-1} cm^{-2})
S	heat capacity of tissue (ml O$_2$ g^{-1} C^{-1})
SA	surface area of entire bat (cm^2)
SA$_{body}$	surface area of bat body (cm^2)
SA$_{wing}$	surface area of bat wing (cm^2)
t_{eu}	euthermic duration (h)
t_{torEWL}	torpor duration based on reduction of total body water (h)
t_{torMax}	maximum time in torpor (h)
t_{torTMR}	torpor duration based on metabolic rate (h)
T_a	ambient hibernaculum temperature (°C)
T_b	bat body temperature (°C)
T_{eu}	euthermic bat temperature (°C)
T_{lc}	lower critical temperature (°C)
T_{tor}	torpid body temperature (°C)
T_{torMin}	minimum defended T_b in torpor (°C)
TMR$_{min}$	mass-specific minimum torpid metabolic rate (ml O$_2$ g^{-1} h^{-1})
WVP_{air}	water vapor pressure in the air (kPa)
WVP_{bat}	water vapor pressure at the bat skin surface (kPa)

Keywords

Acknowledgements

Abstract

Introduction and Objectives
Hibernating bat species across North America face a dangerous introduced environmental pathogen, *Pseudogymnoascus destructans*, which causes white-nose syndrome (WNS). WNS is an imminent extinction threat to susceptible bat species found on Department of Defense installations and neighboring lands. Our goal was to predict the impacts of WNS and fill the critical knowledge gaps for western bat species. Our objectives to meet this goal included the following: (1) collect hibernation physiological and environmental data, (2) apply a mechanistic WNS bioenergetics survivorship model to characterize species-level risk, (3) integrate the model with spatial data to evaluate future scenarios, and (4) disseminate our scientific findings.

Technical Approach
We hypothesized variation in WNS mortality among hibernating species was related to species-level bioenergetic traits and environmental factors and we tested our hypothesis using empirical data and bioenergetic models. In advance of WNS arrival, our team collected or compiled existing physiological data on 3073 bats, representing 13 species, across 14 sites in the West. Microclimate measurements were also compiled or collected from hibernacula. We evaluated these new data for inter- and intraspecific energetic profiles, conducted modeling analyses of environmental and climate factors that affect hibernation conditions, and applied the survivorship model to predict survival in the presence of WNS and future climate change.

Results
The project has succeeded in collecting high-quality bioenergetics and environmental data on bat hibernation and has used these data to develop predictive models of WNS susceptibility in western bats. Our data were the first to establish valuable pre-WNS reference points for the hibernation physiology of over a dozen western bat species. We did not observe significant differences in hibernation physiology within species, but we did observe significant differences of rates of evaporative water loss among species and the temperature range where minimum torpid metabolic rate is used. Our mechanistically informed species distribution models allowed us to predict the role of WNS and changing climate on spatial survivorship of western species, including that the majority of the species we studied will be negatively impacted by WNS.

Benefits
Our project significantly contributes to real world proactive management strategies for WNS by improving our scientific understanding of (1) which western species, (2) populations, and (3) habitats are likely to be associated with high WNS mortality. This information is central to conducting efficient and effective surveillance and monitoring across the large western landscape as well as to deploy WNS interventions and to track potential evolutionary rescue.
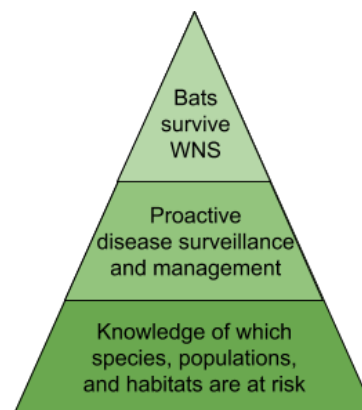
Executive Summary

<u>Introduction</u>

White-nose syndrome (WNS) is a rapidly spreading infectious disease that has led to high mortality rates in multiple hibernating bat species across eastern and central North America. Scientists have estimated WNS killed approximately six million bats in just the first six years after the pathogen was first detected in New York state. WNS presents a potential extinction threat to susceptible species found on Department of Defense (DoD) installations with associated Endangered Species Act listing implications on use of diverse military training environments and thereby military readiness. *Myotis septentrionalis* (Northern-long eared bat) is already listed as threatened in the United States and *M. septentrionalis*, *M. lucifugus*, and *Perimyotis subflavus* are listed as endangered in Canada because of WNS. Despite a higher diversity of bats found in the West, unique aspects of western geography, climate, lack of past research, and accessibility makes conserving bats in the face of WNS in the West an especially difficult challenge.

The causal agent of WNS is a psychrophilic fungus, *Pseudogymnoascus destructans*, a free-living environmental pathogen. The fungus grows best between 7-18 ˚C with high humidity (Verant et al. 2012; Marroquin et al. 2017), which overlaps with subterranean roost conditions typically used by hibernating bats. Bats are infected in hibernacula and can spread fungal spores via bat to bat transmission (Knudsen et al. 2013). The extent of detected WNS as of August 2019 is shown in Figure E1.
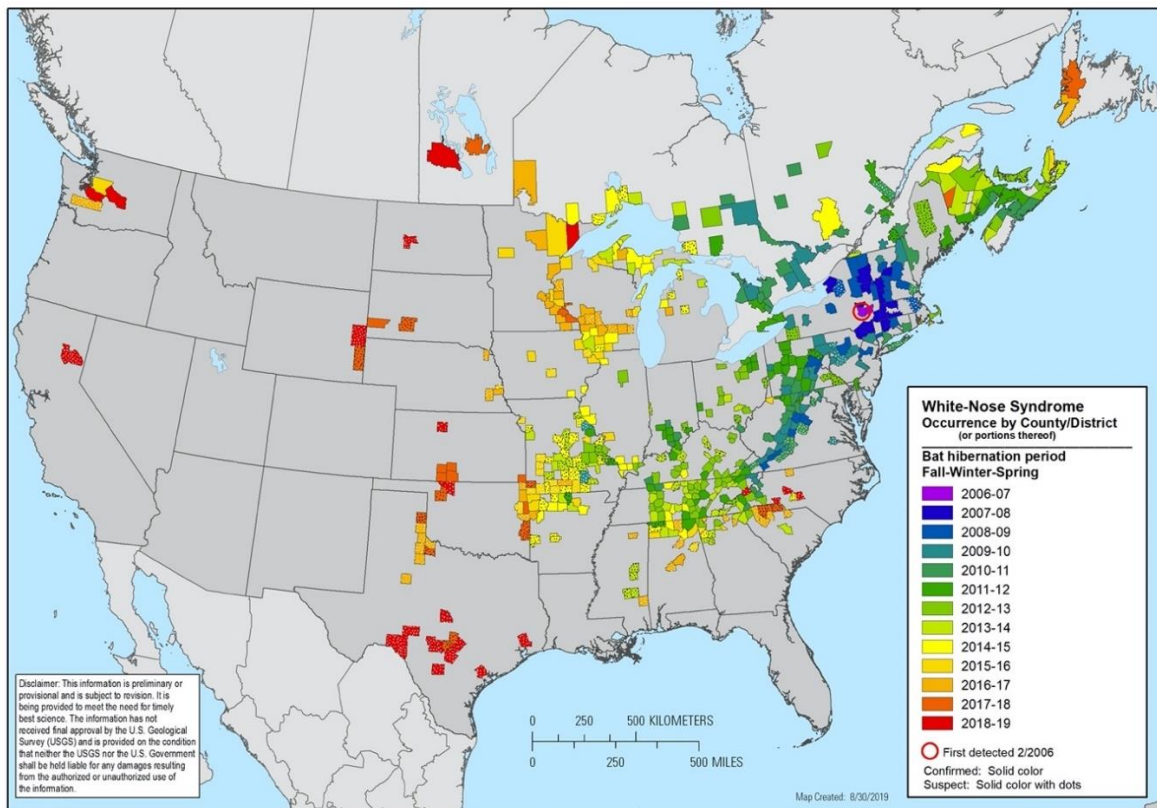
Figure E1. Map of white-nose syndrome (WNS) occurrence as of August 2019 (most recent map available from whitenosesyndrome.org).

Hibernation is composed of bouts of torpor, during which bat body temperature approaches low ambient temperatures to limit the consumption of finite metabolic resources. Torpor is periodically interrupted by energy intensive periods of arousal during which hibernators return to euthermic body temperature (Hayman et al. 2017). Hibernators arouse for a variety of proposed reasons (for a review see Carey 1993 and citations within), including the need to eliminate metabolic waste, regain water balance, or mate. While arousals represent a small fraction of the total time spent in hibernation, they account for the majority of energy consumed, with a single arousal costing as much as 5% of total overwinter energetic costs (Thomas et al. 1990).

During hibernation the fungus erodes wing tissue (Cryan et al. 2010) and causes a cascade of bioenergetic impacts (Verant et al. 2014; Warnecke et al. 2013). The established conceptual model of WNS disease progression is that bats with WNS have greater evaporative water loss, more frequent arousals, and overall greater energy expenditure. WNS mortality occurs during the later stages of hibernation and diseased bats appear emaciated from more frequent energy-consuming arousals (Reeder et al. 2012; Warnecke et al. 2012). Subsequently, an energetic-based framework was central to our motivation to first measure and analyze physiological traits of western bats and then to parameterize advanced bioenergetics-based models to better characterize the WNS threat to western bat species.

Objectives
Our goal was to predict the impacts of WNS and fill the critical ecological, physiological, behavioral, and environmental knowledge gaps for western species before WNS arrived. To achieve this goal our objectives were to: (1) collect robust morphometric, bioenergetic, and hibernacula environmental data on up to five western North American bat species representing different hibernating behaviors and geographic settings at three to five sites each year; (2) examine the transferability of a mechanistic WNS bioenergetics survivorship model (based on host, pathogen, and environmental characteristics) developed for bat species affected by WNS in the East to a set of five representative bat species found in the West; (3) develop approaches that integrate the mechanistic WNS survivorship model with species distribution models to evaluate the presence of WNS with plausible scenarios of non-stationary conditions (e.g. climate change) and to explore the sensitivity of the integrated model to different parameters and data availability; and (4) disseminate knowledge and findings through scientific meetings and peer-reviewed literature.

Technical Approach
We hypothesized the differential mortality due to WNS observed among hibernating species was related to species-level bioenergetic traits and environmental factors and we tested our hypothesis using empirical data and bioenergetic models. In advance of WNS arrival, our team collected or compiled existing basic morphometric trait data on 3073 bats, representing 13 species, across 14 sites in Alberta, British Columbia, Colorado, Montana, Northwest Territories, Nevada, Oklahoma, Oregon, Texas, and Utah. Respirometry and body composition data (measured by quantitative magnetic resonance) were collected or compiled for a subset of 506 and 249 bats respectively, sufficient for respirometry analysis of 12 species, and microclimate measurements were also compiled or collected from hibernacula. We evaluated these new data for inter- and intraspecific energetic profiles. To further characterize susceptibility and understand geographic patterns of susceptibility we conducted several modeling analyses of

3

environmental and climate factors that affect hibernation conditions. First, we compiled subterranean temperatures from caves and mines across the western United States and Canada to: a) quantify the hypothesized relationship between mean annual surface temperature and subterranean temperature and how it is influenced by measurable site attributes, and b) use readily available gridded data to predict and continuously map the range of temperatures that may be available in caves and mines. Second, we created spatial models of host traits and using *M. lucifugus* as a surrogate, assessed previous definitions of the duration of winter hibernation and created an improved estimation thereof, based on data compiled from published literature, public databases, local experts, and our own fieldwork. Third, we applied the mechanistic survivorship model to predict winter survival of nine western bat species in the presence of WNS. Building on these first three analyses we then incorporated the mechanistic survivorship estimate as a predictor, along with landscape attributes, e.g. topography, surface attributes, and below-ground attributes, in an ecological niche model to estimate the current occurrence probability of focal western species across western North America. Lastly, we updated these estimates under conditions of WNS exposure and future climate change to project their combined impacts on this system.

Results and Discussion
Empirical assessment of physiological WNS risk among and between western bat species
Given the bioenergetic underpinnings of WNS disease progression during hibernation, how hibernation physiology varies among western populations of species with broad distributions can help us understand WNS susceptibility across species ranges. We studied this question by comparing the physiology of two hibernating bat species, *M. lucifugus* and *Corynorhinus townsendii*, at sites across their large geographic ranges (McGuire et al. In Review). Despite large geographic distances and climatic variation among our study sites, we found no evidence of intraspecific variation, or local adaptation, in torpid metabolic rate. The conclusion for evaporative water loss was generally consistent with the finding for torpid metabolic rate, but notably there were site differences in water loss. In general, we did not find strong evidence for local adaptation and intraspecific variation in hibernation physiology, as measured by torpid metabolic rate and water loss, two key parameters for understanding hibernation physiology, which suggests these physiological traits will not vary across a species' range. This knowledge can also lessen the financial and logistic challenges associated with collecting physiological trait data from multiple widespread populations, given measurements collected at one site will likely be representative of other populations.

There are a handful of hibernating bats species in the East that have shown no sign of *P. destructans* or limited WNS disease pathology so differences in physiological traits among western bat species may help explain differential susceptibility to WNS. Bats are a diverse group with species that hibernate in a wide variety of conditions, but historically hibernation research has focused mostly on two species with little known about the hibernation physiology of other species. We studied 13 species of free-living bats, including hibernating populations spread over thousands of kilometers, representing diverse hibernation contexts (McGuire et al. In Review). We again measured two key parameters for understanding the energetics of hibernation, torpid metabolic rate and evaporative water loss, across a range of hibernation temperatures. The minimum defended temperature varied among species, but when measured within the appropriate temperature range all species had similar torpid metabolic rate. Conversely,

4

evaporative water loss varied among species, which clustered into two groups (Figure E2). Our results suggest there are two general hibernation strategies in North American bats, representing high and low evaporative water loss groups. Notably, species that have suffered large population declines due to WNS fall in the high evaporative water loss group, and those species that are less affected fall in the low evaporative water loss group (Figure E2).
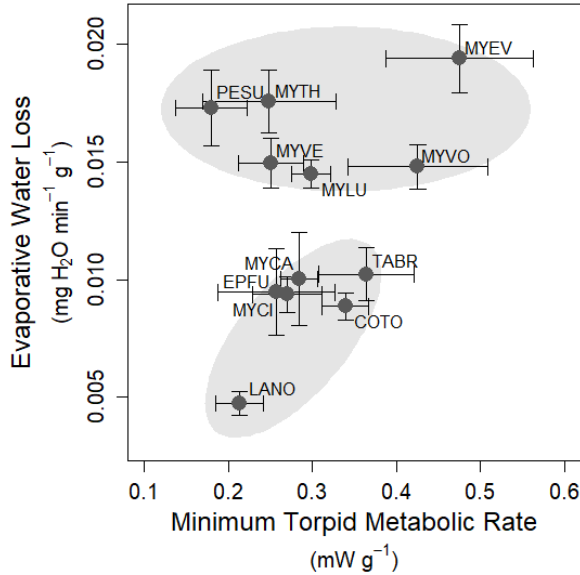
Figure E2. Within the range of temperatures at which minimum torpid metabolic rate was measured, evaporative water loss varied among species but not minimum torpid metabolic rate. Cluster analysis revealed a high and low evaporative water loss cluster. Grey ovals are presented for visual interpretation with the upper oval including species highly impacted by white-nose syndrome (WNS) and the lower oval including species less impacted by WNS. Species codes indicate the first two letters of the genus and the specific epithet.

Advances in modeling bioenergetic WNS survivorship

We built a refined bioenergetic WNS survivorship model that incorporated the latest science by improving the cooling sub-model and adding fungal growth and evaporative water loss parameters (Haase et al. 2019a, 2019b). We then validated the model for *M. lucifugus* (Haase et al. 2019b), a well-studied species, before parameterizing it with existing and new data for nine western species (Haase et al. In Review). On one hand we found all five small *Myotis* species, including *M. ciliolabrum, M. evotis*, *M. lucifugus*, *M. thysanodes*, and *M. volans* that are adapted to surviving in hibernacula at or near saturation were not predicted to survive (Figure E3). On the other hand we found *E. fuscus*, *C. townsendii*, and *M. velifer*, species that are adapted to drier environments and are bigger, all had higher survival than the five *Myotis* species. Saturated conditions, typically used by smaller bats, are less energetically costly for healthy individuals, but lead to greater fungal growth rates and thus higher mortality, which suggests a potential trade-off between water conservation and fat conservation in regards to WNS. These results highlight some key predictors of interspecific survival among western bat species and provide a framework to assess impacts of WNS as the fungus continues to spread into western North America.

5

Figure E3.
Difference between predicted days until fat exhaustion and predicted winter duration (with standard deviation error bars).
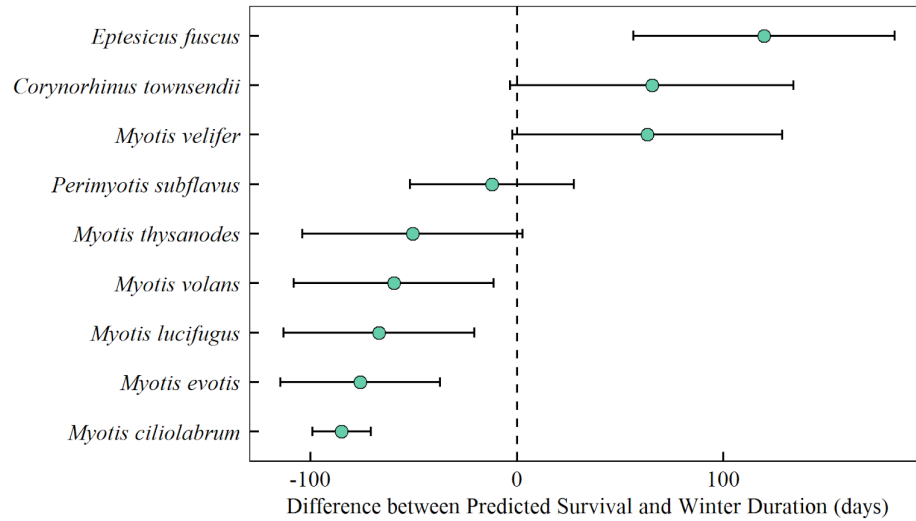
With the more widely studied *M. lucifugus* we examined two of the three most critical parameters governing overwinter survival for hibernators, the duration of winter hibernation and the amount of fat stores taken into hibernation (Hranac et al. In Review). The lack of any previous broad-scale estimates for the duration of winter hibernation highlights the usefulness of our best model which included latitude, elevation, and the number of days in frost. Moreover, we found the additional fat requirements for *M. lucifugus* to survive WNS were considerable and indicate that western *M. lucifugus* populations, especially those along the Rocky Mountains, Alberta, British Columbia, and Alaska, will require similar increases in energetic expenditure when affected by WNS as the eastern populations (Figure E4). In other words, if the increase in energy expenditure results in the same pattern of mortality, *M. lucifugus* populations in the West may be expected to suffer mortality events similar to those experienced in eastern populations (Frick et al. 2010, 2015).
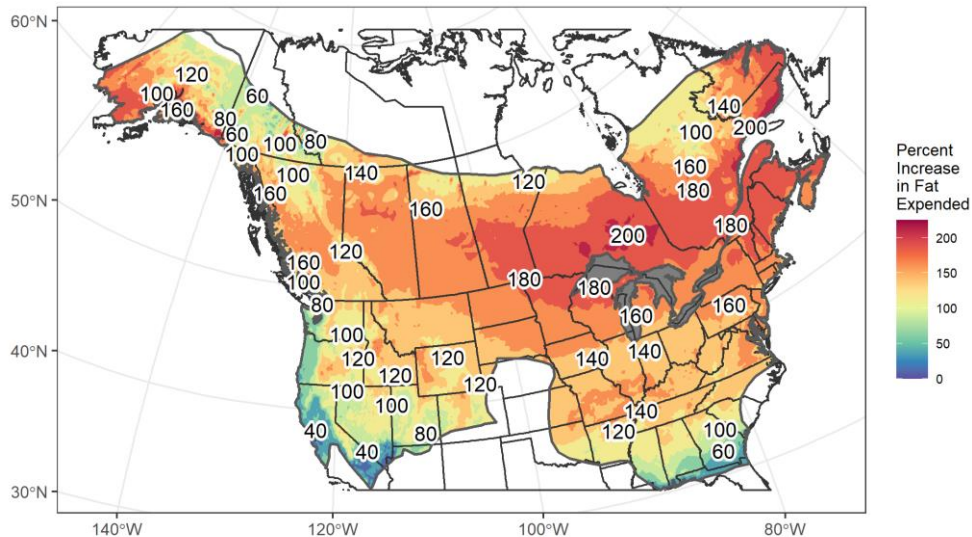
Figure E4. Relative increase (%) in fat stores used over a predicted hibernation period when infected with *Pseudogymnoascus destructans* compared with healthy bats when hibernating at the best available temperature predicted to occur within caves and mines and 98% relative humidity.

Mapping western species winter distributions

We mapped five western species winter ranges to better understand the distribution of suitable bat hibernacula across the West and to inform targeted monitoring and management practices. These distributions can also provide a baseline for estimating which species and populations may be hardest hit by the advance of WNS and climate change. To do so, we integrated a bioenergetic model-based estimate of winter survivorship (Haase et al. 2019b; Hranac et al. In Review) with additional landscape attributes into a correlative species distribution modeling approach and identified important predictors of winter hibernaculum selection (Figure E5). Among species the importance and shape of the relationships varied, as expected, with important predictors including land cover, topography, winter survival capacity, and access to caves and mines. An exciting take-away was the finding that occurrence of bat hibernacula can, in part, be predicted from above ground landscape attributes, and is not dictated by below-ground measures alone for which spatial data are lacking. This finding suggests there is considerable room to scientifically improve existing range maps for bats that currently do little more than draw lines around presence observations.
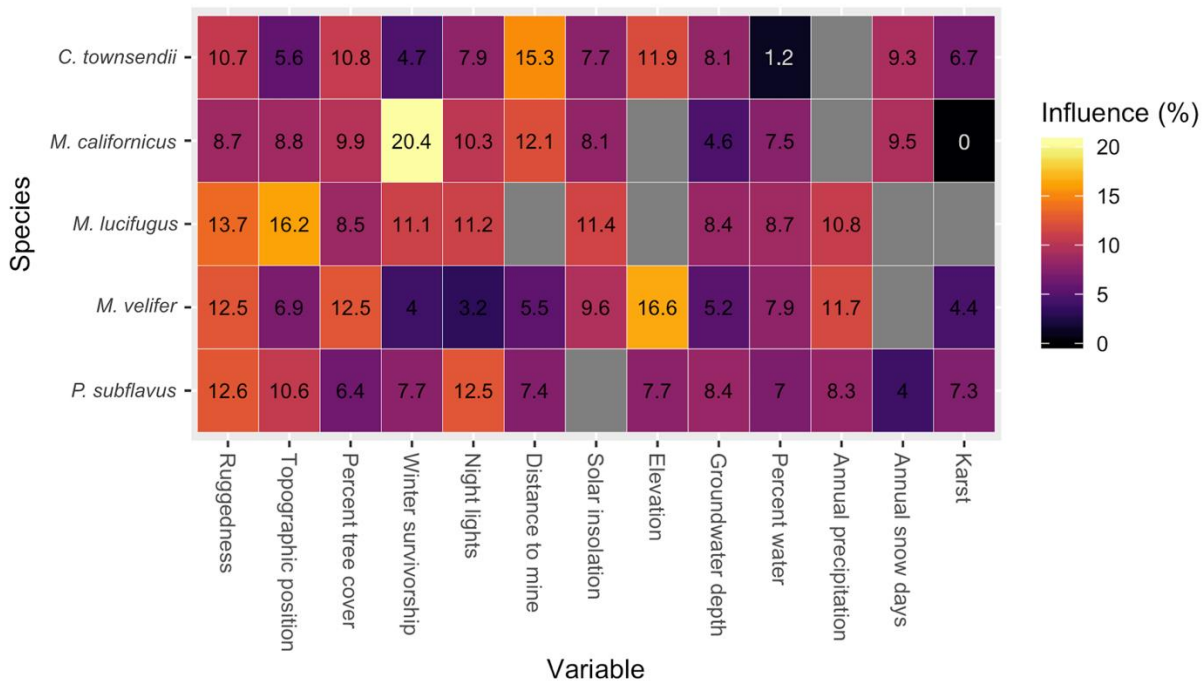
Figure E5. Final predictor influences in boosted regression tree (BRT) models estimating winter species distributions of bat species *Corynorhinus townsendii*, *Myotis californicus*, *M. lucifugus*, *M. velifer*, and *Perimyotis subflavus* across the United States and Canada. Brighter colors indicate higher influence; predictors that were dropped from a given model are shown in gray. Variables are ordered by their average influence across species (decreasing left to right).

Implications of climate change and WNS on western species distributions

Lastly for five species we examined a range of 2050 climate change scenarios on two key climate parameters used in the spatial bioenergetic model, mean annual surface temperature, used to estimate the best available temperature predicted to occur in a cave or mine (McClure et al. 2020), and frost-free period, used to estimate the duration of winter (McClure et al. In Prep). Our results indicate general agreement among the scenarios for these two parameters and that climate change may act to 'rescue' many bat populations from negative WNS outcomes. The

caveats are that those populations will need to persist through 2050 and that warming may not protect all species in all portions of their range (McClure et al. In Review). Our predictions of species distributions in the presence of *P. destructans* and future climate conditions can help managers to better anticipate the species- and place-specific impacts of these stressors, individually and synergistically, across the West (Figure E6).
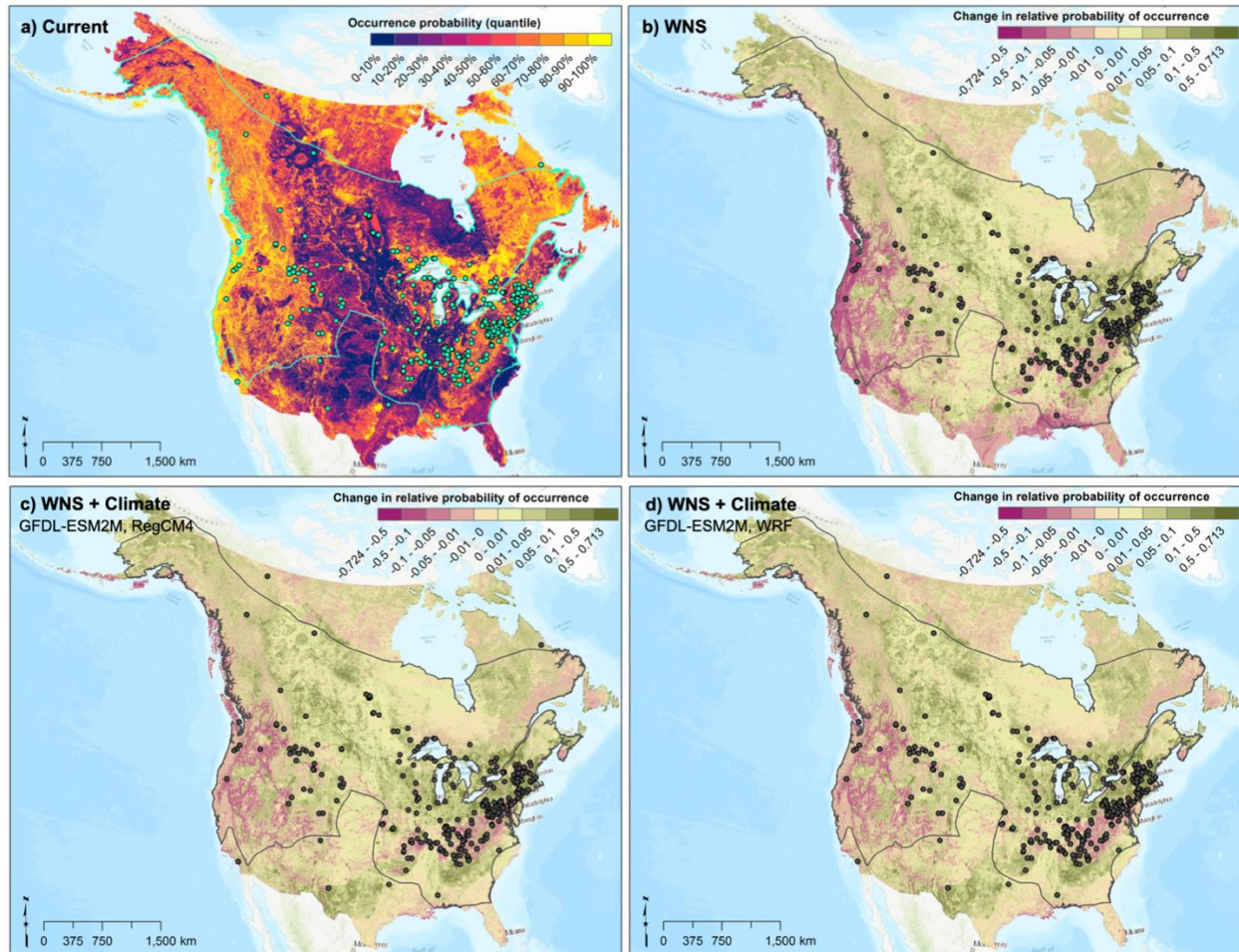
Figure E6. a) Current occurrence probability of *Myotis lucifugus* and change in relative probability of occurrence given b) exposure to white-nose syndrome (WNS), and exposure to WNS under projected mid-century climate conditions. Future climate scenarios shown here were driven by dynamically-downscaled regional climate models c) RegCM4 and d) WRF, each of which was run on boundary conditions defined by the GFDL-ESM2M global circulation model. Darker green indicates a projected increase in occurrence probability; darker purple indicates a projected decrease. The species' current known range (gray outline) and points of recorded winter occurrence (gray points) are overlaid.

Implications for Future Research and Benefits

In total our study included 13 species of diverse bats that cover a wide range of hibernation behaviors and physiology across the western United States and Canada. Some of these species like *M. lucifugus* and *E. fuscus* have been the focus of previous studies, but historically there has been very little hibernation research on many of the species in our study. Our massive data collection effort stands alone as an important contribution to bat conservation. This baseline data would not have been collected if not for this study. Future comparable studies will be very

challenging to conduct because of restrictions that come with species listings and the presence of the fungus in western locations.

Our empirical and bioenergetic modeling analyses revealed evaporative water loss is an important risk factor for WNS susceptibility. Combined with our other central finding of a general lack of local bioenergetic adaptations, it suggests WNS risk due to evaporative water loss will not vary across a species' range, nor will it vary significantly between fall and mid-winter (the latter fieldwork being very logistically difficult). It also means researchers do not have to spend a lot of time and effort measuring this trait at different sites in different biomes to assess the risk of a species we did not measure, and that they can have greater confidence when making inferences across the range (with appropriate caution).

The physiological responses we measured across a range of temperatures provide some indication of the conditions that may be preferred by each species. Again our study was the first to measure and assess torpid metabolic rate across species and sites. From a physiological standpoint it is fascinating some species tolerated temperatures that approached freezing. There is an important caveat that we did not actually measure these conditions *in situ*, we measured them in a mason jar, but this is the best anyone can accomplish with available technology.

Our extensive modeling effort generated resources and tools that are fundamental to allocating WNS disease monitoring, research, and monitoring resources at range-wide scales. We mapped and characterized surface and subterranean attributes of winter bat distributions as well as mapped range-wide relative probability of occurrence under present conditions without WNS and change given occurrence of WNS and climate change scenarios. Models are only as good as the available data, and our study has captured the present state of knowledge while leaving ample documentation and room to incorporate future advancement in our understanding of the system. The effort revealed important knowledge gaps including limited or missing data on species occurrence, duration of winter, and bat behaviors that impact energetics during hibernation. With our integrated host-environment-pathogen modeling effort we generated a comprehensive list of at risk species that should be prioritized for surveillance and changes in hibernation behavior. If shifts to colder winter roost sites are observed this would be a positive development as recent studies of remnant populations in the East offer a glimmer of hope that genetic adaptations and evolutionary rescue may be underway.

New emerging research on this system and contributions from our project will help inform the future directions of bat research and conservation efforts that, if they succeed, will help keep bats and military exercises on the same landscapes. First, hibernating bat species can no longer be lumped together in a group. As our work and other efforts show, each species will have its own unique hibernation strategy and susceptibility to WNS that will mix elements of hibernation physiology and immune responses to *P. destructans*. Second, evolution is likely our best WNS intervention as long as it occurs, 'fast enough to arrest population decline and allow population recovery before extinction ensues' (Gonzalez et al. 2013). Our hibernation energetic findings indicate that critical differences in survival may hinge on small shifts of roost temperature and humidity, fat stores, and arousal frequency or torpor bout duration (Haase et al. 2019b; Haase et al. In Review; Hranac et al. In Review; Lilley et. al. 2016; Cheng et al. 2019). It will be incumbent upon us to retain as much of the existing natural variability both within and among

populations as possible because the distribution of the potential survival traits remains unknown. Third, funding for bat ecology is bat survival research because the science behind evolutionary rescue holds that, 'abundance, variation, and dispersal have pronounced and repeatable effects on the rescue of populations and communities' (Bell et al. 2017). The DoD should support efforts like the North American Bat Monitoring Program and other efforts that are essential to understand variation of bat habitat use in space and time alongside non-WNS stressors. Fourth, WNS interventions can be customized to the West where the United States federal government manages 47% of the land area across 11 contiguous western states (excluding Alaska). Acting independently or together, the Department of the Interior, Department of Agriculture, Department of Defense, state, as well as tribal land-management agencies are positioned to be significant bat conservation stakeholders which would greatly amplify the value of proactive measures designed to support diverse populations of bats.

In sum, proactive actions to retain the diversity of at-risk species across the West should be taken now and while reducing as much as possible other simultaneous threats such as habitat loss and fragmentation, loss of water sources, and climate change. To give susceptible species the best chance at evolutionary rescue, we need policies that protect populations and conserve the greatest amount of genetic diversity. The initial surveillance and containment response effort provided much needed time for us to understand this threat, but the spread of the fungal pathogen across North America now appears inevitable. To protect susceptible bat species in the West (and those in the East) we can start applying what we have learned in the preceding years, redouble our scientific and conservation efforts, and seek opportunities for broader western coalitions and effective conservation policies.

Objectives

White-nose syndrome (WNS), a disease caused by the fungal pathogen *Pseudogymnoascus destructans*, has resulted in widespread mortality in bat populations in the East and presents a serious wildlife management challenge to Department of Defense (DoD) installations in the West. As WNS is a disease affecting the energetics of hibernating bats and caused by an environmental pathogen there are strong linkages between environmental conditions and pathogen dynamics on the landscape. Subsequently our project addresses WNS in response to the FY 2016 SON, 'to improve our fundamental and applied understanding of how non-stationary conditions of land cover, land use, management practices, climate change, and vector population dynamics may affect pathogen exposure pathways and ultimately impact wildlife and military personnel in training environments on DoD installations in the U.S. and its territories.'

Our project's purpose was to develop the science to help identify western bat species, under present or future environmental conditions, that are susceptible to WNS and thereby species of management concern for DoD. The main conservation threat is the potential for WNS to cause local, regional, or continental extirpation of susceptible species. Our working hypotheses were designed to examine our understanding of the WNS threat to western bats. We anticipated that (H1a) survivorship will differ among representative western species. (H1b) Survivorship will differ within species across locations. Geographic location will influence survivorship, such that (H1c) hibernacula microclimate and (H1d) hibernation periods will alter the impact of WNS. (H2a) Climate change will alter the range and hibernation behaviors of western bat species, (H2b) climate and landscape changes that reduce bat resources will further harm populations impacted by WNS, and (H2c) WNS will present a bottleneck for populations that may not survive long enough for climate change to offer any reprieve.

These hypotheses informed our four main technical objectives:
1) Collect robust morphometrics, bioenergetics, and hibernacula environmental data on up to five western North American bat species representing different hibernating behaviors and geographic settings at three to five sites each year.
2) Examine the transferability of the mechanistic WNS bioenergetics survivorship model (based on host, pathogen, and environmental characteristics) developed for bat species affected by WNS in the East to a set of five representative bat species found in the West.
3) Develop approaches that integrate the mechanistic WNS survivorship model with species distribution models to evaluate the presence of WNS with plausible scenarios of non-stationary conditions (e.g. climate change) and to explore the sensitivity of the integrated model to different parameters and data availability.
4) Disseminate knowledge and findings through scientific meetings and peer-reviewed literature.

Background

At the beginning of this project the scientific community lacked in-depth ecological, physiological, and behavioral information on many western species that could be used to proactively strengthen bat conservation approaches to address white-nose syndrome (WNS) impacts. A multi-host disease of bats, WNS had caused unprecedented mortality (>90% for some species) in hibernating populations in eastern North America (Frick et al. 2010; Langwig et al. 2012). The pathogen, *Pseudogymnoascus destructans*, was discovered at a single site in New York in 2006 and by 2015 it had spread to 27 states and five Canadian provinces and was continuing to spread westward (United States Fish & Wildlife Service 2014). As long as movement of the fungus continued at pace, there was a limited window of time to acquire critical ecological and bioenergetics information about bat species living on or near Department of Defense (DoD) lands in the West (Maher et al. 2012). Notably, the fungus made a large jump across the country to Washington state in March 2016 before our study began in the fall of 2016. Western North America has greater bat species diversity than the East (19 species in the East, 31 species in the West) (Adams 2003; Harvey et al. 2013) and far less was known about the physiology of bats west of the Rocky Mountains due to mountainous, less accessible, and less urbanized habitats (Adams 2003). There are a variety of bat species known to be found on western DoD installations (*Antrozous pallidus*, *Corynorhinus townsendii*, *Eptesicus fuscus*, *Eumops perotis*, *Lasiurus blossevillii*, *Myotis spp.*, *M. californicus*, *M. ciliolabrum*, *M. velifer*, *M. volans*, *M. yumanensis*, *Parastrellus hesperus*, *Perimyotis subflavus* and *Tadarida brasiliensis*) through acoustic monitoring or captures. This effort assessed the threat of WNS to western bats so that the military can continue to steward these species on installations while maintaining readiness and training activities.

We built our study on an existing strong conceptual model of WNS epidemiology and disease progression. Bats are infected with *P. destructans* through direct contact with other contaminated bats and through environmental exposure in hibernacula where the fungus persists (Lorch et al. 2011). The closest genetic relatives of *P. destructans* were found in European caves, where it is endemic but not associated with mortality (Puechmaille et al. 2011; Wibbelt et al. 2010). *P. destructans* grows well in environments used by hibernating bats (<20 ˚C), though it is not reliant on bats for survival or growth (Reynolds et al. 2015; Verant et al. 2012). Dispersing bats (hosts and vectors) and humans (vectors) carrying spores of *P. destructans* from infected or contaminated caves (reservoirs) contaminate new hibernacula. Once a cave is infected with *P. destructans*, it is anticipated to remain so for decades (Reynolds et al. 2015). The contribution of long-distance bat or anthropogenic transport (e.g., cavers, researchers) of *P. destructans* fungal spores appeared rare, as the spatial pattern of spread is more diffuse, associated with migration, local mixing, and movement among hibernacula (Maher et al. 2012; Wright and Moran 2011).

At the time our project began, research showed that the change in host physiology during hibernation drove the seasonal transmission dynamics of *P. destructans* (Langwig et al. 2015). The competency of different bat species as vectors is not well understood, but is likely related to species-specific interactions between host physiology and host response to *P. destructans* infection. Diagnostic symptoms of WNS have occurred primarily in hibernating bat species (*M. lucifugus*, *M. septentrionalis*, *M. sodalis*, *M. grisescens*, *M. leibii*, *E. fuscus* and *P. subflavus*) and there are some species on which *P. destructans* was found in the absence of any disease

pathology (see below) (United States Fish & Wildlife Service 2016). Notably, hibernation alone was not a sufficient predictor of WNS vulnerability, as a handful of hibernating bats species in the East have shown no sign of *P. destructans* or limited WNS disease pathology (United States Fish & Wildlife Service 2016). The potential for local, regional, or continental extirpation of WNS susceptible bats is the core conservation threat (WNS National Plan Writing Team 2011). As a direct result of WNS *M. septentrionalis* was listed as threatened in the United States, and Canada has legally protected *M. lucifugus*, *M. septentrionalis*, and *P. subflavus* as endangered species (COSEWIC 2013; Department of the Interior: Fish and Wildlife Service 2013; United States Fish & Wildlife Service 2014). Independent of WNS, western states have already recognized several bat species whose population viability is threatened (e.g., *M. thysanodes*, *M. ciliolabrum*, *C. townsendii*, *Euderma maculatum*).
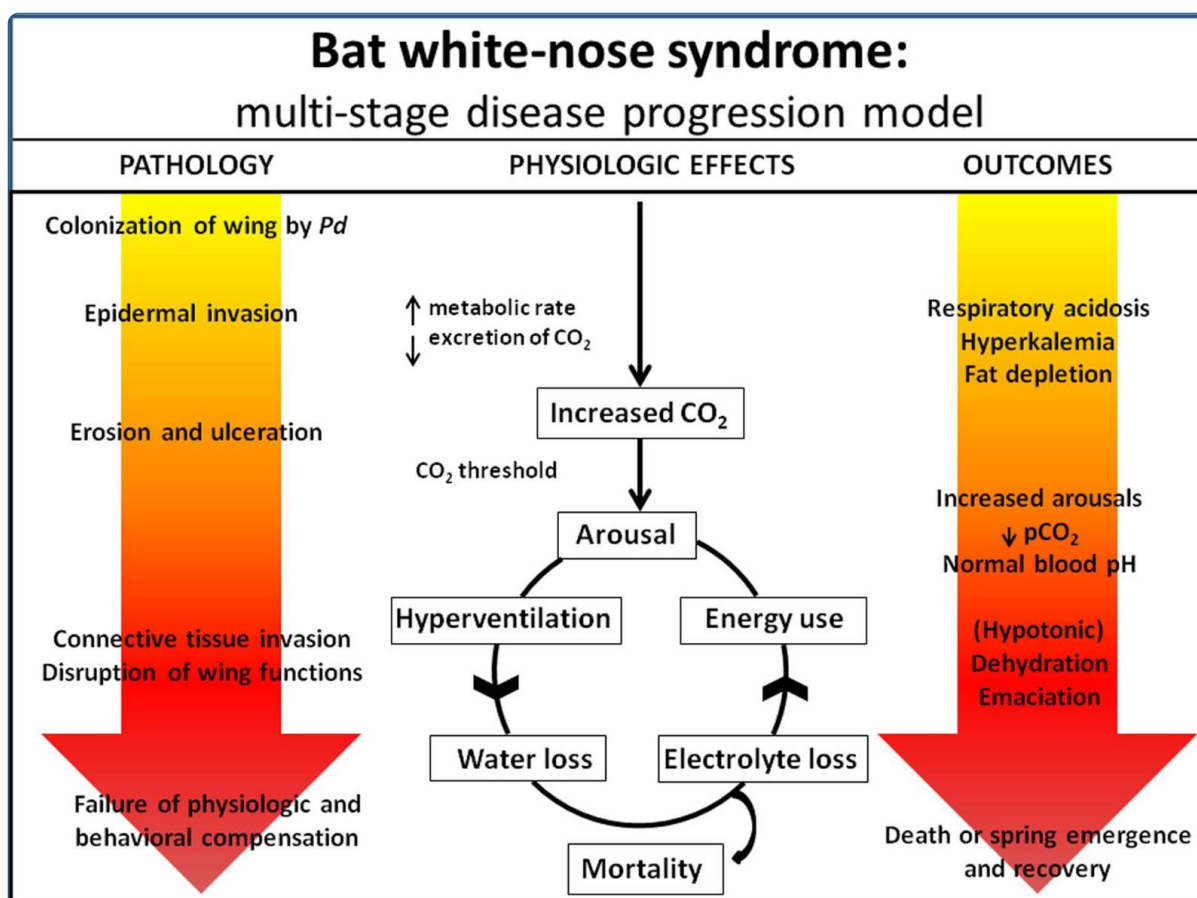
Figure 1. White-nose syndrome (WNS) disease progression model showing pathology, physiologic effects, and outcomes (Verant et al. 2014).

The conceptual model of WNS disease progression is central to understanding the motivation behind our bioenergetics-based models. Figure 1, from Verant et al. (2014), shows WNS pathology, physiological effects, and outcomes. Once infected, bats die from disruptions of homeostasis, including increased energy expenditure and water loss (McGuire et al. 2014; Reeder et al. 2012). Energy depletion, due to frequent arousals during hibernation, is believed to

be the proximate cause of death for bats infected with *P. destructans* (Johnson et al. 2014; Reeder et al. 2012; Warnecke et al. 2012). Healthy bats spend most of hibernation in torpor with body temperatures near ambient, with occasional arousals to normal body temperature (euthermia) (Humphries et al. 2002; Thomas et al. 1990). WNS-associated mortality occurs during the later stages of hibernation and diseased bats appear emaciated from more frequent energy-consuming euthermic arousals (Reeder et al. 2012; Warnecke et al. 2012). Host condition (amount of stored fat) entering hibernation depends on bat physiology and habitat quality; individuals with sufficient energy stores and optimal microclimate and physiological strategy should be able to survive *P. destructans* infection. In general, metabolic rates are known to differ among species as dictated by body size (e.g. Hayssen and Lacy 1985). Prior to our project, what was less clear was whether or not mass-specific torpid metabolic rate varied between or among bat species. One study had suggested this metabolic rate may differ within a bat species during hibernation along a latitudinal cline but only at more extreme temperatures (Dunbar and Brigham 2010). No one had examined mass-specific torpid metabolic rate across multiple species or within western populations, and we targeted this value for measurement in our study because physiologically the metabolic rate at which fat stores are consumed is critical to surviving winter and WNS. Related, water balance appears to be disrupted in WNS-affected bats, and dehydration may be the trigger for energy-consuming arousals and flights related to thirst (Cryan et al. 2010; McGuire et al. 2014; Thomas and Cloutier 1992; Willis et al. 2011). A bioenergetics framework was crucial to build a systematic understanding of WNS impacts within the context of non-stationary conditions across the West. For example, ambient temperature is an important determinant of the hibernaculum environment and bat hibernation periods, which can directly influence WNS disease progression by (1) increasing or decreasing the energy budget needed to survive the fungal infection or (2) affecting disease severity by altering the growth rate of the pathogen.

The available research prior to our study on *P. destructans* spread and impacts on bat species in the West only offered only a partial picture of the system because it discounted species-specific WNS disease susceptibility and progression. An initial model that estimated year-of-infection by county fitted a model based on diffusive spread and presence of caves and duration of winter (mean days < 10°C) suggested that the fungus would cross central Nebraska around 2016 (Maher et al. 2012). This model lacked spatial resolution for large western counties, did not differentiate among bat species and ignored host bioenergetics. Alves et al. (2014) took a simple ecological niche modeling approach which relied primarily on land classes and precipitation that predicted limited *P. destructans* occurrence in the West. The authors assumed all bats (25 species) would be impacted across their North American range and ignored the critical role of bat bioenergetics in disease susceptibility.

Summarily, approaches prior to our study patently oversimplified species and populations with intrinsic physiological and behavioral characteristics, or extrinsic climate conditions that could minimize pathogen transmission and disease severity and serve as potential refugia. Our project recognized that the joint physiological and ecological niche occupied by hosts and the pathogen could drive transmission pathways and WNS severity. On the one hand, if larger fat stores, lower torpid metabolic rates and less frequent arousals, for example, increase survival during WNS infection, high elevation western mountains or northern locations could act as refugia from WNS. On the other hand, southern hibernacula are characterized by shorter hibernation periods

and reduced growing period for the fungus, but warmer microclimate and consequently higher fungal growth rate (Verant et al. 2012). Interpretation of the potential impact of WNS in these and other scenarios (e.g. dry versus humid environments during hibernation) required an integrated approach considering characteristics of the host, pathogen, and environment. Such climate-based responses, which are directly linked to species and population-specific bioenergetics, had important implications for species susceptibility and mitigation activities.

At the time we began our project, WNS-related resources were predominantly focused on disease outbreak areas in the East, leaving us ill-prepared to manage WNS in the West. This meant that conservation and wildlife health communities did not yet have baseline ecological, physiological or behavioral data to begin to frame an understanding of WNS impacts as it expanded its range and host distribution. For example, we did not know whether western populations of species affected in the East would respond differently; how new species would be affected by WNS; how climate change would affect WNS outcomes; whether or not western bats would be able to adapt or evolve; or if land managers would be able to alter hibernaculum transmission or limit disease severity.

To address these western WNS knowledge gaps and to support the DoD's capacity to steward at risk species our project laid out and achieved four scientific objectives. First we set out to collect robust data, leaning heavily on field missions and pulling in existing data sets when possible, on western bat morphology, bioenergetics, and hibernacula environments. Our second objective focused on refining and developing a WNS bioenergetic survivorship model and the parameterizing it with data from western bats. The third objective was to incorporate the survivorship model into spatial maps and to predict impacts of climate change on this disease system. Objective four was the culmination of these efforts, disseminating the knowledge and findings through scientific research and the peer-reviewed literature.

Materials and Methods

Field collection of bat energetic data and hibernaculum data
Much of the bat energetic data required to parameterize the mechanistic model of WNS survivorship did not exist and needed to be collected. Hence, a fundamental component of the project was to gather field energetic data on at least five species of bats (*C. townsendii*, *E. fuscus*, and *Myotis* spp.). Species were initially targeted based on variation in host traits which will likely affect WNS disease outcome and the ability to achieve target sample sizes. We also compiled, standardized, and analyzed available data from prior efforts in Canada. No physiological, morphometric, or environmental variables required transformations prior to analysis.

Permitting and partners
In the United States all procedures were approved by the Texas Tech University Institutional Animal Care and Use Committee (protocol 16031–05). We obtained permits from the Montana Department of Fish, Wildlife & Parks (2016–104, 2017–018, and 2018–008), Colorado Parks and Wildlife (16TR2172, 17TR2172, 18TR2172, and 19TR2172), Nevada Department of Wildlife (497636), Oklahoma Wildlife Conservation Department (6765, 6839, and 7243), Utah Division of Wildlife Resources (2COLL10094), Texas Parks and Wildlife Department (SPR-0416-115), and the National Park Service (ORCA-2018-SCI-0001). A written approval was also received from the University of Central Oklahoma Selman Living Lab Committee. In Canada, bat handling and the procedures for measuring metabolic rates of bats both for this project and collected prior to this project conformed to the guidelines of the Canadian Council on Animal Care and were permitted by Alberta Environment and Parks (17-214 and 18-016), British Columbia Ministry of Forests, Lands and Natural Resource Operations (MRCB15-163558), Northwest Territories Department of Environment and Natural Resources (WL500648), Government of Northwest Territories Wildlife Care Committee (NWTWCC 2018-015), and Parks Canada (WB2018-020 and WB-2018-28777). The field teams practiced WNS decontamination protocols (United States Fish & Wildlife Service 2016) and coordinated as much as possible with existing bat surveys to minimize bat-handling and disturbance events during hibernation. Opportunistic surveillance for WNS and non-invasive diagnostics included consultation with state agencies and the U.S. Geological Survey (USGS) National Wildlife Health Center. When indicated, we submitted swab samples from bat wings to test for the presence of *P. destructans* (National Wildlife Health Center 2013). To help our agency and management partners protect, conserve, and manage cave resources, and in accordance with the National Caves and Cave Resources Management and Protection Act, we have adopted a data management policy to not disclose precise locations of our study sites in publicly-available publications and reports.
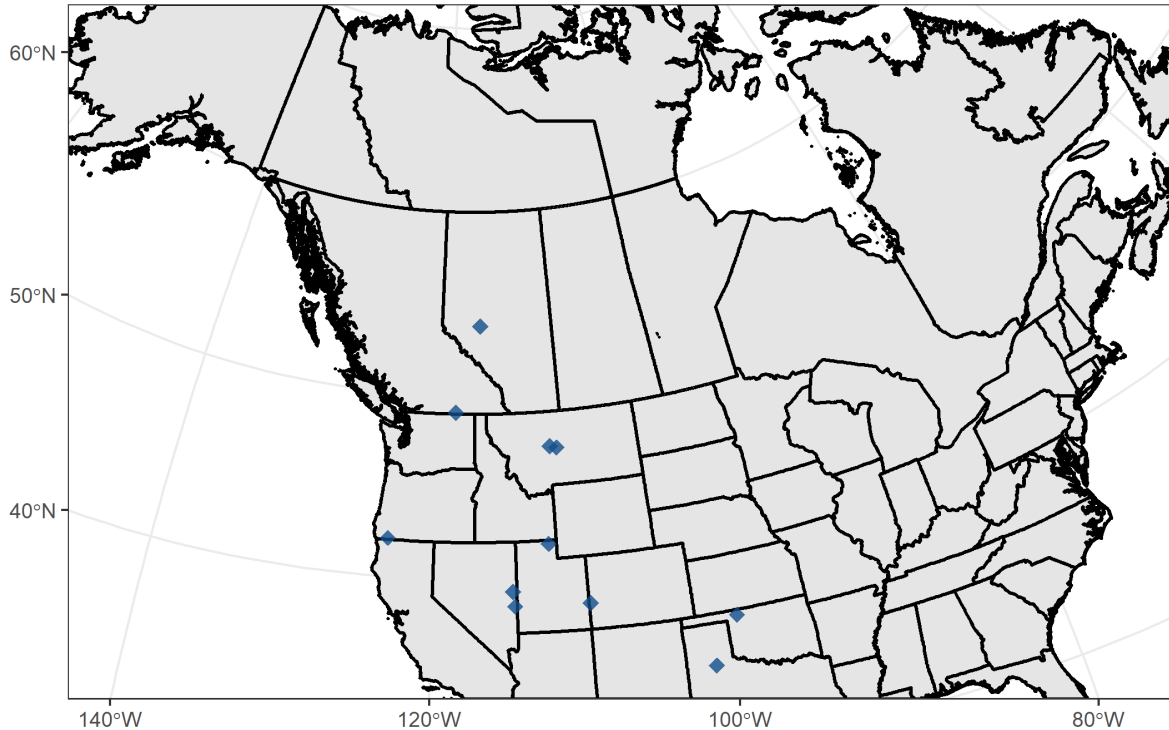
Figure 2. Project-supported field sampling sites.

General overview

Project supported fieldwork was conducted at eleven sites spread across nine western states or provinces (Alberta, British Columbia, Colorado, Montana, Nevada, Oklahoma, Oregon, Texas, and Utah) (Figure 2). During fall and winter fieldwork, we gathered data about energetics and body composition of bats prior to hibernation as well as hibernaculum environmental conditions. The team identified species using region-specific field identification keys (e.g., Shorr and Navo 2014). We captured bats during the pre-hibernation (September - November) swarming and mid-hibernation (January - February) periods with mist nets or harp traps placed near bat activity or at the cave entrance and hand-captured bats from hibernaculum walls during mid-hibernation (Figure 3). We transported bats in cloth bags to a mobile laboratory near the field site where we completed all measurements. It is difficult to determine age late in the swarming season and impossible during hibernation, but any bats we suspected to be sub-adults were excluded from our analysis and therefore we make the assumption that all individuals in our study were adults. We weighed each bat (± 0.1 g), measured forearm length as a standard measure of body size (± 0.1 mm), and for a subset of bats used a quantitative magnetic resonance (QMR) body composition analyzer (Echo-MRI-B, Echo Medical Systems, Houston, TX; McGuire and Guglielmo 2010), to non-invasively measure fat mass, lean mass, and total body water (Figure 4).

Figure 3. *Corynorhinus townsendii* (Townsend's big-eared bat) hibernating on a mine wall (top; K. Raff) and a pair in hand ready for sampling (bottom).

Figure 4. An *Eptesicus fuscus* (big brown bat) resting in a QMR chamber before a 2-minute scan to quantitatively measure lean, fat, and total body water (Bobbitt/USFS).

Respirometry protocol and calculations of TMR and EWL
We measured torpid metabolic rate (TMR) and evaporative water loss (EWL) using open-flow respirometry (Lighton 2008; Figure 5). We used two respirometry systems (Sable Systems International, North Las Vegas, Nevada, USA), each capable of measuring seven animal chambers and a baseline channel (14 animals total). After morphometric measurements and QMR scans were completed, we selected the heaviest individuals for respirometry, maintaining an equal sex ratio. We placed each bat inside a sealed 350 mL glass chamber with 0.2 µm filters (Cole-Parmer, #15945-42) placed in-line to filter potential *P. destructans* contamination from incurrent and excurrent airstreams. Each chamber contained a wire lattice cage to provide a roosting surface, and we added mineral oil to the bottom of the chamber to prevent bat excretions from biasing water vapor pressure (WVP) measurements. The chambers were housed inside a dark, temperature-controlled (±0.5°C) cabinet (PELT-5, Sable Systems International).

We scrubbed incurrent air stream (drawn from outside ambient air) with Drierite® (W.A. Hammond Drierite Co. LTD, Xenia, Ohio) to remove water vapor, sodium bicarbonate (Sigma-Aldrich cat no: 72073) to remove CO_2, and finally magnesium perchlorate (Sigma-Aldrich cat no: 222283) to remove additional water vapor released from the CO_2 scrub. We held bats at 10 °C for 12 h prior to the start of measurements to allow bats to settle and enter steady-state torpor following capture and handling disturbance. We used a dew point generator (DG-4; Sable

19

Systems) to maintain humidity (approximately 85% RH) during the settling phase. We maintained flow rate (flowbar FB-8; Sable Systems) at approximately 300 mL/min during settling, and reduced flow rate to 100 – 120 mL/min when bats entered torpor. We sequentially monitored each bat using a multiplexer (RM-8; Sable Systems), continuously rotating among bats for the duration of the respirometry measurements. During the settling phase we cycled through bats at 10 min intervals. Following 12 h of settling, we switched to a stream of dry air to avoid potential condensation at the low saturated water vapor pressure associated with low temperatures. We cycled through bats and the baseline reference channel at 3 min intervals during the measurement phase, starting at 10 °C and sequentially reducing temperature to 8, 5, and 2 °C. Prior to any field measurements we confirmed that 3 min accounted for the washout period at our measurement flow rates. Each temperature treatment was maintained for approximately 3 hr, corresponding to 7 – 8 measurements of TMR and EWL per bat at each temperature. Excurrent air was subsampled at 75 mL/min and passed through a Field Metabolic System (FMS; Sable Systems International) that measured WVP and excurrent CO_2. We increased flow rates to ~300 mL/min to provide adequate flow to bats that aroused during measurements and if bats did not return to torpor they were removed from the experiment to prevent unnecessary stress and depletion of fat stores. Upon completion of measurements we offered water and a high calorie nutritional supplement (Nutrical, Tomlyn Veterinary Science) to each bat before release.

We processed respirometry recordings in Expedata (Sable Systems), correcting for lag times between analyzers and temporal drift. We selected the mean minimum fractional concentration of CO_2 for each measurement at each temperature for further calculations. Because torpid bats have extremely low metabolic rates, and because of greater sensitivity of CO_2 sensors compared to O_2 sensors, we calculated metabolic rate from CO_2 using equation 10.5 from Lighton (2008). All measurements were made after 12 h of settling time, ensuring all bats were post-absorptive and therefore we assumed fat metabolism (respiratory quotient $= 0.7$) in all our calculations. We converted CO_2 values to mW using the oxyjoule equivalent method (Lighton 2008) and report mass-specific values (mWg^{-1}) to account for variation in body size among species. We quality checked all measurements and excluded values from bats that were not torpid or if there was an erroneous measurement (values < 0.25 mWg^{-1} or > 2 mWg^{-1}) and selected the minimum TMR measurement at each temperature for each individual for further analyses. We calculated water vapor density from WVP using equation 10.10 from Lighton (2008) and converted to EWL (mg H_2O h^{-1}) by multiplying water vapor density by flow rate.
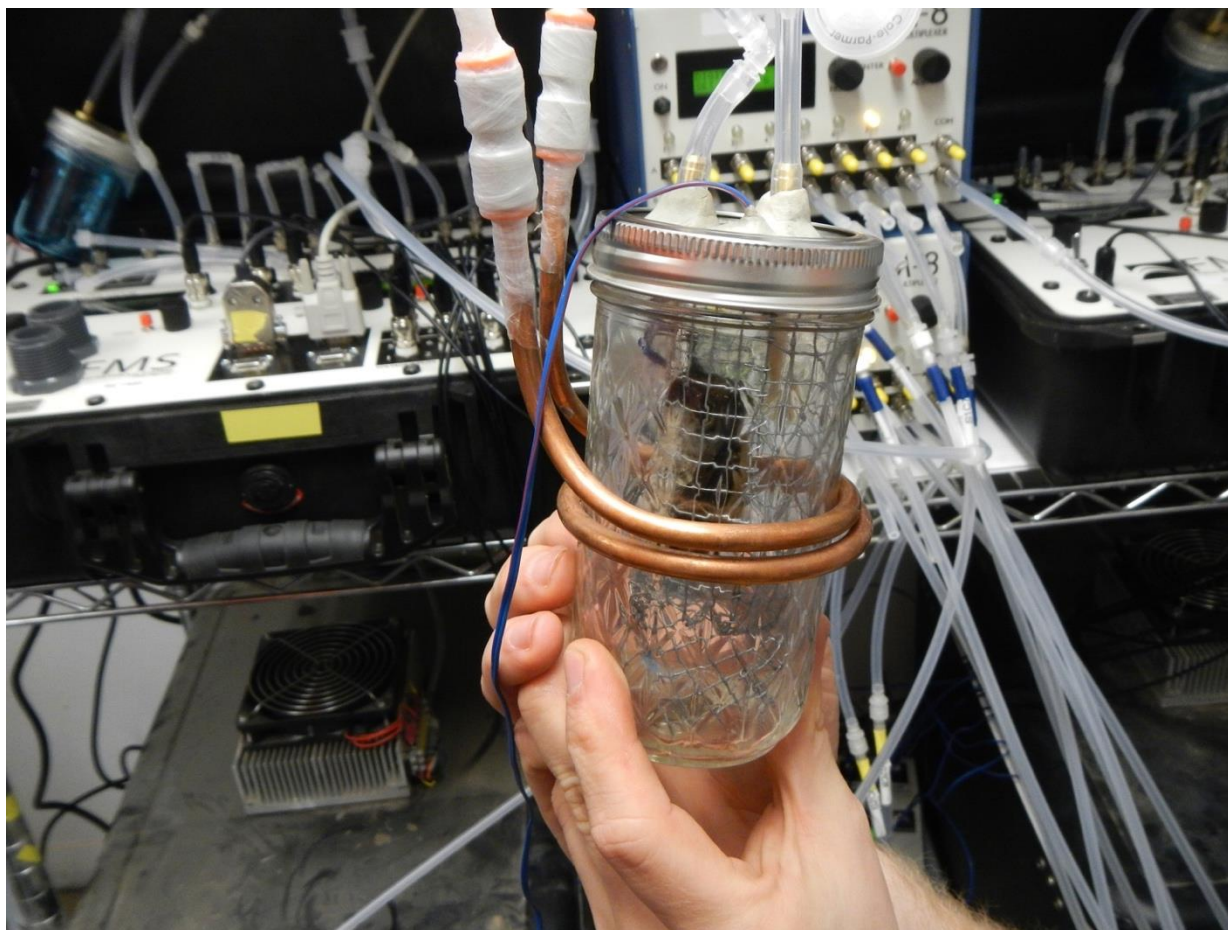
Figure 5. Bat positioned inside a respirometry chamber but outside the temperature controlled-cabinet (Bobbitt/USFS).

Measurement of temperature and relative humidity at hibernation sites

At nine sites we deployed two types of units to measure environmental conditions of hibernacula. Depending on the configuration of the site (i.e., number of chambers or roosting sites), these include up to 10 temperature-only data loggers (iButton DS1922L-F5 or DS1921G, Thermochron) and up to five combination temperature and humidity data loggers (S-THB-M008 or U23-001, Onset HOBO Data Loggers). A HOBO logger was attached to a tree outside the hibernaculum to record surface conditions, while inside the loggers were suspended by copper wire near the cave surface. iButtons were wrapped with a monolayer of Parafilm (Bemis Company, Inc., Neenah, Wisconsin, USA) to prevent water damage, and placed in a small section of pantyhose hung from the cave surface such that the iButton was suspended in the air column. We calibrated all iButtons from -5 to 35 °C in a glycol bath (Haak A25B, Fisher Scientific, Hampton, New Hampshire). HOBO loggers were not independently calibrated, however comparison with paired, calibrated iButton data revealed no difference in observed temperature between logger types (Figure 6). Both types of data loggers were programmed to collect data at 3 h intervals from late fall through spring. We calculated water vapor deficit from microclimate data by calculating the difference between saturated and observed water vapor pressure (WVP) for a given temperature and the measured WVP, as calculated from the temperature and relative humidity measured with HOBO loggers (see Kurta 2014). At Clarity Tunnel we measured ambient temperature outside and inside the roost every 20 min by placing

21

temperature data loggers (Kestrel DROP2; Kestrel Instruments, Boothwyn, Pennsylvania) ~8 m outside the tunnel entrance and ~30 m inside the tunnel.
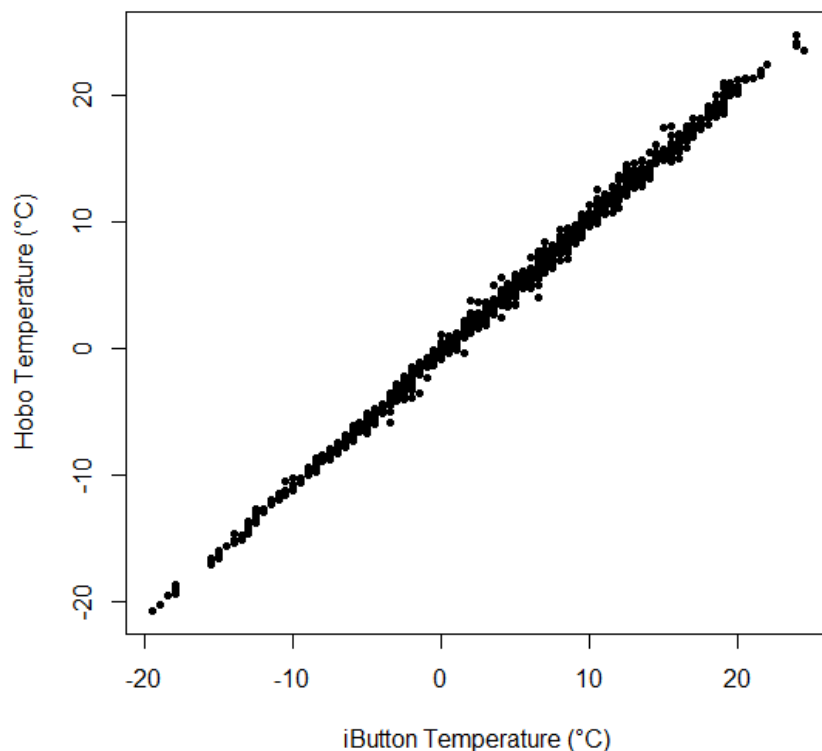
Figure 6. Graph of iButton unit temperature measurements against co-located HOBO unit temperature measurements at the Paradox site in Colorado. The high degree of correlation suggests the different units are well calibrated.

Torpor bout duration with temperature-sensitive transmitters
We deployed temperature-sensitive radiotelemetry on bats at Phoenix Mine, Cadomin Cave, Lick Creek Cave, Piermont Mine, Big Chief Mine, Logan Cave, Old Dry Wolf Cave, Selman Cave, Clarity Rail Tunnel, and Paradox Mine to record torpor bout durations or arousal frequencies during winter sampling for a small number of bats. Willis and Brigham (2003) found that skin temperatures are a good approximation for body temperature for small bats because of their small body size. We placed data logging receivers (Sensorgnome, Lotek SRX400, or Lotek SRX800 depending on site) powered by deep-cycle marine batteries within the hibernaculum at locations where bats were expected to hibernate. We placed 3-element Yagi antennas at either targeted locations based on information from local land managers and/or covered large sections of the hibernaculum with up to 10 antennas in different parts of the hibernaculum. Prior to deployment, all transmitters were calibrated at five points between 5 °C and 42 °C in a temperature-controlled cabinet (PELT-5, Sable Systems International) against a previously calibrated thermocouple. We generated a unique calibration curve and correction equation for each transmitter to convert pulse intervals to skin temperature data (T_{sk}). The receiver recorded the pulse rate of each tag for 15 sec at 7.5 min intervals or less, depending on the number of tags deployed, and cycled through each tag every 30 min to extend battery life. We selected 20 – 30 bats for telemetry observation at a given site. In the United States sites, this included 172 bats

targeted for respirometry. We attached a radio-transmitter (US: 0.36 g, Pip3 temperature-sensitive transmitter, Lotek Wireless, Canada; Canada: ~0.47 g; BD-2NT, LB-2NT, or BD-2XT, Holohil Systems Ltd., Canada) by trimming a small amount of fur in the intrascapular region and affixing the transmitter with non-toxic surgical adhesive (e.g., veterinary grade cyanoacrylate, surgical latex adhesive). Glue was expected to hold for approximately 40 days, after which the transmitter would fall off before the bats emerged in the spring (Halsall et al. 2012). At Cadomin, large banks of batteries were flown in and out by helicopter with two data logging Lotek receivers deployed to record transmitters from January through April. The receiver cycled through all frequencies (n = 20) for up to 1 min each, resulting in each frequency being sampled at least every 20 min. For United States sites we used a power-saving receiver and data-logging technology, a new application of Sensorgnome hardware and software that we developed specifically for the data needs and logistical constraints of our project.

Torpor bout duration using modified iButtons and Recco reflectors
We affixed modified iButtons to bats in Cadomin Cave and Phoenix Mine. The former is a significant hibernaculum for *M. lucifugus* in Alberta and the latter is a newly discovered hibernaculum for hundreds of *C. townsendii* bats near the Greenwood area of British Columbia. We remodeled the iButtons to decrease the circuit board size, use a smaller battery, and replaced the metal housing with only a thin layer of bright yellow Plastidip (Plasti Dip International). These iButtons were modified by adapting the instructions included in Reeder et al. (2012) and then a small RECCO (00-RS-30-CL for insects/small mammals) reflector was attached to assist with locating and recovery. Twenty units were then attached to bats at each of these locations using a small amount of latex or veterinary grade cyanoacrylate glue with anticipation that they would fall off by the end of winter when the bats start to fly around frequently. These units were deployed mid-winter in both locations. Tags were recovered in spring using a RECCO receiver (RECCO Model R9) to locate them; when roosting bats were seen with tags still attached, they were removed and downloaded.

Acoustic monitoring at Lick Creek and Selman Living Lab
At Selman Living Lab we deployed two ultrasonic acoustic monitors (Roost Logger, Titley Scientific, Columbia, Missouri, USA) outside two cave entrances in November 2017 to measure winter activity. We placed acoustic detectors in locations that would record activity near the entrances of the cave, while minimizing the likelihood of detecting activity inside the hibernaculum. The acoustic loggers operated in triggered mode between 30 min before sunset and 30 min following sunrise. Once triggered, loggers recorded for 5 sec unless an additional call was detected. We extracted calls using AnalookW software (version 4.2n, Titley Scientific, Columbia, Missouri, USA) and counted the number of files generated per day. For analysis, we used breakpoint regression to determine when bat activity was dramatically reduced during winter. Through this analysis we determined two breaks: December 7 and February 4. Before December 7 bats were actively swarming and after February 4 emergence from hibernation had begun, thus examining activity outside this time period would not provide a meaningful evaluation of winter activity. We then used linear regression to determine the association between temperature and echolocation activity during this winter period. We manually vetted a subset (n = 50) of call files to confirm that they were produced by *M. velifer*. Given dominance of *M. velifer* at this hibernaculum (n = 100,000 *M. velifer*, n = 70 *P. subflavus*) and that the call

characteristics of *M. velifer* do not overlap with other common species in this area we are confident that virtually all echolocation calls were produced by *M. velifer*.

We used the same acoustic monitoring methods at Lick Creek Cave in Montana. However, there are several species of hibernating bats at Lick Creek Cave, all with overlapping echolocation call characteristics. Because we were not interested in species-specific calls, but rather aimed to use calls as an index of winter duration, we counted passes that contained calls of *Myotis* species (minimum frequency > 30 kHz). We were also not interested in the number of individual bats passing the detector, but rather if there was general activity outside the cave; we thus used a threshold of 50 passes day-1 to determine the onset and end of the hibernation period.

Empirical analyses of bat hibernation physiology
1. Intraspecific variation in hibernation physiology
We first considered variation in hibernation physiology among populations of species distributed over large geographic ranges. We studied this question by comparing the physiology of *M. lucifugus* and *C. townsendii* for which we have data from multiple sites across a large geographic range. We hypothesized that variation in environmental conditions across populations could affect hibernation strategies. We made two alternate predictions. If widely distributed species are locally adapted to regional environmental conditions, we predicted we would observe physiological differences among sites. Alternatively, if populations from throughout the species range seek out and select similar hibernacula then we predicted we would not observe differences across our study sites.

We compared *M. lucifugus* from hibernacula in Montana, Alberta, and Northwest Territories, including the most northerly known hibernaculum for the species. We conducted the *C. townsendii* fieldwork at sites in Colorado, Utah, Nevada, Oregon, and British Columbia. We characterized the climate at each of our study sites based on 1981 – 2010 climate normals (National Oceanic and Atmospheric Administration, Environment and Climate Change Canada).

The analysis we report here considered mass-specific metabolic rates (mWg^{-1}) for ease of comparison with other literature and other accompanying studies, but the qualitative outcomes are not affected whether using mass-specific or whole animal measurements. We used linear mixed models to analyze our data following the procedures described by Zuur et al. (2009). We suspected we might observe greater variance in metabolic rate at either the highest or lowest temperatures due to individual physiological thresholds. Therefore, we included a variance structure in our analysis which allowed for a heterogeneous variance among temperatures. We included a random effect of individual to account for repeated measures and tested for the main effects of temperature, sex, season, site, and the interactions of temperature and site and temperature and sex (in case bats from different sites or sexes responded differently to temperature), followed by Tukey's post-hoc tests for pairwise comparisons of significant effects. For all main effects we assessed statistical significance at $\alpha = 0.05$, but in post-hoc comparisons we considered pairwise differences if p-value < 0.10. All statistical analysis was conducted in R (v 3.6.3; R Core Development Team 2020) and individual bat level data are provided in Appendix A1.

2. Interspecific variation in hibernation physiology

We tested for interspecific variation in hibernation physiology among the 13 species of hibernating bats in our dataset from 14 field sites across the western United States and Canada. We sampled populations of hibernating bats that were taxonomically, ecologically, and geographically diverse. Therefore, we predicted that torpid metabolic rate and evaporative water loss would vary among species. However, we were particularly interested in seeing whether species grouped together into a smaller number of general physiological strategies rather than having to individually consider each species separately. For this analysis we included data from all 13 species of bats at 14 sites across the western United States and Canada, including sites in Northwest Territories, Alberta, British Columbia, Montana, Oregon, Utah, Nevada, Colorado, Oklahoma, and Texas.

For each species, we first assessed whether most individuals remained torpid at lower temperatures, or if individuals aroused below some temperature. The subset of torpid individuals was used for analysis of TMR. We used linear mixed effects models to test for differences in metabolic rate across temperatures for each species (following Zuur et al. 2009). We included a random effect of individual to account for repeated measurements, and allowed for heterogeneity of variance among temperatures, which is expected if individuals vary in their response to low temperature. Not all species were tested during both swarming and hibernation, and sample size was limited in some seasons. Where sample size permitted we tested for an effect of season, otherwise seasons were combined for analysis. We compared metabolic rate across temperatures to determine minimum defended temperature ($T_{defended}$; temperature below which metabolic rate increases), minimum torpid metabolic rate (TMR_{min}) and the temperature range over which TMR_{min} was measured (range over which TMR did not vary based on post-hoc comparisons). We calculated evaporative water loss (EWL) from the same range of temperatures as minimum metabolic rate. As for analysis of intraspecific variation, we report mass-specific metabolic rate here for comparisons among species, but analysis of whole-animal metabolic rate results in qualitatively similar results.

To compare TMR_{min} and EWL among species we conducted two analyses. The temperature range of TMR_{min} varied among species, and there were repeated measurements of individuals at different temperatures within that range. Therefore, we randomly selected one measurement per individual and used linear models to test for a difference in TMR_{min} or EWL among species, repeated this process 1,000 times and used a one-tailed one sample t-test to determine whether the mean p-value was < 0.05. We also used cluster analysis to test for similarity among groups of species (kmeans function in R, centered and scaled data) based on TMR_{min} and EWL. We did not measure EWL for *M. yumanensis* and therefore this species is excluded from cluster analysis. Individual bat level data are provided in Appendix A2.

3. Lean mass contribution to hibernation energetics and water balance
Most studies of hibernation energetics have focused on the use of fat as the primary energy substrate, and studies that consider condition indices implicitly or explicitly assume that changes in lean mass are negligible. However, protein catabolism may play an important role in hibernation that has been underappreciated to date. Gross changes in whole animal lean mass have not been quantified and few studies have considered the role of protein catabolism in hibernation.

We hypothesized that hibernators rely in part on protein catabolism (McGuire et al. In Review). Following from this hypothesis, we tested two predictions. First, we predicted that lean mass would be increased leading into hibernation, as animals deposit both fat and lean mass to survive winter. Second, we predicted that whole-animal lean mass would decrease during hibernation. Finally, differences in the timing of reproductive investment often lead to differences in energetic strategies between sexes, where females have reduced energy expenditure relative to males (Willis 2017). Therefore, we also considered sex effects in lean mass deposition and use. If males use more energy during hibernation (e.g., more frequent arousals or higher metabolic rates), we predicted that lean mass would represent a greater contribution to the hibernation budget of males.

Across all QMR body composition measurements made for the entire project, there were data quality issues at many sites. The magnetic fields used in QMR measurement are temperature-sensitive and we struggled to maintain stable temperatures at many of our field sites. For example, maintaining stable room temperature in our field trailer in Montana in February proved to be impossible. We filtered the QMR dataset, excluding all values where the combined mass of fat and lean tissue did not represent an appropriate proportion of total body mass, whether too low (<0.85) or too high (>0.975). Following this filtering, two QMR body composition datasets remained with sufficient sample size for this analysis: *M. velifer* in Oklahoma (pre-hibernation swarming) and *C. townsendii* in Nevada (pre-hibernation swarming and mid-hibernation). The two Nevada sites were within ~75 km and therefore we combined data from both in our analysis. Forearm length was statistically greater in female *M. velifer* ($t_{90.4} = 2.10$, p-value = 0.04), but was < 1% greater than male *M. velifer* forearm length (< 0.5 mm difference) and therefore we assume there was no biologically relevant difference in body size. Similarly, *C. townsendii* forearm length was statistically greater in females ($t_{63.0} = 2.63$, p-value = 0.01), but was only 1.5% greater than male forearm length (< 1 mm difference) and therefore we assume that there was no biologically relevant difference in body size.

For the *M. velifer* dataset we used linear models to compare body composition between sexes. We used analysis of covariance to determine whether bats deposited lean mass prior to hibernation, and whether there were differences between sexes in the relative deposition of fat and lean mass. With fat or lean mass as a response variable and body mass as a predictor variable, the slope of the relationship describes the relative contribution of fat or lean to total mass gain. With this approach, we determined what proportion of each gram of increasing body mass came from fat or lean mass. If bats deposited only fat, then the slope of the lean mass regression should be zero, otherwise the slopes should both be < 1 and add up to approximately one assuming that all mass gain is either fat or lean mass.

To investigate changes in fat and lean mass through hibernation, we compared body composition of *C. townsendii* during fall swarming and mid-hibernation. We used linear models to compare body composition between sexes and seasons. We used changes in fat and lean mass of male and female *C. townsendii* to illustrate the potential impacts of different contributions of lean mass to energy and water budgets in hibernation. We calculated relative energetic contribution (lean = 5.3 kJ g^{-1}, fat = 37.6 kJ g^{-1} wet mass basis) and water production (lean = 0.82 g H_2O produced g^{-1} wet mass, fat = 1.10 g H_2O g^{-1}) with values from Jenni and Jenni-Eiermann (1998). All calculations are based on the mean values for males and females in the two seasons. We used

propagation of error to carry uncertainty estimates through multiple calculations, resulting in proportionally large errors after the final calculations. These values are strictly numerical calculations and not meant to be interpreted in a statistical comparison, therefore the large uncertainty is less important than the calculated values for comparison. Individual bat level data are provided in Appendix A3.

4. Tadarida brasiliensis (Mexican free-tailed bats) case study
The inclusion of *T. brasiliensis mexicana* in our dataset is notable because this species is not typically considered as a hibernator. Populations in the south-central United States are renowned for making long-distance migrations to southern Mexico in winter. However, there is increasing recognition that subsets of the summer breeding population forgo migration and overwinter in Texas. Our study is the first to examine the physiology of hibernation in this species, including considerations of how these individuals may be affected by WNS. Furthermore, as a highly mobile species, *T. brasiliensis* is particularly relevant to consider as a possible natural vector of long distance spread of the pathogen.

The current framework of winter bat ecophysiology and WNS is heavily biased towards northern latitudes and extreme conditions where insectivorous bats face a critical lack of prey during winter months (e.g., Davis and Hitchcock 1964, 1965; Thomas 1995; Boyles et al. 2008; McGuire et al. 2009; Jonasson and Willis 2011; Jonasson and Willis 2012; Czenze et al. 2013; Day and Tomasi 2014; Hayman et al. 2016; McGuire et al. 2016). Less is known about situations where bats remain active to varying degrees in winter. While long, harsh winters at northern latitudes necessitate obligate hibernation, winter is relatively mild at southern latitudes and torpor expression may be flexible with environmental conditions. *T. brasiliensis* are a subtropical species where most individuals migrate south for winter (with implications for movement of the pathogen), but small remnant populations forgo migration and overwinter. There is evidence for the presence of *P. destructans* infection in *T. brasiliensis*, but to date there has been no diagnostic indications of WNS and no study of their hibernation ecophysiology.

We hypothesized this species uses facultative hibernation to persist through winter and that the bats use heterothermy ranging from daily to multi-day periods depending on ambient temperature. We predicted that *T. brasiliensis* bats are capable of deep torpor, as observed in other hibernating bats, but that they would have a minimum defended temperature higher than northern hibernators.

Methods for *T. brasiliensis* followed the same general methods described above with one exception. When measured prior to hibernation no bats tolerated the 2 °C condition (i.e., all bats aroused from torpor), therefore we used slightly higher temperatures in February (12 °C, 10 °C, 8 °C, and 5 °C). We used mass-specific values of TMR and EWL in this analysis, but as noted for other analyses above, using whole animal metabolic rate did not qualitatively change the interpretation of the results. To objectively estimate the minimum defended temperature, we used a piecewise mixed-effects model with R package '*lme4*' following methods described by Thompson et al. (2015) to estimate the breakpoint of the temperature-response curve. For this analysis we included metabolic rate as the response variable, actual ambient temperature (T_a) experienced by the animal as a fixed effect, and individual as a random effect.

As noted above, we used temperature-sensitive radiotelemetry to monitor skin temperature (T_{sk}) of hibernating bats. We included only T_{sk} readings with at least three consecutive data points within 5 min. We excluded occasional aberrant readings by only including T_{sk} values where changes in body temperature were less than or equal to the highest published rates of T_{sk} change for insectivorous bats (2.7 °C/min; Menzies et al. 2016). We used the torpor onset threshold method to distinguish between periods of torpor and euthermia (Willis 2007). To investigate if animals remained torpid longer during harsher weather, we used a linear model to examine the relationship between torpor bout duration and the minimum T_a outside the roost during the torpor bout. Individual bat level data are provided in Appendix A4.

Improving the energetic costs of cooling model
Calculating energetic costs from first principles
We modelled the energetic cost of cooling (E_{cool}) as a function of the difference between euthermic and torpid body temperature (T_b), the decrease in metabolic rate over that temperature range, and the cooling rate. We assumed that cooling occurred passively; that is, the reduction in metabolic rate is due to an effect of temperature, rather than physiological inhibition (but see Geiser 2016, 2004).

We calculated the total cost of cooling as the energy required for metabolism during steady-state torpor, plus the additional costs to maintain metabolism above torpid T_b as the body cools from euthermic T_b (Prothero and Jürgens 1986; Strunk 1971). We calculated this change using Q_{10}, or the change in metabolic rate over a 10 °C change in temperature, with a scaling equation with body mass (M_b; g) (Geiser 1988):

$$Q_{10} = 3.82 - 0.507 \log_{10} M_b \tag{1}$$

The cost of cooling was calculated as the sum of this reduction in euthermic metabolic rate in response to the difference between torpid and euthermic T_b, and the metabolic rate of steady-state torpor:

$$E_{cool} = D_{cool} \left[TMR_{min} + \left(RMR \cdot Q_{10}^{\frac{T_{tor} - T_{eu}}{10}} \right) \right] \tag{2}$$

where TMR_{min} is the mass-specific minimum torpid metabolic rate (ml O_2 g^{-1} h^{-1}), RMR is the mass-specific resting metabolic rate at ambient temperature (T_a; °C) (ml O_2 g^{-1} h^{-1}), T_{tor} and T_{eu} are torpid and euthermic T_b (°C), respectively, and D_{cool} is the duration of the cooling phase (h). We estimated RMR by increasing allometrically predicted BMR (Schmidt-Nielsen, 1984; Speakman and Thomas 2003) in response to T_a and scaled by euthermic thermal conductance (C_{eu}):

$$RMR = BMR + C_{eu}(T_{eu} - T_a) \tag{3}$$

The duration of the cooling phase (D_{cool}) was determined by the cooling rate (CR) and the temperature difference between T_b:

$$D_{cool} = \frac{\log(T_{eu} - T_{tor})}{CR} \tag{4}$$

We assumed that cooling followed an exponential decay (Newton 1701). Therefore we modeled the rate of cooling as a derivation from Newton's Law of Cooling (Henshaw 1968; Kleiber 1972; Newton 1701; Strunk, 1971), which assumes the rate of heat loss from a body is directly proportional to body size, conductance, and temperature difference between the body and the surrounding environment (Bakken 1976a; Prothero and Jürgens 1986). We calculated the cooling rate as:

$$CR = \frac{C_{eu} \cdot M_b^{0.67} \cdot \log(T_{eu} - T_a)}{S \cdot M_b} \tag{5}$$

where C is the thermal conductance during euthermia (ml O_2 g^{-1} $°C^{-1}$ h^{-1}), $M_b^{0.67}$ represents the surface area of the animal as defined by body mass, $T_{eu} - T_a$ is the difference between euthermic T_b and T_a (°C), and S is the specific heat of animal tissue (0.1728 ml O_2 g^{-1} $°C^{-1}$; Hart 1951). By taking the log of the temperature difference in both Equations 4 and 5, we account for the exponential change in the rate of cooling as T_b is reduced to torpid body temperature. Rather than estimating an instantaneous cooling rate, this equation allowed for the consideration of body size and insulation of the animal (i.e. thermal conductance), as well as environmental influences (e.g., rapid cooling in cold environments).

Validating the cooling model
To validate the cooling equation, we compiled data from published papers that presented metabolic rate and skin temperature curves over time and compared the total energetic cost of torpor entry (i.e., cooling) with modeled cost (Table 11). For publications where data was only presented in figures, we used plot digitizing software (WebPlotDigitizer 4.1; https://apps.automeris.io/wpd) to extract metabolic rate and skin temperature over the period of cooling. We calculated the mean of euthermic and torpid skin temperatures and defined the onset of cooling when skin temperature dropped at least 2 °C below mean euthermic skin temperature and the end of cooling when skin temperature was within 0.5 °C of mean torpid skin temperature. We extracted the metabolic rate for the cooling curve at one-hour intervals from the start and end of cooling and summed the values over the entire cooling period.

Using Equation 2, we then modeled the energetic cost of cooling given morphometric, physiological, and environmental parameters reported in each publication. We obtained body mass, torpid and euthermic T_b, and thermal conductance (if available) for each species; if thermal conductance was not available, we calculated conductance using methodology described by McNab (1980) and Speakman and Thomas (2003). RMR was predicted using Equation 3 and TMR was predicted using the Q_{10} decrease in BMR in response to torpid T_b (Geiser 1988). One publication (Wang, 1978) reported cooling costs for multiple individuals over three ranges of T_a. Therefore, we calculated the mean cost for each temperature range over individuals (for the measured cost) and temperatures (for modeled cost). In instances where multiple data sources existed for the same species (as in the case of *M. lucifugus*), we chose the source that reported as many model parameters as possible.

We compared our modeled values to measured values using linear regression in R version 3.3.3 (R Development Core Team 2019). We assumed that if our cooling model adequately represented measured cooling cost, the slope of the relationship would not be different than 1 (Glantz and Slinker 2000). We did not run a sensitivity analysis of the model to changes in

parameters, as a preliminary analysis showed that the model was sensitive to all parameters equally.

We examined the relationship between mass-specific cooling cost and both body size and thermal conductance to determine the effects of each variable on cooling. We also determined if a scaling relationship with body size and mass-specific cooling cost existed with cooling rate, similar to the relationships observed with warming rate (Geiser and Baudinette 1990; McKechnie and Wolf 2004).

Comparison between 67% proportion and cooling model
We compared the energetic cost of cooling for 53 species (Appendix A5) using both our cooling model (Equation 2) and the commonly-assumed 67% proportion of warming cost. We defined the energy required to warm from torpor to euthermia (E_{warm}) as a function of the cost to raise the temperature of animal tissue from torpid to euthermic T_b (McKechnie and Wolf 2004), in addition to the metabolic costs required to balance heat lost to the environment over the period of warming (Cryan and Wolf 2003). Thus, the cost of warming was calculated as:

$$E_{warm} = S \cdot (T_{eu} - T_{tor}) + D_{warm}[C_{eu}(T_{eu} - T_a)] \qquad (6)$$

where D_{warm} is the duration of time required to warm from torpid to euthermic T_b (h). Assuming warming occurs linearly (Cryan and Wolf 2003; McKechnie and Wolf 2004), we calculated D_{warm} as:

$$D_{warm} = \frac{T_{eu} - T_{tor}}{WR} \qquad (7)$$

where WR is the warming rate for the species (°C h^{-1}). We obtained warming rates for each species from multiple sources (Geiser and Baudinette 1990; Hirshfeld and O'Farrell 1976; Menzies et al. 2016; Willis 2008). All other model parameters were acquired as described above.

We compared both estimates of cooling, predicted from Equation 2 and estimated as 67% of warming, using linear regression. If 67% of warming sufficiently described the cost of cooling, we assumed the slope of the relationship not to be different from 1 (Glantz and Slinker 2000). We regressed the difference between the two estimates against body mass to examine differences in predicted cooling costs in the context of body size.

Hibernation energetic model
The mechanistic hibernation model we use in this project is a refined version of the Hayman et al. (2016) model (which builds on Humphries et al. 2002 and Thomas et al. 1990) with a few critical amendments. The core model is built upon the idea that we can (a) predict the amount of energy required for a bat to survive winter and by (b) comparing that to the length of winter at a location we can (c) predict whether a bat could survive at that location. The source code from the original publication was extracted and is now available as a draft open source R package (R Team 2016) at github.com/cReedHranac/batwintor. Model refinements included the addition of body mass in the arousal and cooling equations (see above; Haase et al. 2019a), rewarming calculations based on species specific rates (recently published by Menzies et al. 2016), and accounting for energy lost as heat when bats are in the rewarming period. An additional major

refinement was the inclusion of evaporative water loss in the calculation of: torpor duration, *P. destructans* fungal growth on torpor duration, and fungal growth on evaporative water loss (Figure 7).
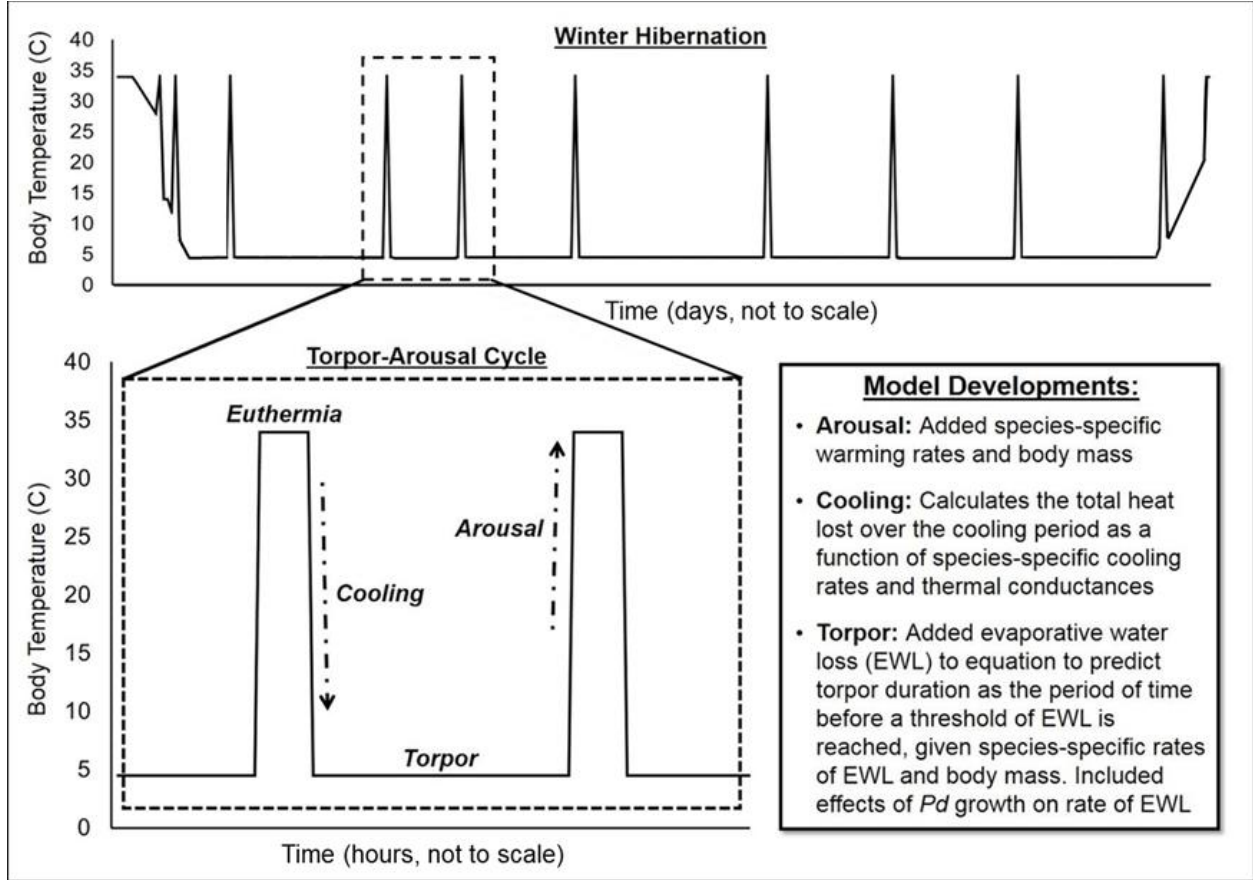
Figure 7. Typical arousal patterns during winter hibernation (above, not to scale) and the elements of a torpor-arousal cycle (lower left). The total energetic costs of torpor and arousals are calculated by the mechanistic White-nose syndrome (WNS) survivorship model for specific temperature and humidity conditions and evaluated against energy stores (i.e., body fat) that bats have going into hibernation to predict how long bats can hibernate. WNS increases the number arousals and overall energetic expenditure of diseased bats, leading to starvation. New model developments from our project are highlighted in the text box (lower right).

Core hibernation energetic model components

We modeled energy expended during a torpor-arousal bout (E_{bout}) as a function of the energetic cost of torpor (E_{tor}) and torpor bout duration (t_{tor}), cost of euthermia (E_{eu}) and euthermic duration per arousal bout (t_{eu}), and the energy required to warm (E_{warm}) and cool (E_{cool}) to and from euthermia:

$$E_{bout} = E_{eu} \cdot t_{eu} + E_{warm} + E_{cool} + E_{tor} \cdot t_{tor} \tag{8}$$

We estimate the energetic costs of cooling (E_{cool}) and warming (E_{warm}) as described above in Equations 2 and 6, respectively.

While bats are euthermic, the amount of energy expended is dependent on their resting metabolic rate; bats lose heat to the environment as a function of the differential between T_a and the lower critical temperature (T_{lc}), and the thermal conductance of euthermic tissue (C_{eu}). Therefore, the energetic cost of euthermia (E_{eu}) is essentially the basal metabolic rate (BMR), plus any additional cost due to temperatures outside the thermoneutral zone:

$$E_{eu} = BMR + (T_{lc} - T_a) \cdot C_{eu} \tag{9}$$

We estimated BMR (ml O_2 g^{-1} h^{-1}) as a function of body mass (M_b in g) from a scaling equation derived for bats (Thomas et al. 1990):

$$log_e BMR = 1.0895 + 0.744\, log_e M_b \tag{10}$$

We estimated C_{eu} (ml O_2 g^{-1} C^{-1} h^{-1}) using methodology described by McNab (1980) and estimated the mean time in euthermia during each arousal (t_{eu}) from the published literature (Thomas and Geiser 1997).

We modeled the energetic costs of torpor (E_{tor}) as a function of T_a and torpid metabolic rate. When hibernaculum temperature is above minimum defended torpor temperature, energy expenditure can be calculated based on the Q_{10} effect (Kallen 1964). Once hibernaculum temperature falls below the minimum defended temperature, E_{tor} depends on torpid metabolic rate and torpid thermal conductance (C_t):

$$E_{tor} = TMR_{min} \cdot Q_{10}^{(T_a - T_{torMin})/10}, \qquad if\ T_a > T_{torMin} \tag{11}$$

$$E_{tor} = TMR_{min} + (T_{torMin} - T_a) \cdot C_t, if\ T_a \leq T_{torMin} \tag{12}$$

Incorporating evaporative water loss into the hibernation energetics model
We incorporated a mechanistic link between EWL and torpor bout duration. We estimated torpor bout duration (t_{tor}) in two ways: 1) as a function of torpid metabolic rate in response to T_a as described in Hayman et al. (2016), and 2) as a function of EWL. Our revised model uses the shorter of the two estimates given hibernaculum conditions, either arousing as a consequence of EWL or TMR, whichever comes first. By including both calculations in our estimates of torpor bout duration, we considered both the effect of EWL and metabolism on torpor physiology (Geiser and Kenagy 1988; Thomas and Geiser 1997)

To estimate torpor bout duration as a function of metabolic rate (t_{torTMR}), we modified the existing equations developed by Hayman et al. (2016) that scale maximum possible time in torpor (t_{torMax}) by the effects of metabolic rate given T_a:

$$t_{torTMR} = t_{torMax}/Q_{10}^{\left(\frac{T_a - T_{torMin}}{10}\right)} \qquad if\ T_a > T_{torMin} \tag{13}$$

$$t_{torTMR} = \frac{t_{torMax}}{1 + (T_{torMin} - T_a) \cdot \left(\frac{C_t}{TMR_{min}}\right)} \qquad if\ T_a \leq T_{torMin} \tag{14}$$

where Q_{10} is the change in metabolism with a 10 °C change in temperature (Geiser 2004), T_{torMin} is the minimum defended T_b in torpor, TMR_{min} is the associated metabolic rate at T_{torMin}, and C_t is the thermal conductance during torpor. Minimum defended T_b (Hanus 1959; Speakman et al. 1991; Brack and Twente 1985) and the maximum time in torpor (t_{torMax}) were estimated from literature (Brack and Twente 1985), and minimum torpid metabolic rate and thermal conductance were measured in the field using respirometry.

To calculate torpor bout duration as a function of EWL (t_{torEWL}), we assumed bats arouse when the total body water pool was depleted to a threshold (Thomas and Cloutier 1992). The hourly rate of total EWL (mg H_2O h^{-1}) is comprised of both cutaneous and respiratory rates of EWL and is dependent on the water vapor pressure deficit between the bat and the surrounding environment. The hourly rate of cutaneous evaporative water loss (CEWL; mg H_2O h^{-1}) is a function of the difference between water vapor pressure at the surface of the bat and the environment (ΔWVP):

$$\Delta WVP \ = \ WVP_{bat} \ - \ WVP_{air} \tag{15}$$

where WVP_{bat} is the water vapor pressure at the skin surface and WVP_{air} is the water vapor pressure of the surrounding air (both in kPa). We assumed WVP_{bat} was at saturation, which can be calculated as:

$$WVP_{bat} \ = \ 0.611 \ \cdot \ e^{\left[\frac{17.503 \cdot T_b}{(T_b + 240.97)}\right]} \tag{16}$$

where T_b is the body temperature of the bat in torpor (Campbell and Norman 1998). We then calculated WVP_{air} at T_a and given relative humidity. We modeled cutaneous EWL as a function of ΔWVP and the area-specific rate of EWL from bodily tissue (rEWL; mg H_2O h^{-1} cm^{-2} per ΔWVP^{-1}) across the surface area (SA; cm^2) of the bat:

$$CEWL \ = \ SA \ \cdot \ rEWL \ \cdot \ \Delta WVP \tag{17}$$

We used a surface area scaling equation (Gouma et al. 2012) to calculate body surface area (SA_{body}) and photos of bat wings to estimate the total surface area of the wings and tail (SA_{wing}; Haase et al. 2019b). Assuming that a furred body and naked wing have biophysical differences that would affect cutaneous EWL, we used different values of the area-specific rate of EWL for the body ($rEWL_{body}$) and wing ($rEWL_{wing}$), estimated from respirometry (Supporting Information). Therefore, we rewrote Equation 17 as:

$$CEWL \ = \ \left[\left(SA_{body} \cdot rEWL_{body}\right) + \left(SA_{wing} \cdot rEWL_{wing}\right)\right] \cdot \Delta WVP \tag{18}$$

Respiratory EWL (REWL; mg H_2O h^{-1}) is a function of the saturation deficit between inspired and expired air. We assumed that inspired air is at T_a and is expired as saturated air at torpid T_b (Thomas and Cloutier 1992). Therefore, we calculated respiratory EWL as:

$$REWL \ = \ respired \ air \ volume \ \cdot \ saturation \ deficit \tag{19}$$

The volume of air that a bat breathes per hour was calculated as a function of the respiration rate of oxygen (i.e. TMR_{min}) in ml O_2 g^{-1} h^{-1} and body mass:

$$respired\ air\ volume\ =\ \frac{TMR_{min} \cdot M_b}{0.2095 \cdot 0.30 \cdot 10^3} \tag{20}$$

assuming the fractional concentration of oxygen in air is 0.2095 and that oxygen extraction efficiency is 30% (Thomas and Cloutier 1992). Using the ideal gas law (Campbell and Norman 1998), we converted the water vapor pressure deficit (ΔWVP; Equation 15) from kPa to mg L^{-1} to determine the saturation deficit.

We validated the rate of total EWL (cutaneous EWL and respiratory EWL) by comparing modeled EWL (from Equations 17 and 19) to measured EWL from each individual during our respirometry procedures. We used individual body mass (Equations 17-18), metabolic rate (Equations 19-20), area-specific rate of EWL (Equations 17-18), and predicted surface area given body mass (Equations 17-18). We modeled the hourly rate of total EWL given the measured T_a and WVP experienced by each individual. We used linear regression to compare modeled EWL to measured EWL rates, assuming that if the model was accurate, the slope of the relationship should be equal to 1.

Given total EWL, we calculated torpor bout duration (t_{torEWL}) based on the reduction of the total body water pool, setting the threshold at 2.7% of lean mass (assuming no body water in fat stores):

$$t_{torEWL} = \frac{0.027 \cdot Lean\ Mass \cdot 1000}{CEWL + REWL} \tag{21}$$

Including the effects of fungal growth on hibernation
We further adjusted the hibernation model by including a link between fungal growth and reduced torpor bout duration through an increase in both metabolic rate and EWL (modifying Equations 13-14, 21). We first altered the estimation of torpor bout duration from T_a (t_{torTMR}; Equations 13 and 14) by scaling t_{torTMR} by the proportion the bat wing surface affected by the fungus. When fungal growth > 0, t_{torTMR} was calculated as:

$$t_{torTMR}\ =\ \left[\frac{t_{torMax}}{Q_{10}^{\left(\frac{T_a - T_{torMin}}{10}\right)}} \right] \Bigg/ \left(\frac{area_{Pd}}{SA_{wing}} \right) \qquad \text{if } T_a > T_{torMin} \tag{22}$$

$$t_{torTMR}\ =\ \left[\frac{t_{tor-max}}{1 + (T_{torMin} - T_a) \cdot \left(\frac{c_t}{TMR_{min}} \right)} \right] \Bigg/ \left(\frac{area_{Pd}}{SA_{wing}} \right) \quad \text{if } T_a \leq T_{torMin} \tag{23}$$

where $area_{Pd}$ is the area (cm^2) of fungal growth calculated as a function of T_b and relative humidity given equations from Hayman et al. (2016).

We adjusted the calculation of torpor bout duration in response to EWL (t_{torEWL}; Equation 21) by increasing CEWL and REWL as a function of fungal growth. We used data from McGuire et al. (2017), who directly measured an increase in TMR and EWL in *M. lucifugus* infected with *P.*

destructans (Haase et al. 2019b). We increased CEWL by including a linear increase to the rate of EWL of bat wings (rEWL$_{wing}$) in response to the proportion the bat wing surface affected by the fungus (from Equation 21):

$$CEWL_{wing} = \left[\left(SA_{body} \cdot rEWL_{body} \right) + \left(SA_{wing} \cdot \left[rEWL_{wing} + \left(0.16 \cdot \frac{area_{Pd}}{SA_{wing}} \cdot 100 \right) \right] \right) \right] \cdot \Delta WVP \quad (24)$$

where 0.16 is the rate of increase in rEWL$_{wing}$, given the proportion the bat wing surface affected by the fungus, determined from data presented in McGuire et al. 2017 (see also Haase et al. 2019b). REWL also is hypothesized to increase in response to fungal growth with an increase in TMR; we included this linear increase by adjusting Equation 23:

$$respired\ air\ volume = \frac{\left[TMR_{min} + \left(0.015 \cdot \frac{area_{Pd}}{SA_{wing}} \cdot 100 \right) \right] \cdot M_b}{0.2095 \cdot 0.30 \cdot 10^3} \quad (25)$$

where 0.015 is the linear increase of torpid metabolic rate given the proportion the bat wing surface affected by the fungus (Haase et al. 2019b).

To validate the adjustment to the estimation of torpor bout duration in response to fungal growth (Equations 22-23, 25), we used an independent dataset of skin temperature measurements from a captive hibernation study by McGuire et al. (2020). Skin temperature data were measured from thirteen *M. lucifugus* infected with *P. destructans* prior to hibernating in a controlled environment (T$_a$ = 7 °C, relative humidity = 98%). Using methodology from Jonasson and Willis (2012), we defined torpor and arousal periods based on cut-off temperatures and calculated the total time in each hibernation phase. We then estimated torpor bout duration (Equations 22-25) at each measured torpor bout from each individual given individual morphometric parameters (initial body mass, predicted surface area). We estimated TMR from body mass and T$_b$ (Speakman and Thomas 2003) and allowed for variation in lean mass (to determine threshold of body water) by sampling from a normal distribution with mean and standard deviation from our capture data. We predicted fungal growth area at each torpor bout given the time since inoculation and equations 2-4 in Hayman et al. (2016). We then used a linear model to compare modeled torpor bout duration to measured torpor bout duration, assuming that if the prediction was accurate, the slope of the relationship should be equal to 1. To determine if including EWL improved our description of torpor expression, we also predicted torpor bout duration without the contribution of EWL using only Equations 22-23. We then compared these predictions to measured bout duration to determine model accuracy. Finally, we compared the R^2 values of both fitted relationships to determine which model had better precision in predicting torpor bout duration.

Estimation of total fat loss and survival for M. lucifugus in Montana
Using our modified hibernation model and model parameters obtained from literature (Appendix A6) and our field captures (Appendix A7), we estimated time until total fat exhaustion for *M. lucifugus* over the range of hibernaculum microclimate conditions measured at our field site. Torpor bout duration changes with body condition and fungal growth so we used differential equations to estimate energy consumption over the winter. We assumed that bats require energy

to arouse at the end of hibernation and to leave the hibernaculum in order to obtain food. Therefore, we included energy required to warm (E_{warm}) and spend 24 h in euthermia (24 x E_{eu}) at the end of winter hibernation. We used the lsoda function of the *deSolve* package, which allowed torpor bout duration to change over time given fungal growth, bat parameters (Appendix A6), and hibernaculum microclimate. We converted total energy consumed over time from ml $O_2\,g^{-1}$ to the amount of fat expended (g) as:

$$fat_{winter} = (E_{winter} \cdot 19.6)/(37.6 \cdot 1000) \tag{26}$$

assuming that 1 ml O_2 releases 19.6 J of energy and the energy content of fat is 37.6 J mg^{-1} (Boyles and Brack 2009). We calculated time until fat exhaustion (t_{fatEx}) as the time when total fat exhaustion (fat_{winter}), became greater than mean fat stores measured during our fall field captures. Finally, we compared the estimated t_{fatEx} for both healthy and infected bats over the range of hibernaculum conditions to the duration of winter for central Montana estimated from our acoustic data. We assumed that mortality would occur if t_{fatEx} was less than winter duration; that is, the mean fat stores did not provide enough fat for a bat to survive through winter, as measured above.

Validation of evaporative water loss calculations and hibernation energetic model sensitivity
We validated the entirety of the hibernation energetic model by comparing measured mass loss from 56 free-living hibernating *M. lucifugus* (Norquay and Willis, unpublished data, but see Norquay et al. (2013) for description of capture methodology and locations) to predicted fat loss from our model. We used this dataset because data from captive animals may not accurately reflect field conditions of free-living animals. We used individuals in which mass was measured during both swarming (August-September) and emergence (April-May). We estimated fat loss using the bioenergetic model for the time between swarming and emergence capture dates, given the hibernaculum conditions where each bat was captured (Bilecki 2003; Czenze and Willis 2015). We took the mean and standard deviation of T_a and water vapor pressure of each capture location and sampled random values from a normal distribution for each individual. We estimated TMR from body mass and T_b (Speakman and Thomas 2003) and allowed for variation in lean mass by sampling from a normal distribution set at the mean and standard deviation from our capture data. We compared estimated fat loss with measured mass loss (assuming all mass change is due to fat loss) using linear regression, assuming if the two values were the same, the slope of the relationship would be no different than 1. We also predicted fat loss for the validation dataset given the hibernation model without the inclusion of EWL; more specifically, we only included Equations 13-14 in our calculations of torpor bout duration. We compared these predictions to measured mass loss and determined both model accuracy (slope = 1) and precision (R^2) to compare against our modified model including EWL.

Following Hayman et al. 2016, we used a multi-parameter sensitivity analysis to assess the impact of each parameter on estimations of time until mortality. Using Latin hypercube sampling in R package *lhs* (Carnell 2016), we created 100 random parameter sets sampled from a uniform distribution of potential values ranging from 10% lower or higher than the default value (Appendix A6). By constraining the minimum and maximum values of the parameters, and including a joint distribution within the Latin hypercube sampling, we considered the potential for correlations between parameters. We determined the relative importance of each variable by

comparing partial rank correlation coefficients (PRCC) values. Positive PRCC values indicate an increase in the model output with an increase in the parameter value, while negative PRCC values indicate a decrease in the model output with an increase in parameter value (Hayman et al. 2016).

Inter-species WNS survivorship estimates
Individual-based hibernation energetics model
Using a combination of field data and energetic modeling, we predicted the probability of winter survival with WNS and determined the influence of host, pathogen, and environmental factors on predicted survival. We used an individual-based modeling framework to allow for variation in bat morphology and physiology and in hibernaculum microclimate. We ran the hibernation energetics model for 100 bats within 100 winters for a total of 10,000 bat-runs of fat expenditure per species. We first characterized a hibernaculum microclimate environment for each species by randomly selecting temperature and water vapor deficit values from normal distributions fitted to the mean and standard deviation from our measured microclimate data from the sampling location associated with that species (Table 1). We determined winter duration for the sampling location given estimates from our winter duration predictive model (see below). We randomly selected body mass, proportion fat mass, and proportion lean mass from normal distributions fitted to the mean and standard deviation of our measured morphometric data for that species to characterize a bat (Table 2). TMR values were randomly pulled from a log-normal distribution fitted to the mean-log and standard deviation of our respirometry measurements. The hibernation energetics model was run for each bat, and if the starting fat mass was not expended over the duration of winter at a site, then survival occurred. For each hibernaculum microclimate environment, we repeated the random selection of bat characteristics 100 times to create a population of 100 bats. We then repeated the 100 bat-runs for 100 hibernaculum environments. We calculated the probability of survival for each species over the 100 independent winter environments as the number of bats that had enough fat mass for predicted energy expenditure over the winter in each population (n = 10,000 individuals total per species). We then designated species groups from our interspecific analyses.

Table 1. Site information for each hibernaculum location, including winter duration and microclimate conditions. Temperature (Ta), relative humidity (RH), and water vapor deficit (dWVP) mean and standard deviation (in brackets) are reported for all data logger locations within the hibernaculum and at the specific location where bats were observed.

State	Site Type	Winter Duration (days)	Across All Data Loggers			At Recorded Bat Locations		
			Ta (°C)	RH (%)	dWVP (kPa)	Ta (°C)	RH (%)	dWVP (kPa)
Montana	Cave	184 ± 12	5.8 [7.0]	90.2 [19.4]	0.17 [0.42]	4.8 [0.4]	100.0 [0.9]	0.00 [0.01]
Montana	Cave	199 ± 16	4.1 [6.1]	78.6 [19.4]	0.27 [0.25]	5.9 [0.6]	100.0 [0.1]	0.00 [0.00]
Nevada	Mine	169 ± 12	6.5 [4.0]	47.6 [17.1]	0.54 [0.27]	7.9 [1.7]	55.1 [18.0]	0.48 [0.23]
Nevada	Mine	172 ± 12	13.4 [7.1]	42.9 [16.2]	1.09 [0.85]	7.6 [1.6]	43.9 [10.6]	0.58 [0.11]
Oklahoma	Cave	134 ± 18	10.2 [5.2]	88.2 [18.1]	0.17 [0.38]	9.5 [2.2]	89.4 [15.8]	0.05 [0.17]
Oklahoma	Cave	134 ± 18	10.2 [5.2]	88.2 [18.1]	0.17 [0.38]	8.8 [2.1]	96.6 [4.9]	0.03 [0.03]
Colorado	Mine	152 ± 23	5.2 [5.2]	78.6 [19.4]	0.21 [0.27]	10.0 [6.9]	57.1 [18.4]	0.61 [0.49]
Oregon	Cave	125 ± 14	5.7 [2.8]	95.7 [12.6]	0.06 [0.21]	6.5 [1.2]	87.0 [5.6]	0.12 [0.05]
Utah	Cave	172 ± 16	10.6 [9.7]	68.8 [19.0]	0.59 [0.61]	2.3 [5.9]	99.8 [1.1]	0.00 [0.00]

Table 2. Morphometric and physiological parameters, including mass-specific torpid metabolic rate (TMR) and the area-specific rate of evaporative water loss (rEWL) used in the individual-based model. The number of samples (N) and standard deviation (in brackets) for each parameter are also reported.

Species	Body Mass (g)	N	Proportion Fat Mass	Proportion Lean Mass	N	TMR (ml O_2 h^{-1} g^{-1})	rEWL (mg H_2O h^{-1} cm^{-2})	N
Corynorhinus townsendii	11.0 [1.0]	136	0.22 [0.05]	0.69 [0.05]	148	0.05 [0.05]	0.13 [0.20]	149
Eptesicus fuscus	19.3 [2.2]	13	0.26 [0.07]	0.64 [0.01]	2	0.04 [0.07]	0.11 [0.10]	8
Myotis ciliolabrum	5.7 [0.4]	33	0.29 [0.03]	0.61 [0.04]	15	0.03 [0.02]	0.16 [0.19]	23
Myotis evotis	7.7 [0.5]	205	0.26 [0.04]	0.63 [0.04]	42	0.06 [0.07]	0.24 [0.18]	13
Myotis lucifugus	8.1 [0.8]	214	0.28 [0.03]	0.63 [0.04]	19	0.04 [0.04]	0.35 [0.20]	66
Myotis thysanodes	9.4 [1.0]	43	0.28 [0.02]	0.63 [0.03]	10	0.03 [0.01]	0.29 [0.14]	11
Myotis velifer	15.6 [1.8]	388	0.29 [0.06]	0.65 [0.05]	184	0.06 [0.08]	0.20 [0.19]	33
Myotis volans	8.7 [0.9]	83	0.23 [0.05]	0.66 [0.05]	16	0.07 [0.08]	0.29 [0.15]	12
Perimyotis subflavus	6.9 [0.7]	79	0.33 [0.09]	0.62 [0.08]	5	0.02 [0.02]	0.34 [0.20]	29

Determining the effect of microclimate, morphology, and physiology on WNS survival
Given research on survival from WNS, we developed multiple hypotheses to explain variation in survival among species. We already understand that fat is a critical factor required for survival (Cheng et al. 2019); therefore we held the proportion of fat constant across species to test for the relative influence of other factors. If pre-hibernation body mass is a driver of survival, then body mass should be a strong predictor and result in higher survival of larger species. Greater body mass reduces the surface area per unit volume for an individual which results in less heat and evaporative water lost to the environment. Thus heavier bats would be able to survive the greater energetic costs associated with WNS. On the other hand, hibernaculum temperature can affect torpid metabolic rate, torpor bout duration, and fungal growth, with colder hibernaculum temperatures potentially decreasing the energetic costs of torpor and fungal growth (Geiser 2004). The benefit of colder temperatures may not only be the direct effect of lower torpid metabolic rate, but rather indirect effects of longer intervals between reaching the physiological triggers of arousals (e.g. dehydration, accumulation of nitrogenous wastes, etc.; French 1982; Prendergast et al. 2002; Ben-Hamo et al. 2013). If this relationship is driving bat survival, then we expect hibernaculum temperature and torpid metabolic rate to be strong predictors and reflect negative relationships with survival. Finally, hibernaculum water vapor deficit may reduce fungal growth to a point that bats that hibernate in drier conditions may experience reduced mortality from WNS. We hypothesize that if this interaction between hibernaculum water vapor deficit, fungal growth, and evaporative water loss drives survival, then both hibernaculum water vapor deficit and evaporative water loss should be strong predictors of survival.

We characterized a hibernaculum microclimate environment for each species by randomly selecting temperature and relative humidity values from normal distributions fitted to the mean and standard deviation from our measured microclimate data from the sampling location (where the bats were found roosting) within the site associated with that species (Table 1). Each temperature and relative humidity combination represented "winter" conditions for each species. We used relative humidity, rather than water vapor deficit to characterize the hibernaculum microclimate in order to prevent impossible water vapor deficit and temperature combinations. We then converted to water vapor deficit once the microclimate was characterized. We combined the microclimate data across sites for species found at multiple sites, as previous analyses indicates no site-specific variation in morphology or physiology (see section on intraspecific analyses). We defined the specific microclimate conditions measured by the data loggers that were closest to the roosting locations of each species at our sampling sites. We assume that these conditions represent the conditions most bats experienced during hibernation at these sites, though note that bats could move freely around the hibernaculum. Using our measured morphometric and physiological data for each species, we randomly selected body mass from a normal distribution fitted to the mean and randomly selected minimum torpid metabolic rate from a lognormal distribution fitted to the mean-log and standard deviation. Due to the limited availability of fat and lean mass measurements across species, we assumed pre-hibernation fat stores were 25% of body mass and lean mass was 65%.

We ran the hibernation energetics model for the predicted winter duration for each bat and determined if survival occurred by comparing the fat mass going into and emerging from hibernation; if the starting fat mass was not expended during the hibernation period, then survival occurred. For each winter run (i.e., hibernaculum temperature and relative humidity combination selected), we repeated the random selection of bat characteristics 100 times to

create a population of 100 bats. Given the 100 winters and 100 bats per winter, we calculated energy expenditure over hibernation 10,000 times for each species. We calculated the probability of survival for each species over the 100 winters as the number of bats that had enough fat mass for predicted energy expenditure over the winter in each population. As the hibernation energetics model calculates the number of days until total fat expenditure, we also calculated the difference between predicted winter duration and predicted winter survival for each species. This difference allows us to visualize the variation in survival for each species, as well as how much more time each species could potentially survive in the hibernaculum environment post spring emergence as a proxy of body condition on emergence.

To test our survival predictions, we fit a linear model to the probability of survival with body mass, mass-specific torpid metabolic rate, mass-specific evaporative water loss, hibernaculum temperature, and hibernaculum water vapor deficit as predictors. Because mass-specific evaporative water loss and hibernaculum water vapor deficit are mechanistically linked, we fit two models, one with mass-specific evaporative water loss and one with hibernaculum water vapor deficit, and selected the model with the highest adjusted R^2 value. We then calculated the partial correlation coefficient (PCC; Baba et al. 2004) and squared semi-partial correlation coefficient (SPCC; Kim 2015) for each covariate. Both the PCC and the SPCC measure the correlation between a covariate of question and the dependent variable, with the effect of the other covariates removed in some form. The SPCC compares the unique variation of a single covariate with the dependent variable, without the influence of the other variables on the covariate (Kim 2015), while the PCC compares the unique variation of the covariate to the unique variation of the dependent variable (with all other variable impacts removed; Baba et al. 2004). The squared SPCC reflects the variation in the dependent variable explained by the covariate in question, not including the variance in the dependent variable explained by other covariates. Therefore, we determined which variables (hibernaculum temperature and water vapor deficit, mass-specific minimum torpid metabolic rate, mass-specific evaporative water loss, and body mass) explained the most variation in survival with WNS and fulfilled our predictions.

We were also interested in how these variables differed among species and if there was any significant variation in survival during hibernation with WNS. We first performed a multiple comparisons Kruskal-Wallis rank sum test of differences to test for pairwise differences between species. We also calculated Tukey Honest Significant Differences to determine pairwise differences in body mass, mass-specific torpid metabolic rate, and mass-specific evaporative water loss between species. We assume that if there are differences between species, there will be differences between the same species sharing the strong predictor traits defined by the SPCC.

Spatial variation in *M. lucifugus* survivorship
The survival of any hibernating species depends on three key factors: the duration of overwinter hibernation, the rate of energy expenditure, and the amount of fat stores taken into the hibernation period. As we have previously assessed the metabolic rate at which a hibernator will expend energy, we also sought to refine estimates of the other two components. To do such, we compiled body mass and bat emergence data from a variety of sources including literature, acoustic surveys, and publicly available datasets, and solicited data-based estimates from local bat researchers across North America (Figure 8, Appendix A8 and Appendix A9). The study region for this analysis was restricted to temperate North America (above the Tropic of Cancer

and below the Arctic Circle) although the published range of *M. lucifugus* extends into the Arctic (International Union for Conservation of Nature [IUCN] 2016).
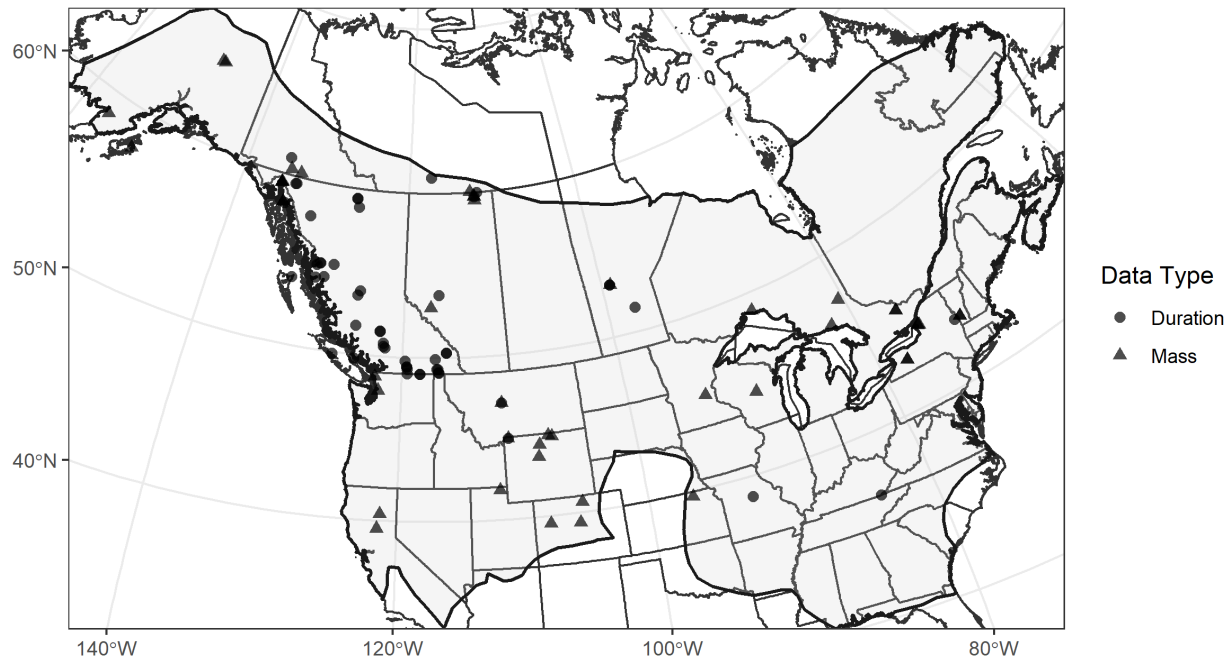
Figure 8. Locations of *Myotis lucifugus* body mass and hibernation duration data across temperate North America. Records of the duration of hibernation (o), pre-hibernation body mass (Δ) and the reported species range via IUCN (black outline with grey shaded interior).

Hibernation duration

Acoustic bat recorders (Songmeter SM2+BAT; Wildlife Acoustics, MA, USA) were deployed by Wildlife Conservation Society Canada (WCS-C) to record bat activity across western Canada between 2008 and 2016. Microphones (either SMX-US or SMX-U1) were placed on 12 to 18 ft tall telescoping poles above likely hibernation or commuting areas (e.g. riverbanks, cliff ridge tops) starting as early as mid-August. Acoustic activity was typically recorded throughout the duration of the winter and data were retrieved between mid-March and mid-May. Recordings were manually analyzed using AnaLookW software (version 4.2n, Titley Scientific, Columbia, Missouri, USA) and customized noise-filters were used to pull files containing bat pulses. The occurrence of at least two bat echolocation pulses in a file was required to identify the recording as a 'bat pass', and the number of passes were summed nightly. The 'start' of the winter hibernation period was defined by the last three night window between August 15 and December 31, in which greater than 10 passes were identified, while the 'end' of the winter hibernation period was defined by the first three night window between March 1 and May 15 in which greater than 10 passes were recorded. Activity rates during the winter are generally low and therefore the 10 pass threshold proved effective in detecting immergence and emergence dates based on field observations (C.L.L. personal observation), although similar conclusions were made with varying pass thresholds, as the changes in activity were typically abrupt and thus easily recognized in the datasets. In locations where bat activity was consistently low throughout

42

the year (spring and fall nightly activity often failing to exceed 10 passes), winter hibernation 'start' and 'end' points were defined by date of the last and first bat recordings, respectively. For sites with multiple years of data, we took the mean immergence and emergence dates. Additionally, spatially explicit records of immergence, and emergence were collected from the literature, which generally reported the average day of entrance or emergence, although some data were presented only as the duration of hibernation. Where sex-specific dates were given for a location, dates were averaged as insufficient data existed to complete a sex-specific analysis. Finally, additional data were solicited from bat researchers across northern North America where few records were available from other sources (Appendix A8).

Spatial covariates. Due to the correlation between ambient temperature and insect activity (Mellanby 1939), we used climatic covariates to explain the relationship between food resources and the onset of hibernation, rather than photoperiod-based metrics. The first (herein "*Original*") definition of hibernation duration used in other work (Humphries et al. 2002) was the number of days per year where mean nightly temperature from 12 a.m. to 6 a.m. was below freezing. The alternative spatial covariate layers we hypothesized to be related to the duration of winter are: degrees latitude North (Northing; Frick and Hijmans 2017); elevation (digital elevation model [DEM]; Wang et al. 2016); number of days of frost annually ($Days_{frost}$; Wang et al. 2016); number of days with an average temperature below freezing annually ($Days_{freeze}$; Wang et al. 2016), and number of days outside of the growing season annually ($Days_{ngrow}$; Wang et al. 2016). All spatial data were re-projected to the same 1 km^2 resolution, cropped, and masked to the study extent.

Modeling framework. All covariates were regressed against the duration of winter hibernation in univariate models and in multivariate models adjusting for Northing or Northing + DEM. From initial model fits, externally studentized residuals were computed to identify outliers. These residuals were converted to p-values and adjusted for multiple testing using Holm's method (Holm 1978). Observations with adjusted p-values (<0.5) across multiple models were excluded, and subsequent models refitted using reduced data. Generalized linear models (GLM) were then fit with the modified data set and model selection was assessed by Akaike Information Criterion (AIC). Model residuals were assessed for spatial auto-correlation using Moran's I from the spdep R package (Bivand and Wong 2018). As no correlation of residuals was observed, the top model by AIC was predicted back across the study extent to create a continuous estimate for the duration of winter.

Body mass and composition
The data required to directly assess the variation in body fat spatially for *M. lucifugus* prior to hibernation do not exist, so instead we relied upon scaling fat with body mass. To do this we 1) identified a relationship between body mass and body fat; and, 2) used a spatial GLM to predict the body mass and then pre-hibernation fat available spatially through the body mass - body fat relationship.

To estimate the relationship between body mass and body fat, we used body composition datasets obtained by quantitative magnetic resonance analysis (QMR, Guglielmo et al. 2011). These datasets included pre-hibernation body mass of Eastern (New York, Vermont; McGuire et

al. 2018) and Western (Montana, this study) *M. lucifugus* populations. We assessed the data for equal means of lean body mass and then fit a linear model to predict fat mass from body mass. We compiled pre-hibernation body mass data for *M. lucifugus* from (VertNet 2020), existing literature, our own study, and solicited the same western researchers mentioned above. Records obtained from VertNet were filtered to include only those with spatial referencing, mass, and those that were recorded between September and December in an attempt to select only records from the pre-hibernation 'swarming' period (Appendix A9). We then used the same outlier identification, covariate and AIC model selection methodology described above for hibernation duration. Residuals from the top model were tested for spatial correlation as described and a spatially weighted GLM was generated using the glmmfields package (Anderson and Ward 2019). The top model was then projected across the distribution of *M. lucifugus* and the linear relationship between pre-hibernation fat mass and body mass was applied to create a spatial data layer representing estimated fat stores across the species distribution.

Spatial variation in hibernation survival
We used a mechanistic hibernation energetics model to estimate the total cost of hibernation for a hibernating bat as previously described. For our analyses, we used previously published parameter values for *M. lucifugus* with the exception of arousal duration, which was set to 2.2 h (French 1985; CLL, unpublished data) and body mass and proportion fat mass were set to the average values calculated from the QMR dataset.

We used these estimates of over-winter energy expenditure in conjunction with spatially varying estimates of hibernation duration and pre-hibernation fat resources as parameters in two ways. First, we used 'optimal' roosting conditions of 4 °C and 98% relative humidity based on observations reported in the literature, assuming these conditions to be available throughout the study extent (Table 5). These microclimatic conditions are thought to provide for the longest possible hibernation duration, a hypothesis that is supported by our recent findings (Haase et al. 2019b). We also considered instances in which the optimal roost temperature may not exist within hibernacula and bats would instead use the best available temperatures (i.e., closest to optimal). Subterranean temperatures in caves and mines are known to deviate from mean annual surface temperature (˚C; MAST) due to a variety of factors (Perry 2013), and it is thought that hibernating bats select particular roosting temperatures from the range of temperatures available within a given hibernaculum. To estimate the closest available temperature to the optimal temperature at any given location we used a spatially explicit model of subterranean winter temperatures as described below (McClure et al. 2020). This flexible approach best captured our assumption that bats will select roosts within hibernacula that offer their preferred temperature when possible but will likely tolerate warmer or cooler temperatures when necessary, especially at the margins of their ranges. Unfortunately, the same information does not exist for relative humidity, and therefore we used the optimal fixed 98% relative humidity for both the optimal and best available temperature scenarios in our analyses.

Combining our estimates of hibernation duration with the dynamic hibernation model results using the aforementioned sets of temperature and humidity conditions, we generated estimates of the amount of fat required to survive hibernation for each of our 1 km^2 cells. We then used this to create a "survival capacity" metric calculated by subtracting the predicted fat required to survive hibernation from the predicted fat available prior to hibernation. This value can also be generated

by estimating the maximal number of days a bat can be expected to hibernate under each of the roosting conditions and subtracting the predicted duration of winter. In either case positive values would indicate a bat's ability to survive hibernation with excess fat, while negative values indicate the depletion of fat stores prior to the end of the hibernation period and this metric was created for healthy bats and bats infected with *P. destructans*.

Finally, we compared the predicted amount of fat required by healthy bats against the fat required by infected bats to estimate the relative increase of energetic costs of *P. destructans* on *M. lucifugus* as a percentage (the difference between resources required to survive hibernation when infected and when healthy in grams of fat, divided by grams of fat required to survive hibernation as healthy bat, multiplied by 100).

All analyses were performed in R (R Core Development Team 2017), with spatial handling tools from *raster* (Hijmans 2016) and *sp* packages (Pebesma et al. 2016). All custom code and data are available at github.com/cReedHranac/winTor. The energetic model code is available from github.com/cReedHranac/batwintor.

Cave and mine microclimate estimation
Subterranean microclimate data
We compiled temperature data collected from caves and mines (139 unique sites, including 75 caves and 64 mines) across western North America (nine states, two Canadian provinces) between 2006 and 2019 (Figure 9) from several data providers: WCS Canada (Jason Rae), Colorado Parks and Wildlife (David Klute), Nevada Department of Wildlife (Jason Williams), Oregon Caves National Monument (Ivan Yates), The Nature Conservancy (Katie Gillies), Wyoming Game and Fish Department (Laura Beard), Jessica Oster (Vanderbilt University), and one published source (Oster et al. 2012). We only included datasets for which site location was provided with positional error < 10 km. Data were collected using a temperature loggers (iButton, Onset HOBO loggers), which recorded temperature at subdaily intervals that varied by site. Many sites contained multiple loggers, placed at a range of distances from the site entrance (479 total loggers, mean of 3.4 per site; Figure 10). Some datasets were accompanied by metadata describing key attributes that may influence temperature at the logger placement site (e.g., distance from site entrance, description of site size or shape, site geology), or other logger placement details (e.g., wall, crevice, or ceiling). Although many loggers recorded humidity as well as temperature, logger saturation, a phenomenon in which the logger fails to accurately record humidity after reaching readings of 100% humidity, precluded the use of data from the majority of loggers. Therefore, we focused only on temperature here.
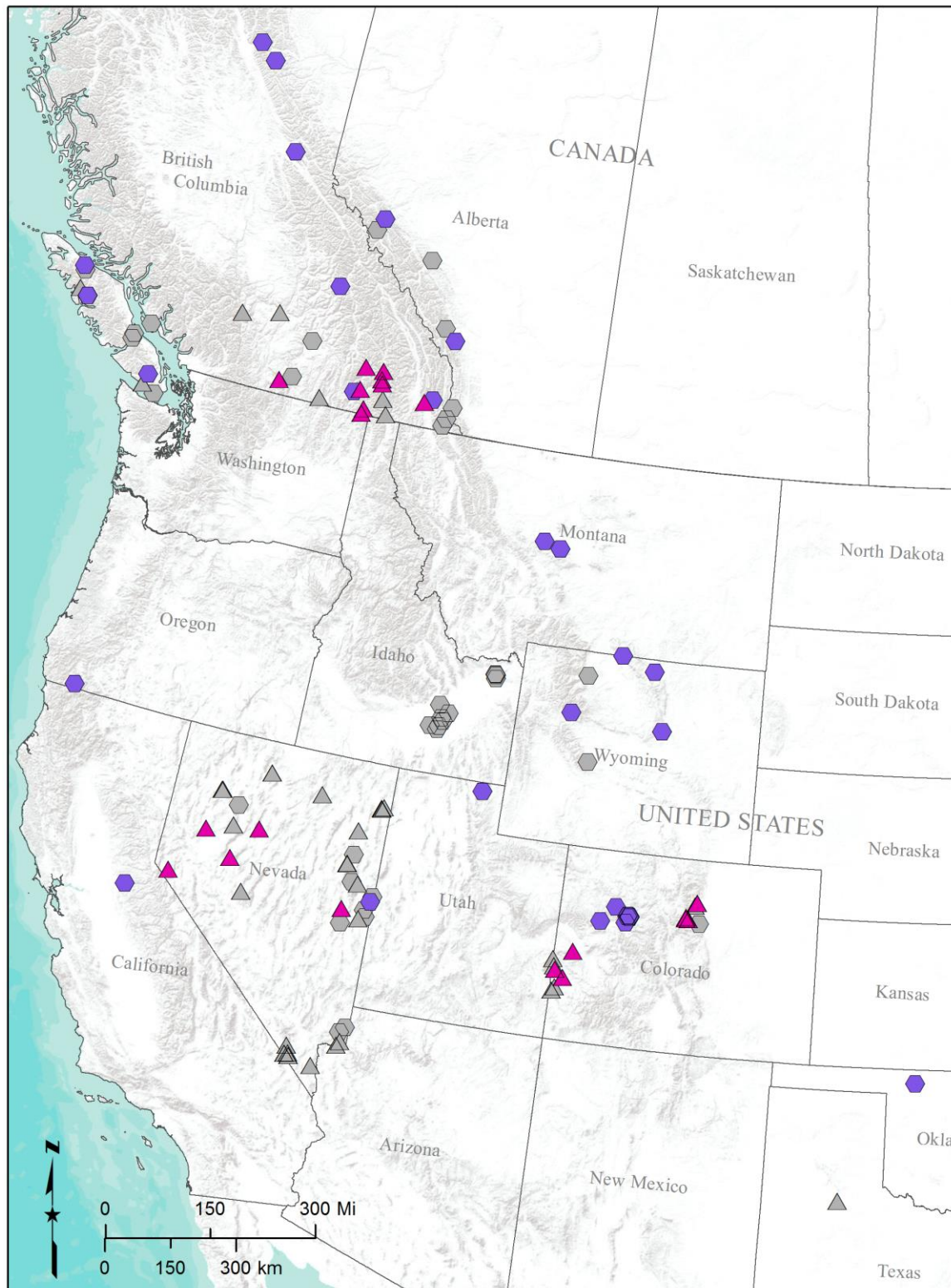
Figure 9. Sites at which subterranean temperatures were recorded. Data were sourced from both caves (hexagons) and mines (triangles). Sites at which no logger distances from site entrances were recorded are shown in gray and were not used in the analysis.
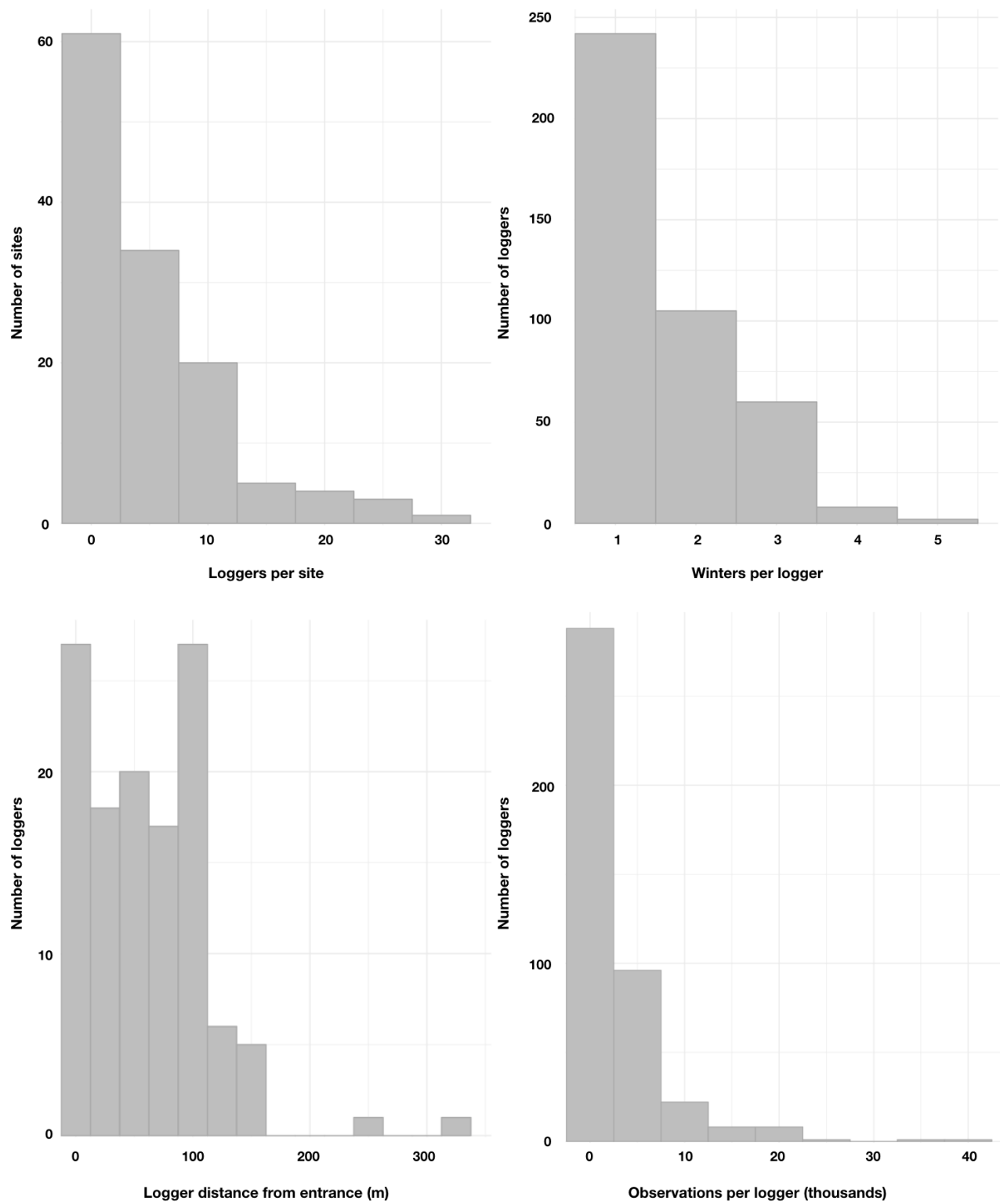
Figure 10. Distribution of a) logger counts per sites, b) winters recorded per logger, c) distance of loggers from site entrances, and d) observation counts per logger (prior to subsampling).

We first screened all logger temperature data for deployment errors, particularly evident recording of surface temperature prior to and following placement of the logger at the site. We restricted our analysis to data recorded during the core winter months of December through February to restrict analysis to a consistent time frame that can be considered winter at all sites across the broad latitudinal range of our study. For loggers deployed over multiple winters, we summarized each winter period separately. Winter periods during which fewer than 14 days of readings were recorded were excluded from analysis (resulting in 131 sites, 427 loggers, and 699 logger-winters). We further restricted our dataset to loggers for which distance from the site entrance was provided, or for which cave maps were provided that could be used to generate a logger placement distance (54 sites, 156 loggers, 202 logger-winters). Recorded distances ranged from 0 to 324 m from the site entrance (median = 61 m).

Because the compiled and filtered raw logger dataset contained greater than 1.2 million observations, which were highly variable in their distribution across loggers (Figure 10) as well as their frequency and regularity of recording, we conducted all analyses using a stratified random sample from the raw logger temperature dataset. We selected 250 records from each unique logger so as to retain all sites and loggers; for loggers with fewer than 250 records (19 loggers; 5%), all records were selected (Appendix A10). Model results were insensitive to this choice of sample size. All logger data processing and analysis was conducted in R (version 3.4.1; R Core Development Team 2019).

Surface climate (present day) and landscape data
We derived MAST and predictors representing key landscape attributes using Google Earth Engine, a cloud-based computing platform supporting large-scale analysis on an extensive catalog of remotely sensed, climatological, and other geospatial datasets (Gorelick et al. 2017). We estimated MAST at each cave site using the DayMet Version 3 dataset (Thornton et al. 2019), which provides gridded daily surface temperature at 1-km resolution (1980-2018). Daily mean temperature was first calculated as the mean of daily minimum and maximum temperature. We then estimated MAST as the 20-year (1998-2018) mean of daily mean temperatures.

We also derived site-level landscape predictors that are believed to impact winter cave temperatures (Perry 2013). We extracted elevation of each site from the Shuttle Radar Topography Mission (SRTM) digital elevation model at 30-m resolution (Farr et al. 2007). Based on elevation, we derived a multiscale topographic position index (TPI), in which canyon and valley bottoms have low position and peaks and ridges have high position. Using a moving-window approach, TPI was calculated as the elevation of a focal raster cell minus the mean elevation within a given neighborhood surrounding the focal cell. We calculated TPI for three neighborhood sizes (500 m, 5 km, and 25 km squares), then averaged these to produce a multiscale index. We extracted Continuous Heat-Insolation Load Index (CHILI), a surrogate for effects of solar insolation and topographic shading (e.g., due to slope aspect) on evapotranspiration, from the Global ALOS CHILI product at 90 m resolution (Theobald et al. 2015). Percent tree cover was extracted from the Terra MODIS Vegetation Continuous Fields product (NASA 2019), which estimates percent tree cover within 250-m resolution pixels. We estimated the mean annual number of snow days at 500-m resolution from the MODIS Snow Cover dataset (V6; Hall et al. 2016) by averaging the number of days per year with at least 10% snow cover over the most recent 5-year period available (2014-2018), as well as mean annual

snowpack (snow water equivalent (SWE) on April 1) for the same time period at 1-km resolution from DayMet (V3; Thornton et al. 2019). We sampled groundwater table depth estimated from compiled point observations gap-filled with a mechanistic groundwater flow model (Fan et al. 2013) as a proxy for the likelihood of water flow within caves or mines, assuming that flow was more likely at sites with shallower (i.e., closer to the surface) groundwater.

Analysis of surface-subterranean temperature relationships
We quantified how well MAST approximates subterranean temperatures and the extent to which subterranean temperatures also depend on distance from the site entrance and other site attributes described above. Based on Perry (2013), we hypothesized a positive relationship between MAST and winter subterranean temperatures, but that caves would tend to be colder than mines (due to greater airflow) (Table 3). We further hypothesized that subterranean temperatures and their relationship with MAST would depend strongly on distance from the site entrance, as evidenced by a significant positive relationship between recorded temperatures and distance from entrance and a significant interaction between entrance distance and MAST. We hypothesized that other site attributes would have negligible effects on subterranean temperatures. However, if effects were detected, we hypothesized that subterranean temperatures would be cooler at higher latitude sites (due to lower winter subterranean temperatures with more pronounced seasonality compared to tropical latitudes); higher elevation sites (although this effect is likely to be confounded with MAST); sites at low topographic positions (due to temperature inversions in canyons and valley bottoms); sites with greater forest cover (due to reduced ground temperatures); and sites with shallower groundwater (due to increased likelihood of water flow). We hypothesized that subterranean temperatures would be warmer at sites with high solar insolation (due to increased ground temperatures). We did not assess the influence of within-cave or within-mine attributes (e.g., volume, length, number of entrances, logger position (i.e., wall, ceiling, crevice)) because these attributes were not consistently described in enough source datasets to draw reliable inferences.

Table 3. Summary of hypothesized influences of mean annual surface temperature (MAST) and site attributes on subterranean winter temperatures (T).

Attribute	Direction	Rationale
MAST	+	Insulation from outside fluctuations keeps T stable at MAST
Distance from entrance	+	Reduced flow of cold air from surface keeps T closer to MAST
Mines relative to caves	+	Mines often have simpler internal structure with less airflow
Latitude	-	Stronger seasonality at high latitudes drives T further from MAST
Elevation	-	MAST is lower at high elevations due to air expansion; likely to be confounded with MAST
Topographic position	-	Low topographic position (canyons, valleys) may result in cold air sinks
Solar insolation (aspect)	+	Greater sun exposure can increase ground temperature
Vegetation cover	-	Greater tree cover can decrease ground temperature
Snow cover	?	Snow cover may insulate caves; flow of snowmelt may reduce T
Water flow (groundwater depth)	-	Flow of cold water may decrease T; water flow may be more likely where the water table is shallower

We screened predictors for multicollinearity based on pairwise correlations and variance inflation factors, removing predictors that caused standard thresholds of 0.7 and 4.0, respectively, to be exceeded (Belsley 1991; Booth et al. 1994). All predictor values were centered and rescaled prior to model fitting. We then fit a linear mixed effects model with fixed effects that included all remaining predictors and an interaction term between MAST and distance from entrances. We included random intercept terms for sites and loggers nested within sites to control for the non-independence of repeated temperature observations from the same logger and for conditions unique to each site that could not be measured. We also accounted for non-constant variance in temperature among loggers as a function of distance from site entrance using an exponential covariance structure, hypothesizing that recorded temperatures would be more variable closer to site entrances. We used analysis of variance (ANOVA) to assess whether inclusion of random effects and a variance component was warranted.

Using a model averaging approach and an information-theoretic framework (Burnham and Anderson 2002), we then fit all additive subsets of this global model to draw multi-model inference regarding predictive relationships and relative importance of predictors using the MuMIn package (Bartón 2018) for R. Multi-model inference produces parameter and error estimates that are not conditional on any one model, which is particularly advantageous when multiple models have similar weights of evidence, or probability of best explaining the data (Burnham and Anderson 2002, 2004; Symonds and Moussali 2011). All-subsets model averaging is recommended over selection of candidate model sets, provided there is strong logic for potential inclusion of each of the predictors considered (Symonds and Moussali 2011), and has been repeatedly demonstrated to support more robust inference compared to selection of a single 'best' model (Burnham and Anderson 2004; Wasserman 2000). The subset of models carrying 95% of the AIC weight were averaged based on their relative AIC weights, using a shrinkage estimation approach to produce unconditional parameter estimates that are not biased away from zero (Lukacs et al. 2010). Our final inferential model was derived from this 95% confidence set. We computed model-averaged regression coefficients, unconditional standard errors (SEs), 95% confidence intervals, and cumulative AIC weights of evidence as a measure of variable importance (Burnham and Anderson 2002, 2004).

Prediction of available subterranean temperature ranges
We used the model-averaged result above to predict mean winter subterranean temperature conditions potentially available across the western United States and Canada, given the presence of a cave or mine of sufficient depth to create a stable dark zone. First, as an illustrative example, we mapped the range of mean winter subterranean temperatures predicted to be available in caves and in mines continuously across western North America, with ranges defined by distance from the site entrance of 10 m and 100 m. These distances were chosen to represent an arbitrary minimum distance from a site entrance at which bats tolerant of temperature fluctuations might be expected to hibernate and a distance well into the stable dark zone, respectively, but the model can be applied to any distance or range of distances defined by a particular research question or management need.

To assess potential utility of the model relative to use of MAST alone as a proxy for subterranean temperature, we used a general estimate of the optimal temperature range for

vespertilionid bat hibernation (2 – 10 °C; reviewed in Perry 2013) to restrict our mapped results to areas where caves or mines, if present and of sufficient depth, would be most likely to offer suitable hibernation conditions, and compared the resulting window to that produced by MAST alone. We also summarized model-predicted temperatures and MAST at known hibernacula to the far north and south of our region of interest (Alberta (n=34) and Texas (n=21)) to assess the model's capacity to estimate more plausible ambient hibernaculum temperatures (i.e., more frequently within the above optimal temperature range) than MAST alone. Finally, we summarized model-predicted temperatures and MAST at winter *M. lucifugus* point locations (n=90) collected from a variety of sources (Table 4) and assessed their alignment with the distribution of ambient temperatures observed in *M. lucifugus* hibernacula (n=32) reported in the literature (Table 5).

Table 4. Sources of winter occurrence records of *Myotis lucifugus* used to assess the plausibility of modeled cave and mine temperatures.

Source	Unique locations
Montana Natural Heritage Program[1]	41
Global Biodiversity Information Facility (GBIF)[2]	16
USGS Bat Population Database (BPD)[3]	16
USGS Biodiversity Information Serving Our Nation (BISON)[4]	10
C. Lausen et al., unpublished data	3
NatureServe[5]	2
S. Olson et al., unpublished data	2

[1]Montana Natural Heritage Program. 2020. Bat Morphometric and Point Observation Databases. Accessed: 02/11/2020; [2]GBIF.org (11 January 2018) GBIF Occurrence Download https://doi.org/10.15468/dl.yokg9g; [3]United States Geological Survey. 2003. Bat Population Database. Available: http//www.fort.usgs.gov/products/data/bpd/bpd.asp. Accessed: 11/11/2017; [4]Core Science Analytics, Synthesis, & Libraries Program of the U.S. Geological Survey (USGS), 2012, Biodiversity Information Serving Our Nation (BISON): U.S. Geological Survey. Available: https://bison.usgs.gov. Accessed 12/28/2016; [5]NatureServe. 2019. NatureServe Central Databases. Arlington, Virginia. USA.

Table 5. Summary of published literature reporting ambient temperatures observed in hibernacula of *Myotis lucifugus*. Sources with a single estimate typically represent the reported mean observed temperature; multiple estimates represent observations at multiple sites or multiple visits over the course of a winter.

Source	State or Province	Number of estimates
Hitchcock 1949	ON, QC	3
Layne 1958	IL	1
Pearson 1962	IL	1
Davis and Hitchcock 1964	NY	1
Henshaw and Folk Jr. 1966	KY	1
Martin et al. 1966	NY	1
Fenton 1970	ON	1
Fenton 1972	ON	1
McManus 1974	NJ	1
Brack 2007	OH	1
Boyles et al. 2007	OH	2
Langwig et al. 2012	NY	10
Vanderwolf et al. 2012	NB	1
Storm and Boyles 2011	NY	1
Jonasson and Willis 2012	MB	4
Kurta and Smith 2014	MI	1
Reimer 2014	AB	1

Bat species distribution models
Winter occurrence data for five focal species
We selected five focal species for our analyses: *C. townsendii*, *M. californicus*, *M. lucifugus*, *M. velifer*, and *P. subflavus*. These species were chosen because occurrence data and field-measured metabolic parameters were available for estimating survivorship, and because they were representative of variability in known distributions and habitat requirements among hibernating bats in the West, which we broadly define here as bats with all or a portion of their range extending west of the Mississippi River (Figure 11; National Atlas of the United States 2011).
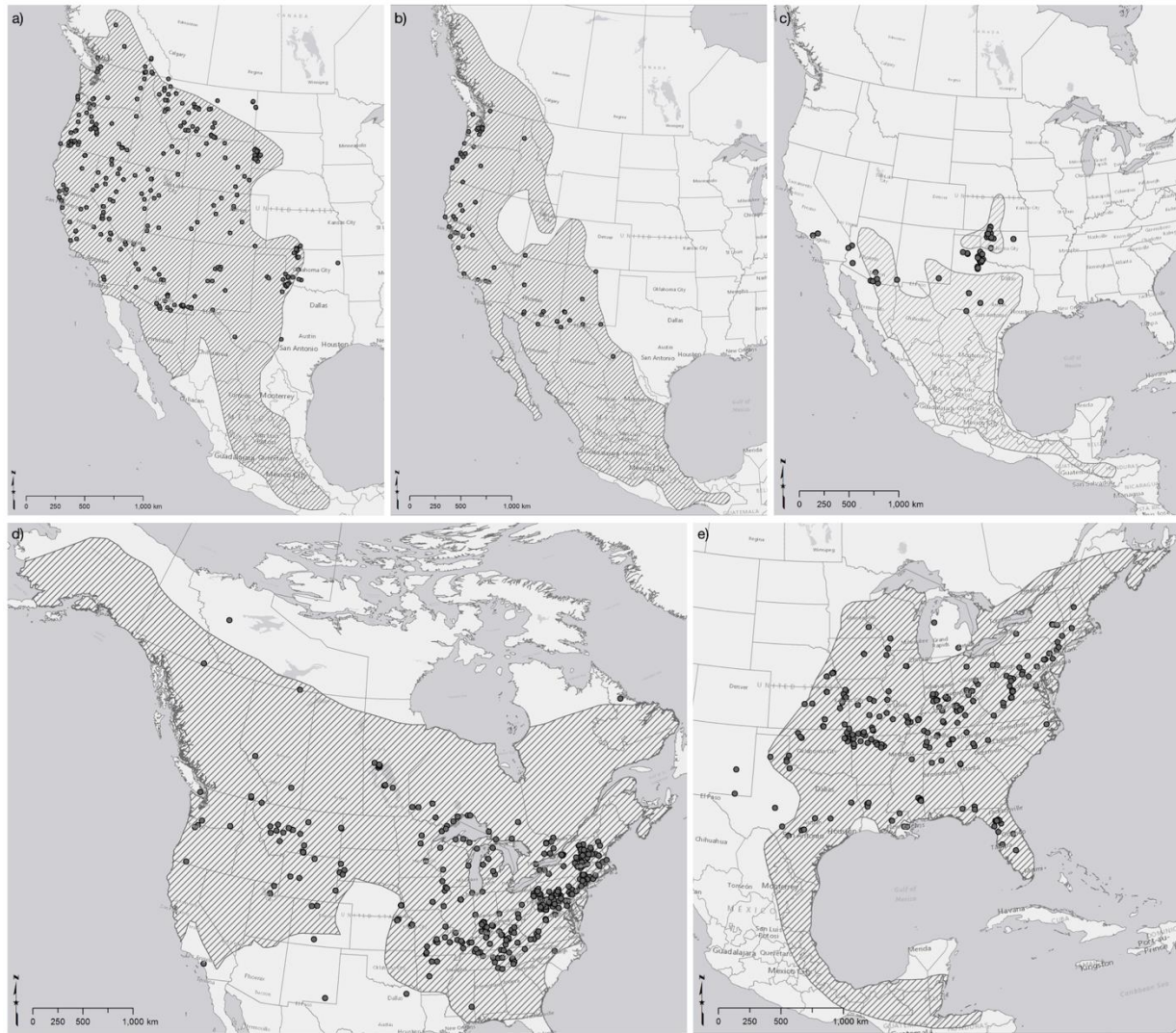
Figure 11. Current geographic range maps overlaid with winter presence locations available to inform species distribution models across the United States and Canada for five focal species: a) *Corynorhinus townsendii*, b) *Myotis californicus*, c) *M. velifer*, d) *M. lucifugus*, and e) *Perimyotis subflavus*.

We compiled occurrence data for these species from multiple sources, including online databases of museum records (VertNet 2016, Biodiversity Information Serving Our Nation [BISON; USGS 2012]), online repositories of vetted public and scientific observations (Global Biodiversity Information Facility [GBIF.org 2018], Bat Population Database [BPD; USGS 2003]), data associated with published literature (Ports and Bradley 1996; Kuenzi et al. 1999; Dubois and

Monson 2007), data obtained from multiple Natural Heritage Programs (NatureServe 2019), and data collected in our own field studies (unpublished data). Many of these sources include thousands of occurrence records for each focal species, but the vast majority of records (>85%) were observed during summer or fall swarming, when bats are more readily observed. Even in bats that do not migrate seasonally, selection of hibernacula microclimates and of the habitat mosaic surrounding hibernacula is expected to differ from selection of summer roosts (Smeraldo et al. 2018). Moreover, due to the sensitivity of hibernaculum locations to disturbance or exploitation, along with the difficulty of detecting torpid bats in hibernacula, winter bat location data were difficult to come by and limited in number (Table 6).

Table 6. Occurrence data available to inform winter species distribution models for five bat species across the United States and Canada after filtering to unique winter locations. Total records include all raw observations compiled from multiple sources. Winter records were selected based on a spatially explicit model of winter duration informed by bat immergence and emergence observations (see winter duration section above, Hranac et al. In Review). Unique records were counted after dissolving repeat winter observations (e.g., across multiple studies or survey dates) at a given location.

Species	Total	Winter	Unique
Corynorhinus townsendii	8959	1637	355
Myotis californicus	5920	596	89
Myotis lucifugus	14946	2113	442
Myotis velifer	11152	1688	72
Perimyotis subflavus	7024	2722	284

We included only in-hand observations (i.e., no acoustic detections) since 1948 (to match the earliest availability of gridded climate data) with location error < 5 km. Because we were interested only in winter distributions associated with hibernacula use, we filtered the compiled dataset to observations recorded during what we defined as winter in a spatially explicit manner. Using a model of winter duration informed by immergence and emergence observations at sites throughout North America (see winter duration section above, Hranac et al. In Review), we estimated the start and end of winter hibernation in a given location (at 1-km resolution) by centering this duration estimate on the winter solstice, then selected only occurrence records falling within this window. Lastly, we dissolved repeat observations (e.g., across multiple studies or survey dates) to a single record for a given site (with unique sites defined to the nearest thousandth of a degree of latitude and longitude).

Predictor variables for five focal species
We identified landscape attributes potentially influencing bat hibernaculum selection based on the published literature and our own knowledge of bat ecology (Table 7, Figure 12). We selected publicly available datasets representing these predictors with sufficient spatial extent to encompass our compiled occurrence data (United States and Canada, with northern extent limit defined by the Arctic Circle). Where multiple candidate datasets were available, we chose those with the highest spatial resolution and/or temporal range that best encompassed our occurrence data. The scale at which bats perceive and respond to landscape attributes may vary among species, attributes, and locales (see Bellamy et al. 2013; Ducci et al. 2015). We therefore followed the example of these studies and others in deriving predictor variables at multiple spatial scales (i.e., over different neighborhood sizes) where applicable for comparison. All

55

predictors were derived and/or sampled using Google Earth Engine, a cloud-based computing platform supporting large-scale analysis on an extensive catalog of remotely sensed, climatological, and other geospatial datasets (Gorelick et al. 2017).

Table 7. Summary of predictors considered in winter species distribution models for bat species *Corynorhinus townsendii*, *Myotis californicus*, *M. lucifugus*, *M. velifer*, and *Perimyotis subflavus* across the United States and Canada.

Predictor	Source data	Resolution	Neighborhood size
Winter survivorship	Haase et al. 2019b, Hranac et al. In Review	1 km	--
Distance to mines	USGS MRDS[1], BC MinFile[2]	1 km	--
Mine density	USGS MRDS, BC MinFile	1 km	25 km
Karst	Weary and Doctor 2014, Salkeld and Walton 2019	1 km	--
Elevation	ALOS[3] Digital Surface Model v2 (Tadono et al. 2014)	30 m	--
Ruggedness	ALOS Digital Surface Model v2 (Tadono et al. 2014)	30 m	500 m, 5 km, 25 km, multiscale
Topographic position	ALOS Digital Surface Model v2 (Tadono et al. 2014)	30 m	500 m, 5 km, 25 km, multiscale
Solar insolation	ALOS Digital Surface Model v2, Theobald et al. 2015	30 m	500 m, 5 km, 25 km, multiscale
Annual precipitation	DayMet v3 (Thornton et al. 2019)	1 km	--
Annual snow days	MODIS[4] Global Daily Snow Cover v6 (Hall et al. 2016)	500 m	--
Percent water	JRC[5] Yearly Water Classification v1 (Pekel et al. 2016)	30 m	500 m, 5 km, 25 km, multiscale
Groundwater depth	Fan et al. 2013	1 km	--
Percent tree cover	MODIS Vegetation Continuous Fields (NASA[6] 2019)	250 m	5 km, 25 km
Night lights	DMSP Radiance-Calibrated OLS[7] v4 (NOAA[8] 2016)	30 arcsec	--

[1]United States Geological Survey Mineral Resources Data System; [2]British Columbia Mineral Inventory; [3]Advanced Land Observing Satellite; [4]Moderate Resolution Imaging Spectroradiometer; [5]Joint Research Centre; [6]National Aeronautics and Space Administration; [7]Defense Meteorological Satellite Program-Operational Linescan System; [8]National Oceanic and Atmospheric Administration
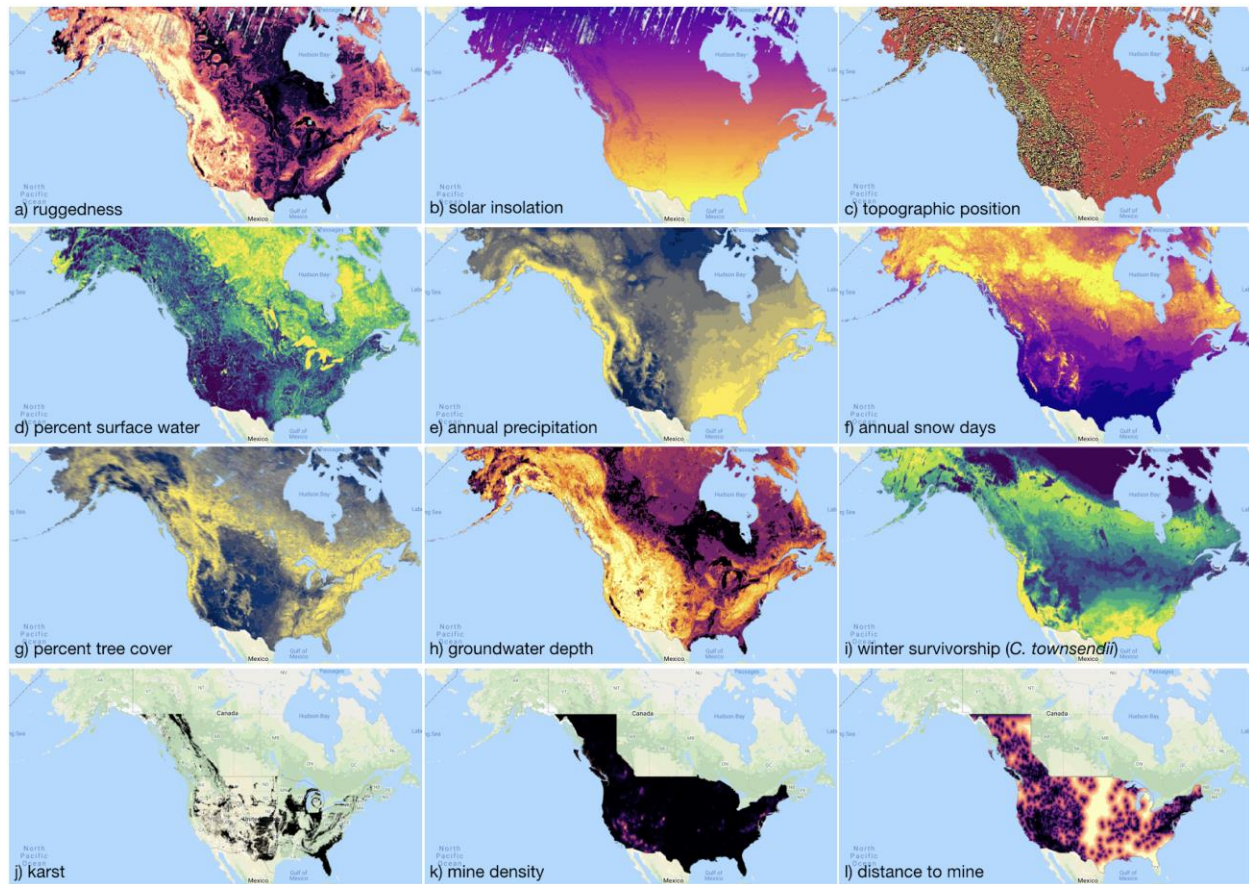
Figure 12. Maps of predictor variables used to fit winter species distribution models for bat species *Corynorhinus townsendii*, *Myotis californicus*, *M. lucifugus*, *M. velifer*, and *Perimyotis subflavus* across the United States and Canada (a-i) or, where continuous spatial data were not available for all provinces, across the United States and British Columbia (j-l). Data for karst and mines (j-l) was not available in other Canadian provinces, but this only impacts models for *M. lucifugus* as other focal species have either no, or only limited distribution in these provinces. In all panels, warmer, brighter colors represent higher values.

Survivorship. We estimated species-specific, spatially explicit winter survivorship relative to the duration of winter. These estimates were based on an existing bioenergetic model of bat winter survivorship, recently updated and parameterized for western bat species. Full details are elsewhere (see hibernation energetic model section above, Haase et al. 2019b; Hranac et al. In Review), but briefly, the model uses the hypothesized energetic requirements of bats in torpor to dynamically model torpor bouts for the duration of a predicted winter under specified hibernaculum conditions. For *M. lucifugus*, torpor consumes approximately eighty times less energy per unit time than euthermia, whereas the infrequent but periodic arousals to euthermic temperatures use the majority of energy stores, with each arousal consuming approximately 5% of total overwinter energetic costs (Thomas et al. 1990). In this model, ambient temperature was set to the species specific best available temperature and relative humidity was set at a fixed 95% relative humidity and we spatially interpolated the model results across the study extent to predict the fat mass expected to remain at the end of winter at each 1-km^2 raster cell. Higher, positive predicted values are expected to correspond to high survivorship, while low or negative values indicate areas where bats are unlikely to survive.

Topography. We derived a number of topographic covariates from the global ALOS Digital Surface Model (DSM version 2.2; Tadono et al. 2014) at 30-m resolution, including elevation, topographic ruggedness, and topographic position. Topographic ruggedness was quantified as the standard deviation of elevation values within a given radius around each focal raster cell. Similarly, topographic position was quantified as the difference between the elevation of each focal raster cell and the mean of elevation values within a given radius, such that high values are associated with peaks and ridges and low values are associated with valleys and canyon bottoms (e.g., Guisan et al. 1999; Dickson and Beier 2007). We also extracted CHILI, a surrogate for effects of solar insolation and topographic shading on evapotranspiration, also derived from the global ALOS DSM at 90-m resolution by Theobald et al. (2015). We used a moving window approach to derive topographic ruggedness and position at three spatial scales (diameter = 500 m, 5 km, 25 km), then the resulting values were averaged to create 'multiscale' metrics. We took the focal mean of CHILI values over these multiple scales as well.

Surface attributes. We derived percent tree cover from the Terra MODIS Vegetation Continuous Fields (VCF) product, which estimates sub-pixel-level surface vegetation cover globally, including percent tree cover, on an annual basis (250-m resolution; NASA 2019). Because data were not available for the entire temporal range of our occurrence data, we used data for the most recent year available (2015). We estimated percent tree cover at two aggregated scales (diameter = 5 km, 25 km). We used global nighttime lights imagery from the Defense Meteorological Program (DMSP) Operational Line-Scan System (OLS) (Radiance-Calibrated, V4) as a proxy for relative intensity of human development (30-arcsec resolution; NOAA 2016). We estimated availability of surface water based on the Joint Research Center (JRC) Yearly Water Classification History (V1), which maps the location and seasonality of surface water from Landsat 5, 7, and 8 imagery (30-m resolution; Pekel et al. 2016). We estimated the percent cover of seasonal or permanent surface water at three spatial scales (diameter = 500 m, 5 km, 25 km), focusing on the most recent year for which data were available (2015) because the data do not span the entire temporal range of our occurrence dataset. We estimated frequency of snow cover based on the MODIS Global Daily Snow Cover product (V6; Hall et al. 2016), which estimates percent snow cover of each 500-m pixel on a daily basis. We counted the average number of days per year with at least 10% snow cover over the 5-year period from July 2013 to June 2018. We quantified precipitation using the DayMet dataset (V3; Thornton et al. 2019), which provides gridded daily precipitation data at 1-km resolution. We estimated mean annual total precipitation by summing daily values annually then averaging the most recent five years available (2013-2018) to favor consistency with the temporal range of other available predictor data.

Below-ground attributes. To represent potential availability of karst features that may provide suitable hibernacula, we relied on a map of karst and pseudokarst features across the United States produced by Weary and Doctor (2014) derived from state geological survey maps and USGS integrated geologic map databases (1:24,000 to 1:500,000 resolution). We merged this with an equivalent dataset for British Columbia provided by the Ministry of Forests, Lands, Natural Resource Operations and Rural Development (1:250,000 resolution) (Forest Analysis and Inventory 2019). We did not differentiate among karst types, instead creating a simple binary indicator of karst presence vs. absence in raster format (1-km resolution). We also estimated availability of mines as potential hibernacula, using mine site locations available from the USGS

Prospect- and Mine-Related Features database (v4, available for all but northeastern states; Horton and San Juan 2019) and the Mineral Resources Data System (MRDS, used for northeastern states; USGS 2016), and from the MINFILE Production Database for British Columbia (British Columbia Geological Survey 2019). We included only mineral resource sites classified as mines (Mine-Related Features and MRDS) or as producing at one time (MINFILE). We derived two measures of mine availability: distance to the nearest mine and density of mines within 50 km of each focal raster cell (1-km resolution), calculated using a Gaussian kernel density function (sigma = 25 km). Karst and mine data were not available for other Canadian provinces; these predictors were not included in models for species with ranges spanning these areas (i.e., *M. lucifugus*). Finally, we estimated groundwater depth from a global water table depth model that gap-filled point observations with a mechanistic groundwater model (1-km resolution; Fan et al. 2013).

Model fitting for five focal species
We estimated species-specific relative probability of occurrence during winter using boosted regression trees (BRT; De'Ath 2007; Elith et al. 2008). A BRT (a.k.a. gradient boosting machine or stochastic gradient boosting) is an ensemble approach that combines regression trees, which relate a response to predictors by recursive binary splits of the data, and boosting, in which inference is drawn from the relative strength of many possible models rather than fitting a single parsimonious model. This method offers advantages over more traditional linear regression approaches in that a variety of response data and model forms can be accommodated (e.g., Gaussian, binomial, Poisson); different types of predictor variables (e.g., continuous, ordinal, categorical) can be included with no need for transformation or outlier removal; nonlinear relationships are easily captured; and interactions between predictors are handled automatically. Furthermore, overfitting is well-controlled through the use of cross-validation as BRT models are 'grown' (Elith et al. 2006, 2008). Importantly, a number of studies (e.g., Elith et al. 2006; Wisz et al. 2008; Oppel et al. 2012; Maiorano et al. 2013) have shown strong BRT predictive performance relative to other species distribution model (SDM) approaches (e.g., generalized linear models, generalized additive models, climatic envelope models, maximum entropy).

We follow the approach detailed by Elith et al. (2008) for application of BRT to species distribution modeling. One key difference in our application is that we make use of presence-only data rather than presence-absence data. Use of presence-only data, in which sites where the focal species was absent are not known with certainty, requires a shift in model assumptions and inference. Presence-absence models compare landscape attributes of sites at which the species was known to be present and absent to estimate the absolute probability of occurrence at any unobserved site given its climate and/or landscape characteristics (Guisan and Zimmerman 2000; Manly et al. 2007). Without absence data, attributes of presence locations must instead be compared to randomly-sampled 'background' (a.k.a. 'pseudo-absence') locations (e.g., Ferrier et al. 2002). In this case, presence is assessed relative to availability and the species' absence at sampled background locations is not guaranteed. This shift in comparison fundamentally alters the inferences that can be made from the model: we cannot estimate the absolute probability of focal species occurrence (i.e., 80% probability of occurrence at a given site), but we can estimate, or rank, the relative probability of occurrence (Keating and Cherry 2004; but see Phillips and Elith 2011; Royle et al. 2012).

We sampled 'background' locations from extents that were broadly inclusive of each species' known range in an effort to sufficiently capture the environmental conditions limiting their distributions (western United States and Canada for *C. townsendii, M. californicus*; United States and Canada for *M. lucifugus*; United States for *M. velifer, P. subflavus* [Razgour et al. 2016]). Because bats were more likely to have been observed in locations already known to harbor bats and that are more accessible (e.g., closer to population centers, accessible by roads, and in less rugged topography; Graham et al. 2004), we generated background points so as to replicate and thus control for this inherent spatial bias (after Hertzog et al. 2014). We first created a bias grid based on the kernel density of occurrence locations (Venables 2002) using the MASS package for R, then generated background points with probability dictated by occurrence density (e.g., Figure 13). We generated three background points for every occurrence point as a balance between achieving coverage of available habitat and not swamping the presence locations or artificially inflating sample size. Finally, we sampled all candidate predictor variables at each presence and background location.
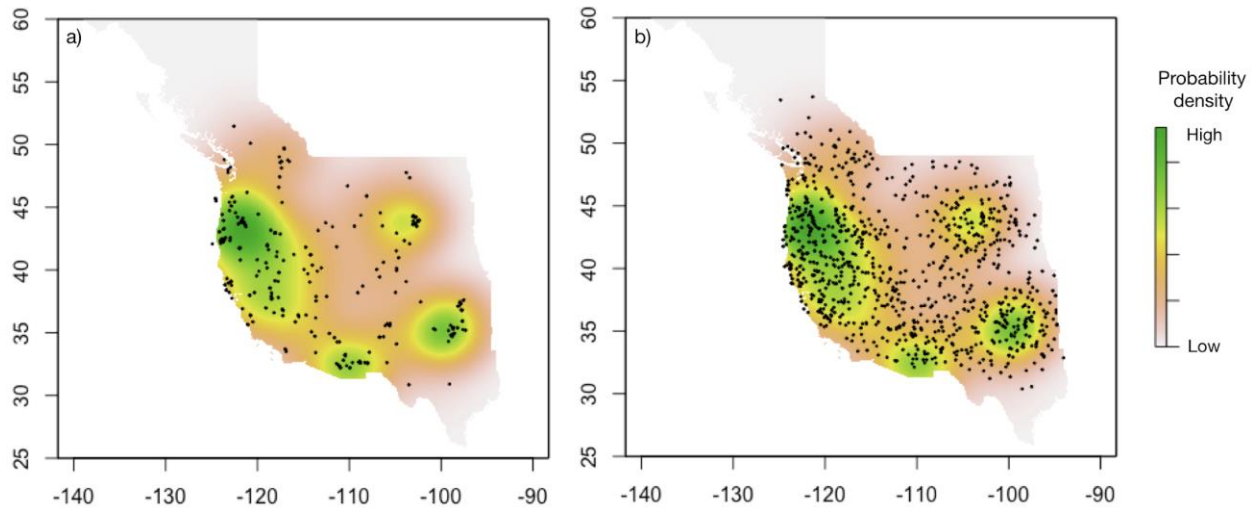
Figure 13. To correct for bias in species occurrence data used to fit winter species distribution models for bat species *Corynorhinus townsendii*, *Myotis californicus*, *M. lucifugus*, *M. velifer*, and *Perimyotis subflavus* across the United States and Canada, a) presence locations were used to generate a bias grid (i.e., kernel density surface), which was in turn used to b) probabilistically generate background locations that were subject to the same spatial patterns of bias. This example illustrates these steps for *C. townsendii*.

To identify the most appropriate scale for each predictor (i.e., the scale at which habitat selection was most evident), we first fit univariate generalized additive models (GAM; Yee and Mitchell 1991) for each predictor. We chose GAM for this preliminary predictor selection step to not constrain the form of the response (as with linear regression). We selected the best performing scale for each predictor based on a comparison of AIC scores across each scale at which the predictor was sampled. We then assessed pairwise correlations and variance inflation factors across the resulting set of predictors and excluded those causing standard thresholds of 0.7 and 4.0, respectively, to be exceeded to avoid multicollinearity (Belsley 1991; Booth et al. 1994). We also excluded mine density from further consideration due to its poorer AIC-based performance across all focal species compared to distance from mines.

61

We fit and calibrated each BRT model using the stepwise cross-validation process detailed by Elith et al. (2008) and accompanying R scripts (in Appendix S3 of Elith et al. 2008). We adjusted the model learning rate to ensure that a minimum of 1000 trees were fit, then calibrated the tree complexity (range: 3 – 5) and bag fraction (range: 0.5 – 0.7) to minimize deviance. We tested for the benefits of dropping uninformative model terms based on estimated reduction in deviance. We then used this 'optimized' model to assess the relative contribution of each predictor, plot the relationship between each predictor and relative occurrence probability, and evaluate model performance. We evaluated the model's fit to the training data (iteratively partitioned in the cross-validation process) based on the mean proportion of deviance explained in each cross-validation iteration, and assessed predictive performance based on the predictive deviance (Elith et al. 2008). Because our models were fit using presence-background data, we do not follow Elith et al. (2008) in reporting cross-validated area under the receiver operating curve (AUC), as use of this metric to evaluate presence-background models is flawed by 'contamination' of background sites with unobserved presence (Boyce et al. 2002, Jimenez-Valverde 2012; Escobar 2018). As a final modeling step, we applied the optimized model to predictor values in each 1-km cell of the extent of interest for each species to predict and map relative probability of occurrence (Elith et al. 2008; see 'Spatial variation in hibernation survival' methods above). We summarized the percentile ranks of occurrence probability values predicted for presence and background locations as an additional assessment of predictive performance. All model fitting and prediction were conducted in R (version 3.4.1; R Core Development Team 2019). A data repository for this analysis is found in Appendix A11.

Impacts of climate change on bats and WNS

We sought to estimate the change in five focal bat species' probability of occurrence (estimated under current conditions in 'Bat species distribution models' above) under two future scenarios: a) exposure to *P. destructans*, and b) exposure to *P. destructans* along with climate change. To estimate bats' probability of occurrence given exposure to *P. destructans*, we needed to run the bioenergetic model with parameters capturing the influence of the hibernaculum environment (temperature and humidity) on fungal growth and the resulting impact of the fungus on bat hibernation physiology. To estimate bats' probability of occurrence given the additional impacts of climate change, we needed to run the bioenergetic model with the *P. destructans* growth parameters above as well as projected future climate parameters (future available temperatures and future winter duration; Figure 14). Here, we focus on methods used to integrate future climate scenarios into the bioenergetic model and subsequently SDMs because *P. destructans* growth parameters are fully described under the section on the hibernation energetics model above.
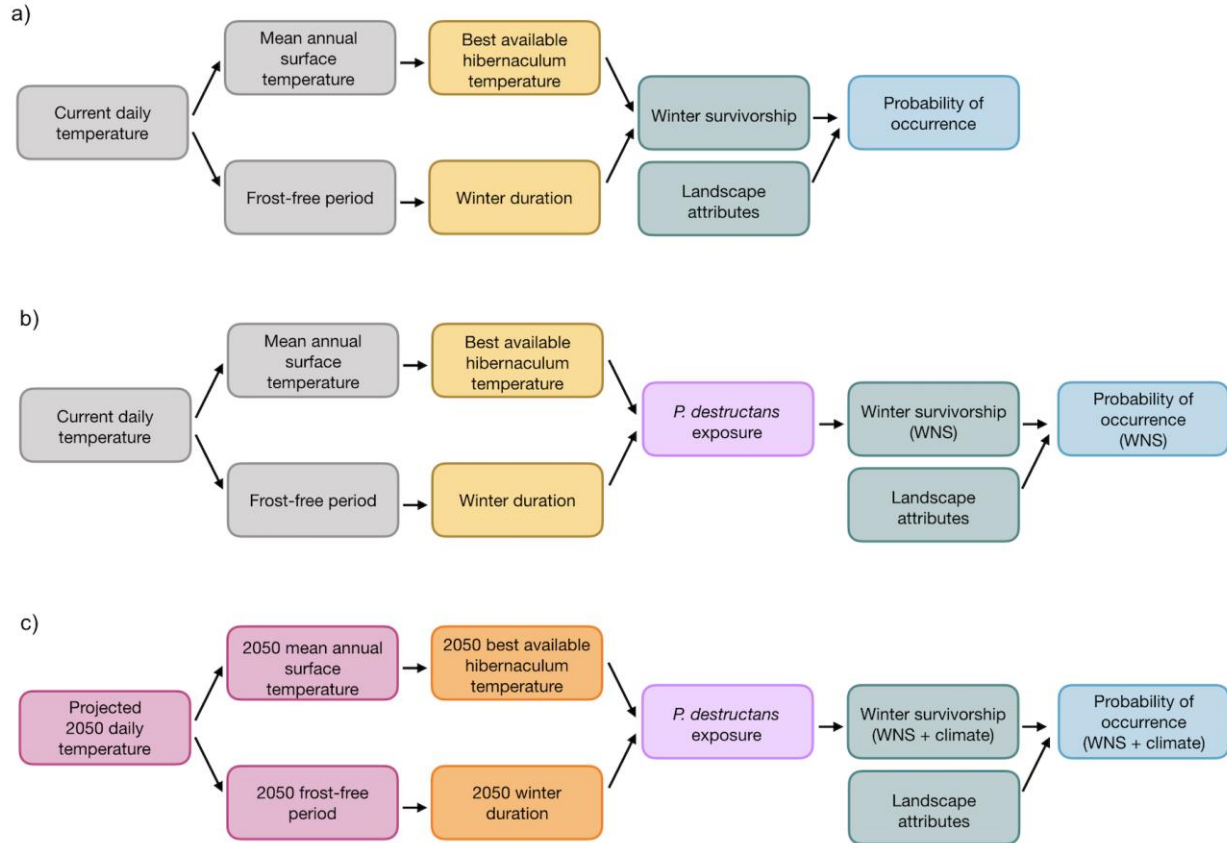
Figure 14. Flowchart schematic comparing development of species distribution models (SDMs) for five focal species under a) current conditions, b) exposure to *Pseudogymnoascus destructans*, and c) exposure to *P. destructans* and projected climate change.

We first projected daily temperatures at midcentury (2050) under a range of possible climate futures at high spatial resolution (1-km), which could then be used to derive our climate parameters of interest. Global climate models (GCMs) model the energy budget of the earth system and the impact of external factors such as solar input and greenhouse gas emissions, simulating global patterns and processes across the earth's major climate system components (atmosphere, ocean, sea ice, and land surface) to project future climate attributes (e.g., temperature, precipitation) under possible future scenarios of carbon and other heat-trapping gas concentrations. Regional climate models (RCMs) mechanistically (i.e., dynamically) downscale coarse GCM projections by resolving processes that occur at finer resolutions than GCM grid sizes (≥100 km) within a more limited geographic scope (Kotamarthi et al. 2016). They account for the effects of e.g., complex topography and coastlines, and simulate hydrologic processes at scales more relevant to decision-making (25 – 50 km). However, these outputs are still too coarse for many applications. GCM and RCM projections can be further statistically downscaled using a variety of approaches. Although many methods exist and vary considerably in their complexity, they all fundamentally aim to account for differences between model simulations applied to historical periods and observed climate attributes during those periods, then apply those statistical adjustments to future projections (Kotamarthi et al. 2016).

The NA-CORDEX Program data archive (Mearns et al. 2017), hosted by the National Center for Atmospheric Research (NCAR), contains output from RCMs run over a domain covering most

63

of North America using boundary conditions from multiple Coupled Model Intercomparison Project 5 (CMIP5) GCMs (Figure 15). These projections span a range of possible climate futures in terms of greenhouse gas concentration scenarios and projected severity of future change, as well as performance in capturing regionally important drivers and processes.

	CRCM5 (UQAM)	CRCM5 (OURANOS)	RCA4	RegCM4	WRF	CanRCM4	HIRHAM5	RCP	ECS (°C)
ERA-Int	0.44° 0.22° 0.11°	0.22°	0.44°	50km 25km	50km 25km	0.44° 0.22°	0.44°		
HadGEM2-ES				50km 25km	50km* 25km*			4.5	4.6
HadGEM2-ES								8.5	4.6
CanESM2	0.44°		0.44°			0.44° 0.22°		4.5	3.7
CanESM2	0.44° 0.22°	0.22°	0.44°			0.44° 0.22°		8.5	3.7
MPI-ESM-LR	0.44°							4.5	3.6
MPI-ESM-LR	0.22° 0.44°	0.22°		50km* 25km*	50km 25km			8.5	3.6
MPI-ESM-MR								4.5	3.4
MPI-ESM-MR	0.44° 0.22°							8.5	3.4
EC-EARTH†			0.44°					2.6	~3.3
EC-EARTH†			0.44°				0.44°	4.5	~3.3
EC-EARTH†			0.44°				0.44°	8.5	~3.3
GFDL-ESM2M								4.5	2.4
GFDL-ESM2M		0.22°		50km 25km	50km* 25km*			8.5	2.4
Access	PoC	PoC	ESGF	PoC	PoC	CCCma	ESGF		
Institution	UQAM	OURANOS	SMHI	Iowa State *NCAR	U Arizona *NCAR	CCCma	DMI		
Modeler	K. Winger	S. Biner	G. Nikulin	R. Arritt *M. Bukovsky	H-I Chang *M. Bukovsky	J. Scinocca	O. Christensen		

Figure 15. Matrix overview of projected climate information available via NA-CORDEX.

The NA-CORDEX data archive includes outputs from two RCMs that offer 25 km spatial resolution and span the complete range (2.4 – 4.6 °C) of GCM equilibrium climate sensitivity (ECS), an emergent property of GCMs that serves as a metric of relative severity of projected change. These are the Regional Climate Model 4 (RegCM4) (Giorgi et al. 2012) and the Weather Research and Forecasting (WRF) model (Skamarock et al. 2008) (Figure 15). These models differ in their underlying sub-models and -processes (see https://na-cordex.org/rcm-characteristics), which may mean that each best represents the meteorological phenomena driving future climate change in different subregions of North America. Kotamarthi et al. (2016) suggest that it is critical to understand the phenomena that are most relevant to climate impacts of interest when selecting the most appropriate downscaling tool. In the Mountain West, complex terrain is the primary driver of climate, with midlatitude cyclones, katabatic winds,

monsoons, and associated air-mass thunderstorms being the most prominent resulting phenomena. The maritime climate along the Pacific coast also produces midlatitude cyclones, as well as orographic lifting and atmospheric rivers (Kotamarthi et al. 2016).

For each of the above RCMs, we selected downscaled outputs run on boundary conditions from two GCMs - GFDL-ESM2M (Equilibrium Climate Sensitivity, ECS = 2.4 °C) and HadGEM2-ES (ECS = 4.6 °C) - in order to span the range of available models' climate sensitivity (Figure 15). This approach is in keeping with the recommendation from Kotamarthi et al. (2016) to use output from multiple GCMs with different physical parameterizations to cover a broader range of model uncertainty. Thus, in total, we consider four possible climate futures (2 RCMs x 2 GCMs).

We used newly-generated versions of these outputs (Seth McGinnis, unpublished data) that were bias-corrected using a multivariate quantile mapping method (Cannon 2018), using DayMet temperatures as the observed dataset (Thornton et al. 2019). Because dynamically downscaled RCMs were still considerably coarser (25-km) than our desired spatial resolution (1-km), outputs were further statistically downscaled by spatially interpolating to 1-km, applying an adiabatic lapse rate correction based on elevation (Seth McGinnis, UCAR, pers. comm.).

To estimate survivorship under future conditions, we first derived 30-year means centered on the year 2050 for MAST and duration of the frost-free period (as described above) for each of our four climate scenarios. Future MAST estimates were then used to estimate the best available hibernaculum temperature likely to be available in any given location for a given species using the subterranean temperature model described in the cave and mine microclimate estimation section above. Similarly, future frost-free period estimates were used to estimate hibernation-specific winter duration (i.e., time between immergence and emergence) as described under the winter duration section above. The bioenergetic survivorship model was then run for each of our five focal species under each future scenario using these projected future climate parameters.

Predictions of future survivorship under each scenario were then used as predictors in the SDMs described in 'Bat species distribution models' above for each of our five focal species. We then estimated and mapped the change in occurrence probability between current conditions and each future scenario simply as the difference in occurrence probability for each raster cell.

Results and Discussion

Empirical analyses of bat hibernation physiology

1. Intraspecific variation in hibernation physiology

Our *M. lucifugus* study sites represented a latitudinal gradient of approximately 1,500 km (Figure 16; McGuire et al. In Review). Similarly, we collected measurements from *C. townsendii* at hibernacula over a region that spanned 1,200 km north to south, and 1,200 km from east to west, including one of the northernmost hibernacula known for the species (Figure 16). Although it was not our explicit aim to test for variation along specific environmental gradients, the *M. lucifugus* sites spanned a wide temperature gradient and *C. townsendii* sites included both arid sites and much more mesic sites (Table 8).
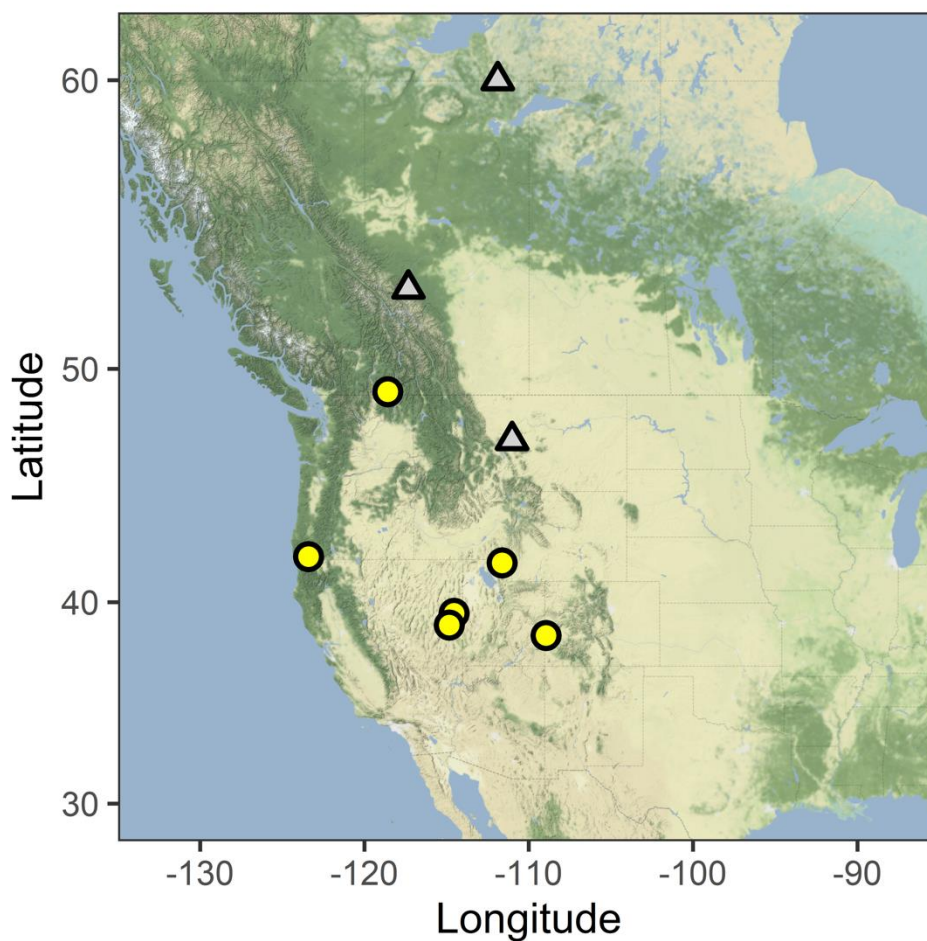
Figure 16. Study sites for *Myotis lucifugus* are indicated in grey triangles and span approximately 1,500 km (approximately 13 degrees of latitude) and study sites for *Corynorhinus townsendii* are indicated in yellow circles and span approximately 1,200 km east to west, and 1,200 km north to south. For both species, the most northern sites are among the most northerly known hibernacula for the species. Map created with ggmap package in R (Kahle and Wickham 2013) using map tiles from Stamen Design (maps.stamen.com; CC BY 3.0).

Table 8. We collected measurements from *Corynorhinus townsendii* at six sites and from *Myotis lucifugus* at three sites. Sites for *M. lucifugus* had a notable temperature gradient, while precipitation varied widely among sites for *C. townsendii*. Among *C. townsendii* sites, the most mesic site received approximately 6.5 times more precipitation than the most arid site. Among *M. lucifugus* sites, temperature decreased with latitude and the mean annual temperature at the most northern site was below freezing. All climate data from 1981 – 2010 climate normals. Hibernation duration estimates are calculated from Hranac et al. (In Review). We do not report precise locations of these sensitive sites, but general locations are illustrated in Figure 16.

Site	Annual Precipitation (mm)	Mean Annual Temperature (°C)	Coldest Month[1] (°C)	Warmest Month[2] (°C)	Predicted Hibernation Duration (days)
Corynorhinus townsendii sites					
Nevada[3]	248	7.2	-11.7	30.9	120
Colorado	338	10.3	-9.5	33.9	89
Utah	501	9	-8.4	31.1	127
British Columbia	535	8	-7.2	28.7	139
Oregon	1597	13.2	0.6	34.6	81
Myotis lucifugus sites					
Montana	563	6.3	-9.7	27.5	154
Alberta	599	4.1	-11.7	22.7	170
Northwest Territories	354	-1.8	-27	23.3	205

1. Mean of daily minimum temperature for the coldest month of the year, based on 1981 – 2010 climate normals.

2. Mean of daily maximum temperature for the warmest month of the year, based on 1981 – 2010 climate normals.

3. The two sites in Nevada were in relatively close proximity and are characterized by a single weather station.

1.1 Corynorhinus townsendii. Our analysis included data for 152 *C. townsendii* from six different sites (sample size ranged from 10 – 47 bats per site). Our dataset included a similar sex ratio among sites (test for equality of proportions; χ^2 = 10.0, df = 5, p-value = 0.07) with a female bias across sites (number females ≥ males at all sites; binomial test p-value = 0.0001). Models of torpid metabolic rate were better supported when they included heterogeneous variance among temperatures (likelihood ratio = 32.38, df = 3, p-value < 0.0001) and the random effect of individual (likelihood ratio = 100.92, df = 1, p-value < 0.0001). Torpid metabolic rate was related to temperature (likelihood ratio = 12.84, df = 3, p-value = 0.005) but the effect of temperature did not vary among sites (site:temperature interaction, likelihood ratio = 22.30, df = 15, p-value = 0.10) or between sexes (sex:temperature interaction, likelihood ratio = 1.70, df = 3 p-value = 0.64). Torpid metabolic rates measured in winter were slightly greater (0.1 mW g^{-1}) than when measured during swarming (likelihood ratio = 4.85, df 1, p-value = 0.03), but given that no similar effect was observed for evaporative water loss and no seasonal effects for *M. lucifugus* (below) were observed, this may be a spurious result. Torpid metabolic rate did not vary among sites (likelihood ratio = 6.85, df = 5, p-value = 0.23) or between sexes (likelihood ratio = 0.15, df = 1, p-value = 0.70) . Torpid metabolic rate was greater at 2 °C than either 5 or 8 °C and torpid metabolic rate at 10 °C was intermediate, suggesting decreasing torpid metabolic rate to a minimum metabolic rate (0.33 ± 0.03 mW g^{-1}) over the range of 5 – 8 °C (Figure 17 a) and minimum defended temperature between 2 and 5 °C.

Trends for evaporative water loss generally followed those observed for torpid metabolic rate. For evaporative water loss, there was better support for models that included heterogeneous variance among temperatures (likelihood ratio = 107.10, df = 3, p-value < 0.0001) and the random effect of individual (likelihood ratio = 57.51, df = 1, p-value < 0.0001). Evaporative water loss varied across temperatures (likelihood ratio = 19.03, df =3, p-value = 0.0003) but the effect of temperature did not differ among sites (site:temperature interaction; likelihood ratio = 15.84, df = 15, p-value = 0.39) or between sexes (sex:temperature interaction; likelihood ratio = 4.49, df = 3, p-value = 0.21). Evaporative water loss did not differ between seasons (likelihood ratio = 2.60, df = 1, p-value = 0.11) or sexes (likelihood ratio = 2.74, df = 1, p-value = 0.10). Minimum evaporative water loss (0.010 ± 0.0007 mg H$_2$O min^{-1} g^{-1}) was measured at 5 – 8 °C (Figure 17 b), which was the same temperature range observed for minimum torpid metabolic rate. There was one pairwise difference in evaporative water loss among sites (likelihood ratio = 13.05, df = 5, p-value = 0.02), with lower evaporative water loss measured in British Columbia compared to Colorado. There were no other differences among sites.
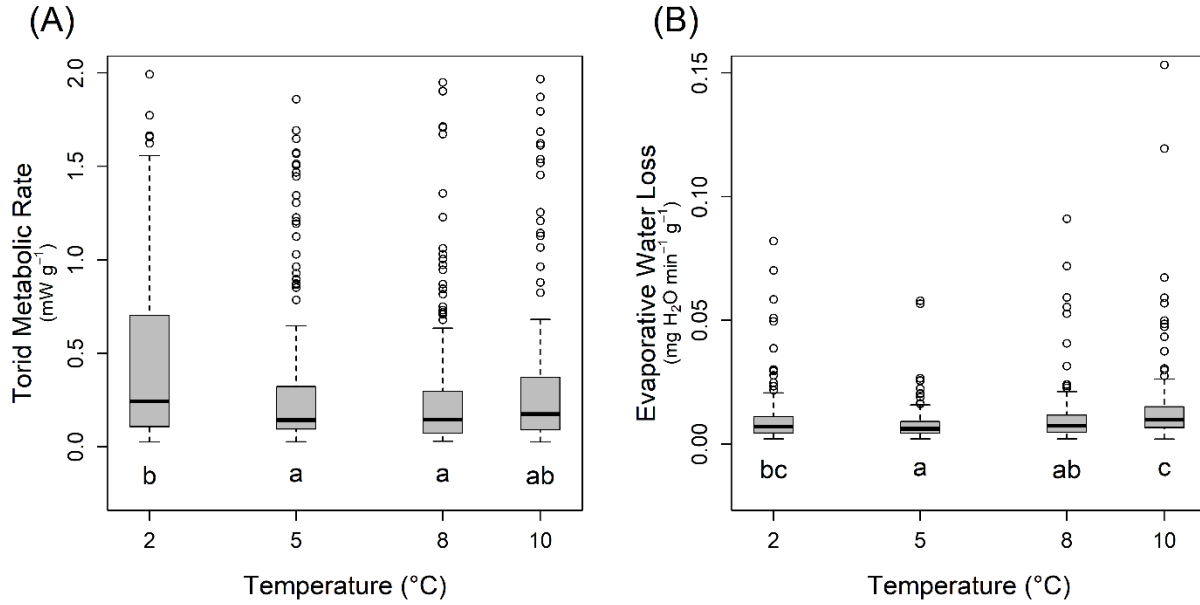
Figure 17. a) *Corynorhinus townsendii* (n = 152) torpid metabolic rate did not vary across six sites, nor did the relationship between site and temperature vary across sites. Minimum metabolic rate was measured between 5 – 8 °C and metabolic rate increased at 2 °C. Measurements made during mid-winter were greater than measurements made during pre-hibernation swarming, but both seasons have been combined here for visual simplicity and comparison with *Myotis lucifugus* (below). b) A similar pattern was observed for evaporative water loss. Minimum evaporative water loss was measured between 5 – 8 °C. There were generally no differences among sites, except for one pairwise difference between sites in British Columbia and Colorado, but sites have been combined here for visual simplicity. In both plots, temperatures indicated with the same letter did not differ.

1.2 Myotis lucifugus. Our analysis included data for 99 *M. lucifugus* from three different sites (sample size ranged from 20 – 40 bats per site). Our dataset included males and females at all sites, but sex ratio varied among sites (test for equality of proportions; $\chi^2 = 10.0$, df = 5, p-value = 0.07), with heavy male bias in Montana and Northwest Territories (binomial test; p-value < 0.0001) and an even sex ratio in Alberta (binomial test: p-value = 0.87). In Montana we conducted fieldwork during pre-hibernation swarming and mid-winter hibernation, but at the Alberta and Northwest Territories sites we only conducted pre-hibernation fieldwork. In an analysis of just data from Montana, torpid metabolic rate did not differ between fall and winter (likelihood ratio = 0.83, df = 1, p-value = 0.36). Therefore, we pooled swarming and hibernation data in Montana and did not include season in comparison among the three sites. As for *C. townsendii*, there was better support for models that included a random effect of individual (likelihood ratio = 27.33, df = 1, p-value < 0.0001) and allowed for differences in variance among temperatures (likelihood ratio = 22.17, df = 3, p-value = 0.0001). Torpid metabolic rate varied among temperatures (likelihood ratio = 15.21, df = 3, p-value = 0.002), but the effect of temperature did not vary among sites (site:temperature interaction; likelihood ratio = 7.06, df = 6, p-value = 0.32) or between sexes (sex:temperature interaction; likelihood ratio = 6.04, df = 3, p-value = 0.11). There were no differences in torpid metabolic rate among sites (likelihood ratio = 3.21, df = 2, p-value = 0.20) or between sexes (likelihood ratio = 0.04, df = 1, p-value = 0.84). Torpid metabolic rate was greater at 10 °C than at any of 8, 5, or 2 °C (Figure 18 a). Minimum metabolic rate was 0.30 ± 0.02 mW g^{-1} and the absence of an increase in metabolic rate at the

lower tested temperatures indicates the minimum defended temperature is < 2 °C, the coldest temperature we tested at.

Evaporative water loss models that included the random of effect of individual and heterogeneous variance structure were better supported (likelihood ratio = 19.74, df = 1, p-value < 0.0001; likelihood ratio = 67.74, df = 3, p-value < 0.0001). There was a marginally significant interaction between site and temperature (likelihood ratio = 12.96, df = 6, p-value = 0.044) but upon inspection the interaction was driven only by slightly greater EWL at the Alberta site at 8 °C and did not indicate any broader patterns of variation among temperatures or sites. After excluding the potentially spurious site by temperature interaction, evaporative water loss did not differ between sexes (likelihood ratio = 1.95, df = 1, p-value = 0.16) but was related to temperature (likelihood ratio = 19.75, df = 3, p-value = 0.0002) with greater evaporative water loss at 10 °C than either 8 or 5 °C (Figure 18 b). There was one site effect; bats from Montana had greater evaporative water loss than either of the other two sites (likelihood ratio = 13.81, df = 2, p-value = 0.001) but the difference was relatively minor (Figure 18 b). Minimum evaporative water loss (calculated at 5 and 8 °C across all sites) was 0.018 ± 0.001 mg H_2O min^{-1} g^{-1}.
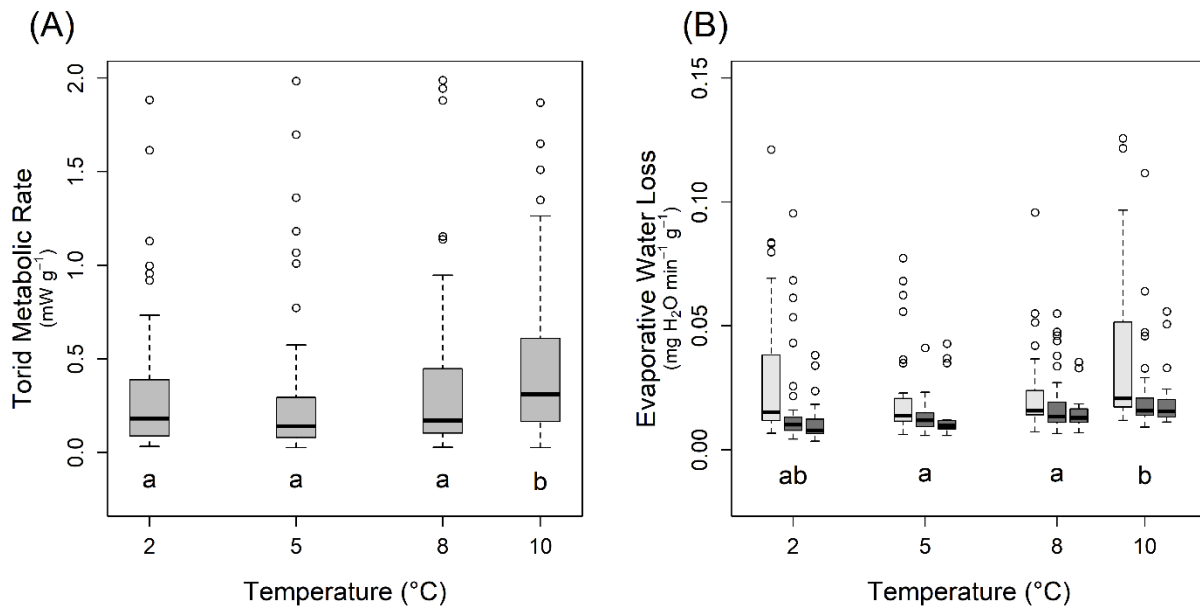
Figure 18. a) *Myotis lucifugus* (n = 99) torpid metabolic rate did not vary across three sites, nor did the relationship between site and temperature vary across sites. Minimum metabolic rate was measured between 2 – 8°C. b) Minimum evaporative water loss was measured between 5 – 8°C. Evaporative water loss was greater in Montana (light grey) than either Alberta or Northwest Territories (dark grey). In both plots, temperatures indicated with the same letter did not differ.

1.3. Discussion of intraspecific variation. Despite large geographic distances and climatic variation among our study sites, we found no evidence of intraspecific variation, or local adaptation, in torpid metabolic rate (McGuire et al. In Review). Torpid metabolic rate did not vary among sites, nor did the relationship between torpid metabolic rate and temperature. There are few studies that have previously considered similar comparisons, with mixed results. In two studies which contrasted populations across evaporative water loss gradients, there was little to no variation in metabolic rate among populations (Klüg-Baerwald and Brigham 2017; Gearhart

70

et al. 2020), consistent with the findings in our study. However, Dunbar and Brigham (2010) found variation in torpid metabolic rate among populations of hibernating *E. fuscus*. However, notably, the differences in metabolic rates among populations were only observed at the coldest and warmest temperatures tested, both of which were outside the range of temperatures we considered in our study. In the range of 5 – 10°C, torpid metabolic rate did not vary among the populations considered by Dunbar and Brigham (2010), similar to our findings. Our objective was to test hibernation physiology over a range of biologically relevant temperatures that might be regularly experienced by hibernating bats. We might have observed intraspecific variation if we included temperatures farther below the minimum defended temperature. However, assuming preferred microclimates are available, hibernators should select temperatures slightly above those that result in minimum metabolic rate (Boyles and McKechnie 2010; Boyles et al. 2020), but note that additional factors affect hibernation strategies, including sex (Jonasson and Willis 2011; Czenze et al. 2017) and body condition (Boyles et al. 2007). Therefore, we conclude that within the range of temperatures which are likely to be preferred during hibernation, there is no evidence for intraspecific variation in torpid metabolic rate.

The conclusion for evaporative water loss was generally consistent with the finding for torpid metabolic rate, but notably there were site differences in water loss. Among *C. townsendii* the relationship between water loss and temperature was consistent across populations, but there was one pairwise combination of sites (British Columbia and Colorado) that differed in evaporative water loss. Similarly, for *M. lucifugus*, evaporative water loss was greater in Montana than at the other sites. Other than these specific comparisons, there was no variation in water loss among sites for either species. Considering biologically relevant conditions, the evidence for intraspecific variation in evaporative water loss is even less compelling. We measured evaporative water loss in dry air, partially because of methodological constraints (the challenge of maintaining humidity below saturation at low temperatures) but also because measuring in dry air exacerbates potential differences in evaporative water loss among groups (Klüg-Baerwald and Brigham 2017; McGuire et al. 2017). Even in naturally experienced arid conditions, free-living animals would experience less water stress than exposed to in our experimental protocol, and the potential differences among populations would be further diminished under real world conditions. Indeed, this was exactly the finding in a study of hibernating *E. fuscus* that only observed a difference in evaporative water loss between an arid and a mesic population when measured in dry air; when measured under higher humidity, there was no difference observed in evaporative water loss (Klüg-Baerwald and Brigham 2017).

However, the potential for more pronounced differences in evaporative water loss (even if minimal) than torpid metabolic rate is consistent with previous studies (Klüg-Baerwald and Brigham 2017; Gearhart et al. 2020). Furthermore, variation in evaporative water loss but not torpid metabolic rate may reflect a physical difference among populations rather than a difference in a physiological process (Klüg-Baerwald and Brigham 2017). We measured total evaporative water loss, which consists of both respiratory and cutaneous water loss. Respiration is related to metabolic rate, and therefore differences in total evaporative water loss in the absence of differences in metabolic rate likely reflect differences in cutaneous water loss (Klüg-Baerwald and Brigham 2017; McGuire et al. 2017; Gearhart et al. 2020). Total water loss during torpor is thought to be primarily driven by cutaneous water loss (Thomas and Cloutier 1992), due to low respiration rates and greatly increased surface area due to wing and tail membranes and

large ears. Studies of hibernating bats often consider evaporative water loss as an important driver of hibernation energetics and success (Thomas and Geiser 1997; Willis et al. 2011; Ben-Hamo et al. 2013; Boratyński et al. 2015; Klüg-Baerwald and Brigham 2017; Haase et al. 2019b). The lipid composition of the stratum corneum plays an important role in cutaneous water loss (Muñoz-Garcia et al. 2012; Pannkuk et al. 2015; Ben-Hamo et al. 2016), and this may be an important avenue for future studies considering intraspecific variation in hibernation physiology.

Although the two species in our study have very large geographic ranges encompassing a wide gradient of environmental challenges, we did not find evidence for local adaptation. Rather, we suggest it is likely that rather than being locally adapted to different climate conditions, hibernating bats may be able to find suitable hibernacula with generally consistent microclimate across their range. This is particularly plausible for hibernating bats because of their ability to fly long distances in search of suitable hibernacula. Behavior may be more important than physiology and bats may be able to behaviorally select suitable hibernacula rather than physiologically specializing on locally variable conditions during hibernation. However, it is important not to extrapolate this finding. As environmental conditions extend beyond the range of preferred conditions, differences among widespread populations may become apparent. Populations at range margins are often limited by the availability of suitable environmental conditions, and this is indeed the case for hibernating bats (Humphries et al. 2002). An important consideration in our site selection was to include populations of both species at the northern limit of the species distribution (Northwest Territories for *M. lucifugus* and southern British Columbia for *C. townsendii*).

Approaching the northern distribution limit *M. lucifugus* prepare differently for hibernation and enter hibernation with substantially larger fat stores than more southern populations (McGuire et al. 2016; this study – Northwest Territories 10.0 g, Alberta 8.4 g, and Montana 7.7 g). The heaviest bats of both species were in our northernmost study sites. Additionally the more northern *M. lucifugus* were longer in forearm supporting other studies (Lausen et al. 2008), with Montana bats having nearly 2 mm shorter forearms than the bats at the Canadian sites. Although the northern *M. lucifugus* populations in our study did not differ from more southern populations in torpid metabolic rates, they did show minor differences in EWL, with the northern two sites having slightly lower EWL than the Montana site.

Our torpid metabolic rate results suggest that populations of these two geographically widespread species of bats are hibernating within their preferred range of conditions despite their geographic spread. However, there may be extreme unknown populations that are forced to hibernate outside of their preferred range and this may become increasingly true as climates shift. Distributions of suitable hibernacula may be altered by global climate change. Subterranean hibernacula are buffered from surface conditions and the resulting stable microclimate is an important factor in the selection by hibernating bats (Perry 2013). However, the conditions in hibernacula are predicted by a variety of factors at the surface (McClure et al. 2020), many of which will be affected by global climate change. If hibernacula with preferred microclimate conditions become harder to find, hibernating bats may be pushed beyond the range of conditions they typically prefer, and potential differences among populations may become more pronounced.

2. Interspecific variation in hibernation physiology

There were 13 species in our dataset (McGuire et al. In Review), including hibernating individuals of two species not normally considered to be hibernators (*Lasionycteris noctivagans* and *T. brasiliensis*). Sample sizes, sampling locations, body mass, and respirometry results are summarized in Appendix A12. TMR was slightly greater in winter than during swarming for *C. townsendii* (likelihood ratio = 4.38, df = 1, p-value = 0.04), but there was no seasonal effect for any other species we could test (*M. ciliolabrum*, *M. lucifugus*, *M. velifer*, *P. subflavus*; all p-value > 0.36). Species varied in their response to temperature, with some species arousing at colder temperatures (Figure 19 a) and other species maintaining consistently low TMR across all temperatures measured (Figure 19 b). The temperature range of TMR_{min} varied among species (Figure 20 a). The highest minimum defended temperature (between 5 – 8 °C) was observed for *T. brasiliensis* and *P. subflavus*, while *E. fuscus*, *L. noctivagans*, *M. californicus*, *M. ciliolabrum*, and *M. lucifugus* maintained TMR_{min} to < 2 °C (Figure 20 a; statistical results of temperature effects included in Appendix A12). When measured within the temperature range of TMR_{min}, EWL varied among species (n = 1,000 random draws, mean linear model p-value < 0.0001, one-sample t-test t_{999} = 11681, p-value < 0.0001) but TMR_{min} did not vary among species (n = 1,000 random draws, mean linear model p-value = 0.12, one-sample t_{999} = 25.1, p-value > 0.99). Accordingly, cluster analysis indicated either two or three groups (depending on subjective interpretation of cluster analysis elbow plot) based on evaporative water loss (Figure 20 b). *L. noctivagans* had noticeably lower EWL than all other species and may represent a separate cluster, but we conservatively present just high EWL and low EWL clusters here.
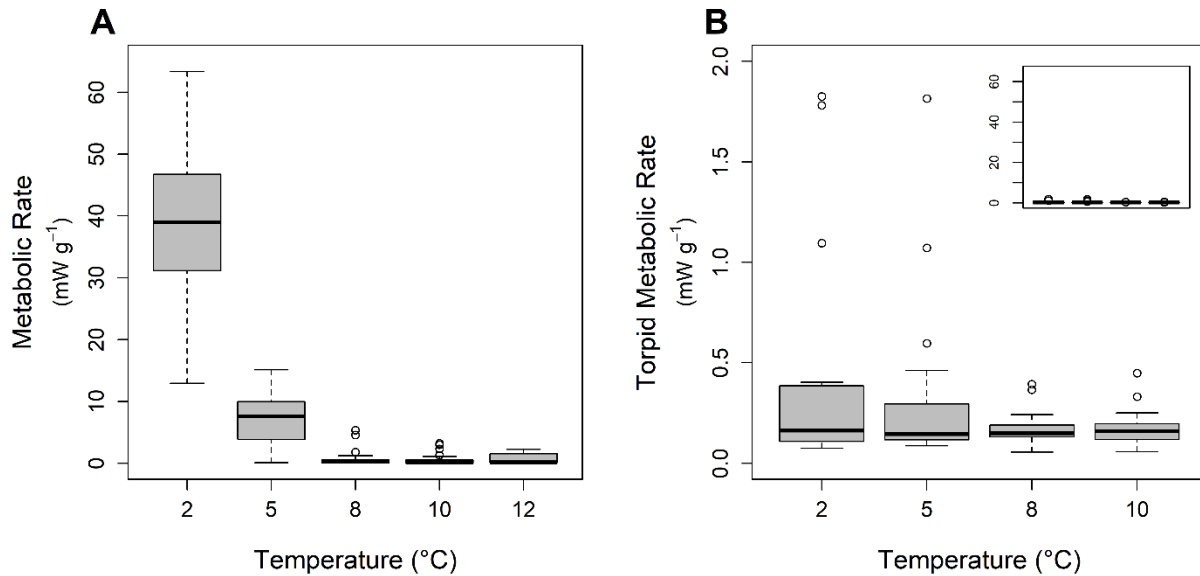
Figure 19. Examples of metabolic responses to decreasing temperature. a) The minimum defended temperature for *Tadarida brasiliensis* was between 5 – 8 °C. Below 8 °C bats aroused from torpor as reflected by the high mass-specific metabolic rate. Between 8 – 12 °C bats remained torpid, and torpid metabolic rate (TMR) did not vary over this range. Most species in our study did not arouse at colder temperatures, but we often detected increased torpid metabolic rate at colder temperatures. b) The minimum defended temperature for *Myotis ciliolabrum* was < 2 °C and we did not detect any differences in TMR over the range 2 – 10 °C. Note the very low metabolic rate of torpid bats (typical of most bats in our study); the inset in panel B plots the same data, but on the same scale as panel A for comparison.
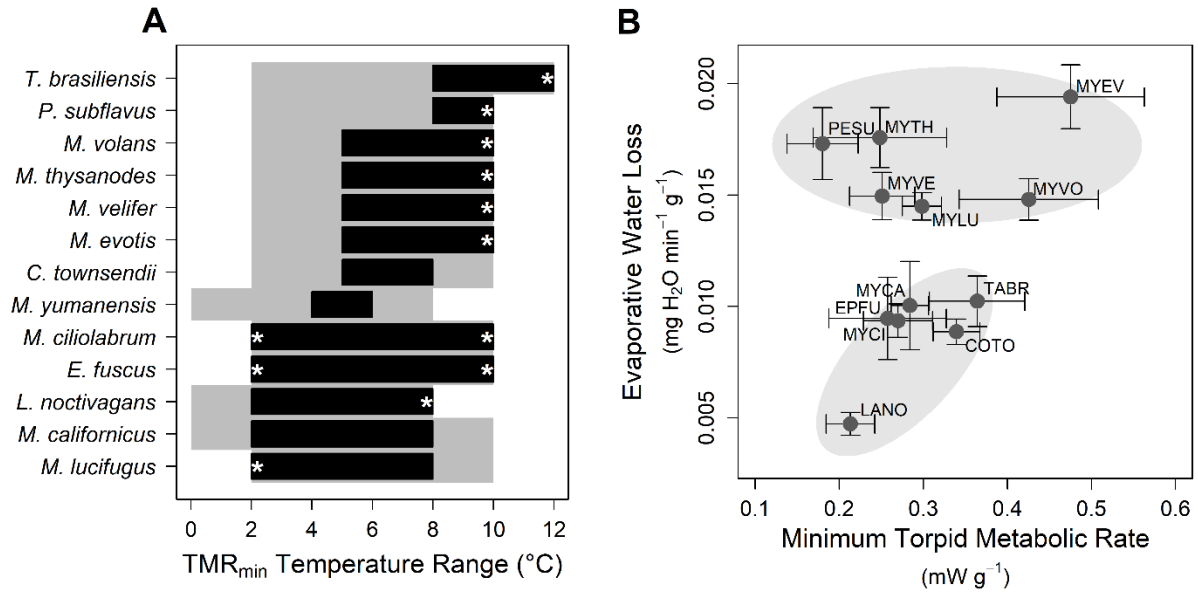
Figure 20. Variation in temperature responses, minimum torpid metabolic rate (TMR$_{min}$), and evaporative water loss (EWL) among species. a) Minimum defended temperature and the range of temperatures which resulted in TMR$_{min}$ varied among species. Grey area represents the temperature range over which the species was tested, the black bars represent the temperature range over which TMR$_{min}$ was measured. The lower end of the black boxes represents the estimated minimum defended temperature, but note that asterisks highlight cases where the TMR$_{min}$ temperature range reached either the upper or lower limit of the tested temperature range. b) Within the range of temperatures at which TMR$_{min}$ was measured, evaporative water loss (EWL) varied among species but not TMR$_{min}$. Cluster analysis revealed a high evaporative water loss (EWL) cluster and a low EWL cluster (note EWL was not measured for *Myotis yumanensis*, therefore excluded from cluster analysis). Grey ovals are presented for visual interpretation. Species codes indicate the first two letters of the genus and the specific epithet: *Tadarida brasiliensis* (TABA), *Perimyotis subflavus* (PESU), *Myotis volans* (MYVO), *Myotis thysanodes* (MYTH), *Myotis velifer* (MYVE), *Myotis evotis* (MYEV), *Corynorhinus townsendii* (COTO), *Myotis yumanensis* (MYYU), *Myotis ciliolabrum* (MYCI), *Eptesicus fuscus* (EPFU), *Lasionycteris noctivagans* (LANO), *Myotis californicus* (MYCA), and *Myotis lucifugus* (MYLU). The difference in EWL but not TMR$_{min}$ is supported by statistical tests for each (see main text).

Most previous studies of hibernation physiology have focused primarily on a single species, often one of a small number of relatively well-studied species. Our study included 13 species of bats hibernating across the western United States and Canada. Some of these species (e.g., *M. lucifugus* and *E. fuscus*) have been the focus of previous study, but there has been little hibernation research on many of the species in our study. Furthermore, we also included species that may not typically be considered hibernators to encompass a potentially wider range of hibernation physiology. Through most of their range *L. noctivagans* are long-distance migrants (McGuire et al. 2012) but in the Pacific northwest they are found hibernating in caves and mines. Similarly, *T. brasiliensis* populations in Texas and nearby states are renowned for migrating long-distances to overwinter in Mexico (Villa and Cockrum 1962) but the species is now recognized as a partial migrant with some individuals hibernating overwinter in Texas (Kunkel et al. 2020). Therefore, the species included in our study encompass diversity in taxonomy, ecology, and geography.

Physiological responses across a range of temperatures provide some indication of the conditions that may be preferred by each species. Some species in our study tolerated temperatures that approached freezing. We did not observe an increase in TMR at the coldest temperature tested (2

°C) for *M. lucifugus*, *M. ciliolabrum*, or *E. fuscus*. Similarly, we did not observe increased TMR at 2 °C for *L. noctivagans* or *M. californicus* but when the temperature decreased to freezing (0 °C, not tested for all species) TMR increased as expected to avoid freezing. In contrast, some species from some of our southern sites did not tolerate colder temperatures. We observed an increase in TMR at temperatures < 8 °C for *P. subflavus*, a species commonly found hibernating in southern states where temperatures are warmer (e.g., Texas, Louisiana, Mississippi; Jones and Pagels 1968; Sandel et al. 2001). For *T. brasiliensis*, a species where most individuals migrate south in winter (Kunkel et al. 2020, In Prep), the response was even more pronounced, with bats arousing from torpor at temperatures < 8 °C. Understanding how different species respond to colder temperatures can help to understand geographic distribution in winter (McClure et al. in prep). Hibernaculum temperatures are driven by surface temperature and a variety of other important factors (McClure et al. 2020). Ultimately species distributions are determined, at least in part, by physiological limitations and environmental constraints and winter conditions limit the distribution of hibernating species (Humphries et al. 2002).

The breadth of temperatures over which TMR_{min} is maintained may reflect niche breadth and the ability of species to hibernate under a broader range of environmental conditions. Although TMR declines with decreasing ambient temperature to $T_{defended}$, at low temperatures the decrease is relatively minor and variation among individuals resulted in a range of temperatures over which we did not detect variation in TMR. Two species in our study were notable in the breadth of the TMR_{min} temperature range, with no evidence for increased TMR across the entire range of temperatures tested for either *E. fuscus* or *M. ciliolabrum*. However, for nine of 13 species in our study, we did not detect increased metabolic rate at the highest temperatures tested. We aimed to identify the lowest defended temperature and to reduce the measurement duration and disturbance to the study animals, and therefore focused on colder temperatures. Future study at either a wider range of temperatures, or at warmer temperatures will help to identify potential interspecific variation in niche breadth.

While $T_{defended}$ and the temperature range of TMR_{min} varied among species, there was no difference in TMR_{min} across species. If measured within the appropriate temperature range for each species, all species had similar TMR. Species that hibernate in comparatively warmer regions may be adapted to warmer temperatures (e.g., *T. brasiliensis*) and species that hibernate in comparatively colder regions may be adapted to colder temperatures (e.g., *M. lucifugus*) but each can achieve comparably low TMR within their respective temperature ranges. Across the broad geographic range of our study, winter duration varies widely (Hranac et al. In Review). Rather than variation in TMR, our results suggest that hibernating bats are more likely to cope with variation in the energetic demand of hibernation by adjusting the amount of fat stored for hibernation, and the frequency of energetically costly periodic arousals. Indeed, among the most northerly studied populations, bats have exceptionally large fat stores (McGuire et al. 2016) and exceptionally long torpor bouts (Czenze et al. 2017).

In general, our analysis suggests two general hibernation strategies based on EWL. While TMR_{min} was comparable among species, species clustered into two groups based on EWL. One group was characterized by high EWL, and the other low EWL. The hibernation strategy adopted by a species is not likely to be phylogenetically driven. Phylogenetic inertia (closely related species with similar phenotypes) may partially explain differences in hibernation strategy, but is not likely the primary driver. Most *Myotis* species had high EWL but there are species from the

same genus in both groups. Similarly, temperature preference (greater potential EWL in warm conditions; Kurta 2014) is not likely an important driver of hibernation strategy. Species in the low EWL cluster are found at both the top and bottom of the temperature ranking (Figure 20 a). We suggest that adaptation to environmental conditions or behavioral adaptation to select specific conditions are the most likely factors in determining which hibernation strategy is adopted by a species. Although not all species can be easily categorized as occurring in either mesic or arid habitats, species that tend to be found in more mesic regions were in the high EWL group (e.g., *M. lucifugus*, *P. subflavus*), while species from more arid regions were in the low EWL group (e.g., *C. townsendii*, *T. brasiliensis*). Notably, while minimal, the only indication of intraspecific variation among our study sites was in EWL, and not TMR (see above section '1. Intraspecific variation in hibernation physiology'), consistent with previous studies (Klüg-Baerwald and Brigham 2017; Gearhart et al. 2020). Maintaining water balance is critical for survival, but differences in EWL may also affect the energetic cost of hibernation. Periodic arousals account for the large majority of the energetic cost of hibernation (Thomas et al. 1990) and EWL may be an important driver of arousal frequency (Thomas and Geiser 1997; Haase et al. 2019b). Consequently differences in the energetics of hibernation among species are likely to be driven by the frequency of arousals (possibly driven by EWL) and not energetic costs during torpor bouts.

We describe two hibernation strategies, high and low EWL, but these may not be strict groupings. In our dataset *L. noctivagans* had notably lower EWL than any of the other species in the low EWL group and may represent a third cluster with especially low EWL. Alternatively, hibernating species may best be represented along a continuous gradient of EWL. Future studies including additional species will reveal whether there are physiological and morphological tradeoffs that give rise to two distinct hibernation strategies, or whether our dataset simply doesn't include species with intermediate EWL.

Interspecific differences in hibernation strategy may be an important driver of distribution patterns, disease risk, and provide a starting point for understanding the potential impacts of climate change. Hibernating bats in North America are threatened by WNS, a fungal disease introduced to North America (Frick et al. 2015; Willis 2015). The sites in our study had not yet been affected by WNS, but the disease is rapidly spreading into western North America. Many of the species in our study have not yet been exposed to WNS and there is interest in predicting which species may be more or less susceptible to the disease. Some of the species in our study occur in eastern North America where WNS is widespread, but are not equally impacted (Frick et al. 2015). Notably, the species in our study that have been heavily impacted in the east (*M. lucifugus*, *P. subflavus*) were included in the high EWL group, while the species that have been less affected in the east (*C. townsendii*, *E. fuscus*) were included in the low EWL group. This is consistent with the growing recognition of the importance of EWL in the impacts of WNS (Willis et al. 2011; McGuire et al. 2017; Haase et al. 2019b). As climate change alters environmental conditions, and WNS spreads across the west, the interspecific differences in hibernation physiology that we observed will contribute to species differences in response to these threats.

Our study included 13 species with data collected from field sites spread >2,800 km from North to South, and > 2,000 km from East to West. Conducting studies on this scale is logistically challenging, but provides key insights into the physiological differences that underlie

differentiation among species. Previous studies focused on a few 'model' species have undoubtedly provided fundamental insights into the biology of hibernation, but we provide insight into variation in hibernation among species. Furthermore, doing this work in the field is extremely complicated, but provides best estimates of natural measurements of these parameters, and not values from individuals that may be habituated to captivity. Meta-analyses make it possible to compare data collected over the course of multiple studies, but in the Anthropocene (Voigt and Kingston 2016) the landscape is rapidly changing, both literally and figuratively. Understanding variability in physiological limitations is critical to understanding adaptive potential and how species, assemblages, communities, and ultimately ecosystem processes will be affected by the numerous stressors they face.

3. Lean mass contribution to hibernation energetics and water balance

We recorded data from 184 *M. velifer* during swarming, including 52 females and 132 males (McGuire et al. In Review). Female body mass (15.4 ± 0.3 g) was greater (Figure 21 a; $F_{1,182} = 26.15$, p-value < 0.0001) than male body mass (14.0 ± 0.1 g), including more fat (Figure 21 b; $F_{1,182} = 69.38$, p-value < 0.0001) but not more lean mass (Figure 21 c; $F_{1,182} = 3.00$, p-value = 0.08). There was a significant interaction between sex and body mass for both fat ($F_{1,180} = 15.99$, p-value < 0.0001) and lean mass ($F_{1,180} = 8.47$, p-value = 0.004), indicating that males and females differed in the relative contribution of fat and lean to body mass (Figure 21 d, e). Each gram of body mass increase in males was comprised of 0.59 ± 0.03 g of fat and 0.38 ± 0.03 g of lean, compared with 0.77 ± 0.03 g fat and 0.25 ± 0.03 g lean in females.
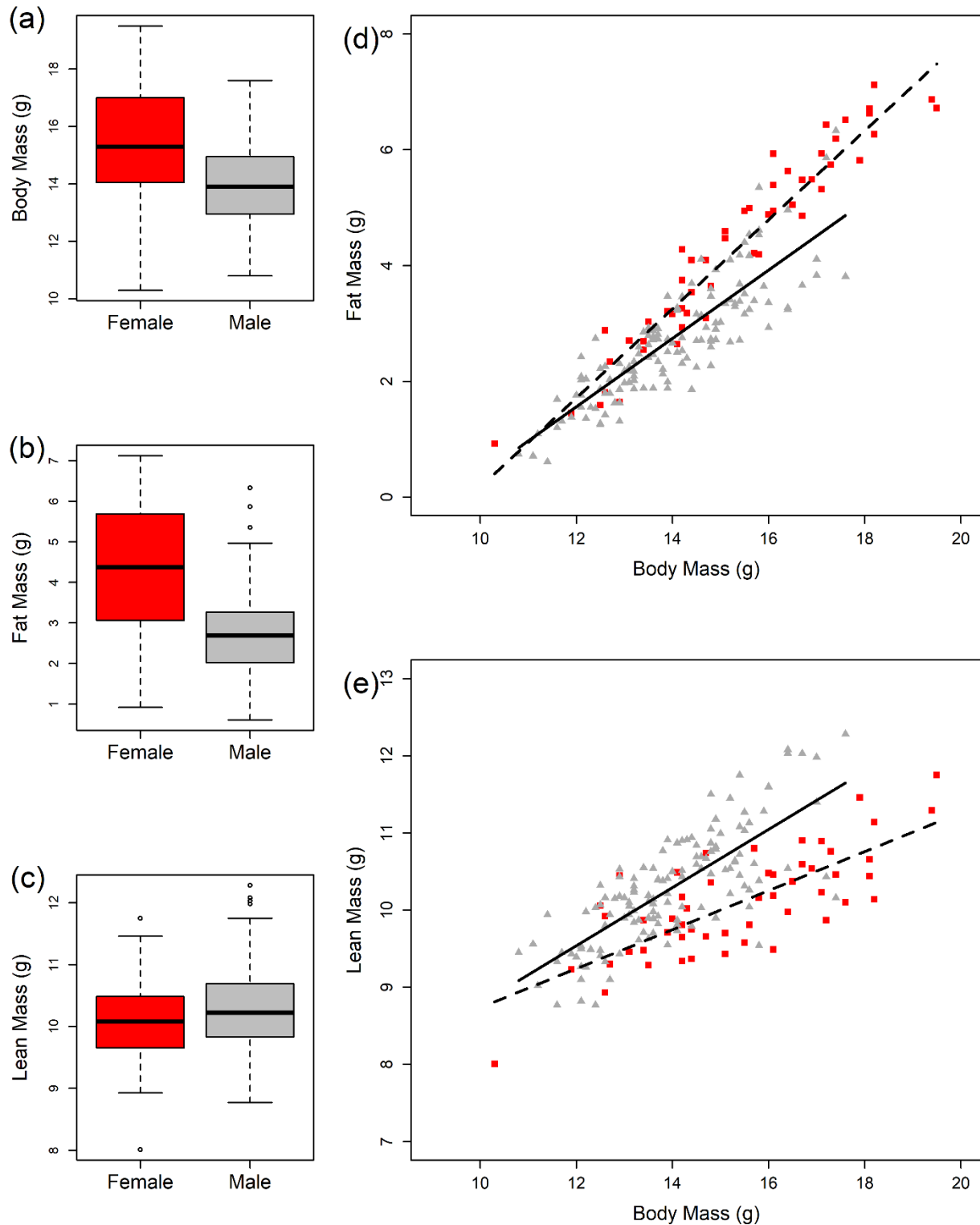
Figure 21. Body composition of *Myotis velifer* during pre-hibernation swarming in Oklahoma. a) Females weighed more than males b) driven by larger fat stores. c) There was no difference in lean mass of males and females. Females and males differed in the relative contributions of fat and lean to body mass gain. d) Females (red squares, dashed line) deposited relatively more fat (female: 0.77 g fat per g body mass increase, male: 0.59 g fat per g body

mass increase) than males (grey triangle, solid line). e) Conversely, males deposited relatively more lean mass than females (male: 0.38 g lean per g body mass, female: 0.25 g lean per g body mass).

Body composition of *C. townsendii* was related to sex and season. As expected, fat mass decreased during hibernation (Figure 22 a; $F_{1,62} = 69.45$, p-value < 0.0001). Males had less fat than females ($F_{1,62} = 16.39$, p-value = 0.0001), but the change in fat did not differ between sexes (sex:season interaction; $F_{1,61} = 0.65$, p-value = 0.42). Lean mass also decreased during hibernation, as predicted (Figure 22 b; $F_{1,62} = 4.52$, p-value = 0.037). Sex patterns for lean mass were the same as for fat mass, with greater lean mass in females ($F_{1,62} = 14.96$, p-value = 0.0003) but no difference between sexes in the way lean mass changed during hibernation (sex:season interaction; $F_{1,61} = 0.60$, p-value = 0.44).

Our statistical results did not suggest a difference between sexes in the decreases of fat or lean mass but visual examination (Figure 22 b) might suggest a greater decrease in lean mass for males than females. The calculations that follow are not meant to imply that this difference exists (our statistical analysis suggests it does not) but rather to illustrate the energetic and water balance consequences of a biologically relevant scenario of increased lean mass catabolism. The overall change in fat and lean mass was similar for males and females, but males catabolized more lean and less fat than females (Table 9). Lean mass accounted for approximately 18% of mass change in females, compared with 35% of mass change in males. Due to the higher energy density of fat, females consequently produced more energy than males. Lean mass accounted for approximately 3% of the energy budget of females compared with 7% of the energy budget of males. Total water production was similar, but lean mass accounted for 29% of water production in males compared to only 14% in females. After accounting for the water that would be required to excrete the urea produced in protein catabolism, net water production was approximately four times greater in females than males, despite producing approximately the same amount of total water. Note that net water production was substantially less than total water production in both sexes.
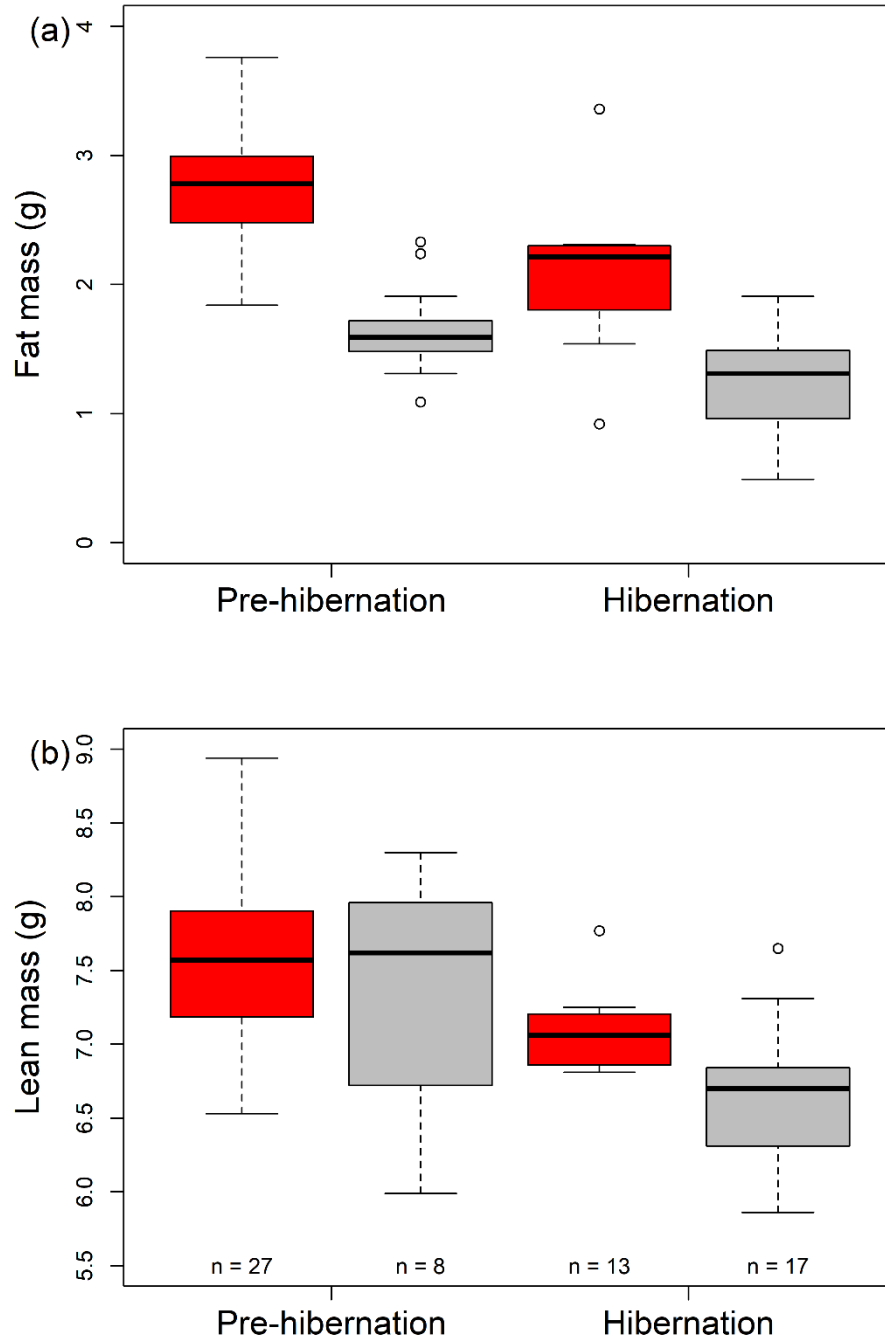
Figure 22. Body composition of *Corynorhinus townsendii* measured during pre-hibernation swarming and mid-hibernation in Nevada. a) In both seasons, females (red boxes) had greater fat mass than males (grey boxes) and fat mass predictably declined through hibernation. There was no sex by season interaction, indicating that the seasonal pattern of fat decrease was the same in both sexes. b) The same pattern was observed for lean mass. Females had more lean mass than males in both seasons, and lean mass decreased through hibernation. As for fat, there was no interaction to suggest a difference in the seasonal pattern of lean mass use between sexes.

Table 9. Calculations of the contribution of fat and lean to energy and water balance in hibernating *Corynorhinus townsendii* (Townsend's big-eared bats). Note that statistical comparison (Figure 22) does not support a difference in the relative contribution of fat and lean between males and females, but we have used the means for each group in these calculations to illustrate the potential impact of biologically relevant scenarios of lean mass catabolism in hibernation. All values here are numerical calculations based on mean fat and lean mass measured for males and females, with error propagation with each calculation. Total mass change was similar for females and males, but males catabolized more lean mass and less fat than females. Consequently, lean mass contributed a smaller proportion of the energy budget and females produced more energy. Total water production was similar, but the water required to excrete the urea produced by protein catabolism resulted in smaller net water production in males. Despite similar total water production, net water production was approximately four times greater in females.

	Female	Male
Mass		
Pre-hibernation lean mass (g)	7.58 ± 0.11	7.10 ± 0.11
Pre-hibernation fat mass (g)	2.72 ± 0.08	2.12 ± 0.25
Hibernation lean mass (g)	7.34 ± 0.21	6.63 ± 0.12
Hibernation fat mass (g)	1.65 ± 0.10	1.25 ± 0.10
Decrease in lean mass (g)	0.23 ± 0.24	0.48 ± 0.16
Decrease in fat mass (g)	1.07 ± 0.13	0.87 ± 0.27
Decrease in lean + fat mass (g)	1.30 ± 1.09	1.34 ± 0.99
Lean mass contribution to mass change (%)	17.9 ± 18.9	35.4 ± 14.5
Energy		
Energy from lean (kJ)	1.23 ± 1.27	2.52 ± 0.85
Energy from fat (kJ)	40.04 ± 4.80	32.60 ± 9.96
Total energy production (kJ)	41.27 ± 4.96	35.12 ± 10.00
Lean contribution to energy (%)	2.98 ± 3.10	7.18 ± 3.17
Water		
Water from lean (mL)	0.19 ± 0.20	0.39 ± 0.13
Water from fat (mL)	1.17 ± 0.14	0.95 ± 0.29
Total water production (mL)	1.36 ± 0.24	1.34 ± 0.32
Lean contribution to water (%)	13.97 ± 14.65	29.04 ± 11.99
Net water production (mL)	0.81 ± 0.62	0.21 ± 0.50

The two datasets in our analysis illustrate the importance of lean mass for hibernating bats. Lean mass accounted for 25 – 38% of pre-hibernation body mass increase in *M. velifer*, and decreased substantially through hibernation in *C. townsendii*. Fat is the most important energy substrate, but our results indicate that lean mass dynamics in hibernating bats are greater than have previously been considered. Many studies, whether implicitly or explicitly, have assumed that lean mass change is negligible, and that most or all mass change is due to fat.

The importance of fat as the primary energy substrate is clear, but changes in lean mass may result from, and contribute to, multiple functions. Fat may be stored as triglycerides in adipose tissue, and carbohydrates may be stored as glycogen in the liver (though carbohydrate metabolism is thought to not represent an important component of the energetics of hibernation). For lean mass, there is no storage molecule or tissue, but rather changes in lean mass represent changes in the mass of functional tissues. Hyperphagic bats may adaptively increase fat mass by eating more and converting ingested nutrients to fatty acids for storage. Increased lean mass prior to hibernation is likely the consequence of functional changes in muscles and organs. One likely scenario is muscle hypertrophy as a consequence of load carrying. Flight performance is compromised when carrying heavy loads (MacAyeal et al. 2011), and as bats fatten for hibernation they may require larger muscles to maintain flight efficiency (as observed in migrating birds which also must fly while carrying large fuel loads; Piersma 1998). Alternatively, or coincidentally, hyperphagic bats may increase the size of the digestive tract to facilitate rapid assimilation of ingested nutrients (McGuire et al. 2013). Larger digestive organs would represent an increase in lean mass, which would similarly contribute to a load carrying effect. Regardless of the mechanism of lean mass increase, the consequence is that hibernating bats have larger lean mass stores available during hibernation. The load carrying effect is also consistent with spring demands. After many weeks or months of hibernation, bats weigh less and therefore no longer require extra muscle mass to support flight. Therefore, lean mass catabolism is possible due to functional increases in lean tissues prior to hibernation, and the decreased load carrying capacity required when emerging from hibernation in spring.

The available literature is consistent with hibernating animals catabolizing both muscle and digestive organs during hibernation. Fasting-related reductions in the digestive tract are expected and have been demonstrated in several species of hibernators (Carey 1990; Paksuz 2014). Notably, intestinal mass of thirteen-lined ground squirrels (*Ictidomys tridecemlineatus*) and alpine marmots (*Marmota marmota*) decreases in hibernation, but begins to decline prior to hibernation (Carey 1990; Hume et al. 2002), suggesting that in bats, lean mass increases prior to hibernation may be a unique consequence of the load carrying requirements of flight. Similarly, studies have shown decreases in muscle and kidney mass during hibernation (Yacoe 1983). While decreases in muscles and digestive organs come at a functional cost, if these tissues were increased due to autumn load carrying and hyperphagia demands, then the excess capacity that is not required in spring would allow for partial catabolism of these tissues (e.g., for gluconeogenesis or metabolic water production, see below) with minimal functional consequence upon emergence in spring. However, changes in the muscle fiber composition of gastrocnemius but not pectoralis muscles in hibernating bats suggests that lean mass is not catabolized equally among tissues and differential changes preserve priority functionality (Brigham et al. 1990). In other biological systems lean mass catabolism can result in important functional consequences. For example, migrating birds that catabolize digestive tissues while crossing ecological barriers have reduced foraging ability upon arrival at refuelling stopovers (Piersma 1998; Karasov and Pinshow 2000). If perturbation of normal hibernation patterns (e.g., by disease such as WNS; McGuire et al. 2017) leads to increased lean mass catabolism, it is possible that hibernators may emerge in spring with exhausted nutrient stores and digestive systems that are functionally compromised.

Fat remains the primary fuel source for hibernation, but the contribution of protein is not negligible. In our example calculations protein contributed 3 to 7% of the energy budget of

hibernating bats. Sex differences in the contribution of lean mass to energy and water budgets may be important to consider. In *M. velifer*, males put on proportionately more lean mass than females, and in *C. townsendii* our calculations illustrated potential sex differences in the role of lean mass catabolism. Sex differences in the relative deposition of lean mass suggest it is not simply a consequence of increased load carrying capacity, but may represent an adaptive strategy. The "Thrifty Female" (Jonasson and Willis 2011) and "Frisky Male" (Czenze et al. 2017) hypotheses suggest that sex-differences in hibernation energetic strategies result from differences in the timing of reproductive investment. Copulation occurs in fall, and while females must emerge in spring in sufficient condition to support pregnancy, males have low energetic demands in spring and therefore may face weaker selection for strict energy budgeting during hibernation compared to females (Willis 2017). Males generally arouse more frequently than females (e.g., Jonasson and Willis 2011; Czenze et al. 2017), possibly in search of additional mating opportunities (Gustafson 1979), which likely results in greater protein catabolism. The rate of protein catabolism is greatly reduced during torpor compared to periodic arousals (Yacoe 1983). Therefore, contrary to the general consideration of 'protein sparing' strategies described in the starvation literature (McCue 2010), the relatively greater lean mass deposition in male *M. velifer* may be an adaptive strategy to support increased arousal frequency during hibernation, consistent with the greater calculated contribution of lean mass in hibernating male *C. townsendii*.

One of the major differences of using protein as a fuel instead of fat is the lower energy density and greater water produced by burning protein. On a dry mass basis, protein has lower energy density than fatty acids (39.6 kJ g^{-1} dry mass for lipids compared with 17.8 kJ g^{-1} in proteins). But the apparent difference in energy density is further exacerbated by the high water content of lean tissues. Adipose tissue contains only ~ 5% bound water by weight, compared with 70% for protein. This relationship accentuates the already lower energy density of protein compared to fatty acids. Water is further produced as a byproduct of metabolism (metabolic water production), such that when combining bound and metabolic water production, fat provides more water on a wet tissue basis (1.05 g H_2O per g wet tissue for lipids, 0.82 g H_2O g^{-1} for protein). But when calculated on an equivalent energy basis, protein catabolism yields ~ 5x more water than fat.

Our study demonstrates that lean mass is dynamic in hibernating bats, with hibernating bats increasing lean mass in advance of hibernation and catabolizing lean mass during hibernation. The lack of a storage tissue for protein makes the functional considerations of lean mass deposition and catabolism important to consider. Furthermore, sex-differences suggest that protein catabolism contributes to adaptive strategies of male and female hibernating bats. We have presented ideas and hypotheses, but there remain many opportunities for investigations of the previously underappreciated role of protein catabolism in hibernation. Protein contributes a small, but not negligible amount to the energy budget of hibernation, but may have many impacts on gluconeogenesis, water balance, and indirect effects on energetics through effects on arousal frequency.

4. Tadarida brasiliensis (Mexican free-tailed bats) case study
We captured 28 *T. brasiliensis* (14 pre-hibernation, 14 hibernation). The overwintering population was almost exclusively comprised of males, and all individuals in our analysis were male. Bats readily entered torpor during the acclimation period of respirometry. Metabolic rate

did not differ between seasons ($F_{1,106} = 2.34$, p-value = 0.13) but varied across temperatures ($F_{4,106} = 89.13$, p-value < 0.001). Minimum defended temperature was the highest observed among all species in our study. Metabolic rate did not differ among 8 °C, 10 °C, and 12 °C (all p-values > 0.05) but increased when T_a was lowered to 5 °C and again when T_a was lowered to 2 °C (all p-values < 0.001) (Figure 20). Therefore minimum defended temperature was between 5 - 8 °C. Based on the mixed effects breakpoint model, we estimated the minimum defended temperature to be 5.9 °C (95% CI 5.8 - 6.1 °C).

We deployed temperature-sensitive transmitters on 30 bats in February 2019 (all males) but only successfully recorded data from four. All bats used torpor each day of the field study and three of the four exhibited at least one torpor bout lasting > 24 h (Table 10). Patterns of torpor varied between milder periods where bats aroused in the evening at dusk and departed the roost (Figure 23 a) and colder periods when bats remained torpid for multiple days (Figure 23 b). Maximum torpor bout duration ranged from 12.3 – 126.0 h (0.5 – 5.3 days) while median bout duration ranged from 10.2 – 36.2 hr. Bats used longer torpor bouts in colder weather ($F_{1,20} = 7.58$, p-value = 0.012).

Table 10. Male *Tadarida brasiliensis* used torpor daily, and in some cases for multiple days, during winter.

Bat ID	Body mass (g)	# days of data	# torpor bouts	Max torpor bout duration (h)	Median torpor bout duration (h)	Mean minimum torpid T_{sk} (°C) ± SE
109	10.3	12	8	55.5	22.4	10.4 ± 1.51
110	10.6	13	5	126.0	36.2	8.52 ± 1.2
117	14.4	4	3	32.0	15.3	8.53 ± 1.0
123	13.8	8	7	12.3	10.2	8.84 ± 0.7
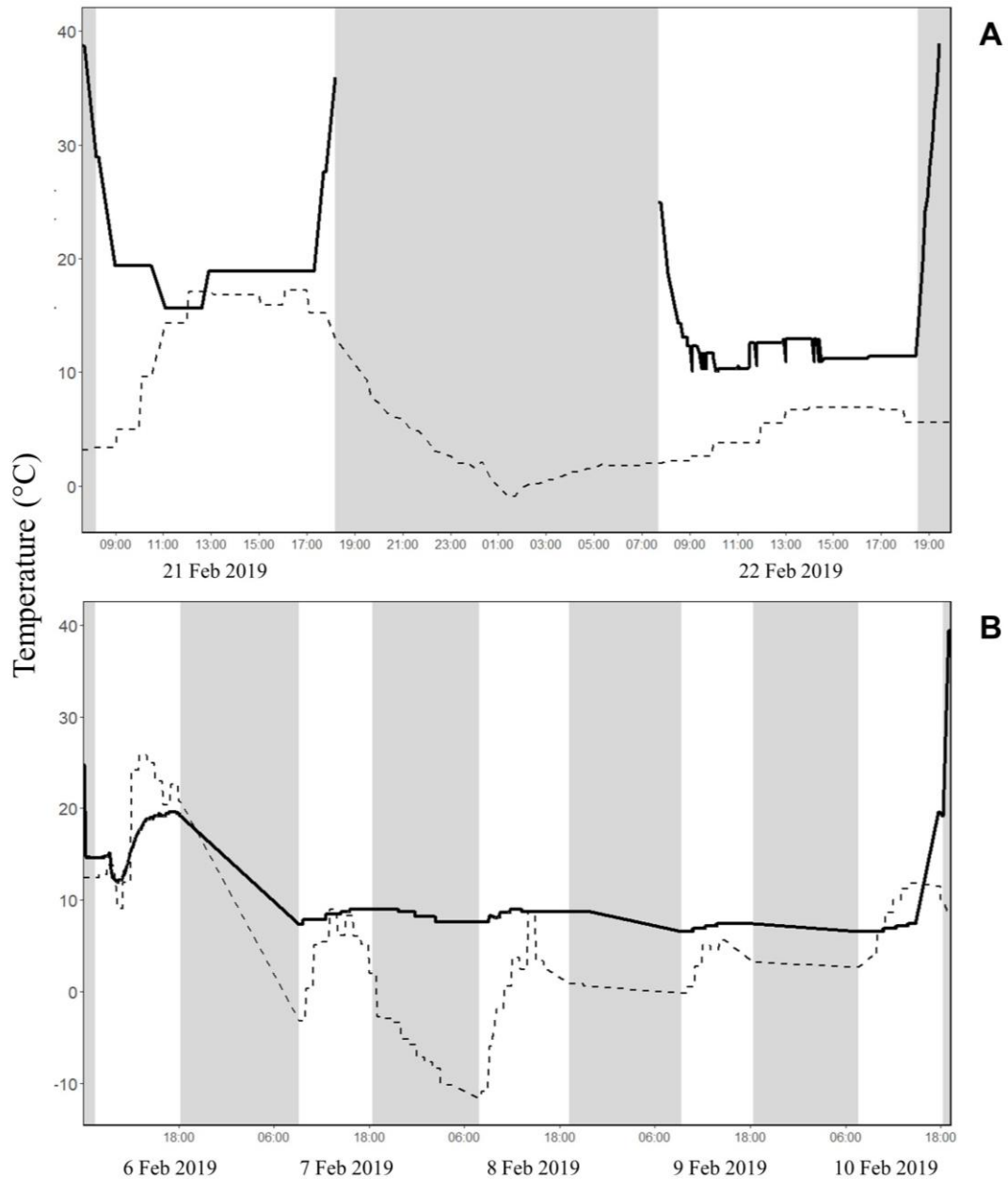
Figure 23. *Tadarida brasiliensis* exhibited both single a) and multi-day b) torpor bouts in response to varying environmental conditions. Solid lines denote T_{sk} while dashed lines denote T_a outside the roost. Shaded areas represent the nighttime period between sunset and sunrise.

This case study of hibernation physiology of *T. brasiliensis*, adds to a small, but growing, body of literature studying hibernation away from north temperate regions with implications for WNS susceptibility and pathogen spread (Kunkel 2020; Kunkel et al. In Prep). Our observations that *T. brasiliensis* alternated between daily and multi-day torpor lends support to the framework that hibernation energetics are governed by balancing trade-offs (Boyles et al. 2020). With relatively mild winters at this study site, *T. brasiliensis* varied the duration of torpor bouts in response to varying environmental conditions. In other research we have shown that bats remained active on

warmer winter nights without foraging (Kunkel 2020), indicating flexibility in the need to minimize energy expenditure. This dynamic hibernation strategy is a southern extension of the latitudinal gradient of hibernation patterns seen in other bat species (Dunbar and Brigham 2010; McGuire et al. 2016) and agrees with evidence of torpor avoidance (Willis 2017; Boyles et al. 2020). This work builds on the growing body of evidence showing environmental variability influences hibernation phenotype and provides valuable context for future studies of hibernation physiology and behavior.

Minimum defended temperature was 5.9 °C, which predicts *T. brasiliensis* should select winter roosts which do not experience frequent drops in below 5.9 °C. The minimum defended temperature measured is comparable to other sub-tropical hibernating bat species (e.g., 6 °C for *T. aegyptiaca* (Cory Toussaint et al. 2010), 6.7°C for *T. teniotis* (Marom et al. 2006); 7.3 °C for *Nyctophilus bifax* (Stawski et al. 2009)) and higher than typical northern hibernating bats (e.g., 1.3 °C for *M. lucifugus* (Jonasson and Willis 2012) and 1.0 °C for *E. fuscus* (Willis et al. 2005)). Although we were unable to access the roosting locations of free-living bats to directly measure roost microclimate, the telemetry data provides some insight. Assuming T_{sk} is approximately equal to T_a (as is typical for roosting heterotherms; Ruf and Geiser 2015), the bats we observed consistently selected microclimates above the minimum defended temperature as mean minimum torpid T_{sk} was 8.5 – 10.4 °C (Table 10). Metabolic rate did not differ between 8 – 12 °C (Figure 20), suggesting bats selected roost microclimates which were within the range of temperatures that would minimize energy expenditure while maintaining a safety margin above their minimum defended temperature.

While bats overwintering in temperate regions typically exhibit extended bouts of torpor, we recorded daily torpor by all four bats monitored and multi-day bouts in three of the four bats. Like other subtropical bats (e.g., Stawski et al. 2009), *T. brasiliensis* aroused from torpor during warm winter nights. However, this did not preclude bats from entering prolonged torpor during cold periods. Because bats remained torpid longer in colder weather, our findings indicate this species uses facultative hibernation and adjusts heterothermy use with environmental changes. In additional research not presented here, we found that winter activity is not associated with foraging at this site and thus roost departures may serve alternative purposes such as drinking or roost switching. It is unclear how frequently this species uses daily or multi-day torpor on a long-term scale, but our small sample size indicates heterothermy is used extensively.

As the southern United States is predicted to warm significantly in the next century (Intergovernmental Panel on Climate Change 2018) it is likely the energetic costs of overwintering will decrease, perhaps leading to range expansion and decreased propensity to migrate in this species. The frequency of overwintering increased in the last 50 years and it is estimated this pattern will continue (Weaver et al. 2015). Expansion of overwintering raises concerns of WNS pathogen infection and transmission. As subtropical migrants, *T. brasiliensis* have not been considered threatened by WNS, but this may change if overwintering range and hibernation behavior increases in the future. Since we only observed short-term facultative hibernation, we suggest *T. brasiliensis* are at low risk of WNS-induced population declines but their ability for extensive travel (> 50 km/night; Davis et al. 1962; Williams et al. 1973) suggests this species may accelerate the transmission of the fungal pathogen which causes this disease.

Arousal Frequencies
In the United States sites, arousal data from temperature sensitive transmitters were not obtained due to the movement of bats out of the range of detection of the receiving dataloggers. Only a single logger recorded any data, but the recordings were not extensive enough to calculate arousal frequencies. This was also the case for the Canadian mine site (Phoenix Mine). Arousals were documented in both years (2017 and 2018) from radiotransmittered *M. lucifugus* in Cadomin Cave site in Alberta, Canada, and in 2018 from *C. townsendii* using attached modified iButtons in Phoenix Mine, British Columbia, Canada. At Cadomin Cave (radio-telemetry), the mean torpor bout duration of *M. lucifugus* was 23.3 ± 15.2 SD days, mean arousal duration was 1.74 ± 1.3 SD hours, and the mean number of arousals during the period monitored was 1.2 ± 0.4 SD per bat (n = 22 bats; 27 arousals documented; mean monitoring period 37 days). At Phoenix Mine (modified iButtons), *C. townsendii* mean torpor bout duration was 21.4 ± 11.3 SD days, mean arousal duration was 0.75 ± 1.1 SD hours, and the mean number of arousals during the period monitored was 3.4 ± 1.5 SD per bat (five bats; 17 arousals documented; mean monitoring period 75 days).

Improving the energetic costs of cooling model
Cooling cost from our model was not different from measured cost (slope = 0.99 [0.93, 1.04], $F_{1,7}$ = 1220, p-value = < 0.001, R^2 = 0.99; Table 11, Figure 24). Mass-specific costs of cooling ranged from 0.36 ml O_2 g^{-1} in the Northern birch mouse (*Sicista betulina* [10 g]), one of the smallest species, to 41.9 ml O_2 g^{-1} in the short-beaked echidna (*Tachyglossus aculeatus* [4600 g]), the largest species in our dataset. Warming ranged from 2.8 ml O_2 g^{-1} in the bicolored shrew (*Crocidura leucodon* [12 g]) to 26.4 ml O_2 g^{-1} in the arctic ground squirrel (*Urocitellus parryii* [406 g]). Cooling was more energetically costly than warming in four species (*Marmota flaviventris*, *M. broweri, M. marmota,* and *T. aculeatus*), all of which had low thermal conductance values (< 0.05 ml O_2 g^{-1} $°C^{-1}$ h^{-1}), large body sizes (>2000 g), and thus slow cooling rates (< 0.5 °C h^{-1}).

Table 11. Measured and modeled costs (ml O2 g^{-1}) of cooling into torpor from euthermia. Measured costs are reported from the referenced papers and modeled costs are from Equation 2.

Species	T_a	Measured Costs	Modeled Costs	Data Reference
Erinaceus europaeus	5	4.73	4.65	Webb and Ellison 1998
Glis glis	4	2.65	2.86	Wilz and Heldmaier 2000
Marmota flaviventris	6	9.25	8.53	Armitage et al. 2003
Marmota marmota	7	3.76	3.86	Heldmaier et al. 2004
Urocitellus richardsonii	13 – 15	4.22*	4.50 **	Wang 1978
Urocitellus richardsonii	8 – 10	3.16*	3.85**	Wang 1978
Urocitellus richardsonii	2 – 6	4.09*	3.98**	Wang 1978
Zapus princeps	5	5.09	5.17	Cranford 1983

*mean over all individuals
**mean over all temperatures
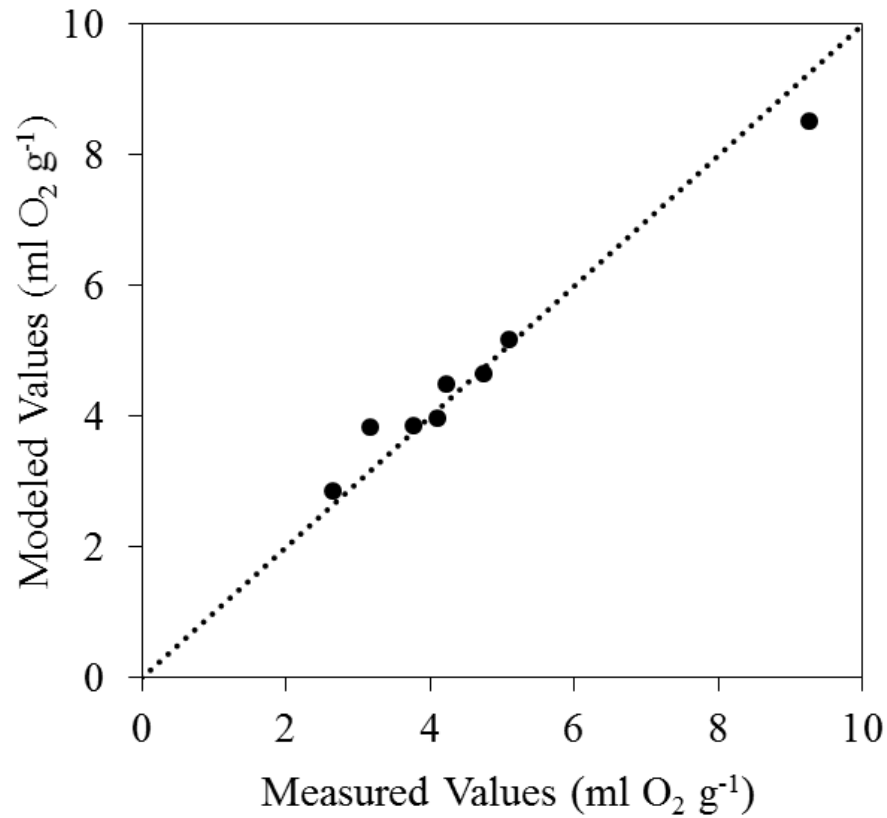
Figure 24. Measured and modeled cooling cost (ml O2 g^{-1}) of hibernating species used to validate a cooling cost model. Dashed line represents 1:1 line. Modeled cost was not different from measured cost (slope = 0.99 [0.939, 1.04], $F_{1,7}$ = 1220, p-value = <0.001, R^2 = 0.99).

Both body mass and thermal conductance were significant predictors of mass-specific cooling cost ($F_{1,51}$ = 226.4, p-value < 0.001, R^2 = 0.90), with body mass and thermal conductance accounting for 88.9% and 10% of the variation in cooling cost across species, respectively. Mass-specific cooling cost decreased with increased cooling rate ($F_{1,51}$ = 506.4, p-value < 0.001, R^2 = 0.91; Figure 25 a), and cooling rate was inversely proportional to body mass ($F_{1,51}$ = 611.1, p-value < 0.001, R^2 = 0.92; Figure 25 b).
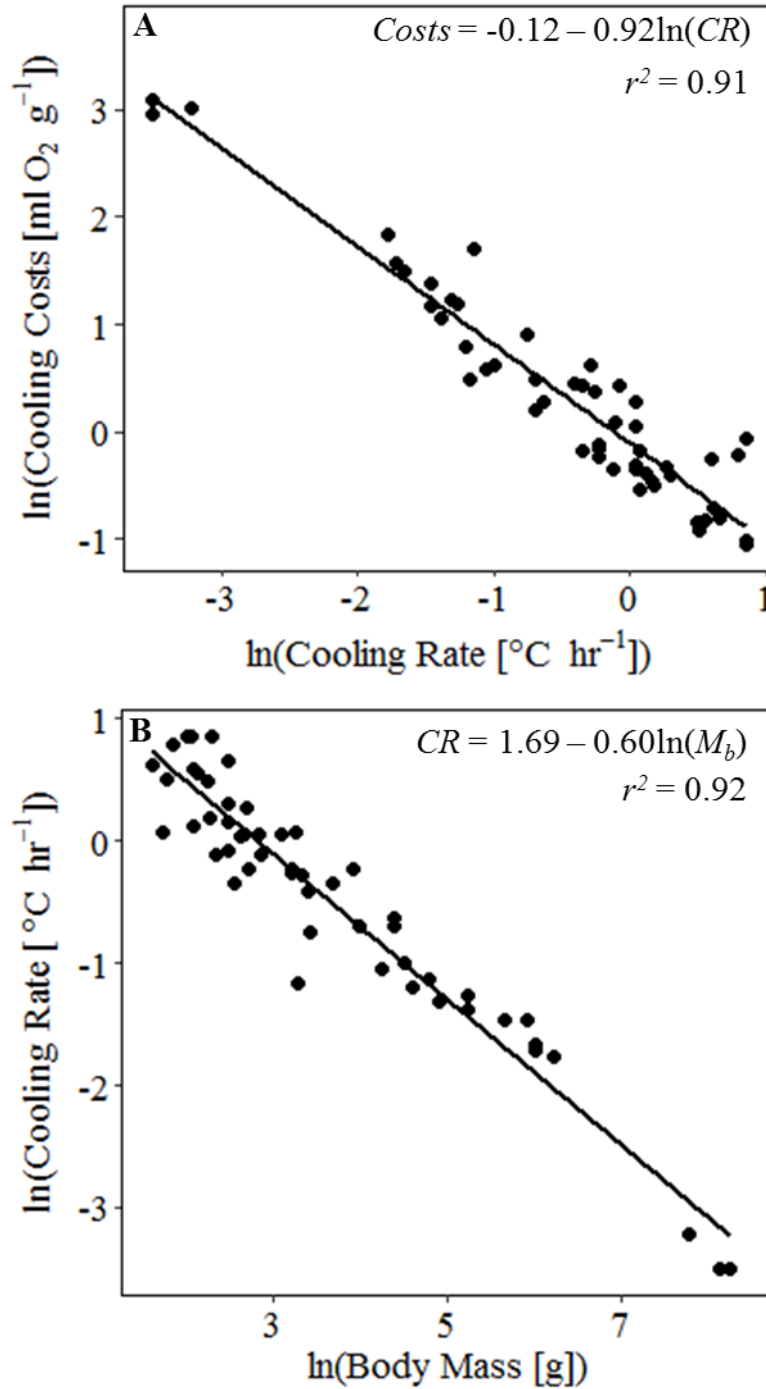
Figure 25. Relationship between cooling rate (CR; °C h^{-1}) and a) body mass (g) and b) mass-specific cooling cost per arousal (ml O2 g^{-1}) for 55 mammalian hibernators.

The oft-used 67% proportion of warming cost estimate of cooling cost (Appendix A13) did not describe cooling cost across taxa (slope = 0.07 [-0.03, 0.16], $F_{1,51}$ = 1.83, p-value = 0.18, R^2 = 0.03; Figure 26 a). Body mass, however, explained 47% of the variation in the difference between the two calculations ($F_{1,51}$ = 44.36, p-value < 0.001; Figure 26 b). The mean cooling cost was 47.9 ± 18% of warming cost, ranging from 3.8% in *Perognathus longimembris* (8.4 g),

the little pocket mouse, to 383% in *T. aculeatus* (4600 g). Cooling cost represented 67% of warming cost in all ground squirrel species and one other species of similar body size: *Callospermophilus lateralis* (137 g, 58% [48 – 68%]) , *Cricetus cricetus* (370 g, 76% [66 – 86%]), *Ictidomys mexicanus* (190 g, 74% [64 – 84%]), *I. tridecemlineatus* (190 g, 70% [60 – 80%]), *Otospermophilus beecheyi* (502 g, 57% [47 – 67%]), *Spermophilus citellus* (290 g, 58% [48 – 68%]), *U. parryii* (406 g, 60% [50 – 70%]), and *U. richardsonii* (406 g, 67% [57 – 77%]).
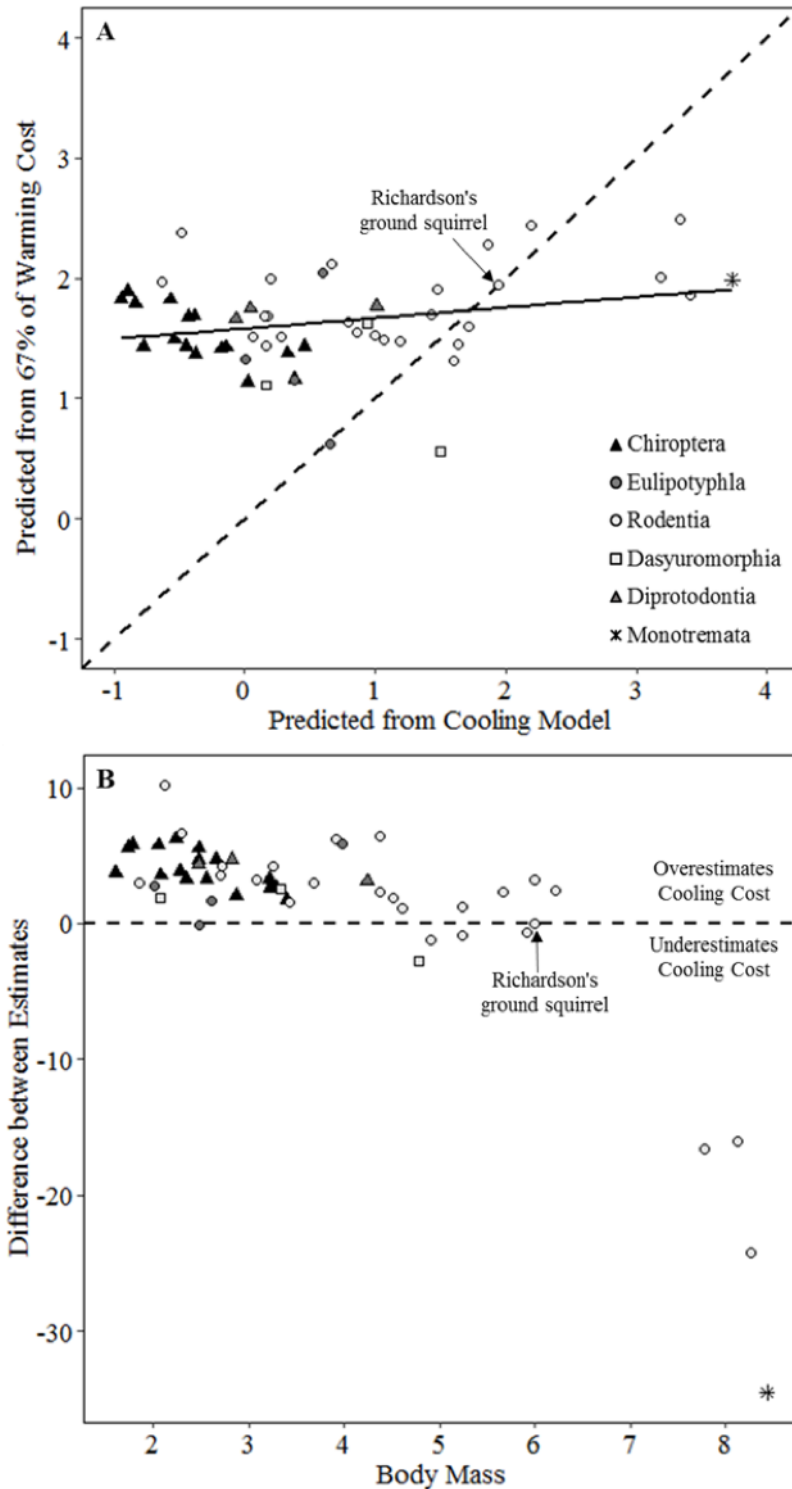
Figure 26. a) Energetic cost of cooling (ln[ml O2 g^{-1}]) for 53 mammalian species grouped by order and predicted from our cooling model and estimated from the commonly assumed 67% of warming costs. Dashed line represents one-to-one relationship between estimates and solid line is the fitted relationship. b) Relationship of the difference between cooling cost estimates (predicted from 67% of warming cost – cooling model; ml O2 g^{-1}) and body mass (ln[g]). Dashed line represents no difference between estimates.

The common assumption that the cost of cooling is equal to 67% of the cost of warming during arousal in hibernation is not broadly applicable across taxa. The cost of cooling scaled with body mass, which was expected given the relationship between the rate of heat loss and surface area to volume ratio (Bakken, 1976a, 1976b). Consequently, cooling rate was inversely related to mass-specific cooling cost (Figure 25 a), suggesting cooling rate, as a function of body size and thermal conductance, is an important factor in hibernation energetics.

We attributed the mismatch between the two estimates of cooling cost to the fact that the 67% proportion relied on metabolic measurements from a squirrel species (*U. richardsonii*), which has a body mass that is not representative of the body size of most hibernating mammals. Due to the scaling relationship between body mass and surface area (Schmidt-Nielsen 1984), smaller species have a greater amount of surface exposed to the environment per unit volume compared to larger species (Kleiber 1972; Strunk 1971). Greater surface area leads to greater heat loss and thus faster cooling rates, which we observed in the relationship between cooling rate and body mass (Figure 25 b). Therefore, the estimated 67% of the cost of warming overestimated the cost of cooling in species smaller than ground squirrels and underestimated the cost of cooling in larger species (Figure 26). The fact that most of the variation in the relationship between both cooling cost calculations was described by body mass also supports these patterns. Incorporating both body size and surface area (scaled from body mass) in the calculation of cooling cost leads to more accurate estimates of the differences in cooling across taxa.

The physiological mechanisms behind the cooling and warming processes also suggest it is inappropriate to estimate cooling cost from warming estimates. Warming is considered to be an active process in our analysis, where animals increase T_b using endogenous heat production to warm tissues (Geiser 2004; but see discussion of passive rewarming below). In placental mammals, brown adipose tissue provides high metabolic heat production for nonshivering thermogenesis (Smalley and Dryer 1963; Smith and Hock 1963), while non-placentals (monotremes and marsupials) and birds generate heat by shivering (Johnston 1971; Schmidt-Nielsen 1987). Nonshivering thermogenesis has been reported to produce as much heat as shivering in species that do both (Janský 2008), but the energetic costs of brown fat consumption compared to muscular activity required by shivering have yet to be compared. Differences in the efficiency between these two processes may potentially lead to interspecific differences in warming costs, which makes assumptions inaccurate for some species.

In contrast with active warming, our model assumed that entry into torpor was a passive process – that is, cooling was driven by heat loss rather than active metabolic suppression (Snapp and Heller 1981). Snapp and Heller (1981) observed that the rate of metabolism decreases in response to temperature, i.e. the Q_{10} effect, supports the hypothesis that most mammals passively enter torpor. However, active metabolic inhibition (e.g. suppression of enzyme activity) may be required for deep torpor (Geiser 2004, 2016). If active suppression is required for the cooling phase to occur, then cooling rate would also be driven by the ability to inhibit metabolism rather than just body size and thermal conductance. Due to the uncertainty behind when and in which species metabolic inhibition occurs, we assumed passive cooling, and did not account for any changes to metabolic rate. However, our model can be revised to include alterations to input parameters (e.g. metabolic rate) if active suppression alters metabolic rate for a species of interest.

A common assumption used to predict the energetic cost of cooling may not represent cooling cost of all hibernators due to interspecific variation in body size, thermal conductance, and T_a exposure. We considered how mechanisms differed between the cooling and warming processes and how these differences may lead to a mismatch between the assumed proportion and modeled costs. We found that cooling rate scaled linearly with body mass and was a strong predictor of overall cooling cost. Our model allows for generalization of energetic cost for multiple taxa using species-specific physiological and morphometric parameters, and for predictions over variable environmental conditions. Accurate predictions are especially important in the context of wildlife conservation, as is the case with predicting the energetic effects of WNS on bat species across North America.

Refinement of the hibernation energetic model

We captured 183 *M. lucifugus* over the capture periods of 2016 – 2018 (140 during fall, 43 during winter; Appendix A7; Table 12). There was minimal variation in hibernaculum microclimate measured by the HOBO and iButton loggers within the hibernaculum (temperature: mean = 4.80 ± 0.60 °C, range = 2.77 – 5.68 °C; water vapor pressure deficit: mean = 0.11 ± 0.26 kPa, range = 0.00 – 2.57 kPa) across winters. We found all bats roosting in the cathedral room, where hibernaculum microclimate was stable throughout the winter (T_a = 4.8 °C, RH = 100%). Activity decreased < 50 passes day-1 by mid-October (mean date among years 14 October) and increased beyond 50 passes day-1 by mid-April (mean date among years 13 April). We therefore concluded that hibernation duration in central Montana was 181 days.

Table 12. Morphometric and physiological data measured from *Myotis lucifugus* captured at a hibernaculum in central Montana. N = sample size, TMR: mass-specific torpid metabolic rate, EWL: mass-specific evaporative water loss.

Variable	Value ± SD	N
Body mass (g)	8.30 ± 0.98	176
Fat mass (g)	2.09 ± 0.74	65
Lean mass (g)	4.56 ± 0.72	65
TMR (ml O_2 g^1 h^{-1})	0.03 ± 0.02	49
EWL (mg H_2O g^{-1} h^{-1})	0.93 ± 0.60	49

Measured EWL from our respirometry procedures in dry air (0% relative humidity) ranged from 0.31 to 1.53 mg H_2O h^{-1} g^{-1} (mean: 0.71 ± 0.25 mg H_2O h^{-1} g^{-1}) depending on temperature and individual. Our model accurately predicted EWL for *M. lucifugus* in Montana ($F_{1,61}$ = 570.3, p-value < 0.001, slope = 0.97 [0.89, 1.06]; Figure 27). Given the hibernaculum conditions measured at the roosting location (T_a = 4.8 °C, RH = 100%), we predicted EWL from *M. lucifugus* as 0.06 ± 0.40 mg H_2O h^{-1} g^{-1} in healthy bats. *P. destructans* had no impact on EWL early in infection, but by late hibernation had increased EWL to 2.19 mg H_2O h^{-1} g^{-1}.

Our model accurately estimated torpor bout duration in captive bats infected with *P. destructans* ($F_{1,32}$ = 18.64, p-value = 0.0001, slope = 0.65 [0.43, 1.16]; Figure 27), but the estimates had a wide variance and lacked precision (only 25% of the variation in the data was explained by the

model). Without the inclusion of EWL, however, the model did not accurately describe torpor bout duration ($F_{1,32}$ = 0.40, p-value = 0.53, slope = -0.15 [-0.59, 0.30]) and did not describe variation in the data (R^2 = 0.02). We therefore predicted torpor bout duration using our modified model including EWL. For healthy bats, torpor bouts lasted 16.10 ± 5.04 days within the microclimate conditions of the hibernaculum at the field site (range: 4.54 – 18.3 days). Torpor bouts ranged from < 1 day to 18.3 days (mean: 6.20 ± 5.40 days) for bats infected with *P. destructans*.

Our modified hibernation model accurately predicted mass loss in healthy wild bats ($F_{1,47}$ = 74.38, p-value < 0.0001, slope = 0.87 [0.67, 1.07]; Figure 27). Though there was a lack of individual metabolic rate and EWL data for the bats used in this validation procedure, our model still explained 62% of the variation in the dataset. Our model was also more precise than the hibernation model that lacked EWL, which was not accurate ($F_{1,47}$ = 1.04, p-value = 0.84, slope = -0.02 [-0.18, 0.15]) and described less than 1% of the variation in the data. Using the model with EWL, the mean time until total fat exhaustion for healthy *M. lucifugus* predicted in the hibernaculum microclimate conditions at our field site in Montana was 317.5 ± 105.50 days at a rate of 0.006 ± 0.002 g day^{-1}. Bats were predicted to survive for over 360 days in the microclimate selected for roosting (T_a = 4.8 °C, RH = 100%). The shortest time until fat exhaustion (176 days) was at the warmest temperature available in the hibernaculum (5.5 °C) and lowest humidity (90%). Almost all other available microclimate conditions within the hibernaculum (2 – 5 °C and > 90% RH) result in predicted hibernation duration greater than winter duration (181 days).

Our sensitivity analysis revealed that fat loss was influenced by host-specific parameters, including body mass, the proportions of body mass comprised of fat and lean mass, and parameters that influenced EWL, including wing surface area and the area-specific rates of cutaneous EWL (Figure 28). Model parameters that were most influential to survival were physical traits that vary both within and among species. There was little effect of metabolic rate during torpor or euthermia, nor time spent euthermic.
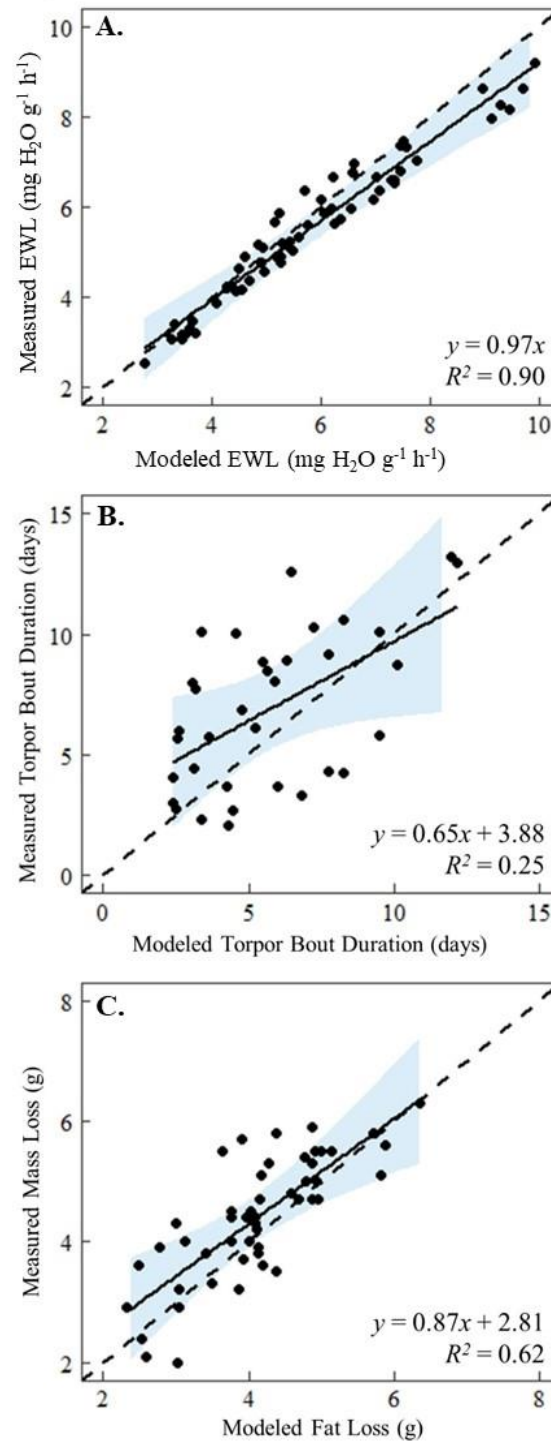
Figure 27. Comparison of measured and modeled a) evaporative water loss (EWL), b) torpor bout duration, and c) fat loss in *Myotis lucifugus*. EWL and fat loss were measured/modeled in healthy bats, while torpor bout duration was measured/modeled in bats that were inoculated with *Pseudogymnoascus destructans*. Dashed lines represent one-to-one line and solid lines represent fitted relationships with 95% confidence intervals (shaded blue).
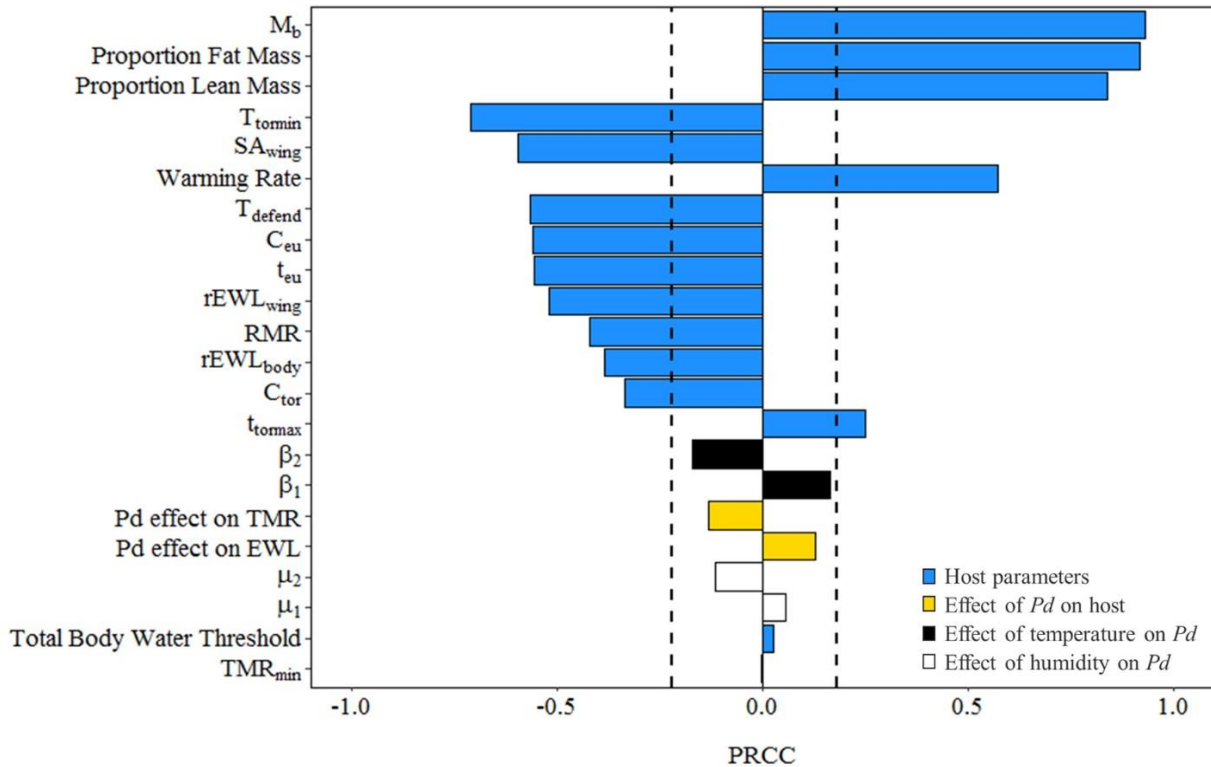
Figure 28. Sensitivity analyses for model calculating total fat exhaustion in hibernating bats infected with *Pseudogymnoascus destructans*. Dashed lines signify confidence intervals ($\alpha = 0.05$). Positive PRCC values indicate an increase in predicted time until total fat exhaustion with an increase in parameter value; negative values indicate a decrease in predicted time until fat exhaustion with an increase in parameter value.

We showed complete survival capacity (100% survival) in the entire microclimate space inhabited by healthy *M. lucifugus* in a cave system in central Montana (Figure 29). The shortest time until fat exhaustion (176 days) was at the warmest temperature available in the hibernaculum (5.5 °C) and lowest humidity (90%). Almost all other available microclimate conditions within the hibernaculum (2 – 5 °C and > 90% RH) result in predicted hibernation duration greater than winter duration (181 days). Unfortunately, these hibernaculum temperatures and predicted torpor bout durations are comparable to hibernacula inhabited by highly impacted *M. lucifugus* populations in WNS-affected regions. Our results reflect these trends, as almost all microclimate conditions available at our field site resulted in mortality for infected bats, and suggest that *M. lucifugus* within the Montana cave system would be highly impacted by WNS. Within the hibernaculum conditions available at our field site, we predicted a higher and more variable rate of fat loss (range: 0.006 – 0.32 g day^{-1}) for infected bats. However, our model predicts a small window of microclimate space that would allow for survival, where cooler temperatures and moderate humidity reduce fungal growth, resulting in longer torpor bout duration and decreased arousal frequency. These results are consistent with observations of WNS-affected bats roosting in colder temperatures compared to unaffected bats (Reeder et al. 2012; Storm et al. 2011).
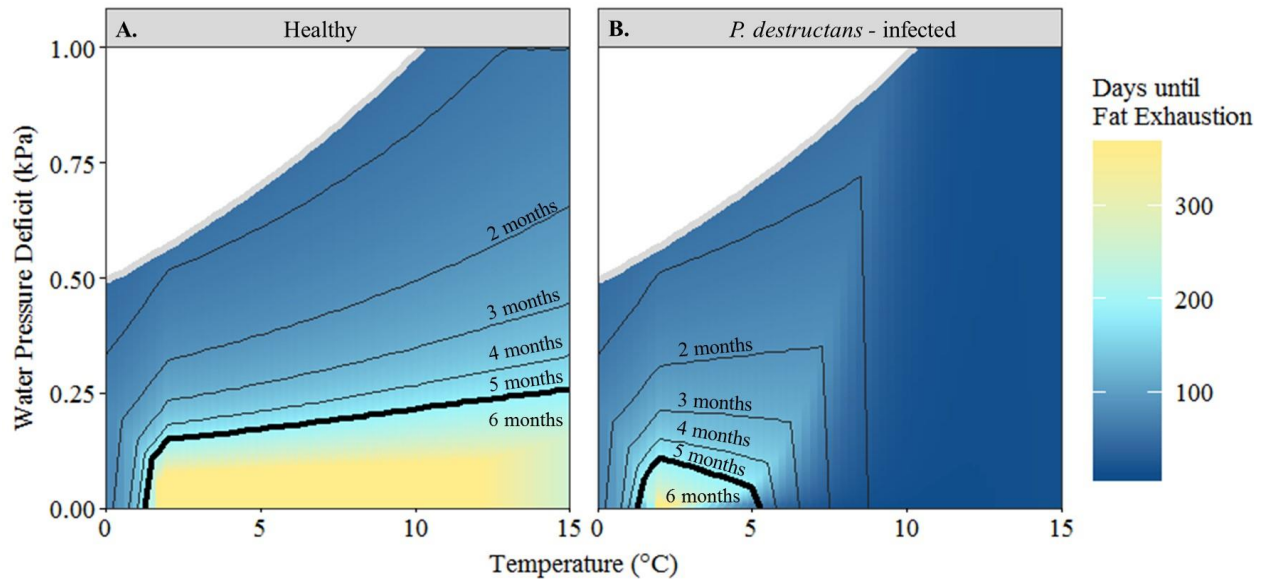
Figure 29. Predicted number of days until fat exhaustion for a) healthy b) *Pseudogymnoascus destructans* - infected little brown bats (*Myotis lucifugus*) over a range of hibernaculum temperature (°C) and water vapor deficit (kPa) values. Contours represent hibernaculum conditions that allow survival for specific winter duration (in months); dark black contour indicates six months, the estimated hibernation duration at our study site in central Montana. White area bounded by grey line represents impossible parameter space for each temperature (e.g. at 2 °C, air is saturated at 0.50 kPa and cannot hold more water).

Our model supports the role of EWL as a driver of periodic arousals in hibernation, and contributes to addressing one of the longest-standing questions in hibernation biology. It also showcases how interactions between host and pathogen physiology, and the environment can exacerbate or mitigate the costs of a disease. The model allows for species-specific parameterization and interspecific variation in morphometrics, physiology, and roosting habitats, suggesting that morphometric and physiological data from western bat species is needed. With this modified hibernation energetics model, we now have the tool to assess the potential impact of WNS on populations that have different hibernation behaviors than previously impacted species.

Inter-species WNS survivorship estimates

Our application of hibernation modeling to empirical field data allows for the estimation of survival from WNS across multiple species groups in varying hibernacula. We confirm our predictions that hibernaculum water vapor deficit and body mass are strong predictors of susceptibility to WNS. Species that are adapted to drier environments have higher survival than those that are adapted to surviving in hibernacula at or near saturation. Saturated conditions, though less energetically costly for healthy individuals, lead to greater fungal growth rates and thus higher mortality, which suggests a trade-off between water conservation and fat conservation in regards to WNS. There were species differences in survival during hibernation with WNS predicted at our sampling sites ($X^2 = 529.6$, df = 8, p-value < 0.001, critical difference = 117.53). There were no differences in survival between *M. velifer* and *E. fuscus* (observed difference = 90.10 days) nor *M. velifer* and *C. townsendii* (observed difference = 82.38 days). All three species survived winter with WNS for most, if not all, of the modeled environmental conditions (Figure 30). *E. fuscus* survived in all scenarios and contained enough fat to hibernate

for an additional 120 days in hibernation past the predicted spring emergence date. *M. velifer* and *C. townsendii* survived for most of the scenarios, but not all. Both species had enough fat to survive an additional month in hibernation, on average. There was no difference in survival among all small *Myotis* species, including *M. ciliolabrum, M. evotis*, *M. lucifugus*, *M. thysanodes*, and *M. volans*. These five species were not predicted to survive in most of the microclimate scenarios and model predictions showed mortality between 3 – 4 months of hibernation. *M. thysanodes* had high mortality, but was predicted to survive in some microclimate scenarios. *P. subflavus* had a wide range of survival across microclimate scenarios, but on average, did not have enough fat to survive hibernation. There were no patterns of differences in body mass, mass-specific torpid metabolic rate, mass-specific evaporative water loss, or hibernaculum microclimate, as we predicted.
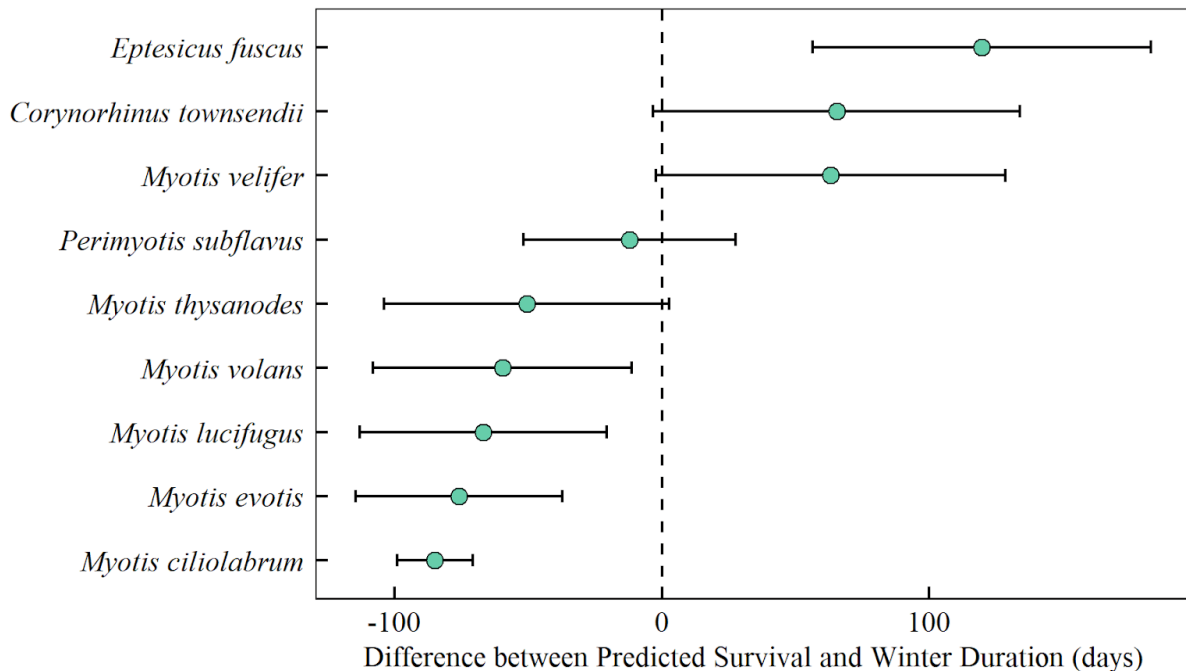
Figure 30. Difference between predicted days until fat exhaustion and predicted winter duration (with standard deviation error bars). All small *Myotis* species, including *M. ciliolabrum*, *M. evotis*, *M. lucifugus*, *M.thysanodes*, and *M. volans*, did not exhibit differences in predicted survival at our measured sampling sites. Additionally, *M. velifer* did not differ from *Corynorhinus townsendii* nor *Eptesicus fuscus* in predicted survival.

Hibernaculum temperature and water vapor deficit, mass-specific minimum torpid metabolic rate, mass-specific evaporative water loss, and body mass explained 58% of the variation in winter survival with WNS. Hibernaculum water vapor deficit explained more variation (9.0%) than mass-specific evaporative water loss (1.5%) and thus the model with water vapor deficit explained more overall variation in survival (adjusted $R^2 = 0.89$) compared to mass-specific evaporative water loss (adjusted $R^2 = 0.75$) (Figure 31). Body mass (p-value = 0.004) and hibernaculum water vapor deficit (p-value = 0.043) were the only significant predictors of the probability of survival through hibernation with WNS. When assessing each covariate alone, water vapor deficit (8.27%) and body mass (47.0%) explained over half of the variation in survival, while the other covariates explained less than 4%. According to the estimated parameter values, high humidity and smaller body mass resulted in decreased survival with WNS.
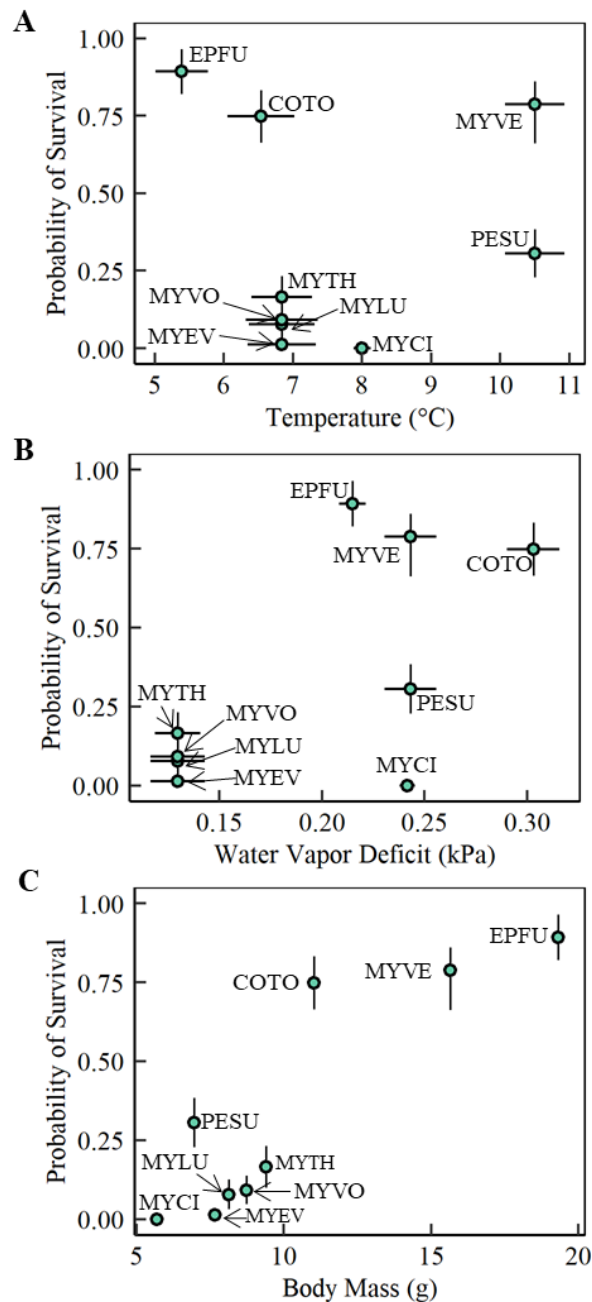
Figure 31. Predicted survival over hibernation with white-nose syndrome in response to a) hibernaculum temperature (°C), b) hibernaculum water vapor deficit (kPa), and c) body mass (g) of nine species: *Corynorhinus townsendii* (COTO), *Eptesicus fuscus* (EPFU), *Myotis ciliolabrum* (MYCI), *Myotis evotis* (MYEV), *Myotis lucifugus* (MYLU), *Myotis thysanodes* (MYTH), *Myotis velifer* (MYVE), *Myotis volans* (MYVO), and *Perimyotis subflavus* (PESU).

The relationship between predicted survival and hibernaculum water vapor deficit demonstrates how microclimate can mitigate WNS susceptibility. Our results are comparable to empirical studies which associate population declines with humid environments. Suboptimal environments

for fungal growth are potentially suboptimal environments for bat hibernation given bat physiology and behavior.

Insights on winter duration and spatial variation in hibernation survival
Hibernation duration
The acoustics dataset provided 34 observations for the duration of hibernation across western Canada. An additional seven observations were gleaned from literature and 11 research groups provided observations of hibernation duration for *M. lucifugus,* providing estimations at 49 unique locations (Figure 8, Appendix A8). The top model for hibernation duration included latitude (Northing), elevation (DEM), and the number of days in frost ($Days_{frost}$), but with only the latter two variables identified as significant terms. Residuals were not significantly correlated (Moran's I: -0.0036, p-value = 0.354) and no spatial corrections were needed. Given we were interested in prediction, we kept the model despite the non-significant, and co-linear terms. The selected model outperformed the original *a priori* estimate of the duration of winter (*Original*, ΔAIC 19.06; Hayman et al. 2016; Table 13). Median predicted hibernation duration was ~179 days (mean = 169.16, sd = 45.36). Maximum hibernation duration across the study extent was estimated at ~289 days in the upper portions of Manitoba, Ontario, and Quebec, 45 days longer than the longest observation in the training data (from Manitoba, Canada (Norquay and Willis 2014); Figure 32). Despite this 95% of all cells had a predicted hibernation duration below 225 days, and only 5% of cells predicted a duration below 80 days.
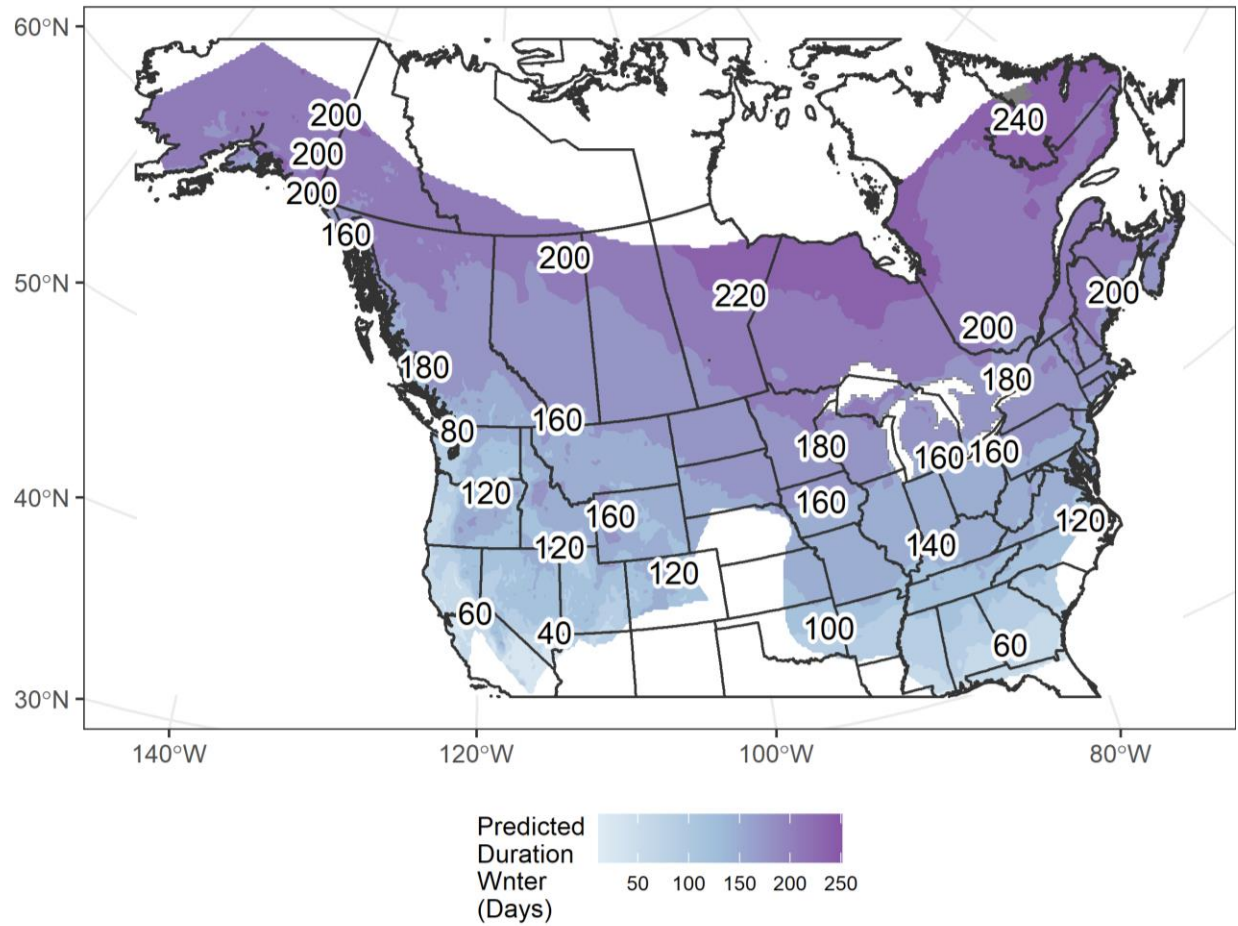
Figure 32. Predicted hibernation duration across temperate North America for *Myotis lucifugus*. Maximum hibernation duration (289 days) was predicted in the northern reaches of Manitoba, Ontario, and Quebec Canada. The central 95% of all values fell between 80 – 224 days.

Body mass

There was no statistical difference in pre-hibernation lean body mass between any of the populations sampled with the QMR as seen in Figure 33. As such, any spatial variation in body mass is likely due to differences in body fat. Pre-hibernation fat stores were strongly related to body mass (fat mass = -2.839 + 0.597 x body mass; $F_{1,171}$ = 826.7, p-value = < 0.001, adjusted R^2 = 0.8276; Figure 33).
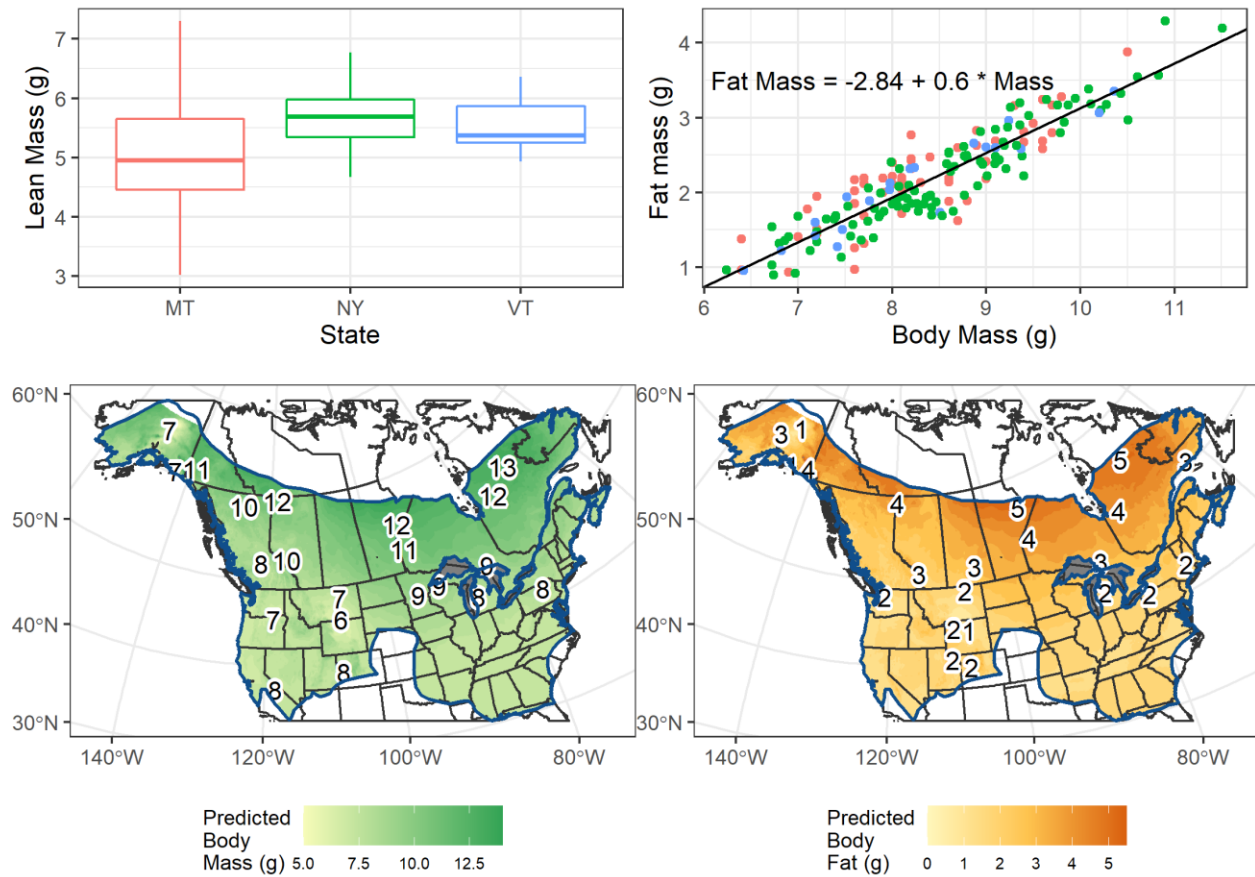
Figure 33. Body fat and mass data comparison for *Myotis lucifugus*. Top left: Comparison of lean body mass by state. Top right: Linear relationship between body fat and body mass. Each point represents an individual bat and colors indicate the state each record originated from. Bottom left: Predicted mass of *M. lucifugus* across the species' distribution. Bottom right: Predicted pre-hibernation body fat resources resulting from the application of the linear relationship between fat mass and body mass.

We obtained 47 observations of pre-hibernation body mass (Appendix A9) representing 43 unique cell locations and one outlier observation was removed from further analysis, leaving 42 locations. The top performing model included latitude (Northing) and the number of days below freezing (Days$_{freeze}$), although the model including latitude, number of annual days below freezing, and elevation performed similarly (ΔAIC < 2; Table 13). Across the distribution of *M. lucifugus*, the median predicted pre-hibernation body mass was 8.65 g (mean = 9.14 g, sd = 1.84 g) and 95% of the cells predicted values between 7.04 g – 12.52 g. Median pre-hibernation fat stores were predicted at 2.32 g (mean = 2.61 g, sd = 1.10 g) with 95% of cells predicting available fat available ranging between 1.36 g and 4.63 g.

Localized clines in body size and body mass of *M. lucifugus* have previously been recorded (Lacki et al. 2015; Lausen et al. 2008). However, when we compare more detailed metrics of body composition, lean mass, and body fat content, these clines are better understood: the lean mass of bats generally stays consistent while the difference in body mass is due to increases in fat. Our model selection suggests that variation in the duration of winter hibernation may in part drive variation in both body mass and fat stores across the range of the species. The relationships

between mass (and thus fat) and latitude and days below freezing also suggest stronger selection pressure for heavier bats in more extreme conditions. While still useful, the relationship between the selected abiotic variables and body mass of bats showed strong spatial autocorrelations among residuals, and there may be additional continental scale drivers or local determinants not investigated in this study.

The scaling relationship identified between pre-hibernation fat stores and body mass is a departure from the fixed 30% value used in previous energetic modeling studies (Hayman et al. 2016; Humphries et al. 2002), and is supported by contemporary findings (Cheng et al. 2019). More localized body mass – body fat relationships may exist, yet without increased data resolution, drivers of the true relationship will remain difficult to assess. Here we assumed bats did not forage during hibernation, but some bats (primarily from southern hibernacula) have been known to forage over winter (Thomas and Cloutier 1992). Without data, we were required to assume bats relied exclusively on pre-hibernation fat stores.

Table 13. Model selection by AIC for alternative spatial models. Terms included degrees of latitude North (Northing), elevation as represented by a digital elevation model (DEM), number of days in frost per year (Days$_{frost}$), number of days below freezing during a year (Days$_{freeze}$), the number of days outside of the growing season (Days$_{ngrow}$), and the original *a priori* estimate from Hayman et al. 2016 (*Original*). Best model values are underlined and is the difference between the respective model and the corresponding top model (underlined).

Covariate Structure	Hibernation Duration		Body Mass	
	AICc	ΔAIC	AICc	ΔAIC
DEM	523.01	33.72	172.73	10.16
Northing	515.44	26.16	172.24	9.67
Days$_{frost}$	490.02	0.73	164.22	1.66
Days$_{freeze}$	507.77	18.48	168.58	6.02
Days$_{ngrow}$	494.90	5.61	163.59	1.03
Original	508.35	19.06	167.46	4.89
Northing + DEM	514.68	25.39	174.67	12.11
Northing + Days$_{frost}$	491.46	2.18	166.65	4.08
Northing + Days$_{freeze}$	509.83	20.55	169.85	7.28
Northing + Days$_{ngrow}$	497.05	7.76	162.57	0.00
Northing + *Original*	510.36	21.07	167.97	5.40
Northing + DEM + Days$_{frost}$	489.29	0.00	164.78	2.21
Northing + DEM + Days$_{freeze}$	511.95	22.67	168.05	5.48
Northing + DEM + Days$_{ngrow}$	499.17	9.88	164.32	1.76
Northing + DEM + *Original*	512.59	23.30	167.63	5.07

Overwinter hibernation survival

Overall, our energetic model predicted nearly ubiquitous survival of uninfected bats throughout the range of *M. lucifugus* with < 0.0001% of cells falling below the threshold for survival. Our results found that 95% of all uninfected bats roosting at 4 ˚C and 98% relative humidity during hibernation would only require 0.21 – 0.60 g of fat to survive the duration of hibernation (median = 0.48, mean = 0.45 g, sd = 0.12). When considering the amount of fat that bats were taking into hibernation this meant that the median bat emerged with 1.85 g of body fat remaining (mean = 2.16 g, sd = 1.01 g) and the heaviest 95th percentile of bats had up to 4.05 g of fat remaining.

Considering these residual fat values in the terms of days spent in hibernation, the median bat would have sufficient fat resources to survive an additional 181 days (mean = 190.83 days, sd = 45.35 days) and those bats with < 4 g of fat remaining could be capable of surviving another 280 days in those optimal roosting conditions.

When *P. destructans* infection was included into the optimal roosting conditions, the median value of fat required to survive hibernation was increased by 0.72 g to 1.21 g (mean = 1.16 g, *sd* = 0.45) and the residual fat values dropped to a median of 1.22 g (mean = 1.45 g, sd = 0.76). In total 95% of bats were predicted to emerge with between 0.61 – 2.93 g of fat remaining after the duration of hibernation. Translating the fat values into days, the median value was reduced ~135 days to 45.63 days (mean = 55.41 days, sd = 45.35 days). Mortality of bats prior to the end of the hibernation period was predicted in 4.82% of the cells where the survival capacity of hibernating bats fell below zero and are visible in the northeastern provinces of Canada (Figure 34).
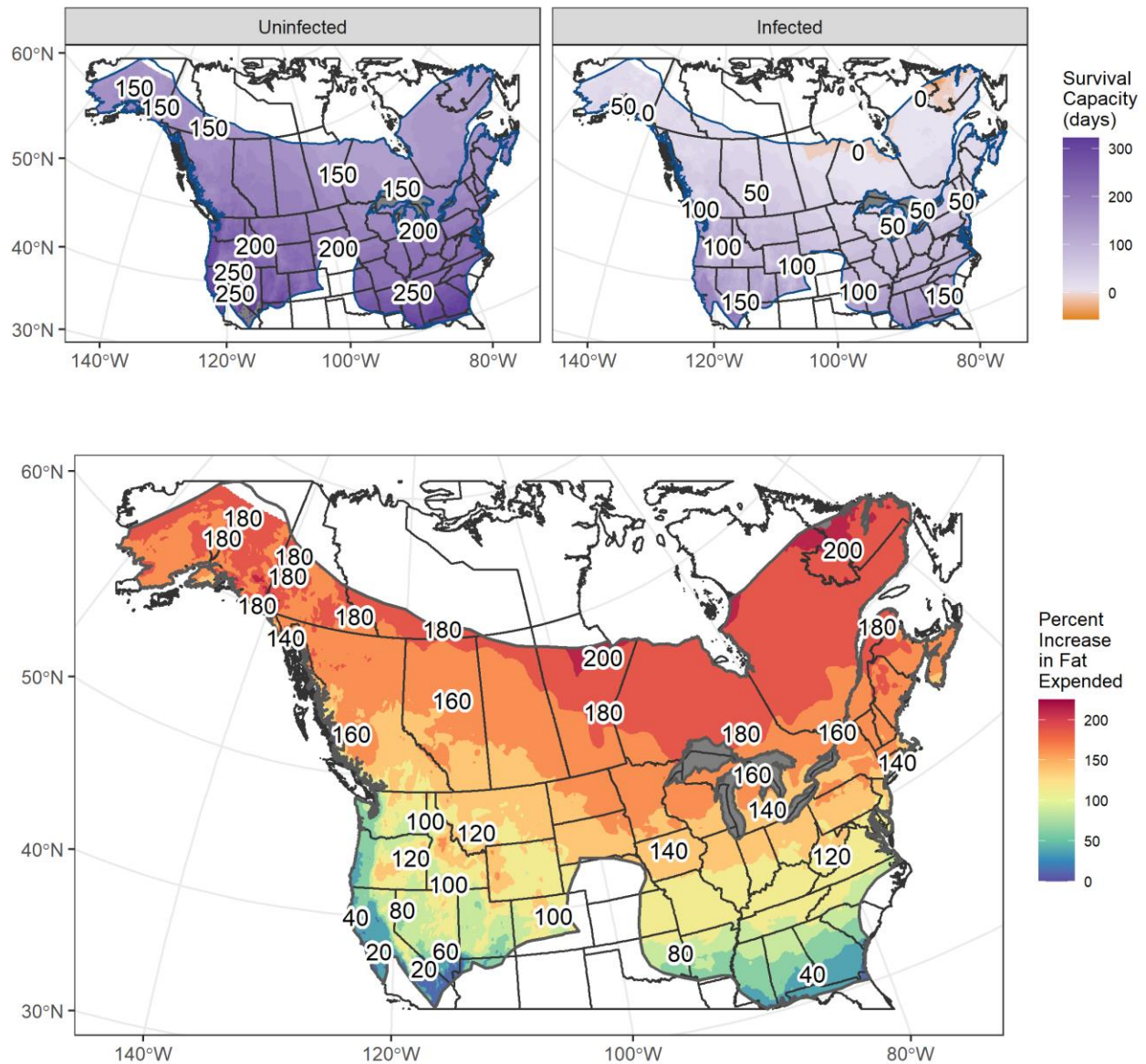
Figure 34. Top row: Predicted survival capacity for *Myotis lucifugus* hibernating at 4 ˚C and 98% relative humidity. Survival capacity (in days) is calculated by subtracting the maximal days in hibernation that an individual can tolerate based upon prehibernation fat stores from the predicted duration of winter. Positive values (purple) suggest that bats will likely survive the duration of hibernation under those conditions for the duration of winter while values below 0 imply that the fat stores were insufficient for survival. Uninfected bats are on the left, and bats infected with *Pseudogymnoascus destructans* are on the right. Bottom: Relative increase (%) in fat used over a predicted hibernation period when infected with *P. destructans* compared with healthy bats.

The majority of the predicted best available subterranean hibernacula were expected to have available temperatures at or above 4 °C. Despite this, 32.64% of cells fell below that temperature, and 6.44% of cells fell below the lower critical temperature of 2 °C that *M. lucifugus* defends during hibernation (Figure 35).
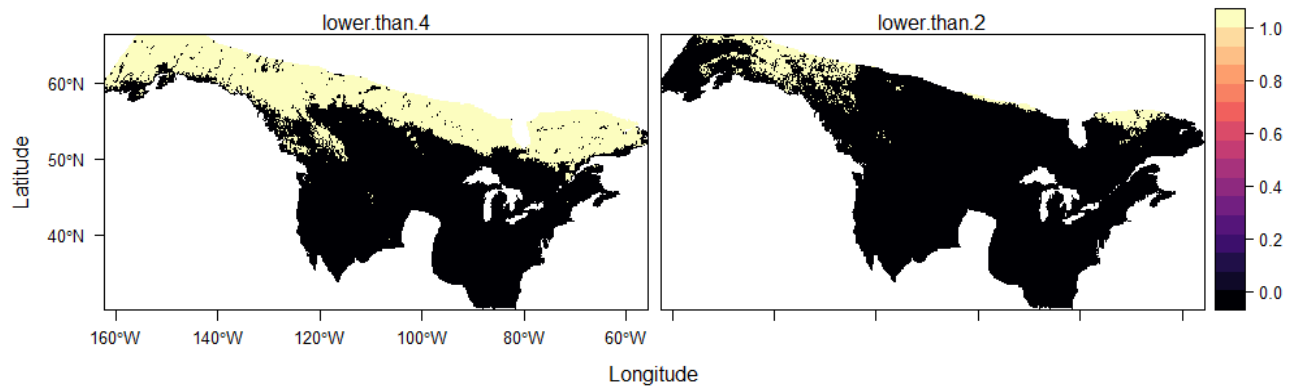
Figure 35. Predicted best available roosting temperatures. Left, yellow pixels indicate areas where the best available temperature is below 4 °C. Right, yellow pixels indicate where temperatures were predicted to be below 2 °C.

Despite these lower than optimal temperatures, *M. lucifugus* was predicted to survive across most of its distribution with only 0.5% of cells predicted to fall below the survival threshold, primarily around Denali National Park in Alaska. Median fat required to survive hibernation as an uninfected bat dropped 0.71 g to 1.11 g (mean = 1.41 g, sd = 0.93) with a nearly identical 95% interior range. When including infection with *P. destructans*, the hibernation energetics model predicted the median fat required for hibernation increased 0.72 g to 1.21 g, (mean = 1.20 g, sd = 0.40 g). Similar to optimal roosting conditions infection resulted in 4.74% of cells falling below the survival threshold, although the geographic distribution of where mortality is likely to occur was different as highlighted in Figure 36.
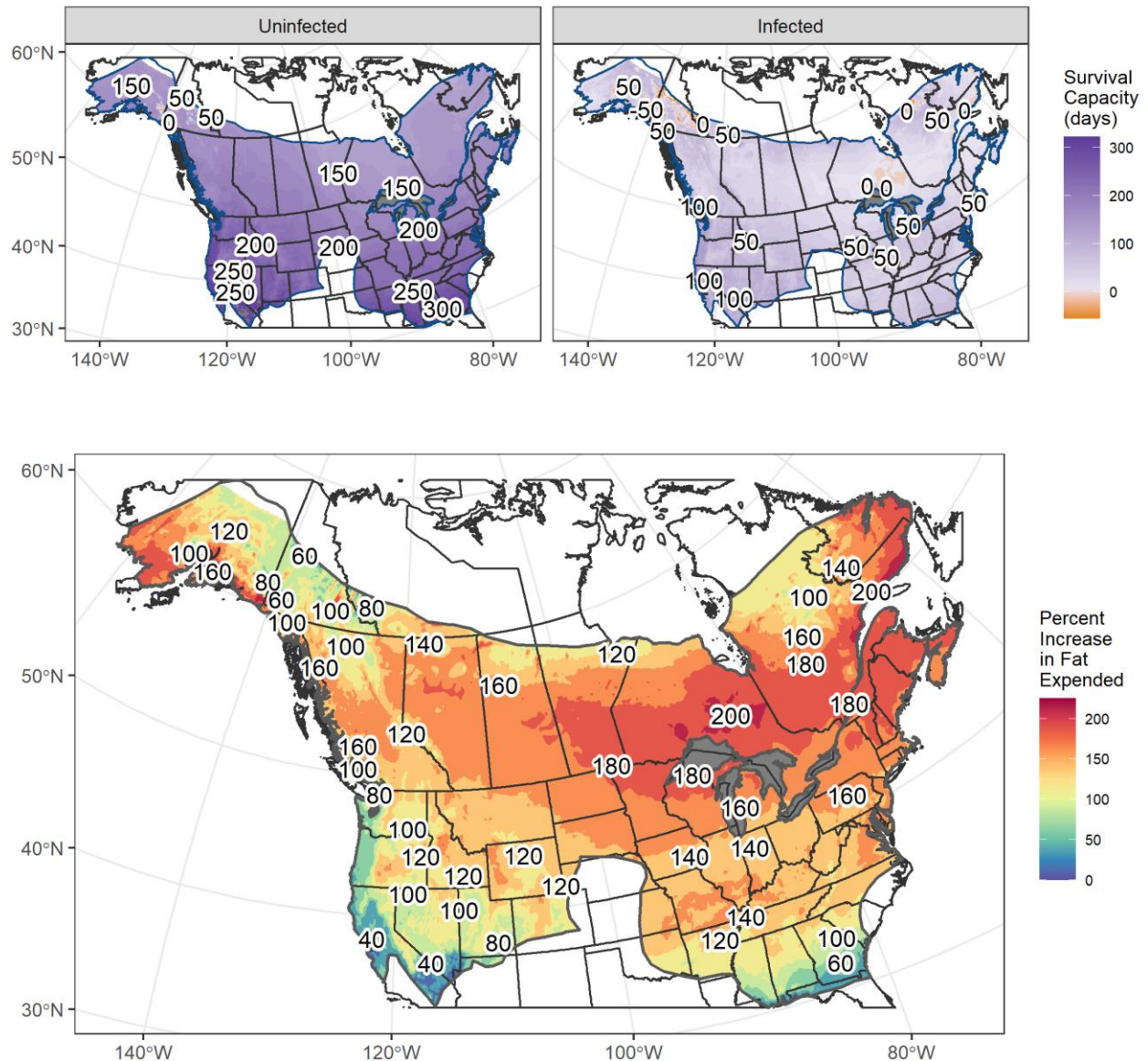
Figure 36. Top row: Predicted survival capacity for *Myotis lucifugus* hibernating at the best available temperature predicted to exist in caves or mines and 98% relative humidity. Survival capacity (in days) is calculated by subtracting the maximal days in hibernation that an individual can tolerate based upon pre-hibernation fat stores from the predicted duration of winter. Positive values (purple) suggest that bats will likely survive the duration of hibernation under those conditions for the duration of winter while values below 0 imply that the fat stores were insufficient for survival. Uninfected bats are on the left, and bats infected with *Pseudogymnoascus destructans* are on the right. Bottom: Relative increase (%) in fat stores used over a predicted hibernation period when infected with *P. destructans* compared with healthy bats when hibernating at the best available temperature predicted to occur within caves and mines and 98% relative humidity.

While neither of the considered hibernation conditions predict large areas to drop below the survival threshold, the increased percent of fat needed to hibernate with *P. destructans* highlights the metabolic consequences of infection. At 4 ˚C and 98% relative humidity, bats were predicted to expend a median of 154% more body fat resources to hibernate while infected for the same

duration of winter (Appendix A14). Overall, 95% of infected bats are predicted to increase their metabolic expenditure between ~66% and 195% compared to their healthy counterparts. Hibernating at the predicted best available temperature suggested similar increases in the energy expended, however again the geographic distribution of where the greatest increases occurred were different than those observed under static conditions.

Discussion on winter duration
Here we examined the spatial variation in hibernation duration across North America, created estimates of the fat stores bats take into the hibernation period, and applied an updated model of hibernation energetics (Haase et al. 2019b) to estimate the overwinter fat necessary for *M. lucifugus* to survive the duration of hibernation. By comparing the required fat and the fat available, we were able to predict survival of *M. lucifugus* across its distribution for two different ecological situations; one in which bats roost within their most preferred conditions, and one in which they roost in the best conditions predicted to be available. Finally, we modeled the possible impact of *P. destructans* infection, in particular to understand the implications for western *M. lucifugus* populations where bats have yet to be impacted by WNS.

Winter hibernation duration is a key determinant of the overwintering survival for any hibernating species. While local variation in winter onset due to unique landscape features may create refugia where bats may persist later than or emerge from hibernation earlier than average, the lack of any previous broad-scale estimates for this critical variable highlights the need for this study. Prior work (Hayman et al. 2016; Humphries et al. 2002) had defined the hibernation period *a priori* as the yearly number of nights with a mean nightly temperature below freezing. Our results suggest that substantial improvements in the estimation of hibernation duration can be made by including elevation, latitude, and the number of days with frost. The number of days of frost, rather than the number of days freezing, and the counter-intuitive negative coefficients for both Northing (-0.45) and DEM (-0.04) in the model suggest that there is more nuance to the relationship between bats and low temperatures than currently understood. Our model is potentially biased in part by the over-representation of Canadian data, low elevation sites, and the collinearity of elevation and latitude with other explanatory variables. Notably, however, when included in univariate models, the coefficient signs regress as expected with the coefficients increasing with latitude and elevation; yet the univariate models do not predict hibernation duration as well and had higher AIC scores. Because we were interested in prediction, we kept the best model by AIC, but clearly more work is required to understand what predicts overwinter duration in bats. Also, there were few estimates of hibernation duration from the western-most states and the more southern latitudes within the species' distribution. These factors likely impacted model results in unpredictable ways and highlights the need for additional data collection.

Species such as *M. lucifugus* may not hibernate across their broadest summer distribution, but likely rather seek out locations with more favorable conditions to overwinter. The maximum winter hibernation duration predicted within the IUCN distribution of *M. lucifugus* was a month and a half longer than the longest observation within our dataset and this did not consider the portion of the species' distribution that extended into the Arctic Circle. In all probability, bats likely do not overwinter within these regions for multiple reasons. First, while our survival models predict that an uninfected bat could survive the longest predicted hibernation winter

duration, the necessary roosting microclimate conditions may not exist on the landscape (McClure et al. 2020). A series of complex interactions between surface features (e.g., slope, aspect, elevation, suitable crevices) or cave features (e.g., number of entrances, air flow, depth) ultimately define when and where suitable hibernacula conditions exist for hibernation (Perry 2013; McClure et al. 2020). These site level determinants of microclimate conditions make it difficult to define a relationship between landscape-level features and the available subterranean conditions and create challenges in attempting to predict where suitable hibernacula conditions exist (Perry 2013; McClure et al. 2020). Despite this, our use of modeled subterranean temperatures offers an improvement over assuming either static optimal conditions or MAST used in Hayman et al. 2016. Second, and perhaps more importantly, regions where extended winters reduce the summer active period to < 100 days likely create significant challenges to reproductive success. With a gestation period of ~60 days (O'Farrrell and Studier 1973; Kurta et al. 1989), a female bat would be hard pressed to gestate, nurse, and wean young, while still allowing the young of the year time to fatten sufficiently to survive such an extended hibernation period. These results highlight the fact that only a subset of summer distributions may be suitable for overwinter survival, an idea rarely considered in the definition of bat species' distributions.

Localized clines in body size and body mass of *M. lucifugus* have previously been recorded (Lacki et al. 2015; Lausen et al. 2008). However, when we compare more detailed metrics of body composition, lean mass, and body fat content, these clines are better understood: the lean mass of bats generally stays consistent while the difference in body mass is due to increases in fat. Our model selection suggests that variation in the duration of winter hibernation may in part drive variation in both body mass and fat stores across the range of the species. The relationships between mass (and thus fat) and latitude and days below freezing also suggest stronger selection pressure for heavier bats in more extreme conditions. While still useful, the relationship between the selected abiotic variables and body mass of bats showed strong spatial autocorrelations among residuals, and there may be additional continental scale drivers or local determinants not investigated in this study.

The scaling relationship identified between pre-hibernation fat stores and body mass is a departure from the fixed 30% value used in previous energetic modeling studies (Hayman et al. 2016; Humphries et al. 2002), and is supported by contemporary findings (Cheng et al. 2019). More localized body mass – body fat relationships may exist, yet without increased data resolution, drivers of the true relationship will remain difficult to assess. Here we assumed bats did not forage during hibernation, but some bats (primarily from southern hibernacula) have been known to forage over winter (Thomas and Cloutier 1992). Without data, we were required to assume bats relied exclusively on pre-hibernation fat stores.

For our modelled roost conditions, virtually all uninfected *M. lucifugus* were capable of surviving the estimated duration of winter. Observed rates of survival among uninfected overwintering bats is high (Boyles and Brack 2009) and bats are likely capable of overwintering across most of their summer distribution where suitable hibernacula exist. These results are an improvement over previous models which did not predict survival where hibernation duration was greater than six months (Hayman et al. 2016) despite our prediction that some 51% of the study extent may experience winters longer than that. In previous models, roosting microclimatic space was derived exclusively from surface metrics (i.e., MAST and relative humidity). Our use

of a static, optimal roosting scenario served as a baseline for a best available temperature scenario which provided more biologically relevant conditions for *M. lucifugus* as bats have been known to preferentially roost in these conditions when available (Haase et al. 2019a; CLL, unpublished data; Thomas and Cloutier 1992). In areas where WNS has devastated hibernating colonies of *M. lucifugus*, available microclimates are often warmer with temperatures reaching 10 °C (Perry 2013), which has a significant impact on energy expenditure during hibernation (Figure 37). Despite this, our predictions for overwinter survival using estimates of the best roosting temperatures available suggest that survival may still be possible, provided that bats use the coldest areas within the cave or mine system. In a rare ray of hope, all of the hibernation temperatures that we recorded in the West were well below the 10 °C mark, with hibernating *M. lucifugus* in northeastern Alberta and Northwest Territories roosting at ~2°C and 100% relative humidity (CLL, unpublished data). While the high relative humidity is generally beneficial to the growth of *P. destructans* (and thereby a promoter of WNS pathology), the cooler temperatures may slow fungal growth in comparison to the warmer roosts of the eastern United States.
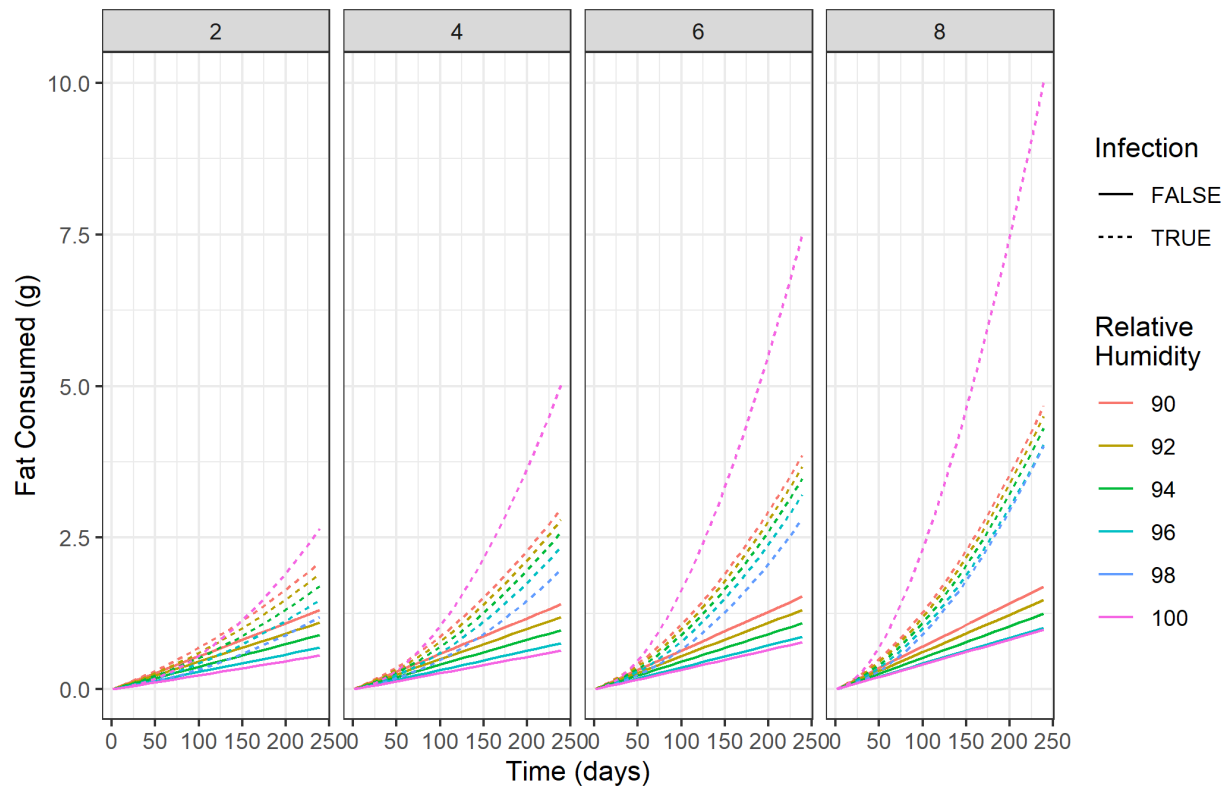
Figure 37. Rate of energy expenditure at various roosting conditions for *Myotis lucifugus*. Each panel is a unique temperature (°C), and relative humidity is depicted by line color. Infectious status is denoted by line type with solid lines representing uninfected bats and dashed lines represent bats infected with *Pseudogymnoascus destructans*.

Our model predicted uninfected bats to emerge from hibernation with remaining fat quantities far greater than the amount of fat thought to be needed to hibernate for the entire duration of winter. Some of this may be an artifact of our modeling, as we may be missing additional energetic costs such as flight during the arousal periods or sex-related differences, and we do not model deviance from the most optimal arousal patterns that can result from arousals of individuals sharing the hibernacula (neighbor-initiated arousals; Czenze et al. 2017; Hayman et al. 2017;

Jonasson and Willis 2012; Turner et al. 2015). Alternatively, remaining fat stores may be retained as a buffer against adverse abiotic conditions experienced after emergence, especially among females that undergo pregnancy immediately upon exit from hibernation (Czenze et al. 2017; Johnson et al. 2017) and whose reproductive success stands to benefit from a longer growing season. Early emergence would provide a selective advantage to the young of the year, as even one or two extra weeks foraging on the landscape could increase fat stores, making them more prepared for hibernation (Reynolds and Kunz 2000). As of yet, little is known about the energetic demands of the emergent bats as they return to the landscape, and accurate parameterization of this factor could significantly change our definition of survival capacity and increase our estimates of WNS-related mortality.

Modeled hibernation survival predictions of bats infected with *P. destructans* at either 4 ˚C and 98% relative humidity or using the best available temperature do not match observations from the eastern United States where mass mortality events have occurred due to WNS (Blehert et al. 2009; Frick et al. 2010, 2015). While our analysis did demonstrate infection with *P. destructans* dramatically increases the amount of energy expended during hibernation, nearly 95% of all cells analyzed predicted survival despite infection. Interestingly, however, the areas with the greatest increase in hibernation energy expenditure using the best available temperature were much more in line with regions where bat populations have experienced the greatest mortality.

Irrespective of the absolute values for survival predicted within this work, our modeling predicts that western *M. lucifugus* populations, especially those along the Rocky Mountains, Alberta, British Columbia, and Alaska will require similar increases in energetic expenditure when affected by WNS as the eastern populations. Thereby, if the increase in energy expenditure results in the same pattern of mortality, *M. lucifugus* populations in the West may be expected to suffer mortality events similar to those experienced in eastern populations (Frick et al. 2010, 2015). The long duration winters, especially in northern British Columbia, northern Alberta, Alaska, Yukon, Northwest Territories, and portions of the Rocky Mountains, may result in severe WNS-associated pathology and disruption to hibernation physiology, although use of cool available hibernacula microclimates in some of these areas may slow fungal growth (Reeder et al. 2012; Verant et al. 2014); identifying and describing roosting microclimates in these areas will allow for better predictive models at a regional scale. Some northern hibernacula may provide a refugia for *M. lucifugus* infected with WNS, but to better determine this, microclimate availability needs to be known, and spring energy requirements quantified. For example, if gleaning of arthropod prey in spring is typically required for successful reproduction in northern latitude *M. lucifugus* (Kaupas and Barclay 2018; Talerico, 2008), then this extra energy expenditure associated with gleaning (Norberg and Rayner 1987) may require additional fat stores and WNS-related mortality rate may in fact be higher than predicted. Additionally, even if WNS related mortality is not directly observed, reproductive success may decline resulting in more long-term population decline.

The outputs of the energetic model that we applied are sensitive to a number of parameters and assumptions (Haase et al. 2019b). The hibernation energetic model is largely derived from first principles and deviations in parameters, especially those defining the frequency or duration of arousal (cluster-based arousal, partial arousals, disturbances, etc. Carey 1993) or increasing these costs (e.g. increased number of mid-winter flights or disease pathophysiology), have the potential to alter the amount of resources required to survive hibernation. Roost microclimates

are important to survival predictions and impact bat energetic and fungal growth dynamics (Marroquin et al. 2017), and further study is required to understand how relative humidity may vary across the landscape and within hibernacula. Additionally, western bats hibernate differently than eastern populations with more solitary hibernators as opposed to the large hibernation colonies that were frequent in the East prior to the arrival of WNS (Langwig et al. 2012; Speakman and Thomas 2003). Arousals account for > 90% of total energy expended during the hibernation period, and the lower probability of neighbor-initiated arousals in the West may play a significant role in reducing the disruption of hibernation physiology among western populations (Czenze et al. 2013).

Overall, this work represents an effort to iteratively refine both individual and landscape models of bat hibernation physiology and the impacts of WNS on bat populations. By specifically addressing the spatial heterogeneity of both abiotic phenomena and host traits, we offer some of the most detailed predictions for the potential impacts of WNS on *M. lucifugus* as *P. destructans* continues to spread through western North America.

Cave and mine microclimate estimation
Surface-subterranean temperature relationships
The final inferential model is summarized in Table 14. Elevation and snowpack were dropped from the model due to high collinearity with MAST. MAST and distance from site entrance were the most important predictors of subterranean temperatures, followed by whether the site was a cave or a mine. As predicted, we observed a positive relationship between MAST and subterranean temperature, such that an increase of 1 standard deviation (2.82 °C) in MAST corresponded to a 1.67 °C increase in subterranean temperature (95% CI: 0.785 – 2.55). Similarly, subterranean temperatures increased with distance from site entrances, such that an increase of 1 standard deviation (53.4 m) in distance from the site entrance corresponded to a 1.62 °C increase in temperature (95% CI: 1.16 – 2.08). However, these positive effects of MAST and distance from site entrance on subterranean temperature were not strictly additive, as suggested by a negative interaction term (-0.32 °C; 95% CI: -0.970 – 0.327), though the confidence interval on this estimate did include zero. After controlling for these influences, mines tended to be warmer than caves (by 3.08 °C; 95% CI: 1.22 – 4.94). Other landscape predictors, such as elevation, topographic position, and solar insolation, had less discernible effects on subterranean cave temperatures as evidenced by lower variable importance, smaller standardized coefficients, and confidence intervals that spanned zero.

Table 14. Summary of the inferential model, including model-averaged coefficient estimates (on standardized scale), unconditional standard errors (SE), 95% confidence intervals (CI), and cumulative AIC weights for predictors used to estimate subterranean temperatures.

Parameter	Estimate	SE	95% CI		AIC weight
Intercept	2.75	0.612	1.555	3.955	--
Distance from entrance	1.62	0.236	1.159	2.083	1.00
MAST	1.67	0.451	0.785	2.553	1.00
Site Type (Mine)	3.08	0.949	1.216	4.936	1.00
MAST * Distance from entrance	-0.32	0.331	-0.970	0.327	0.64
Solar Insolation	0.14	0.316	-0.478	0.761	0.36
Snow Days	0.18	0.407	-0.619	0.975	0.35

Percent Tree	-0.09	0.285	-0.646	0.470	0.30
Multiscale TPI	0.10	0.301	-0.490	0.691	0.30
Groundwater Depth	-0.07	0.297	-0.657	0.508	0.28

ANOVA model comparisons indicated that inclusion of random intercept terms for loggers nested within sites, as well as distance from entrance as a covariance parameter, was warranted (Table 15). This parameter's coefficient, estimated as -0.614 in the top-ranked model, indicated that as predicted, variance in observed subterranean temperature decreased with increasing distance from site entrances. The top-ranked model was 56.8 AIC units better (i.e., lower) than a null model containing random intercept terms for loggers nested within sites and exponential covariance structure, but was 86022.6 AIC units better than a null model with no random effects or covariance structure. These results suggest that the fixed effects of MAST, distance from site entrance, and other site characteristics approximated the data well; however, explicitly accounting for residual spatial structure in the data dramatically improved model performance.

Table 15. Results of ANOVA model comparisons assessing the need for inclusion of random intercepts and covariance structure.

Comparison	Purpose	dAIC	likelihood ratio	p-value
fixed + **random effects** *vs.* fixed effects	Test need for random effects	46472.0	46476.0	<0.0001
fixed + random effects + **covariance structure** *vs.* fixed + random effects	Test need for covariance structure	26718.1	26720.1	<0.0001
fixed + random effects + covariance structure *vs.* null model	Test overall model performance	86022.6	86036.6	<0.0001
fixed + random effects + covariance structure *vs.* random effects + covariance structure	Test contribution of fixed effects	56.8	64.8	<0.0001

Mapping predicted available temperature ranges
By applying the inferential model to predictor values at each 1-km raster cell across western North America, we mapped mean winter temperatures predicted to be available in caves and mines if such features exist at any given site, at distances of 10 m and 100 m from site entrances as bracketing examples (Figure 38); species tolerant of temperature fluctuations can be found as close as 10 m to site entrances (e.g., *C. townsendii*; C. Lausen, *pers. comm.*), whereas 100 m is representative of the stable dark zone selected by many species for hibernation (McClure et al. Forthcoming). We also mapped MAST across the same extent for comparison (Figure 38 e). These maps reiterate that predicted mine temperatures are warmer than predicted cave temperatures at a given distance from the site entrance and that for a given site type (cave or mine), temperatures were warmer with increasing distance from site entrance. We also show that modeled temperatures were more moderate than MAST; they were warmer than MAST in cold regions, and colder than MAST in warm regions.

113
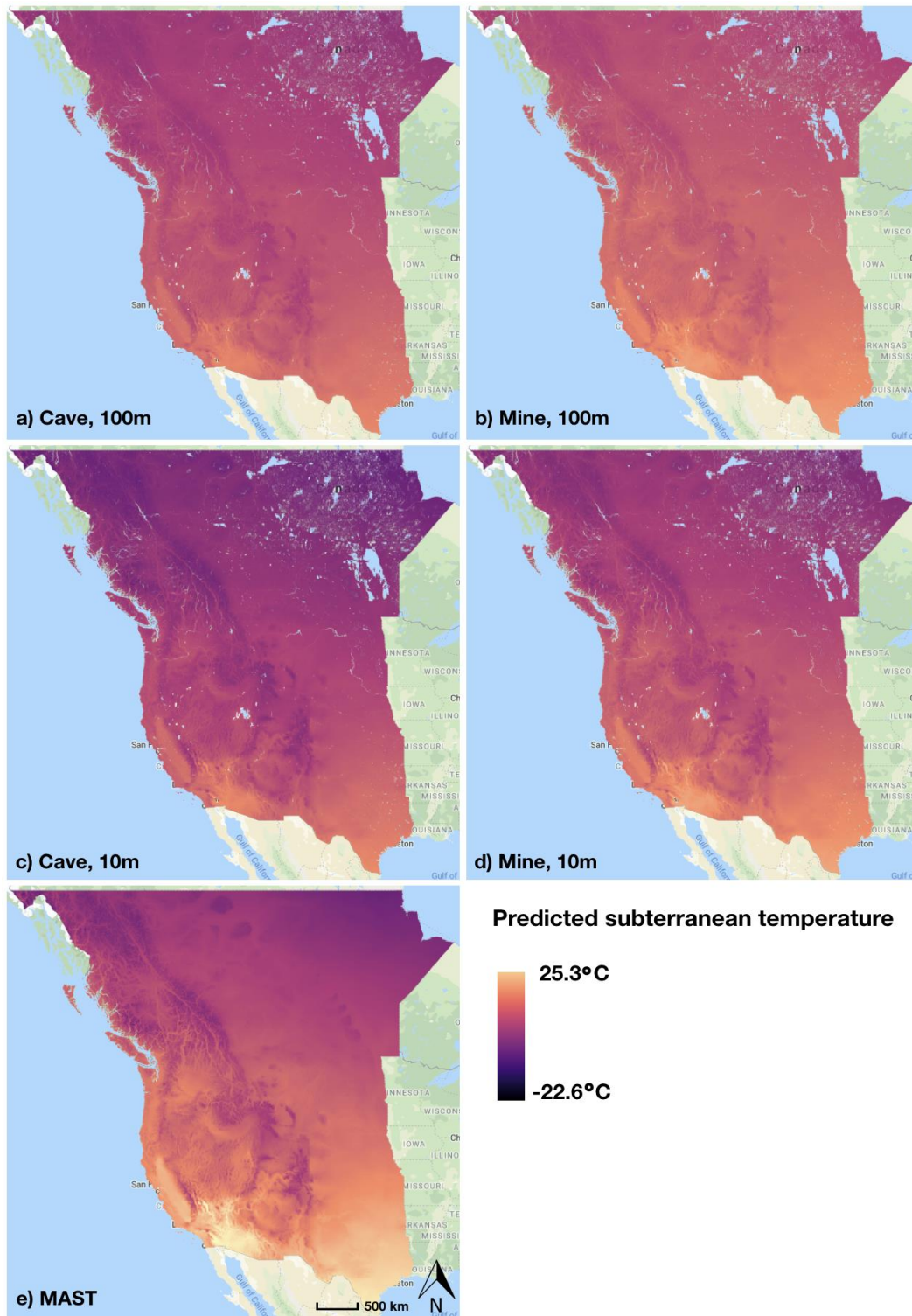
Figure 38. Maps of model-predicted subterranean temperatures 100 m into a) caves and b) mines; 10 m into c) caves and d) mines; and predicted by e) MAST alone.

To relate these maps back to vespertilionid bat hibernation, we masked areas where mean temperatures of 2 – 10 °C are not predicted to be found anywhere between 50 m and 100 m from

the site entrance (where bats other than *C. townsendii* typically hibernate; C. Lausen, *pers. comm.*), again comparing these 'hibernation-suitable windows' to those predicted based solely on MAST (Figure 39). We show considerably broader windows of potentially suitable hibernation conditions using our model of subterranean temperature compared to that approximated by MAST. Notably, our model more frequently predicts suitable conditions at known hibernacula in Alberta and Texas that MAST alone would predict to be unsuitable (Figure 40). Similarly, our model consistently predicts conditions within and centered on the range of hibernaculum temperatures tolerated by *M. lucifugus* as reported in the literature at sites where *M. lucifugus* has been observed in winter (Figure 41; Tables 4 – 5).
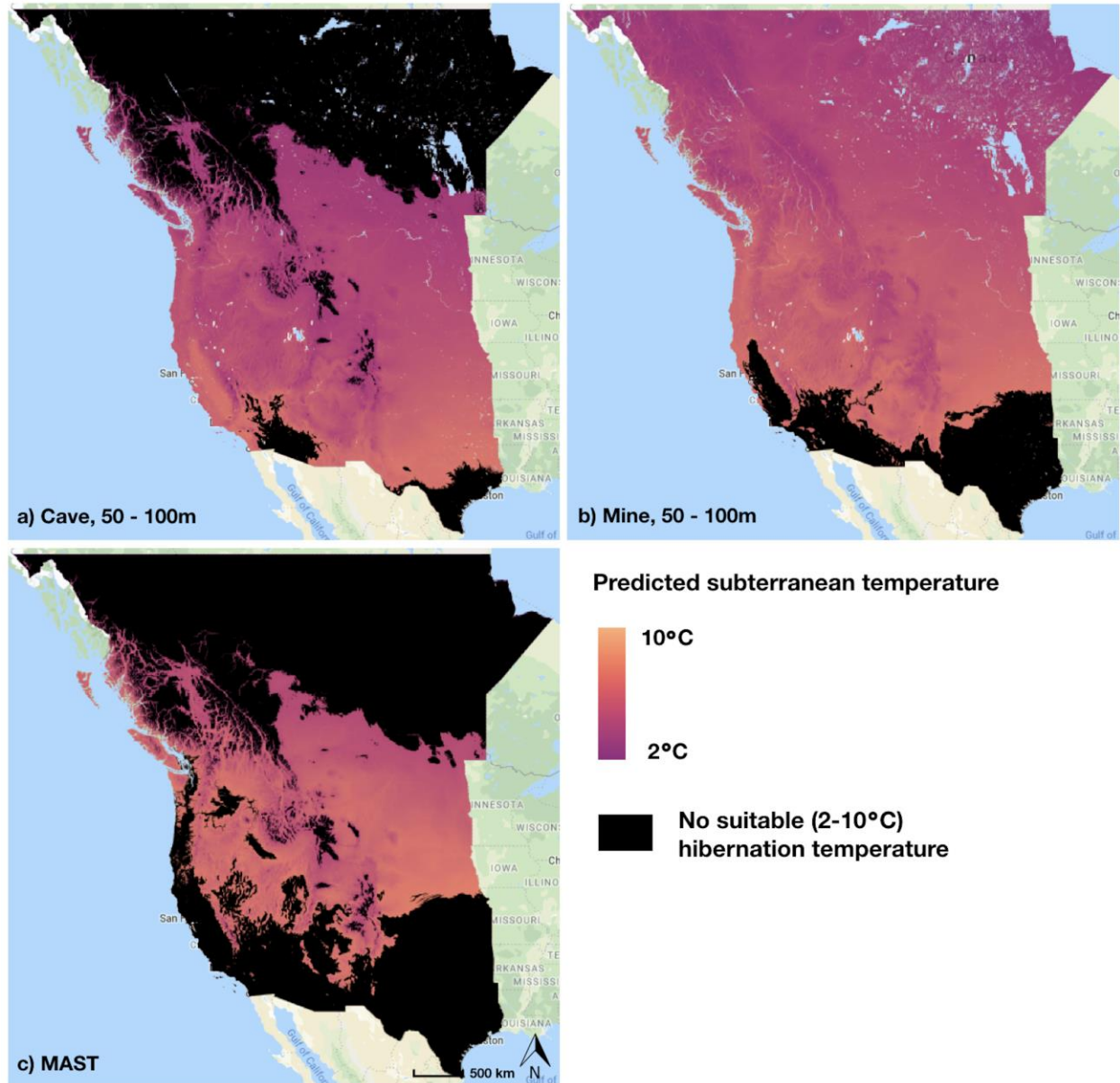
Figure 39. Model-predicted windows of hibernation-suitable temperatures ($2 - 10\ °C$) for a) caves ($50 - 100$ m) and b) mines ($50 - 100$ m), and predicted by c) MAST alone. These maps illustrate the performance of the models compared to MAST alone. Parameterizing the model with species- or guild-specific hibernation information provides an estimate of region-wide potential suitability of hibernaculum conditions under present or future climate.

115
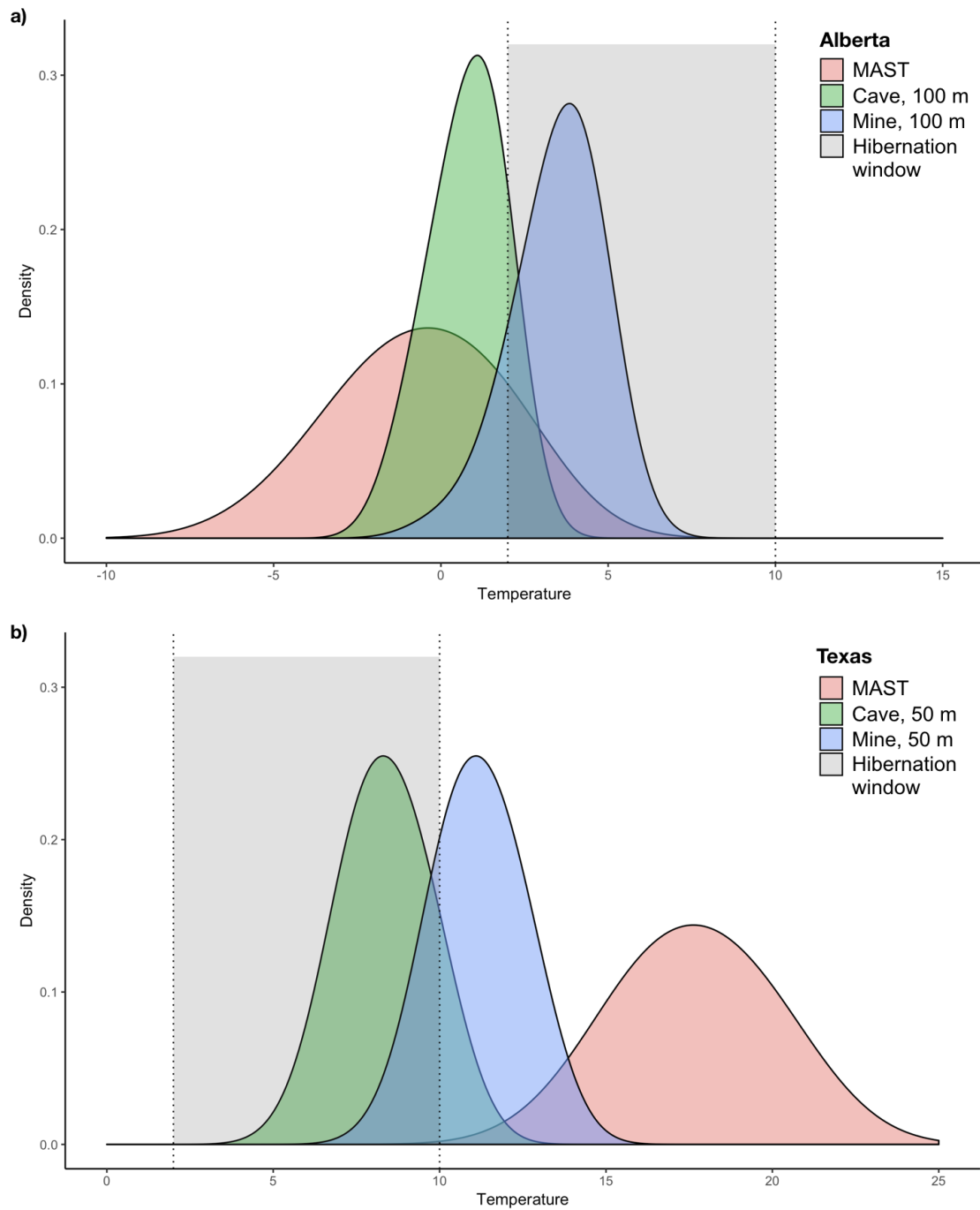
Figure 40. Density of model-predicted temperatures for caves (green) and mines (blue) and MAST (pink) at known hibernacula in a) Alberta and b) Texas. The estimated range of suitable hibernation temperatures for most vespertilionid bats $(2 - 10°C)$ is shown in gray.
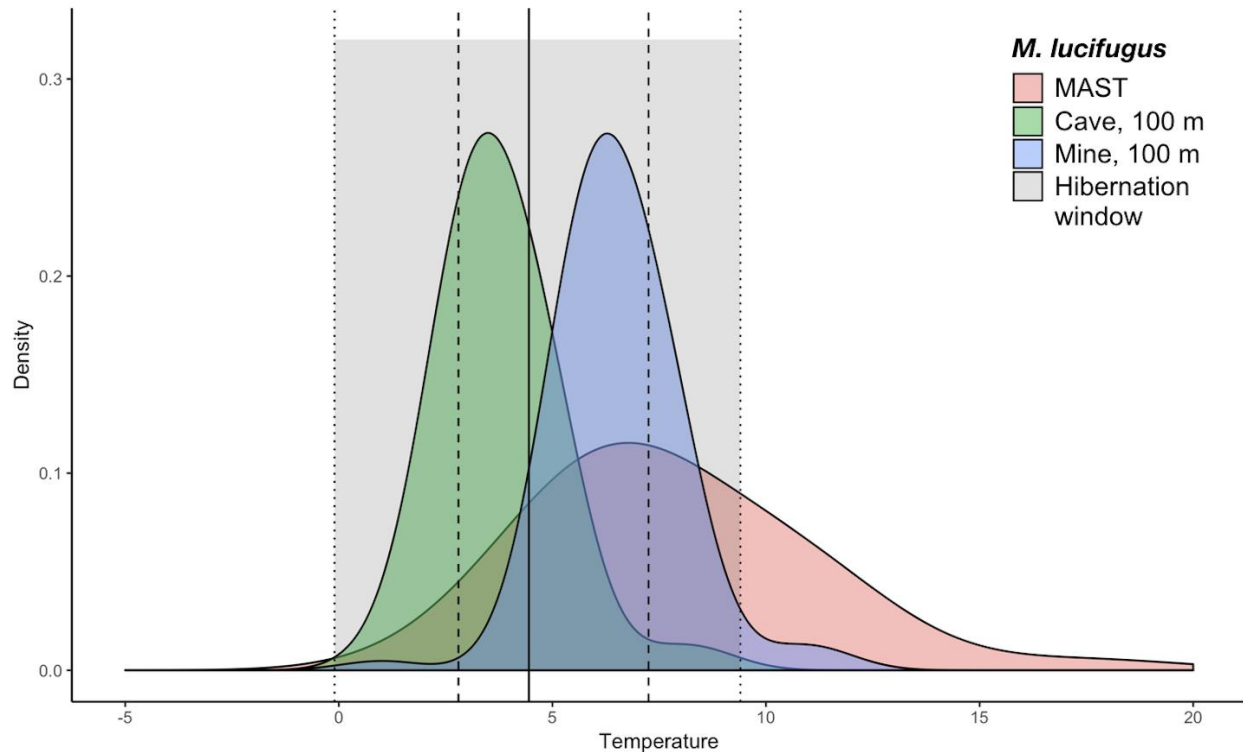
Figure 41. Density of model-predicted temperatures for caves (green) and mines (blue) and MAST (pink) at winter occurrence locations of *Myotis lucifugus*. The range of hibernation temperatures tolerated by *M. lucifugus* estimated from published literature is shown in gray, along with the median of the distribution (solid line) and interquartile range (dashed lines).

Discussion of cave and microclimate estimation

The central aim of this study was to quantitatively test the qualitative relationships between subterranean temperature, MAST, and site attributes presented by Perry (2013), using what is to our knowledge the largest set of available cave microclimate data compiled to date. We confirmed that although MAST is a strong determinant of subterranean temperature, MAST alone is a fairly poor direct proxy for ambient temperature of caves and mines. Caves, in particular, tended to be colder in winter than MAST would suggest, and temperatures deviated more from MAST as one approaches cave and mine entrances, becoming both colder and more variable. This has important implications when estimating the conditions likely to be experienced by hibernating bats in a given location. MAST is often used as a proxy for subterranean temperature in the absence of ground-based data (e.g., Grieneisen 2011; Hayman et al. 2016). Our results demonstrate that better estimates of ambient subterranean temperatures can be made by accounting for site type (cave vs. mine), distance from site entrance, and other landscape attributes that tend to drive subterranean temperatures below MAST. This holds despite inescapable variability around predicted means due to aspects of site configuration, such as number of entrances that would modulate airflow, that could not be accounted for here.

Many site attributes discussed by Perry (2013) had little or no detectable effect on cave and mine temperatures in our compiled dataset. Our failure to detect these relationships may have been due to any effects of surface-level landscape attributes (i.e., topography, vegetation, snow cover) dampening with greater distances from site entrances. Our ability to detect these relationships may also have been obscured by noise in the data resulting from the coarse resolution of

remotely-sensed metrics (i.e., 30-m to 1-km) and/or spatial error in reported site locations, although any such noise is likely minimal relative to real variation in subterranean temperatures within and among sites. This natural variability is likely driven by variability in site configuration attributes (e.g., cave size, number and orientation of entrances, placement of loggers on walls vs. in crevices) that were generally not recorded or reported in the datasets available to us.

Our analysis focused on estimation of subterranean temperature, but temperature is only one determinant of suitable subterranean conditions. It has been widely hypothesized that hibernaculum humidity impacts the hibernation physiology of bats (Willis et al. 2011; McGuire et al. 2017), as well as habitat suitability for other subterranean species. Thus, a location that exhibits a suitable temperature regime may not be usable for some bat species that require high humidity to hibernate normally, which includes numerous species under threat from WNS (Langwig et al. 2012). However, it is likely that hibernating bats adaptively use high-humidity micro-refugia inside hibernacula (e.g., crevices, blind adits) to avoid otherwise excessively dry conditions, thereby increasing the suitability of a site through fine-scale selection of structure and substrate. Hibernacula that contain water, whether standing, flowing, or seeping, are also more likely to offer sufficiently humid conditions. Humidity is also a critical determinant of suitable conditions for growth of *P. destructans* (Marroquin et al. 2017) and the severity of its physiological effects on hibernating bats (Cryan et al. 2010). Consequently, it is important for future monitoring efforts to reliably record humidity and for future analyses to estimate how subterranean humidity may vary with surface conditions and site attributes as the present study has done for temperature, although this may prove an unavoidably difficult task as current loggers saturate and fail in the high-humidity conditions of most hibernacula.

Our model enables prediction of mean ambient winter temperature expected to be available at any given location and distance into a cave or mine, should such a feature exist. Together with knowledge about the locations and conditions within hibernacula that bats tend to select, we can approximate the mean conditions experienced during hibernation and where suitable conditions are likely to occur. However, we do not recommend application of the model at the individual site level. Given the limited nature of the available data, the model is intended for use in understanding general patterns and predicting over broad geographic extents. Although the model outperforms MAST alone for predicting ambient hibernaculum temperatures, it remains a coarse estimate that should be treated as a hypothesis to be further tested and refined as additional data become available. Cave microclimates are complex over space and time, as is selection of microclimate conditions by bats during hibernation. Cave and mine attributes, such as the number and orientation of entrances, amount of airflow, whether the site includes refugia from microclimatic variation (e.g., rock crevices or blind adits), as well as how hibernating animals dynamically use these features (i.e., by moving among different locations within a hibernaculum throughout the winter) will influence the suitability of a site on a finer scale than our model can resolve. Some bat species (e.g., *M. lucifugus*) require hibernacula with highly stable microclimates (Thomas and Cloutier 1992), whereas other species (e.g., *E. fuscus*) tolerate a wider range of or more variable microclimates (Klüg-Baerwald and Brigham 2017). Intra-specific temperature preference and tolerance may vary geographically (Klüg-Baerwald and Brigham 2017) and may also depend on whether hibernating bats are solitary or clustered (Langwig et al. 2012; Boratyński et al. 2015). These factors may contribute to selection of

hibernacula depending more on the specific morphology of the site that governs temperature variability than on average ambient temperature.

Despite these considerations, we suggest that our approach is the best available given the data, offering a clear improvement over MAST as a simple proxy for understanding the relationship between surface and subterranean conditions at this scale. Furthermore, our model's ability to predict a range of mean available temperatures over a range of distances from site entrances may more reasonably capture the range of temperatures resulting from the complexity described above in habitat selection and hibernaculum use than MAST alone. MAST has been used widely as a proxy for subterranean temperature, e.g., to estimate susceptibility of *M. lucifugus* to WNS (Grieneisen 2011) and to predict duration of winter survivorship given species-specific physiology and exposure to WNS (Hayman et al. 2016). Our model offers a refinement to this generalization that we suggest can improve inference and prediction in similar future studies. We also suggest that the more feasible hibernaculum temperatures predicted by our model can aid prediction of species occurrence in a given region should a sufficiently deep cave or mine exist. Our model may also be applied to smaller, shallower features used by some species as hibernacula (e.g., crevices and depressions) by assuming a minimal distance from site entrance, though results of this application should be interpreted with caution because the model was not informed by data from these types of features. Although predicted hibernation-suitable windows (e.g., Figure 39) are likely to be geographically broad for many species, these could be further refined by, e.g., karst, known mine locations, or other landscape attributes of known importance to a focal species to help target survey and monitoring efforts for potential hibernacula.

We strongly recommend that future monitoring efforts and field studies of subterranean microclimate record not only temperature and humidity at multiple sites and at multiple positions within a given cave or mine, but also record site attributes (e.g., distance from entrance, number of entrances, presence of water, airflow, etc.) in a standardized manner. This would enable future analyses to improve understanding of surface-subterranean relationships and to more fully account for the influence of site characteristics when estimating microclimate conditions. Spatial predictions of suitable hibernaculum conditions would also be improved by integrating both temperature and humidity and their relationships with surface conditions and site attributes. In turn, the combination of estimated temperature and humidity ranges for a given potential hibernaculum would better support prediction of *P. destructans* impacts on the bat species that may occur there. And although the present study has focused on estimating hibernaculum conditions for bats, we expect this information to have important applications to other cave fauna that are poorly understood and far understudied relative to bats but that may be highly dependent on particular subterranean conditions to persist (Mammola et al. 2019).

Our study offers an improved understanding of the determinants of subterranean climate and an improved ability to predict subterranean temperatures. We suggest that further refinement can be achieved by more standardized collection of cave and mine attribute data that may influence subterranean climate, and that similar assessments of patterns in humidity are needed to more fully understand and predict subterranean conditions for cave dwelling organisms. This information has the potential to improve understanding of the distributions and unique habitat needs of not only hibernating bats, but also a variety of poorly studied cave-obligate species, many of which are rare and endemic. Furthermore, we suggest that a quantitative understanding

of the link between surface and subterranean climate can help researchers and managers to better anticipate and plan for the impacts of future climate change on subterranean environments and the species they support, as well as how changes in climate may impact disease spread (see section 'Impacts of climate change on bats and WNS'). Although we have focused on the importance of subterranean climate for bat hibernaculum suitability in western North America, with implications for the severity of WNS impacts as the disease spreads through this region, our approach and findings are applicable to subterranean environments in other temperate regions and to the wide range of organisms that depend on them.

Bat species distribution models
After filtering the compiled dataset to unique winter locations, an average of 240 presence locations per species (range: 72 – 450) were available to fit SDMs (Table 6; McClure et al. In Review). Of the neighborhood sizes compared, moderate to large neighborhoods (5-km, 25-km diameter) tended to capture the scale at which bats responded to landscape attributes better than a small neighborhood (500-m), but scale of selection for each attribute varied among species (Appendix A16). Sampling landscape predictors at finer resolution (1-km) tended to produce stronger relationships with bat occurrence than coarse-resolution sampling (10-km), and the tendency for each predictor to perform best at either a fine or coarse sampling resolution was fairly consistent across species (Appendix A16).

Optimal BRT parameters varied among species, but higher tree complexity (4 – 5) and higher bag fractions (0.6 – 0.7) were favored (Table 16). Model performance was fairly similar across species, with a mean of 54.7 – 74.4% of the total deviance in the training data explained and predictive deviance of 0.753 – 0.881. The model for *M. californicus* had the best fit to the data (74.4% deviance explained), while the model for *C. townsendii* had the best predictive performance (0.753 ± 0.027 predictive deviance). The model for *P. subflavus* had the poorest performance in terms of both fit (54.7% deviance explained) and predictive performance (0.881 ± 0.027 predictive deviance).

Table 16. Final boosted regression tree (BRT) model parameters and performance metrics for winter species distribution models for bat species *Corynorhinus townsendii*, *Myotis californicus*, *M. lucifugus*, *M. velifer*, and *Perimyotis subflavus* across the United States and Canada.

Species	Tree complexity	Bag fraction	N trees	Mean total deviance	Mean residual deviance	Mean deviance explained	Predictive deviance (± SE)	Mean predicted percentile (presence)	Mean predicted percentile (background)
C. townsendii	5	0.7	3400	1.122	0.391	65.2	0.753 ± 0.026	89.4	53.6
M. californicus	4	0.7	1850	1.106	0.283	74.4	0.782 ± 0.072	94.6	56.8
M. lucifugus	5	0.6	4500	1.141	0.409	64.2	0.836 ± 0.024	80.3	43.4
M. velifer	3	0.6	1800	1.125	0.318	71.7	0.759 ± 0.041	83.7	38.7
P. subflavus	5	0.5	2300	1.126	0.51	54.7	0.881 ± 0.027	88.0	58.1

We found considerable interspecific differences in the relative influence of each predictor on occurrence probability (Figure 42). Ruggedness, topographic position, and percent tree cover were among the most consistently strong contributors, based on mean relative influence across species (11.64% ± 1.96 SD, 9.62% ± 4.14 SD, and 9.62% ± 2.31 SD, respectively). Winter survivorship, on average, also had high influence, but its influence varied considerably across species (9.58% ± 6.67 SD). Karst had the lowest influence overall (mean 4.6% ± 3.31 SD, though it was not considered in the *M. lucifugus* model).
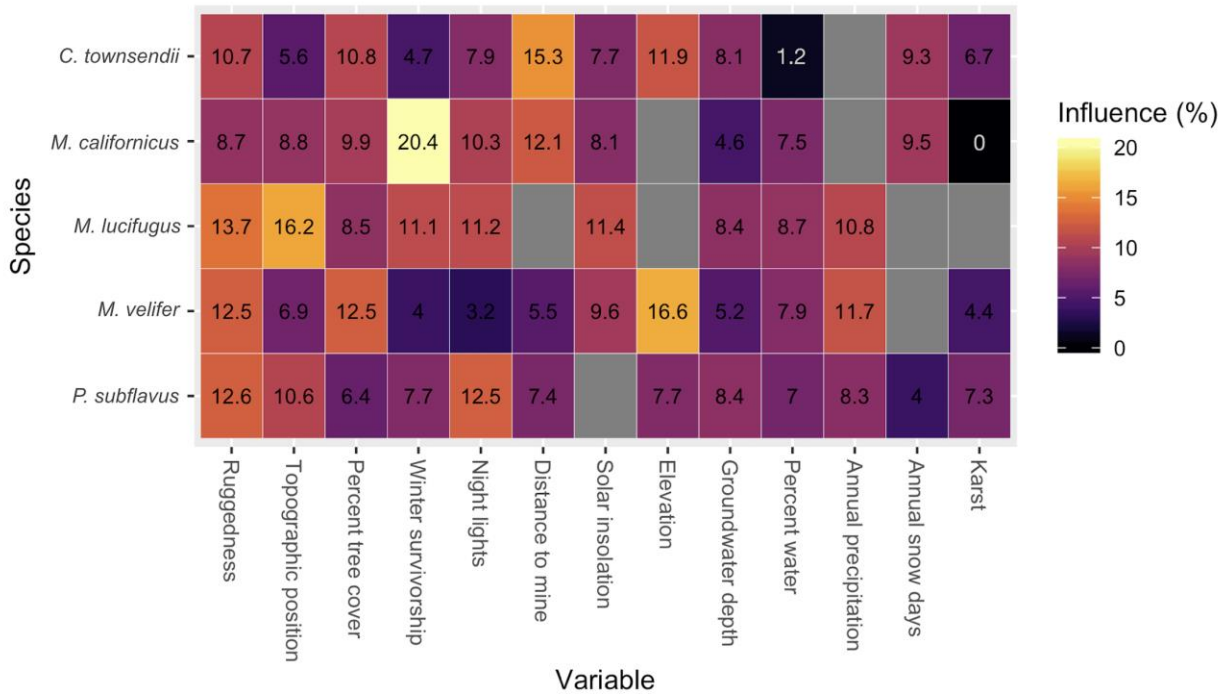

Figure 42. Final predictor influences in boosted regression tree (BRT) models estimating winter species distributions of bat species *Corynorhinus townsendii*, *Myotis californicus*, *M. lucifugus*, *M. velifer*, and *Perimyotis subflavus* across the United States and Canada. Brighter colors indicate higher influence; predictors that were dropped from a given model are shown in gray. Variables are ordered by their average influence across species (decreasing left to right).

Consistency in a predictor's degree of influence across species did not necessarily correspond to similar relationships between that predictor and relative occurrence probability among species (Figure 43). The effect of ruggedness was fairly consistent among species, with low relative occurrence probability predicted in very flat, open areas (very low ruggedness). *M. velifer,* and particularly *P. subflavus* appeared to favor low topographic positions (i.e., canyon bottoms); *M. lucifugus* also showed this pattern, in addition to an avoidance of open, flat topography (topographic position ~0). Relationships with solar insolation and elevation varied widely. For example, *C. townsendii* showed some preference for low elevations with high insolation, while *M. velifer* selected for low elevation, low insolation sites and *P. subflavus* preferred higher elevations (elevation was excluded from models for *M. californicus* and *M. lucifugus* due to high

collinearity with other predictors). Occurrence probability generally increased with predicted winter survivorship, as expected, particularly in species for which survivorship had strong influence (*M. californicus, M. lucifugus, P. subflavus*). Similarly, occurrence probability was generally higher with greater tree cover and fewer days of snow annually. The shape and direction of responses to groundwater depth, surface water, and annual precipitation (excluded from *C. townsendii* and *M. californicus* models due to collinearity) were highly variable. Before correcting for bias in presence locations, night lights were a strong predictor of most species' occurrence, but this relationship primarily reflected the distribution of sampling effort, not distribution of the species of interest. Still, even after correcting for sampling bias closer to human habitation, all species had very low relative probability of occurrence where night light intensity was lowest (darkest). However, in all species the rest of the response curve is quite flat, indicating minimal lingering effect of night lights in the models. Similarly, occurrence probability tended to be highest very close to mines, but beyond a minimum distance, the presence of mines had little effect on species distributions. Three species showed evidence of a preference for karst features (karst could not be considered for *M. lucifugus* due to missing karst data in portions of the species' range).
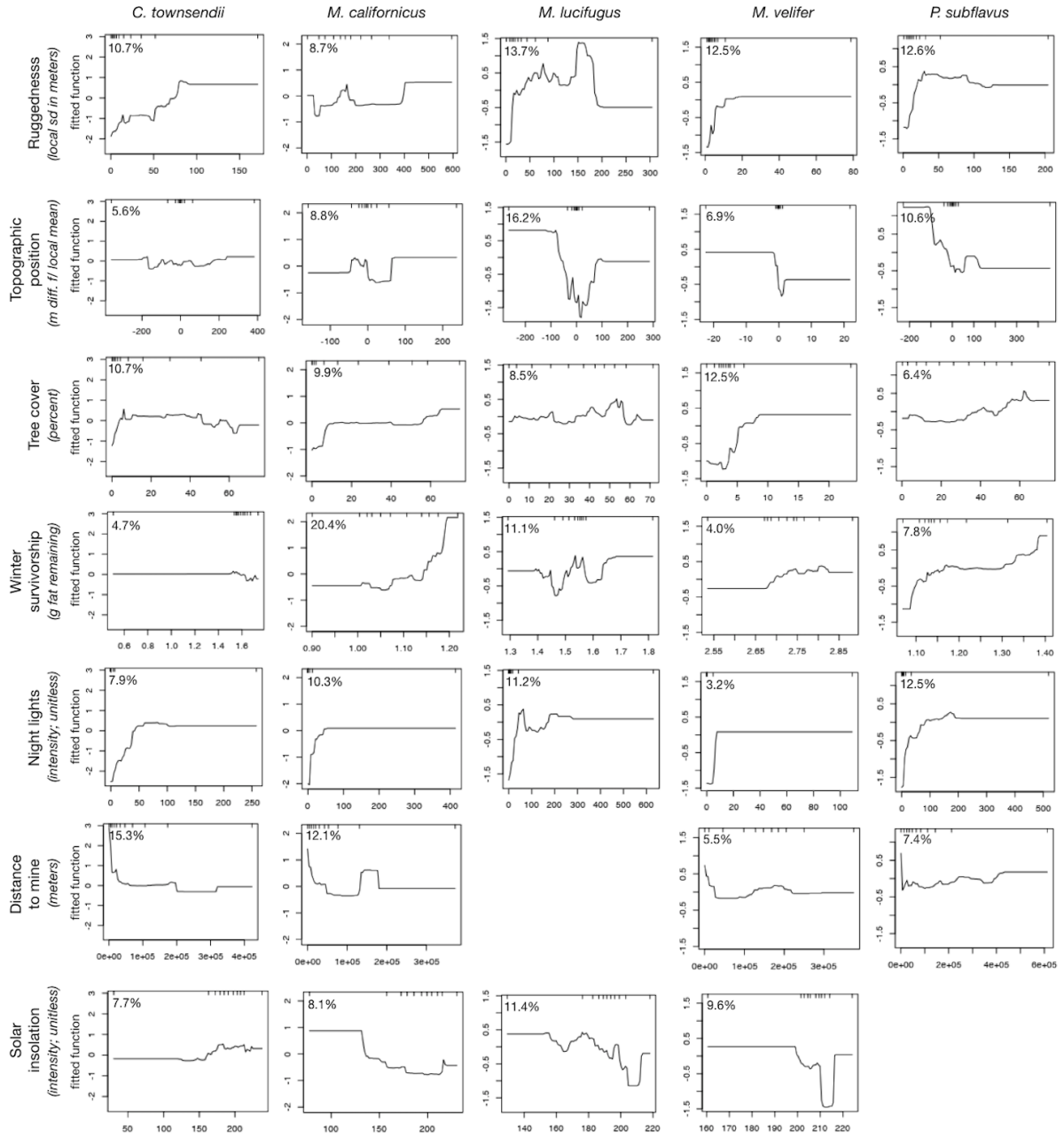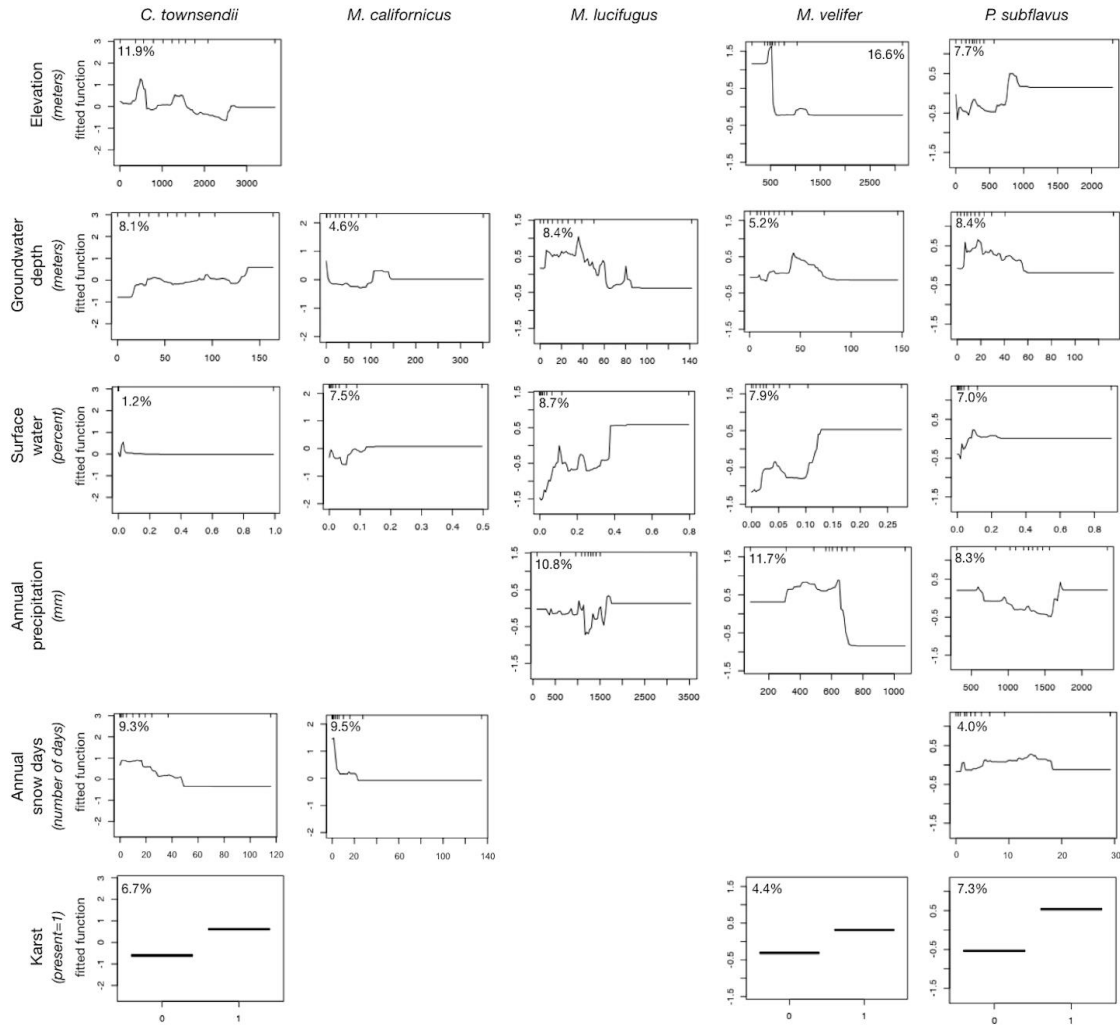
Figure 43. Fitted probability of occurrence functions for each predictor from boosted regression tree (BRT) models estimating winter species distributions of bat species *Corynorhinus townsendii*, *Myotis californicus*, *M. lucifugus*, *M. velifer*, and *Perimyotis subflavus* in the United States and Canada. Variables are ordered by their average influence across species; percentages indicate the relative influence of each predictor in the model. Rug plots (i.e., tic marks) indicate the deciles of the distribution of predictor values represented in the full presence/background location dataset.

We observed high relative probability of occurrence at presence locations compared to background locations, as expected (Appendix A16, Figures 44 – 49). The mean percentile rank of predicted occurrence probability at presence locations ranged from 80.3 (*M. lucifugus*, *M. velifer*) to 94.6 (*M. californicus*), 29.9 - 45 percentile points higher than the mean values predicted for background locations. In some cases, conspicuous exclusions and inclusions evident in existing species range extents (e.g., exclusion of Great Plains for *C. townsendii*, exclusion of Texas panhandle and mid-Atlantic coast for *M. lucifugus*, inclusion of Great Salt Lake area for *M. californicus*, inclusion of Arizona's Sky Islands for *M. velifer*) are mirrored by low and high predicted probabilities, respectively. Often, areas outside the focal species' known ranges have high predicted occurrence probability, reflecting the similarity of landscape attributes in these areas to those of known presence locations. Conversely, areas with low

occurrence probability often occur within the species' known ranges, highlighting the generalized nature of simple polygon range extent estimates.

Figure 44. Predicted relative probability of occurrence of *Corynorhinus townsendii* (predictive deviance = 0.753 ± 0.026) across the western United States and British Columbia. The species' current range extent (turquoise outline) and winter occurrence locations used to fit the model are overlaid (turquoise points). Occurrence probability is scaled using a quantile symbolization to reflect the fact that predictions represent relative occurrence probability; while absolute values cannot be reliably interpreted relative to one another, percentile ranking is permitted (i.e., yellow areas of the maps represent the 10% by area of the mapped landscape with the highest occurrence probability, regardless of the underlying distribution of values).

126

Figure 45. Predicted relative probability of occurrence of *Myotis californicus* (predictive deviance = 0.782 ± 0.072) across the western United States and British Columbia. The species' current range extent (turquoise outline) and winter occurrence locations used to fit the model are overlaid (turquoise points).
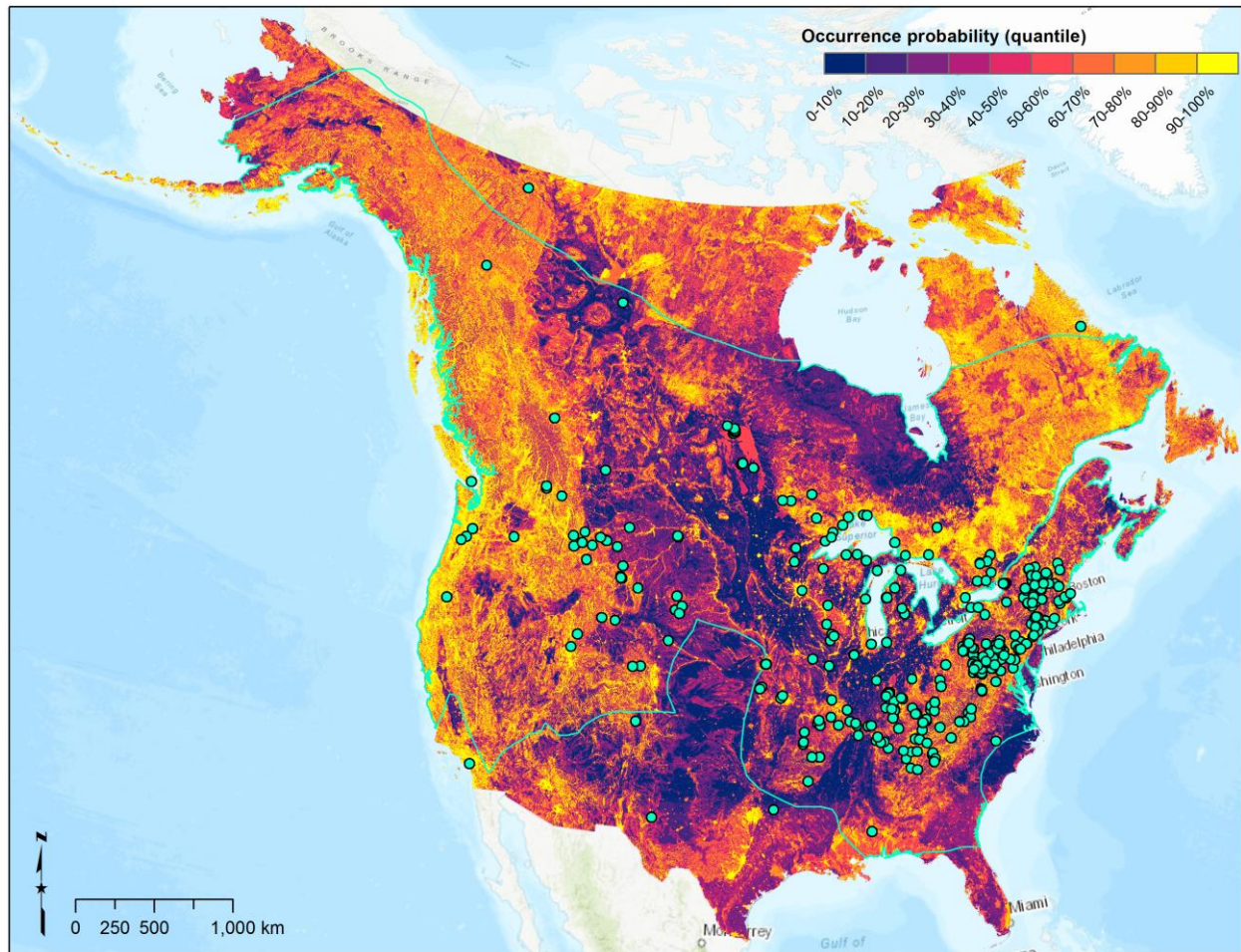
Figure 46. Predicted relative probability of occurrence of *Myotis lucifugus* (predictive deviance = 0.836 ± 0.024) across the United States and Canada (below the Arctic Circle). The species' current range extent (turquoise outline) and winter occurrence locations used to fit the model are overlaid (turquoise points).
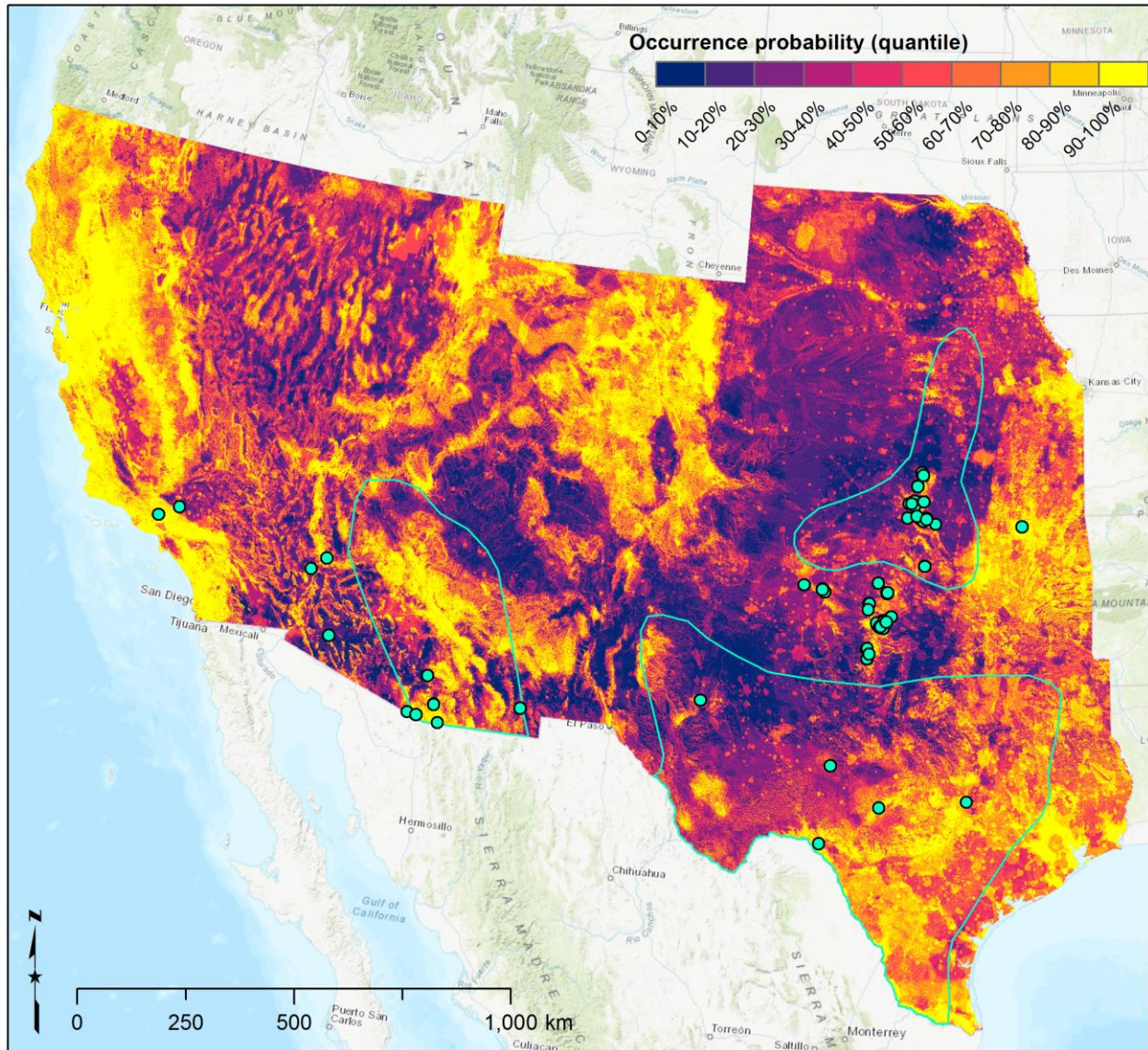
Figure 47. Predicted relative probability of occurrence of *Myotis velifer* (predictive deviance = 0.759 ± 0.041) across the southwestern United States. The species' current range extent (turquoise outline) and winter occurrence locations used to fit the model are overlaid (turquoise points).
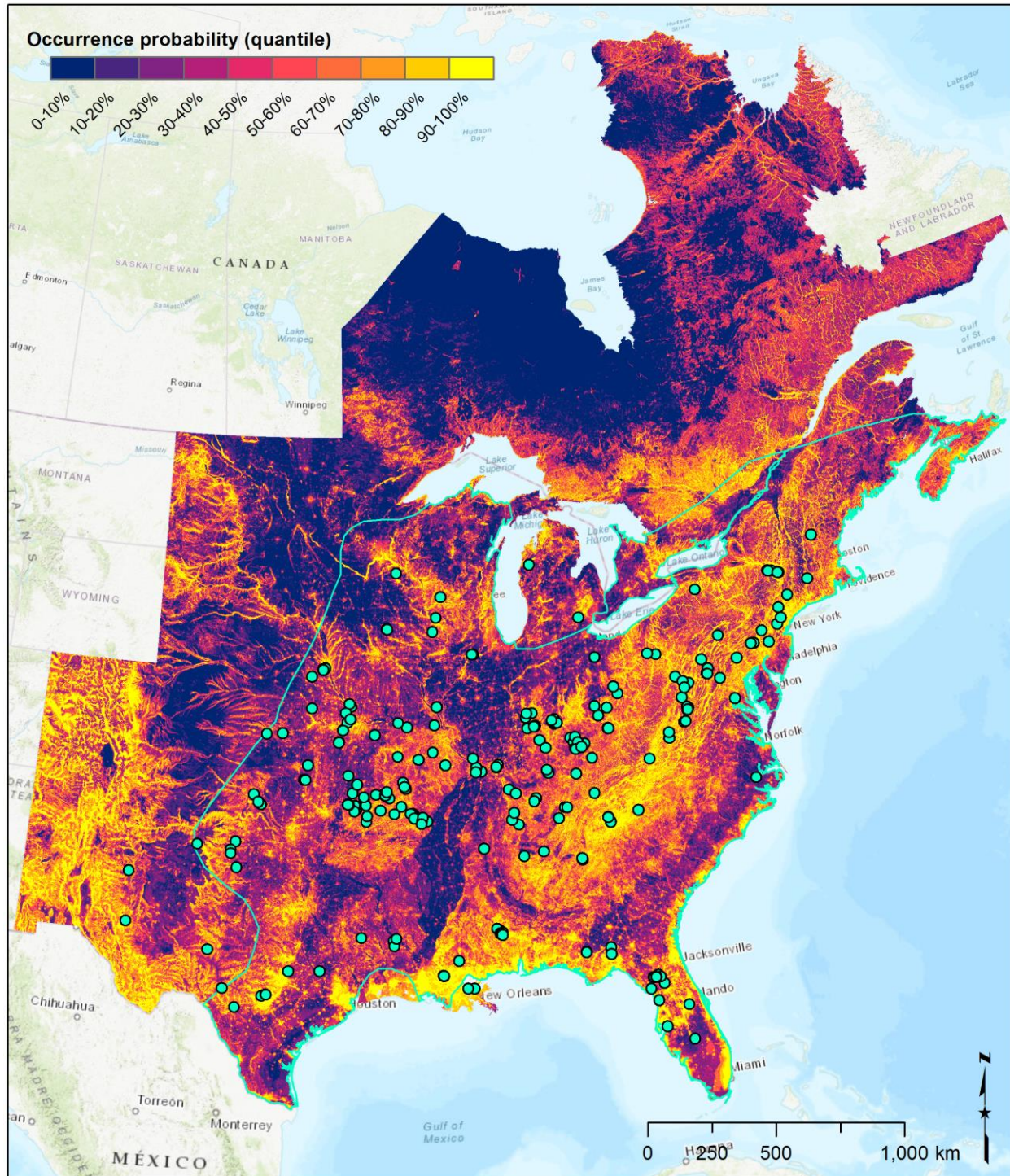
Figure 48. Predicted relative probability of occurrence of *Perimyotis subflavus* (predictive deviance = 0.881 ± 0.027) across the eastern and central United States and eastern Canada. The species' current range extent (turquoise outline) and winter occurrence locations used to fit the model are overlaid (turquoise points).
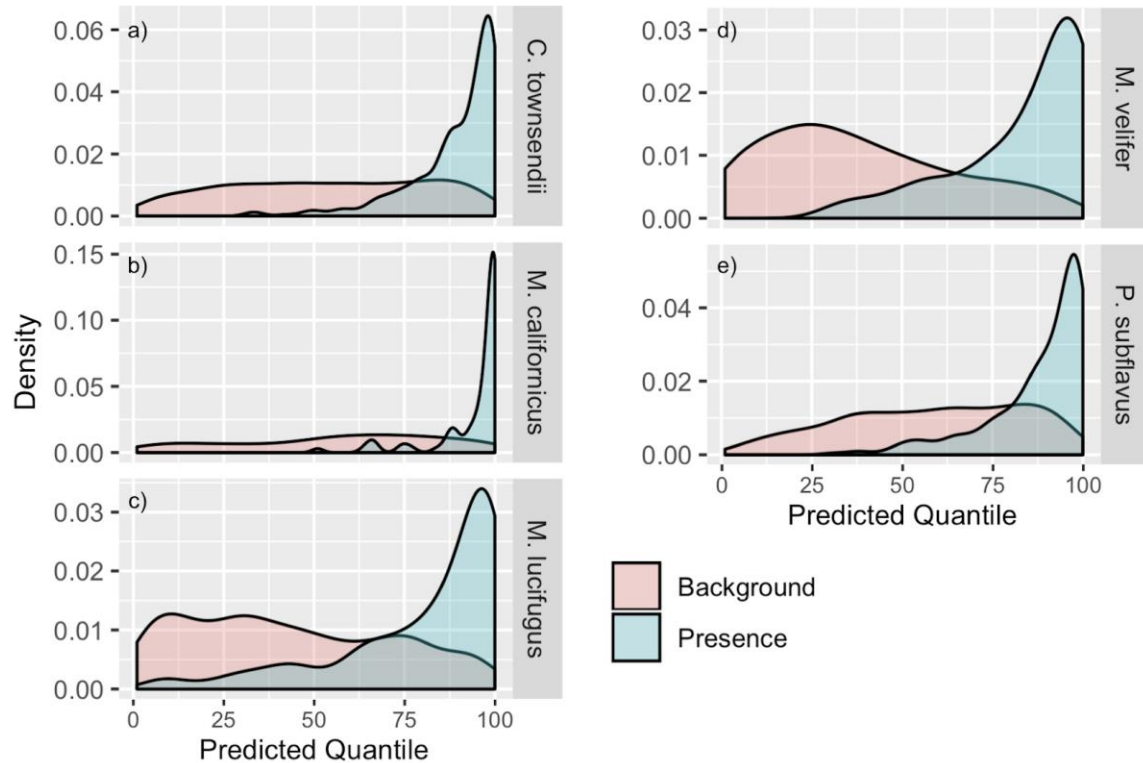
Figure 49. Distributions of predicted relative probability of occurrence of a) *Corynorhinus townsendii*, b) *Myotis californicus*, c) *M. lucifugus*, d) *M. velifer*, and e) *Perimyotis subflavus* in the United States and Canada at presence locations (green) compared to background locations (pink).

This study provides insights into the drivers and spatial patterns of bat hibernaculum selection in the West, a topic that is poorly understood, yet critical for advancing bat research, conservation, and management of WNS impacts. We demonstrate that the nature and scale of bats' responses to the landscape when selecting hibernacula varies among species and across different landscape attributes. Our results point to ranges of landscape attribute values where each focal species may be most likely to hibernate and highlight the importance of protecting mine features as hibernacula for multiple species. Importantly, our findings indicate that topographic attributes are important predictors of hibernaculum selection, suggesting that bat winter occurrence can, in part, be predicted from readily mapped above-ground features. We also found that our mechanistic estimate of winter survivorship contributed to prediction of winter occurrence probability for all focal species; in one case (*M. californicus*), it was by far the strongest predictor.

Because so little is known about how bats choose winter hibernacula and bat winter distributions in the West have never been modeled, we felt it was important to use methods that allow for flexible, nonlinear relationships between predictors and relative probability of occurrence. Peaks in our modeled response curves may help to identify ranges of preferred attributes (e.g., preferred elevation bands or density of forest cover). Flat portions of response curves may indicate an absence of selection (e.g., beyond a threshold distance, bats don't care how far they are from the nearest mine) or they may indicate ranges of attribute values where we simply have no data (see wide gaps in decile rug plots on response curves, Figure 43). Our use of bias

correction when generating background locations (Hertzog et al. 2014) impacted model results and was important given the opportunistic sampling of winter bat locations reflected in the public databases we relied on. Prior to bias correction, night lights were a strong predictor of most species' occurrence probability and suggested a preference for more intense night lights, but this uncorrected result would have reflected the distribution of sampling effort rather than the ecology of the focal species.

Although topographic attributes were often strong predictors of hibernaculum selection, preferred topographic characteristics (e.g., high versus low topographic position) varied among species. Karst presence was a weak predictor, perhaps because we did not consider differential selection among different types or depths of karst, or because the available map of karst features does not necessarily indicate where karst features are accessible to bats via caves or crevices. Mines were clearly important features for several species, and their relative influence appeared to scale sensibly with species' tendency to use mines: influence was lowest for *M. velifer* (cave myotis), which is more frequently found in caves. Our models suggest the importance of generating and making public spatial karst and mine datasets in other Canadian provinces to better predict occurrence for *M. lucifugus* and other species frequently found in mines in these regions. Our results support the preservation of western mines as critical winter habitat for which there are significant opportunities to enhance existing protected area status (Weller et al. 2018).

Our mechanistic winter survivorship estimate (see section 'Insights on winter duration and spatial variation in hibernation survival') contributed to all species' predicted occurrence, but to varying degrees. The direction of the relationship between survivorship and relative occurrence probability was positive overall, as expected, but its strength varied among species. This complex, model-based estimate of survivorship is unavoidably subject to uncertainty, but it has greater direct relevance to winter bat distributions than generic climate metrics (e.g., mean surface temperature) with no mechanistic link to bat physiology. Future quantitative comparisons between predictions from this mechanistic predictor and those generated using standard, off-the-shelf climate predictors may be of interest. We also see worthwhile opportunities to continue honing this survivorship model as additional empirical data for parameterization become available (e.g., for estimating species-specific, spatially explicit winter duration, better estimating subterranean temperatures and humidity experienced by hibernating bats and how they respond physiologically).

The maps of relative occurrence probability presented here (Figures 44 – 48) should help to guide future work to survey and monitor western bat populations, inform future conservation efforts, and provide a baseline for understanding potential impacts of future change, namely the spread of WNS through the West and climate change. These maps should be interpreted with care outside the known range of each species, as places with predictor values similar to those currently occupied will be highlighted but other limits on species distributions (e.g., historic spread processes, species interactions) may exist that were not captured here. Occurrence probability of generalist species with broad geographic ranges is particularly difficult to model effectively (Hernandez et al. 2006; Razgour et al. 2016). Predictive maps for such species (e.g., *M. lucifugus*, *P. subflavus*), which have lower predictive performance, should be interpreted with caution. Still, we expect that these maps can be useful for considering the potential occurrence of the focal species in areas predicted to be suitable beyond their coarsely mapped range extents,

which are likely inaccurate or out of date in some areas. Places that are predicted to have low occurrence probability may in fact be unlikely to support hibernacula, or they may simply have attributes not well represented in our presence data. These areas should be considered in the context of existing knowledge of the focal species and their hibernation patterns: Do these places lack karst or mine features, topographic relief, or trees to shelter hibernating bats? Or are they simply remote and characterized by rare landscape features that were underrepresented in our sample? It is also important to recognize that mapped occurrence probabilities are relative values. We cannot estimate absolute occurrence probability from the available data, and our estimates may not be strictly proportional to absolute probability. The predicted values should be interpreted as rank probabilities, as reflected by the quantile symbology used in our maps (Figures 43 – 48).

These are complex models based on relatively small sample sizes, so uncertainty remains and portions of the predictor space are undersampled. We may also be missing key predictors that we simply don't yet understand to be important for hibernaculum selection or cannot map continuously with currently available spatial data. Future efforts to improve on these models would benefit from additional winter location data (particularly for species other than *C. townsendii* and *M. lucifugus*) in novel locations. Future survey efforts could perhaps target places predicted to be highly suitable but where no occurrence data exist (e.g., *M. californicus* in the Great Salt Lake region, *M. velifer* in south Texas and northeast Arizona), or places with landscape characteristics not well represented in the current sample. Absence data would improve the robustness of distribution models considerably (e.g., in comprehensive survey and monitoring efforts, which species were searched for but not found?), although reliable absences would be extremely difficult to obtain (due to low detection probabilities that vary with survey techniques and site characteristics).

Winter hibernation is clearly a critical part of temperate bats' annual cycle, yet it is largely a black box for many species; we have only limited knowledge of where these widely-distributed species go for approximately half the year or what drives them there. This lack of understanding of the ecology of these species hinders conservation and management responses to ongoing and future threats to their persistence. Insights from SDMs are valuable for locating, studying, and managing species with low detectability (Razgour et al. 2016). SDMs may also help to define winter critical habitat for bats, as they have for other species (Heinrichs et al. 2010; Brotons et al. 2004). Unlike the East, there has simply not been a 'where' on which to focus conservation policy in the West; models like ours could begin to fill this gap.

Impacts of climate change on bats and WNS
Mean projected climate parameters (MAST and frost-free period) among the four climate scenarios assessed are mapped in Figure 50, along with the inter-scenario range and the mean projected change in each parameter from current conditions. Spatial patterns in the mean parameter values reflect latitudinal, topographic, and coastal influences on temperature and frost-free period, as expected. We observed high agreement among climate scenarios (i.e., low inter-scenario range) for projected MAST, with increasing disagreement at very high latitudes. Disagreement among climate scenarios in length of the frost-free period was higher in places and more sporadic, likely reflecting a stronger influence of topography. Projected change in MAST increased with latitude and with elevation, while projected change in frost-free period was more

spatially variable, with the largest increases in the Appalachian region and localized portions of the West coast.

Projected changes in probability of occurrence for each of five focal species under future scenarios are mapped in Figures 51 – 55. We focus on projections from SDMs in which the survivorship predictor accounted for at least 5% of the boosted regression tree (BRT) model fit (Figure 42), which included models for *M. californicus, M. lucifugus*, and *P. subflavus*. Projections from SDMs to which survivorship contributed less than 5% (*C. townsendii, M. velifer*) are expected to be less useful because little clear relationship between known species occurrences and survivorship emerged.

Generally, as expected, probability of occurrence was projected to decline following exposure to *P. destructans* (with the exception of *C. townsendii*, Figure 54). However, projected occurrence probability increased for most species in most places when climate change was also considered. The greatest projected declines with *P. destructans* exposure were typically in areas with the highest occurrence probability under current conditions (i.e., the areas currently expected to be most suitable for a given species). Spatial patterns in climate impacts were more variable. For *M. californicus*, we projected moderate declines in occurrence probability in British Columbia, but a strong increase in other high occurrence probability portions of the range. For *M. lucifugus*, we projected decreases in the severity of declines, but climate change had little impact on areas already expected to remain stable or experience increased occurrence probability. In contrast, we observed thresholding behavior in *P. subflavus* such that projected rangewide declines under *P. destructans* exposure were replaced by a marked increase in occurrence probability in the southeast given climate change. This threshold appears to follow and is thus probably driven by spatial patterns in the frost-free period (Figure 50). We do not interpret projected changes under each future scenario for *C. townsendii* or *M. velifer* because the low contribution of winter survivorship estimates to SDM fits appear to result in unreliable and counterintuitive behavior of models for these species (Figures 54-55).

All four climate scenarios showed close agreement regarding future changes in occurrence probability. This agreement may be driven by one or more factors. First, derived estimates of MAST and frost-free period may not be sensitive to differences among scenarios in projected daily temperatures. This appears to be more true for MAST than for frost-free period (Figure 50) and is not surprising given that calculation of the frost-free period is threshold dependent (i.e., definition of the frost-free period is dependent on the first and last day of the year on which a precise threshold temperature is reached). Second, the subterranean temperature model and/or winter duration model may not be sensitive to MAST and frost-free period parameters, respectively. This is unlikely in the case of the subterranean temperature model, given that MAST is the model's strongest predictor. It is also unlikely in the case of the winter duration given that inclusion of frost-free period as a predictor improved the model by 25.39 AIC units (Table 13). Third, the survivorship model may not be sensitive to variation in the best available temperature estimate derived from the subterranean temperature model and/or our estimate of winter duration. We suggest that derivation of the 'best available' temperature for a given species at a given location from the subterranean temperature model likely absorbs the majority of the variability among climate scenarios. Finally, SDMs may not be sensitive to variation in

survivorship estimates. SDM sensitivity to survivorship is expected to be directly related to the contribution of the survivorship predictor to the BRT model for a given species (Figure 42).

Although all climate scenarios produced very similar projections of future change in occurrence probability, differences were apparent in some places for most species. For *M. californicus*, differences were most apparent along the Pacific coast near the California-Oregon border and around the state of Oklahoma (Figure 51). For *P. subflavus*, the location of the threshold between increasing and decreasing occurrence probability fluctuated across the Appalachian region among scenarios (Figure 53). Model disagreement was also evident in Oklahoma for *C. townsendii* and *M. velifer*, as well as the Columbia Plateau of eastern Washington and the Sierra Nevada range of California, respectively (Figures 54 – 55).

We suggest that our predictions of species distributions in the presence of *P. destructans* and future climate conditions can help managers to better anticipate the species- and place-specific impacts of these stressors, individually and synergistically, across the West. Our findings suggest that mid-century climate change may 'rescue' many bat populations from the deleterious effects of *P. destructans.* However, given the pace of *P. destructans'* spread from the East and its recent leap to Washington state (USFWS 2020), this rescue effect may arrive too late for many hibernacula. Furthermore, a warming climate is not predicted to shield all species in all areas (e.g., *M. californicus* in British Columbia, *M. lucifugus* in mountainous regions, *P. subflavus* in the northeastern United States). It is therefore important that managers continue to strive for effective conservation strategies as *P. destructans* continues to spread in order to minimize mortality.

Our results may help to inform placement of passive acoustic detectors for monitoring as *P. destructans* continues to spread and the climate continues to warm. For example, monitoring of bat populations could be targeted in areas where our projections suggest that suitable hibernation conditions are likely to be lost and that occurrence probability is likely to decline (vulnerable hibernacula). Conversely, these efforts could target hibernacula that are likely to be retained (potential refugia). Our prediction may also enable assessment of the distribution of at-risk and stable hibernacula across federal, state, and private lands to guide engagement strategies for conservation. Additionally, they may help managers to prepare for possible range expansions into or contractions from their jurisdictions under future climate conditions.
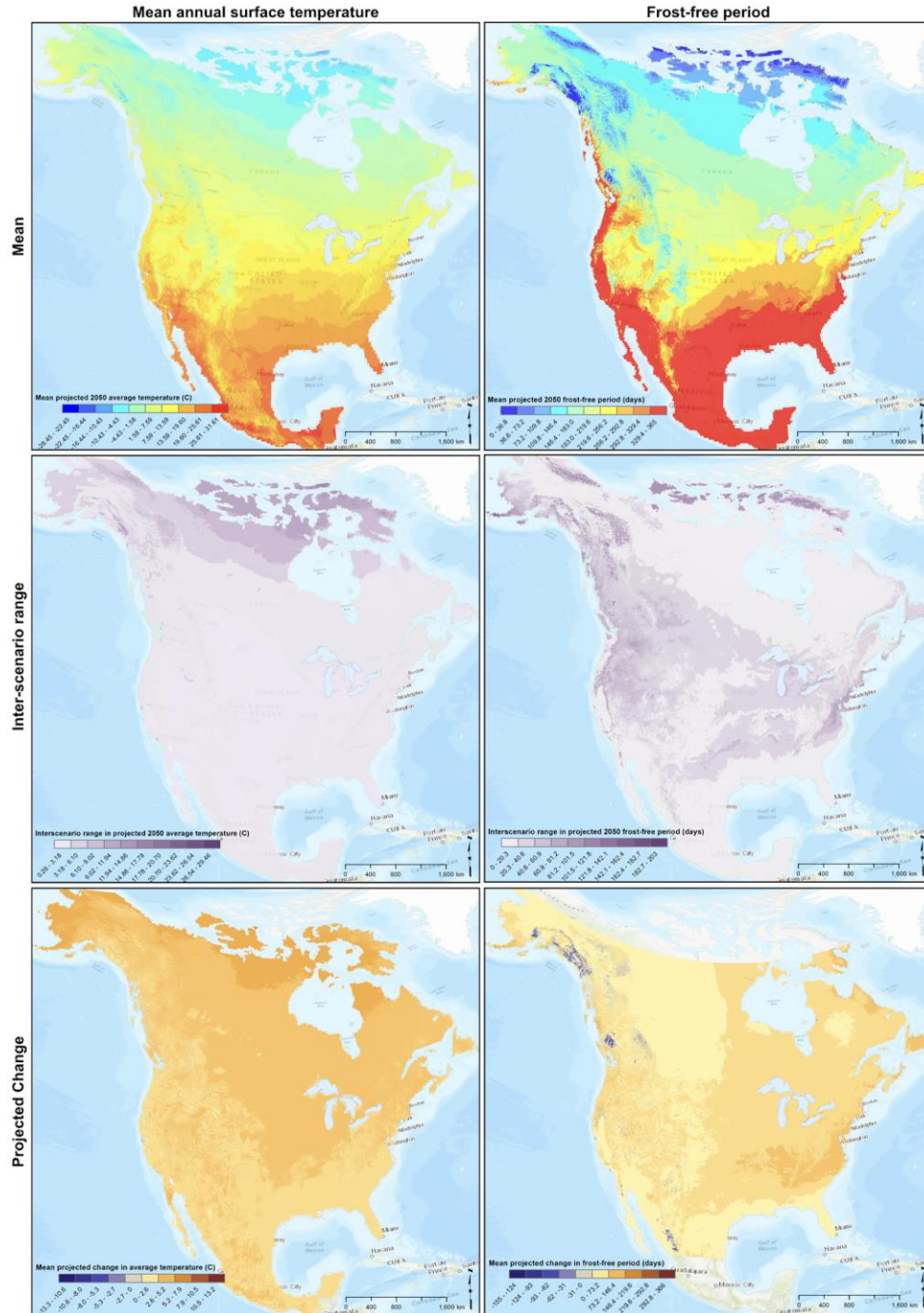
Figure 50. Projected mid-century climate conditions (30-year averages centered on 2050) used to parameterize bioenergetic survivorship models: mean annual surface temperature (left) and duration of frost-free period (right). Survivorship estimates were subsequently used as predictors of occurrence probability in species distribution models for five focal bat species. Future climate scenarios were driven by each combination of two global circulation models (GCMs): GFDL-ESM2M and HadGEM2-ES, and two dynamically-downscaled regional climate models (RCMs): RegCM4 and WRF. We show the mean (top) and range (center) among the four scenarios as well as the mean projected change from current conditions (bottom).
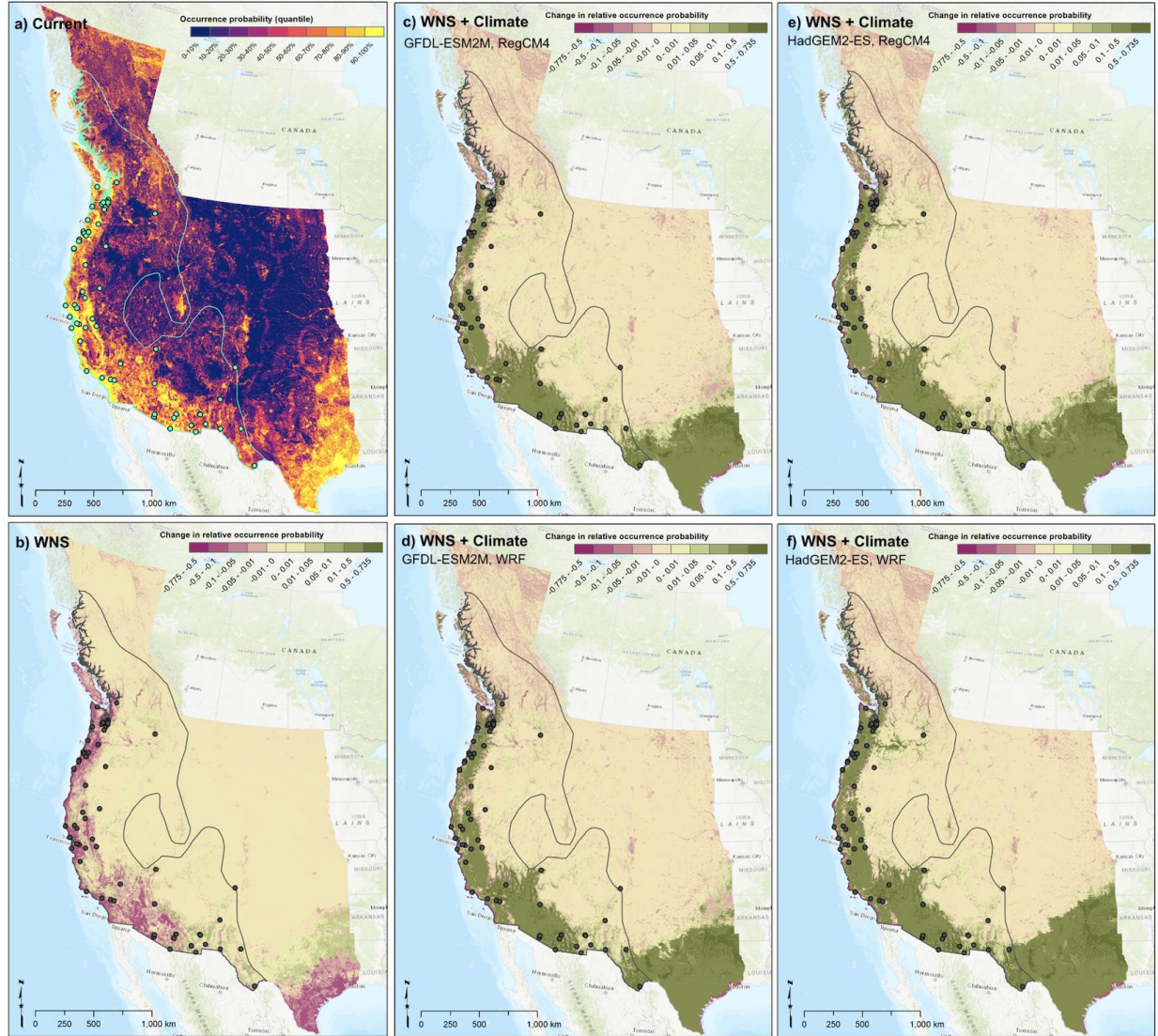
Figure 51. a) Current occurrence probability of *Myotis californicus* and change in relative probability of occurrence given b) exposure to white-nose syndrome (WNS), and exposure to WNS under projected mid-century climate conditions. Future climate scenarios shown here were driven by each combination of dynamically-downscaled regional climate models c,e) RegCM4 and d,f) WRF run on boundary conditions defined by the c,d) GFDL-ESM2M and e,f) HadGEM2-ES global circulation model. Darker green indicates a projected increase in occurrence probability; darker purple indicates a projected decrease. The species' current known range (gray outline) and points of recorded winter occurrence (gray points) are overlaid.
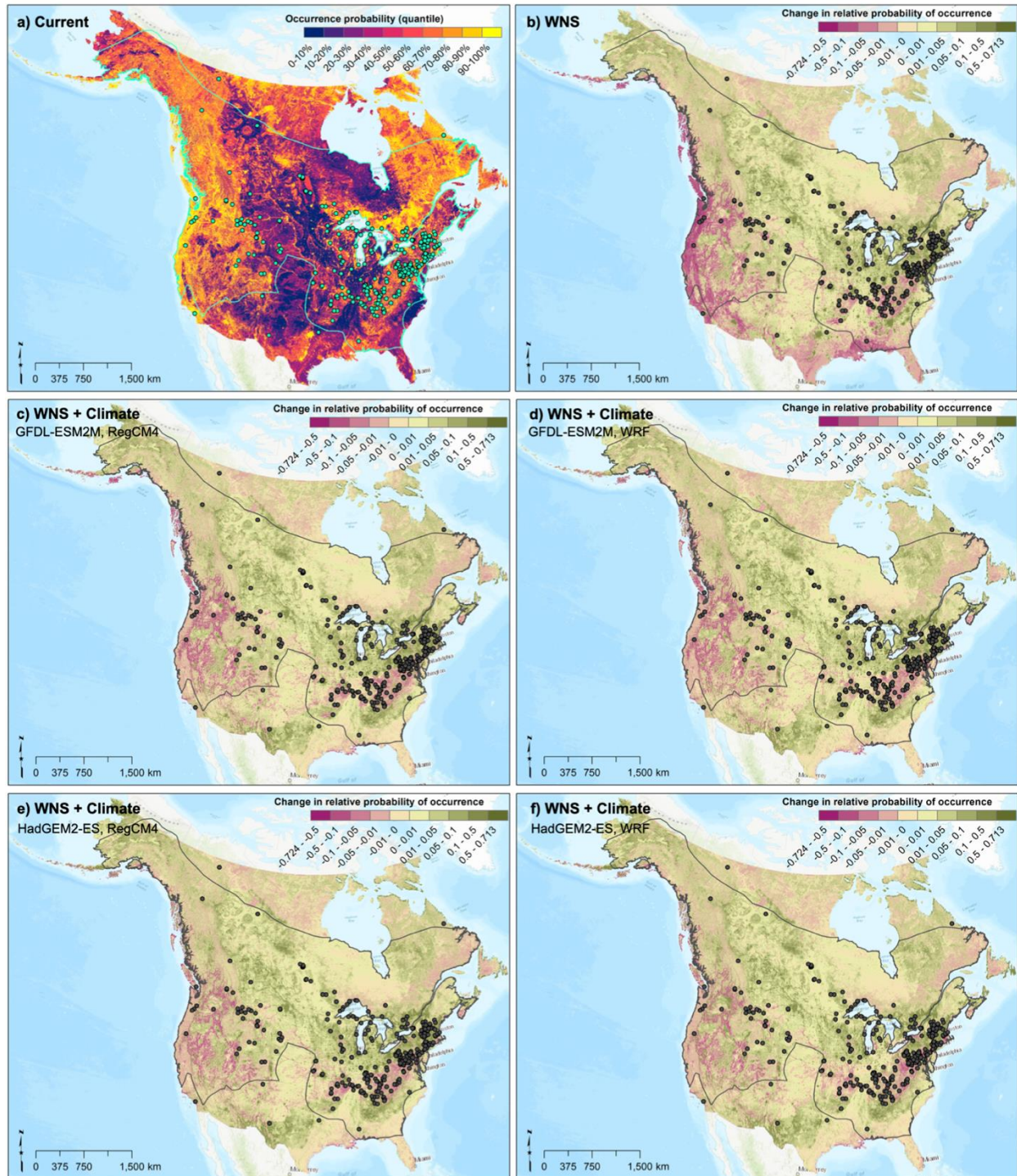
Figure 52. a) Current occurrence probability of *Myotis lucifugus* and change in relative probability of occurrence given b) exposure to white-nose syndrome (WNS), and exposure to WNS under projected mid-century climate conditions. Future climate scenarios shown here were driven by each combination of dynamically-downscaled regional climate models c,e) RegCM4 and d,f) WRF run on boundary conditions defined by the c,d) GFDL-ESM2M and e,f) HadGEM2-ES global circulation model. Darker green indicates a projected increase in occurrence probability; darker purple indicates a projected decrease. The species' current known range (gray outline) and points of recorded winter occurrence (gray points) are overlaid.

Figure 53. a) Current occurrence probability of *Perimyotis subflavus* and change in relative probability of occurrence given b) exposure to white-nose syndrome (WNS), and exposure to WNS under projected mid-century climate conditions. Future climate scenarios shown here were driven by each combination of dynamically-downscaled regional climate models c,e) RegCM4 and d,f) WRF run on boundary conditions defined by the c,d) GFDL-ESM2M and e,f) HadGEM2-ES global circulation model. Darker green indicates a projected increase in occurrence probability; darker purple indicates a projected decrease. The species' current known range (gray outline) and points of recorded winter occurrence (gray points) are overlaid.
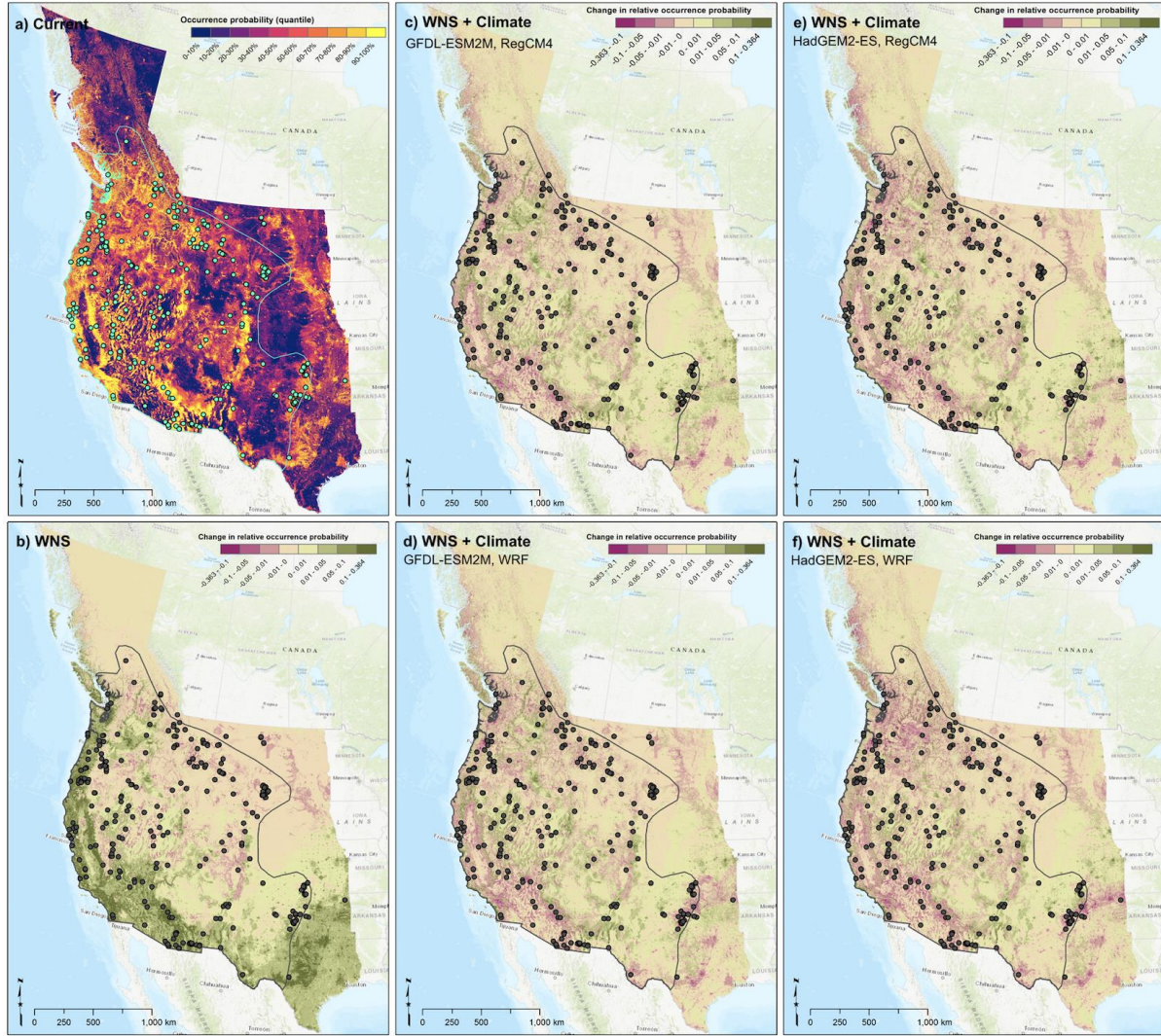
Figure 54. a) Current occurrence probability of *Corynorhinus townsendii* and change in relative probability of occurrence given b) exposure to white-nose syndrome (WNS), and exposure to WNS under projected mid-century climate conditions. Future climate scenarios shown here were driven by each combination of dynamically-downscaled regional climate models c,e) RegCM4 and d,f) WRF run on boundary conditions defined by the c,d) GFDL-ESM2M and e,f) HadGEM2-ES global circulation model. Darker green indicates a projected increase in occurrence probability; darker purple indicates a projected decrease. The species' current known range (gray outline) and points of recorded winter occurrence (gray points) are overlaid.
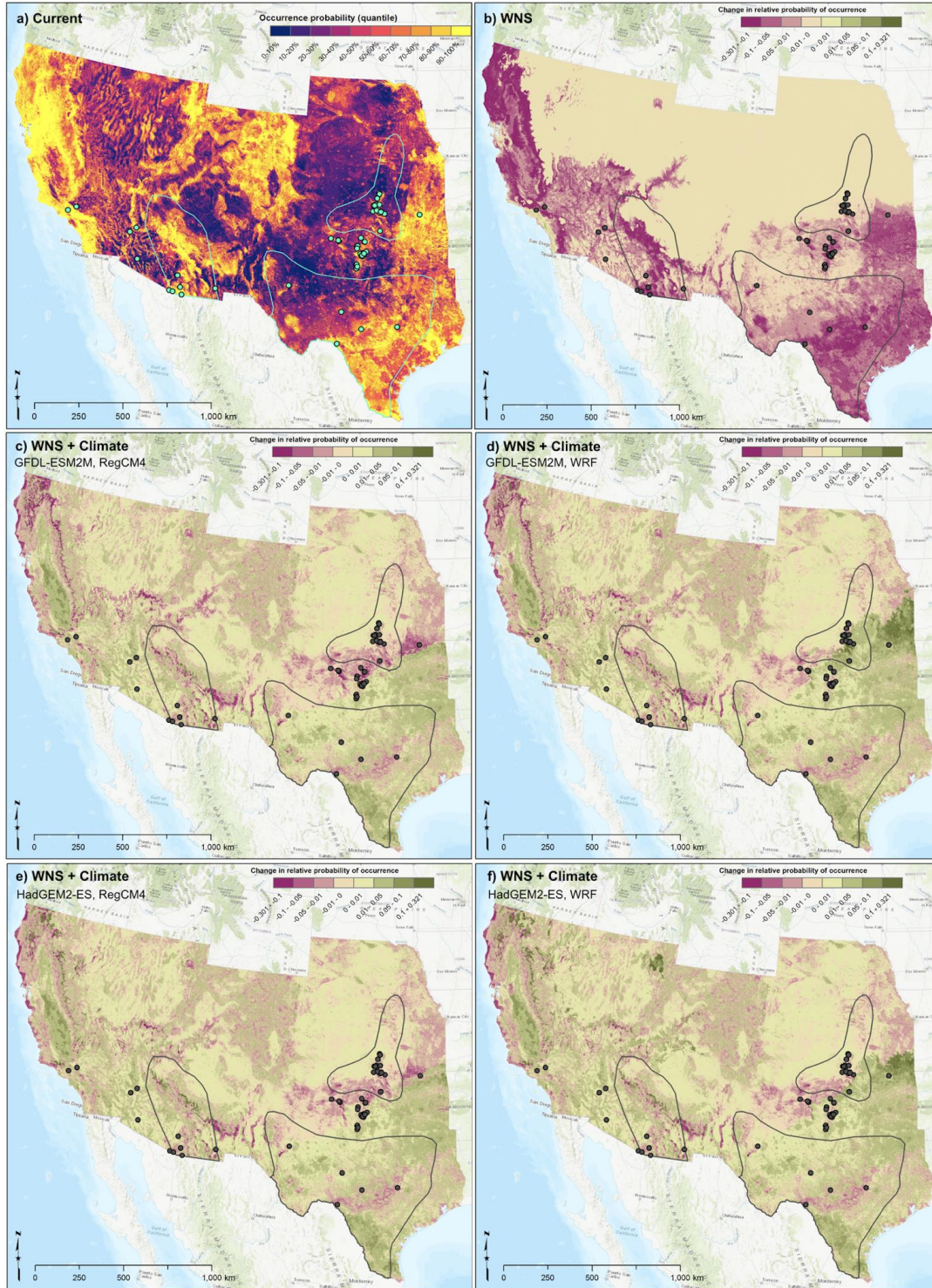
Figure 55. a) Current occurrence probability of *Myotis velifer* and change in relative probability of occurrence given b) exposure to white-nose syndrome (WNS), and exposure to WNS under projected mid-century climate conditions. Future climate scenarios shown here were driven by each combination of dynamically-downscaled regional climate models c,e) RegCM4 and d,f) WRF run on boundary conditions defined by the c,d) GFDL-ESM2M and e,f) HadGEM2-ES global circulation model. Darker green indicates a projected increase in occurrence probability; darker purple indicates a projected decrease. The species' current known range (gray outline) and points of recorded winter occurrence (gray points) are overlaid.

Conclusions and Implications for Future Research

<u>Conclusions and main findings</u>
Our project set ambitious scientific objectives to measure, for the first time, key bioenergetic parameters of western bats. We then combined these new data with existing data sets that we compiled or sourced to improve or create models that revealed our best scientific understanding of the environmental conditions and host attributes that contribute to WNS susceptibility. We generated species-level predictions about WNS outcomes in the West and made spatial projections about survivorship that leveraged both environmental attributes and the estimates of winter survival from a refined bioenergetic model. Below we revisit our three main scientific objectives and share our main conclusions and findings for each. Over the course of the project, various research results were shared with the larger scientific, bat management, and WNS-response communities through attending scientific and WNS management meetings and publishing findings in peer-reviewed scientific journals. We remain committed to sharing the remaining results and findings widely in these same venues (see Appendix B materials for a summary of these communication efforts).

Objective 1
Collect robust morphometrics, bioenergetics, and hibernacula environmental data on up to five western North American bat species representing different hibernating behaviors and geographic settings at three to five sites each year.

- Species with broad geographic ranges may experience variable environmental conditions throughout their range leading to local adaptation. Variation among populations reflects potential adaptability with implications for populations impacted by disease, climate change, and other anthropogenic influences. However, behavior may counteract divergent selection among populations. We examined intraspecific variation in hibernation physiology in *M. lucifugus* (little brown myotis) and *C. townsendii* (Townsend's big-eared bat), two species of bats with large geographic ranges. We studied *M. lucifugus* at three hibernacula which spanned a latitudinal gradient of 1,500 km, and *C. townsendii* from six hibernacula spread across 1,200 km latitude and similar longitude. We found no difference in torpid metabolic rate among populations of either species, nor was there a difference in the effect of ambient temperature among sites. Similarly, EWL was similar among populations of both species, though for *C. townsendii* there was one pairwise site difference and for *M. lucifugus* one site differed from the others. We suggest the general lack of regional variation is a consequence of behavior. As volant animals, bats can travel relatively long distances in search of preferred microclimates for hibernation. Despite dramatic macroclimate differences among populations, hibernating bats are able to find preferred microclimate conditions within their range, resulting in similar selection pressures among populations spread across wide geographic ranges. This suggests the energetic consequences of WNS infection will be range-wide within species.

- Hibernation is a taxonomically diverse phenomenon among mammals, and occurs across a wide range of geographic and ecological contexts. However, most studies have focused on a relatively small number of species, few studies consider more than one species and typically bat studies have targeted *M. lucifugus*. Multi-species studies can identify

important differences from commonly studied species, and provide insight into general patterns of hibernation strategies and in the case of bats, potential physiological WNS risk factors. We studied 13 species of free-living bats, including hibernating populations spread over thousands of kilometers, representing diverse hibernation contexts. We measured TMR and EWL (two key parameters for understanding the energetics of hibernation) across a range of hibernation temperatures. The minimum defended temperature varied among species, but when measured within the appropriate temperature range, all species had similar torpid metabolic rate. Conversely, EWL varied among species, which clustered into two groups. Our results suggest there are two general hibernation strategies in North America bats, representing high and low evaporative water loss groups. Notably, species that have suffered large population declines due to WNS fall in the high EWL group, and those species that are less affected fall in the low EWL group.

- Hibernation requires balancing energy and water demands over periods of several months with no food intake for many species. Many studies have considered the importance of fat for hibernation energy budgets but protein catabolism has received less attention, and whole animal changes in lean mass have not previously been considered. We predicted hibernating bats deposit lean mass prior to hibernation, and while fat provides the major energy source, hibernating bats would catabolize protein with implications for energy and water budgets. We further predicted that males and females would differ in the deposition and use of lean mass due to reproductive differences. We used QMR body composition analysis to measure fat and lean mass in two systems of hibernating bats. First, we considered the body composition of *M. velifer* (cave myotis) during pre-hibernation swarming. Second, we compared *C. townsendii* measured during pre-hibernation swarming and in mid-winter. We illustrated the functional consequences of protein catabolism by calculating the relative contributions of lean mass to mass change, energetics, and water production in male and female *C. townsendii*. *M. velifer* deposited lean mass prior to hibernation, with males depositing relatively more (38% of mass gain) than females (25% of mass gain). In *C. townsendii*, females had more fat and lean mass than males in both seasons, and lean mass decreased substantially through hibernation. Although lean mass accounted for 18 or 35% of mass loss (in females and males respectively), it only contributed 3 and 7% of the energy budgets. Combining fat and lean catabolism, net water production was much less than gross water production when accounting for water required to excrete urea. Mammals generally cannot catabolize protein for metabolic water production due to the water cost of excreting urea. However, we propose a variation on the protein-for-water strategy whereby hibernators could benefit from protein catabolism by temporally compartmentalizing the benefits to periods of torpor, and costs to periodic arousals. Combined, our analyses demonstrate that lean mass is dynamic in hibernation, and changes in lean mass have important functional consequences for energy and water budgets, which may have possible implications on the energetics of surviving WNS.

- Hibernation requires animals to balance the energetic benefits with the physiological costs incurred with prolonged torpor use. While long, harsh winters at northern latitudes necessitate obligate hibernation, winter is relatively mild at southern latitudes and torpor expression may be flexible with environmental conditions. *T. brasiliensis mexicana*

143

(Mexican free-tailed bats) are a subtropical species where most individuals migrate south for winter, but small remnant populations forgo migration and overwinter. We hypothesized that this species uses facultative hibernation to persist through winter and predicted bats use heterothermy ranging from daily to multi-day periods depending on ambient temperature. We also predicted that *T. brasiliensis* are capable of deep torpor, as observed in other hibernating bats, but that they would have a minimum defended temperature higher than northern hibernators. We used open-flow respirometry on bats at five temperatures between 2 °C and 12 °C to establish a temperature-response curve and attached temperature-sensitive radiotransmitter to free-living bats to quantify torpor use. Bats used deep torpor and began to defend body temperature, on average, at 5.9 °C, a similar temperature to other subtropical bat species but higher than northern hibernating bats. Free-living bats used torpor ranging from a few hours to 5.5 days, with torpor bout duration increasing in colder weather. This work adds to the growing body of research about the diversity of hibernation strategies, particularly facultative hibernation at lower latitudes, and allows us to assess the WNS susceptibility and vector potential of this partially migratory and more southern species.

Objective 2
Examine the transferability of the mechanistic WNS bioenergetics survivorship model (based on host, pathogen, and environmental characteristics) developed for bat species affected by WNS in the East to a set of five representative bat species found in the West.

- Warming and euthermic costs are regularly included in energetic models, but although cooling to torpid body temperature is an important phase of the torpor-arousal cycle, it is often overlooked in energetic models. When included, cooling cost is assumed to be 67% of warming cost, an assumption originally derived from a single study that measured cooling cost in ground squirrels. Since this study, the same proportional value has been assumed across a variety of hibernating species, including its use in the Hayman et al. (2016) model that we set out to parameterize for western bats. However, no additional values had been derived, so we derived a model of cooling cost from first principles and validated the model with empirical energetic measurements. We compared the assumed 67% proportional cooling cost with our model-predicted cooling cost for 53 hibernating mammals. Our results indicate that using 67% of warming cost only adequately represents cooling cost in ground squirrel-sized mammals. In smaller species, this value overestimates cooling cost and in larger species, the value underestimates cooling cost. Our model now allows for the generalization of energetic costs for multiple species using species-specific physiological and morphometric parameters, and for predictions over variable environmental conditions.

- Hibernation consists of extended durations of torpor interrupted by periodic arousals. The 'dehydration hypothesis' proposes that hibernating mammals arouse to replenish water lost through evaporation during torpor. Arousals are energetically expensive, and increased arousal frequency can alter survival throughout hibernation. Yet we lack a means to assess the effect of EWL, determined by animal physiology and hibernation microclimate, on torpor bout duration and subsequent survival. WNS causes increased frequency of arousals during hibernation and EWL has been hypothesized to contribute to this increased arousal frequency. *P. destructans* grows well in humid hibernaculum

environments and damages wing tissue important for water conservation. Here, we integrated the effect of EWL on torpor expression in our hibernation energetics model, including the effects of fungal infection, to determine the link between EWL and survival. We collected field data for *M. lucifugus,* a species that experiences high mortality from WNS, to gather parameters for the model. In saturating conditions, we predicted healthy bats experience minimal mortality. Infected bats, however, suffer high fungal growth in highly saturated environments, leading to exhaustion of fat stores before spring. Our results suggest that host adaptation to humid environments leads to increased arousal frequency from infection, which drives mortality across hibernaculum conditions. We predicted almost complete mortality for *M. lucifugus* within the current hibernaculum conditions of a Montana cave system, in part because the high humidity selected by hibernating bats also results in high fungal growth. Our modified hibernation model provides a tool to assess the interplay between host physiology, hibernaculum microclimate, and diseases such as WNS on winter survival.

- Caves and other subterranean features provide unique environments for many species. The importance of cave microclimate is particularly relevant at temperate latitudes where bats make seasonal use of caves for hibernation. WNS has brought renewed interest in bat hibernation and hibernaculum conditions that lead to catastrophic bat population declines. A recent review synthesized current understanding of cave climatology, exploring the qualitative relationship between cave and surface climate with implications for hibernaculum suitability. However, we realized a more quantitative understanding of the conditions in which bats hibernate and how they may promote or mediate WNS impacts was required. We compiled subterranean temperatures from caves and mines across the western United States and Canada to: a) quantify the hypothesized relationship between MAST and subterranean temperature and how it is influenced by measurable site attributes, and b) use readily available gridded data to predict and continuously map the range of temperatures that may be available in caves and mines. Our analysis supports qualitative predictions that subterranean winter temperatures are correlated with MAST, that temperatures are warmer and less variable farther from the surface, and that even deep within caves temperatures tend to be lower than MAST. Effects of other site attributes (e.g., topography, vegetation, precipitation) on subterranean temperatures were not detected. We then assessed the plausibility of model-predicted temperatures using knowledge of winter bat distributions and preferred hibernaculum temperatures. Our model unavoidably simplifies complex subterranean environments, and is not intended to explain all variability in subterranean temperatures. Rather, our results offer researchers and managers improved broad-scale estimates of the geographic distribution of potential hibernaculum conditions compared to reliance on MAST alone. Later, we used this information to better support range-scale estimation of winter bat distributions and projection of likely WNS impacts across the West.

- While we worked to improve hibernation energetics models we also critically examined spatial heterogeneity in host traits linked to survival. To do so, we developed predictive spatial models of body mass for the *M. lucifugus* and reassessed previous definitions of the duration of winter hibernation. Using data from published literature, public databases, local experts, and our own fieldwork, we fit a series of generalized linear models with

hypothesized abiotic drivers to create distribution-wide predictions for the duration of winter and pre-hibernation body fat. Our results provide improved estimations of the duration of winter hibernation and identify a scaling relationship between body mass and body fat allowing us to create the first continuous estimates of pre-hibernation body mass and fat across the species distribution. We used these results and a mechanistic hibernation energetic model to create spatially varying winter fat use estimates for *M. lucifugus*. These results predict that WNS mortality of *M. lucifugus* in western North America may be comparable to the substantial die-off observed in eastern populations.

- In multi-host disease systems, differences in mortality between species may reflect variation in host physiology, morphology, and behavior. In systems where the pathogen can persist in the environment, microclimate conditions, and the adaptation of the host to these conditions, may also impact mortality. We assessed the effects of body mass, torpid metabolic rate, evaporative water loss, and hibernaculum temperature and water vapor deficit on predicted overwinter survival of bats infected by *P. destructans*. We used our refined hibernation energetics model in an individual-based model framework to predict the probability of survival of nine bat species at eight sampling sites across North America. The model predicts time until fat exhaustion as a function of host characteristics, hibernaculum microclimate, and fungal growth. We fit a linear model to determine relationships with each variable and predicted survival and semi-partial correlation coefficients to determine the major drivers in variation in bat survival. Six of the species modeled were predicted to not survive WNS, including all five small *Myotis species* and *P. subflavus* (tricolored bat). We found host body mass and hibernaculum water vapor deficit explained over half of the variation in survival with WNS across species. These results indicate that larger bats that roost in drier conditions are less susceptible to the disease due to increased fat stores and roosting conditions that are unsuitable for the fungus that causes WNS. Our results highlight some key predictors of interspecific survival among western bat species and provide a framework to assess impacts of WNS as the fungus continues to spread into western North America.

Objective 3
Develop approaches that integrate the mechanistic WNS survivorship model with species distribution models to evaluate the presence of WNS with plausible scenarios of non-stationary conditions (e.g. climate change) and to explore the sensitivity of the integrated model to different parameters and data availability.

- Western North America hosts the highest bat diversity in the United States and Canada, yet little is known about western hibernacula and western bats' hibernation behavior. An improved understanding of where bats hibernate in the West and the conditions that create suitable hibernacula is critical if land managers are to anticipate and address the conservation needs of WNS-susceptible species in the United States and Canada. We estimated the relative probability of occurrence during winter across the ranges of five bat species occurring in the West. We estimated winter survival capacity from our mechanistic survivorship model based on bat bioenergetics and climate conditions. Leveraging the Google Earth Engine platform for spatial data processing, we used boosted regression trees to integrate these survivorship estimates with key landscape

attributes and relate them to bat occurrence data in a hybrid correlative-mechanistic approach. We show that winter survival capacity, topography, land cover, and access to caves and mines are important predictors of winter hibernaculum selection, but the shape and relative importance of these relationships vary among species. Our findings suggest that the occurrence of bat hibernacula can, in part, be predicted from readily mapped above-ground features, and is not only dictated by below-ground characteristics for which spatial data are lacking. Furthermore, our mechanistic estimate of winter survivorship was among the strongest predictors of winter occurrence probability across focal species.

- Our findings not only offer an improved understanding of the likely winter distribution of bats occurring in the West, but also a baseline for assessing the potential species-level impacts of *P. destructans* as well as future climate change. Using our hybrid species distribution model, we substituted survivorship under current conditions with survivorship given exposure to *P. destructans,* under both current climate conditions and four future climate scenarios derived from multiple regional climate models run on boundary conditions derived from multiple global circulation models. We demonstrate that in general, occurrence probability is expected to decline following exposure to *P. destructans,* but that projected changes in climate may offer a rescue effect for many species in some or all of their ranges. We observed minimal variability in both the magnitude and spatial patterns in these projections among climate scenarios. However, managers must consider whether these potential positive effects of a warming climate for bat survivorship will arrive soon enough to benefit bats exposed to *P. destructans* and should design monitoring and conservation efforts accordingly.

Implications for future research and conservation efforts
As a bat-killing pathogen reaches new western species and populations, how do we effectively build on what the scientific and management community has learned? Since it appeared in 2006 we have acquired an astounding amount of knowledge about the pathogen, hibernating bat species as hosts, their interactions, and the environmental conditions that influence both. With the increased funding for bat research due to this disease threat, our understanding of basic bat biology, physiology, and ecology has expanded. Augmenting the foundational research that began in 2006, recent studies of remnant populations in the East offer a glimmer of hope that genetic adaptations and evolutionary rescue may be underway. There is also new physiological trait data and research on western hibernating bats from this project showing how certain environmental niches could allow some bats to survive the energetic consequences of the infection. Combined, these findings support the need for proactive interventions for existing populations to reduce other simultaneous threats such as habitat loss and fragmentation, loss of water sources, and climate change. To give susceptible species the best chance at evolutionary rescue, we will need policies that protect populations and conserve the greatest amount of genetic diversity. The initial surveillance and containment response effort provided much needed time for us to understand this threat, but the spread of the fungal pathogen across North America now appears inevitable. To protect susceptible bat species in the West (and those in the East) we can start applying what we have learned in the preceding years, redouble our scientific and conservation efforts, and seek opportunities for broader western coalitions and effective conservation policies.

Hibernating bat species are diverse and unique (and so are their responses to WNS)

147

As the outbreak grew, it was clear that not all exposed species experienced high mortality. Diagnostic symptoms of WNS occurred in some hibernating bat species and in the remainder, *P. destructans* was detected in the absence of, or in the presence of limited disease pathology (United States Fish & Wildlife Service 2020). This contradiction was one of the motivating questions behind this project. Traits associated with roost microclimates, bat morphology, physiology, behavior, and immune response were hypothesized as possible explanations for the differentiation. Complicating matters, beyond roost microclimate and basic morphologic data, prior to this project, there was very little science on the risk factors that could inform the interspecies susceptibility debate. We moved the science forward on interspecies susceptibility, likely linked to both hibernation ecophysiology and immune responses to *P. destructans* infection (Bernard et al. 2020), by measuring key bioenergetic parameters of 13 western bat species. EWL appears to be disrupted in WNS-affected bats, and in particular our efforts show it appears that species with high rates of water loss are those that preferentially select roost sites with high humidity, where the fungus also grows well (Haase et al. In Review). Prior to our contributions, the hibernation literature (and even our own thinking) was heavily biased towards a focus on traits of fat and metabolic, but our collective work has raised the profile of the importance of EWL and how non-fat components might come into play for water balance. There are now also indications of differential immune responses among species. A new transcriptome study tracked the regulation of immune and defense genes in infected versus control tissues from individual bats and reported *M. lucifugus* (high WNS mortality) and *M. myotis* (European species, no WNS mortality) both mounted a more systematic host immune response than *E. fuscus* (low WNS mortality), which mounted an 'extremely localized response' (Davy et al. 2020). The authors point to phylogenetic-based differences in host immune response and micro-flora known to be associated with *E. fuscus* that inhibit *P. destructans* growth as possible explanations.

Evolution as an intervention
Hopefully, and counter to initial extinction projections, some populations of *M. lucifugus*, persist and may even be increasing at sites that experienced massive WNS population crashes (Dobony and Johnson, 2018; Langwig et al. 2015; Maslo et al. 2015; Langwig et al. 2012; Frick et al. 2015; Frank et al. 2019). Evolutionary rescue is 'the idea that evolution might occur sufficiently fast enough to arrest population decline and allow population recovery before extinction ensues' (Gonzalez et al. 2013). In early support of evolutionary rescue, Auteri and Knowles (2020) examined the genome of *M. lucifugus* survivors and non-survivors for single nucleotide polymorphisms and found changes in genes associated with torpor arousals, fat breakdown, and vocalizations. These initial findings will need further scientific replication and scrutiny, but altogether these are hopeful indications that eco-evolutionary dynamics may at least help some populations of *M. lucifugus* and perhaps other species overcome WNS (Bell 2017).

The mechanism of evolutionary rescue is the genetic selection of host traits, physiological, immune or otherwise, that influence the survival outcome of *P. destructans* infection. An underlying assumption of evolutionary rescue is that some proportion of individuals have a genotype and phenotype that results in WNS survival. Selected traits will depend on existing natural variability within the population and their probability of occurrence. The hibernation energetics of susceptible bat species indicate that critical differences in survival may hinge on small shifts of roost temperature and humidity, fat stores, and arousal frequency or torpor bout

duration (Haase et al. 2019b; Haase et al. In Review; Hranac et al. In Review; Lilley et al. 2016 Cheng et al. 2019). For example, our energetic model of *M. lucifugus* at a hibernaculum in central Montana predicted high mortality but also suggested a small survival window exists, where cooler temperatures would reduce fungal growth and greater fat mass would prolong survival (Haase et al. 2019b; Hranac et al. In Review). Observations of mean torpor bout duration shifting from 7.6 days during the first year of severe mortality to 14.7 and 12.9 days in years six and seven, respectively, is potential evidence of physiological adaptation (Frank et al. 2019). Evidence of fungal load reductions in surviving eastern *M. lucifugus* populations also suggests resistance to the pathogen may have developed (Langwig et al. 2012, 2017). That resistance may be immune-related or associated with shifting attributes of clustering, density, and microclimate that reduce fungal growth (Langwig et al. 2012). That said, evolution or adaptations to survive WNS may not be occurring in all populations or species. A precautionary approach to retain as much of the existing natural variability both within and among populations as possible is warranted because the distribution of potential survival traits remains unknown.

Keep in mind the survival of western species and populations will be dependent on their ability to cope with other significant population threats, including but not limited to WNS, and the capacity for adaptation. WNS has already placed some species in a population bottleneck (Langwig et al. 2012; Lilley et al. 2016) and it may yet result in extinctions. At present almost all bat evolutionary rescue research has focused on a single species, *M. lucifugus*, and it is not clear if the beneficial traits will evolve in all threatened, diseased or otherwise, populations or species. However, if there is sufficient population size and diversity of western bat species, evolution may allow susceptible species to escape this bottleneck and overcome WNS as well as other threats (Bell et al. 2017; Maslow and Fefferman 2015; Frank et al. 2019).

We should all keep in mind that any recovery will be slow: a typical insectivorous bat population of 10,000 bats that suffered a 10% population decline would take ~100 years to rebound assuming pre-WNS rates of population growth (Langwig et al. 2012). Even if trajectories are positive, stochastic events may result in extirpations or extinction, and the former may indicate the subsequent need for translocations or accepting a new species assemblage equilibrium.

Bat ecology research is bat survival research
Like many other threatened species, we are playing catchup and it will be necessary to keep growing our ecological knowledge of bat species. The science behind evolutionary rescue holds that, 'abundance, variation, and dispersal have pronounced and repeatable effects on the rescue of populations and communities' (Bell et al. 2017). We need greater understanding of these baseline attributes and more science that studies how threats impact these attributes.
As a starting point we need more information on the diverse ecology of western bat species, including habitat type and range size requirements, and dynamics throughout the year. For example, systematic range-wide efforts like the North American Bat Monitoring Program (NABat) are essential to understand variation of bat habitat use in space and time. NABat is one standardized methodology to collect acoustic bat occurrence data that has not yet reached its full operational potential, but its unbiased sampling approach promises to provide much improved estimates of species summer occurrence across North America (Rodhouse et al. 2015). For winter habitat, a recent effort documented nearly 3,000 known western cave and mine hibernacula along with population trends, but it was a retrospective study limited to analyses of

C. townsendii and *Myotis* at the genus level (Weller et al. 2018). Accurate species range maps and habitat needs are essential to build the information on western bat ecology needed to design effective conservation policies. For the WNS threat, just as important as where species are found is how they overcome the energetic challenge of hibernation. Our first-of-its-kind study measured critical baseline aspects of hibernation physiology across 13 species at sites from Texas to northern Canada, from Oklahoma to Oregon (McGuire et al. In Review). Combining our empirical data with a bioenergetic model of winter hibernation, we identified interspecific differences of water loss and associated bioenergetic costs that elevated WNS susceptibility (Haase et al. In Review). Further risk assessments and refined range maps can help prioritize western species for research and lands for conservation action.

We need more granular ecological science too. Outstanding research questions for western species include the use of non-traditional hibernacula, like exposed rock outcrops or talus slopes, patterns of co-roosting, winter activity patterns, and intra-annual movement patterns. Related to dispersal and the potential for bats to move survival traits to new populations, technology may soon be small enough to provide a clearer understanding of bat movement patterns throughout the year (Weller et al. 2016; Castle et al. 2015; Taylor et al. 2017).

We also need to bolster research on the understudied threats to western populations (Jones et al. 2009; Voigt et al. 2016) that may present additional selective sweeps alongside the pressure of a selection for WNS survival traits. Stressful environments are known to further impede evolutionary rescue and amplify extinction risk (Seltmann et al. 2017; Lachapelle et al. 2017; Davy et al. 2016). Climate change is a global threat and source of uncertainty that will alter both summer and winter bat habitat, perhaps with likely more immediate effects on drought and water availability in the arid West but it could also help abate the energetic stress of WNS (Adams et al. 2010; Jones et al. 2009; McClure et al. 2020). Then there are the unknown impacts of habitat and wetland loss on high-quality roosting and foraging habitat (Korine et al. 2016; Jung and Threlfall 2016; Fuller et al. 2020; United States Environmental Protection Agency 2016). A critical open question is whether global insect declines, driven by habitat loss and pollution from pesticides and fertilizers, compromise bat prey biomass and consequently fat stores (Forister et al. 2019; Sánchez-Bayo et al. 2019; Lister and Garcia 2018; Hallmann et al. 2017; Jones et al. 2009; Cheng et al. 2019). More fundamentally, we do not know if bat populations are presently limited by prey availability and researchers have yet to rigorously tackle the potential threat of pesticides on bat prey species and overall health. This overwhelming lack of knowledge about proposed threats is a threat unto itself that further compounds efforts to conserve bats (Frick et al. 2019).

There is clearly a lot of scientific discovery ahead, and an urgent need to fill knowledge gaps and synthesize findings with an ever-shortening window to gain additional pre-WNS baseline data. Once listed, well-intentioned regulations for endangered species can end up impeding research and create perverse incentives to obscure the presence of listed species to avoid restrictions and requirements, whether real or perceived. If species are protected, policies should be made with consideration for how they will impact research and management interventions necessary to advance conservation priorities.

Customize interventions for the West

First and foremost, the basic rule of do no harm applies, but we should not shirk from improvisation either. Creative use of proactive bat conservation research and measures that support the adaptive capacity of susceptible western species is likely to help reduce the risk of extinction from WNS and other threats. A precautionary principle approach to evolutionary rescue necessitates instituting strong conservation measures that maintain and support all populations of susceptible species, not just those in regions where WNS is currently endemic. The western WNS response has an unprecedented opportunity to leverage proactive interventions across vast amounts of land that are under public land management. The United States federal government manages 47% of the land area across 11 contiguous western states (excluding Alaska), versus just 4% in the remaining lower 48 (Poschman et al. 2014). Acting independently or together, the Department of the Interior, Department of Agriculture, Department of Defense, state, as well as tribal land-management agencies are positioned to be significant bat conservation stakeholders. The size of western public and tribal land allotment would amplify the value of any proactive measures implemented on federal and tribal lands.

Current federal species listings due to WNS focus solely on species already in a tailspin and the United States and Canada have implemented different levels of protection (Table 17). Why not place proactive protections for at-risk western bat species at the federal, state, or provincial level now, whether or not they have shown dramatic declines? And if a species is listed, regulations should cover whole population conservation, the genetic diversity of the species, and remnant populations. Only *M. septentrionalis* has received Endangered Species Act protections in the United States due to WNS and as a threatened species, the main restrictions only apply to areas already affected by WNS (Table 17).

Table 17. Summary of existing policy tools compared against an ideal proactive policy tool designed to support evolutionary rescue.

Policy tool	Covers WNS threatened species not yet in rapid decline	Whole population conservation	Designed to protect genetic diversity and remnant populations	Restrictions against incidental take
United States Endangered Species Act 4(d) rule for *Myotis septentrionalis*	No	No	No	Limited*
Canada Species at Risk Act listings for *M. lucifugus*, *Perimyotis subflavus*, & *M. septentrionalis* under section 41(1)	No	Yes	Yes	Limited†
Proactive policy	Yes	Yes	Yes	Yes

*Incidental take of *M. septentrionalis* (northern long-eared bat) outside of hibernacula resulting from activities other than tree removal is not prohibited' (https://www.fws.gov/midwest/endangered/mammals/nleb/pdf/FRnlebFinal4dRule14Jan2016.pdf).
†Allows permitting of activities in which incidental take will occur.

The Recovering America's Wildlife Act of 2019 to 'amend the Pittman-Robertson Wildlife Restoration Act to make supplemental funds available for management of fish and wildlife species of greatest conservation need as determined by State fish and wildlife agencies, and for other purposes' (https://www.congress.gov/bill/116th-congress/house-bill/3742/text) is currently under congressional review. Such funds could be channeled to proactive bat conservation efforts to help avert future listings.

Moving into 2020 and beyond, land managers at any level in the United States and Canada should make a concerted effort to evaluate proposed activities for impacts on bat species that are susceptible to WNS, to avoid or minimize those impacts, and to sponsor research when impacts are unknown. For example in 2020, the Arkansas Game and Fish Commission amended a state wildlife management regulation to ban nuisance bat killing unless rabies testing was indicated due to a potential exposure (https://www.agfc.com/en/wildlife-management/nuisance-wildlife/). Integrated pest-management plans and policies should require non-lethal exclusionary measures to remove nuisance bats from structures with exceptions for cases of potential rabies exposure. Monitoring and testing, when possible, will be critical to track disease progression and extinction threats. Early *P. destructans* detection sets a starting point for monitoring and attributing subsequent impact. Survival rate data can help us understand specific drivers of survival or mortality in susceptible species (DiRenzo et al. 2018).

COVID-19 has also introduced new challenges to managing bats, with some agencies recommending euthanasia of bats coming in contact with humans, and cessation of rehabilitation in some states (e.g., Association of Fish & Wildlife Agencies 2020). With the widescale accessibility of personal protective equipment, and a deeper understanding of the spread of the SARS-CoV-2 virus, these reactionary lethal policies were later partially lifted in some jurisdictions, but this shines light on the unpreparedness to deal with wildlife disease issues as it pertains to species at risk and species that are otherwise protected.

We should carefully evaluate each tech-based disease management strategy for the western context. These include biological or chemical agents that target the fungus, vaccination of bats, genetic engineering of host or pathogen that reduces mortality (i.e. CRISPR-type methods), or mechanically changing microclimate bat environments (USFWS 2020). Many existing strategies are not suited to the dispersed and inaccessible nature of western bats (i.e. direct treatment hibernaculum sites, vaccinations). At minimum there needs to be full transparency of an intervention's benefits, risks, efficacy, and long-term costs. Risks now include potentially altering the natural trajectory of evolutionary rescue. While much remains unknown about the potential of evolutionary rescue, it should be considered just as feasible as other tech-based interventions that likewise remain unproven, and it is the only real long-term sustainable solution among available options. Other interventions that provide a short-term benefit could wind up being a net-loss if they offset an evolutionary rescue process. These same considerations apply to more supportive interventions, such as those inoculating bats with local probiotics to reduce fungal growth or those seeking to improve spring maternal survival with 'hot boxes'. Western agency managers are going to face tough decisions to optimize management objectives and balance risk and uncertainty. Structured decision making processes have been used to help managers navigate the WNS intervention problem space (Bernard et al. 2020), i.e. whether to invest in costly treatments and/or invest in proactive conservation measures. The Achilles' heel

of structured decision making is that it relies on available information and research to inform options, and managers, as the name implies are liable to choose a short-term intervention over what may appear to be a passive 'do nothing' outcome. In reality, precautionary principle proactive approaches are really 'do more' results with interventions designed to support diverse populations of bats.

It is only a matter of time before all North American bat species are exposed to *P. destructans.* The potential of evolutionary rescue warrants greater proactive conservation actions than have been considered. Bold action is needed, including extended protections on state, federal, private, and tribal western lands to at-risk species, support for more fundamental or baseline research on bats, and a willingness to keep trying new things.

Literature Cited

Literature Cited

Adams, R., 2003. Bats of the Rocky Mountain West: natural history, ecology and conservation. University Press of Colorado, Boulder, CO.

Adams, R.A., 2010. Bat reproduction declines when conditions mimic climate change projections for western North America. Ecology, 91(8), 2437–2445. https://doi.org/10.1890/09-0091.1

Alves, D.M.C.C., Terribile, L.C., Brito, D., 2014. The potential impact of white-nose syndrome on the conservation status of North American bats. PLoS One, 9(9), 1–7. https://doi.org/10.1371/journal.pone.0107395

Anderson, S.C., Ward, E.J., 2019. Black swans in space: modeling spatiotemporal processes with extremes. Ecology, 100(1), e02403. https://doi.org/10.1002/ecy.2403

Armitage, K.B., Blumstein, D.T., Woods, B.C., 2003. Energetics of hibernating yellow-bellied marmots (*Marmota flaviventris*). Comparative Biochemistry and Physiology Part A: Molecular & Integrative Physiology, 134(1), 101–114. https://doi.org/10.1016/S1095-6433(02)00219-2

Association of Fish & Wildlife Agencies. Voluntary interim guidance for bat-related activities in response to COVID-19 Version 1.0 (April 13, 2020) https://www.fishwildlife.org/application/files/1915/9230/2350/Covid-19_Guidance_for_Bats_4-13-2020a11.docx

Auteri, G.G., Knowles, L.L., 2020. Decimated little brown bats show potential for adaptive change. Scientific Reports, 10, 3023. https://doi.org/10.1038/s41598-020-59797-4

Baba, K., Shibata, R., Sibuya, M., 2004. Partial correlation and conditional correlation as measures of conditional independence. Australian & New Zealand Journal of Statistics, 46(4), 657–664. https://doi.org/10.1111/j.1467-842X.2004.00360.x

Bakken, G.S., 1976a. A heat transfer analysis of animals: unifying concepts and the application of metabolism chamber data to field ecology. Journal of Theoretical Biology, 60(2), 337–384. https://doi.org/10.1016/0022-5193(76)90063-1

Bakken, G.S., 1976b. An improved method for determining thermal conductance and equilibrium body temperature with cooling curve experiments. Journal of Thermal Biology, 1(3), 169–175. https://doi.org/10.1016/0306-4565(76)90009-7

Bartón, K., 2018. MuMIn: Multi-model inference. R package version 1.42.1. http://cran.r-project.org/package=MuMIn

Bell, G., 2017. Evolutionary rescue. Annual Review of Ecology, Evolution, and Systematics, 48(1), 605–627. https://doi.org/10.1146/annurev-ecolsys-110316-023011

Bellamy, C., Scott, C., Altringham, J., 2013. Multiscale, presence-only habitat suitability models: Fine-resolution maps for eight bat species. Journal of Applied Ecology, 50(4), 892–901. https://doi.org/10.1111/1365-2664.12117

Belsley, D.A., 1991. Conditioning diagnostics. John Wiley & Sons, Inc.

Ben-Hamo, M., Muñoz-Garcia, A., Williams, J.B., Korine, C., Pinshow, B., 2013. Waking to drink: rates of evaporative water loss determine arousal frequency in hibernating bats. Journal of Experimental Biology, 216, 573–577. https://doi.org/10.1242/jeb.078790

Bernard, R.F., Reichard, J.D., Coleman, J.T.H., Blackwood, J.C., Verant, M.L., Segers, J.L., Lorch, J.M., White, J., Moore, M.S., Russell, A.L., Katz, R.A., Lindner, D.L., Toomey, R.S., Turner, G.G., Frick, W.F., Vonhof, M.J., Willis, C.K.R., Grant, E.H.C., 2020. Identifying research needs to inform white-nose syndrome management decisions. Conservation Science and Practice, 2(8), 1–17. https://doi.org/10.1111/csp2.220

Bilecki, L.C., 2003. Bat hibernacula in the karst landscape of Central Manitoba: protecting critical wildlife habitat while managing for resource development. Master's Thesis, University of Manitoba. http://hdl.handle.net/1993/3794

Bivand, R.S., Wong, D.W.S., 2018. Comparing implementations of global and local indicators of spatial association. Test, 27, 716–748. https://doi.org/10.1007/s11749-018-0599-x

Blehert, D.S., Hicks, A.C., Behr, M., Meteyer, C.U., Berlowski-Zier, B.M., Buckles, E.L., Coleman, J.T.H., Darling, S.R., Gargas, A., Niver, R., Okoniewski, J.C., Rudd, R.J., Stone, W.B., 2009. Bat white-nose syndrome: an emerging fungal pathogen? Science, 323(5911), 227–227. https://doi.org/10.1126/science.1163874

Booth, G.D., Niccolucci, M.J., Schuster, E.G., 1994. Identifying proxy sets in multiple linear regression: an aid to better coefficient interpretation. Research paper INT (USA).

Boratyński, J.S., Willis, C.K., Jefimow, M., Wojciechowski, M.S., 2015. Huddling reduces evaporative water loss in torpid Natterer's bats, *Myotis nattereri*. Comparative Biochemistry and Physiology Part A: Molecular & Integrative Physiology, 179, 125–132. https://doi.org/10.1016/j.cbpa.2014.09.035

Boyce, M.S., Vernier, P.R., Nielsen, S.E., Schmiegelow, F.K., 2002. Evaluating resource selection functions. Ecological Modelling, 157(2–3), 281–300. https://doi.org/10.1016/S0304-3800(02)00200-4

Boyles, J.G., Dunbar, M.B., Storm, J.J., Brack, V., 2007. Energy availability influences microclimate selection of hibernating bats. Journal of Experimental Biology, 210(24), 4345–4350. https://doi.org/10.1242/jeb.007294

Boyles, J.G., Storm, J.J., Brack Jr, V., 2008. Thermal benefits of clustering during hibernation: a field test of competing hypotheses on *Myotis sodalis*. Functional Ecology, 22(4), 632–636. https://doi.org/10.1111/j.1365-2435.2008.01423.x

Boyles, J.G., Brack, V., 2009. Modeling Survival Rates of Hibernating Mammals with Individual-Based Models of Energy Expenditure. Journal of Mammalogy, 90, 9–16. https://doi.org/10.1644/08-MAMM-A-205.1

Boyles, J.G., McKechnie, A.E., 2010. Energy conservation in hibernating endotherms: Why "suboptimal" temperatures are optimal. Ecological Modelling, 221(12), 1644–1647. https://doi.org/10.1016/j.ecolmodel.2010.03.018

Boyles, J.G., Johnson, J.S., Blomberg, A., Lilley, T.M., 2020. Optimal hibernation theory. Mammal Review, 50(1), 91–100. https://doi.org/10.1111/mam.12181

Brack, V., Twente. J.W., 1985. The duration of the period of hibernation of three species of vespertilionid bats. Canadian Journal of Zoology, 63(12), 2952–2954. https://doi:10.1139/z85-442

Brack, V., 2007. Temperatures and locations used by hibernating bats, including *Myotis sodalis* (Indiana Bat), in a limestone mine: implications for conservation and management. Environmental Management 40, 739–746. https://doi.org/10.1007/s00267-006-0274-y

Brigham, R., Ianyzzo, C., Hamilton, N., Fenton, M., 1990. Histochemical and biochemical plasticity of muscle fibers in the little brown bat, *Myotis lucifugus*. Journal of Comparative Physiology B, 160(2), 183–186. https://doi:10.1007/bf00300951

British Columbia (BC) Geological Survey, 2019. MINFILE Production Database. Ministry of Energy, Mines and Petroleum Resources. https://catalogue.data.gov.bc.ca/dataset/minfile-production-database

Brotons, L., Manosa, S., Estrada, J., 2004. Modelling the effects of irrigation schemes on the distribution of steppe birds in Mediterranean farmland. Biodiversity Conservation, 13(5), 1039–1058. https://doi:10.1023/b:bioc.0000014468.71368.35

Burnham, K.P., Anderson, D.R., 2002. Model selection and multimodel inference: a practical information-theoretic approach. Springer Science & Business Media.

Burnham, K.P., Anderson, D.R., 2004. Multimodel inference: understanding AIC and BIC in model selection. Sociological Methods & Research, 33(2), 261–304. https://doi.org/10.1177/0049124104268644

Campbell, G.S., Norman, J.M., 1998. An Introduction to Environmental Biophysics. Springer-Verlag, New York.

Cannon, A.J., 2018. Multivariate quantile mapping bias correction: an N-dimensional probability density function transform for climate model simulations of multiple variables. Climate dynamics 50(1–2), 31–49. https://doi.org/10.1007/s00382-017-3580-6

Carey, C., 1993. Why do hibernators periodically arouse? Overview. Life in the Cold: Ecological, Physiological and Molecular Mechanism. Westview, Boulder, Colorado, 25–34.

Carey, H.V., 1990. Seasonal changes in mucosal structure and function in ground squirrel intestine. American Journal of Physiology-Regulatory, Integrative and Comparative Physiology, 259, R385–R392. https://doi.org/10.1152/ajpregu.1990.259.2.R385

Carnell, R., 2016. Package lhs: Latin Hypercube Samples. Available from http://lhs.r-forge.r-project.org

Castle, K.T., Weller, T.J., Cryan, P.M., Hein, C.D., Schirmacher, M.R., 2015. Using sutures to attach miniature tracking tags to small bats for multimonth movement and behavioral studies. Ecology and Evolution, 5(14), 2980–2989. https://doi.org/10.1002/ece3.1584

Cheng, T.L., Gerson, A., Moore, M.S., Reichard, J.D., DeSimone, J., Willis, C.K.R., Frick, W.F., Kilpatrick, A.M., 2019. Higher fat stores contribute to persistence of little brown bat populations with white-nose syndrome. Journal of Animal Ecology, 88(4), 591–600. https://doi.org/10.1111/1365-2656.12954

Cory Toussaint, D.C., McKechnie, A.E., Van der Merwe, M., 2010. Heterothermy in free-ranging male Egyptian free-tailed bats (*Tadarida aegyptiaca*) in a subtropical climate. Mammalian Biology, 75(5), 466–470. https://doi.org/10.1016/j.mambio.2009.06.001

COSEWIC, 2013. COSEWIC assessment and status report on the little brown myotis *Myotis lucifugus*, northern myotis *Myotis septentrionalis* and tri-colored bat *Perimyotis subflavus* in Canada www.registrelep-sararegistry.gc.ca/default_e.cfm (accessed 01.12.15)

Cranford, J.A., 1983. Body temperature, heart rate and oxygen consumption of normothermic and heterothermic western jumping mice (*Zapus princeps*). Comparative Biochemistry and Physiology Part A: Physiology, 74(3), 595-599. https://doi.org/10.1016/0300-9629(83)90553-4

Cryan, P.M., Wolf, B.O., 2003. Sex differences in the thermoregulation and evaporative water loss of a heterothermic bat, Lasiurus cinereus, during its spring migration. Journal of Experimental Biology, 206, 3381–3390. https://doi.org/10.1242/jeb.00574

Cryan, P.M., Meteyer, C.U., Boyles, J.G., Blehert, D.S., 2010. Wing pathology of white-nose syndrome in bats suggests life-threatening disruption of physiology. BMC Biology, 8(1), 135. https://doi.org/10.1186/1741-7007-8-135

Czenze, Z.J., Park, A.D., Willis, C.K.R., 2013. Staying cold through dinner: cold-climate bats rewarm with conspecifics but not sunset during hibernation. Journal of Comparative Physiology B, 183, 859–866. https://doi.org/10.1007/s00360-013-0753-4

Czenze, Z.J., Willis, C.K.R., 2015, Warming up and shipping out: arousal and emergence timing in hibernating little brown bats (*Myotis lucifugus*). Journal of Comparative Physiology B, 185, 575–586. https://doi:10.1007/s00360-015-0900-1

Czenze, Z.J., Jonasson, K.A., Willis, C.K., 2017. Thrifty females, frisky males: Winter energetics of hibernating bats from a cold climate. Physiological and Biochemical Zoology, 90, 502–511. https://doi.org/10.1086/692623

Davis, R.B., Herreid, C.F., Short, H.L., 1962. Mexican free-tailed bats in Texas. Ecological Monographs, 32(4), 311–346. https://doi.org/10.2307/1942378

Davis, W.H., Hitchcock, H.B., 1964. Notes on sex ratios of hibernating bats. Journal of Mammalogy, 45(3), 475–476. https://doi.org/10.2307/1377426

Davis, W.H., Hitchcock, H.B., 1965. Biology and migration of the bat, *Myotis lucifugus*, in New England. Journal of Mammalogy, 46(2), 296–313. https://doi.org/10.2307/1377850

Davy, C.M., Mastromonaco, G.F., Riley, J.L., Baxter-Gilbert, J.H., Mayberry, H., Willis, C.K.R., 2017. Conservation implications of physiological carry-over effects in bats recovering from white-nose syndrome. Conservation Biology 31(3), 615–624. https://doi.org/10.1111/cobi.12841

Davy, C.M., Donaldson, M.E., Bandouchova, H., Breit, A.M., Dorville, N.A.S., Dzal, Y.A., Kovacova, V., Kunkel, E.L., Martínková, N., Norquay, K.J.O., Paterson, J.E., Zukal, J., Pikula, J., Willis, C.K.R., Kyle, C.J., 2020. Transcriptional host–pathogen responses of *Pseudogymnoascus destructans* and three species of bats with white-nose syndrome. Virulence 11(1), 781–794. https://doi.org/10.1080/21505594.2020.1768018

Day, K.M., Tomasi, T.E., 2014. Winter energetics of female Indiana bats, *Myotis sodalis*. Physiological and Biochemical Zoology, 87(1), 56–64. https://doi.org/10.1086/671563

De'Ath, G., 2007. Boosted trees for ecological modeling and prediction. Ecology, 88(1), 243–251. https://doi.org/10.1890/0012-9658(2007)88[243:BTFEMA]2.0.CO;2

Department of the Interior: Fish and Wildlife Service, Endangered and Threatened Wildlife and Plants; 12-Month Finding on a Petition to List the Eastern Small-Footed Bat and the Northern Long-Eared Bat as Endangered or Threatened Species; Listing the Northern Long-Eared Bat as an Endangered Species. Federal Register. 78, 61046–61080 (2013).

Dickson, B.G., Beier, P., 2007. Quantifying the influence of topographic position on cougar, *Puma concolor*, movement in southern California, USA. Journal of Zoology, 271(3), 270–277. https://doi.org/10.1111/j.1469-7998.2006.00215.x

DiRenzo, G. V., Zipkin, E.F., Grant, E.H.C., Royle, J.A., Longo, A. V., Zamudio, K.R., Lips, K.R., 2018. Eco-evolutionary rescue promotes host–pathogen coexistence. Ecological Applications 28(8), 1948–1962. https://doi.org/10.1002/eap.1792

Dobony, C.A., Johnson, J.B., 2018. Observed resiliency of little brown myotis to long-term white-nose syndrome exposure. Journal of Fish and Wildlife Management. 9(1), 168–179. https://doi.org/10.3996/102017-JFWM-080

Dubois, J.E., Monson, K.M., 2007. Recent distribution records of the little brown bat, *Myotis lucifugus*, in Manitoba and Northwestern Ontario. The Canadian Field-Naturalist, 121(1), 57–61. http://dx.doi.org/10.22621/cfn.v121i1.393

Ducci, L., Agnelli, P., Di Febbraro, M., Frate, L., Russo, D., Loy, A., 2015. Different bat guilds perceive their habitat in different ways: a multiscale landscape approach for variable selection in species distribution modelling. Landscape Ecology, 30(10), 2147–2159. https://doi.org/10.1007/s10980-015-0237-x

Dunbar, M.B., Brigham, R.M., 2010. Thermoregulatory variation among populations of bats along a latitudinal gradient. Journal of Comparative Physiology B, 180(6), 885–893. https://doi.org/10.1007/s00360-010-0457-y

Elith, J., Graham, C.H., Anderson, R.P., Dudík, M., Ferrier, S., Guisan, A., Hijmans, R.J., Huettmann, F., Leathwick, J.R., Lehmann, A., Li, J., Lohmann, L.G., Loiselle, B.A., Manion, G., Moritz, C., Nakamura, M., Nakazawa, Y., Overton, J. McC., Peterson, A.T., Phillips, S.J., Richardson, K.S., Scachetti-Pereira, R., Schapire, R.E., Soberón, J., Williams, S., Wisz, M.S., Zimmermann, N. E., 2006. Novel methods improve prediction of species' distributions from occurrence data. Ecography, 29(2), 129–151. https://doi.org/10.1111/j.2006.0906-7590.04596.x

Elith, J., Leathwick, J.R., Hastie, T., 2008. A working guide to boosted regression trees. Journal of Animal Ecology, 77(4), 802–813. https://doi.org/10.1111/j.1365-2656.2008.01390.x

Escobar, L.E., Qiao, H., Cabello, J., Peterson, A.T., 2018. Ecological niche modeling re-examined: A case study with the Darwin's fox. Ecology and Evolution, 8(10), 4757–4770. https://doi.org/10.1002/ece3.4014

Fan, Y., Li, H., Miguez-Macho, G., 2013. Global patterns of groundwater table depth. Science, 339(6122), 940–943. https://doi.org/10.1126/science.1229881

Farr, T.G., Rosen, P.A., Caro, E., Crippen, R., Duren, R., Hensley, S., Kobrick, M., Paller, M., Rodriguez, E., Roth, L., Seal, D., Shaffer, S., Shimada, J., Umland, J., Werner, M., Oskin, M., Burbank, D., Alsdorf, D., 2007. The shuttle radar topography mission. Reviews of Geophysics, 45(RG2004), 1–13. https://doi.org/10.1029/2005RG000183

Fenton, M.B., 1970. Population studies of *Myotis lucifugus* (Chiroptera: Vespertilionidae) in Ontario. Toronto, Canada: The Royal Ontario Museum. Available: https://www.biodiversitylibrary.org/item/111399

Fenton, M.B., 1972. Distribution and over-wintering of *Myotis leibii* and *Eptesicus fuscus* (Chiroptera: Vespertilionidae) in Ontario. The Royal Ontario Museum, Life Sciences Occassional Papers 21, 1-8. https://doi.org/10.5962/bhl.title.60742

Ferrier, S., Watson, G., Pearce, J., Drielsma, M., 2002. Extended statistical approaches to modelling spatial pattern in biodiversity in northeast New South Wales. I. Species-level modelling. Biodiversity and Conservation, 11(12), 2275–2307. https://doi.org/10.1023/A:1021302930424

Forest Analysis and Inventory, 2019. Reconnaissance Karst Potential Mapping. Ministry of Forests, Lands, Natural Resource Operations and Rural Development. https://catalogue.data.gov.bc.ca/dataset/reconnaissance-karst-potential-mapping.

Forister, M.L., Pelton, E.M., Black, S.H., 2019. Declines in insect abundance and diversity: We know enough to act now. Conservation Science and Practice, 1(8), 1–8. https://doi.org/10.1111/csp2.80

Frank, C.L., Davis, A.D., Herzog, C., 2019. The evolution of a bat population with white-nose syndrome (WNS) reveals a shift from an epizootic to an enzootic phase. Frontiers in Zoology, 16(1), 1–9. https://doi.org/10.1186/s12983-019-0340-y

French, A.R., 1982. Effects of temperature on the duration of arousal episodes during hibernation. Journal of Applied Physiology, 52(1), 216–220. https://doi.org/10.1152/jappl.1982.52.1.216

French, A.R., 1985. Allometries of the durations of torpid and euthermic intervals during mammalian hibernation: A test of the theory of metabolic control of the timing of changes in body temperature. Journal of Comparative Physiology B, 156, 13–19. https://doi.org/10.1007/BF00692921

Frick, S.E., Hijmans, R.J., 2017. WorldClim 2: New 1-km spatial resolution climate surfaces for global land areas. International Journal of Climatology, 37(12), 4302–4315. https://doi.org/10.1002/joc.5086

Frick, W.F., Pollock, J.F., Hicks, A.C., Langwig, K.E., Reynolds, D.S., Turner, G.G., Butchkoski, C.M., Kunz, T.H., 2010. An emerging disease causes regional population collapse of a common North American bat species. Science, 329(5992), 679–82. https://doi.org/10.1126/science.1188594

Frick, W.F., Puechmaille, S.J., Hoyt, J.R., Nickel, B.A., Langwig, K.E., Foster, J.T., Barlow, K.E., Bartonicka, T., Feller, D., Haarsma, A.J., Herzog, C., Horacek, I., Van der Kooij, J., Mulkens, B., Petrov, B., Reynolds, R., Rodrigues, L., Stihler, C.W., Turner, G.G., Kilpatrick, A.M., 2015. Disease alters macroecological patterns of North American bats. Global Ecology and Biogeography, 24(7), 741–749. https://doi.org/10.1111/geb.12290

Frick, W.F., Kingston, T., Flanders, J., 2019. A review of the major threats and challenges to global bat conservation. Annals of the New York Academy of Sciences, 1469(1), 1–21. https://doi.org/10.1111/nyas.14045

Fuller, N.W., McGuire, L.P., Pannkuk, E.L., Blute, T., Haase, C.G., Mayberry, H.W., Risch, T.S., Willis, C.K., 2020. Disease recovery in bats affected by white-nose syndrome. Journal of Experimental Biology, 223(6), jeb211912. https://doi.org/10.1242/jeb.211912

GBIF.org, 2018. GBIF Occurrence Download https://doi.org/10.15468/dl.yokg9g, https://doi.org/10.15468/dl.nbukht, https://doi.org/10.15468/dl.qbxz8c, https://doi.org/10.15468/dl.5pln8k, https://doi.org/10.15468/dl.mr3sre, https://doi.org/10.15468/dl.oxobig, https://doi.org/10.15468/dl.bewazl, https://doi.org/10.15468/dl.kt8pum, https://doi.org/10.15468/dl.7aati8 (accessed 11.01.18).

Gearhart, C., Adams, A.M., Pinshow, B., Korine, C., 2020. Evaporative water loss in Kuhl's pipistrelles declines along an environmental gradient, from mesic to hyperarid. Comparative Biochemistry and Physiology Part A: Molecular & Integrative Physiology, 240, 110587. https://doi.org/10.1016/j.cbpa.2019.110587

Geiser, F., 1988. Reduction of metabolism during hibernation and daily torpor in mammals and birds: temperature effect or physiological inhibition? Journal of Comparative Physiology B, 158(1), 25–37. https://doi.org/10.1007/BF00692726

Geiser, F., Kenagy, G.J., 1988. Torpor duration in relation to temperature and metabolism in hibernating ground squirrels. Physiological Zoology, 61(5), 442–449. https://www.jstor.org/stable/30161266

Geiser, F., Baudinette, R.V., 1990. The relationship between body mass and rate of rewarming from hibernation and daily torpor in mammals. Journal of Experimental Biology, 151, 349–359.

Geiser, F., 2004. Metabolic rate and body temperature reduction during hibernation and daily torpor. Annual Review of Physiology, 66, 239–74. https://doi.org/10.1146/annurev.physiol.66.032102.115105

Geiser, F., 2016. Conserving energy during hibernation. Journal of Experimental Biology, 219(14), 2086–2087. https://doi.org/10.1242/jeb.129171

Giorgi, F., Coppola, E., Solmon, F., Mariotti, L., Sylla, M.B., Bi, X., Elguindi, N., Diro, G.T., Nair, V., Giuliani, G., Turuncoglu, U.U., 2012. RegCM4: model description and preliminary tests over multiple CORDEX domains. Climate Research, 52, 7–29. https://doi.org/10.3354/cr01018

Glantz, S., Slinker, B., 2000. Primer of applied regression & analysis of variance, 2nd ed. McGraw-Hill Education/Medical, New York.

Gorelick, N., Hancher, M., Dixon, M., Ilyushchenko, S., Thau, D., Moore, R., 2017. Google Earth Engine: Planetary-scale geospatial analysis for everyone. Remote Sensing of Environment, 202, 18–27. https://doi.org/10.1016/j.rse.2017.06.031

Gouma, E., Simos, Y., Verginadis, I., Lykoudis, E., Evangelou. A., Karkabounas, S., 2012. A simple procedure for estimation of total body surface area and determination of a new value of Meeh's constant in rats. Laboratory Animals, 46(1), 40–45. https://doi:10.1258/la.2011.011021

Graham, C.H., Ferrier, S., Huettman, F., Moritz, C., Peterson, A.T., 2004. New developments in museum-based informatics and applications in biodiversity analysis. Trends in Ecology and Evolution, 19(9), 497–503. https://doi.org/10.1016/j.tree.2004.07.006

Grieneisen, L. 2011. Hibernacula microclimate and white-nose syndrome susceptibility in the little brown myotis (*Myotis lucifugus*). Master's Thesis. Bucknell University, Lewisburg, Pennsylvania, USA.

Guglielmo, C.G., McGuire, L.P., Gerson, A.R., Seewagen, C.L., 2011. Simple, rapid, and non-invasive measurement of fat, lean, and total water masses of live birds using quantitative magnetic resonance. Journal of Ornithology, 152, 75–85. https://doi.org/10.1007/s10336-011-0724-z

Guisan, A., Weiss, S.B., Weiss, A.D., 1999. GLM versus CCA spatial modeling of plant species distribution. Plant Ecology, 143(1), 107–122. https://doi.org/10.1023/A:1009841519580

Gustafson, A., 1979. Male reproductive patterns in hibernating bats. Reproduction, 56(1), 317–331. https://doi.org/10.1530/jrf.0.0560317

Haase, C.G., Fuller, N.W., Hranac, C.R., Hayman, D.T.S., Olson, S.H., Plowright, R.K., McGuire, L.P., 2019a. Bats are not squirrels: Revisiting the cost of cooling in hibernating mammals. Journal of Thermal Biology, 81, 185–193. https://doi.org/10.1016/j.jtherbio.2019.01.013

Haase, C.G., Fuller, N.W., Hranac, C.R., Hayman, D.T.S., McGuire, L.P., Norquay, K.J.O., Silas, K.A., Willis, C.K.R., Plowright, R.K., Olson, S.H., 2019b. Incorporating evaporative water loss into bioenergetic models of hibernation to test for relative influence of host and pathogen traits on white-nose syndrome. PLoS One,14, e0222311. https://doi.org/10.1371/journal.pone.0222311

Haase, C.G., Fuller, N.W., Dzal, Y.A., Hranac, C.R., Hayman, T.S., Lausen, C.L., McGuire, L.P., Silas, K.A., Olson, S.H., Plowright, R.K., 2021. Body mass and hibernation microclimate may predict bat susceptibility to white-nose syndrome. Ecology and Evolution 11. https://doi.org/10.1002/ece3.7070

Hall, D.K., Salomonson, V.V., Riggs, G.A., 2016. MODIS/Terra Snow Cover Daily L3 Global 500m Grid. Version 6. Boulder, Colorado USA: NASA National Snow and Ice Data Center Distributed Active Archive Center. https://developers.google.com/earth-engine/datasets/catalog/MODIS_006_MOD10A1

Hallmann, C.A., Sorg, M., Jongejans, E., Siepel, H., Hofland, N., Schwan, H., Stenmans, W., Müller, A., Sumser, H., Hörren, T., Goulson, D., de Kroon, H., 2017. More than 75 percent decline over 27 years in total flying insect biomass in protected areas. PLoS One, 12(1), e0185809. https://doi.org/10.1371/journal.pone.0185809

Halsall, A.L., Boyles, J.G., Whitaker, J.O., 2012. Body temperature patterns of big brown bats during winter in a building hibernaculum. Journal of Mammalogy, 93(2), 497–503. https://doi.org/10.1644/11-MAMM-A-262.1

Hanus, K., 1959. Body temperatures and metabolism of bats at different environmental temperatures. Physiologia Bohemoslovaca. 8: 250–259.

Hart, J.S., 1951. Calorimetric determination of average body temperature of small mammals and its variation with environmental conditions. Canadian Journal of Zoology, 29(3), 224–233. https://doi.org/10.1139/z51-021

Harvey, M.J., Altenbach, J.S., Best, T.L., 2013. Bats of the United States and Canada. Johns Hopkins University Press.

Hayman, D.T.S., Pulliam, J.R.C., Marshall, J.C., Cryan, P.M., Webb, C.T., 2016. Environment, host, and fungal traits predict continental-scale white-nose syndrome in bats. Science Advances, 2(1), e1500831–e1500831. https://doi.org/10.1126/sciadv.1500831

Hayman, D.T.S., Cryan, P.M., Fricker, P.D., Dannemiller, N.G., 2017. Long-term video surveillance and automated analyses reveal arousal patterns in groups of hibernating bats. Methods in Ecology and Evolution, 8(12), 1813–1821. https://doi.org/10.1111/2041-210X.12823

Hayssen, V., Lacy, R.C., 1985. A reexamination of basal metabolic rates in mammals: taxonomic differences in the allometry of BMR and body mass. Comparative Biochemistry and Physiology, 81A(4), 741–754. https://doi.org/10.1016/0300-9629(85)90904-1

Heinrichs, J.A., Bender, D.J., Gummer, D.L., Schumaker, N.H., 2010. Assessing critical habitat: evaluating the relative contribution of habitats to population persistence. Biological Conservation, 143(9), 2229–2237. https://doi.org/10.1016/j.biocon.2010.06.009

Heldmaier, G., Ortmann, S., Elvert, R., 2004. Natural hypometabolism during hibernation and daily torpor in mammals. Respiratory Physiology & Neurobiology, 141(3), 317–329. https://doi.org/10.1016/j.resp.2004.03.014

Henshaw, R.E., Folk Jr, G.E., 1966. Relation of thermoregulation to seasonally changing microclimate in two species of bats (*Myotis lucifugus* and *M. sodalis*). Physiological Zoology, 39(3), 223–236. https://doi.org/10.1086/physzool.39.3.30152849

Henshaw, R.E., 1968. Thermoregulation during hibernation: application of Newton's law of cooling. Journal of Theoretical Biology, 20(1), 79–90. https://doi.org/10.1016/0022-5193(68)90093-3

Hernandez, P.A., Graham, C.H., Master, L.L., Albert, D.L., 2006. The effect of sample size and species characteristics on performance of different species distribution modeling methods. Ecography, 29(5), 773–785. https://doi.org/10.1111/j.0906-7590.2006.04700.x

Hertzog, L.R., Besnard, A., Jay-Robert, P., 2014. Field validation shows bias-corrected pseudo-absence selection is the best method for predictive species-distribution modelling. Diversity and Distributions, 20(12), 1403–1413. https://doi.org/10.1111/ddi.12249

Hijmans, R.J., 2016. raster: Geographic Data Analysis and Modeling. R Package version 2.5-8.

Hirshfeld, J.R., O'Farrell, M.J., 1976. Comparisons of differential warming rates and tissue temperatures in some species of desert bats. Comparative Biochemistry and Physiology Part A: Physiology, 55(1), 83–87. https://doi.org/10.1016/0300-9629(76)90127-4

Hitchcock, H.B., 1949. Hibernation of bats in southeastern Ontario and adjacent Quebec. Canadian Field-Naturalist, 63, 47–59.

Holm, S., 1978. Board of the Foundation of the Scandinavian Journal of Statistics A Simple Sequentially Rejective Multiple Test Procedure Author (s): Sture Holm. Published by: Wiley on behalf of the Board of the Foundation of the Scandinavian Journal of Statistics, 6(2), 65–70. https://www.jstor.org/stable/4615733

Horton, J.D., San Juan, C.A., 2019. Prospect- and Mine-Related Features from U.S. Geological Survey 7.5- and 15-Minute Topographic Quadrangle Maps of the United States (ver. 4.0, November 2019): U.S. Geological Survey data release. https://doi.org/10.5066/F78W3CHG

Hranac, C.R., Haase, C.G., Fuller, N.W., McClure, M.L., Marshall, J.C., Lausen, C.L., McGuire, L.P., Olson, S.H., Hayman, D.T.S., In Review. What is winter? Modelling spatial variation in bat host traits and hibernation and their implications for overwintering energetics. Ecology and Evolution. In preprint: https://doi.org/10.22541/au.161185857.74191912/v1

Hume, I., Beiglbock, C., Ruf, T., Frey-Roos, F., Bruns, U., Arnold, W., 2002. Seasonal changes in morphology and function of the gastrointestinal tract of free-living alpine marmots, *Marmota marmota*. Journal of Comparative Physiology B, 172(3), 197–207. https://doi.org/10.1007/s00360-001-0240-1

Humphries, M.M., Thomas, D.W., Speakman, J.R., 2002. Climate-mediated energetic constraints on the distribution of hibernating mammals. Nature, 418(6895), 313–316. https://doi.org/10.1038/nature00828

Intergovernmental Panel on Climate Change. 2018. Global Warming of 1.5° C: An IPCC Special Report on the Impacts of Global Warming of 1.5° C Above Pre-Industrial Levels and Related Global Greenhouse Gas Emission Pathways, in the Context of Strengthening the Global Response to the Threat of Climate Change, Sustainable Development, and Efforts to Eradicate Poverty. Intergovernmental Panel on Climate Change.

International Union for Conservation of Nature (IUCN), 2016. Terrestrial Mammals Red List Spatial Data. IUCN Red List Threat. Species.

Janský, L., 2008. Non-shivering thermogenesis and its thermoregulatory significance. Biological Reviews, 48(1), 85–132. https://doi.org/10.1111/j.1469-185X.1973.tb01115.x

Jenni, L., Jenni-Eiermann, S., 1998. Fuel supply and metabolic constraints in migrating birds. Journal of Avian Biology, 29(4), 521–528. https://doi.org/10.2307/3677171

Jimenez-Valverde, A., 2012. Insights into the area under the receiver operating characteristic curve (AUC) as a discrimination measure in species distribution modelling. Global Ecology and Biogeography 21(4), 498–507. https://doi.org/10.1111/j.1466-8238.2011.00683.x

Johnson, J.S., Reeder, D.M., McMichael, J.W., Meierhofer, M.B., Stern, D.W.F., Lumadue, S.S., Sigler, L.E., Winters, H.D., Vodzak, M.E., Kurta, A., Kath, J.A., Field, K.A., 2014. Host, pathogen, and environmental characteristics predict white-nose syndrome mortality in captive little brown myotis (*Myotis lucifugus*). PLoS One 9(11), e112502. https://doi.org/10.1371/journal.pone.0112502

Johnson, J.S., Treanor, J.J., Lacki, M.J., Baker, M.D., Falxa, G.A., Dodd, L.E., Waag, A.G., Lee, E.H., 2017. Migratory and winter activity of bats in Yellowstone National Park. Journal of Mammalogy, 98(1), 211–221. https://doi.org/10.1093/jmammal/gyw175

Johnston, D.W., 1971. The absence of brown adipose tissue in birds. Comparative Biochemistry and Physiology Part A: Physiology, 40(4), 1107–1108. https://doi.org/10.1016/0300-9629(71)90298-2

Jonasson, K.A., Willis, C.K., 2011. Changes in body condition of hibernating bats support the thrifty female hypothesis and predict consequences for populations with white-nose syndrome. PLoS One, 6(6), e21061. https://doi.org/10.1371/journal.pone.0021061

Jonasson, K.A., Willis, C.K., 2012. Hibernation energetics of free-ranging little brown bats. Journal of Experimental Biology, 215, 2141–2149. https://doi.org/10.1242/jeb.066514

Jones, C., Pagels, J., 1968. Notes on a population of *Pipistrellus subflavus* in southern Louisiana. Journal of Mammalogy, 49(1), 134–139. https://doi.org/10.2307/1377741

Jones, G., Jacobs, D.S., Kunz, T.H., Wilig, M.R., Racey, P.A., 2009. Carpe noctem: The importance of bats as bioindicators. Endangered Species Research, 8(1–2), 93–115. https://doi.org/10.3354/esr00182

Jung, K., Threlfall, C. G., 2016. Urbanisation and its effects on bats – A global meta-analysis in: Voigt, C.C., Kingston, T. (Eds.), Bats in the anthropocene: conservation of bats in a changing world. Springer International Publishing, Cham. https://doi.org/10.1007/978-3-319-25220-9_8

Kahle, D., Wickham, H., 2013. ggmap: Spatial Visualization with ggplot2. The R journal, 5, 144-161.

Kallen, F.C., 1964. Some aspects of water balance in the hibernating bat, in: Annales Academie Scientiarum Fennicae, A4 Biologica. Suomalainen Tiedeakatemia, 259–267.

Karasov, W.H. Pinshow, B., 2000. Test for physiological limitation to nutrient assimilation in a long-distance passerine migrant at a springtime stopover site. Physiological and Biochemical Zoology, 73(3), 335–343. https://doi.org/10.1086/316746

Kaupas, L.A., Barclay, R.M.R., 2018. Temperature-dependent consumption of spiders by little brown bats, *Myotis lucifugus*, but not northern long-eared bats, *Myotis septentrionalis*, in northern Canada. Canadian Journal of Zoology, 96(3), 261–268. https://doi.org/10.1139/cjz-2017-0123

Keating, K.A., Cherry, S., 2004. Use and interpretation of logistic regression in habitat-selection studies. The Journal of Wildlife Management, 68(4), 774–789. http://dx.doi.org/10.2193/0022-541X(2004)068[0774:UAIOLR]2.0.CO;2

Kim, S., 2015. ppcor: An R package for a fast calculation to semi-partial correlation coefficients. Communications for Statistical Applications and Methods, 22(6), 665–674. https://doi.org/10.5351/CSAM.2015.22.6.665

Kleiber, M., 1972. Body size, conductance for animal heat flow and Newton's law of cooling. Journal of Theoretical Biology, 37(1), 139–150. https://doi.org/10.1016/0022-5193(72)90120-8

Klüg-Baerwald, B.J., Brigham, R.M., 2017. Hung out to dry? Intraspecific variation in water loss in a hibernating bat. Oecologia, 183(4), 977–985. https://doi.org/10.1007/s00442-017-3837-0

Knudsen, G.R., Dixon, R.D., Amelon, S.K., 2013. Potential spread of white-nose syndrome of bats to the Northwest: epidemiological considerations. Northwest Science, 87(4), 292–306. https://doi.org/10.3955/046.087.0401

Korine, C., Adams, R., Russo, D., Fisher-Phelps, M., Jacobs, D., 2016. Bats and water: anthropogenic alterations threaten global bat populations, in: Voigt, C.C., Kingston, T. (Eds.), Bats in the anthropocene: conservation of bats in a changing world. Springer International Publishing, Cham, pp. 215–241. https://doi.org/10.1007/978-3-319-25220-9_8

Kotamarthi, R., Mearns, L., Hayhoe, K., Castro, C., Wuebbles, D., 2016. Use of climate information for decision-making and impacts research: state of our understanding. Prepared for the Department of Defense, Strategic Environmental Research and Development Program.

Kuenzi, A.J., Downard, G.T., Morrison, M.L., 1999. Bat distribution and hibernacula use in west central Nevada. The Great Basin Naturalist, 59(3), 213–220. https://doi.org/10.2307/41713112

Kunkel, E.L., 2020. Ecology and energetics of partial migration and facultative hibernation of Mexican free-tailed bats. Master's Thesis, Department of Biological Sciences, Texas Tech University.

Kunkel, E.L., McGuire, L.P., In Prep. Partial migration in Mexican Free-tailed bats. Physiological and Biochemical Zoology.

Kunkel, E.L., Fuller, N.W., McGuire, L.P., In Prep. Facultative hibernation of Mexican Free-tailed bats. Comparative Biochemistry and Physiology Part A: Molecular and Integrative Biology.

Kurta, A., Bell, G.P., Nagy, K.A., Kunz, T.H., 1989. Energetics of pregnancy and lactation in freeranging little brown bats (*Myotis lucifugus*). Physiological Zoology , 62(3), 804–818. https://www.journals.uchicago.edu, https://doi.org/10.1086/physzool.62.3.30157928

Kurta, A., 2014. The misuse of relative humidity in ecological studies of hibernating bats. Acta Chiropterologica, 16(1), 249–254. https://doi.org/10.3161/150811014X683444

Kurta, A., Smith, S.M., 2014. Hibernating bats and abandoned mines in the Upper Peninsula of Michigan. Northeastern Naturalist, 21(4), 587–606. https://doi.org/10.1656/045.021.0407

Lachapelle, J., Colegrave, N., Bell, G., 2017. The effect of selection history on extinction risk during severe environmental change. Journal of Evolutionary Biology, 30(1), 1872–1883. https://doi.org/10.1111/jeb.13147

Lacki, M.J., Dodd, L.E., Toomey, R.S., Thomas, S.C., Couch, Z.L., Nichols, B.S., 2015. Temporal changes in body mass and body condition of cave-hibernating bats during staging and swarming. Journal of Fish and Wildlife Management, 6(2), 360–370. https://doi.org/10.3996/042015-JFWM-033

Langwig, K.E., Frick, W.F., Bried, J.T., Hicks, A.C., Kunz, T.H., Marm Kilpatrick, A., 2012. Sociality, density-dependence and microclimates determine the persistence of populations suffering from a novel fungal disease, white-nose syndrome. Ecology Letters, 15(9), 1050–1057. https://doi.org/10.1111/j.1461-0248.2012.01829.x

Langwig, K.E., Frick, W.F., Reynolds, R., Parise, K.L., Drees, K.P., Hoyt, J.R., Cheng, T.L., Kunz, T.H., Foster, J.T., Kilpatrick, A.M., 2015. Host and pathogen ecology drive the seasonal dynamics of a fungal disease, white-nose syndrome. Proceedings of the Royal Society B: Biological Sciences, 282(1799), 10–12. https://doi.org/10.1098/rspb.2014.2335

Langwig, K.E., Hoyt, J.R., Parise, K.L., Frick, W.F., Foster, J.T., Kilpatrick, A.M., 2017. Resistance in persisting bat populations after white-nose syndrome invasion. Philosophical Transactions of the Royal Society B: Biological Sciences, 372(1712), 20160044. https://doi.org/10.1098/rstb.2016.0044

Lausen, C.L., Delisle, I., Barclay, R.M.R., Strobeck, C., 2008. Beyond mtDNA: nuclear gene flow suggests taxonomic oversplitting in the little brown bat (*Myotis lucifugus*). Canadian Journal of Zoology, 86(7), 700–713. https://doi.org/10.1139/Z08-046

Layne, J., 1958. Notes on mammals of southern Illinois. The American Midland Naturalist, 60(1), 219–254. https://doi.org/10.2307/2422479

Lighton, J.R.B., 2008. Measuring metabolic rates: a manual for scientists. Oxford University Press, Oxford. https://doi.org/10.1093/acprof:oso/9780195310610.001.0001

Lilley, T.M.T., Johnson, J.J.S., Ruokolainen, L., Rogers, E.J., Wilson, C.A., Schell, S.M., Field, K.A., Reeder, D.M., 2016. White-nose syndrome survivors do not exhibit frequent arousals associated with *Pseudogymnoascus destructans* infection. Frontiers in Zoology, 13(12), 1–8. https://doi.org/10.1186/s12983-016-0143-3

Lister, B.C., Garcia, A., 2018. Climate-driven declines in arthropod abundance restructure a rainforest food web. Proceedings of the National Academy of Sciences of the United States of America, 115(44), E10397–E10406. https://doi.org/10.1073/pnas.1722477115

Lorch, J.M., Meteyer, C.U., Behr, M.J., Boyles, J.G., Cryan, P.M., Hicks, A.C., Ballmann, A.E., Coleman, J.T.H., Redell, D.N., Reeder, D.M., Blehert, D.S., 2011. Experimental infection of bats with *Geomyces destructans* causes white-nose syndrome. Nature, 480(7377), 376–378. https://doi.org/10.1038/nature10590

Lukacs, P.M., Burnham, K.P., Anderson, D.R., 2010. Model selection bias and Freedman's paradox. Annals of the Institute of Statistical Mathematics. 62(1), 117–125. https://doi.org/10.1007/s10463-009-0234-4

Macayeal, L.C., Riskin, D.K., Swartz, S.M., Breuer, K.S., 2011. Climbing flight performance and load carrying in lesser dog-faced fruit bats (*Cynopterus brachyotis*). Journal of Experimental Biology, 214, 786–793. https://doi.org/10.1242/jeb.050195

Maher, S.P., Kramer, A.M., Pulliam, J.T., Zokan, M.A., Bowden, S.E., Barton, H.D., Magori, K., Drake, J.M., 2012. Spread of white-nose syndrome on a network regulated by geography and climate. Nature Communications, 3, 1306. https://doi.org/10.1038/ncomms2301

Maiorano, L., Cheddadi, R., Zimmermann, N.E., Pellissier, L., Petitpierre, B., Pottier, J., Laborde, H., Hurdu, B.I., Pearman, P.B., Psomas, A., Singarayer, J.S., 2013. Building the niche through time: using 13,000 years of data to predict the effects of climate change on three tree species in Europe. Global Ecology and Biogeography, 22(3), 302–317. https://doi.org/10.1111/j.1466-8238.2012.00767.x

Mammola, S., Pedro, C., Culver, D.C., Louis, D., Ferreira, R.L., Cene, F., Galassi, D.M., Christian, G., Stuart, H., Humphreys, W.F., Isaia, M., 2019. Scientists' warning on the conservation of subterranean ecosystems. Bioscience, 69(8), 641–650. https://doi.org/10.1093/biosci/biz064

Manly, B.F.L., McDonald, L., Thomas, D.L., McDonald, T.L., Erickson, W.P., 2007. Resource selection by animals: statistical design and analysis for field studies. Springer Science & Business Media.

Marom, S., Korine, C., Wojciechowski, M.S., Tracy, C.R., Pinshow, B., 2006. Energy metabolism and evaporative water loss in the European free-tailed bat and Hemprich's long-eared bat, Microchiroptera: Species sympatric in the Negev Desert. Physiological and Biochemical Zoology, 79(5), 944–956. https://doi.org/10.1086/505999

Marroquin, C.M., Lavine, J.O., Windstam, S.T., 2017. Effect of humidity on development of *Pseudogymnoascus destructans*, the causal agent of bat white-nose syndrome. Northeastern Naturalist, 24(1), 54–64. https://doi.org/10.1656/045.024.0105

Martin, R.L., Pawluk, J.T., Clancy, T.B., 1966. Obervations on the hibernation of *Myotis subulatus*. Journal of Mammalogy, 47(2), 348–349. https://doi.org/10.2307/1378149

Maslo, B., Fefferman, N.H., 2015. A case study of bats and white-nose syndrome demonstrating how to model population viability with evolutionary effects. Conservation Biology, 29(4), 1176-1185. https://doi.org/10.1111/cobi.12485

McClure, M.L., Crowley, D., Haase, C.G., McGuire, L.P., Fuller, N.W., Hayman, D.T.S., Lausen, C.L., Plowright, R.K., Dickson, B.G., Olson, S.H., 2020. Linking surface and subterranean climate:

implications for the study of hibernating bats and other cave dwellers. Ecosphere 11. https://doi.org/10.1002/ecs2.3274

McClure, M.L., Haase, C.G., Crowley, D., Hranac, C.R., Hayman, D.T.S., Mcguire, L.P., Dickson, B.G., Fuller, N.W., Plowright, R.K., Lausen, C.L., Olson, S.H., In Review. A hybrid correlative-mechanistic approach for modeling and mapping winter distributions of western bat species. Journal of Biogeography.

McClure, M.L., Haase, C.G., Crowley, D., Hranac, C.R., Hayman, D.T.S., Mcguire, L.P., Dickson, B.G., Fuller, N.W., Plowright, R.K., Lausen, C.L., Olson, S.H., In Prep. Projecting the compound effects of climate change and white-nose syndrome on western bat species. Climate Change Ecology.

McCue, M.D., 2010. Starvation physiology: reviewing the different strategies animals use to survive a common challenge. Comparative Biochemistry and Physiology Part A: Molecular & Integrative Physiology, 156(1), 1–18. https://doi.org/10.1016/j.cbpa.2010.01.002

McKechnie, A.E., Wolf, B.O., 2004. The energetics of the rewarming phase of avian torpor, in: Barnes, B.M., Carey, H.V. (Eds.), Life in the cold: evolution, mechanisms, adaptation, and applications, International Hibernation Symposium. Institute of Arctic Biology, University of Alaska, Fairbanks, Alaska.

McGuire, L.P., Fenton, M.B., Guglielmo, C.G., 2009. Effect of age on energy storage during prehibernation swarming in little brown bats, *Myotis lucifugus*. Canadian Journal of Zoology, 87(6), 515–519. https://doi.org/10.1139/Z09-041

McGuire, L.P., Guglielmo, C.G., 2010. Quantitative magnetic resonance: a rapid, noninvasive body composition analysis technique for live and salvaged bats. Journal of Mammalogy, 91(6), 1375–1380. https://doi.org/10.2307/40961866

McGuire, L.P., Guglielmo, C.G., Mackenzie, S.A. Taylor, P.D., 2012. Migratory stopover in the long-distance migrant silver-haired bat, *Lasionycteris noctivagans*. Journal of Animal Ecology, 81(2), 377–385. https://doi.org/10.1111/j.1365-2656.2011.01912.x

McGuire, L.P., Fenton, M.B., Guglielmo, C.G., 2013. Phenotypic flexibility in migrating bats: seasonal variation in body composition, organ sizes and fatty acid profiles. Journal of Experimental Biology, 216(Pt 5), 800-8. https://doi.org/10.1242/jeb.072868

McGuire, L.P., Jonasson, K.A., Guglielmo, C.G., 2014. Bats on a budget: Torpor-assisted migration saves time and energy. PLoS One, 9(12), e115724. https://doi.org/10.1371/journal.pone.0115724

McGuire, L.P., Muise, K.A., Shrivastav, A., Willis, C.K., 2016. No evidence of hyperphagia during prehibernation in a northern population of little brown bats, *Myotis lucifugus*. Canadian Journal of Zoology, 94(12), 821–827. https://doi.org/10.1139/cjz-2016-0110

McGuire, L.P., Mayberry, H.W., Willis, C.K.R., 2017. White-nose syndrome increases torpid metabolic rate and evaporative water loss in hibernating bats. American Journal of Physiology-Regulatory, Integrative and Comparative Physiology, 313(6), R680–R686. https://doi.org/10.1152/ajpregu.00058.2017

McGuire, L.P., Kelly, L.A., Baloun, D.E., Boyle, W.A., Cheng, T.L., Clerc, J., Fuller, N.W., Gerson, A.R., Jonasson, K.A., Rogers, E.J., Sommers, A.S., Guglielmo, C.G., 2018. Common condition indices are no more effective than body mass for estimating fat stores in insectivorous bats. Journal of Mammalogy, 99(5), 1065–1071. https://doi.org/10.1093/jmammal/gyy103

McGuire, L.P., Mayberry, H.W., Fletcher, Q.E., Willis, C.K.R., 2020. An experimental test of energy and electrolyte supplementation as a mitigation strategy for white-nose syndrome. Conservation Physiology, 7(1), coz006. https://doi:10.1093/conphys/coz006

McGuire, L.P., Dzal, Y.A., Fuller, N.W., Klüg-Baerwald, B.J., Haase, C.G., Silas, K.A., Willis, C.K.R., Lausen, C.L., Olson, S.H., In Review. Interspecific variation in evaporative water loss, and not metabolic rate, among hibernating bats.

McGuire, L.P., Fuller, N.W., Dzal, Y.A., Haase, C.G., Silas, K.A., Willis, C.K.R., Olson, S.H., Lausen, C.L., In Review. Similar physiology in hibernating bats across broad geographic ranges. Journal of Comparative Physiology B.

McGuire, L.P., Fuller, N.W., Haase, C.G., Silas, K.A., Olson, S.H., In Review. Lean mass dynamics in hibernating bats and implications for energy and water budgets. Physiological and Biochemical Zoology.

McManus, J.J., 1974. Activity and thermal preference of the little brown bat, *Myotis lucifugus*, during hibernation. Journal of Mammalogy, 55(4), 844–846. https://doi.org/10.2307/1379416

McNab, B.K., 1980. On estimating thermal conductance in endotherms. Physiological Zoology, 53(2), 145–156. https://doi.org/10.1086/physzool.53.2.30152577

Mearns, L., McGinnis, S., Korytina, D., Arritt, R., Biner, S., Bukovsky, M., Chang, H.; Christensen, O., Herzmann, D., Jiao, Yanjun., Kharin, S., Lazare, M., Nikulin, G., Qian, Minwei., Scinocca, John., Winger, K., Castro, C., Frigon, A., Gutowski, W., 2017. The NA-CORDEX dataset, version 1.0. NCAR Climate Data Gateway, Boulder CO. https://doi.org/10.5065/D6SJ1JCH

Mellanby, K., 1939. Low temperature and insect activity. Proceedings of the Royal Society B: Biological Sciences, 127(849), 473–487. https://doi.org/10.1098/rspb.1939.0035

Menzies, A.K., Webber, Q.M.R., Baloun, D.E., McGuire, L.P., Muise, K.A., Coté, D., Tinkler, S., Willis, C.K., 2016. Metabolic rate, latitude and thermal stability of roosts, but not phylogeny, affect rewarming rates of bats. Physiology & Behavior, 164(Part A), 361–368. https://doi.org/10.1016/j.physbeh.2016.06.015

Muñoz-Garcia, A., Ro, J., Reichard, J.D., Kunz, T.H., Williams, J. B., 2012. Cutaneous water loss and lipids of the stratum corneum in two syntopic species of bats. Comparative Biochemistry and Physiology Part A: Molecular & Integrative Physiology, 161(2), 208–215. https://doi.org/10.1016/j.cbpa.2011.10.025

National Aeronautics and Space Administration (NASA), 2019. MOD44B Version 6 Vegetation Continuous Fields (VCF). NASA EOSDIS Land Processes Distributed Active Archive Center (LP DAAC). https://lpdaac.usgs.gov/products/mod44bv006/

National Atlas of the United States, 2011. North American Bat Ranges. National Atlas of the United States, Reston, Virginia. https://www.sciencebase.gov/catalog/item/4f4e4814e4b07f02db4dab2e

National Oceanic and Atmospheric Administration (NOAA), 2016. DMSP OLS: Global Radiance-Calibrated Nighttime Lights Version 4, Defense Meteorological Program Operational Linescan System. https://developers.google.com/earth-engine/datasets/catalog/NOAA_DMSP-OLS_CALIBRATED_LIGHTS_V4

National Wildlife Health Center (USGS), Bat white-nose syndrome (WNS)/Pd surveillance submission guidelines winter 2013/2014 (November - April) (2013), pp. 1–26.

NatureServe, 2019. NatureServe Central Databases. Arlington, Virginia. USA.

Newton, I., 1701. Scala graduum caloris, calorum descriptiones & signa (Scale of the degrees of heat). Philosophical Transactions, 22(270), 824–829. https://doi.org/10.1098/rstl.1700.0082

Norberg, U.M., Rayner, J.M., 1987. Ecological morphology and flight in bats (Mammalia; Chiroptera): wing adaptations, flight performance, foraging strategy and echolocation. Philosophical Transactions of the Royal Society B: Biological Sciences, 316(1179), 335–427. https://doi.org/10.1098/rstb.1987.0030

Norquay, K.J., Martinez-Nuñez, F., Dubois, J.E., Monson, K.M., Willis, C.K., 2013. Long-distance movements of little brown bats, *Myotis lucifugus*. Journal of Mammalogy, 94(2), 506–515. https://doi.org/10.2307/23488381

Norquay, K.J.O., Willis, C.K.R., 2014. Hibernation phenology of *Myotis lucifugus*. Journal of Zoology, 294(2), 85–92. https://doi.org/10.1111/jzo.12155

O'Farrrell, M.J., Studier, E.H., 1973. Reproduction, growth, and development in *Myotis thysanodes* and *M. Lucifugus* (Chiroptera: Vespertilionidae). Ecology, 54(1), 18–30. https://doi.org/10.2307/1934371

Oppel, S., Meirinho, A., Ramírez, I., Gardner, B., O'Connell, A.F., Miller, P.I., Louzao, M., 2012. Comparison of five modelling techniques to predict the spatial distribution and abundance of seabirds. Biological Conservation, 156, 94-104. https://doi.org/10.1016/j.biocon.2011.11.013

Oster, J.L., Montañez, I.P., Kelley, N.P., 2012. Response of a modern cave system to large seasonal precipitation variability. Geochimica et Cosmochimica Acta, 91, 92–108. https://doi.org/10.1016/j.gca.2012.05.027

Paksuz, E.P., 2014. The effect of hibernation on the morphology and histochemistry of the intestine of the greater mouse-eared bat, *Myotis myotis*. Acta histochemica, 116(8), 1480–1489. https://doi.org/10.1016/j.acthis.2014.10.004

Pannkuk, E.L., McGuire, L.P., Warnecke, L., Turner, J.M., Willis, C.K. & Risch, T.S., 2015. Glycerophospholipid profiles of bats with white-nose syndrome. Physiological and Biochemical Zoology, 88(4), 425–432. https://doi.org/10.1086/681931

Pearson, E.W., 1962. Bats hibernating in silica mines in southern Illinois. Journal of Mammalogy, 43(1), 27–33. https://doi.org/10.2307/1376877

Pebesma, E., Bivand, R., Rowlingson, B., Gomez-Rubio, V., Hijmans, R., Summer, M., MacQueen, D., Lemon, J., O'Brien, J., 2016. Classes and Methods for Spatial Data. R package version 1.2-3.

Pekel, J.F., Cottam, A., Gorelick, N., Belward, A.S., 2016. High-resolution mapping of global surface water and its long-term changes. Nature, 540(7633), 418. https://doi.org/10.1038/nature20584

Perry, R.W., 2013. A review of factors affecting cave climates for hibernating bats in temperate North America. Environmental Reviews, 21(1), 28–39. https://doi.org/10.1139/er-2012-0042

Phillips, S.J., Elith, J., 2011. Logistic methods for resource selection functions and presence-only species distribution models, in: Proceedings of the 25th AAAI Conference on Artificial Intelligence, 1384–1389.

Piersma, T., 1998. Phenotypic flexibility during migration: optimization of organ size contingent on the risks and rewards of fueling and flight? Journal of Avian Biology, 29(84), 511–520. https://doi.org/10.2307/3677170

Ports, M.A., Bradley, P.V., 1996. Habitat affinities of bats from northeastern Nevada. The Great Basin Naturalist, 56(1), 48–53. https://scholarsarchive.byu.edu/gbn/vol56/iss1/6

Poschman, H., 2014. Public Lands in the West, in: The Book of the States 2014. pp. 459–462.

Prendergast, B.J., Freeman, D.A., Zucker, I., Nelson, R.J., 2002. Periodic arousal from hibernation is necessary for initiation of immune responses in ground squirrels. American Journal of Physiology-Regulatory, Integrative and Comparative Physiology, 282(4), R1054-R1062. https://doi.org/10.1152/ajpregu.00562.2001

Prothero, J., Jürgens, K.D., 1986. An energetic model of daily torpor in endotherms. Journal of Theoretical Biology, 121(4), 403–415. https://doi.org/10.1016/S0022-5193(86)80099-6

Puechmaille, S.J., Wibbelt, G., Korn, V., Fuller, H., Forget, F., Mühldorfer, K., Kurth, A., Bogdanowicz, W., Borel, C., Bosch, T., Cherezy, T., Drebet, M., Görföl, T., Haarsma, A.-J., Herhaus, F., Hallart, G., Hammer, M., Jungmann, C., Le Bris, Y., Lutsar, L., Masing, M., Mulkens, B., Passior, K., Starrach, M., Wojtaszewski, A., Zöphel, U., Teeling, E.C., 2011. Pan-european distribution of white-nose syndrome fungus (*Geomyces destructans*) not associated with mass mortality. PLoS One 6(4), e19167. https://doi.org/10.1371/journal.pone.0019167

R Core Development Team, 2017-2020. R: A language and environment for statistical computing. R Foundation for Statistical Computing, Vienna, Austria. URL: https://www.R-project.org

Razgour, O., Rebelo, H., Di Febbraro, M., Russo, D., 2016. Painting maps with bats: species distribution modelling in bat research and conservation. Hystrix, 27(1). https://doi.org/10.4404/hystrix-27.1-11753

Reeder, D.M., Frank, C.L., Turner, G.G., Meteyer, C.U., Kurta, A., Britzke, E.R., Vodzak, M.E., Darling, S.R., Stihler, C.W., Hicks, A.C., Jacob, R., Grieneisen, L.E., Brownlee, S.A., Muller, L.K., Blehert, D.S., 2012. Frequent arousal from hibernation linked to severity of infection and mortality in bats with white-nose syndrome. PLoS One, 7(6), e38920. https://doi.org/10.1371/journal.pone.0038920

Reimer, J.P., 2014. Bat activity and use of hibernacula in Wood Buffalo National Park, Alberta. Northwestern Naturalist, 95(3), 277-289. https://doi.org/10.1898/13-30.1

Reynolds, S., Kunz, T.H., 2000. Changes in body composition during reproduction and postnatal growth in the little brown bat, *Myotis lucifugus* (Chiroptera: Vespertilionidae). Écoscience, 7(1), 10–17. https://doi.org/10.1080/11956860.2000.11682565

Reynolds, H.T., Ingersoll, T., Barton, H.A., 2015. Modeling the environmental growth of *Pseudogymnoascus destructans* and its impact on the white-nose syndrome epidemic. Journal of Wildlife Diseases, 51(2), 318. https://doi.org/10.7589/2014-06-157

Rodhouse, T.J., Ormsbee, P.C., Irvine, K.M., Vierling, L.A., Szewczak, J.M., Vierling, K.T., 2015. Establishing conservation baselines with dynamic distribution models for bat populations facing imminent decline. Diversity and Distributions, 21(12), 1401–1413. https://doi.org/10.1111/ddi.12372

Royle, J.A., Chandler, R.B., Yackulic, C., Nichols, J.D., 2012. Likelihood analysis of species occurrence probability from presence-only data for modelling species distributions. Methods in Ecology and Evolution, 3(3), 545–554.

Ruf, T., Geiser, F., 2015. Daily torpor and hibernation in birds and mammals. Biological Reviews, 90(3), 891–926. https://doi.org/10.1111/brv.12137

Sánchez-Bayo, F., Wyckhuys, K.A.G., 2019. Worldwide decline of the entomofauna: A review of its drivers. Biological Conservation. 232, 8–27. https://doi.org/10.1016/j.biocon.2019.01.020

Sandel, J.K., Benatar, G.R., Burke, K.M., Walker, C.W., Lacher, T.E., Honeycutt, R.L. 2001. Use and selection of winter hibernacula by the eastern pipistrelle, *Pipistrellus subflavus*, in Texas. Journal of Mammalogy, 829(1), 173–178. https://doi.org/10.1093/jmammal/82.1.173

Schmidt-Nielsen, K., 1984. Scaling: Why is animal size so important?, 1st ed. Cambridge University Press, Cambridge; New York.

Schmidt-Nielsen, K. (Ed.), 1987. Animal Physiology: Adaptation and Environment, 3rd ed. Cambridge University Press, London; New York.

Seltmann, A., Czirják, G.Á., Courtiol, A., Bernard, H., Struebig, M.J., Voigt, C.C., 2017. Habitat disturbance results in chronic stress and impaired health status in forest-dwelling paleotropical bats. Conservation Physiology, 5(1), 1–14. https://doi.org/10.1093/conphys/cox020

Shorr, R., Navo, K., 2014. Key to the bats of Colorado. Accessed October 2017: http://www.cnhp.colostate.edu/teams/zoology/cbwg/batList.asp

Skamarock, W.C., Klemp, J.B., Dudhia, J., Gill, D.O., Barker, D.M., Duda, M.G., Huang, X., Wang, W., Powers, J.G., 2008. A Description of the Advanced Research WRF Version 3. NCAR Technical Note NCAR/TN–475+STR.

Smalley, R.L., Dryer, R.L., 1963. Brown fat: thermogenic effect during arousal from hibernation in the bat. Science, 140(3573), 1333–1334. https://doi.org/10.1126/science.140.3573.1333

Smeraldo, S., Di Febbraro, M., Bosso, L., Flaquer, C., Guixé, D., Lisón, F., Meschede, A., Juste, J., Prüger, J., Puig-Montserrat, X., Russo, D., 2018. Ignoring seasonal changes in the ecological niche of non-migratory species may lead to biases in potential distribution models: lessons from bats. Biodiversity and Conservation, 27(9), 2425–2441. https://doi.org/10.1007/s10531-018-1545-7

Smith, R.E., Hock, R.J., 1963. Brown fat: thermogenic effector of arousal in hibernators. Science 140(3563), 199–200. https://doi.org/10.1126/science.140.3563.199

Snapp, B.D., Heller, H.C., 1981. Suppression of metabolism during hibernation in ground squirrels (*Citellus lateralis*). Physiological Zoology, 54(3), 297–307. https://doi.org/10.1086/physzool.54.3.30159944

Speakman, J.R., Webb, P.I., Racey, P.A., 1991. Effects of disturbance on the energy expenditure of hibernating bats. Journal of Applied Ecology, 28(3), 1087–1104. https://doi.org/10.2307/2404227

Speakman, J.R., Thomas, D.W., 2003. Physiological ecology and energetics of bats, in: Kunz, T.H., Fenton, M.B. (Eds.), Bat Biology. University of Chicago Press, Chicago, 430–490.

Stawski, C., Turbill, C., Geiser, F., 2009. Hibernation by a free-ranging subtropical bat, *Nyctophilus bifax*. Journal of Comparative Physiology B, 179(4), 433–441. https://doi.org/10.1007/s00360-008-0328-y

Storm, J.J., Boyles, J.G., 2011. Body temperature and body mass of hibernating little brown bats *Myotis lucifugus* in hibernacula affected by white-nose syndrome. Acta Theriologica, 56, 123–127. https://doi.org/10.1007/s13364-010-0018-5

Strunk, T.H., 1971. Heat loss from a Newtonian animal. Journal of Theoretical Biology, 33(1), 35–61. https://doi.org/10.1016/0022-5193(71)90215-3

Symonds, M.R., Moussalli, A., 2011. A brief guide to model selection, multimodel inference and model averaging in behavioural ecology using Akaike's information criterion. Behavioral Ecology and Sociobiology, 65(1), 13–21. https://doi.org/10.1007/s00265-010-1037-6

Tadono, T., Ishida, J., Oda, F., Naito, S., Minakawa, K., Iwamoto, H., 2014. Precise global DEM generation by ALOS PRISM, ISPRS. Annals of the Photogrammetry, Remote Sensing and Spatial Information Sciences 2(4), 71–76. https://developers.google.com/earth-engine/datasets/catalog/JAXA_ALOS_AW3D30_V2_2

Talerico, J.M., 2008. The behaviour, diet and morphology of the little brown bat, *Myotis lucifugus*, near the northern extent of its range in Yukon Canada. Master's Thesis, Graduate Studies, University of Calgary. https://doi.org/10.11575/PRISM/14939

Taylor, P.D., Crewe, T.L., Mackenzie, S.A., Lepage, D., Aubry, Y., Crysler, Z., Francis, C.M., Guglielmo, C.G., Hamilton, D.J., Holberton, R.L., Loring, P.H., Norris, D.R., Paquet, J., Ronconi, R.A., Smith, P.A., Smetzer, J., Welch, L., Woodworth, B.K., 2017. The Motus Wildlife Tracking System: a collaborative research network to enhance the understanding of wildlife movement. Avian Conservation and Ecology, 12(1), Article 8. https://doi.org/10.5751/ACE-00953-120108

Theobald, D.M., Harrison-Atlas, D., Monahan, W.B., Albano, C.M., 2015. Ecologically-relevant maps of landforms and physiographic diversity for climate adaptation planning. PloS One, 10(12), e0143619. https://doi.org/10.1371/journal.pone.0143619

Thomas, D.W., Dorais, M., Bergeron, J.M., 1990. Winter energy budgets and cost of arousals for hibernating little brown bats, *Myotis lucifugus*. Journal of Mammalogy, 71(3), 475–479. https://doi.org/10.2307/1381967

Thomas, D.W., Cloutier, D., 1992. Evaporative water loss by hibernating little brown bats, *Myotis lucifugus*. Physiological and Biochemical Zoology, 65(2), 443–456. https://doi.org/10.1086/physzool.65.2.30158262

Thomas, D.W., 1995. Hibernating bats are sensitive to nontactile human disturbance. Journal of Mammalogy, 76(3), 940–946. https://doi.org/10.2307/1382764

Thomas, D.W., Geiser, F., 1997. Periodic arousals in hibernating mammals: is evaporative water loss involved? Functional Ecology, 11(5), 585–591. https://doi.org/10.1046/j.1365-2435.1997.00129.x

Thompson, L.J., Brown, M., Downs, C.T., 2015. Seasonal metabolic variation over two years in an Afrotropical passerine bird. Journal of Thermal Biology, 52, 58–66. https://doi.org/10.1016/j.jtherbio.2015.05.003

Thornton, P.E., Thornton, M.M., Mayer, B.W., Wei, Y., Devarakonda, R., Vose, R.S., Cook, R.B., 2019. Daymet: Daily Surface Weather Data on a 1-km Grid for North America, Version 3. ORNL DAAC, Oak Ridge, Tennessee, USA. https://doi.org/10.3334/ORNLDAAC/1328

Turner, J.M., Warnecke, L., Wilcox, A., Baloun, D., Bollinger, T.K., Misra, V., Willis, C.K.R., 2015. Physiology & Behavior Conspecific disturbance contributes to altered hibernation patterns in bats with white-nose syndrome. Physiology & Behavior, 140, 71–78. https://doi.org/10.1016/j.physbeh.2014.12.013

United States Environmental Protection Agency, 2016. National Wetland Condition Assessment 2011: A Collaborative Survey of the Nation's Wetlands.

United States Fish & Wildlife Service, 2014. Web Page. www.whitenosesyndrome.org (accessed 01.11.14)

United States Fish & Wildlife Service, 2016. National white-nose syndrome decontamination protocol – Version 04.12.2016.

United States Fish & Wildlife Service, 2016. Web Page. www.whitenosesyndrome.org (accessed 01.11.16)

United States Fish & Wildlife Service, 2020. Web Page. www.whitenosesyndrome.org (accessed 09.09.20)

United States Geological Survey (USGS). 2003. Bat Population Database. http://www.fort.usgs.gov/products/data/bpd/bpd.asp

United States Geological Survey (USGS) Core Science Analytics, Synthesis, and Libraries Program, 2012. Biodiversity occurrence data accessed through Biodiversity Information Serving Our Nation (BISON). bison.usgs.gov (accessed 28.12.16, 09.03.17)

United States Geological Survey (USGS), 2016. Mineral Resources Data System. Reston, VA. https://mrdata.usgs.gov/mrds/

Vanderwolf, K.J., McAlpine, D.F., Forbes, G.J., Malloch, D., 2012. Bat Populations and Cave Microclimate Prior to and at the Outbreak of White-Nose Syndrome in New Brunswick. The Canadian Field-Naturalist, 126(2), 125–134. https://doi.org/10.22621/cfn.v126i2.1327

Venables, W.N., Ripley, B.D., 2002. Modern Applied Statistics with S, Fourth edition. Springer, New York.

Verant, M.L., Boyles, J.G., Waldrep, W., Wibbelt, G., Blehert, D.S., 2012. Temperature-dependent growth of *Geomyces destructans*, the fungus that causes bat white-nose syndrome. PLoS One, 7(9), p.e46280. https://doi.org/10.1371/journal.pone.0046280

Verant, M.L., Meteyer, C.U., Speakman, J.R., Cryan, P.M., Lorch, J.M., Blehert, D.S., 2014. White-nose syndrome initiates a cascade of physiologic disturbances in the hibernating bat host. BMC Physiology, 14(1), 10. https://doi.org/10.1186/s12899-014-0010-4

VertNet. 2020. *Myotis lucifugus* occurrence data accessed through VertNet. vertnet.org (accessed 05.05.19)

VertNet. 2016. Biodiversity occurrence data accessed through VertNet. vertnet.org (accessed 14.12.16, 21.12.16, 09.03.17)

Villa, B.R., Cockrum, E.L., 1962. Migration in the guano bat *Tadarida brasiliensis mexicana* (Saussure). Journal of Mammalogy, 43(1), 43–64. https://doi.org/10.2307/1376879

Voigt, C.C., Kingston, T., 2016. Bats in the Anthropocene: conservation of bats in a changing world. Springer Nature.

Wang, L.C.H., 1978. Energetics and field aspects of mammalian torpor: the Richardson's ground squirrel, in: Wang, L.C.H., Hudson, J.W. (Eds.), Strategies in the cold. Academic Press, New York, pp. 109–145.

Wang, T., Hamann, A., Spittlehouse, D., Carroll, C., 2016. Locally downscaled and spatially customizable climate data for historical and future periods for North America. PLoS One, 11(6), 1–17. https://doi.org/10.1371/journal.pone.0156720

Warnecke, L., Turner, J.M., Bollinger, T.K., Lorch, J.M., Misra, V., Cryan, P.M., Wibbelt, G., Blehert, D.S., Willis, C.K.R., 2012. Inoculation of bats with European *Geomyces destructans* supports the novel pathogen hypothesis for the origin of white-nose syndrome. Proceedings of the National Academy of Sciences,109(18), 6999–7003. https://doi.org/10.1073/pnas.1200374109

Warnecke, L., Turner, J.M., Bollinger, T.K., Misra, V., Cryan, P.M., Blehert, D.S., Wibbelt, G., Willis, C.K.R., 2013. Pathophysiology of white-nose syndrome in bats: a mechanistic model linking wing damage to mortality. Biology Letters. 9(4), 20130177–20130177. https://doi.org/10.1098/rsbl.2013.0177

Wasserman, L., 2000. Bayesian model selection and model averaging. Journal of Mathematical Psychology, 44(1), 92–107. https://doi.org/10.1006/jmps.1999.1278

Weary, D.J., Doctor, D.H., 2014. Karst in the United States: a digital map compilation and database: U.S. Department of the Interior, U.S. Geological Survey. https://doi.org/10.3133/ofr20141156

Weaver, S.P., Simpson, T.R., Baccus, J.T., Weckerly, F.W., 2015. Baseline population estimates and microclimate data for newly established overwintering Brazilian free-tailed bat colonies in central Texas. The Southwestern Naturalist, 60(2–3), 151–157. https://doi.org/10.1894/SWNAT-D-14-00022.1

Webb, P.I., Ellison, J., 1998. Normothermy, torpor, and arousal in hedgehogs (*Erinaceus europaeus*) from Dunedin. New Zealand Journal of Zoology, 25(2), 85–90. https://doi.org/10.1080/03014223.1998.9518139

Weller, T.J., Castle, K.T., Liechti, F., Hein, C.D., Schirmacher, M.R., Cryan, P.M., 2016. First direct evidence of long-distance seasonal movements and hibernation in a migratory bat. Scientific Reports, 6(1), 1–7. https://doi.org/10.1038/srep34585

Weller, T.J., Rodhouse, T.J., Neubaum, D.J., Ormsbee, P.C., Dixon, R.D., Popp, D.L., Williams, J.A., Osborn, S.D., Rogers, B.W., Beard, L.O., McIntire, A.M., Hersey, K.A., Tobin, A., Bjornlie, N.L., Foote, J., Bachen, D.A., Maxell, B.A., Morrison, M.L., Thomas, S.C., Oliver, G. V, Navo, K.W., 2018. A review of bat hibernacula across the western United States: Implications for white-nose syndrome surveillance and management. PLoS One 13(10), e0205647. https://doi.org/10.1371/journal.pone.0205647

WNS National Plan Writing Team, A National Plan for Assisting States, Federal Agencies, and Tribes in Managing White-Nose Syndrome in Bats (2011), p. 21.

Wibbelt, G., Kurth, A., Hellmann, D., Weishaar, M., Barlow, A., Veith, M., Prüger, J., Görföl, T., Grosche, L., Bontadina, F., Zöphel, U., Seidl, H.-P., Cryan, P.M., Blehert, D.S., 2010. White-nose syndrome fungus (*Geomyces destructans*) in bats, Europe. Emerging Infectious Diseases, 16(8), 1237–1243. https://doi.org/10.3201/eid1608.100002

Williams, T.C., Ireland, L.C., Williams, J.M., 1973. High altitude flights of the free-tailed bat, *Tadarida brasiliensis*, observed with radar. Journal of Mammalogy, 54(4), 807–821. https://doi.org/10.2307/1379076

Willis, C.K., Brigham, R.M., 2003. Defining torpor in free-ranging bats: experimental evaluation of external temperature-sensitive radiotransmitters and the concept of active temperature. Journal of Comparative Physiology B, 173, 379–389. https://doi.org/10.1007/s00360-003-0343-y

Willis, C.K., Lane, J. E., Liknes, E.T., Swanson, D. L., Brigham, R.M., 2005. Thermal energetics of female big brown bats, *Eptesicus fuscus*. Canadian Journal of Zoology, 83(6), 871–879. https://doi.org/10.1139/z05-074

Willis, C.K., 2007. An energy-based body temperature threshold between torpor and normothermia for small mammals. Physiological and Biochemical Zoology, 80(6), 643–651. https://doi.org/10.1086/521085

Willis, C.K.R., 2008. Do roost type or sociality predict warming rate? A phylogenetic analysis of torpor arousal, in: Lovegrove, B.G., McKechnie, A.E. (Eds.), Hypometabolism in animals: hibernation, torpor and cryobiology. School of Biological and Conservation Sciences, University of KwaZulu-Natal, Pietermaritzburg, pp. 373–384.

Willis, C.K., Menzies, A.K., Boyles, J.G., Wojciechowski, M.S., 2011. Evaporative water loss is a plausible explanation for mortality of bats from white-nose syndrome. Integrative and Comparative Biology, 51(3), 364–373. https://doi.org/10.1093/icb/icr076

Willis, C.K., 2015. Conservation physiology and conservation pathogens: white-nose syndrome and integrative biology for host–pathogen systems. Integrative and Comparative Biology, 55, 631–641.

Willis, C.K., 2017. Trade-offs influencing the physiological ecology of hibernation in temperate-zone bats. Integrative and Comparative Biology, 57(6), 1214–1224. https://doi.org/10.1093/icb/icx087

Wilz, M., Heldmaier, G., 2000. Comparison of hibernation, estivation and daily torpor in the edible dormouse, *Glis glis*. Journal of Comparative Physiology B, 170(7), 511–521. https://doi.org/10.1007/s003600000129

Wisz, M.S., Hijmans, R.J., Li, J., Peterson, A.T., Graham, C.H., Guisan, A., NCEAS Predicting Species Distributions Working Group, 2008. Effects of sample size on the performance of species distribution models. Diversity and Distributions, 14(5), 763–773. https://doi.org/10.1111/j.1472-4642.2008.00482.x

Wright, S.K., Moran, J.R., 2011. Ocean-going vessels: a possible conduit for the introduction of white-nose syndrome fungus (*Geomyces destructans*) into bats in Alaska. Northwestern Naturalist, 92(2), 133–135. https://doi.org/10.1898/1051-1733-92.2.133

Yacoe, M.E., 1983. Protein metabolism in the pectoralis muscle and liver of hibernating bats, *Eptesicus fuscus*. Journal of Comparative Physiology, 152, 137–144.

Yee, T.W., Mitchell, N.D., 1991. Generalized additive models in plant ecology. Journal of Vegetation Science, 2(5), 587-602. https://doi.org/10.2307/3236170

Zuur, A., Ieno, E.N., Walker, N., Saveliev, A.A., Smith, G.M., 2009. Mixed effects models and extensions in ecology with R. Springer Science & Business Media.

Appendices

A. <u>Supporting Data</u>

Appendix A1. Intra-specific species physiology data for McGuire et al. In Review. Full data and metadata available at https://doi.org/dryad.73n5tb2w

Appendix A2. Inter-specific species physiology data for McGuire et al. In Review. Full data and metadata available at https://doi.org/10.5061/dryad.12jm63xwg

Appendix A3. Body composition data for McGuire et al. In Review. Full data and metadata available at https://doi.org/dryad.3r2280gfg

Appendix A4. *Tadarida brasiliensis* data Kunkel et al. In Prep. Full data and metadata available at https://doi.org/10.5061/dryad.12jm63xwg

Appendix A5. Parameters used to apply cooling model across mammalian species: cooling rate (CR; °C h^{-1}), warming rate (WR; °C h^{-1}), body mass (M$_b$; g), thermal conductance (C; ml O$_2$ g^{-1} °C^{-1}), euthermic (T$_{eu}$; °C) and torpid (T$_{tor}$; °C) body temperature, air temperature (T$_a$; °C), and Q$_{10}$ rates.

Species, by Order	CR	WR	M$_b$	C	T$_{eu}$	T$_{tor}$	T$_a$	Q$_{10}$	Reference [Conductance Reference]
Chiroptera									
Chalinolobus gouldii	1.29	84.0	12	0.34	36	6	5	3.27	Hosken and Withers 1997
Corynorhinus townsendii	0.80	91.2[1]	10	0.20	37	9	8	3.32	CGH et al. unpublished data [Speakman and Thomas 2003]
Eptesicus fuscus	0.61	90.0[2]	18	0.20	37	16	15	3.19	Halsall et al. 2012 [Willis 2015]
Lasionycteris noctivagans	0.59	162.0[2]	11	0.15	35	6	5	3.30	Dunbar 2007
Lasiurus borealis	0.46	106.8[2]	13	0.13	35	6	5	3.26	Dunbar and Tomasi 2006
Lasiurus cinereus	0.53	128.4[2]	25	0.18	35	6	5	3.11	Cryan and Wolf 2003
Myotis californicus	1.26	77.4[1]	5	0.26	35	11	10	3.47	CGH et al. unpublished data [Speakman and Thomas 2003]
Myotis lucifugus	1.11	64.0[1]	9	0.26	37	5	4	3.33	Czenze and Willis 2015 [Hayman et al. 2016]
Myotis myotis	0.51	24.2[1]	25	0.20	35	17	16	3.11	Wojciechowski et al. 2007
Myotis nattereri	0.77	63.0[1]	8	0.18	35	10	8	3.36	Hope and Jones 2012 [Speakman and Thomas 2003]
Myotis velifer	0.70	50.0	14	0.20	37	9	8	3.23	CGH et al. unpublished data [Hirshfeld and O'Farrell 1976]
Myotis yumanensis	0.72	27.6	6	0.15	37	9	8	3.44	Licht and Leitner 1967 [O'Farrell and Studier 1970]
Nyctalus noctula	0.21	94.8[1]	27	0.07	37	5	5	3.09	Kayser 1964
Nyctophilus geoffroyi	1.57	80.4[2]	8	0.36	36	6	6	3.37	Geiser and Brigham 2000 [Herreid and Kessel 1967]
Pipistrellus pipistrellus	1.10	57.0[1]	6	0.23	37	6	5	3.43	Kayser 1964
Tadarida brasiliensis	0.90	43.8[1]	12	0.25	36	11	10	3.27	Herreid and Schmidt-Nielsen 1966
Tadarida teniotis	0.45	46.8[1]	30	0.18	35	22	15	3.07	Marom et al. 2006
Dasyuromorphia									
Dasyuroides byrnei	0.21	33.0[1]	120	0.13	34	11	10	2.77	Geiser and Baudinette 1987

Appendix A5, continued

Species, by Order	CR	WR	M_b	C	T_{eu}	T_{tor}	T_a	Q_{10}	Reference [Conductance Reference]
Planigale gilesi	1.19	57.0	8	0.33	33	10	15	3.36	Geiser and Baudinette 1988 [Stone and Purvis 1992]
Sminthopsis macroura	0.50	8.0[1]	28	0.22	34	21	19	3.09	Song et al. 1995
Diprotodontia									
Burramys parvus	0.32	26.4[1]	54	0.14	36	3	2	2.94	Fleming 1985 [Herreid and Kessel 1967]
Cercartetus concinnus	0.70	47.4[1]	17	0.21	34	6	5	3.20	Geiser 1987
Cercartetus lepidus	0.78	54.0[1]	12	0.21	34	6	5	3.27	Geiser 1987
Cercartetus nanus	0.22	24.0[1]	70	0.11	35	6	5	2.88	Song et al. 1997
Eulipotyphla									
Crocidura leucodon	0.61	54.0[1]	12	0.20	36	24	20	3.27	Nagel 1977
Crocidura russula	0.69	54.0[1]	14	0.20	36	19	10	3.24	Nagel 1977
Crocidura suaveolens	1.56	54.0[1]	8	0.37	36	20	10	3.38	Nagel 1977
Erinaceus europaeus	0.19	10.2	505	0.18	34	11	10	2.45	Webb and Ellison 1998
Rodentia									
Baiomys taylori	1.44	20.4	6	0.39	36	22	20	3.41	Hudson 1965
Callospermophilus lateralis	0.18	20.0	137	0.12	35	16	15	2.74	Larkin and Heller 1996 [Snapp and Heller 1981]
Chaetodipus californicus	0.70	54.6	22	0.23	34	11	5	3.14	Tucker 1965
Chaetodipus hispidus	0.47	21.0	40	0.21	38	18	17	3.01	Wang and Hudson 1970
Cricetus cricetus	0.15	30.0[1]	370	0.13	35	10	8	2.52	Waßmer and Wollnik 1997 [Kayser 1964]
Eliomys quercinus	0.34	54.0[1]	80	0.17	33	6	5	2.86	Pajunen, 1970 [Kayser 1964]
Glis glis	0.20	51.0[1]	100	0.11	36	8	8	2.81	Wilz and Heldmaier 2000 [Kayser 1961]
Ictidomys mexicanus	0.18	21.0[1]	190	0.14	36	15	17	2.66	Neumann and Cade 1965 [Snyder and Nestler 1990]
Ictidomys tridecemlineatus	0.16	27.0[1]	190	0.11	35	7	6	2.66	Pohl and Hart 1965 [Aschoff 1981]
Marmota broweri	0.03	2.9	2400	0.04	30	10	2	2.11	Lee et al. 2016
Marmota flaviventris	0.02	2.3	3405	0.04	36	9	8	2.03	Arnold 1988 [Florant and Heller 1977]
Marmota marmot	0.02	5.0[1]	3870	0.04	34	10	7	2.00	Ortmann and Heldmaier 2000 [Kayser 1964]

181

Species, by Order	CR	WR	M_b	C	T_{eu}	T_{tor}	T_a	Q_{10}	Reference [Conductance Reference]
Mesocricetus auratus	0.35	25.8[1]	80	0.17	37	5	4	2.86	Lyman, 1948
Microdipodops pallidus	0.53	48.0[1]	15	0.15	39	9	8	3.22	Bartholomew and MacMillen 1961
Muscardinus avellanarius	0.87	66.0[1]	15	0.26	36	11	10	3.22	Pretzlaff and Dausmann 2012
Rodentia, continued									
Otospermophilus beecheyi	0.11	2.6	502	0.12	32	15	14	2.45	Strumwasser 1959 [Aschoff 1981]
Perognathus longimembris	1.18	24.0[1]	8	0.27	35	5	3	3.35	Bartholomew and Cade 1957
Phodopus sungorus	0.32	8.7	31	0.13	32	18	12	3.07	Heldmaier et al. 2004
Sicista betulina	1.53	72.0[1]	10	0.38	38	6	5	3.31	Johansen and Krog 1959
Spermophilus citellus	0.15	24.0[1]	290	0.11	36	6	1	2.57	Hut et al. 2002) [Aschoff 1981]
Tamias amoenus	0.52	56.0[1]	50	0.21	38	3	1	2.96	Geiser and Kenagy 1988 [Kenagy and Vleck 1982]
Tamias striatus	0.25	60.0[1]	92	0.13	35	6	5	2.82	Neal 1976 [Wang and Hudson 1970]
Urocitellus parryii	0.14	7.0	406	0.11	35	0	-2	2.50	Boyer and Barnes, 1999 [Hock 1960]
Urocitellus richardsonii	0.19	9.4	400	0.17	37	10	10	2.50	Wang 1978) [Snyder and Nestler 1990]
Zapus princeps	0.72	60.0[1]	26	0.25	33	6	5	3.10	Cranford 1983
Monotremata									
Tachyglossus aculeatus	0.01	4.3	4600	0.03	33	2	2	1.96	Grigg et al. 1992 [Nicol and Andersen 2007]

[1](Geiser and Baudinette 1990)
[2](Menzies et al. 2016)

Appendix A6. Parameters for the energetics model for the little brown bat (*Myotis lucifugus*), their units, and the reference.

Parameter Name	Parameter	Value	Units	Reference
Basal metabolic rate	BMR	2.6	ml O_2 g^{-1} h^{-1}	Calculated from Speakman and Thomas 2003
Minimum torpid metabolic rate	TMR_{min}	0.14	ml O_2 g^{-1} h^{-1}	Measured in this study
Lower defended temperature during torpor	$T_{tor-min}$	2	°C	Hock 1951; Hanus 1959; Speakman et al. 1991
Lower critical temperature	T_{lc}	32	°C	Hock 1951; Hanus 1959; Speakman et al. 1991
Euthermic body temperature	T_{eu}	37	°C	Thomas et al. 1990; Hock 1951; Hanus 1959; Speakman et al. 1991
Change in torpid metabolism	Q_{10}	$1.6 + 0.26\,T_a - 0.006T_a^2$	-	Hock 1951
Torpid thermal conductance	C_t	0.20	ml O_2 g^{-1} °C^{-1} h^{-1}	Calculated from McNab 1980
Euthermic thermal conductance	C_{eu}	0.26	ml O_2 g^{-1} °C^{-1} h^{-1}	Calculated from Fenton 1970
Wing surface area	SA_{wing}	19.68	cm^{-2}	Calculated in this study
Body surface area	SA_{body}	39.26	cm^{-2}	Calculated from Gouma et al. 2012
Area-specific rate of evaporative water loss for wing	$rEWL_{wing}$	0.33	mg hr^{-1} ΔWVP^{-1} cm^{-2}	Calculated in this study
Area-specific rate of evaporative water loss for body	$rEWL_{body}$	0.10	mg hr^{-1} ΔWVP^{-1} cm^{-2}	Calculated in this study
Time in euthermia per arousal	t_{eu}	1.10	h	Jonasson and Willis 2012; French 1982, 1985
Maximum time in torpor	$t_{tor-max}$	1300	h	Brack and Twente 1985
Specific heat of tissue	S	0.173	ml O_2 g^{-1} °C^{-1}	Wang 1978
Rewarming rate	WR	0.80	°C min^{-1}	Haase et al. 2019a; Czenze and Willis 2015; Geiser and Baudinette 1990; Hirshfeld and O'Farrell 1976
Body mass	M_b	7.80	g	Measured in this study
Proportion of lean mass	pLean	0.58	g	Measured in this study
Proportion of fat mass	pFat	0.26	g	Measured in this study

Appendix A6, continued

Parameter Name	Parameter	Value	Units	Reference
Proportion of body water threshold	pMass	0.027	mg	Calculated in this study
Humidity-dependent fungal growth parameter	μ_1	1.51×10^{-4}	-	Hayman et al. 2016
Humidity-dependent fungal growth parameter	μ_2	-9.92×10^{-3}	-	Hayman et al. 2016
Temperature-dependent fungal growth parameter	β_1	1.15×10^{-3}	-	Hayman et al. 2016
Temperature-dependent fungal growth parameter	β_2	0.27	-	Hayman et al. 2016

Appendix A7. Lick Creek *M. lucifugus* data for Haase et al. 2019b. Full data and metadata available at https://doi.org/10.5061/dryad.2280gb5n2

Appendix A8. Winter hibernation duration data for *Myotis lucigugus.* Location data was coerced to the center of the cell to protect hibernacula locations. Some dates were given arbitrary years to calculate duration

Latitude	Longitude	Start	End	Winter Duration	Reference
53.12	-99.19	15/09/2018	15/05/2019	242	Czenze and Willis 2015
51.44	-97.38	13/09/2018	15/05/2019	244	Norquay and Willis 2014
53.12	-99.19	15/09/2018	15/05/2019	242	Jonasson and Willis 2012
59.75	-112.20	15/10/2018	15/05/2019	212	Reimer et al. 2014
44.93	-110.67	15/10/2018	10/4/2019	177	Johnson et al. 2016
38.83	-92.29	NA	NA	83	Brack Jr. and Twente 1985
36.61	-83.66	4/12/2018	1/4/2019	118	Hayman et al. 2017
58.30	-134.40	24/10/2018	31/03/2019	158	Karen Blejwas
61.00	-135.00	30/09/2018	18/04/2019	200	Tom Jung
59.60	-133.60	15/10/2018	24/03/2019	160	Cori Lausen
58.90	-125.80	21/10/2018	15/04/2019	176	Cori Lausen
59.40	-126.10	7/10/2018	7/4/2019	182	Cori Lausen
60.00	-111.88	15/10/2018	15/04/2019	182	Sharon Irwin and Cori Lausen
53.80	-116.50	15/09/2018	15/05/2019	242	Cori Lausen
43.24	-73.51	10/10/2018	15/05/2019	217	Davis and Hitchcock 1965
60.96	-117.33	5/10/2018	20/04/2019	197	Joanna Wilson
47.12	-111.00	NA	NA	180	SERDP
51.75	-124.72	15/10/2015	21/03/2016	158	WCS-C Recorder
51.52	-122.29	21/10/2015	27/03/2016	158	WCS-C Recorder
49.12	-116.63	6/11/2012	27/04/2013	172	WCS-C Recorder
55.20	-129.10	28/10/2015	1/3/2016	125	WCS-C Recorder
49.01	-119.50	1/12/2012	11/3/2013	100	WCS-C Recorder
53.88	-124.59	25/09/2015	30/03/2016	187	WCS-C Recorder
51.50	-122.30	22/10/2015	29/03/2016	159	WCS-C Recorder
49.02	-118.34	13/12/2010	4/3/2011	81	WCS-C Recorder
55.24	-127.67	11/10/2014	8/4/2015	179	WCS-C Recorder
54.30	-129.40	4/10/2014	16/03/2015	163	WCS-C Recorder
49.91	-116.90	20/11/2013	27/03/2014	127	WCS-C Recorder
49.30	-116.66	28/12/2014	4/3/2015	66	WCS-C Recorder
54.41	-128.52	3/11/2015	5/3/2016	123	WCS-C Recorder
55.21	-129.14	21/11/2015	25/03/2016	125	WCS-C Recorder
59.43	-126.10	25/09/2015	24/04/2016	212	WCS-C Recorder
50.52	-121.72	26/11/2014	17/04/2015	142	WCS-C Recorder
50.83	-121.88	4/11/2014	18/04/2015	165	WCS-C Recorder
50.63	-121.86	9/12/2014	2/3/2015	83	WCS-C Recorder
50.28	-115.85	31/10/2013	25/03/2014	145	WCS-C Recorder
50.28	-115.85	21/09/2012	26/03/2013	186	WCS-C Recorder
55.06	-129.47	14/10/2014	15/03/2015	152	WCS-C Recorder
49.30	-116.76	17/11/2012	14/03/2013	117	WCS-C Recorder
49.01	-118.35	17/12/2011	14/03/2012	88	WCS-C Recorder

Appendix A8, continued

Latitude	Longitude	Start	End	Winter Duration	Reference
49.78	-119.74	23/10/2013	19/04/2014	178	WCS-C Recorder
49.08	-116.58	17/11/2012	27/04/2013	161	WCS-C Recorder
49.45	-119.56	15/06/2012	31/08/2012	77.5	WCS-C Recorder
49.44	-119.57	16/11/2012	23/03/2013	127	WCS-C Recorder
49.91	-126.65	24/10/2014	1/3/2015	128	WCS-C Recorder
57.90	-131.17	4/10/2015	20/03/2016	168	WCS-C Recorder
49.76	-124.57	3/12/2015	4/3/2016	92	WCS-C Recorder
59.57	-133.70	6/10/2015	2/5/2016	209	WCS-C Recorder
54.07	-131.80	30/12/2014	4/3/2015	64	WCS-C Recorder
53.58	-124.79	18/10/2014	11/3/2015	144	WCS-C Recorder
49.30	-119.55	30/12/2013	4/3/2014	64	WCS-C Recorder

Appendix A9. Spatial body mass data for *Myotis lucifugus*. Locations were obscured to the center of the raster cell from which the data was taken.

Latitude	Longitude	Mass (g)	Reference
39.40	-105.47	8.5	VertNet.org 2014
39.51	-121.55	7	VertNet.org 2014
39.55	-107.79	5.9	VertNet.org 2014
39.72	-96.64	7.3	VertNet.org 2014
40.41	-121.37	7	VertNet.org 2014
40.63	-105.15	7.7	VertNet.org 2014
42.66	-77.96	8.8	VertNet.org 2014
42.69	-77.96	6.9	VertNet.org 2014
43.65	-108.21	5.1	VertNet.org 2014
43.99	-75.93	14.5	VertNet.org 2014
44.00	-75.99	7.35	VertNet.org 2014
44.03	-76.05	9	VertNet.org 2014
44.38	-108.04	6.45	VertNet.org 2014
44.54	-89.56	8.2	VertNet.org 2014
44.80	-106.95	6.9	VertNet.org 2014
44.88	-107.26	5.4	VertNet.org 2014
45.30	-93.58	9.23	VertNet.org 2014
47.91	-122.10	6.45	VertNet.org 2014
48.76	-122.49	6.73	VertNet.org 2014
57.76	-152.52	6	VertNet.org 2014
58.33	-134.60	6.53	VertNet.org 2014
58.33	-134.60	6.65	VertNet.org 2014
58.69	-156.66	6.75	VertNet.org 2014
59.45	-135.32	7.08	VertNet.org 2014
59.45	-135.32	7.43	VertNet.org 2014
59.45	-135.33	7.5	VertNet.org 2014
59.50	-135.26	8.04	VertNet.org 2014
64.84	-147.72	5.6	VertNet.org 2014
64.85	-148.05	5.4	VertNet.org 2014
59.52	-112.22	8.97	WCS Canada
60.05	-112.68	9.91	WCS Canada
59.74	-112.22	9.63	WCS Canada
59.75	-112.20	9.94	WCS Canada
47.12	-111.00	8.22	SERDP
41.81	-111.62	6.72	SERDP
53.03	-117.33	11.21	Schowalter 1980
45.30	-76.90	11.1	McGuire et al. 2009
47.40	-80.44	9.55	Fenton, 1970
53.10	-99.16	12.56	McGuire et al. 2016
43.24	-73.04	9.06	Kunz and T. H. Kunz 1987
43.24	-73.04	9.19	Kunz 1995
45.30	-76.90	10	Fenton 1970
48.98	-87.40	10.3	Fenton 1970

Appendix A9, continued

Latitude	Longitude	Mass (g)	Reference
46.29	-81.86	9.5	Fenton, 1970
44.93	-110.67	7.76	Johnson et al. 2016
6.26	-133.34	11.34	WCS Canada Yukon
60.36	-134.59	8.73	WCS Canada Yukon

Appendix A10. Cave microclimate data for McClure et al. 2020. Full data and metadata available at https://doi.org/10.5061/dryad.51c59zw66

Appendix A11. Species distribution data for McClure et al. In Review. Full data and metadata available at https://doi.org/10.5061/dryad.crjdfn32r

Appendix A12. We collected data from 13 species of hibernating bats, including metabolic rate and evaporative water loss. The range of temperatures at which the lowest torpid metabolic rate (TMR) was recorded varied among species. Within that range of temperatures minimum torpid metabolic rate (TMR$_{min}$) did not vary among species, but species were divided into a high evaporative water loss (EWL) and low EWL cluster.

Species	n	Sites[1]	Body Mass (g)	Range Tested (°C)	Temperature Effect[2]	TMR$_{min}$ (mW g^{-1})	Range TMR$_{min}$ (°C)	T$_{defended}$[3] (°C)	EWL (mg H$_2$O min^{-1} g^{-1})	EWL Cluster
Vespertilionidae										
Corynorhinus townsendii	152	BC, CO, NV$_1$, NV$_2$, OR, UT	10.3 ± 0.1	2 – 10	LR$_3$ = 13.0, p-value = 0.0047	0.33 ± 0.03	5 – 8	2 – 5	0.009 ± 0.001	Low
Eptesicus fuscus	7	MT$_1$	16.7 ± 1.2	2 – 10	LR$_3$ = 1.6, p-value = 0.67	0.25 ± 0.07	2 –10	< 2	0.009 ± 0.002	Low
Lasionycteris noctivagans	23	BC$_2$	12.7 ± 0.2	0 – 8	LR$_4$ = 15.6, p-value = 0.0036	0.15 ± 0.01	2 – 8	0 – 2	0.005 ± 0.001	Low[4]
Myotis californicus	45	BC$_2$	5.7 ± 0.1	0 – 10	LR$_5$ = 22.0, p-value = 0.0005	0.26 ± 0.02	2 – 8	0 – 2	0.010 ± 0.002	Low
Myotis ciliolabrum	23	MT$_1$, NV$_2$	5.0 ± 0.1	2 – 10	LR$_3$ = 6.2, p-value = 0.10	0.26 ± 0.04	2 – 10	< 2	0.009 ± 0.001	Low
Myotis evotis	13	MT$_2$	7.5 ± 0.2	2 – 10	LR$_3$ = 16.7, p-value = 0.0008	0.48 ± 0.09	5 – 10	2 – 5	0.019 ± 0.001	High
Myotis lucifugus	99	MT$_2$, AB, NWT	8.9 ± 0.1	2 – 10	LR$_3$ = 15.2, p-value = 0.0016	0.30 ± 0.02	2 – 8	< 2	0.014 ± 0.001	High
Myotis thysanodes	11	MT$_2$	9.4 ± 0.3	2 – 10	LR$_3$ = 11.2, p-value = 0.011	0.25 ± 0.08	5 – 10	2 – 5	0.018 ± 0.001	High

Appendix A12, continued

Species	n	Sites[1]	Body Mass (g)	Range Tested (°C)	Temperature Effect[2]	TMR_{min} (mW g^{-1})	Range TMR_{min} (°C)	$T_{defended}$[3] (°C)	EWL (mg H_2O min^{-1} g^{-1})	EWL Cluster
Myotis velifer	33	OK	14.4 ± 0.3	2 – 10	LR_3 = 8.0, p-value = 0.046	0.25 ± 0.04	5 – 10	2 – 5	0.015 ± 0.001	High
Myotis volans	12	MT_1, MT_2	9.0 ± 0.2	2 – 10	LR_3 = 10.6, p-value = 0.014	0.43 ± 0.08	5 – 10	2 – 5	0.015 ± 0.001	High
Myotis yumanensis	27	BC_2, BC_3	5.8 ± 0.1	0 – 8	LR_4 = 48.4, p-value < 0.0001	0.20 ± 0.01	4 – 6	2 – 4	n/a[5]	
Perimyotis subflavus	34	OK	7.0 ± 0.1	2 – 10	LR_3 = 17.1, p-value < 0.001	0.18 ± 0.04	8 – 10	5 – 8	0.017 ± 0.002	High
Molossidae										
Tadarida brasiliensis	27	TX	13.4 ± 0.4	2 – 12	LR_4 = 63.2, p-value < 0.0001	0.35 ± 0.06	8 – 12	5 – 8	0.010 ± 0.001	Low

[1]Subscripts identify sites in states or provinces with multiple sites.
[2]LR = likelihood ratio, degrees of freedom indicated in subscript.
[3]Where metabolic rate did not increase at coldest temperature tested, $T_{defended}$ can only be determined as less than the lowest temperature tested. Otherwise $T_{defended}$ is between the range of temperatures indicated.
[4]*L. noctivagans* may represent a third cluster with lower EWL (see Figure 20b), but to be conservative we present only two clusters here.
[5]EWL was not measured for *M. yumanensis*.

Appendix A13: Summary of previous studies that calculated energy expenditure during torpor or arousals, including the various methods by which warming and cooling costs have been considered. Warming models consider the effects of body mass (M_b), specific heat capacity of tissues (S), euthermic (T_{eu}) and torpid (T_b) body temperatures, and resting (RMR) and torpid (TMR) metabolic rates.

Species	Warming Model	Cooling Use	Reference
Various bats	$M_b(T_{eu} - T_{tor})S$	None	Prothero and Jürgens 1986
Myotis lucifugus	$(T_{eu} - T_{tor})S$	67.2% of warming	Thomas et al. 1990
Myotis lucifugus	$(T_{eu} - T_{tor})S$	None	Humphries et al. 2002
Lasiurus cinereus	$M_b(T_{eu} - T_{tor})S + \int_{t_1}^{t_2} C(T_{eu} - T_a)$	None	Cryan and Wolf 2003
Lasiurus cinereus	$[M_b(T_{eu} - T_{tor})S] + D^*_{warm}\left(TMR + \dfrac{RMR - TMR}{2}\right)$	None	Willis et al. 2006
Myotis lucifugus	$(T_{eu} - T_{tor})S$	65% of warming	Frederico 2007
Myotis lucifugus	$(T_{eu} - T_{tor})S$	67% of warming	Boyles and Brack 2009
Myotis lucifugus	$(T_{eu} - T_{tor})S$	67% of warming	Boyles and McKechnie 2010
Various bats	$(T_{eu} - T_{tor})S$	67% of warming	Boyles and Willis 2010
Myotis lucifugus	$(T_{eu} - T_{tor})S$	67% of warming	Jonasson and Willis 2012**
Myotis lucifugus	$(T_{eu} - T_{tor})S$	67% of warming	Ehlman et al. 2013
Myotis lucifugus	None	None	Burles et al. 2014
Lasionycteris noctivagans	$M_b(T_{eu} - T_{tor})S + \int_{t_1}^{t_2} C(T_{eu} - T_a)$	67.2% of warming	McGuire et al. 2014
Various bats	$(T_{eu} - T_{tor})S$	None	Hayman et al. 2016
Myotis lucifugus	$[M_b(T_{eu} - T_{tor})S] + D^*_{warm}\left(TMR + \dfrac{RMR - TMR}{2}\right)$	67.2% of warming	Wilcox and Willis 2016
Myotis lucifugus	$(T_{eu} - T_{tor})S$	67.2% of warming	Czenze et al. 2017

*D_{warm} is defined as the time required to warming tissues, a function of the rate of warming and gradient between euthermic and torpid body temperatures

**Jonasson and Wills (2012) also used models published by Thomas et al. (1990) and Humphries et al. (2002) listed in the table

Appendix A14: Summary of spatial products created for *Myotis lucifugus*. Hibernation duration was predicted in days and defined as the annual period during which bats must hibernate to survive. Pre-hibernation body mass and initial fat mass were predicted from glm models. Fat required refers to the predicted amount of fat required to survive the duration of winter hibernation. Survival capacity is defined as the predicted fat required to survive hibernation – the predicted body fat available for bats going into hibernation and/or the predicted maximal number of days that a bat could hibernate – the duration of winter. Negative values represent a predicted shortfall in the fat required to survive hibernation while positive values indicate a surplus of fat stores remaining at emergence from hibernation. Finally the % increased expenditure represents the increased fat required to survive hibernation between infected and uninfected bats calculated as the difference between predicted fat use of the infected and healthy individuals divided by the healthy multiplied by 100.

Results Layer	Units	Env. Conditions	Pd Infection	Median	Mean	SD	5%	95%	Minimum	Maximum
Hibernation Duration	days	-	-	178.95	169.17	45.35	79.70	224.40	0.00	288.34
Body Mass	grams	-	-	8.64	9.14	1.84	7.04	12.52	4.53	23.27
Body Fat	grams	-	-	2.32	2.61	1.10	1.36	4.63	0.00	11.05
Fat Required	grams	4x98	No	0.48	0.45	0.12	0.21	0.60	0.00	0.77
Fat Required	grams	4x98	Yes	1.22	1.16	0.45	0.35	1.77	0.00	2.71
Fat Required	grams	Best A. x 98	No	0.49	0.49	0.21	0.28	0.60	0.00	7.28
Fat Required	grams	Best A. x 98	Yes	1.21	1.20	0.40	0.51	1.77	0.00	7.28
Survival Capacity	grams	4x98	No	1.84	2.16	1.01	1.07	4.05	-0.50	10.67
Survival Capacity	grams	4x98	Yes	1.22	1.45	0.76	0.61	2.93	-1.36	10.21
Survival Capacity	grams	Best A. x 98	No	1.82	2.12	1.02	1.00	4.05	-3.17	10.47
Survival Capacity	grams	Best A. x 98	Yes	1.11	1.41	0.93	0.35	3.33	-3.26	9.90
Survival Capacity	days	4x98	No	181.05	190.83	45.35	135.60	280.30	71.66	370.79
Survival Capacity	days	4x98	Yes	45.63	55.41	45.35	0.19	144.88	-63.76	235.37
Survival Capacity	days	Best A. x 98	No	181.05	188.79	49.37	134.22	280.07	-175.95	370.79
Survival Capacity	days	Best A. x 98	Yes	45.38	46.86	32.55	0.66	102.67	-175.95	182.56
Increased Expenditure	%	4x98	-	154.42	145.18	41.57	62.66	195.26	0.00	251.46
Increased Expenditure	%	Best A. x 98	-	147.11	142.42	36.52	72.09	192.08	0.00	269.57

Appendix A15: Final predictor sets and their relative influences in boosted regression tree (BRT) models used to estimate winter species distributions of five focal bat species across the United States and Canada, including a) *Corynorhinus townsendii*, b) *Myotis californicus*, c) *Myotis lucifugus*, d) *Myotis velifer*, and e) *Perimyotis subflavus*.

a) *Corynorhinus townsendii*

Variable	Neighborhood size	Sample resolution	Relative influence
Distance to mine	--	10 km	15.32
Elevation	--	10 km	11.94
Percent tree cover	5 km	1 km	10.75
Ruggedness	500 m	1 km	10.65
Annual snow days	--	1 km	9.34
Groundwater depth	--	10 km	8.13
Night lights	--	1 km	7.92
Solar insolation	Multiscale	1 km	7.73
Karst	--	1 km	6.74
Topographic position	5 km	1 km	5.61
Winter survivorship	--	1 km	4.66
Percent water	500 m	1 km	1.2

b) *Myotis californicus*

Variable	Neighborhood size	Sample resolution	Relative influence
Winter survivorship	--	10 km	20.39
Distance to mine	--	1 km	12.13
Night lights	--	1 km	10.33
Percent tree cover	5 km	10 km	9.88
Annual snow days	--	1 km	9.53
Topographic position	Multiscale	10 km	8.83
Ruggedness	25 km	1 km	8.68
Solar insolation	5 km	1 km	8.1
Percent water	25 km	10 km	7.53
Groundwater depth	--	1 km	4.6

c) *Myotis lucifugus*

Variable	Neighborhood size	Sample resolution	Relative influence
Topographic position	Multiscale	1 km	16.22
Ruggedness	Multiscale	1 km	13.68
Solar insolation	25 km	10 km	11.36
Night lights	--	1 km	11.15
Winter survivorship	--	10 km	11.11
Annual precipitation	--	10 km	10.78
Percent water	5 km	1 km	8.73
Percent tree cover	25 km	1 km	8.54
Groundwater depth	--	10 km	8.44

Appendix A15, continued

d) *Myotis velifer*

Variable	Neighborhood size	Sample resolution	Relative influence
Elevation	--	10 km	16.57
Ruggedness	500 m	10 km	12.48
Percent tree cover	25 km	1 km	12.46
Annual precipitation	--	10 km	11.71
Solar insolation	25 km	1 km	9.61
Percent water	25 km	1 km	7.9
Topographic position	500 m	1 km	6.91
Distance to mine	--	10 km	5.51
Groundwater depth	--	10 km	5.24
Karst	--	1 km	4.44
Winter survivorship	--	1 km	3.99
Night lights	--	10 km	3.17

e) *Perimyotis subflavus*

Variable	Neighborhood size	Sample resolution	Relative influence
Ruggedness	5 km	1 km	12.61
Night lights	--	1 km	12.54
Topographic position	25 km	1 km	10.6
Groundwater depth	--	10 km	8.42
Annual precipitation	--	1 km	8.26
Winter survivorship	--	10 km	7.77
Elevation	--	10 km	7.74
Distance to mine	--	10 km	7.37
Karst	--	1 km	7.28
Percent water	5 km	1 km	7.05
Percent tree cover	5 km	1 km	6.4
Annual snow days	--	10 km	3.97

B. List of Scientific/Technical Publications

1. Articles in peer-reviewed journals
   a. In print
      i. Haase, C.G., Fuller, N.W., Hranac, C.R., Hayman, D.T.S., Olson, S.H., Plowright, R.K., McGuire, L.P., 2019. Bats are not squirrels: Revisiting the cost of cooling in hibernating mammals. Journal of Thermal Biology, 81, 185–193. https://doi.org/10.1016/j.jtherbio.2019.01.013
      ii. Haase, C.G., Fuller, N.W., Hranac, C.R., Hayman, D.T.S., McGuire, L.P., Norquay, K.J.O., Silas, K.A., Willis, C.K.R., Plowright, R.K., Olson, S.H., 2019b. Incorporating evaporative water loss into bioenergetic models of hibernation to test for relative influence of host and pathogen traits on white-nose syndrome. PLoS One,14(10), e0222311. https://doi.org/10.1371/journal.pone.0222311
      iii. Fuller, N.W., Haase, C.G., Silas, K.A., Olson, S.H., Mcguire, L.P., 2019. First reported case of diphallia in *Corynorhinus townsendii*. Western North American Naturalist, 79(3), 454–457.
      iv. McClure, M.L., Crowley, D., Haase, C.G., McGuire, L.P., Fuller, N.W., Hayman, D.T.S., Lausen, C.L., Plowright, R.K., Dickson, B.G., Olson, S.H., 2020. Linking surface and subterranean climate: implications for the study of hibernating bats and other cave dwellers. Ecosphere 11. https://doi.org/10.1002/ecs2.3274
      v. Haase, C.G., Fuller, N.W., Dzal, Y.A., Hranac, C.R., Hayman, T.S., Lausen, C.L., McGuire, L.P., Silas, K.A., Olson, S.H., Plowright, R.K., 2021. Body mass and hibernation microclimate may predict bat susceptibility to white-nose syndrome. Ecology and Evolution 11. https://doi.org/10.1002/ece3.7070
   b. Accepted for publication
      i. …
   c. Submitted for publication
      i. Hranac, C.R., Haase, C.G., Fuller, N.W., McClure, M.L., Marshall, J.C., Lausen, C.L., McGuire, L.P., Olson, S.H., Hayman, D.T.S., In Review. What is winter? Modelling spatial variation in bat host traits and hibernation and their implications for overwintering energetics. Ecology and Evolution. In preprint: https://doi.org/10.22541/au.161185857.74191912/v1
      ii. McClure, M.L., Haase, C.G., Crowley, D., Hranac, C.R., Hayman, D.T.S., Mcguire, L.P., Dickson, B.G., Fuller, N.W., Plowright, R.K., Lausen, C.L., Olson, S.H., In Review. A hybrid correlative-mechanistic approach for modeling and mapping winter distributions of western bat species. Journal of Biogeography.
      iii. McClure, M.L., Haase, C.G., Crowley, D., Hranac, C.R., Hayman, D.T.S., Mcguire, L.P., Dickson, B.G., Fuller, N.W., Plowright, R.K., Lausen, C.L., Olson, S.H., In Prep. Projecting the compound effects of climate

change and white-nose syndrome on western bat species. Ecological Applications.

    iv. McGuire, L.P., Fuller, N.W., Haase, C.G., Silas, K.A., Olson, S.H., In Review. Lean mass dynamics in hibernating bats and implications for energy and water budgets. Physiological and Biochemical Zoology.

    v. McGuire, L.P., Fuller, N.W., Dzal, Y.A., Haase, C.G., Silas, K.A., Willis, C.K.R., Olson, S.H., Lausen, C.L., In Review. Similar physiology in hibernating bats across broad geographic ranges. Journal of Comparative Physiology B.

    vi. McGuire, L.P., Dzal, Y.A., Fuller, N.W., Klüg-Baerwald, B.J., Haase, C.G., Silas, K.A., Willis, C.K.R., Lausen, C.L., Olson, S.H., In Review. Interspecific variation in evaporative water loss, and not metabolic rate, among hibernating bats.

    vii. Kunkel, E.L., McGuire, L.P., In Prep. Partial migration in Mexican Free-tailed bats. Physiological and Biochemical Zoology.

    viii. Kunkel, E.L., Fuller, N.W., McGuire, L.P., In Prep. Facultative hibernation of Mexican Free-tailed bats. Comparative Biochemistry and Physiology Part A: Molecular and Integrative Biology.

d. Technical reports (specify whether in print, accepted for publication, or submitted for publication)

    i. NONE

e. Conference or symposium proceedings scientifically recognized and referenced (other than abstracts)

    i. Lausen et al., White-nose syndrome survivorship modelling and probiotic management strategies to conserve bats in British Columbia. Proceedings of Interdisciplinary Approaches to Managing Health of Fish and Wildlife. Meeting, Kimberley, B.C., Columbia Mountains Institute. July 2018. https://cmiae.org/wp-content/uploads/Proceedings_Interdisciplinary-Approaches-to-Managing-Health-of-Fish-and-Wildlife_2018.pdf

f. Conference or symposium abstracts

    i. Hranac et al., Modeling the impact of white-nose syndrome on western bat species, International Bat Research Conference, July 2016

    ii. Olson et al., Assessing white-nose syndrome susceptibility in western bats using a bioenergetic approach, USFWS White-Nose Syndrome Meeting and Workshop, May 2017

    iii. McGuire et al., Energetics disturbance and working with hibernating bats in the face of WNS, New Mexico bat working group, June 2017

    iv. Hranac et al., Modeling the impact of white-nose syndrome on two Western *Myotis* bats, Infectious Disease of Bats Symposium, July 2017

    v. Haase et al., Modeling the influence of evaporative water loss on hibernation energetics and implications for WNS, North American Society for Bat Research Conference, October 2017

    vi. McClure et al., Western bat distributions before and after exposure to WNS: a hybrid correlative-mechanistic modeling approach, North American Society for Bat Research Conference, October 2017

vii. Fuller et al., The other end of the hibernation phenotype spectrum: *Myotis velifer* and hibernation in mild environments, North American Society for Bat Research Conference, October 2017

viii. McGuire et al., Stop using body condition index, North American Society for Bat Research Conference, October 2017

ix. Olson et al., Emerging disease threats to species of importance, The Strategic Environmental Research and Development Program (SERDP) and Environmental Security Technology Certification Program (ESTCP) Symposium, November 2017

x. Olson et al., Assessing white-nose syndrome susceptibility in western bats using a bioenergetic approach, The Strategic Environmental Research and Development Program (SERDP) and Environmental Security Technology Certification Program (ESTCP) Symposium, November 2017

xi. Olson et al., Bioenergetic risk factors for WNS across the West, Montana Bat Working Group Meeting, February 2018

xii. McGuire et al., Regional variation in hibernation phenotype: *Myotis velifer* hibernation at southern latitudes and implications for white-nose syndrome. Society for Integrative and Comparative Biology, Society for Integrative and Comparative Biology, San Francisco, California, USA, 2018 Annual Meeting Abstracts, Integrative and Comparative Biology, Volume 58, Issue suppl_1, March 2018, Pages e265–e458, https://doi.org/10.1093/icb/icy002

xiii. Haase et al., Incorporating evaporative water loss into models of hibernation energetics and implications for white-nose syndrome, USFWS White-Nose Syndrome Meeting and Workshop, June 2018

xiv. McGuire et al., A conceptual framework of hibernation phenotype and interspecific variation in hibernation physiology, USFWS White-Nose Syndrome Meeting and Workshop, June 2018

xv. Fuller et al., Hibernation physiology of a launchpad species, USFWS White-Nose Syndrome Meeting and Workshop, June 2018

xvi. Olson et al., A combined empirical + modeling approach to assess the impact of WNS in the West, USFWS White-Nose Syndrome Meeting and Workshop, June 2018

xvii. McClure et al., Projected impacts of the continued spread of white-nose syndrome (WNS) to Western North American bats, North American Congress for Conservation Biology, Toronto, July 2018

xviii. Fuller et al., Interspecific variations in hibernation physiology and implications for white-nose syndrome in Western bats, North American Society for Bat Research Conference, October 2018

xix. Haase et al., Bats are not squirrels: revisiting the cost of cooling in hibernating mammals, North American Society for Bat Research Conference, October 2018

xx. Olson et al., A combined empirical + modeling approach to assess the impact of WNS in Western North America, The Strategic Environmental Research and Development Program (SERDP) and Environmental

Security Technology Certification Program (ESTCP) Symposium, November 2018

xxi. Olson et al., An empirical and modeling approach to assess the impact of white-nose syndrome in western North America, 24th Annual Meeting of the Southeastern Bat Diversity Network and 29th Annual Colloquium on the Conservation of Mammals in the Southeastern U.S., February 2019

xxii. Haase et al., Application of a new hibernation energetic model: a case study with Montana bats, Montana Bat Working Group Meeting, February 2019

xxiii. Haase et al., Estimating susceptibility of Western bat species to WNS with the application of bioenergetic disease modeling, Western Bat Working Group Meeting, May 2019

xxiv. Olson et al., Update on the study of western bat energetics, Montana Bat Working Group Meeting, February 2020

xxv. Kunkel et al., Partial migration in Mexican free-tailed bats: ecology and bioenergetics of winter residents. Society for Integrative and Comparative Biology, Society for Integrative and Comparative Biology, Austin, Texas, USA, 2020 Annual Meeting Abstracts, Integrative and Comparative Biology, Forthcoming. https://academic.oup.com/icb/pages/symposia

xxvi. Kunkel et al., Ecology and energetics of winter resident Mexican free-tailed bats (*Tadarida brasiliensis mexicana*), 38th Annual Meeting of the Texas Society of Mammalogists, Junction, Texas, February 2020

xxvii. Olson et al., A multi-species evaluation of hibernation physiology and influence on WNS-risk factors, USFWS White-Nose Syndrome Webinar, June 2020

xxviii. Olson et al., Linking surface and subterranean climate: implications for the study of hibernating bats and other cave dwellers, November 2020, White-Nose Syndrome Conference Call for state, federal, provincial agencies, stakeholders and researchers

g. Text books or book chapters
    i. NONE

C. Other Supporting Materials
   All custom code and data for the bioenergetic hibernation model are available at
   github.com/cReedHranac/winTor. The energetic model code is available from
   github.com/cReedHranac/batwintor. The code is being prepared as an R package.

   The compilation of permit reports provided to state permitting agencies (Colorado,
   Montana, Nevada, Oklahoma, Oregon, and Utah) that included analysis of bat capture
   and sampling data by site, an overview of any microclimate data collected, and site-based
   parameterization of the Haase et al. 2019b is included as an attachment.

Colorado Parks and Wildlife
Final Project Report 2016-2019
Under permits 16TR2172, 17TR2172, 18TR2172, and 19TR2172

We caught a total of 120 bats: 105 *Corynorhinus townsendii*, 2 *Eptesicus fuscus*, 9 *Myotis ciliolabrum*, and 4 *M. thysanodes* (Table 1; Appendix) over the sampling period of fall 2016 to winter 2019. During the fall, bats were caught using mist nets and harp traps at the cave entrance. During the winter, bats were hand-captured from cave walls. We determined sex, age, reproductive condition, and wing score and measured forearm length and body mass of each bat. We used quantitative magnetic resonance (QMR; Echo-MRI-B, Echo Medical Systems, Houston, TX) to measure fat mass and lean mass. We measured metabolic rate (TMR) and evaporative water loss (EWL) during torpor using open-flow respirometry. We measured body fat from 63 individuals and processed 40 individuals through respirometry. Body mass and body fat were greater in females compared to males for the species we had both sexes (Figure 1). We only captured *C. townsendii* in both seasons; there was no difference in body mass between seasons, but fat mass was greater in the fall (Figure 2). There were differences between season for both metabolic rate and evaporative water loss (Figure 3) in the one species measured in respirometry (*C. townsendii*).

We measured hibernaculum temperature and relative humidity over each hibernation period using HOBO (Model U23-001, Onset Computer Corporation) and iButton (Model DS1921Z-F5, Maxim Integrated Products) microclimate data loggers. We placed four HOBO and ten iButton loggers throughout the hibernacula in the fall and recorded conditions at 3 h intervals. We collected loggers from the hibernacula in the spring (May) of each year. The mean temperature of the cave was 4.17 °C while the mean relative humidity was 79.03% (Figure 4).

We predicted survival for *C. townsendii* (Figure 5) over the range of environmental conditions experienced in the cave (Figure 5) using a modified hibernation energetics model. Survival was predicted for both healthy individuals and those affected by white-nose syndrome. The modified hibernation energetics model estimates the time until fat exhaustion during hibernation as a function of bat characteristics, hibernaculum microclimate, and *Pseudogymnoascus destructans* growth. Survival was determined by comparing model output time to winter duration – if time until fat exhaustion is greater than winter duration, survival occurs. We validated the model predictions with field and laboratory data and determined model sensitivity to bat characteristics.

We predicted that *C. townsendii* in Paradox Mine will not suffer high mortality rates as we would expect in other areas. Our results suggest that the microclimate conditions available in Paradox Mine are perhaps suboptimal conditions for fungal growth, and therefore may not impact the population as white-nose syndrome would elsewhere.

For further information about our findings please visit www.science4bats.org/publications and review all project associated publications.

Table 1: The number of each species per year captured at Paradox Mine.

Species	Year	Count
Corynorhinus townsendii	2016	29
Corynorhinus townsendii	2017	31
Corynorhinus townsendii	2018	13
Corynorhinus townsendii	2019	32
Eptesicus fuscus	2016	1
Eptesicus fuscus	2018	1
Myotis ciliolabrum	2016	8
Myotis ciliolabrum	2017	1
Myotis thysanodes	2016	3
Myotis thysanodes	2017	1
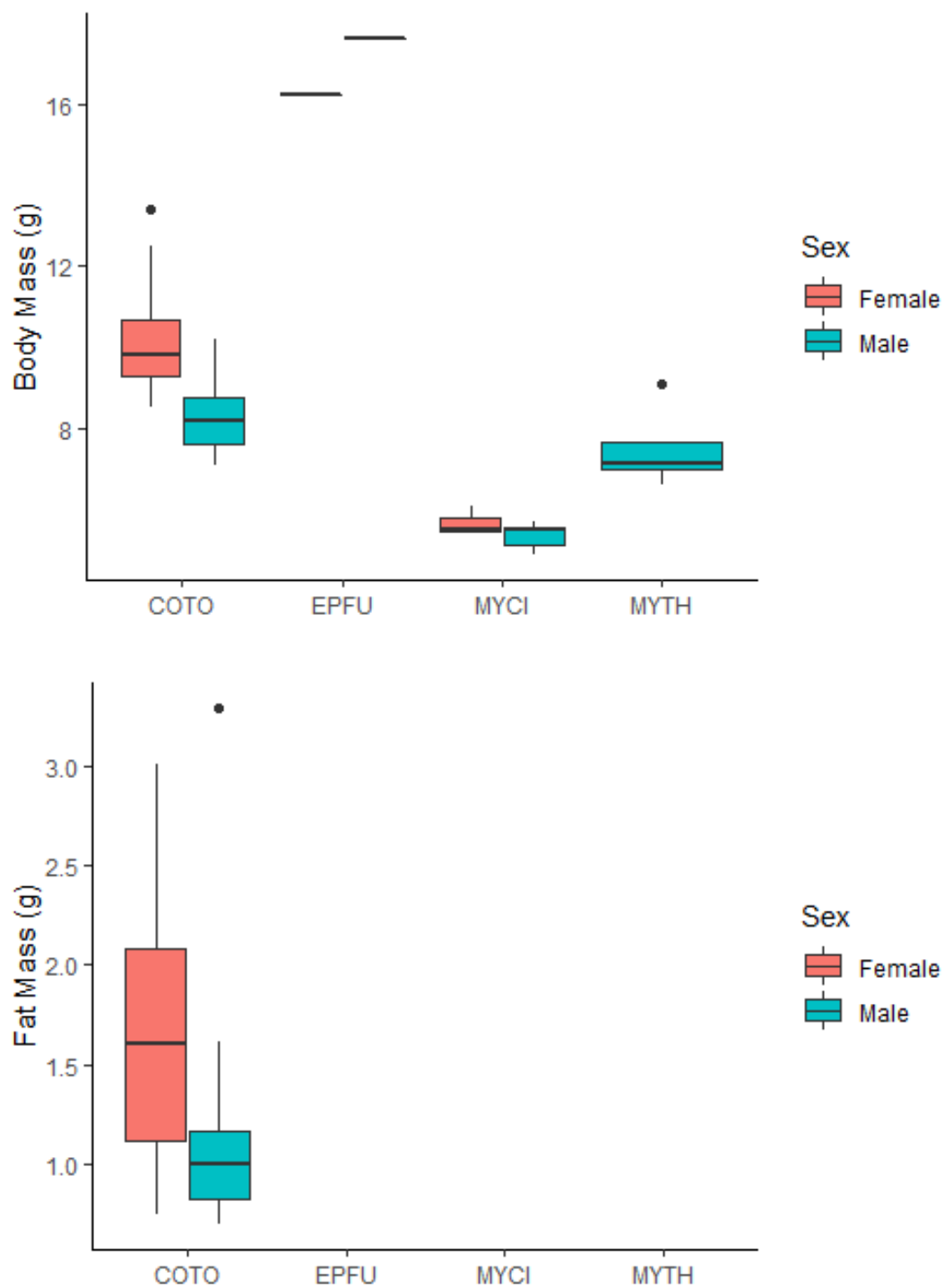
Figure 1. Body mass (top) and fat mass (bottom) by sex for the four species captured at Paradox Mine.
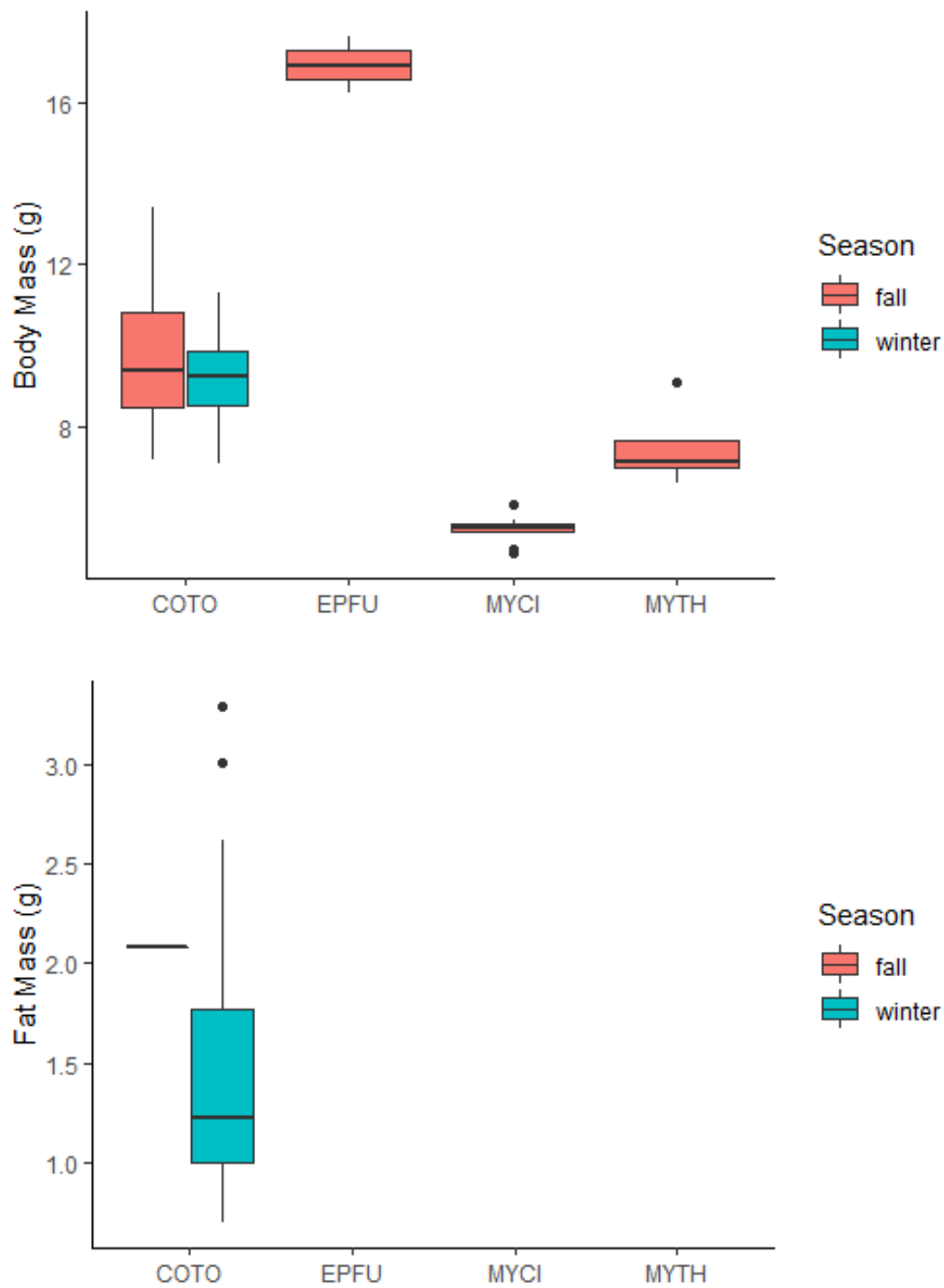
Figure 2. Body mass (top) and fat mass (bottom) by season for the four species captured at Paradox Mine.
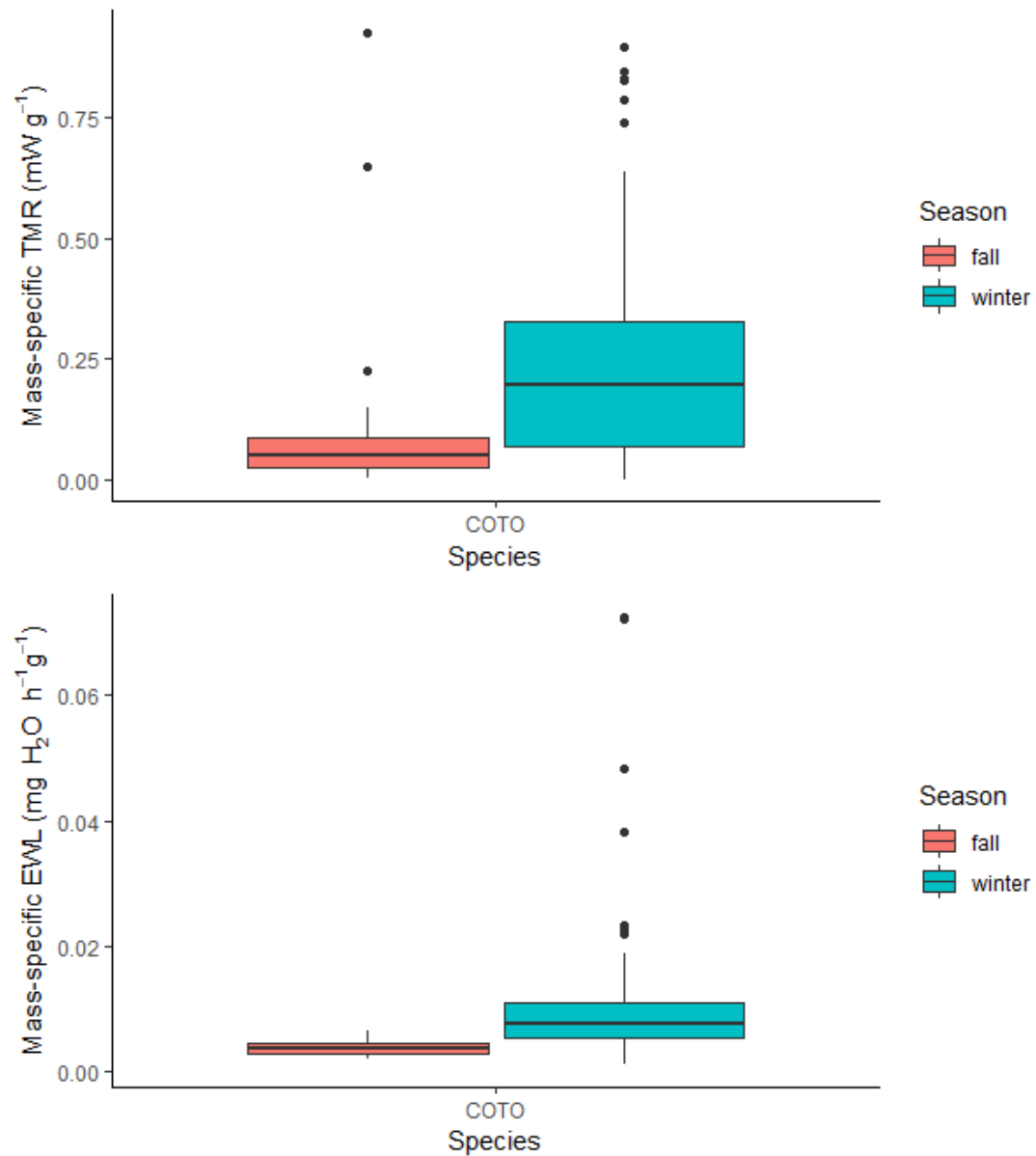
Figure 3. Mass-specific torpor metabolic rate (TMR; top) and mass-specific evaporative water loss (EWL; bottom) by season for COTO captured at Paradox Mine.
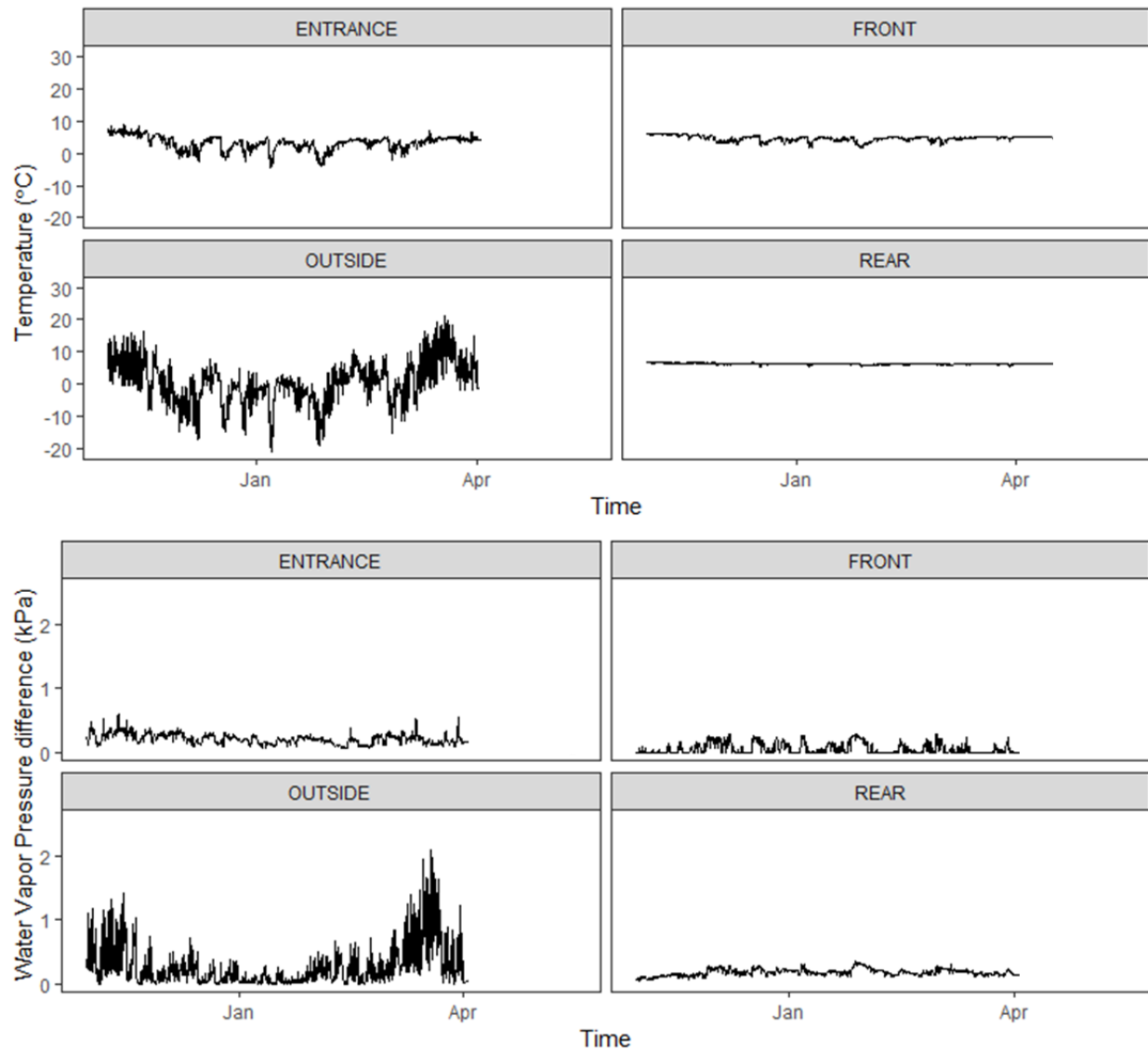
Figure 4: Microclimate (top: temperature, bottom: water vapor pressure difference) at different locations throughout the mine.
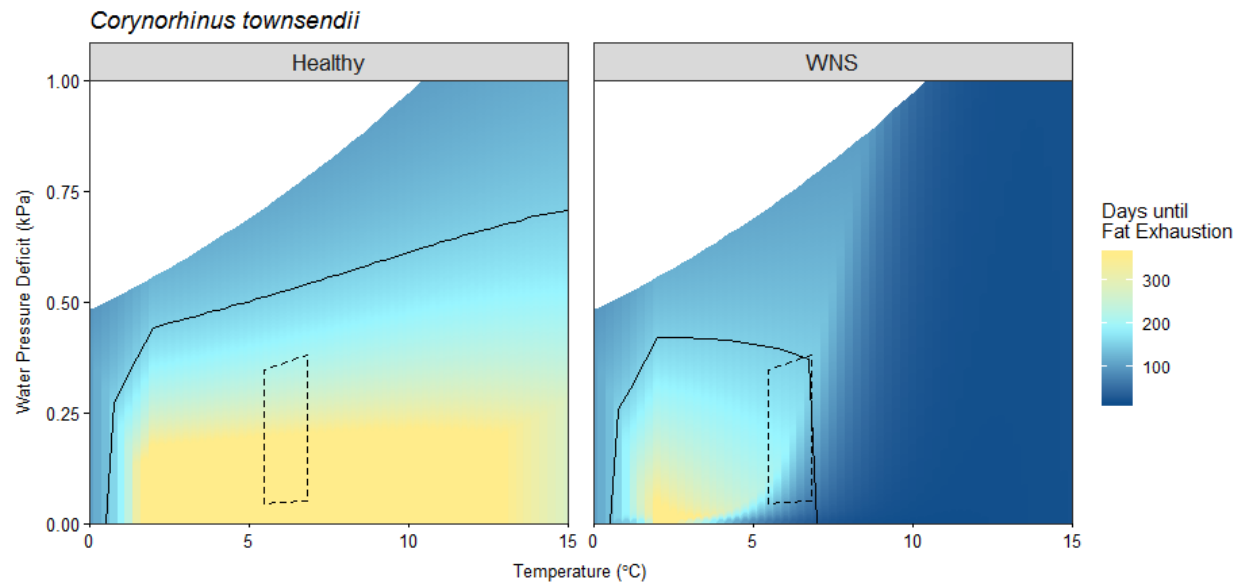
Figure 5: Predicted days until total fat exhaustion for *Corynorhinus townsendii* in Paradox Mine. Solid lines represent days of hibernation duration (152 days) predicted for Paradox and the range of microclimate conditions that would allow survival in this area. Dashed lines represent microclimate conditions measured at the roosting location within the mine. The area where solid and dashed lines overlap is the microclimate conditions available that allow survival. White space represents impossible microclimate space based on the saturation potential for each temperature.

APPENDIX: Morphometric data from species captured at Paradox Mine. Forearm is in mm, mass, fat, and lean mass in g.

Species	Date	Sex	Age	Reproductive Condition	Forearm	Mass	Fat	Lean	Wing Score	Respirometry?
Corynorhinus townsendii	9/26/2016	Male	Adult	Scrotal	44.1	7.9			0	
Corynorhinus townsendii	9/26/2016	Male	Adult	Scrotal	41.2	7.5			0	
Corynorhinus townsendii	9/26/2016	Male	Adult	Scrotal	42.3	9.2			1	
Corynorhinus townsendii	9/26/2016	Female	Adult	Non-reproducing	44.5	9.5			1	
Corynorhinus townsendii	9/26/2016	Female	Adult	Non-reproducing	44.7	9.5			0	
Corynorhinus townsendii	9/26/2016	Male	Adult	Scrotal	42.5	8.2			1	
Corynorhinus townsendii	9/26/2016	Male	Adult	Scrotal	42.1	8.3			0	
Corynorhinus townsendii	9/26/2016	Male	Adult	Scrotal	40.2	7.2			0	
Corynorhinus townsendii	9/26/2016	Male	Adult	Scrotal	42.3	9.1			1	
Corynorhinus townsendii	9/26/2016	Male	Adult	Scrotal	43.3	9.4			0	
Corynorhinus townsendii	9/26/2016	Male	Adult	Scrotal	43	9.2			1	
Corynorhinus townsendii	9/27/2016	Male	Adult	Scrotal	43.1	8.9			0	
Corynorhinus townsendii	9/27/2016	Male	Adult	Scrotal	42.6	8.9			1	
Corynorhinus townsendii	9/27/2016	Male	Adult		40.5	7.2			0	
Corynorhinus townsendii	9/27/2016	Male	Adult	Scrotal	43.7	8.6			0	
Corynorhinus townsendii	9/27/2016	Female	Adult	Non-reproducing	45	8.9			0	
Corynorhinus townsendii	9/27/2016	Male	Adult	Non-reproducing	41.7	7.9			0	
Corynorhinus townsendii	9/27/2016	Male	Adult	Scrotal	42	7.6			0	
Corynorhinus townsendii	9/27/2016	Male	Adult	Non-reproducing	44.1	8.2			0	
Corynorhinus townsendii	9/27/2016	Male	Adult	Non-reproducing	42.3	8.6			0	
Corynorhinus townsendii	9/27/2016	Male	Adult	Non-reproducing	42.7	7.7			0	
Corynorhinus townsendii	9/27/2016	Female	Adult	Non-reproducing	44.5	10.5			1	
Corynorhinus townsendii	9/27/2016	Female	Adult	Non-reproducing	43.3	10.3			0	
Corynorhinus townsendii	9/27/2016	Male	Adult	Non-reproducing	41.8	8.7			3	
Corynorhinus townsendii	9/27/2016	Female	Adult	Non-reproducing	45.2	13.4			1	
Corynorhinus townsendii	9/27/2016	Male	Adult	Scrotal	41.9	9.6			1	
Corynorhinus townsendii	9/29/2016	Female	Adult	Non-reproducing	44.2	10.6			0	
Corynorhinus townsendii	9/29/2016	Male	Adult	Scrotal	40.1	7.6			0	
Corynorhinus townsendii	9/30/2016	Female	Adult	Non-reproducing	44.2	12.3			0	

Species	Date	Sex	Age	Reproductive Condition	Forearm	Mass	Fat	Lean	Wing Score	Respirometry?
Corynorhinus townsendii	2/7/2017	Female	Adult	Non-reproducing	42.5	9.3			1	
Corynorhinus townsendii	2/7/2017	Female	Adult	Non-reproducing	45	9.3			1	
Corynorhinus townsendii	2/7/2017	Female	Adult	Non-reproducing	42	9.3			0	
Corynorhinus townsendii	2/7/2017	Female	Adult	Non-reproducing	44.3	9.1			1	
Corynorhinus townsendii	2/7/2017	Female	Adult	Non-reproducing	45.3	9.5	1.2	3.61	1	yes
Corynorhinus townsendii	2/7/2017	Female	Adult	Non-reproducing	44.6	9.7	0.9	3.93	1	yes
Corynorhinus townsendii	2/7/2017	Male	Adult	Non-reproducing	42.3	10.2	0.8	3.08	0	yes
Corynorhinus townsendii	2/7/2017	Female	Adult	Non-reproducing	43.4	9.5	1.1	3.79	1	yes
Corynorhinus townsendii	2/7/2017	Female	Adult	Non-reproducing	43.8	9.7			3	
Corynorhinus townsendii	2/7/2017	Female	Adult	Non-reproducing	43.2	9.2			1	
Corynorhinus townsendii	2/7/2017	Female	Adult	Non-reproducing	42.6	9			0	
Corynorhinus townsendii	2/7/2017	Female	Adult	Non-reproducing	45.9	10	1.2	3.55	2	yes
Corynorhinus townsendii	2/7/2017	Female	Adult	Non-reproducing	42.8	9			0	
Corynorhinus townsendii	2/7/2017	Female	Adult	Non-reproducing	42.2	8.6			2	
Corynorhinus townsendii	2/7/2017	Male	Adult	Scrotal	43.8	8.6	1	3.17	2	yes
Corynorhinus townsendii	2/7/2017	Female	Adult	Non-reproducing	43.4	8.6			2	
Corynorhinus townsendii	2/7/2017	Female	Adult	Non-reproducing	45.9	10.3	0.8	4.37	1	yes
Corynorhinus townsendii	2/7/2017	Female	Adult	Non-reproducing	42.7	9.6			3	
Corynorhinus townsendii	2/7/2017	Female	Adult	Non-reproducing	44.5	9.1			2	
Corynorhinus townsendii	2/7/2017	Female	Adult	Non-reproducing	43.1	8.5			1	
Corynorhinus townsendii	2/7/2017	Male	Adult	Non-reproducing	42.8	8.3	0.7	4.23	0	yes
Corynorhinus townsendii	2/7/2017	Male	Adult	Non-reproducing	42.3	7.3			0	
Corynorhinus townsendii	2/7/2017	Male	Adult	Non-reproducing	40.4	7.4	0.8	3.41	1	yes
Corynorhinus townsendii	2/7/2017	Female	Adult	Non-reproducing	45.1	9.5	1.1	3.8	0	yes
Corynorhinus townsendii	2/7/2017	Male	Adult	Non-reproducing	42.1	7.3			2	
Corynorhinus townsendii	2/7/2017	Male	Adult	Scrotal	42	7.9	0.7	2.64	2	yes
Corynorhinus townsendii	2/7/2017	Female	Adult	Non-reproducing	45	11.3	1.6	3.6	0	yes
Corynorhinus townsendii	2/7/2017	Female	Adult	Non-reproducing	44.8	9.7			1	
Corynorhinus townsendii	2/7/2017	Male	Adult	Non-reproducing	44.2	8.3	0.8	2.58	0	yes
Corynorhinus townsendii	2/7/2017	Female	Adult	Non-reproducing	42.4	9.7	1	3.91	1	yes
Corynorhinus townsendii	10/13/2017	Female	Adult	Non-reproducing	43.9	10.7	2.1	5.68	1	yes

Species	Date	Sex	Age	Reproductive Condition	Forearm	Mass	Fat	Lean	Wing Score	Respirometry?
Corynorhinus townsendii	10/17/2018	Male	Adult	Scrotal	35	8.8			3	
Corynorhinus townsendii	10/17/2018	Female	Adult	Non-reproducing	44.3	10.8			1	yes
Corynorhinus townsendii	10/17/2018	Female	Adult	Non-reproducing	43.9	10.8			1	yes
Corynorhinus townsendii	10/17/2018	Female	Adult	Non-reproducing	44.3	11.4			0	yes
Corynorhinus townsendii	10/17/2018	Female	Adult	Non-reproducing	43	11.8			1	yes
Corynorhinus townsendii	10/17/2018	Female	Adult	Non-reproducing	44.5	10.9			0	
Corynorhinus townsendii	10/17/2018	Female	Adult	Non-reproducing	45	11.3			0	yes
Corynorhinus townsendii	10/17/2018	Female	Adult	Non-reproducing	44.6	10.8			1	yes
Corynorhinus townsendii	10/17/2018	Female	Adult	Non-reproducing	43.6	10.7			0	yes
Corynorhinus townsendii	10/17/2018	Female	Adult	Non-reproducing	44.7	12.1			1	yes
Corynorhinus townsendii	10/17/2018	Female	Adult	Non-reproducing	43.8	11.9			1	yes
Corynorhinus townsendii	10/17/2018	Female	Adult	Non-reproducing	44.3	12.5			1	yes
Corynorhinus townsendii	10/17/2018	Female	Adult	Non-reproducing	42.1	11			0	yes
Corynorhinus townsendii	1/23/2019	Female	Adult	Non-reproducing	42.2	8.5	1.7	2.77	0	yes
Corynorhinus townsendii	1/23/2019	Female	Adult	Non-reproducing	43.6	7.4	1.4	6.04	1	yes
Corynorhinus townsendii	1/23/2019	Female	Adult	Non-reproducing	42.9	10.4	2.1	4.33	1	yes
Corynorhinus townsendii	1/23/2019	Male	Adult	Non-reproducing	42.3	9.1	1.1	7.96	0	yes
Corynorhinus townsendii	1/23/2019	Female	Adult	Non-reproducing	43.1	9.5	2.2	4.53	0	yes
Corynorhinus townsendii	1/23/2019	Female	Adult	Non-reproducing	42.5	8.2	1.3	6.74	1	yes
Corynorhinus townsendii	1/23/2019	Male	Adult	Scrotal	41.2	7.9	3.3	1.49	2	
Corynorhinus townsendii	1/23/2019	Female	Adult	Non-reproducing	43.6	7.4	1.4	6.04	1	yes
Corynorhinus townsendii	1/23/2019	Female	Adult	Non-reproducing	42.9	10.4	2.1	4.33	1	
Corynorhinus townsendii	1/23/2019	Female	Adult	Non-reproducing	44.1	8.9	1.1	3.72	1	
Corynorhinus townsendii	1/23/2019	Female	Adult	Non-reproducing	44	10.2	1.7	8.26	2	
Corynorhinus townsendii	1/23/2019	Male	Adult	Scrotal	42.8	8.4	1.6	4.57	1	yes
Corynorhinus townsendii	1/23/2019	Female	Adult	Non-reproducing	45.2	9.1			1	yes
Corynorhinus townsendii	1/23/2019	Female	Adult	Non-reproducing	42.8	9.1			1	
Corynorhinus townsendii	1/23/2019	Female	Adult	Non-reproducing	42.4	8.2	1	3.47	1	
Corynorhinus townsendii	1/23/2019	Female	Adult	Non-reproducing	44.1	8.9	1.1	3.72	1	
Corynorhinus townsendii	1/23/2019	Female	Adult	Non-reproducing	44.8	10.3	1.5	3.4	0	yes
Corynorhinus townsendii	1/23/2019	Female	Adult	Non-reproducing	43.6	10.1	1.4	2.37	0	yes
Corynorhinus townsendii	1/23/2019	Female	Adult	Non-reproducing	44.8	9.3	1.9	9.24	2	yes
Corynorhinus townsendii	1/23/2019	Female	Adult	Non-reproducing	43.9	9.9			2	yes
Corynorhinus townsendii	1/23/2019	Female	Adult	Non-reproducing	45	10.2			1	yes

Species	Date	Sex	Age	Reproductive Condition	Forearm	Mass	Fat	Lean	Wing Score	Respirometry?
Corynorhinus townsendii	1/23/2019	Female	Adult	Non-reproducing	43.9	10			1	yes
Corynorhinus townsendii	1/23/2019	Female	Adult	Non-reproducing	45.4	10.6			1	yes
Corynorhinus townsendii	1/23/2019	Female	Adult	Non-reproducing	43.2	9.9	0.8	0.78	1	yes
Corynorhinus townsendii	1/23/2019	Female	Adult	Non-reproducing	44.2	9.6	1.5	3.24	1	
Corynorhinus townsendii	1/23/2019	Female	Adult	Non-reproducing	44.4	9.6	2.4	5.9	1	
Corynorhinus townsendii	1/23/2019	Female	Adult	Non-reproducing	45	10.8	2.3	3.17	0	yes
Corynorhinus townsendii	1/23/2019	Female	Adult	Non-reproducing	44.5	9.2	1.8	6.6	0	
Corynorhinus townsendii	1/23/2019	Male	Adult	Non-reproducing	40.4	7.1	1	5.79	1	
Corynorhinus townsendii	1/23/2019	Female	Adult	Non-reproducing	43	7.8	1.1	6.38	0	
Corynorhinus townsendii	1/23/2019	Female	Adult	Non-reproducing	42.4	9	1.8	5.25	1	
Corynorhinus townsendii	1/23/2019	Female	Adult	Non-reproducing	45	10.3	3	9.99	1	
Corynorhinus townsendii	1/23/2019	Male	Adult	Non-reproducing	41.8	7.3	1	5.28	1	
Corynorhinus townsendii	1/23/2019	Female	Adult	Non-reproducing	44	10.4	2.6	7.79	0	yes
Eptesicus fuscus	9/28/2016	Male	Adult	Scrotal	49.7	17.6			0	
Eptesicus fuscus	10/17/2018	Female	Adult	Non-reproducing	47.1	16.2			1	yes
Corynorhinus townsendii	1/23/2019	Female	Adult	Non-reproducing	43.6	8.9			1	yes
Myotis ciliolabrum	9/27/2016	Female	Adult	Non-reproducing	32.3	6.1			0	
Myotis ciliolabrum	9/27/2016	Male	Adult	Non-reproducing	34	5			1	
Myotis ciliolabrum	9/27/2016	Male	Adult	Non-reproducing	31.6	5.6			0	
Myotis ciliolabrum	9/28/2016	Female	Adult	Non-reproducing	34.8	5.4			0	
Myotis ciliolabrum	9/28/2016	Male	Adult	Non-reproducing	33.9	4.9			1	
Myotis ciliolabrum	9/28/2016	Male	Adult	Scrotal	34.4	5.7			0	yes
Myotis ciliolabrum	10/13/2017	Female	Adult	Non-reproducing	34.6	5.5			0	
Myotis ciliolabrum	9/28/2016	Male	Adult	Non-reproducing	33.1	5.5			0	
Myotis ciliolabrum	9/28/2016	Male	Adult	Non-reproducing	32.7	5.5			0	
Myotis thysanodes	10/13/2017	Female	Adult	Non-reproducing	41.3	6.6			0	
Myotis thysanodes	9/26/2016	Male	Adult	Non-reproducing	42.1	7.2			1	
Myotis thysanodes	9/27/2016	Male	Adult	Non-reproducing	42.9	7.1			1	
Myotis thysanodes	10/13/2017	Male	Adult	Scrotal	42.2	9.1			1	

Montana Department of Fish, Wildlife and Parks
Final Project Report 2016-2018
Under permits 2016-104, 2017-018, and 2018-008

We caught a total of 580 bats: 1 *Corynorhinus townsendii*, 13 *Eptesicus fuscus*, 1 *Lasionycteris noctivagans,* 2 *Myotis ciliolabrum*, 186 *M. evotis*, 214 *M. lucifugus*, 43 *M. thysanodes*, and 98 *M. volans* (Table 1; Appendix) over the sampling period of fall 2016 to fall 2018. During the fall, bats were caught using mist nets and harp traps at the cave entrance. During the winter, bats were hand-captured from cave walls. We determined sex, age, reproductive condition, and wing score and measured forearm length and body mass of each bat. We used quantitative magnetic resonance (QMR; Echo-MRI-B, Echo Medical Systems, Houston, TX) to measure fat mass and lean mass. We measured metabolic rate (TMR) and evaporative water loss (EWL) during torpor using open-flow respirometry. We measured body fat from 325 individuals and processed 108 individuals through respirometry. All bats were released and none were injured in the handling and measurements.

Body mass and body fat did not vary between sexes at Lick Creek Cave (Figure 1) nor Old Dry Wolf (Figure 2). The mean mass for each species did not vary between seasons in Lick Creek (Figure 3), nor Old Dry Wolf (Figure 4) for the species that we captured both seasons. Metabolic rate and evaporative water loss varied differently between seasons depending on sample site (Figures 5-6).

We measured hibernaculum temperature and relative humidity over each hibernation period at each site using HOBO (Model U23-001, Onset Computer Corporation) and iButton (Model DS1921Z-F5, Maxim Integrated Products) microclimate data loggers. We placed four HOBO and ten iButton loggers throughout the hibernacula in the fall and recorded conditions at 3 h intervals. We collected loggers from the hibernacula in the spring (May) of each year. The mean temperature of Lick Creek Cave was 3.65 °C while the mean relative humidity was 93.67% (Figure 7). The mean temperature of Old Dry Wolf Cave was 4.45 °C while the mean relative humidity was 70.90% (Figure 8).

We predicted survival for *M. evotis* (Figure 9), *M. lucifugus* (Figure 9), *M. thysanodes* (Figure 10), *M. volans* (Figure 10), and *E. fuscus* (Figure 11) over the range of environmental conditions experienced in the cave. We also inferred the survival of both species once affected with white-nose syndrome. The modified hibernation energetics model estimates the time until fat exhaustion during hibernation as a function of bat characteristics, hibernaculum microclimate, and fungal growth. Survival is determined by comparing model output time to winter duration – if time until fat exhaustion is greater than winter duration, survival occurs. We validated the model predictions with field and laboratory data and determined model sensitivity to bat characteristics.

For further information about our findings please visit www.science4bats.org/publications and review all project associated publications.

Table 1: The number of each species per year captured in Montana.

Species	Year	Lick Creek	Dry Wolf
Corynorhinus townsendii	2017	1	1
Eptesicus fuscus	2017	5	5
Eptesicus fuscus	2018	8	8
Lasionycteris noctivagans	2018		1
Myotis ciliolabrum	2018	2	2
Myotis evotis	2016	22	1
Myotis evotis	2017	106	
Myotis evotis	2018	77	2
Myotis lucifugus	2016	66	
Myotis lucifugus	2017	93	
Myotis lucifugus	2018	55	
Myotis thysanodes	2016	3	
Myotis thysanodes	2017	20	
Myotis thysanodes	2018	20	
Myotis volans	2016	11	2
Myotis volans	2017	56	
Myotis volans	2018	28	1
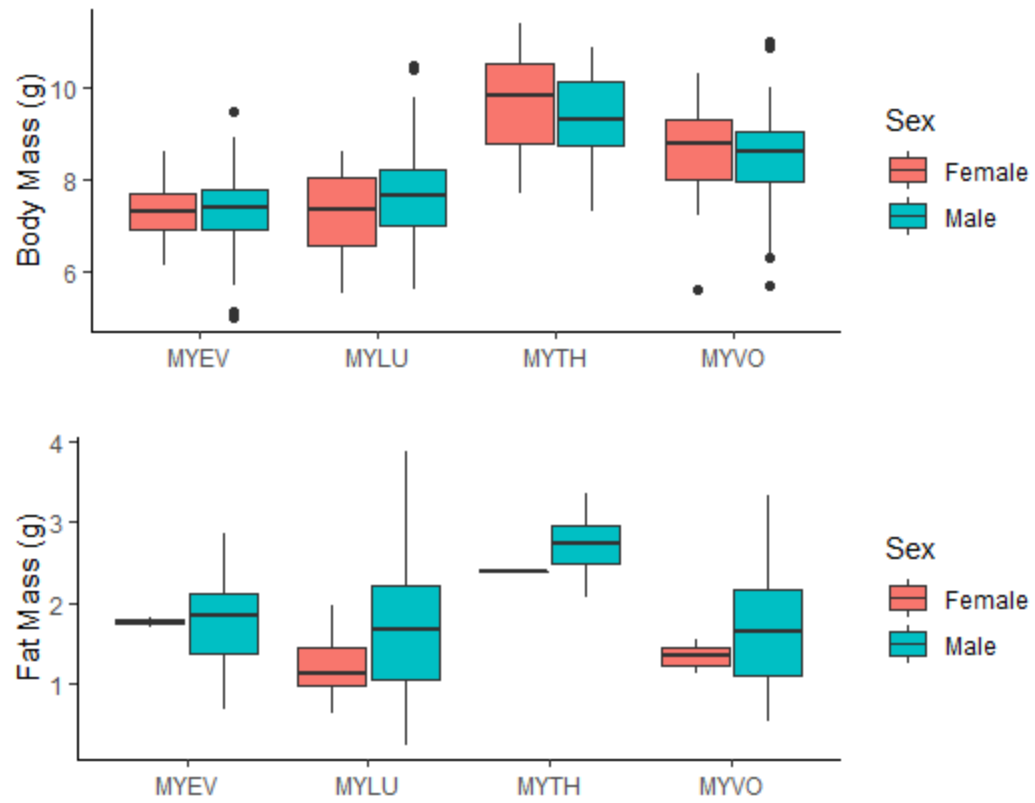
Figure 1. Body mass (top) and fat mass (bottom) by sex for the four species captured at Lick Creek Cave.
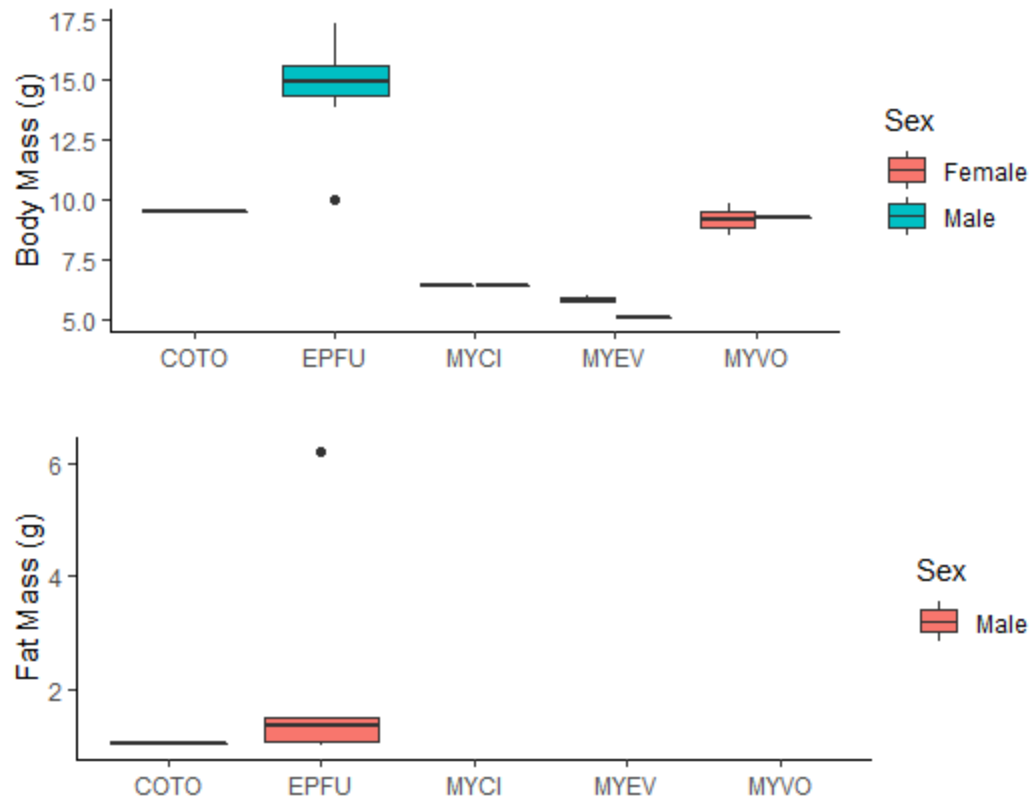
Figure 2. Body mass (top) and fat mass (bottom) by sex for the five species captured at Old Dry Wolf Cave. The single COTO data point was male.
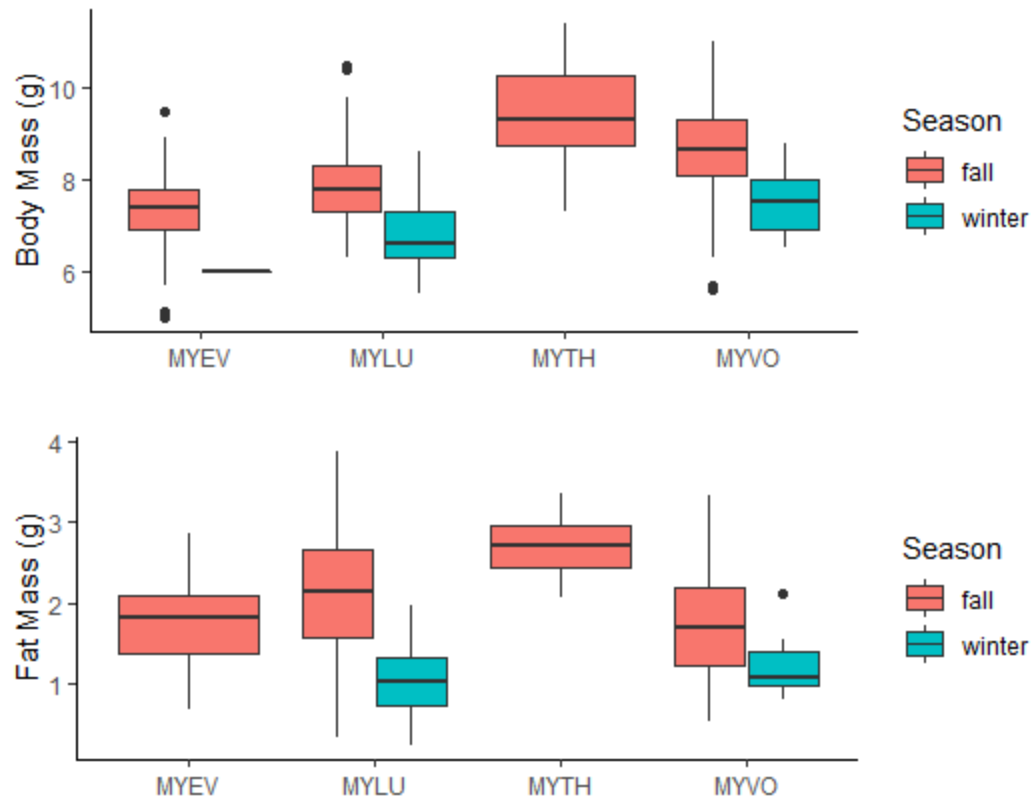
Figure 3. Body mass (top) and fat mass (bottom) by season for the four species captured at Lick Creek Cave.
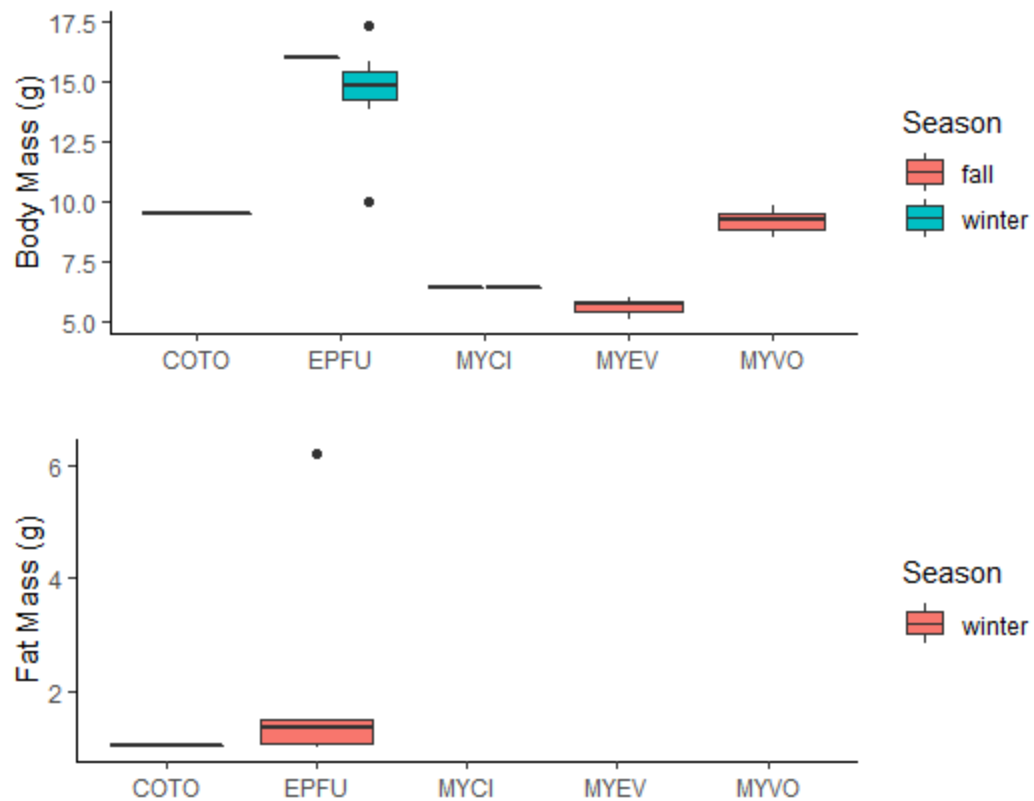
Figure 4. Body mass (top) and fat mass (bottom) by season for the five species captured at Old Dry Wolf Cave. The single COTO was captured during the winter.
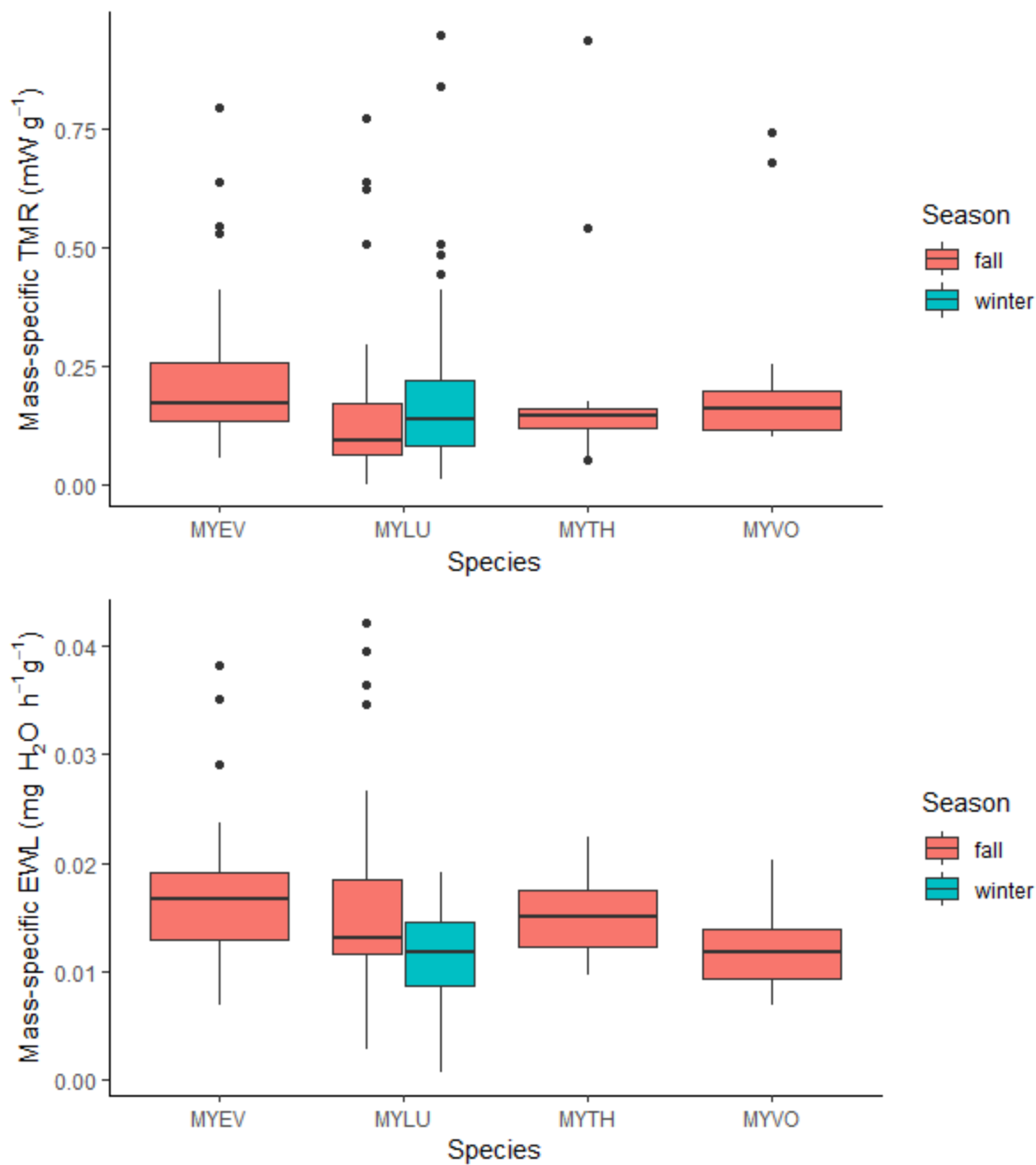
Figure 5. Mass-specific torpor metabolic rate (TMR; top) and mass-specific evaporative water loss (EWL; bottom) by season for the four species captured at Lick Creek Cave.
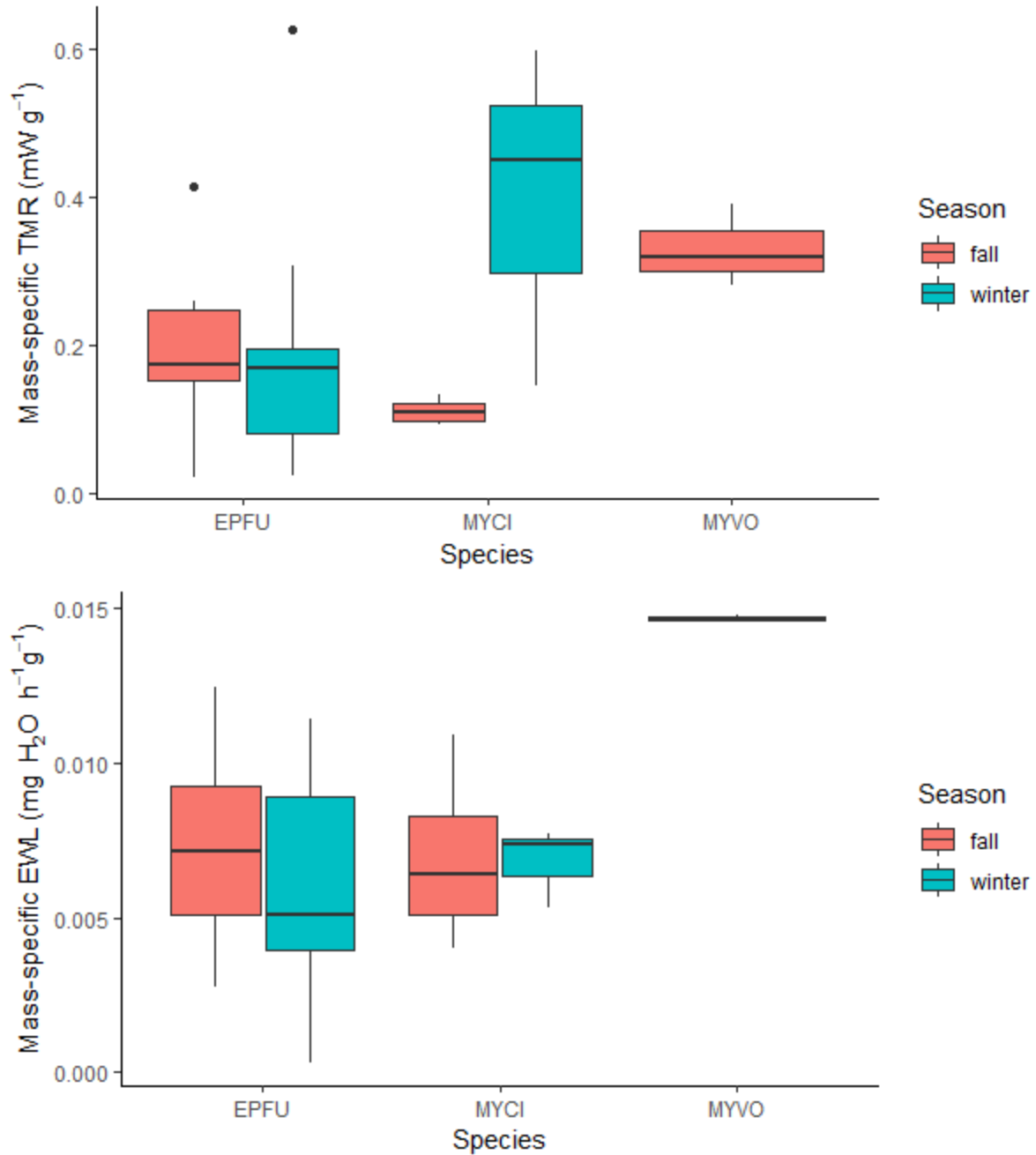
Figure 6. Mass-specific torpor metabolic rate (TMR; top) and mass-specific evaporative water loss (EWL; bottom) by season for three species captured at Old Dry Wolf Cave. The single data point for MYVO is from the fall.
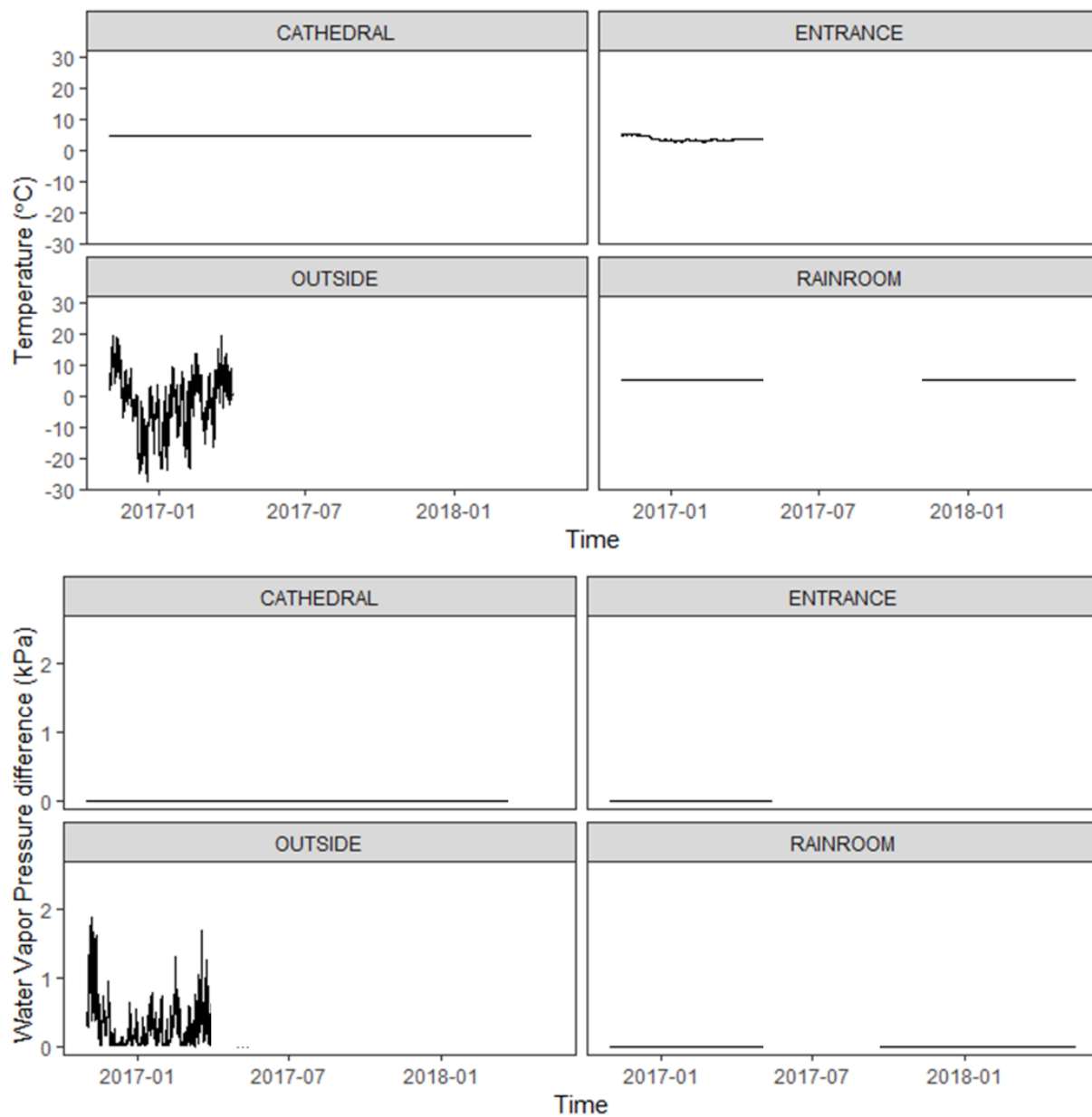
Figure 7: Microclimate (top: temperature, bottom: water vapor pressure difference) at different locations throughout Lick Creek cave.
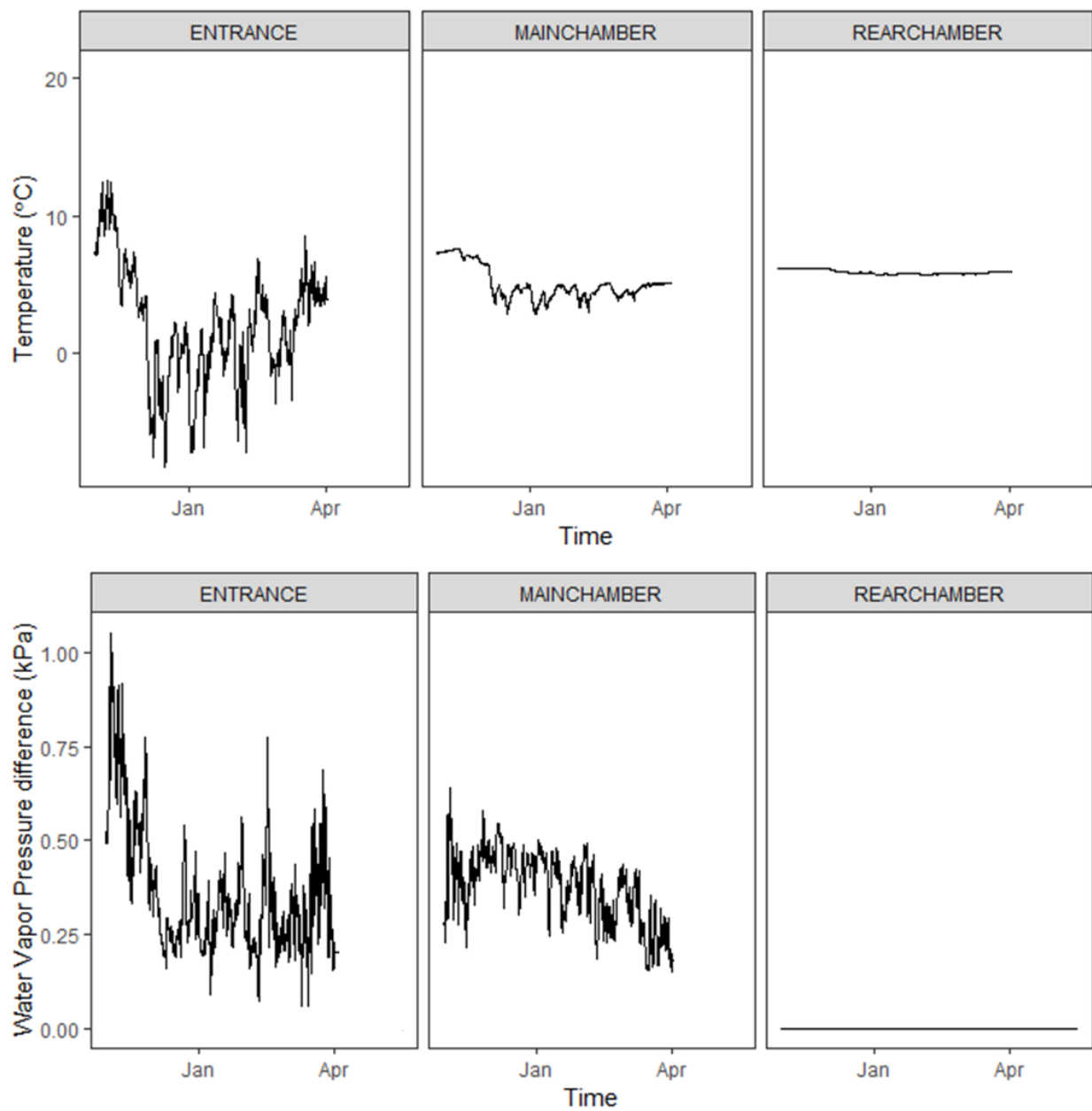
Figure 8: Microclimate (top: temperature, bottom: water vapor pressure difference) at different locations throughout Old Dry Wolf cave.
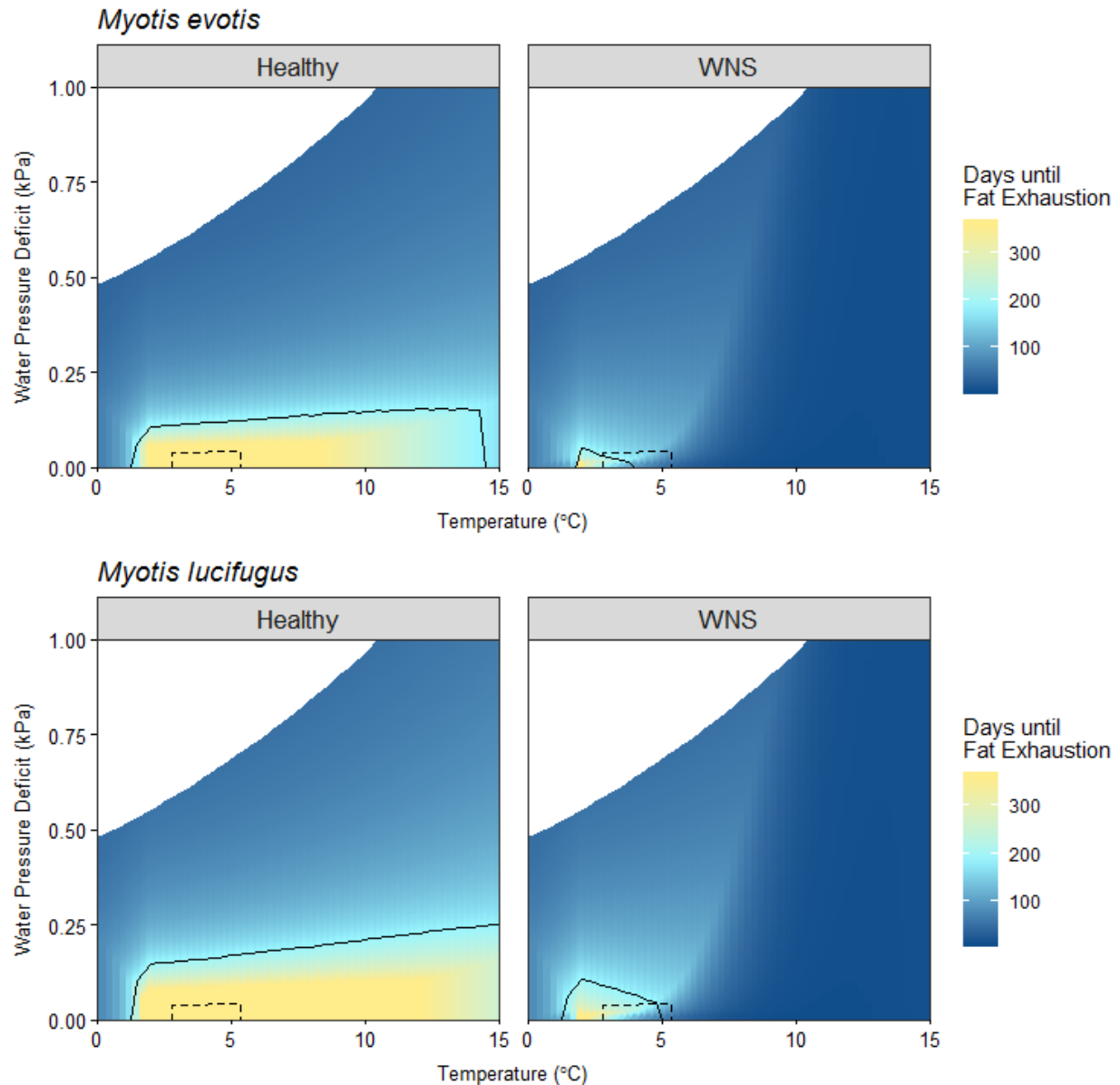
Figure 9: Predicted days until total fat exhaustion for _Myotis evotis_ and _M. lucifugus_ in Lick Creek Cave. Solid lines represent days of hibernation duration (184 days) predicted for Lick Creek Cave and the range of microclimate conditions that would allow survival in this area. Dashed lines represent microclimate conditions measured at the roosting location within the mine. The area where solid and dashed lines overlap is the microclimate conditions available that allow survival. White space represents impossible microclimate space based on the saturation potential for each temperature. Here, _M. evotis_ and _M. lucifugus_ have some microclimate space that would allow for survival from white-nose syndrome (WNS).
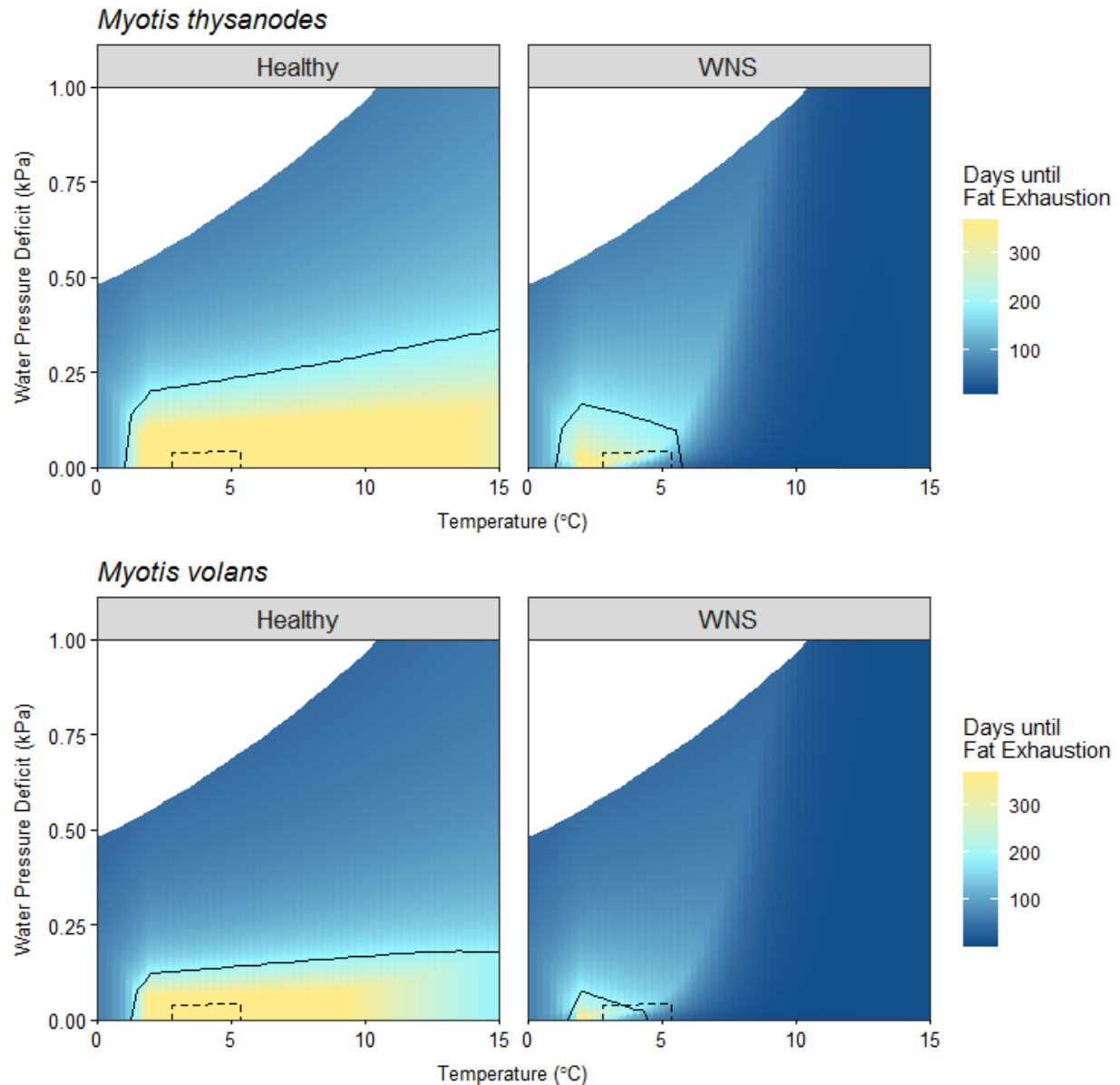
Figure 10: Predicted days until total fat exhaustion for *Myotis thysanodes* and *M. volans* in Lick Creek Cave. Solid lines represent days of hibernation duration (184 days) predicted for Lick Creek Cave and the range of microclimate conditions that would allow survival in this area. Dashed lines represent microclimate conditions measured at the roosting location within the mine. The area where solid and dashed lines overlap is the microclimate conditions available that allow survival. White space represents impossible microclimate space based on the saturation potential for each temperature. Here, *M. thysanodes* and *M. volans* have some microclimate space that would allow for survival from white-nose syndrome (WNS).
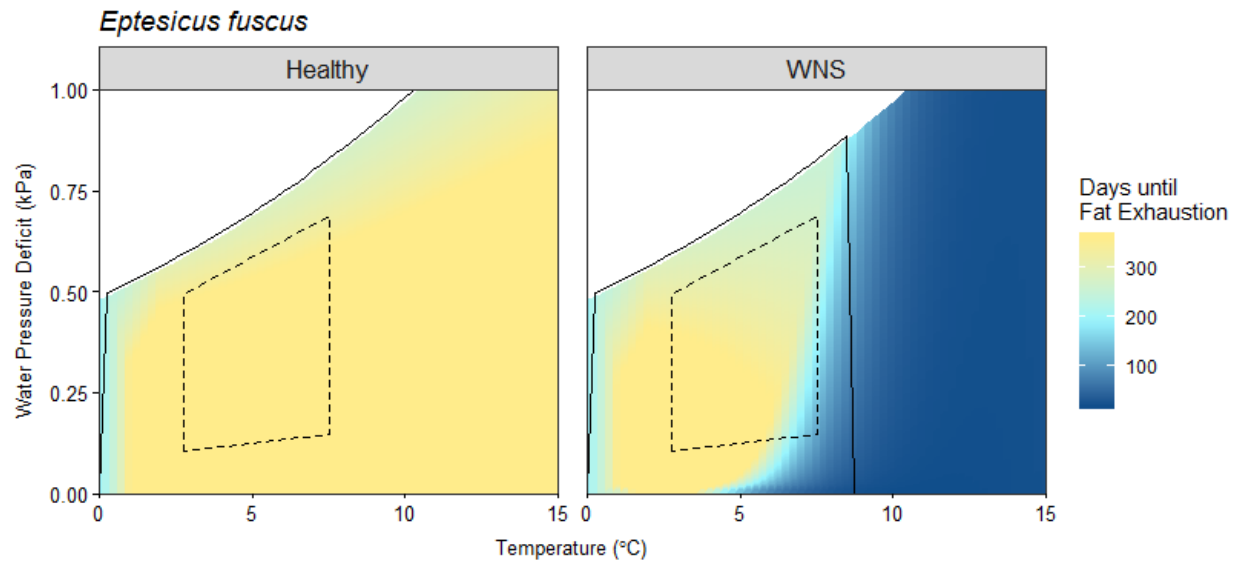
Figure 9: Predicted days until total fat exhaustion for *Eptesicus fuscus* in Dry Wolf Cave. Solid lines represent days of hibernation duration (199 days) predicted for Dry Wolf Cave and the range of microclimate conditions that would allow survival in this area. Dashed lines represent microclimate conditions measured at the roosting location within the mine. The area where solid and dashed lines overlap is the microclimate conditions available that allow survival. White space represents impossible microclimate space based on the saturation potential for each temperature. Here, *E. fuscus* has some microclimate space that would allow for survival from white-nose syndrome (WNS).

APPENDIX: Morphometric data from Lick Creek (LCC) and Old Dry Wolf (ODW). Forearm in mm, mass, fat, and lean mass in g.

Species	Date	Site	Sex	Age	Reproductive?	Forearm	Mass	Fat	Lean	Wing Score	Respirometry?
Corynorhinus townsendii	2/14/2017	ODW	Male	Adult	Scrotal	43.7	9.5	1.07	3.41	0	yes
Eptesicus fuscus	2/14/2017	ODW	Male	Adult	Non-reproducing	45.3	10	1.03	5.36	1	yes
Eptesicus fuscus	2/14/2017	ODW	Male	Adult	Non-reproducing	47	14.9	1.25	4.68	1	
Eptesicus fuscus	2/14/2017	ODW	Male	Adult	Non-reproducing	44.8	15.4	1.5	3.49	1	yes
Eptesicus fuscus	2/14/2017	ODW	Male	Adult	Non-reproducing	47.8	14.7	1.04	2.27	1	
Eptesicus fuscus	2/14/2017	ODW	Male	Adult	Non-reproducing	47.8	15.3	1.49	4.25	1	yes
Eptesicus fuscus	2/13/2017	ODW	Male	Adult	Unknown	44.5	14.1	6.19	4.67	1	yes
Eptesicus fuscus	2/13/2018	ODW	Male	Adult	Unknown	49.9	15.8			1	yes
Eptesicus fuscus	2/13/2018	ODW	Male	Adult	Unknown	47.6	17.3			1	yes
Eptesicus fuscus	2/13/2018	ODW	Male	Adult	Unknown	46.4	14.6			1	yes
Eptesicus fuscus	2/13/2018	ODW	Male	Adult	Unknown	45.5	13.8			2	yes
Eptesicus fuscus	10/1/2018	ODW	Male	Adult	Reproducing	46.4	21.9			1	yes
Eptesicus fuscus	10/1/2018	ODW	Male	Adult	Non-reproducing	45.5	16			0	yes
Eptesicus fuscus	10/1/2018	ODW	Female	Adult	Non-reproducing	47.8	20.4			0	
Lasionycteris noctivagans	10/1/2018	ODW	Female	Adult	Unknown	35.8	6.4				
Myotis ciliolabrum	2/13/2018	ODW	Female	Adult	Unknown	32.7	6.4			1	yes
Myotis ciliolabrum	10/1/2018	ODW	Male	Adult	Non-reproducing	38.6	5.1			0	yes
Myotis evotis	9/19/2016	ODW	Male	Juvenile	Non-reproducing	38	7.1			0	
Myotis evotis	9/21/2016	LCC	Male	Adult	Non-reproducing	37.5				0	
Myotis evotis	9/22/2016	LCC	Male	Adult	Non-reproducing	38.8	6.1			0	
Myotis evotis	9/22/2016	LCC	Male	Adult	Non-reproducing	37.8	5.7			0	
Myotis evotis	9/22/2016	LCC	Male	Adult	Non-reproducing	39.4	7.7			0	
Myotis evotis	9/23/2016	LCC	Female	Adult	Non-reproducing	38.3	6.6			1	
Myotis evotis	9/23/2016	LCC	Male	Adult	Scrotal	37.4	6.7			0	
Myotis evotis	9/23/2016	LCC	Male	Adult	Non-reproducing	37.9	7.5			0	
Myotis evotis	9/23/2016	LCC	Female	Adult	Non-reproducing	38.6	6.9			0	
Myotis evotis	9/23/2016	LCC	Female	Adult	Non-reproducing	39.1	6.6			0	
Myotis evotis	9/23/2016	LCC	Male	Adult	Non-reproducing	38.1	7.4			1	

Species	Date	Site	Sex	Age	Reproductive?	Forearm	Mass	Fat	Lean	Wing Score	Respirometry?
Myotis evotis	9/23/2016	LCC	Male	Adult	Non-reproducing	37.8	7.5			1	
Myotis evotis	9/23/2016	LCC	Male	Adult	Non-reproducing	38.7	7.5			0	
Myotis evotis	9/23/2016	LCC	Male	Adult	Non-reproducing	38.4	7.4			1	
Myotis evotis	9/23/2016	LCC	Male	Adult	Non-reproducing	37.6	6.8			0	
Myotis evotis	9/23/2016	LCC	Male	Juvenile	Non-reproducing	38.4	5			0	
Myotis evotis	9/23/2016	LCC	Male	Adult	Non-reproducing	37.6	6.9			1	
Myotis evotis	9/23/2016	LCC	Male	Juvenile	Non-reproducing	37.5	7.4			1	
Myotis evotis	9/23/2016	LCC	Male	Adult	Non-reproducing	38	5.1			0	
Myotis evotis	9/23/2016	LCC	Female	Juvenile	Non-reproducing	37.5	6.9			1	
Myotis evotis	9/23/2016	LCC	Female	Juvenile	Non-reproducing	38.5	8.2			0	
Myotis evotis	9/23/2016	LCC	Female	Adult	Non-reproducing	39	8			1	
Myotis evotis	9/23/2016	LCC	Male	Juvenile	Non-reproducing	38.5	7.3			0	
Myotis evotis	9/23/2016	LCC	Male	Adult	Non-reproducing	39.5	7.4			1	
Myotis evotis	9/23/2016	LCC	Male	Adult	Non-reproducing	38.5	7.1			0	
Myotis evotis	9/18/2017	LCC	Male	Adult	Non-reproducing	38.5	6.8	1.18	2.9	1	
Myotis evotis	9/18/2017	LCC	Male	Adult	Non-reproducing	38.7	8.9	1.77	4.53	1	
Myotis evotis	9/18/2017	LCC	Male	Adult	Scrotal	38.8	8.9	1.45	2.9	0	
Myotis evotis	9/18/2017	LCC	Male	Adult	Non-reproducing	38.8	6.6	1.26	4.57	1	
Myotis evotis	9/18/2017	LCC	Male	Adult	Non-reproducing	39	6.9	0.78	2.65	1	
Myotis evotis	9/18/2017	LCC	Male	Adult	Non-reproducing	39.1	7.7	0.68	2.94	1	
Myotis evotis	9/18/2017	LCC	Male	Adult	Scrotal	39.3	7.8	1.34	4.42	1	
Myotis evotis	9/18/2017	LCC	Male	Adult	Scrotal	39.3	7.8	1.43	5.2	1	
Myotis evotis	9/18/2017	LCC	Male	Adult	Non-reproducing	38.9	7.5	2.14	4.44	1	
Myotis evotis	9/18/2017	LCC	Male	Adult	Scrotal	38.4	6.9	1.24	3.24	1	
Myotis evotis	9/18/2017	LCC	Male	Adult	Non-reproducing	37.8	7.8	1.2	4.81	1	
Myotis evotis	9/18/2017	LCC	Male	Adult	Non-reproducing	38.5	6.8	1.16	2.5	1	
Myotis evotis	9/18/2017	LCC	Male	Adult	Non-reproducing	38.5	7.8	0.86	4.69	1	
Myotis evotis	9/18/2017	LCC	Male	Adult	Scrotal	39.5	7.8	1.46	3.44	2	
Myotis evotis	9/18/2017	LCC	Male	Adult	Non-reproducing	39.5	8.3	1.96	5.1	1	
Myotis evotis	9/18/2017	LCC	Male	Adult	Scrotal	38.3	7.1	1.08	3.09	1	
Myotis evotis	9/18/2017	LCC	Male	Adult	Scrotal	35.5	7.5	2.09	4.32	1	
Myotis evotis	9/18/2017	LCC	Male	Adult	Non-reproducing	38	7.8	1.37	4.38	1	
Myotis evotis	9/18/2017	LCC	Male	Adult	Non-reproducing	39	8	2.38	4.36	1	
Myotis evotis	9/18/2017	LCC	Male	Adult	Scrotal	38.9	6.6	0.66	3.35	1	

Species	Date	Site	Sex	Age	Reproductive?	Forearm	Mass	Fat	Lean	Wing Score	Respirometry?
Myotis evotis	9/18/2017	LCC	Male	Adult	Non-reproducing	38.5	7.9	2.08	4.86	1	
Myotis evotis	9/18/2017	LCC	Male	Adult	Scrotal	37.3	7.5	1.35	2.55	1	
Myotis evotis	9/18/2017	LCC	Male	Adult	Non-reproducing	36.7	8	2.32	4.67	1	
Myotis evotis	9/18/2017	LCC	Male	Adult	Non-reproducing	37	7.8	1.62	2.87	1	
Myotis evotis	9/18/2017	LCC	Male	Adult	Non-reproducing	38.5	8.1	2.42	4.65	1	
Myotis evotis	9/18/2017	LCC	Male	Adult	Non-reproducing	37.9	7.3	0.81	5.29	1	
Myotis evotis	9/18/2017	LCC	Male	Adult	Scrotal	38.2	6	0.77	4.56	1	
Myotis evotis	9/18/2017	LCC	Male	Adult	Scrotal	38.8	7.5	0.88	3.5	1	
Myotis evotis	9/18/2017	LCC	Male	Adult	Scrotal	37.2	6.2	0.89	4.25	1	
Myotis evotis	9/18/2017	LCC	Male	Adult	Scrotal	38.5	8	1.95	2.84	0	
Myotis evotis	9/18/2017	LCC	Male	Adult	Non-reproducing	38.6	7.7	2.38	4.49	1	
Myotis evotis	9/19/2017	LCC	Male	Adult	Scrotal	36.7	6.9			2	yes
Myotis evotis	9/19/2017	LCC	Male	Adult	Scrotal	38.5	6.5			1	
Myotis evotis	9/20/2017	LCC	Male	Adult	Scrotal	35.7	8			0	
Myotis evotis	9/20/2017	LCC	Male	Adult	Non-reproducing	37.9	6.9			1	yes
Myotis evotis	9/20/2017	LCC	Male	Adult	Non-reproducing	35.6	6.7			1	
Myotis evotis	9/20/2017	LCC	Male	Adult	Scrotal	38.3	6.9			0	
Myotis evotis	9/25/2017	LCC	Male	Adult	Non-reproducing	37.1	7.1			1	
Myotis evotis	9/25/2017	LCC	Male	Adult	Non-reproducing	38.8	7.1			1	
Myotis evotis	9/25/2017	LCC	Male	Juvenile	Non-reproducing	39.3	7.3			1	
Myotis evotis	9/25/2017	LCC	Male	Juvenile	Non-reproducing	35.5	5.9			1	
Myotis evotis	9/25/2017	LCC	Female	Juvenile	Non-reproducing	39.3	7.5			0	
Myotis evotis	9/25/2017	LCC	Male	Adult	Non-reproducing	38.4	7			1	
Myotis evotis	9/25/2017	LCC	Male	Adult	Non-reproducing	39.7	7.7			1	
Myotis evotis	9/25/2017	LCC	Male	Adult	Non-reproducing	38.2	7.8			1	
Myotis evotis	9/25/2017	LCC	Male	Adult	Non-reproducing	38.9	7			1	
Myotis evotis	9/27/2017	LCC	Male	Adult	Non-reproducing	39.1	6.6			1	
Myotis evotis	9/27/2017	LCC	Male	Adult	Non-reproducing	40.1	8.7	2.87	4.74	1	
Myotis evotis	9/27/2017	LCC	Male	Adult	Scrotal	37.8	8	1.94	4.17	1	
Myotis evotis	9/27/2017	LCC	Male	Adult	Non-reproducing	38.2	8	2.14	3.59	2	

Species	Date	Site	Sex	Age	Reproductive?	Forearm	Mass	Fat	Lean	Wing Score	Respirometry?
Myotis evotis	9/27/2017	LCC	Male	Adult	Non-reproducing	36.9	7	2.01	4.26	0	
Myotis evotis	9/27/2017	LCC	Male	Adult	Non-reproducing	39.1	7.2	2.09	4.63	0	
Myotis evotis	9/27/2017	LCC	Male	Adult	Scrotal	39.3	8.2	2.09	4.96	1	
Myotis evotis	9/27/2017	LCC	Male	Adult	Scrotal	38.2	8.1	1.96	4.09	1	
Myotis evotis	9/27/2017	LCC	Male	Adult	Scrotal	38.3	7.6	1.21	3.65	1	
Myotis evotis	9/27/2017	LCC	Male	Adult	Non-reproducing	38.1	7.8	2.25	4.31	1	
Myotis evotis	9/27/2017	LCC	Male	Adult	Scrotal	38	7.5	1.57	3.4	1	
Myotis evotis	9/27/2017	LCC	Female	Adult	Non-reproducing	40.3	7.5	1.82	3.87	1	
Myotis evotis	9/27/2017	LCC	Male	Adult	Scrotal	36.3	7.2	1.84	4.54	1	
Myotis evotis	9/27/2017	LCC	Male	Adult	Non-reproducing	37.1	6.9	1.44	3.5	1	
Myotis evotis	9/27/2017	LCC	Male	Adult	Scrotal	37.3	7	1.81	4.37	1	
Myotis evotis	9/27/2017	LCC	Male	Adult	Non-reproducing	39	7.7	2.01	3.6	0	
Myotis evotis	9/27/2017	LCC	Male	Adult	Scrotal	38	7.9	2	3.8	0	
Myotis evotis	9/27/2017	LCC	Male	Adult	Scrotal	39.2	8	1.98	5.02	1	
Myotis evotis	9/27/2017	LCC	Male	Adult	Scrotal	39.3	7.1	1.15	3.6	1	
Myotis evotis	9/27/2017	LCC	Male	Adult	Scrotal	37.6	7.1	1.84	4.42	1	
Myotis evotis	9/27/2017	LCC	Male	Adult	Scrotal	39.5	8.2	1.94	3.56	1	
Myotis evotis	9/27/2017	LCC	Male	Adult	Scrotal	38.5	7.6	1.73	5.09	1	
Myotis evotis	9/27/2017	LCC	Male	Adult	Scrotal	38.3	7.7	2.18	4.62	1	
Myotis evotis	9/27/2017	LCC	Male	Adult	Scrotal	38.1	7.4	0.84	1.57	1	
Myotis evotis	9/27/2017	LCC	Male	Adult	Non-reproducing	38.1	7.1	1.83	3.81	1	
Myotis evotis	9/27/2017	LCC	Male	Adult	Scrotal	37.1	7.7	2.17	4.72	2	
Myotis evotis	9/27/2017	LCC	Male	Adult	Scrotal	37.1	7.4	1.6	3.53	1	
Myotis evotis	9/27/2017	LCC	Male	Adult	Scrotal	38.9	7.6	1.67	5.04	1	
Myotis evotis	9/27/2017	LCC	Male	Adult	Scrotal	39.5	7.7	1.72	3.89	1	
Myotis evotis	9/27/2017	LCC	Male	Adult	Scrotal	39.2	8	1.98	5.24	1	
Myotis evotis	9/27/2017	LCC	Male	Adult	Scrotal	36.1	6.8	1.29	3.63	1	
Myotis evotis	9/27/2017	LCC	Male	Adult	Scrotal	38.1	7.6	2.01	4.91	1	
Myotis evotis	9/27/2017	LCC	Male	Adult	Scrotal	37.2	6.6	1.54	4.22	1	
Myotis evotis	9/27/2017	LCC	Male	Adult	Scrotal	36.9	6.9	1.36	3.89	1	
Myotis evotis	9/27/2017	LCC	Male	Adult	Scrotal	38.1	7.7	1.65	4.47	1	

Species	Date	Site	Sex	Age	Reproductive?	Forearm	Mass	Fat	Lean	Wing Score	Respirometry?
Myotis evotis	9/27/2017	LCC	Male	Adult	Scrotal	38.7	8	2.03	5.18	1	
Myotis evotis	9/28/2017	LCC	Male	Adult	Scrotal	36.7	7.3	2.27	4.29	1	
Myotis evotis	9/28/2017	LCC	Male	Adult	Scrotal	40.1	8.6	2.29	5.47	1	
Myotis evotis	9/28/2017	LCC	Female	Juvenile	Non-reproducing	39.2	7.2	1.69	3.66	1	
Myotis evotis	9/28/2017	LCC	Male	Adult	Scrotal	38.4	7.1	1.81	4.45	1	
Myotis evotis	9/28/2017	LCC	Male	Adult	Scrotal	38.9	7.6	1.99	4.74	1	
Myotis evotis	9/28/2017	LCC	Male	Adult	Scrotal	38.6	8.8	2.34	5.68	1	
Myotis evotis	9/28/2017	LCC	Male	Adult	Scrotal	38.2	8.2	2.12	3.74	1	
Myotis evotis	9/28/2017	LCC	Male	Adult	Scrotal	38	7.8	1.65	3.82	1	
Myotis evotis	9/28/2017	LCC	Male	Adult	Scrotal	38.2	7.6	2.22	4.68	1	
Myotis evotis	9/28/2017	LCC	Male	Adult	Scrotal	37.4	6.4	1.01	4.61	1	
Myotis evotis	9/28/2017	LCC	Male	Adult	Scrotal	38.2	7	1.38	4.03	1	
Myotis evotis	9/28/2017	LCC	Male	Adult	Scrotal	38.1	8.3	2.16	5.13	1	
Myotis evotis	9/28/2017	LCC	Male	Adult	Scrotal	38.4	7.5	1.95	3.41	1	
Myotis evotis	9/28/2017	LCC	Male	Adult	Non-reproducing	36.1	7.6	2.13	4.68	1	
Myotis evotis	9/28/2017	LCC	Male	Adult	Scrotal	38.4	8.4	1.39	4.4	1	
Myotis evotis	9/28/2017	LCC	Male	Adult	Scrotal	39.7	8.3	2.27	3.53	1	
Myotis evotis	9/28/2017	LCC	Male	Adult	Scrotal	37.6	8	1.49	3.74	1	
Myotis evotis	9/28/2017	LCC	Male	Juvenile	Non-reproducing	36.1	7.2	2.41	4.06	1	
Myotis evotis	9/28/2017	LCC	Male	Adult	Scrotal	37.6	7.8	2.15	4.75	1	
Myotis evotis	9/28/2017	LCC	Male	Adult	Non-reproducing	38.4	8.1	2.16	3.83	1	
Myotis evotis	9/28/2017	LCC	Male	Adult	Scrotal	39.1	8.1	2.13	3.65	1	
Myotis evotis	9/28/2017	LCC	Male	Adult	Scrotal	38.4	7.5	1.68	3.92	1	
Myotis evotis	9/28/2017	LCC	Male	Adult	Non-reproducing	39.4	8.2	1.98	2.89	2	
Myotis evotis	2/22/2018	LCC	Male	Adult	Unknown	38.1	6			1	
Myotis evotis	9/20/2018	LCC	Male	Adult	Non-reproducing	40.2	7.8			0	yes
Myotis evotis	9/20/2018	LCC	Male	Adult	Non-reproducing	39.9	7.9			0	yes
Myotis evotis	9/20/2018	LCC	Female	Adult	Unknown	39.2	7.6			0	yes
Myotis evotis	9/20/2018	LCC	Male	Adult	Scrotal	37	7.3			0	yes
Myotis evotis	9/20/2018	LCC	Male	Adult	Non-reproducing	39.3	6.9			0	yes
Myotis evotis	9/20/2018	LCC	Female	Adult	Unknown	40.6	8			1	yes

Species	Date	Site	Sex	Age	Reproductive?	Forearm	Mass	Fat	Lean	Wing Score	Respirometry?
Myotis evotis	9/20/2018	LCC	Male	Adult	Scrotal	37.1	6.8			0	yes
Myotis evotis	9/20/2018	LCC	Female	Adult	Unknown	39.6	7.3			0	yes
Myotis evotis	9/20/2018	LCC	Male	Adult	Scrotal	38.6	7.1			0	yes
Myotis evotis	9/20/2018	LCC	Male	Adult	Scrotal	28.6	6.1			1	
Myotis evotis	9/20/2018	LCC	Male	Adult	Non-reproducing	37	6.7			0	
Myotis evotis	9/20/2018	LCC	Male	Adult	Scrotal	39.1	6.8			0	
Myotis evotis	9/20/2018	LCC	Male	Adult	Non-reproducing	38	6.3			0	
Myotis evotis	9/20/2018	LCC	Female	Adult	Unknown	37.9	7.6			1	
Myotis evotis	9/20/2018	LCC	Male	Adult	Scrotal	38.6	7.4			0	
Myotis evotis	9/22/2018	LCC	Male	Adult	Non-reproducing	38.5	7.4			1	
Myotis evotis	9/22/2018	LCC	Male	Adult	Non-reproducing	38.1	8.8			0	
Myotis evotis	9/22/2018	LCC	Male	Adult	Scrotal	38.8	9.5			0	
Myotis evotis	9/22/2018	LCC	Male	Adult	Non-reproducing	38.1	6.5			1	
Myotis evotis	9/22/2018	LCC	Male	Adult	Scrotal	39.3	7.4			0	
Myotis evotis	9/22/2018	LCC	Male	Adult	Non-reproducing	38.4	6.9			1	
Myotis evotis	9/22/2018	LCC	Male	Adult	Non-reproducing	38.5	8			0	
Myotis evotis	9/22/2018	LCC	Male	Adult	Scrotal	38.4	7.5			0	
Myotis evotis	9/22/2018	LCC	Male	Adult	Scrotal	37.6	7.4			0	
Myotis evotis	9/22/2018	LCC	Male	Adult	Scrotal	37.5	6.9			0	
Myotis evotis	9/22/2018	LCC	Male	Adult	Non-reproducing	39.2	6.9			0	
Myotis evotis	9/22/2018	LCC	Female	Adult	Non-reproducing	39	8.6			0	
Myotis evotis	9/22/2018	LCC	Male	Adult	Scrotal	39.7	8.6			0	
Myotis evotis	9/22/2018	LCC	Female	Adult	Non-reproducing	40.4	7.2			0	
Myotis evotis	9/22/2018	LCC	Male	Adult	Scrotal	39.3	6.9			0	
Myotis evotis	9/22/2018	LCC	Female	Adult	Non-reproducing	39.5	7.4			0	
Myotis evotis	9/22/2018	LCC	Male	Adult	Non-reproducing	36.9	6.9			0	
Myotis evotis	9/22/2018	LCC	Male	Adult	Non-reproducing	38.6	6.4			0	
Myotis evotis	9/22/2018	LCC	Male	Adult	Non-reproducing	36.5	7.8			0	
Myotis evotis	9/22/2018	LCC	Male	Adult	Scrotal	36	7.2			0	
Myotis evotis	9/22/2018	LCC	Male	Adult	Scrotal	37.8	8.4			0	
Myotis evotis	9/22/2018	LCC	Male	Adult	Scrotal	36.7	7			0	

Species	Date	Site	Sex	Age	Reproductive?	Forearm	Mass	Fat	Lean	Wing Score	Respirometry?
Myotis evotis	9/22/2018	LCC	Male	Adult	Non-reproducing	39.6	8.2			0	
Myotis evotis	9/22/2018	LCC	Male	Adult	Scrotal	38	7.1			1	
Myotis evotis	9/22/2018	LCC	Male	Adult	Non-reproducing	38.9	7			0	
Myotis evotis	9/22/2018	LCC	Male	Adult	Scrotal	38.5	6.7			1	
Myotis evotis	9/22/2018	LCC	Male	Adult	Scrotal	39.9	7.3			1	
Myotis evotis	9/22/2018	LCC	Female	Adult	Non-reproducing	39.3	8.4			1	yes
Myotis evotis	9/22/2018	LCC	Female	Adult	Non-reproducing	37.2	6.3			1	
Myotis evotis	9/22/2018	LCC	Male	Adult	Non-reproducing	39.5	8.1			0	
Myotis evotis	9/23/2018	LCC	Male	Adult	Scrotal	38.2	7.6			0	
Myotis evotis	9/23/2018	LCC	Male	Adult	Scrotal	38.9	7.8			0	yes
Myotis evotis	9/23/2018	LCC	Male	Juvenile	Non-reproducing	38.2	7.1			0	
Myotis evotis	9/23/2018	LCC	Female	Adult	Non-reproducing	29.2	7.7			1	yes
Myotis evotis	9/23/2018	LCC	Female	Adult	Non-reproducing	38.9	7.5			0	
Myotis evotis	9/23/2018	LCC	Female	Juvenile	Non-reproducing	39.4	6.9			0	
Myotis evotis	9/23/2018	LCC	Female	Juvenile	Non-reproducing	37.9	6.1			0	yes
Myotis evotis	9/23/2018	LCC	Female	Adult	Non-reproducing	39.3	7.7			0	
Myotis evotis	9/23/2018	LCC	Male	Adult	Non-reproducing	39.2	7.8			0	yes
Myotis evotis	9/23/2018	LCC	Female	Adult	Non-reproducing	39.6	8.1			0	
Myotis evotis	9/23/2018	LCC	Male	Adult	Scrotal	28.5	7.3			0	
Myotis evotis	9/23/2018	LCC	Female	Adult	Non-reproducing	38.8	7.2			1	
Myotis evotis	9/23/2018	LCC	Male	Adult	Scrotal	37.6	8			0	
Myotis evotis	9/26/2018	LCC	Male	Adult	Scrotal	38.1	7.4			1	
Myotis evotis	9/26/2018	LCC	Male	Adult	Scrotal	36.6	7.2			1	
Myotis evotis	9/26/2018	LCC	Male	Adult	Scrotal	38.9	7.1			1	
Myotis evotis	9/26/2018	LCC	Male	Adult	Scrotal	36.8	6.7			1	
Myotis evotis	9/26/2018	LCC	Female	Adult	Non-reproducing	39.9	6.9			1	
Myotis evotis	9/26/2018	LCC	Male	Adult	Scrotal	37.7	7.1			1	
Myotis evotis	9/26/2018	LCC	Female	Adult	Non-reproducing	38.3	6.8			2	
Myotis evotis	9/26/2018	LCC	Female	Adult	Non-reproducing	38	6.7			1	
Myotis evotis	9/26/2018	LCC	Female	Adult	Non-reproducing	37.6	6.9			1	

Species	Date	Site	Sex	Age	Reproductive?	Forearm	Mass	Fat	Lean	Wing Score	Respirometry?
Myotis evotis	9/26/2018	LCC	Male	Adult	Non-reproducing	37.7	6.7			1	
Myotis evotis	9/26/2018	LCC	Male	Adult	Scrotal	38.3	8.2			2	
Myotis evotis	9/26/2018	LCC	Male	Adult	Scrotal	38	6.7			2	
Myotis evotis	9/26/2018	LCC	Male	Adult	Scrotal	37.3	7			2	
Myotis evotis	9/26/2018	LCC	Male	Adult	Non-reproducing	39.5	7.1			1	
Myotis evotis	9/26/2018	LCC	Male	Adult	Scrotal	39.1	7.3			2	
Myotis evotis	9/26/2018	LCC	Female	Adult	Non-reproducing	38.5	7			1	
Myotis evotis	9/26/2018	LCC	Female	Adult	Non-reproducing	38.5	7			1	
Myotis evotis	9/26/2018	LCC	Male	Adult	Scrotal	38.5	7.3			2	
Myotis evotis	10/1/2018	ODW	Female	Juvenile	Non-reproducing	37.9	5.7			0	
Myotis evotis	10/1/2018	ODW	Female	Juvenile	Non-reproducing	36.8	6			0	
Myotis lucifugus	9/21/2016	LCC	Male	Adult	Non-reproducing	38.2	6.3			0	
Myotis lucifugus	9/21/2016	LCC	Male	Adult	Non-reproducing	37.2	6.5			0	
Myotis lucifugus	9/21/2016	LCC	Male	Adult	Non-reproducing	35	6.3			0	
Myotis lucifugus	9/21/2016	LCC	Male	Adult	Non-reproducing	36.2	6.9			0	
Myotis lucifugus	9/21/2016	LCC	Male	Adult	Non-reproducing	36.3	7.8			1	
Myotis lucifugus	9/21/2016	LCC	Male	Adult	Non-reproducing	37.5	7.5			0	
Myotis lucifugus	9/21/2016	LCC	Male	Adult	Non-reproducing	36.1	7.6			2	
Myotis lucifugus	9/21/2016	LCC	Male	Adult	Non-reproducing	37.5	7.5			0	
Myotis lucifugus	9/21/2016	LCC	Male	Adult	Non-reproducing	35.5	7.5			0	
Myotis lucifugus	9/21/2016	LCC	Male	Adult	Non-reproducing	36.1	8			0	
Myotis lucifugus	9/21/2016	LCC	Female	Juvenile	Non-reproducing	37.4	6.8			0	
Myotis lucifugus	9/21/2016	LCC	Male	Adult	Non-reproducing	37.5	8			0	
Myotis lucifugus	9/21/2016	LCC	Male	Adult	Non-reproducing	38.5	8			0	
Myotis lucifugus	9/22/2016	LCC	Male	Adult	Non-reproducing	36.1	6.6			0	
Myotis lucifugus	9/22/2016	LCC	Male	Adult	Non-reproducing	35.9	6.7			0	
Myotis lucifugus	9/22/2016	LCC	Male	Adult	Non-reproducing	36.6	6.4			0	
Myotis lucifugus	9/22/2016	LCC	Male	Adult	Scrotal	37.7	6.4			0	
Myotis lucifugus	9/22/2016	LCC	Male	Adult	Scrotal	36.1	7.7			0	
Myotis lucifugus	9/22/2016	LCC	Male	Adult	Non-reproducing	38.2	7.3			0	
Myotis lucifugus	9/22/2016	LCC	Male	Adult	Scrotal	36.3	8.8			0	
Myotis lucifugus	9/22/2016	LCC	Male	Adult	Non-reproducing	36	7.4			0	
Myotis lucifugus	9/22/2016	LCC	Male	Adult	Scrotal	35	6.8			0	
Myotis lucifugus	9/22/2016	LCC	Male	Adult	Non-reproducing	34.8	6.4			0	

Species	Date	Site	Sex	Age	Reproductive?	Forearm	Mass	Fat	Lean	Wing Score	Respirometry?
Myotis lucifugus	9/22/2016	LCC	Male	Adult	Scrotal	39	7.8			0	
Myotis lucifugus	9/22/2016	LCC	Male	Adult	Non-reproducing	33.7	6.4			0	
Myotis lucifugus	9/22/2016	LCC	Female	Juvenile	Non-reproducing	36.3	6.6			0	
Myotis lucifugus	9/22/2016	LCC	Male	Adult	Scrotal	37.1	7			0	
Myotis lucifugus	9/22/2016	LCC	Male	Adult	Non-reproducing	37.4	7.2			0	
Myotis lucifugus	9/22/2016	LCC	Male	Adult	Non-reproducing	37.7	7.9			0	
Myotis lucifugus	9/22/2016	LCC	Male	Adult	Scrotal	36.5	7.7			0	
Myotis lucifugus	9/22/2016	LCC	Male	Adult	Non-reproducing	36.9	6.9			1	
Myotis lucifugus	9/22/2016	LCC	Male	Adult	Scrotal	36.3	7.8			0	
Myotis lucifugus	9/22/2016	LCC	Male	Adult	Non-reproducing	36	8.2			0	
Myotis lucifugus	9/23/2016	LCC	Female	Juvenile	Non-reproducing	37.3	7.6			0	
Myotis lucifugus	9/23/2016	LCC	Female	Adult	Non-reproducing	38.1	8.3			0	
Myotis lucifugus	9/23/2016	LCC	Male	Juvenile	Non-reproducing	36.4	8.4			0	
Myotis lucifugus	9/23/2016	LCC	Male	Adult	Non-reproducing	36	7.4			0	
Myotis lucifugus	9/23/2016	LCC	Female	Adult	Non-reproducing	37.9	7.8			0	
Myotis lucifugus	9/23/2016	LCC	Male	Adult	Scrotal	40	8.8			0	
Myotis lucifugus	9/23/2016	LCC	Male	Juvenile	Non-reproducing	35.3	7			0	
Myotis lucifugus	9/23/2016	LCC	Female	Juvenile	Non-reproducing	39	6.9			0	
Myotis lucifugus	9/23/2016	LCC	Female	Juvenile	Non-reproducing	36.6	7.4			0	
Myotis lucifugus	9/23/2016	LCC	Male	Adult	Non-reproducing	37.6	7.6			0	
Myotis lucifugus	9/23/2016	LCC	Male	Adult	Non-reproducing	37.5	8.6			0	
Myotis lucifugus	9/23/2016	LCC	Male	Adult	Non-reproducing	34.1	7.3			1	
Myotis lucifugus	9/23/2016	LCC	Male	Adult	Non-reproducing	37	8.3			1	
Myotis lucifugus	9/23/2016	LCC	Male	Adult	Scrotal	34.5	8.1			1	
Myotis lucifugus	9/23/2016	LCC	Male	Adult	Non-reproducing	37.5	8.2			1	
Myotis lucifugus	9/23/2016	LCC	Male	Adult	Non-reproducing	36.8	7.5			2	
Myotis lucifugus	9/23/2016	LCC	Male	Adult	Non-reproducing	38.4	8.9			0	
Myotis lucifugus	9/23/2016	LCC	Male	Adult	Scrotal	37	8			1	
Myotis lucifugus	9/23/2016	LCC	Male	Adult	Non-reproducing	35.7	7.8			0	
Myotis lucifugus	9/23/2016	LCC	Male	Adult	Non-reproducing	36.1	6.6			1	
Myotis lucifugus	9/23/2016	LCC	Male	Adult	Non-reproducing	37.2	7.3			0	

Species	Date	Site	Sex	Age	Reproductive?	Forearm	Mass	Fat	Lean	Wing Score	Respirometry?
Myotis lucifugus	9/23/2016	LCC	Male	Adult	Non-reproductive	38.3	7.5			0	
Myotis lucifugus	9/23/2016	LCC	Female	Adult	Non-reproducing	38.7	6.8			0	
Myotis lucifugus	9/23/2016	LCC	Male	Adult	Non-reproducing	36.1	7.6			0	
Myotis lucifugus	9/23/2016	LCC	Female	Adult	Non-reproducing	37	7.3			0	
Myotis lucifugus	9/23/2016	LCC	Male	Adult	Non-reproducing	37.8	7.9			0	
Myotis lucifugus	9/23/2016	LCC	Female	Adult	Non-reproducing	35.8	6.3			0	
Myotis lucifugus	9/23/2016	LCC	Male	Adult	Non-reproducing	36.2	7.5			0	
Myotis lucifugus	9/23/2016	LCC	Male	Adult	Non-reproducing	38.1	7.5			0	
Myotis lucifugus	9/23/2016	LCC	Male	Adult	Unknown	37.6	8.1				
Myotis lucifugus	9/23/2016	LCC	Male	Adult	Scrotal	37.7	7.3			0	
Myotis lucifugus	9/23/2016	LCC	Male	Adult	Scrotal	37.5	7			2	
Myotis lucifugus	9/23/2016	LCC	Female	Adult	Non-reproducing	38.5	8.1			0	
Myotis lucifugus	9/23/2016	LCC	Male	Adult	Scrotal	38.4	7.3			1	
Myotis lucifugus	9/23/2016	LCC	Female	Adult	Non-reproducing	36.8	6.8			0	
Myotis lucifugus	2/17/2017	LCC	Female	Adult	Non-reproducing	40	8.1	0.85	2.35	1	
Myotis lucifugus	2/17/2017	LCC	Male	Adult	Non-reproducing	35.2	6.5	0.71	3.8	0	yes
Myotis lucifugus	2/17/2017	LCC	Male	Adult	Non-reproducing	36.3	6.4	0.4	3.7	1	
Myotis lucifugus	2/17/2017	LCC	Male	Adult	Non-reproducing	35.5	6.4	0.85	3.23	2	yes
Myotis lucifugus	2/17/2017	LCC	Male	Adult	Non-reproducing	36.1	6.3	0.67	2.92	1	yes
Myotis lucifugus	2/17/2017	LCC	Male	Adult	Non-reproducing	38.3	6.5	0.52	1.94	1	
Myotis lucifugus	2/17/2017	LCC	Male	Adult	Non-reproducing	36.3	6	1.04	1.81	2	yes
Myotis lucifugus	2/17/2017	LCC	Female	Adult	Non-reproducing	37	6.3	0.62	3.84	1	yes
Myotis lucifugus	2/17/2017	LCC	Female	Adult	Non-reproducing	38.3	8.4	1.96	4.22	1	yes
Myotis lucifugus	2/17/2017	LCC	Female	Adult	Non-reproducing	34.5	5.5	1.11	2.65	2	yes
Myotis lucifugus	2/17/2017	LCC	Female	Adult	Non-reproducing	37.5	7.9	1.22	3.55	2	yes
Myotis lucifugus	2/17/2017	LCC	Male	Adult	Non-reproducing	35.8	5.6	0.23	3.22	0	yes
Myotis lucifugus	2/17/2017	LCC	Female	Adult	Non-reproducing	37.1	6.5	0.63	3.71	3	yes
Myotis lucifugus	2/17/2017	LCC	Male	Adult	Non-reproducing	39.2	8.1	0.73	4.22	1	yes
Myotis lucifugus	2/17/2017	LCC	Male	Adult	Non-reproducing	37.2	6.9	1.36	2.88	1	yes
Myotis lucifugus	2/17/2017	LCC	Male	Adult	Non-reproducing	36	6.1	0.36	3.63	0	yes
Myotis lucifugus	2/17/2017	LCC	Female	Adult	Non-reproducing	36.6	6.4	0.97	2.76	1	yes

Species	Date	Site	Sex	Age	Reproductive?	Forearm	Mass	Fat	Lean	Wing Score	Respirometry?
Myotis lucifugus	2/17/2017	LCC	Male	Adult	Non-reproducing	36	6.5	0.4	2.81	2	
Myotis lucifugus	2/17/2017	LCC	Male	Adult	Non-reproducing	36.1	6	1.03	3.56	1	
Myotis lucifugus	9/18/2017	LCC	Male	Juvenile	Non-reproducing	36.9	7.2	1.37	3.15	1	yes
Myotis lucifugus	9/18/2017	LCC	Male	Adult	Non-reproducing	38.2	7.2	1.44	4.59	1	
Myotis lucifugus	9/18/2017	LCC	Male	Adult	Scrotal	37.2	7.6	0.97	3.02	1	
Myotis lucifugus	9/18/2017	LCC	Male	Adult	Scrotal	37.6	7.9	0.6	3.135	1	
Myotis lucifugus	9/18/2017	LCC	Male	Adult	Scrotal	35.4	6.4	1.38	5.34	1	
Myotis lucifugus	9/18/2017	LCC	Male	Adult	Non-reproducing	37.9	8.6	1.88	3.56	1	
Myotis lucifugus	9/18/2017	LCC	Male	Adult	Non-reproducing	38.4	9.1	2.69	5.59	2	
Myotis lucifugus	9/19/2017	LCC	Male	Juvenile	Non-reproducing	37	8.2			1	yes
Myotis lucifugus	9/19/2017	LCC	Male	Adult	Scrotal	36.2	7.5			1	yes
Myotis lucifugus	9/19/2017	LCC	Male	Adult	Non-reproducing	28.1	8.6			1	yes
Myotis lucifugus	9/19/2017	LCC	Male	Adult	Non-reproducing	36.2	8.6			1	yes
Myotis lucifugus	9/19/2017	LCC	Male	Adult	Non-reproducing	36	8.1			2	yes
Myotis lucifugus	9/19/2017	LCC	Male	Adult	Non-reproducing	36.3	7.4			1	yes
Myotis lucifugus	9/19/2017	LCC	Male	Juvenile	Non-reproducing	36.6	7			1	yes
Myotis lucifugus	9/19/2017	LCC	Male	Adult	Scrotal	37.2	8.3			1	yes
Myotis lucifugus	9/19/2017	LCC	Male	Adult	Scrotal	38.1	9.5	0.33	5.03	1	yes
Myotis lucifugus	9/20/2017	LCC	Male	Adult	Scrotal	35.4	8.6			1	yes
Myotis lucifugus	9/20/2017	LCC	Male	Adult	Scrotal	37.7	8.1			0	
Myotis lucifugus	9/20/2017	LCC	Male	Adult	Non-reproducing	39.2	8.7			2	
Myotis lucifugus	9/20/2017	LCC	Male	Adult	Scrotal	37.1	8.7			1	
Myotis lucifugus	9/20/2017	LCC	Male	Adult	Scrotal	37	7.7			1	
Myotis lucifugus	9/20/2017	LCC	Male	Adult	Non-reproducing	39.3	10.4			1	
Myotis lucifugus	9/25/2017	LCC	Male	Adult	Scrotal	35.2	6.4			1	
Myotis lucifugus	9/25/2017	LCC	Male	Adult	Non-reproducing	35.4	8.3			1	yes
Myotis lucifugus	9/25/2017	LCC	Male	Adult	Scrotal	37.1	8.3			1	yes
Myotis lucifugus	9/25/2017	LCC	Male	Juvenile	Non-reproducing	38.8	7.7			0	yes
Myotis lucifugus	9/25/2017	LCC	Male	Juvenile	Non-reproducing	37.3	8.5			0	yes
Myotis lucifugus	9/25/2017	LCC	Male	Adult	Non-reproducing	36.9	8.1			1	yes
Myotis lucifugus	9/25/2017	LCC	Male	Adult	Scrotal	36.2	8.7			0	yes

Species	Date	Site	Sex	Age	Reproductive?	Forearm	Mass	Fat	Lean	Wing Score	Respirometry?
Myotis lucifugus	9/25/2017	LCC	Male	Adult	Non-reproducing	36.9	7.3	1.76	4.57	0	yes
Myotis lucifugus	9/25/2017	LCC	Male	Adult	Non-reproducing	35.3	8.5	0.96	3.43	0	yes
Myotis lucifugus	9/25/2017	LCC	Male	Adult	Scrotal	37.7	7.4			1	yes
Myotis lucifugus	9/25/2017	LCC	Male	Adult	Non-reproducing	37.2	8.3			1	yes
Myotis lucifugus	9/25/2017	LCC	Male	Adult	Non-reproducing	38.2	7.9			1	yes
Myotis lucifugus	9/25/2017	LCC	Male	Adult	Non-reproducing	37	8			0	yes
Myotis lucifugus	9/27/2017	LCC	Male	Juvenile	Non-reproducing	37	7.3			0	yes
Myotis lucifugus	9/27/2017	LCC	Female	Adult	Non-reproducing	36.5	6.4			1	yes
Myotis lucifugus	9/27/2017	LCC	Male	Juvenile	Scrotal	39	7.4	1.52	4	0	
Myotis lucifugus	9/27/2017	LCC	Male	Adult	Non-reproducing	37.2	7.7	1.69	5.08	1	
Myotis lucifugus	9/27/2017	LCC	Male	Adult	Scrotal	36.5	7.9	2.19	4.86	1	
Myotis lucifugus	9/27/2017	LCC	Male	Adult	Scrotal	38.1	6.9	0.93	5.1	1	
Myotis lucifugus	9/27/2017	LCC	Male	Adult	Non-reproducing	38.2	9.7	3.17	4.69	1	
Myotis lucifugus	9/27/2017	LCC	Male	Adult	Scrotal	37.1	9.7	2.8	4.6	1	
Myotis lucifugus	9/27/2017	LCC	Male	Adult	Non-reproducing	36.2	8.9	2.63	4.5	1	
Myotis lucifugus	9/27/2017	LCC	Male	Adult	Non-reproducing	26.1	7.7	2.08	4.93	2	
Myotis lucifugus	9/27/2017	LCC	Male	Adult	Non-reproducing	35.9	7.6	1.5	4.68	1	
Myotis lucifugus	9/27/2017	LCC	Male	Juvenile	Non-reproducing	37.3	9.3	3.16	5.16	1	
Myotis lucifugus	9/27/2017	LCC	Male	Adult	Non-reproducing	36.3	9	2.18	4.54	1	
Myotis lucifugus	9/27/2017	LCC	Male	Adult	Non-reproducing	38.4	7	1.41	4.06	1	
Myotis lucifugus	9/27/2017	LCC	Male	Adult	Scrotal	36.4	9.4	2.81	5.66	1	
Myotis lucifugus	9/27/2017	LCC	Male	Adult	Scrotal	37.5	8.6	2.14	4.44	1	
Myotis lucifugus	9/27/2017	LCC	Male	Adult	Scrotal	36.9	8.6	2.19	4.64	1	
Myotis lucifugus	9/28/2017	LCC	Male	Adult	Non-reproducing	35.6	7.7	2.19	4.83	1	
Myotis lucifugus	9/28/2017	LCC	Male	Adult	Non-reproducing	37.3	9	2.41	4.5	1	
Myotis lucifugus	9/28/2017	LCC	Male	Adult	Scrotal	35.5	8	2.21	4.88	1	
Myotis lucifugus	9/28/2017	LCC	Male	Adult	Scrotal	38.5	8.8	1.89	3.89	1	
Myotis lucifugus	9/28/2017	LCC	Male	Adult	Non-reproducing	38.4	8	2.12	3.93	1	
Myotis lucifugus	9/28/2017	LCC	Male	Adult	Scrotal	38.2	9.6	3.24	5.39	1	
Myotis lucifugus	9/28/2017	LCC	Male	Adult	Scrotal	35.6	8	2.4	4.82	1	
Myotis lucifugus	9/28/2017	LCC	Male	Adult	Scrotal	37.2	7.1	1.78	3.65	1	

Species	Date	Site	Sex	Age	Reproductive?	Forearm	Mass	Fat	Lean	Wing Score	Respirometry?
Myotis lucifugus	9/28/2017	LCC	Male	Adult	Scrotal	37.2	8.2	2.45	5.02	1	
Myotis lucifugus	9/28/2017	LCC	Male	Adult	Scrotal	37.2	7.2	1.95	4.41	1	
Myotis lucifugus	9/28/2017	LCC	Male	Adult	Scrotal	38.2	8.1	2.04	4.11	1	
Myotis lucifugus	9/28/2017	LCC	Male	Adult	Non-reproducing	36.8	8.9	2.83	5.21	1	
Myotis lucifugus	9/28/2017	LCC	Male	Adult	Scrotal	36.7	8.7	1.62	3.22	1	
Myotis lucifugus	9/28/2017	LCC	Male	Adult	Scrotal	39.2	9.6	2.69	6.01	1	
Myotis lucifugus	9/28/2017	LCC	Male	Adult	Scrotal	37.8	10.5	3.88	5.53	1	
Myotis lucifugus	9/28/2017	LCC	Male	Adult	Scrotal	38.5	8.2	2.77	4.59	0	
Myotis lucifugus	9/28/2017	LCC	Male	Adult	Scrotal	37	7.2	1.51	4.01	3	
Myotis lucifugus	9/28/2017	LCC	Male	Adult	Scrotal	38.1	8.1	1.72	4.33	0	
Myotis lucifugus	9/28/2017	LCC	Male	Adult	Scrotal	36.9	9.5	2.92	4.5	1	
Myotis lucifugus	9/28/2017	LCC	Male	Adult	Scrotal	38.2	9.8	3.28	5.64	1	
Myotis lucifugus	9/28/2017	LCC	Male	Adult	Non-reproducing	38.6	8.1	2.2	4.14	1	
Myotis lucifugus	9/28/2017	LCC	Male	Adult	Non-reproducing	37.1	8.2	2.43	5.25	2	
Myotis lucifugus	2/22/2018	LCC	Female	Adult	Unknown	35.2	6.2	0.98	4	0	
Myotis lucifugus	2/22/2018	LCC	Female	Adult	Unknown	37.1	8.6	1.67	5.89	0	yes
Myotis lucifugus	2/22/2018	LCC	Male	Adult	Unknown	36	6	1.52	3.58	1	
Myotis lucifugus	2/22/2018	LCC	Female	Adult	Unknown	38.4	7.5	1.4	4.79	0	yes
Myotis lucifugus	2/22/2018	LCC	Female	Adult	Unknown	38.3	8.4	1.8	5.71	0	yes
Myotis lucifugus	2/22/2018	LCC	Male	Adult	Unknown	37.3	7.1	1.75	4.39	0	yes
Myotis lucifugus	2/22/2018	LCC	Male	Adult	Unknown	37.7	6.6	0.78	4.94	1	
Myotis lucifugus	2/22/2018	LCC	Female	Adult	Unknown	38	8	1.44	5.77	0	yes
Myotis lucifugus	2/22/2018	LCC	Male	Adult	Unknown	36.6	7.6	1.01	3.84	0	yes
Myotis lucifugus	2/22/2018	LCC	Male	Adult	Unknown	39.9	7	1.16	5.16	1	yes
Myotis lucifugus	2/22/2018	LCC	Male	Adult	Unknown	37	6.8	0.77	3.53	1	yes
Myotis lucifugus	2/22/2018	LCC	Male	Adult	Unknown	35.8	7.1	1.2	4.93	1	yes
Myotis lucifugus	2/22/2018	LCC	Male	Adult	Unknown	36.5	6.1			0	
Myotis lucifugus	2/22/2018	LCC	Male	Adult	Unknown	38.5	6.6			0	
Myotis lucifugus	2/22/2018	LCC	Male	Adult	Unknown	38.4	6.9	1.27	3.74	1	yes
Myotis lucifugus	2/22/2018	LCC	Male	Adult	Unknown	37.2	6.6			0	
Myotis lucifugus	2/22/2018	LCC	Male	Adult	Unknown	36.2	6			0	

Species	Date	Site	Sex	Age	Reproductive?	Forearm	Mass	Fat	Lean	Wing Score	Respirometry?
Myotis lucifugus	2/22/2018	LCC	Male	Adult	Unknown	36.7	6.5			0	
Myotis lucifugus	2/22/2018	LCC	Male	Adult	Unknown	37.9	7.9	0.78	4.56	0	yes
Myotis lucifugus	2/22/2018	LCC	Male	Adult	Unknown	36.6	7.4	1.11	3.6	0	yes
Myotis lucifugus	2/22/2018	LCC	Male	Adult	Unknown	36.6	6.3			3	
Myotis lucifugus	2/22/2018	LCC	Male	Adult	Unknown	37	7.2	1.31	4.93	1	yes
Myotis lucifugus	2/22/2018	LCC	Male	Adult	Unknown	37.4	6.9	1.49	2.55	0	yes
Myotis lucifugus	2/22/2018	LCC	Male	Adult	Unknown	37.6	6.5			0	
Myotis lucifugus	9/20/2018	LCC	Male	Adult	Scrotal	35.6	7			0	
Myotis lucifugus	9/20/2018	LCC	Male	Adult	Non-reproducing	36.7	6.9			0	
Myotis lucifugus	9/20/2018	LCC	Male	Adult	Non-reproducing	36.2	7.8			1	
Myotis lucifugus	9/20/2018	LCC	Male	Adult	Scrotal	37.5	7.5			0	
Myotis lucifugus	9/20/2018	LCC	Male	Adult	Scrotal	38.9	7.4			0	
Myotis lucifugus	9/20/2018	LCC	Male	Adult	Non-reproducing	37.8	7.3			0	
Myotis lucifugus	9/20/2018	LCC	Male	Adult	Non-reproducing	36.4	6.6			1	
Myotis lucifugus	9/20/2018	LCC	Male	Adult	Non-reproducing	36.2	7.8			1	
Myotis lucifugus	9/20/2018	LCC	Male	Adult	Non-reproducing	35.9	7.3			0	
Myotis lucifugus	9/20/2018	LCC	Male	Adult	Scrotal	36.5	7.4			0	
Myotis lucifugus	9/20/2018	LCC	Male	Adult	Scrotal	37.5	7.5			0	
Myotis lucifugus	9/20/2018	LCC	Male	Adult	Non-reproducing	37.2	8.3			0	
Myotis lucifugus	9/22/2018	LCC	Male	Adult	Non-reproducing	38.4	7.9			0	
Myotis lucifugus	9/22/2018	LCC	Male	Adult	Non-reproducing	37.6	8.1			0	
Myotis lucifugus	9/22/2018	LCC	Male	Adult	Scrotal	38.4	7.9			0	
Myotis lucifugus	9/22/2018	LCC	Male	Adult	Non-reproducing	37.5	7.7			0	
Myotis lucifugus	9/22/2018	LCC	Male	Adult	Scrotal	36.2	8.2			0	
Myotis lucifugus	9/22/2018	LCC	Male	Adult	Non-reproducing	38.4	9.4			0	
Myotis lucifugus	9/22/2018	LCC	Male	Adult	Scrotal	38	8.3			0	
Myotis lucifugus	9/22/2018	LCC	Male	Adult	Non-reproducing	37.5	7.6			0	
Myotis lucifugus	9/22/2018	LCC	Male	Adult	Scrotal	37	7.7			0	
Myotis lucifugus	9/22/2018	LCC	Male	Adult	Scrotal	37.7	8.7			0	
Myotis lucifugus	9/22/2018	LCC	Male	Juvenile	Non-reproducing	36.9	9.6			0	
Myotis lucifugus	9/22/2018	LCC	Male	Adult	Scrotal	37.1	7.9			0	
Myotis lucifugus	9/22/2018	LCC	Male	Adult	Scrotal	35.7	7.6			1	
Myotis lucifugus	9/22/2018	LCC	Male	Adult	Non-reproducing	36.7	8.4			0	
Myotis lucifugus	9/22/2018	LCC	Male	Adult	Scrotal	35.6	7.6			1	

Species	Date	Site	Sex	Age	Reproductive?	Forearm	Mass	Fat	Lean	Wing Score	Respirometry?
Myotis lucifugus	9/22/2018	LCC	Male	Adult	Scrotal	35.9	7.7			1	
Myotis lucifugus	9/22/2018	LCC	Male	Adult	Scrotal	35.8	7.6			1	
Myotis lucifugus	9/23/2018	LCC	Male	Adult	Non-reproducing	35.2	6.8			0	
Myotis lucifugus	9/26/2018	LCC	Male	Adult	Scrotal	37.1	8.5			0	
Myotis lucifugus	9/26/2018	LCC	Male	Adult	Scrotal	37.8	9.1			1	
Myotis lucifugus	9/26/2018	LCC	Male	Adult	Scrotal	36.4	8.2			1	
Myotis lucifugus	9/26/2018	LCC	Male	Adult	Scrotal	35.2	7.2			1	
Myotis lucifugus	9/26/2018	LCC	Female	Adult	Non-reproducing	41	8.8			1	
Myotis thysanodes	9/23/2016	LCC	Female	Adult	Non-reproducing	42.9	10.7			1	
Myotis thysanodes	9/23/2016	LCC	Female	Juvenile	Non-reproducing	43.3	11.4			0	
Myotis thysanodes	9/23/2016	LCC	Male	Adult	Non-reproducing	41	9			1	
Myotis thysanodes	9/19/2017	LCC	Female	Adult	Non-reproducing	45.3	10.6			1	
Myotis thysanodes	9/19/2017	LCC	Male	Adult	Non-reproducing	40.4	9.3	2.25	5.7	1	
Myotis thysanodes	9/18/2017	LCC	Male	Adult	Scrotal	43.2	10.6			1	
Myotis thysanodes	9/20/2017	LCC	Male	Adult	Scrotal	39.3	8.3			1	
Myotis thysanodes	9/20/2017	LCC	Male	Adult	Non-reproducing	42.3	9.9			1	
Myotis thysanodes	9/20/2017	LCC	Male	Adult	Non-reproducing	41	9			1	
Myotis thysanodes	9/20/2017	LCC	Male	Adult	Non-reproducing	42	7.3			1	
Myotis thysanodes	9/25/2017	LCC	Male	Adult	Scrotal	41.1	7.7			1	
Myotis thysanodes	9/25/2017	LCC	Male	Adult	Non-reproducing	41.5	8.6	2.07	5.45	0	
Myotis thysanodes	9/27/2017	LCC	Male	Adult	Scrotal	40.8	9.7	2.74	4.83	1	
Myotis thysanodes	9/27/2017	LCC	Male	Adult	Scrotal	41.4	9	2.46	5.71	1	
Myotis thysanodes	9/27/2017	LCC	Male	Adult	Non-reproducing	41.5	10.9	3.37	5.39	1	
Myotis thysanodes	9/27/2017	LCC	Male	Adult	Scrotal	42.9	10.4	2.86	6.46	1	
Myotis thysanodes	9/27/2017	LCC	Male	Adult	Scrotal	41.5	10.3			1	
Myotis thysanodes	9/28/2017	LCC	Male	Adult	Scrotal	42.7	10.6	2.95	4.5	1	
Myotis thysanodes	9/28/2017	LCC	Male	Adult	Non-reproducing	41.5	10.9			0	
Myotis thysanodes	9/28/2017	LCC	Male	Adult	Scrotal	42.9	8.8	2.69	4.06	1	
Myotis thysanodes	9/28/2017	LCC	Female	Adult	Non-reproducing	42.6	9.8	2.99	5.83	1	
Myotis thysanodes	9/28/2017	LCC	Male	Adult	Non-reproducing	42.3	8.8	2.39	4.4	1	
Myotis thysanodes	9/27/2017	LCC	Male	Adult	Scrotal	42.7	10.3			1	
Myotis thysanodes	9/28/2017	LCC	Male	Adult	Non-reproducing	42.2	10.1	3.12	6.04	1	
Myotis thysanodes	9/28/2017	LCC	Male	Juvenile	Non-reproducing	40.4	8.7	2.51	5.21	1	
Myotis thysanodes	9/28/2017	LCC	Male	Adult	Non-reproducing	42.3	9.3			1	
Myotis thysanodes	9/20/2018	LCC	Male	Adult	Non-reproducing	41.4	7.6			0	

Species	Date	Site	Sex	Age	Reproductive?	Forearm	Mass	Fat	Lean	Wing Score	Respirometry?
Myotis thysanodes	9/22/2018	LCC	Male	Adult	Scrotal	42.9	10.4			1	
Myotis thysanodes	9/22/2018	LCC	Female	Adult	Non-reproducing	42.4	10.4			1	
Myotis thysanodes	9/23/2018	LCC	Female	Adult	Non-reproducing	43	9.6			0	yes
Myotis thysanodes	9/23/2018	LCC	Female	Adult	Non-reproducing	41.3	8.7			0	yes
Myotis thysanodes	9/23/2018	LCC	Male	Adult	Non-reproducing	41.8	9.4			0	yes
Myotis thysanodes	9/23/2018	LCC	Male	Adult	Scrotal	42.3	10.2			0	yes
Myotis thysanodes	9/23/2018	LCC	Male	Adult	Non-reproducing	41	8.9			0	
Myotis thysanodes	9/23/2018	LCC	Male	Adult	Non-reproducing	41.2	8.6			0	yes
Myotis thysanodes	9/23/2018	LCC	Male	Adult	Non-reproducing	42.3	9.5			0	yes
Myotis thysanodes	9/23/2018	LCC	Male	Adult	Non-reproducing	42.6	10.2			0	yes
Myotis thysanodes	9/23/2018	LCC	Male	Adult	Non-reproducing	42.7	7.7			1	
Myotis thysanodes	9/23/2018	LCC	Female	Adult	Non-reproducing	41.4	7.7			0	yes
Myotis thysanodes	9/23/2018	LCC	Female	Adult	Non-reproducing	41.5	9.3			0	yes
Myotis thysanodes	9/26/2018	LCC	Male	Adult	Non-reproducing	42.3	9.2			0	yes
Myotis thysanodes	9/26/2018	LCC	Male	Adult	Non-reproducing	44.5	10.1			0	yes
Myotis thysanodes	9/26/2018	LCC	Female	Adult	Non-reproducing	42.1	10.5			0	yes
Myotis thysanodes	9/26/2018	LCC	Female	Adult	Non-reproducing	43.7	9.3			1	yes
Myotis thysanodes	9/26/2018	LCC	Male	Adult	Scrotal	40.2	8.8			0	yes
Myotis thysanodes	9/26/2018	LCC	Male	Adult	Non-reproducing	39.5	8.3			1	yes
Myotis thysanodes	9/26/2018	LCC	Male	Adult	Non-reproducing	37.7	9.2			0	yes
Myotis thysanodes	9/19/2018	ODW	Male	Adult	Non-reproducing	40.2	9.8			1	
Myotis volans	9/20/2016	ODW	Female	Adult	Non-reproducing	38.8	8.8			0	
Myotis volans	9/21/2016	LCC	Male	Adult	Non-reproducing	37.8	8			0	
Myotis volans	9/22/2016	LCC	Female	Adult	Non-reproducing	38.5	9.7			0	
Myotis volans	9/22/2016	LCC	Male	Adult	Non-reproducing	37.2	7.2			0	
Myotis volans	9/22/2016	LCC	Male	Adult	Non-reproducing	37.5	8.7			0	
Myotis volans	9/23/2016	LCC	Male	Adult	Non-reproducing	39.5	9			0	
Myotis volans	9/23/2016	LCC	Female	Adult	Non-reproducing	39.5	8			1	
Myotis volans	9/23/2016	LCC	Female	Adult	Non-reproducing	39.1	9.3			1	
Myotis volans	9/23/2016	LCC	Male	Adult	Non-reproducing	37.4	8.8			0	
Myotis volans	9/23/2016	LCC	Male	Adult	Non-reproducing	38.8	11			0	

Species	Date	Site	Sex	Age	Reproductive?	Forearm	Mass	Fat	Lean	Wing Score	Respirometry?
Myotis volans	9/23/2016	LCC	Male	Adult	Non-reproducing	39.3	10.9			0	
Myotis volans	2/17/2017	LCC	Male	Adult	Non-reproducing	38.1	7.5	0.97	4.38	0	
Myotis volans	2/17/2017	LCC	Male	Adult	Non-reproducing	40.2	8.8	1.55	3.57	1	
Myotis volans	2/17/2017	LCC	Female	Adult	Non-reproducing	37.5	8.1	1.34	2.62	1	
Myotis volans	2/17/2017	LCC	Male	Adult	Non-reproducing	38	6.5	1.05	2.97	1	
Myotis volans	2/17/2017	LCC	Male	Adult	Non-reproducing	36.2	6.8	0.79	2.38	1	
Myotis volans	2/17/2017	LCC	Male	Adult	Scrotal	39	8.9	1.54	5.77	1	
Myotis volans	9/18/2017	LCC	Male	Adult	Non-reproducing	38.1	8.8	1.09	4.24	1	
Myotis volans	9/18/2017	LCC	Male	Adult	Non-reproducing	38.1	7.9	1.22	3.68	1	
Myotis volans	9/18/2017	LCC	Male	Adult	Scrotal	38.5	5.7	0.51	5.53	1	
Myotis volans	9/18/2017	LCC	Male	Adult	Non-reproducing	38.9	7.6	1.02	5.47	1	
Myotis volans	9/18/2017	LCC	Male	Adult	Non-reproducing	37.6	7.8	1.54	3.81	1	
Myotis volans	9/18/2017	LCC	Male	Adult	Non-reproducing	39.3	8.2	0.85	4.26	1	
Myotis volans	9/18/2017	LCC	Male	Adult	Non-reproducing	39.4	7.6	0.96	5.33	1	
Myotis volans	9/18/2017	LCC	Male	Adult	Scrotal	40.2	9.3	1.64	2.77	1	
Myotis volans	9/18/2017	LCC	Male	Adult	Scrotal	38.2	8.6	1.25	3.685	1	
Myotis volans	9/18/2017	LCC	Male	Adult	Scrotal	34.4	8.7	2.25	5.22	1	
Myotis volans	9/18/2017	LCC	Male	Adult	Non-reproducing	40	8.5	1.06	5.89	1	
Myotis volans	9/18/2017	LCC	Male	Adult	Non-reproducing	38.3	8	0.77	3.3	1	
Myotis volans	9/18/2017	LCC	Male	Adult	Scrotal	39.4	10	2.17	4.163	1	
Myotis volans	9/18/2017	LCC	Male	Adult	Scrotal	37.2	8.1	1.22	4.32	1	
Myotis volans	9/18/2017	LCC	Male	Adult	Non-reproducing	38.1	7.9			1	
Myotis volans	9/18/2017	LCC	Male	Adult	Scrotal	39.2	8.5	1.17	4.19	1	
Myotis volans	9/19/2017	LCC	Male	Adult	Scrotal	38.1	7.9			1	
Myotis volans	9/19/2017	LCC	Male	Adult	Non-reproducing	39.1	8.1			1	yes
Myotis volans	9/20/2017	LCC	Male	Adult	Non-reproducing	38.4	9.3			1	yes
Myotis volans	9/25/2017	LCC	Male	Adult	Scrotal	39.3	7			1	
Myotis volans	9/25/2017	LCC	Male	Adult	Non-reproducing	37.7	8.4			0	
Myotis volans	9/25/2017	LCC	Male	Adult	Non-reproducing	38.4	8.5			1	
Myotis volans	9/25/2017	LCC	Male	Adult	Scrotal	40.3	9.5			1	
Myotis volans	9/25/2017	LCC	Male	Adult	Scrotal	39	9.3			1	

Species	Date	Site	Sex	Age	Reproductive?	Forearm	Mass	Fat	Lean	Wing Score	Respirometry?
Myotis volans	9/25/2017	LCC	Male	Adult	Scrotal	39.7	8.4			1	
Myotis volans	9/25/2017	LCC	Female	Adult	Non-reproducing	39.4	10.3			1	
Myotis volans	9/25/2017	LCC	Male	Juvenile	Non-reproducing	38.5	7.5			0	
Myotis volans	9/27/2017	LCC	Male	Adult	Scrotal	39.3	8.5	1.48	4.53	1	
Myotis volans	9/27/2017	LCC	Male	Adult	Non-reproducing	38.1	8.4	1.73	5.71	1	
Myotis volans	9/27/2017	LCC	Male	Adult	Non-reproducing	39	9.6	2.18	6.3	1	
Myotis volans	9/27/2017	LCC	Male	Adult	Scrotal	40.4	9.4	2.27	6.16	1	
Myotis volans	9/27/2017	LCC	Male	Adult	Scrotal	37.1	8.4	1.82	5.72	0	
Myotis volans	9/27/2017	LCC	Male	Adult	Scrotal	39.5	8.9	1.78	4.99	2	
Myotis volans	9/27/2017	LCC	Male	Adult	Scrotal	39.4	10	3.33	5.76	1	
Myotis volans	9/27/2017	LCC	Male	Adult	Scrotal	38	7.6	1.27	4.12	1	
Myotis volans	9/27/2017	LCC	Male	Adult	Scrotal	39.9	9	1.66	4.06	1	
Myotis volans	9/27/2017	LCC	Male	Juvenile	Non-reproducing	37.3	6.3	0.99	4.58	1	
Myotis volans	9/27/2017	LCC	Male	Adult	Scrotal	38.6	8.6	1.82	4.69	1	
Myotis volans	9/27/2017	LCC	Male	Adult	Scrotal	37.2	8.6	2.2	5.64	1	
Myotis volans	9/27/2017	LCC	Male	Adult	Scrotal	38.2	9.4	2.74	4.68	1	
Myotis volans	9/27/2017	LCC	Male	Adult	Scrotal	38.1	8.6	2.41	5.29	1	
Myotis volans	9/27/2017	LCC	Male	Adult	Scrotal	38.6	8.2	1.67	5.71	1	
Myotis volans	9/28/2017	LCC	Male	Adult	Scrotal	37.4	8.9	2.13	3.94	1	
Myotis volans	9/28/2017	LCC	Male	Adult	Non-reproducing	37.5	9.5	2.27	4.425	1	
Myotis volans	9/28/2017	LCC	Male	Adult	Scrotal	37.6	9.8	2.75	6.13	1	
Myotis volans	9/28/2017	LCC	Male	Adult	Scrotal	37.3	8	1.7	5.34	1	
Myotis volans	9/28/2017	LCC	Male	Adult	Scrotal	39.1	9	1.92	6.2	1	
Myotis volans	9/28/2017	LCC	Male	Adult	Scrotal	39	9.9	2.86	4.25	1	
Myotis volans	9/28/2017	LCC	Male	Adult	Scrotal	38.3	8.7	2.31	5.44	1	
Myotis volans	9/28/2017	LCC	Male	Adult	Scrotal	38.5	9.5			1	
Myotis volans	9/28/2017	LCC	Male	Adult	Unknown	38.4	7.7	2.12	4.31	1	
Myotis volans	2/22/2018	LCC	Male	Adult	Unknown	40.2	8.1			1	
Myotis volans	2/22/2018	LCC	Male	Adult	Unknown	39	7.5			1	
Myotis volans	2/22/2018	LCC	Female	Adult	Unknown	38.5	7.2	1.11	5.11	1	
Myotis volans	2/22/2018	LCC	Male	Adult	Unknown	39	6.6	0.95	4.83	1	

Species	Date	Site	Sex	Age	Reproductive?	Forearm	Mass	Fat	Lean	Wing Score	Respirometry?
Myotis volans	9/20/2018	LCC	Male	Adult	Scrotal	39.1	8.5			1	yes
Myotis volans	9/20/2018	LCC	Male	Adult	Scrotal	39.9	8.6			0	yes
Myotis volans	9/20/2018	LCC	Male	Adult	Scrotal	39.6	8.9			0	yes
Myotis volans	9/20/2018	LCC	Female	Adult	Unknown	40.7	9.4			0	yes
Myotis volans	9/20/2018	LCC	Male	Adult	Scrotal	38.4	8.9			0	yes
Myotis volans	9/22/2018	LCC	Female	Adult	Non-reproducing	38.6	8.2			0	
Myotis volans	9/22/2018	LCC	Male	Adult	Non-reproducing	39.2	8.6			0	
Myotis volans	9/22/2018	LCC	Female	Juvenile	Scrotal	38.8	5.6			0	
Myotis volans	9/22/2018	LCC	Male	Adult	Non-reproducing	37.3	6.4			1	
Myotis volans	9/22/2018	LCC	Male	Adult	Non-reproducing	38.7	8.7			0	
Myotis volans	9/22/2018	LCC	Male	Adult	Scrotal	37.2	8.2			0	
Myotis volans	9/22/2018	LCC	Male	Adult	Scrotal	36.6	9.1			1	
Myotis volans	9/22/2018	LCC	Male	Adult	Scrotal	37.7	9.3			1	
Myotis volans	9/23/2018	LCC	Female	Adult	Scrotal	39	10.3			1	
Myotis volans	9/23/2018	LCC	Male	Adult	Scrotal	39	9			0	
Myotis volans	9/26/2018	LCC	Male	Adult	Non-reproducing	37.7	9.2			0	yes
Myotis volans	9/26/2018	LCC	Male	Adult	Non-reproducing	39.6	8.6			0	yes
Myotis volans	9/26/2018	LCC	Male	Adult	Scrotal	39.3	7.5			0	
Myotis volans	9/26/2018	LCC	Female	Adult	Non-reproducing	38.3	8.8			1	yes
Myotis volans	9/26/2018	LCC	Female	Juvenile	Non-reproducing	38.2	7.8			0	
Myotis volans	9/26/2018	LCC	Male	Adult	Scrotal	38.9	20.2			1	yes
Myotis volans	9/26/2018	LCC	Female	Adult	Non-reproducing	39.6	9			1	yes
Myotis volans	9/26/2018	LCC	Female	Adult	Non-reproducing	41.9	10			1	yes
Myotis volans	10/1/2018	ODW	Female	Adult	Non-reproducing	48.7	8.5			0	yes

Nevada Department of Wildlife
Final Project Report 2017 – 2019
Under permit # 497636

We caught a total of 245 bats: 170 *Corynorhinus townsendii*, 2 *Eptesicus fuscus*, 71 *Myotis ciliolabrum*, and 2 *M. volans* (Table 1; Appendix) over the sampling period of fall 2017 to winter 2019. . During the fall, bats were caught using mist nets and harp traps at the cave entrance. During the winter, bats were hand-captured from cave walls. We determined sex, age, reproductive condition, and wing score and measured forearm length and body mass of each bat. We used quantitative magnetic resonance (QMR; Echo-MRI-B, Echo Medical Systems, Houston, TX) to measure fat mass and lean mass. We measured metabolic rate (TMR) and evaporative water loss (EWL) during torpor using open-flow respirometry. We measured body fat from 216 individuals and processed 89 individuals through respirometry. Body mass and body fat varied between sexes at Piermont Mine (Figure 1) and somewhat varied between sexes at Big Chief mine (Figure 2). The mean mass for each species varied between seasons at both Piermont (Figure 3) and Big Chief mines (Figure 4) for the species that we captured both seasons. There was not much difference in metabolic rate among *C. townsendii* between seasons at Piermont Mine, but evaporative water loss was different between seasons (Figure 5). These trends were also reflected at Big Chief Mine for *C. townsendii* and *M. ciliolabrum* (Figure 6).

We predicted survival for *C. townsendii* and *M. ciliolabrum* (Figure 7) over the range of environmental conditions experienced in the cave. We also inferred the survival of both species once affected with white-nose syndrome. The modified hibernation energetics model estimates the time until fat exhaustion during hibernation as a function of bat characteristics, hibernaculum microclimate, and fungal growth. Survival is determined by comparing model output time to winter duration – if time until fat exhaustion is greater than winter duration, survival occurs. We validated the model predictions with field and laboratory data and determined model sensitivity to bat characteristics.

We predict that *M. ciliolabrum* will have high mortality in Piermont – that is, we predict that bats will run out of fat stores prior to the conclusion of hibernation. *C. townsendii,* however, are predicted to survival in greater microclimate space and will survive in specific areas of the hibernaculum. Note, however, that these predictions are made from the mean body mass, fat mass, and lean mass measured in Nevada, and thus we would expect that 50% of the population to have greater fat mass than the "average" bat described here.

For further information about our findings please visit www.science4bats.org/publications and review all project associated publications.

Table 1: The number of each species per year captured in Nevada.

Species	Year	Piermont	Big Chief
Corynorhinus townsendii	2017	28	
Corynorhinus townsendii	2018	62	43
Corynorhinus townsendii	2019	24	13
Eptesicus fuscus	2018	1	1
Myotis ciliolabrum	2017	23	
Myotis ciliolabrum	2018	3	21
Myotis ciliolabrum	2019	7	17
Myotis volans	2017	2	
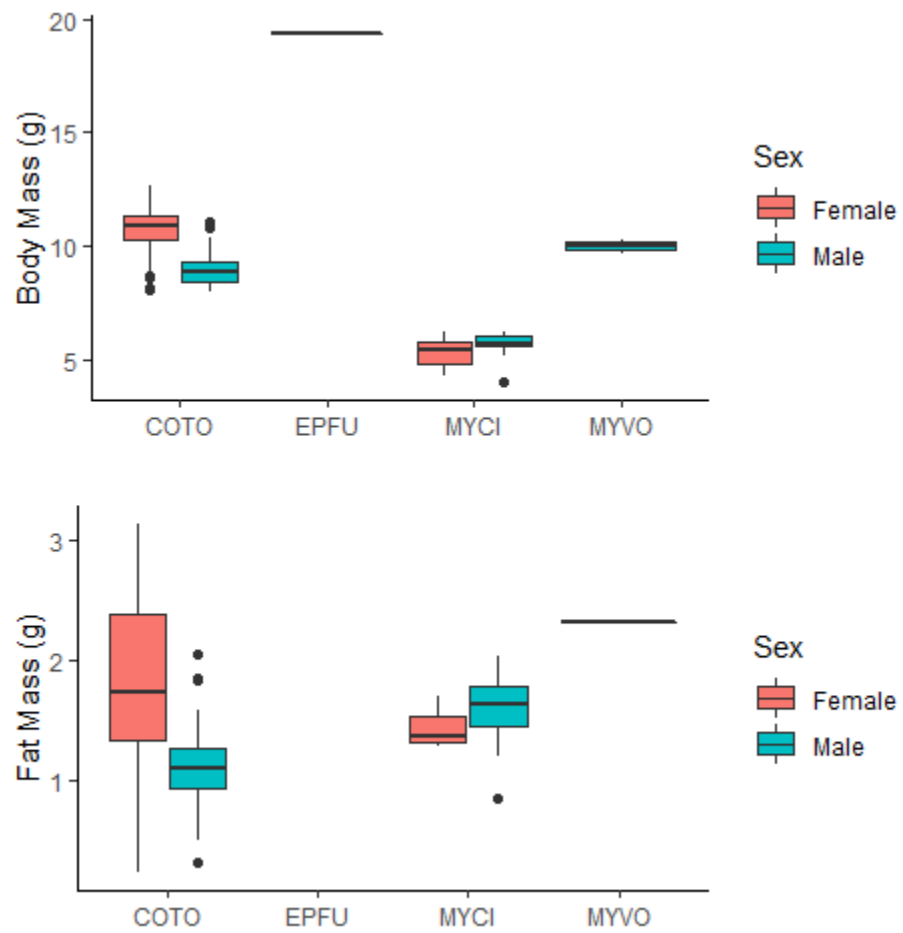
Figure 1. Body mass (top) and fat mass (bottom) by sex for the four species captured at Piermont Mine. The single EPFU and MYVO data points were females.
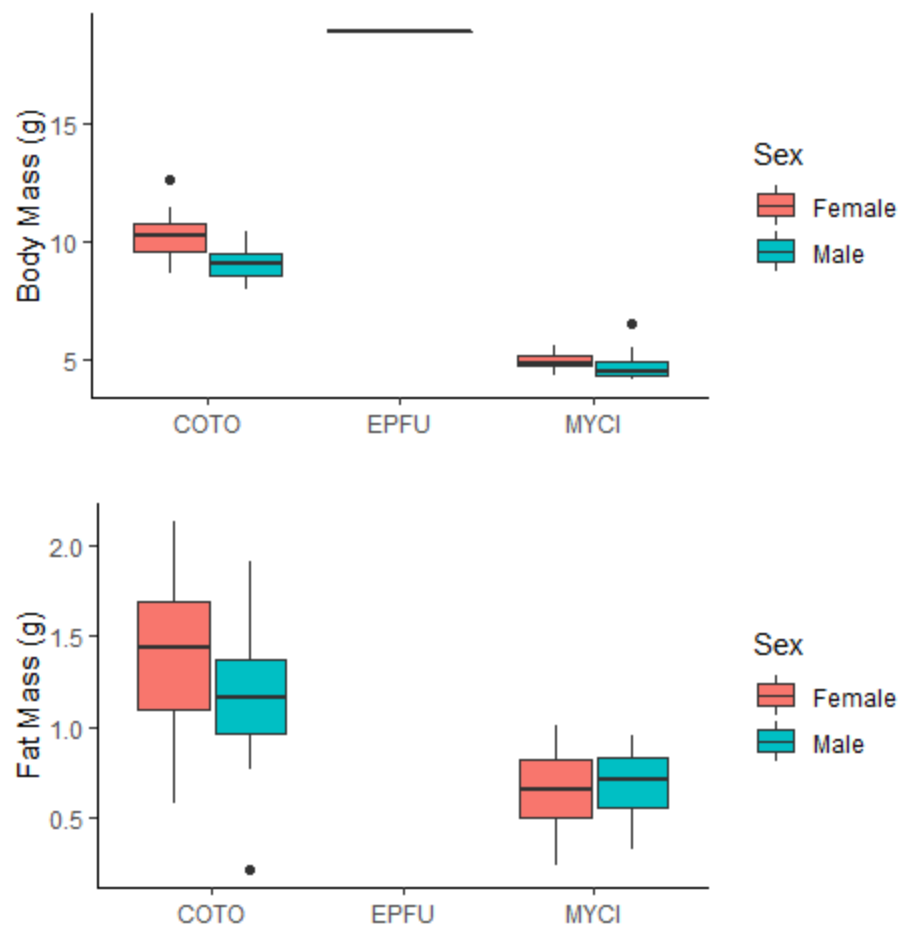
Figure 2. Body mass (top) and fat mass (bottom) by sex for the five species captured at Big Chief Mine. The single EPFU data point was male.
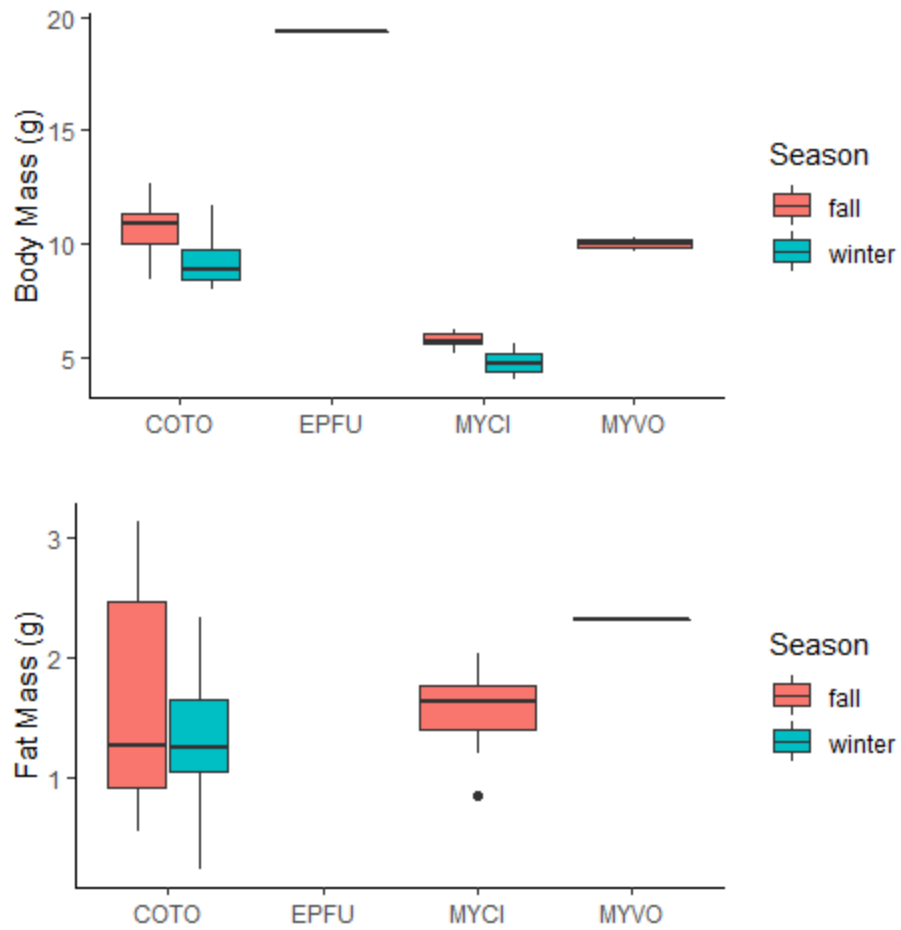
Figure 3. Body mass (top) and fat mass (bottom) by season for the four species captured at Piermont Mine. The single EPFU and MYVO data points were captured in the fall.
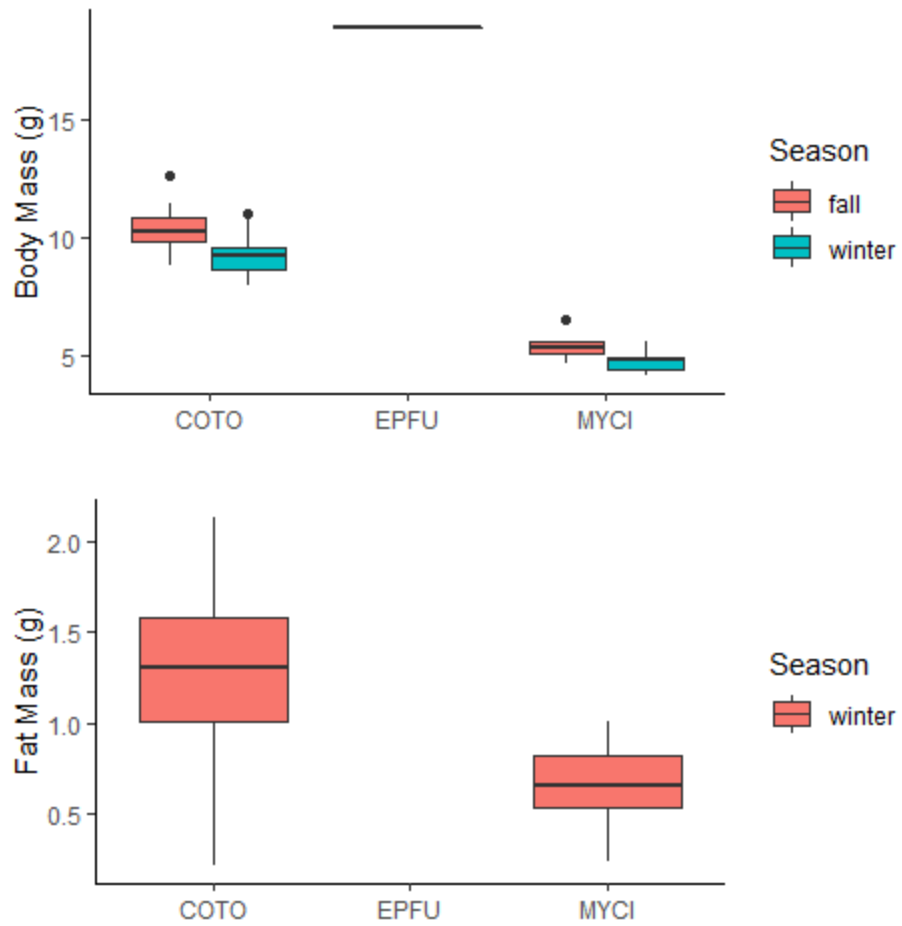
Figure 4. Body mass (top) and fat mass (bottom) by season for the three species captured at Big Chief Mine. The single EPFU data point was in the fall.
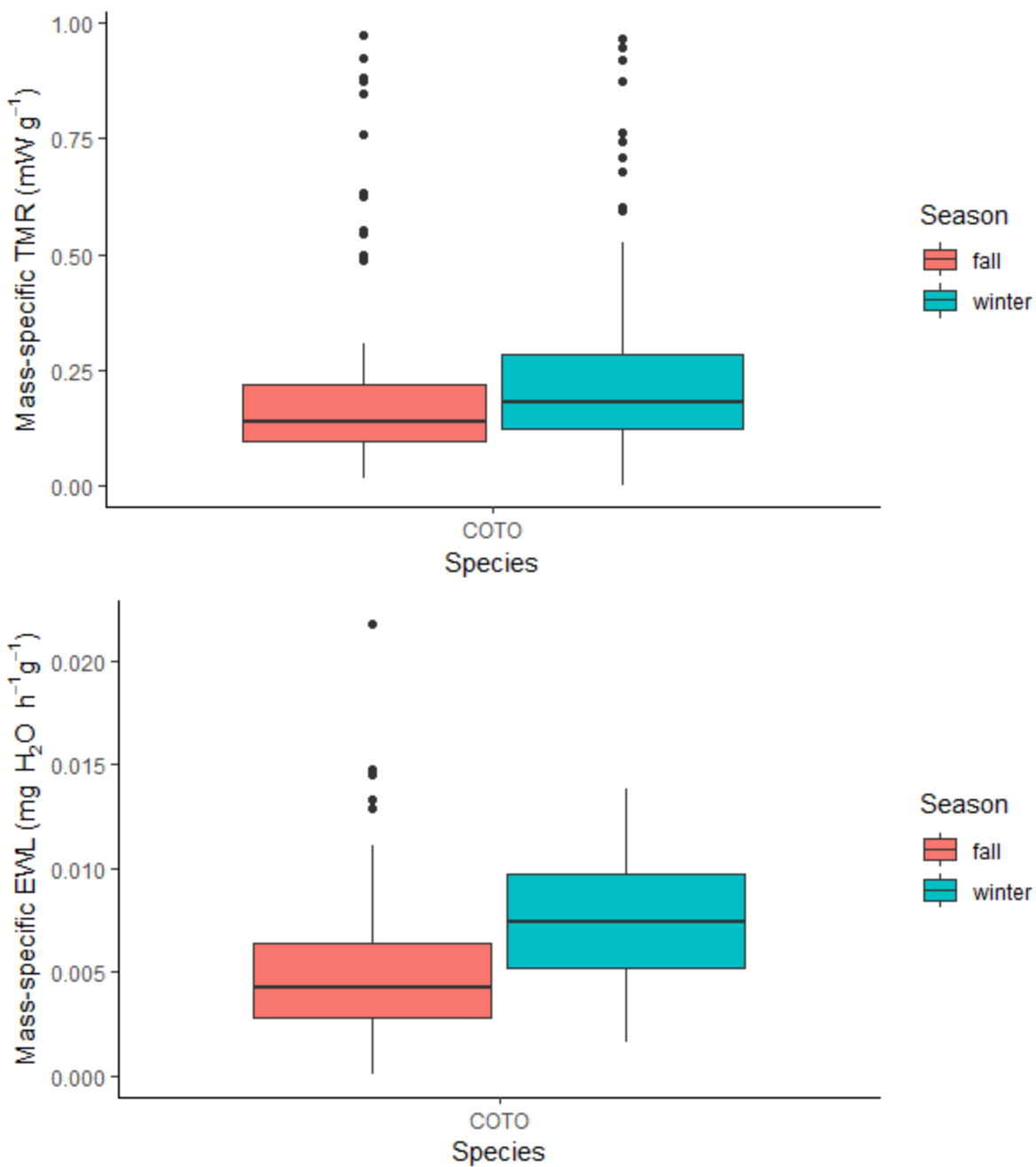
Figure 5. Mass-specific torpor metabolic rate (TMR; top) and mass-specific evaporative water loss (EWL; bottom) by season for COTO captured at Piermont Mine.
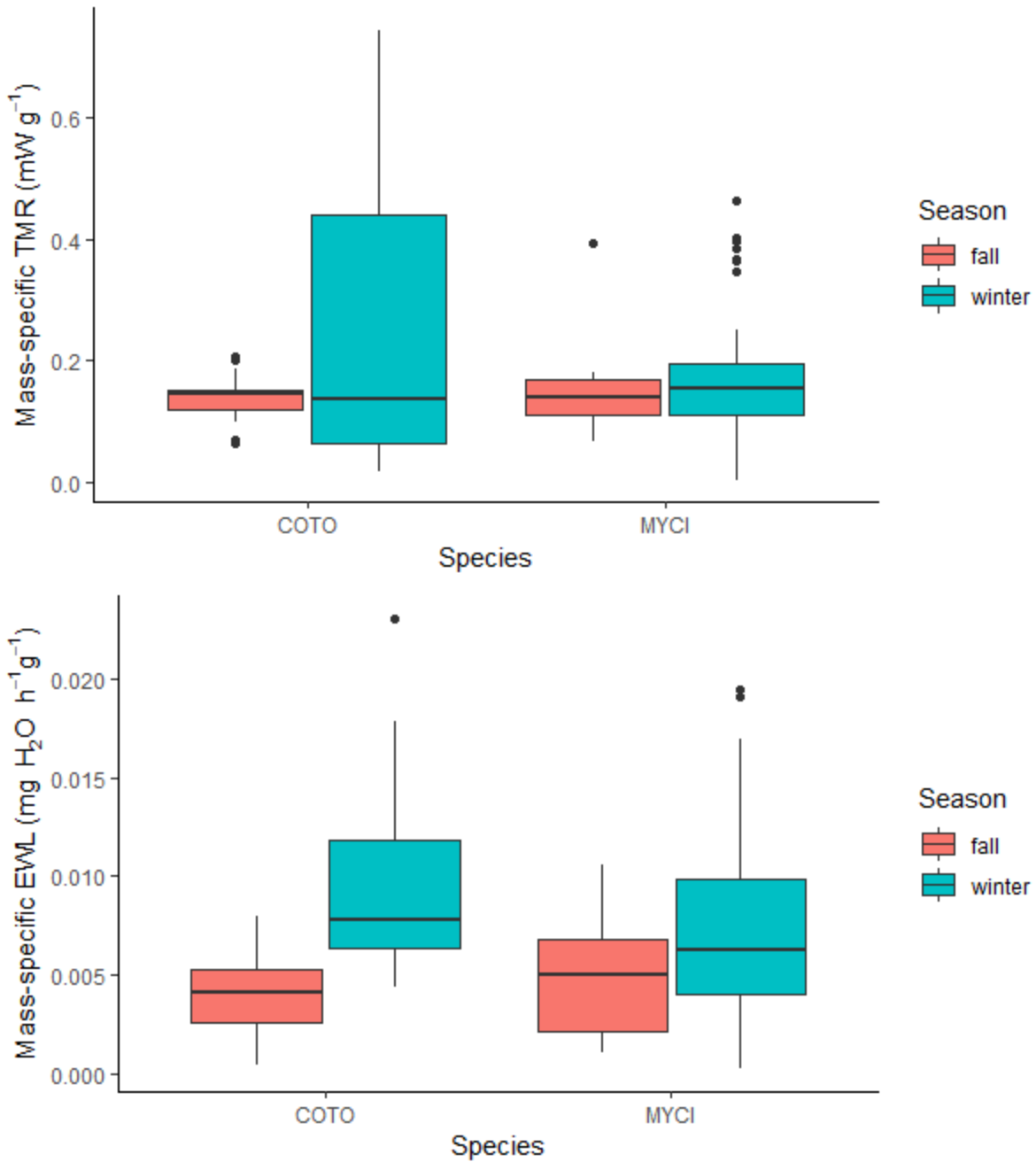
Figure 6. Mass-specific torpor metabolic rate (TMR; top) and mass-specific evaporative water loss (EWL; bottom) by season for the two species captured at Big Chief Mine.
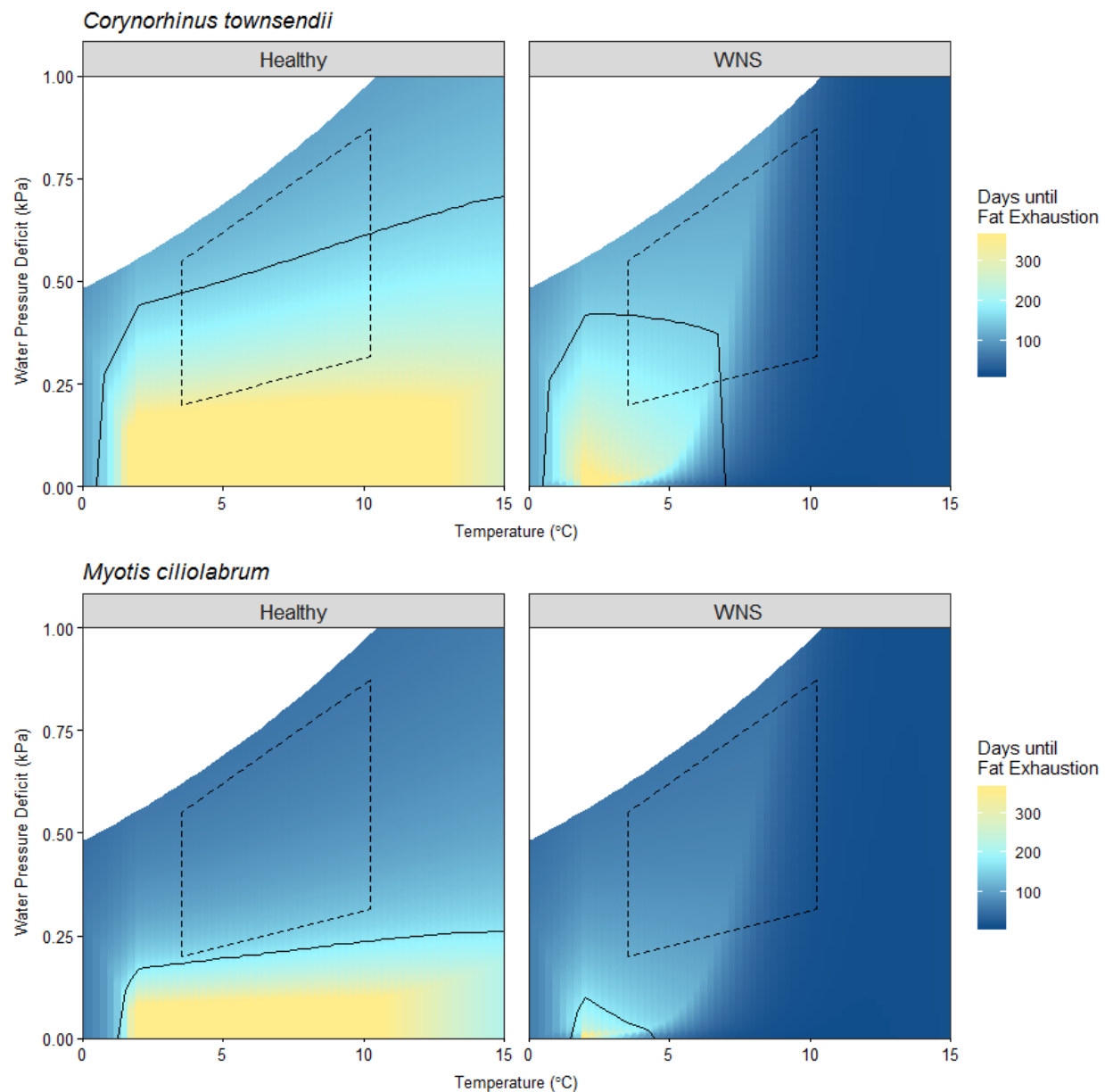
Figure 7: Predicted days until total fat exhaustion for *Corynorhinus townsendii* and *Myotis ciliolabrum* in Piermont Mine. Solid lines represent days of hibernation duration (172 days) predicted for Piermont Mine and the range of microclimate conditions that would allow survival in this area. Dashed lines represent microclimate conditions measured at the roosting location within the mine. The area where solid and dashed lines overlap is the microclimate conditions available that allow survival. White space represents impossible microclimate space based on the saturation potential for each temperature.

APPENDIX: Morphometric data from Piermont (PMM) and Big Chief (BCM). Forearm in mm, mass, fat, and lean mass in g.

Species	Date	Site	Sex	Age	Reproductive?	Forearm	Mass	Fat	Lean	Wing Score	Respirometry?
Corynorhinus townsendii	10/7/2017	PMM	Female	Adult	Non-reproducing	46.5	12.2	2.54	4.07	0	
Corynorhinus townsendii	10/7/2017	PMM	Female	Adult	Non-reproducing	43.9	11	2.39	7.17	0	
Corynorhinus townsendii	10/7/2017	PMM	Male	Adult	Scrotal	44.6	10.2	0.92	7.77	0	
Corynorhinus townsendii	10/7/2017	PMM	Male	Adult	Scrotal	43.3	9.5	1.12	5.93	0	
Corynorhinus townsendii	10/7/2017	PMM	Female	Adult	Non-reproducing	46.1	11.9	2.77	7.76	1	
Corynorhinus townsendii	10/7/2017	PMM	Male	Adult	Scrotal	42.7	8.4	0.89	4.3	0	
Corynorhinus townsendii	10/7/2017	PMM	Male	Adult	Scrotal	43.4	9.2	0.54	5.39	0	
Corynorhinus townsendii	10/7/2017	PMM	Female	Adult	Non-reproducing	46.6	11.3	2.84	7.45	0	
Corynorhinus townsendii	10/7/2017	PMM	Male	Adult	Scrotal	45	9.1	0.67	4.71	0	
Corynorhinus townsendii	10/7/2017	PMM	Female	Adult	Non-reproducing	45.4	11.8	3.15	7.21	0	
Corynorhinus townsendii	10/7/2017	PMM	Female	Adult	Non-reproducing	42.5	8.9	0.98	4.62	1	
Corynorhinus townsendii	10/7/2017	PMM	Male	Adult	Scrotal	44.3	8.4	0.54	4.53	1	
Corynorhinus townsendii	10/7/2017	PMM	Male	Adult	Scrotal	45.2	10.2	1.27	6.04		
Corynorhinus townsendii	10/7/2017	PMM	Male	Adult	Scrotal	43.3	9.3	1.54	6.81	1	
Corynorhinus townsendii	10/7/2017	PMM	Male	Adult	Scrotal	44.6	10.4	1.26	5.26	0	
Corynorhinus townsendii	10/8/2017	PMM	Female	Adult	Non-reproducing	46	11.7			1	yes
Corynorhinus townsendii	10/8/2017	PMM	Female	Adult	Non-reproducing	44.9	11.3			1	yes
Corynorhinus townsendii	10/8/2017	PMM	Female	Adult	Non-reproducing	45.3	12			1	yes
Corynorhinus townsendii	10/8/2017	PMM	Female	Adult	Non-reproducing	45.7	11			1	yes
Corynorhinus townsendii	10/8/2017	PMM	Female	Adult	Non-reproducing	44.2	12			1	yes
Corynorhinus townsendii	10/8/2017	PMM	Female	Adult	Non-reproducing	46.5	12.7			1	yes
Corynorhinus townsendii	10/8/2017	PMM	Female	Adult	Non-reproducing	44.5	11.8			0	yes
Corynorhinus townsendii	10/8/2017	PMM	Female	Adult	Non-reproducing	44.3	10.6			1	yes
Corynorhinus townsendii	10/8/2017	PMM	Male	Adult	Scrotal	43	8.6			0	yes
Corynorhinus townsendii	10/8/2017	PMM	Male	Adult	Scrotal	45	9.3			1	yes
Corynorhinus townsendii	10/8/2017	PMM	Female	Adult	Non-reproducing	45.3	9.9			0	yes
Corynorhinus townsendii	10/8/2017	PMM	Male	Adult	Scrotal	43.1	9.1			1	yes
Corynorhinus townsendii	10/8/2017	PMM	Female	Adult	Non-reproducing	43.1	10.3			0	yes

Species	Date	Site	Sex	Age	Reproductive?	Forearm	Mass	Fat	Lean	Wing Score	Respirometry?
Corynorhinus townsendii	1/29/2018	PMM	Male	Adult	Scrotal	43.7	9	1.065	2.725	1	
Corynorhinus townsendii	1/29/2018	PMM	Male	Adult	Unknown	43.5	9	0.3	5.23	0	
Corynorhinus townsendii	1/29/2018	PMM	Male	Adult	Scrotal	43.7	9.6	0.9	3.95	0	yes
Corynorhinus townsendii	1/29/2018	PMM	Male	Adult	Scrotal	42.3	8.4	1.1	5.51	0	
Corynorhinus townsendii	1/29/2018	PMM	Female	Adult	Unknown	45	10.8	1.81	7.32	1	yes
Corynorhinus townsendii	1/29/2018	PMM	Male	Adult	Scrotal	42.9	9.5	1.59	5.01	0	yes
Corynorhinus townsendii	1/29/2018	PMM	Female	Adult	Unknown	45.9	10.6	2.24	7.32	1	yes
Corynorhinus townsendii	1/29/2018	PMM	Female	Adult	Unknown	45.7	11	0.83	3.25	1	yes
Corynorhinus townsendii	1/29/2018	PMM	Male	Adult	Scrotal	43.1	8.1	1.08	5.77	0	
Corynorhinus townsendii	1/29/2018	PMM	Male	Adult	Unknown	43.6	8	1.41	5.1	1	
Corynorhinus townsendii	1/29/2018	PMM	Female	Adult	Unknown	45.9	10.2	2.33	6.49	1	yes
Corynorhinus townsendii	1/29/2018	PMM	Female	Adult	Unknown	44.3	9.2	1.32	6.36	2	
Corynorhinus townsendii	1/29/2018	PMM	Female	Adult	Unknown	45	8.2	1.83	5.4	1	yes
Corynorhinus townsendii	1/29/2018	PMM	Male	Adult	Scrotal	44.8	8.8	0.98	4.02	1	
Corynorhinus townsendii	1/29/2018	PMM	Male	Adult	Unknown	44	8.9	1.85	6.04	1	yes
Corynorhinus townsendii	1/29/2018	PMM	Male	Adult	Unknown	40.7	8.1	1.16	4.5	1	
Corynorhinus townsendii	1/29/2018	PMM	Male	Adult	Scrotal	44.8	9.2			1	yes
Corynorhinus townsendii	1/29/2018	PMM	Female	Adult	Unknown	43.1	9	1.48	6.8	1	
Corynorhinus townsendii	1/29/2018	PMM	Female	Adult	Unknown	44.2	8.9	1.24	4.89	3	
Corynorhinus townsendii	1/29/2018	PMM	Male	Adult	Unknown	44.4	8.1	0.49	6.64	1	
Corynorhinus townsendii	1/29/2018	PMM	Female	Adult	Unknown	44.2	9.8	1.375	4.07	1	yes
Corynorhinus townsendii	1/29/2018	PMM	Male	Adult	Non-reproducing	44.5	8.8	1.05	4.01	0	
Corynorhinus townsendii	1/29/2018	PMM	Female	Adult	Unknown	41.8	8.1	0.22	6.02	1	
Corynorhinus townsendii	1/29/2018	PMM	Female	Adult	Unknown	44.5	8.6	1.83	5.28	1	
Corynorhinus townsendii	1/29/2018	PMM	Female	Adult	Unknown	44.9	8.7	1.65	5.99	1	
Corynorhinus townsendii	1/29/2018	PMM	Male	Adult	Non-reproducing	45.1	8.9	1.23	3.17	0	yes
Corynorhinus townsendii	1/29/2018	PMM	Male	Adult	Unknown	43.6	8.9	1.23	4.91	1	
Corynorhinus townsendii	1/29/2018	PMM	Female	Adult	Unknown	46.1	11.1	1.59	8.15	1	yes
Corynorhinus townsendii	1/29/2018	PMM	Female	Adult	Unknown	46.6	10.2	0.93	7.62	1	yes
Corynorhinus townsendii	1/29/2018	PMM	Male	Adult	Unknown	44	9.1	2.05	4.16	0	yes

Species	Date	Site	Sex	Age	Reproductive?	Forearm	Mass	Fat	Lean	Wing Score	Respirometry?
Corynorhinus townsendii	2/1/2018	BCM	Male	Adult	Unknown	43	9.1	1.91	5.86	0	yes
Corynorhinus townsendii	2/1/2018	BCM	Male	Adult	Unknown	43.1	8.3	1.13	4.85	0	
Corynorhinus townsendii	2/1/2018	BCM	Female	Adult	Unknown	44.7	9.5	0.65	2.79	1	yes
Corynorhinus townsendii	2/1/2018	BCM	Male	Adult	Unknown	44.9	8.9	0.98	6.78	0	
Corynorhinus townsendii	2/1/2018	BCM	Male	Adult	Unknown	46.4	9.9	1.72	6.45	0	
Corynorhinus townsendii	2/1/2018	BCM	Female	Adult	Unknown	42.9	7.9	0.21	5.43	1	
Corynorhinus townsendii	2/1/2018	BCM	Male	Adult	Scrotal	45.5	9.2	1.35	4.82	2	
Corynorhinus townsendii	2/1/2018	BCM	Female	Adult	Unknown	45	10.3	2.14	5.91	0	yes
Corynorhinus townsendii	2/1/2018	BCM	Male	Adult	Unknown	43.2	8.4	1.22	5.96	1	
Corynorhinus townsendii	2/1/2018	BCM	Female	Adult	Unknown	44.1	9.4	1.64	4.43	0	
Corynorhinus townsendii	2/1/2018	BCM	Male	Adult	Unknown	42.9	8.6	0.79	6.84	1	
Corynorhinus townsendii	2/1/2018	BCM	Male	Adult	Unknown	44.9	9	1.34	6.31	0	
Corynorhinus townsendii	2/1/2018	BCM	Male	Adult	Scrotal	46.1	9.1	1.2	6.42	0	
Corynorhinus townsendii	11/3/2018	PMM	Female	Adult	Non-reproducing	44.1	10.8			1	
Corynorhinus townsendii	11/3/2018	PMM	Female	Adult	Non-reproducing	42.8	10.5			1	
Corynorhinus townsendii	11/3/2018	PMM	Male	Adult	Non-reproducing	42.7	9.9			0	
Corynorhinus townsendii	11/3/2018	PMM	Female	Adult	Non-reproducing	44.2	10.7			1	
Corynorhinus townsendii	11/3/2018	PMM	Female	Adult	Non-reproducing	43.8	10.9			0	
Corynorhinus townsendii	11/3/2018	PMM	Female	Adult	Non-reproducing	45.9	12			0	yes
Corynorhinus townsendii	11/3/2018	PMM	Female	Adult	Non-reproducing	45.3	10.4			0	
Corynorhinus townsendii	11/3/2018	PMM	Female	Adult	Non-reproducing	45.2	11.1			0	
Corynorhinus townsendii	11/3/2018	PMM	Female	Adult	Non-reproducing	44.8	10.4			0	
Corynorhinus townsendii	11/3/2018	PMM	Female	Adult	Non-reproducing	45.8	10.8			1	
Corynorhinus townsendii	11/3/2018	PMM	Male	Adult	Non-reproducing	44.2	10.7			1	
Corynorhinus townsendii	11/3/2018	PMM	Female	Adult	Non-reproducing	43.8	10.6			1	
Corynorhinus townsendii	11/3/2018	PMM	Female	Adult	Non-reproducing	45	10.3			0	
Corynorhinus townsendii	11/3/2018	PMM	Female	Adult	Non-reproducing	44.8	10.4			0	
Corynorhinus townsendii	11/3/2018	PMM	Female	Adult	Non-reproducing	44.9	10.8			1	
Corynorhinus townsendii	11/3/2018	PMM	Female	Adult	Non-reproducing	46.9	11.2			0	
Corynorhinus townsendii	11/3/2018	PMM	Female	Adult	Non-reproducing	45.2	11.1			0	
Corynorhinus townsendii	11/3/2018	PMM	Male	Adult	Non-reproducing	43.3	11.1			0	
Corynorhinus townsendii	11/3/2018	PMM	Female	Adult	Non-reproducing	44.5	11.1			0	
Corynorhinus townsendii	11/3/2018	PMM	Female	Adult	Non-reproducing	46	12.1			1	yes

Species	Date	Site	Sex	Age	Reproductive?	Forearm	Mass	Fat	Lean	Wing Score	Respirometry?
Corynorhinus townsendii	11/3/2018	PMM	Male	Adult	Scrotal	43	9.3			1	
Corynorhinus townsendii	11/3/2018	PMM	Female	Adult	Non-reproducing	45	11.4			1	yes
Corynorhinus townsendii	11/3/2018	PMM	Female	Adult	Non-reproducing	44.5	10.9			0	
Corynorhinus townsendii	11/3/2018	PMM	Female	Adult	Non-reproducing	47.4	11.7			1	yes
Corynorhinus townsendii	11/3/2018	PMM	Female	Adult	Non-reproducing	45.1	12			0	yes
Corynorhinus townsendii	11/3/2018	PMM	Female	Adult	Non-reproducing	45	11.1			0	
Corynorhinus townsendii	11/3/2018	PMM	Female	Adult	Non-reproducing	43.9	11.3			0	yes
Corynorhinus townsendii	11/3/2018	PMM	Female	Adult	Non-reproducing	44.5	10.9			1	
Corynorhinus townsendii	11/3/2018	PMM	Female	Adult	Non-reproducing	44	11.8			1	yes
Corynorhinus townsendii	11/3/2018	PMM	Female	Adult	Non-reproducing	46.9	11.2			1	yes
Corynorhinus townsendii	11/3/2018	PMM	Male	Adult	Scrotal	42.4	10			0	
Corynorhinus townsendii	11/3/2018	PMM	Female	Adult	Non-reproducing	44.3	11.3			0	yes
Corynorhinus townsendii	11/3/2018	PMM	Female	Adult	Non-reproducing	43.2	11.3			0	
Corynorhinus townsendii	11/3/2018	PMM	Male	Adult	Non-reproducing	42.9	9.7			1	
Corynorhinus townsendii	11/3/2018	PMM	Female	Adult	Non-reproducing	42.8	11.3			0	yes
Corynorhinus townsendii	11/3/2018	PMM	Male	Adult	Non-reproducing	42.6	9.3			0	
Corynorhinus townsendii	11/3/2018	BCM	Female	Adult	Non-reproducing	41.7	10.8			0	
Corynorhinus townsendii	11/3/2018	BCM	Male	Adult	Non-reproducing	41.6	8.8			0	yes
Corynorhinus townsendii	11/3/2018	BCM	Female	Adult	Non-reproducing	44.2	11.2			0	
Corynorhinus townsendii	11/3/2018	BCM	Male	Adult	Scrotal	43.7	9.7			0	yes
Corynorhinus townsendii	11/5/2018	BCM	Male	Adult	Non-reproducing	43.6	9.8			0	
Corynorhinus townsendii	11/5/2018	BCM	Female	Adult	Non-reproducing	45.1	10.7			1	
Corynorhinus townsendii	11/5/2018	BCM	Male	Adult	Scrotal	44.2	10			0	yes
Corynorhinus townsendii	11/5/2018	BCM	Male	Adult	Scrotal	44	9.7			0	
Corynorhinus townsendii	11/5/2018	BCM	Female	Adult	Non-reproducing	43.6	9.9			0	
Corynorhinus townsendii	11/5/2018	BCM	Female	Adult	Non-reproducing	44.6	11.3			0	
Corynorhinus townsendii	11/5/2018	BCM	Female	Adult	Non-reproducing	45.2	11.4			0	
Corynorhinus townsendii	11/5/2018	BCM	Female	Adult	Non-reproducing	43.3	9.7			0	
Corynorhinus townsendii	11/5/2018	BCM	Female	Adult	Non-reproducing	46.2	11			0	yes
Corynorhinus townsendii	11/5/2018	BCM	Male	Adult	Non-reproducing	42.7	10.4			0	

Species	Date	Site	Sex	Age	Reproductive?	Forearm	Mass	Fat	Lean	Wing Score	Respirometry?
Corynorhinus townsendii	11/5/2018	BCM	Male	Adult	Scrotal	44	10.1			0	
Corynorhinus townsendii	11/5/2018	BCM	Male	Adult	Non-reproducing	42	9.4			0	
Corynorhinus townsendii	11/5/2018	BCM	Female	Adult	Non-reproducing	43.1	10.3			0	
Corynorhinus townsendii	11/5/2018	BCM	Female	Adult	Non-reproducing	44.3	10.2			0	yes
Corynorhinus townsendii	11/5/2018	BCM	Female	Adult	Non-reproducing	45.4	12.6			0	yes
Corynorhinus townsendii	11/5/2018	BCM	Female	Adult	Non-reproducing	42.6	10.2			0	
Corynorhinus townsendii	11/5/2018	BCM	Female	Adult	Non-reproducing	45.5	9.8			0	yes
Corynorhinus townsendii	1/28/2019	PMM	Female	Adult	Non-reproducing	45.2	9.1			0	yes
Corynorhinus townsendii	1/28/2019	PMM	Male	Adult	Scrotal	41.5	8.6			0	
Corynorhinus townsendii	1/28/2019	PMM	Male	Adult	Non-reproducing	43.2	8.6			2	
Corynorhinus townsendii	1/28/2019	PMM	Male	Adult	Scrotal	43.4	8.1			0	
Corynorhinus townsendii	1/28/2019	PMM	Female	Adult	Non-reproducing	44.9	10.8			0	yes
Corynorhinus townsendii	1/28/2019	PMM	Female	Adult	Non-reproducing	46.4	11.7			1	yes
Corynorhinus townsendii	1/28/2019	PMM	Male	Adult	Scrotal	45.1	8			0	
Corynorhinus townsendii	1/28/2019	PMM	Male	Adult	Non-reproducing	42.5	8.5			0	
Corynorhinus townsendii	1/28/2019	PMM	Male	Adult	Non-reproducing	44.3	10.5			0	yes
Corynorhinus townsendii	1/28/2019	PMM	Female	Adult	Scrotal	43.2	8.2			0	
Corynorhinus townsendii	1/28/2019	PMM	Female	Adult	Non-reproducing	44.5	9.5			1	yes
Corynorhinus townsendii	1/28/2019	PMM	Male	Adult	Scrotal	43.6	8.2			1	
Corynorhinus townsendii	1/28/2019	PMM	Male	Adult	Non-reproducing	44	8.8			1	yes
Corynorhinus townsendii	1/28/2019	PMM	Male	Adult	Non-reproducing	44.6	9.8			1	yes
Corynorhinus townsendii	1/28/2019	PMM	Female	Adult	Non-reproducing	45.7	9.8			0	yes
Corynorhinus townsendii	1/28/2019	PMM	Male	Adult	Non-reproducing	45.2	10			0	yes
Corynorhinus townsendii	1/28/2019	PMM	Female	Adult	Non-reproducing	46	9.7			1	yes
Corynorhinus townsendii	1/28/2019	PMM	Male	Adult	Non-reproducing	44.5	8.6			0	yes
Corynorhinus townsendii	1/28/2019	PMM	Male	Adult	Scrotal	42.6	8.7			0	yes
Corynorhinus townsendii	1/28/2019	PMM	Male	Adult	Scrotal	41.9	8.1			0	yes
Corynorhinus townsendii	1/28/2019	PMM	Male	Adult	Scrotal	42.9	8.6			0	yes
Corynorhinus townsendii	1/28/2019	PMM	Male	Adult	Non-reproducing	44.1	8.4			1	

Species	Date	Site	Sex	Age	Reproductive?	Forearm	Mass	Fat	Lean	Wing Score	Respirometry?
Corynorhinus townsendii	2/1/2019	BCM	Male	Adult	Non-reproducing	43	8.8	1.4	6.72	0	
Corynorhinus townsendii	2/1/2019	BCM	Male	Adult	Scrotal	42.6	8.5	0.76	6.84	0	
Corynorhinus townsendii	2/1/2019	BCM	Male	Adult	Non-reproducing	44.9	9.8	1.63	7.65	0	
Corynorhinus townsendii	2/1/2019	BCM	Male	Adult	Scrotal	43.9	8.3	1.1	6.58	0	
Corynorhinus townsendii	2/1/2019	BCM	Female	Adult	Non-reproducing	44.5	10.7	1.91	8.03	0	
Corynorhinus townsendii	2/1/2019	BCM	Female	Adult	Non-reproducing	44.5	10.2	1.56	7.94	0	
Corynorhinus townsendii	2/1/2019	BCM	Female	Adult	Non-reproducing	46.1	11	1.72	8.3	1	
Corynorhinus townsendii	2/1/2019	BCM	Female	Adult	Non-reproducing	44	9.4	1.49	7.31	0	
Corynorhinus townsendii	2/1/2019	BCM	Male	Adult	Scrotal	43.7	8.5	1.37	6.46	0	
Corynorhinus townsendii	2/1/2019	BCM	Male	Adult	Non-reproducing	44.6	9.4	1.31	7.62	1	
Corynorhinus townsendii	2/1/2019	BCM	Female	Adult	Non-reproducing	44.8	9.3	1.31	6.83	0	
Corynorhinus townsendii	2/1/2019	BCM	Male	Adult	Non-reproducing	45.6	8.4	0.96	7.04	1	
Corynorhinus townsendii	2/1/2019	BCM	Female	Adult	Non-reproducing	45.3	10.2	1.69	7.96	1	
Corynorhinus townsendii	2/1/2018	BCM	Male	Adult	Scrotal	44.8	8.9	0.81	3.83	1	yes
Corynorhinus townsendii	2/1/2018	BCM	Female	Adult	Unknown	44.8	8.6	0.58	5.29	0	
Corynorhinus townsendii	2/1/2018	BCM	Female	Adult	Unknown	43.9	9.5	1.39	6.72	1	
Corynorhinus townsendii	2/1/2018	BCM	Female	Adult	Unknown	45.5	10.2	1.09	7.68	1	yes
Corynorhinus townsendii	2/1/2018	BCM	Male	Adult	Unknown	44.6	9.1	1.1	6.49	0	
Corynorhinus townsendii	2/1/2018	BCM	Male	Adult	Unknown	43.1	8.3	0.96	6.12	0	
Corynorhinus townsendii	2/1/2018	BCM	Female	Adult	Unknown	45.1	9.7	1.1	2.2	0	yes
Corynorhinus townsendii	2/1/2018	BCM	Male	Adult	Unknown	44.9	9.3	1.65	6.7	0	yes
Corynorhinus townsendii	2/1/2018	BCM	Female	Adult	Unknown	44.5	9.2	1.02	5.82	0	
Corynorhinus townsendii	2/1/2018	BCM	Female	Adult	Unknown	42.6	9.3	1.49	6.49	0	
Eptesicus fuscus	11/5/2018	BCM	Male	Adult	Non-reproducing	46.2	18.9			0	
Eptesicus fuscus	11/3/2018	PMM	Female	Adult	Non-reproducing	48	19.4			1	
Myotis ciliolabrum	10/7/2017	PMM	Male	Adult	Non-reproducing	33.4	5.5	1.20	2.67	0	
Myotis ciliolabrum	10/7/2017	PMM	Male	Adult	Scrotal	33.1	5.6	1.67	3.37	0	
Myotis ciliolabrum	10/7/2017	PMM	Male	Adult	Scrotal	31.8	5.7	1.37	3.02	0	
Myotis ciliolabrum	10/7/2017	PMM	Male	Adult	Scrotal	31.6	5.7	1.43	3.26	0	
Myotis ciliolabrum	10/7/2017	PMM	Male	Adult	Scrotal	31.3	5.7	1.47	3	0	

Species	Date	Site	Sex	Age	Reproductive?	Forearm	Mass	Fat	Lean	Wing Score	Respirometry?
Myotis ciliolabrum	10/7/2017	PMM	Male	Adult	Scrotal	31.7	5.6	1.74	3.15	0	
Myotis ciliolabrum	10/7/2017	PMM	Male	Adult	Scrotal	31.1	5.7	1.6	2.49	0	
Myotis ciliolabrum	10/7/2017	PMM	Male	Adult	Scrotal	33.8	5.5	0.85	2.18	0	
Myotis ciliolabrum	10/7/2017	PMM	Male	Adult	Scrotal	33.9	5.8	1.63	3.34	0	
Myotis ciliolabrum	10/7/2017	PMM	Male	Adult	Scrotal	32.5	6.2	1.83	2.74	0	
Myotis ciliolabrum	10/7/2017	PMM	Male	Adult	Scrotal	31	5.8	1.88	3.29	0	
Myotis ciliolabrum	10/7/2017	PMM	Male	Adult	Non-reproducing	34.2	5.9	1.7	3.59	0	
Myotis ciliolabrum	10/7/2017	PMM	Female	Adult	Non-reproducing	34.9	6.2	1.36	1.83	0	
Myotis ciliolabrum	10/7/2017	PMM	Male	Adult	Scrotal	31.2	5.7	1.5	2.44	0	
Myotis ciliolabrum	10/7/2017	PMM	Male	Adult	Scrotal	34.1	6.1	1.64	3.61	0	
Myotis ciliolabrum	10/7/2017	PMM	Male	Adult	Scrotal	33.2	6.1	2.04	3.39	1	
Myotis ciliolabrum	10/7/2017	PMM	Male	Adult	Scrotal	32.9	5.7	1.46	2.69	1	
Myotis ciliolabrum	10/7/2017	PMM	Male	Adult	Scrotal	33.7	6.1	1.64	3.74	1	
Myotis ciliolabrum	10/7/2017	PMM	Male	Adult	Scrotal	32.7	6.1	1.82	3.81	1	
Myotis ciliolabrum	10/7/2017	PMM	Male	Adult	Scrotal	32.7	6.1	1.78	3.56	1	
Myotis ciliolabrum	10/7/2017	PMM	Male	Adult	Scrotal	32.4	5.2	1.21	2.45	1	
Myotis ciliolabrum	10/7/2017	PMM	Female	Adult	Non-reproducing	34.9	5.8	1.28	3.8	1	
Myotis ciliolabrum	10/7/2017	PMM	Male	Adult	Scrotal	32.7	5.6	1.8	3.39	1	
Myotis ciliolabrum	2/1/2018	BCM	Female	Adult	Unknown	34.4	5.2	0.65	4.04	1	yes
Myotis ciliolabrum	2/1/2018	BCM	Female	Adult	Unknown	33.2	5.6	0.82	4.09	1	yes
Myotis ciliolabrum	2/1/2018	BCM	Female	Adult	Unknown	32.1	4.6	0.87	2.32	1	
Myotis ciliolabrum	2/1/2018	BCM	Female	Adult	Unknown	35.1	4.8	0.48	3.58	1	
Myotis ciliolabrum	2/1/2018	BCM	Male	Adult	Unknown	32.5	4.4	0.86	1.91	0	
Myotis ciliolabrum	2/1/2018	BCM	Female	Adult	Unknown	33.1	5.1	0.81	3.77	1	yes
Myotis ciliolabrum	2/1/2018	BCM	Female	Adult	Unknown	34.5	4.7	0.48	2.95	0	
Myotis ciliolabrum	2/1/2018	BCM	Female	Adult	Unknown	34.7	4.9	0.94	2.79	0	yes
Myotis ciliolabrum	2/1/2018	BCM	Male	Adult	Unknown	32.9	4.8	0.71	3.61	1	
Myotis ciliolabrum	2/1/2018	BCM	Female	Adult	Unknown	34.4	4.7	0.5	3.63	1	
Myotis ciliolabrum	2/1/2018	BCM	Male	Adult	Unknown	32.9	4.5	0.82	2.9	1	yes
Myotis ciliolabrum	2/1/2018	BCM	Male	Adult	Unknown	32.8	4.1	0.52	2.98	1	

Species	Date	Site	Sex	Age	Reproductive?	Forearm	Mass	Fat	Lean	Wing Score	Respirometry?
Myotis ciliolabrum	2/1/2018	BCM	Male	Adult	Unknown	31.7	4.1	0.32	2.88	0	
Myotis ciliolabrum	2/1/2018	BCM	Male	Adult	Unknown	31.4	4.3	0.95	1.91	1	yes
Myotis ciliolabrum	11/3/2018	PMM	Female	Adult	Non-reproducing	33.5	5.4			1	
Myotis ciliolabrum	11/3/2018	PMM	Female	Adult	Non-reproducing	33.7	5.7			1	
Myotis ciliolabrum	11/3/2018	PMM	Male	Adult	Non-reproducing	32.3	5.3			1	
Myotis ciliolabrum	11/5/2018	BCM	Female	Adult	Non-reproducing	34.4	4.8			0	yes
Myotis ciliolabrum	11/5/2018	BCM	Female	Adult	Non-reproducing	32.5	5.3			0	yes
Myotis ciliolabrum	11/5/2018	BCM	Female	Adult	Non-reproducing	33.5	4.6			0	yes
Myotis ciliolabrum	11/5/2018	BCM	Male	Adult	Non-reproducing	32	5.6			0	yes
Myotis ciliolabrum	11/5/2018	BCM	Male	Adult	Non-reproducing	33.5	5.3			0	
Myotis ciliolabrum	11/5/2018	BCM	Female	Adult	Non-reproducing	32.7	5.5			1	yes
Myotis ciliolabrum	11/5/2018	BCM	Male	Adult	Non-reproducing	32.1	6.5			1	yes
Myotis ciliolabrum	1/28/2019	PMM	Female	Adult	Non-reproducing	35.1	4.4			0	
Myotis ciliolabrum	1/28/2019	PMM	Female	Adult	Non-reproducing	34.4	4.7			0	
Myotis ciliolabrum	1/28/2019	PMM	Male	Adult	Non-reproducing	32.8	4			0	
Myotis ciliolabrum	1/28/2019	PMM	Female	Adult	Non-reproducing	34	5			0	
Myotis ciliolabrum	1/28/2019	PMM	Female	Adult	Non-reproducing	33.4	4.3			0	
Myotis ciliolabrum	1/28/2019	PMM	Female	Adult	Non-reproducing	33.6	5.3			0	
Myotis ciliolabrum	1/28/2019	PMM	Female	Adult	Non-reproducing	34.3	5.6			1	
Myotis ciliolabrum	2/1/2019	BCM	Female	Adult	Non-reproducing	33.1	4.4	0.23	3.85	0	
Myotis ciliolabrum	2/1/2019	BCM	Male	Adult	Non-reproducing	32.4	4.9	0.56	4.25	0	yes
Myotis ciliolabrum	2/1/2019	BCM	Male	Adult	Non-reproducing	33.2	4.2	0.79	3.46	3	
Myotis ciliolabrum	2/1/2019	BCM	Female	Adult	Non-reproducing	33.2	5.1	0.74	4.58	0	yes
Myotis ciliolabrum	2/1/2019	BCM	Female	Adult	Non-reproducing	33.6	5	0.85	4.08	1	yes
Myotis ciliolabrum	2/1/2019	BCM	Female	Adult	Non-reproducing	32	4.8	0.54	4.09	1	yes
Myotis ciliolabrum	2/1/2019	BCM	Male	Adult	Non-reproducing	33.8	4.9	0.62	4.16	1	yes
Myotis ciliolabrum	2/1/2019	BCM	Male	Adult	Non-reproducing	34	4.6	0.79	3.95	0	yes
Myotis ciliolabrum	2/1/2019	BCM	Female	Adult	Non-reproducing	34.7	5.5	1.01	4.48	0	yes
Myotis ciliolabrum	2/1/2019	BCM	Female	Adult	Non-reproducing	34.5	4.8	0.55	4.17	0	yes
Myotis ciliolabrum	2/1/2019	BCM	Female	Adult	Non-reproducing	34.6	4.3	0.63	3.68	1	yes

Species	Date	Site	Sex	Age	Reproductive?	Forearm	Mass	Fat	Lean	Wing Score	Respirometry?
Myotis ciliolabrum	2/1/2019	BCM	Female	Adult	Non-reproducing	33.2	4.8	0.66	4.18	0	yes
Myotis ciliolabrum	2/1/2019	BCM	Male	Adult	Non-reproducing	30.4	4.3	0.55	4.16	0	yes
Myotis ciliolabrum	2/1/2019	BCM	Male	Adult	Non-reproducing	33	4.1	0.57	3.65	1	
Myotis ciliolabrum	2/1/2019	BCM	Female	Adult	Non-reproducing	34.7	4.5	0.49	4.13	1	yes
Myotis ciliolabrum	2/1/2019	BCM	Female	Adult	Non-reproducing	35.7	5.2	0.49	4.65	1	yes
Myotis ciliolabrum	2/1/2019	BCM	Male	Adult	Scrotal	33.2	4.9	0.91	4.17	1	yes
Myotis volans	10/7/2017	PMM	Male	Adult	Scrotal	38.2	10.3	2.32	6.86	0	yes
Myotis volans	10/8/2017	PMM	Male	Adult	Scrotal	37.8	9.7			1	

Oklahoma Department of Wildlife Conservation
Final Project Report 2016-2018
Under permit #s 6765, 6839, 7243

We caught a total of 563 bats: 3 *Corynorhinus townsendii*, 1 *Eptesicus fuscus*, 418 *Myotis velifer*, and 141 *Perimyotis subflavus* (Table 1; Appendix) over the sampling period of fall 2016 to winter 2018. During the fall, bats were caught using mist nets and harp traps at the cave entrance. During the winter, bats were hand-captured from cave walls. We determined sex, age, reproductive condition, and wing score and measured forearm length and body mass of each bat. We used quantitative magnetic resonance (QMR; Echo-MRI-B, Echo Medical Systems, Houston, TX) to measure fat mass and lean mass. We measured metabolic rate (TMR) and evaporative water loss (EWL) during torpor using open-flow respirometry. We measured body fat from 359 individuals and processed 83 individuals through respirometry. Body mass and body fat were greater in females for each species compared to males (Figure 1). The mean mass for each species varied between seasons (Figure 2), with both body mass and fat mass greater in the fall compared to winter. Metabolic rate was not different between seasons, but evaporative water loss showed differences, depending on species (Figure 3).

We measured hibernaculum temperature and relative humidity over each hibernation period at each site using HOBO (Model U23-001, Onset Computer Corporation) and iButton (Model DS1921Z-F5, Maxim Integrated Products) microclimate data loggers. We placed four HOBO and ten iButton loggers throughout the hibernacula in the fall and recorded conditions at 3 h intervals. We collected loggers from the hibernacula in the spring (May) of each year. The mean temperature of the cave was 10.23 °C while the mean relative humidity was 88.17% (Figure 4).

We predicted survival for *Myotis velifer* and *Perimyotis subflavus* (Figure 5) over the range of environmental conditions experienced in the cave. We also inferred the survival of both species once affected with white-nose syndrome (Figure 5). The modified hibernation energetics model estimates the time until fat exhaustion during hibernation as a function of bat characteristics, hibernaculum microclimate, and fungal growth. Survival is determined by comparing model output time to winter duration – if time until fat exhaustion is greater than winter duration, survival occurs. We validated the model predictions with field and laboratory data and determined model sensitivity to bat characteristics.

For further information about our findings please visit www.science4bats.org/publications and review all project associated publications.

Table 1: The number of each species per year captured at Selman Living Lab.

Species	Year	Count
Corynorhinus townsendii	2016	2
Corynorhinus townsendii	2017	1
Eptesicus fuscus	2017	1
Myotis velifer	2016	195
Myotis velifer	2017	223
Perimyotis subflavus	2016	6
Perimyotis subflavus	2017	104
Perimyotis subflavus	2018	31
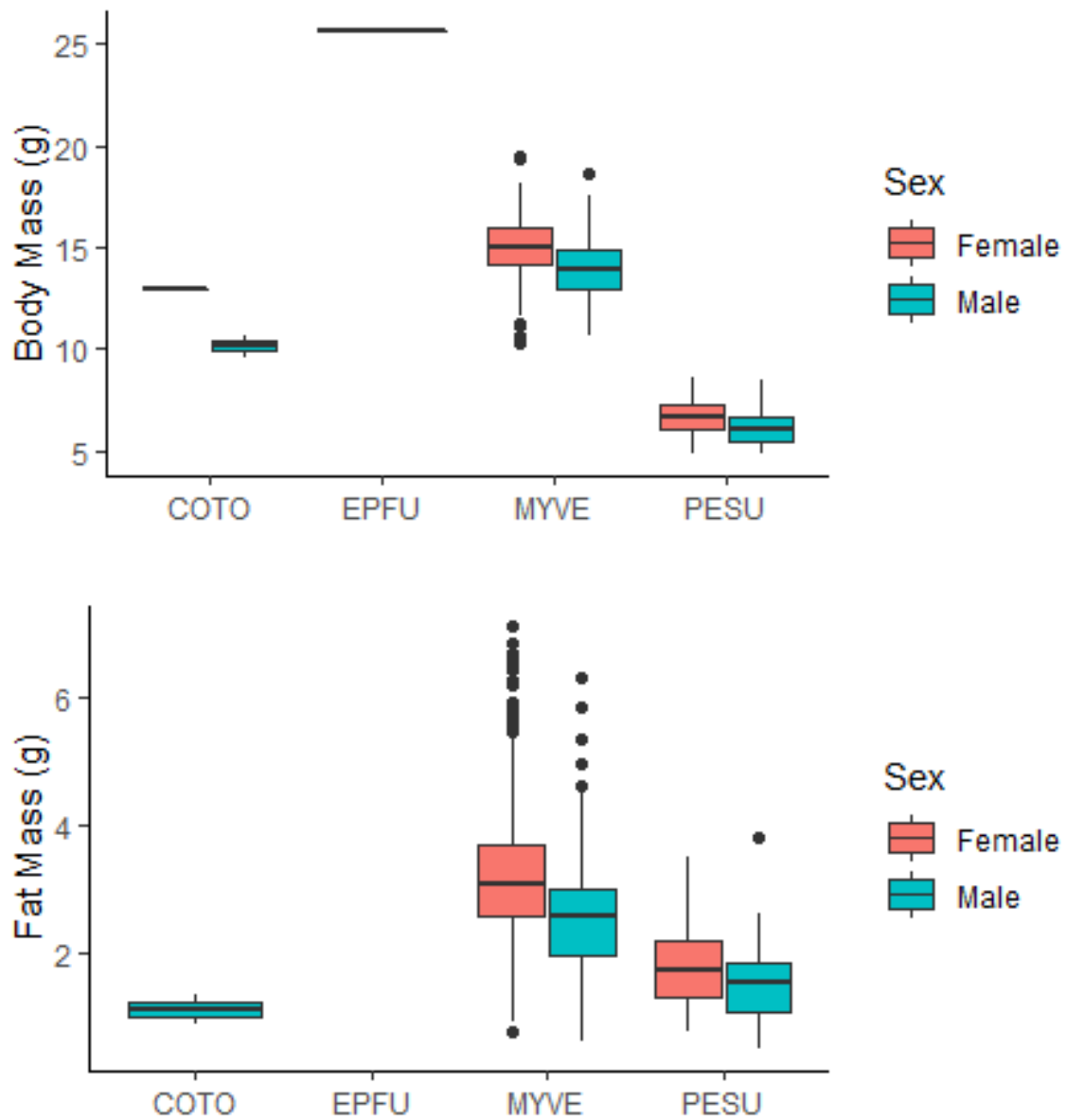
Figure 1. Body mass (top) and fat mass (bottom) by sex for the four species captured at Selman Living Lab. The single EPFU data point was a male.
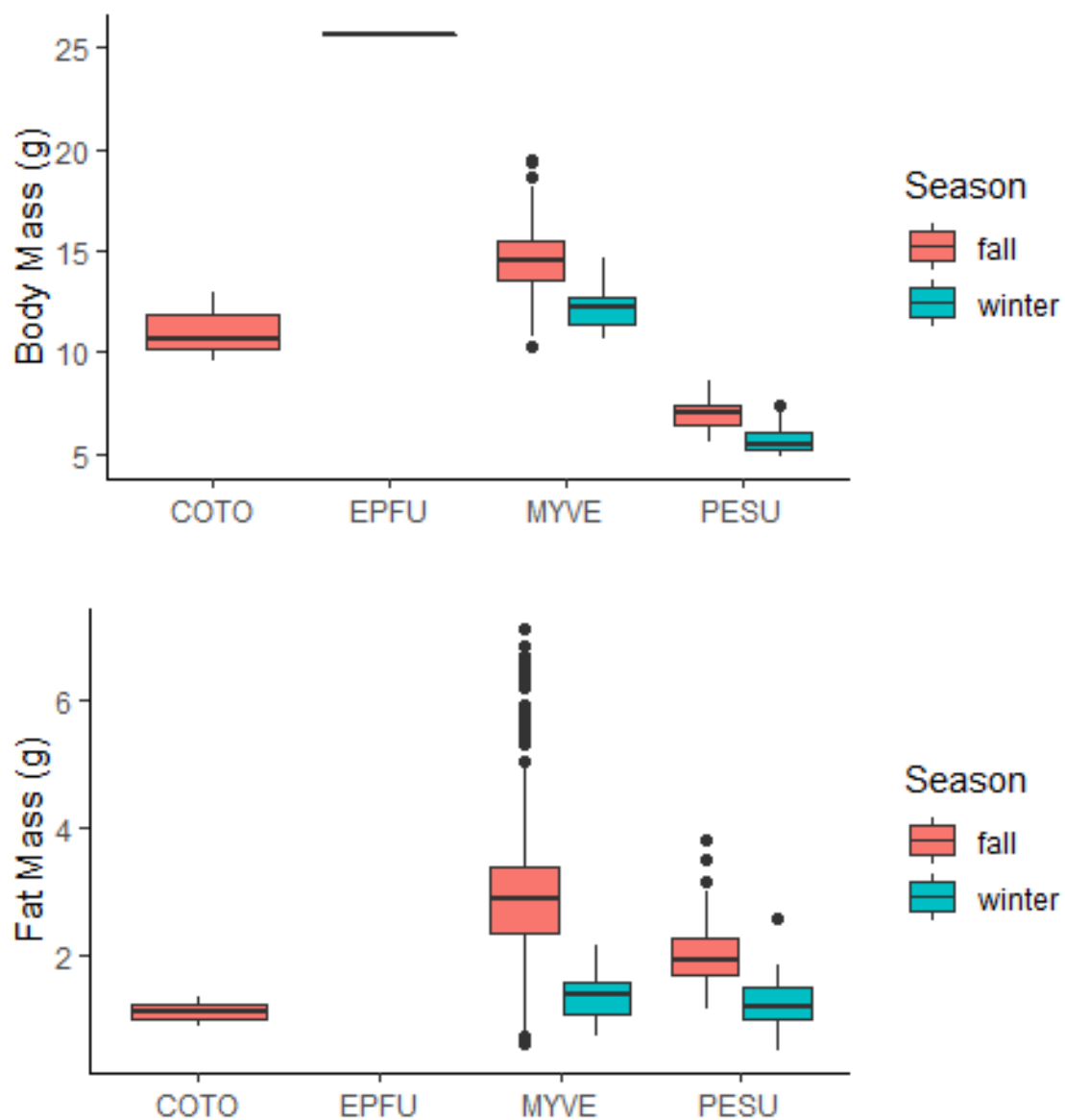
Figure 2. Body mass (top) and fat mass (bottom) by season for the four species captured at Selman Living Lab. The single EPFU data point was during the fall.
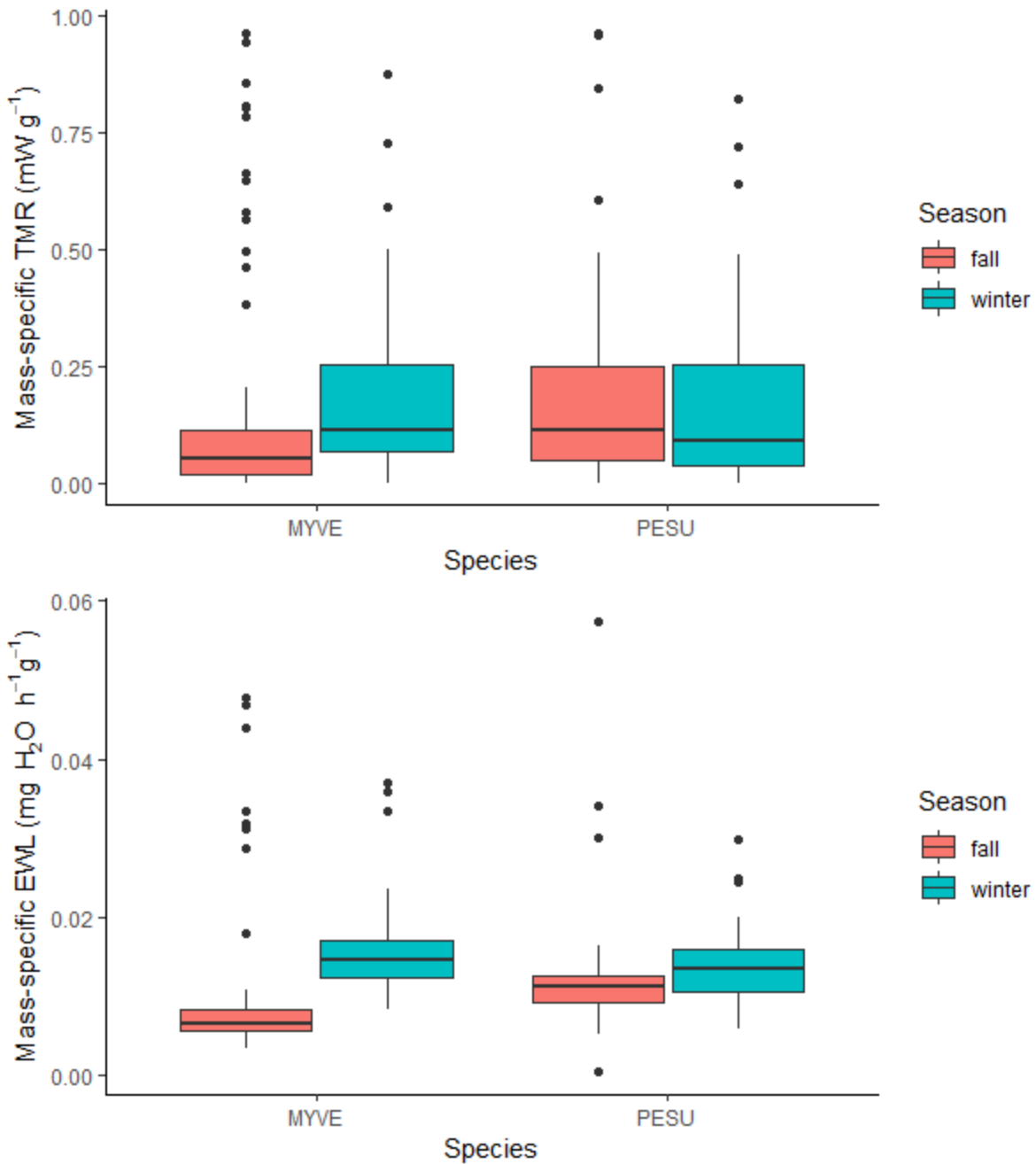
Figure 3. Mass-specific torpor metabolic rate (TMR; top) and mass-specific evaporative water loss (EWL; bottom) by season for two species captured at Selman Living Lab.
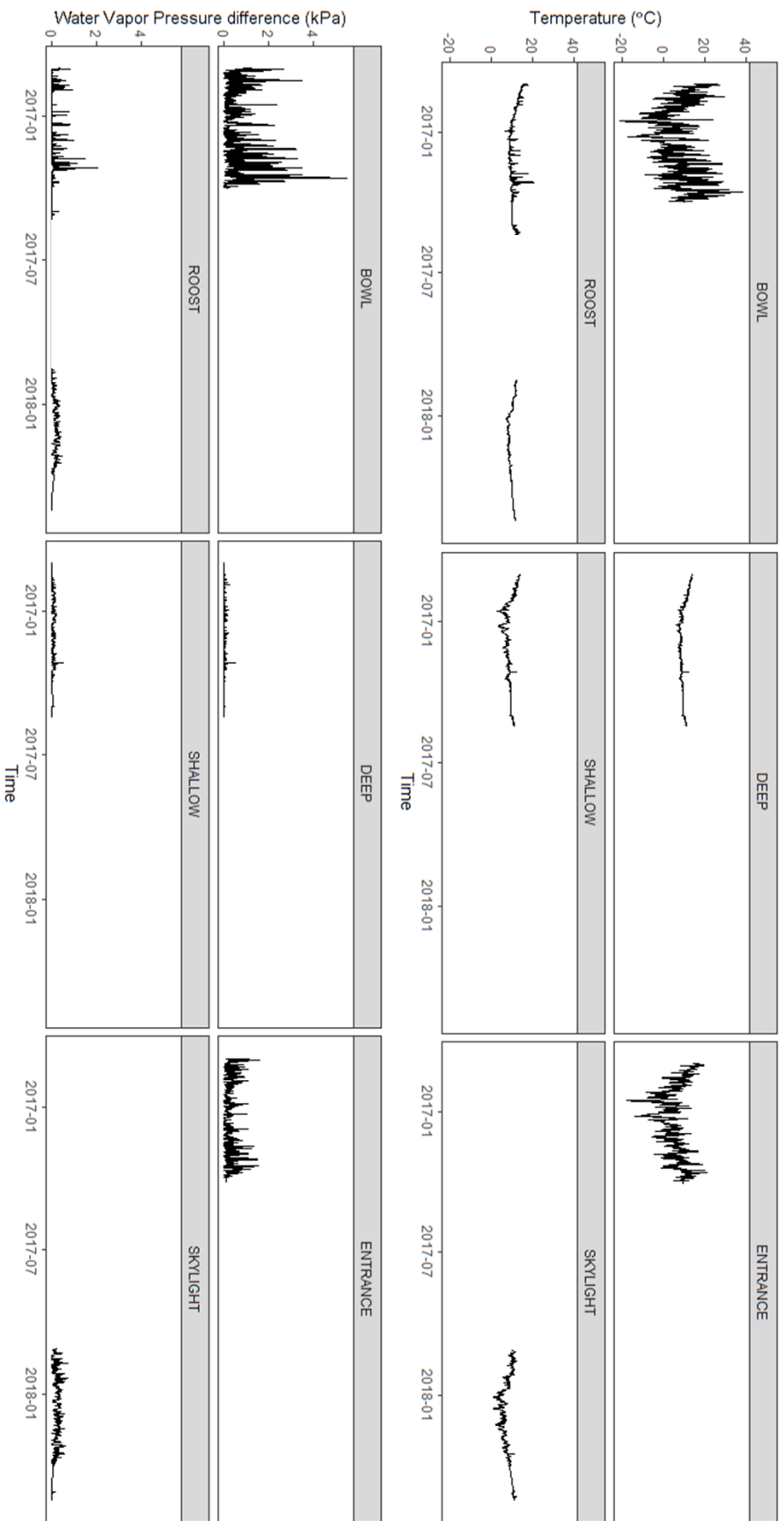
Figure 4: Microclimate (top: temperature, bottom: water vapor pressure difference) at different locations throughout the cave.
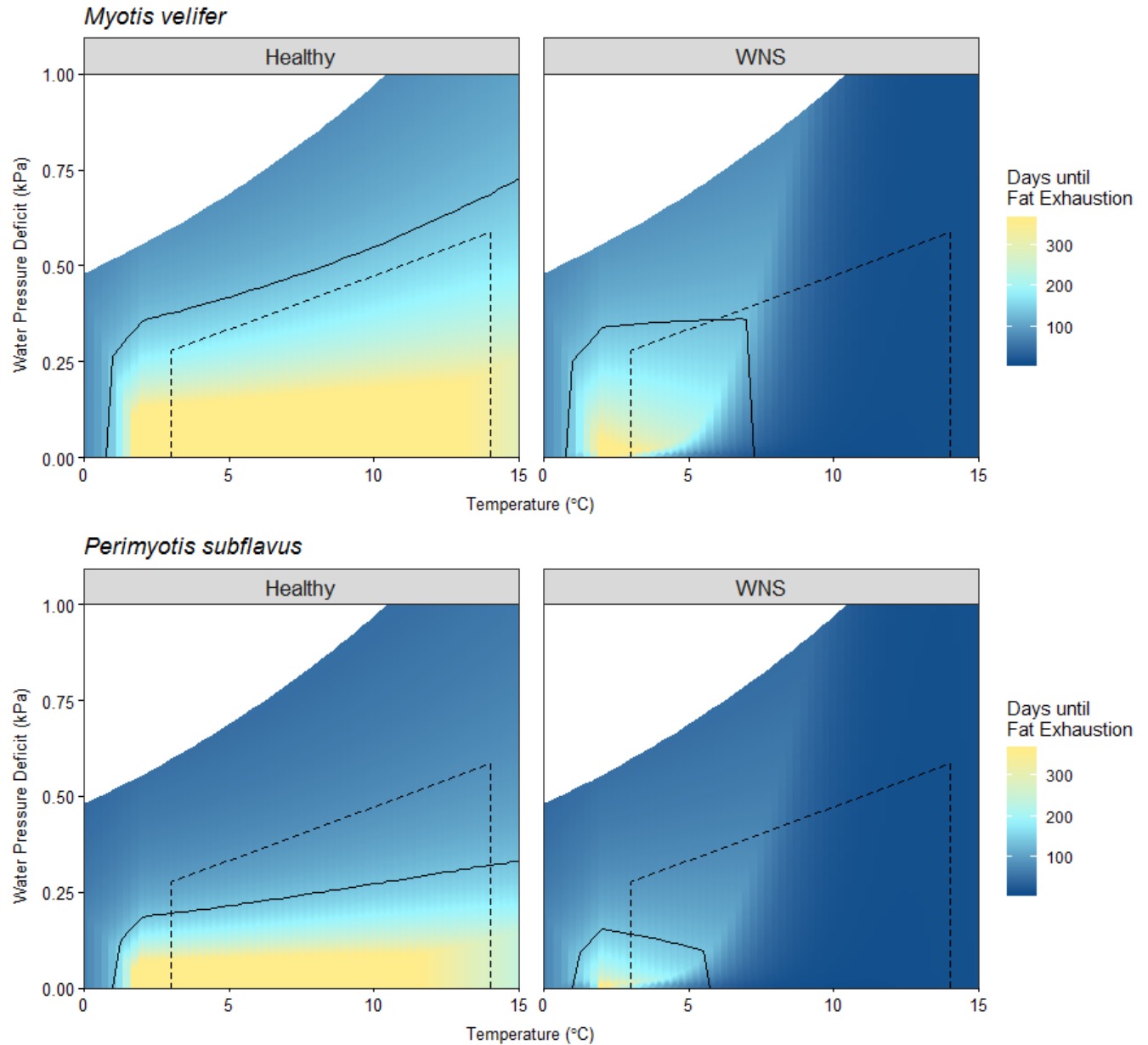
Figure 5: Predicted days until total fat exhaustion for *Myotis velifer* and *Perimyotis subflavus* in Selman Living Lab Cave. Solid lines represent days of hibernation duration (134 days) predicted for Selman Living Lab Cave and the range of microclimate conditions that would allow survival in this area. Dashed lines represent microclimate conditions measured at the roosting location within the mine. The area where solid and dashed lines overlap is the microclimate conditions available that allow survival. White space represents impossible microclimate space based on the saturation potential for each temperature. Here, *M. velifer* and *P. subflavus* have some microclimate space that would allow for survival from white-nose syndrome (WNS).

APPENDIX: Morphometric data from species captured at Selman Living Lab. Forearm is in mm, mass, fat, and lean mass are in g.

Bat Species	Date	Sex	Age	Reproductive?	Forearm	Mass	Fat	Lean	Wing Score	Respirometry?
Perimyotis subflavus	1/28/2017	Male	Adult	Non-reproducing	35.7	4.9	1.16	2.76	0	
Perimyotis subflavus	1/28/2017	Female	Adult	Non-reproducing	34.7	4.8	1.31	2.47	2	
Perimyotis subflavus	1/28/2017	Female	Adult	Non-reproducing	33.6	5.9	1.17	4	1	
Perimyotis subflavus	1/28/2017	Female	Adult	Non-reproducing	34.3	5.5	1.06	3.52	0	
Perimyotis subflavus	1/28/2017	Male	Adult	Non-reproducing	33.3	5.1	1.04	3.36	1	
Perimyotis subflavus	1/28/2017	Male	Adult	Non-reproducing	33.8	4.9	1.54	2.58	2	
Perimyotis subflavus	1/28/2017	Female	Adult	Non-reproducing	33.4	5.2	1.48	2.69	1	yes
Perimyotis subflavus	1/28/2017	Male	Adult	Non-reproducing	34.1	5.2	1.01	3.54	2	
Perimyotis subflavus	1/28/2017	Female	Adult	Non-reproducing	33.9	5.4	1.14	3.38	0	
Perimyotis subflavus	1/28/2017	Female	Adult	Non-reproducing	33.9	5.4	1.11	3.02	0	
Perimyotis subflavus	1/28/2017	Female	Adult	Non-reproducing	33.4	5.1	0.96	3.13	1	
Perimyotis subflavus	1/28/2017	Female	Adult	Non-reproducing	35.1	6.2	1.57	3.66	0	yes
Perimyotis subflavus	1/28/2017	Female	Adult	Non-reproducing	34.4	5.6	0.77	3.63	1	
Perimyotis subflavus	1/28/2017	Female	Adult	Non-reproducing	33.3	5.3	1.49	2.65	0	yes
Perimyotis subflavus	1/28/2017	Male	Adult	Non-reproducing	34.6	4.9	1.07	3.06	2	
Perimyotis subflavus	1/28/2017	Female	Adult	Non-reproducing	34	4.9	1.1	2.66	2	
Perimyotis subflavus	1/28/2017	Male	Adult	Non-reproducing	32.8	5.2	1.08	3.26	1	
Perimyotis subflavus	1/28/2017	Male	Adult	Non-reproducing	34.2	5.3	0.48	4.1	0	
Perimyotis subflavus	1/28/2017	Male	Adult	Non-reproducing	35	6	1.33	3.79	1	yes
Perimyotis subflavus	1/28/2017	Female	Adult	Non-reproducing	34.1	6.8	1.76	3.96	1	yes
Myotis velifer	2/25/2017	Female	Adult	Non-reproducing	45.8	13.1	1.69	7.57	1	yes
Myotis velifer	2/25/2017	Male	Adult	Reproducing	45.9	12.5	1.14	6.11	1	
Myotis velifer	2/25/2017	Male	Adult	Non-reproducing	46.5	12.6	1.67	5.77	1	yes
Myotis velifer	2/25/2017	Female	Adult	Non-reproducing	44.4	12.1	1.29	7.42	1	
Myotis velifer	2/25/2017	Female	Adult	Non-reproducing	47.3	10.7	0.78	4.34	1	
Myotis velifer	2/25/2017	Female	Adult	Non-reproducing	44	12.6	1.36	4.56	1	
Myotis velifer	2/25/2017	Female	Adult	Non-reproducing	45.5	12.1	1.42	6.19	1	
Myotis velifer	2/25/2017	Female	Adult	Non-reproducing	44	11.7	1.04	5.32	1	
Myotis velifer	2/25/2017	Female	Adult	Non-reproducing	44.5	12.6	1.18	3.48	1	
Myotis velifer	2/25/2017	Female	Adult	Non-reproducing	45.1	12.7	1.61	7.16	1	yes
Myotis velifer	2/25/2017	Male	Adult	Non-reproducing	45.5	11.1	0.74	5.64	1	
Myotis velifer	2/25/2017	Male	Adult	Non-reproducing	46.3	13.8	1.72	5.22	2	yes
Myotis velifer	2/25/2017	Male	Adult	Non-reproducing	45	11	1.38	4.75	1	

Bat Species	Date	Sex	Age	Reproductive?	Forearm	Mass	Fat	Lean	Wing Score	Respirometry?
Myotis velifer	2/25/2017	Female	Adult	Non-reproducing	45.6	12.3	1.51	3.83	1	
Myotis velifer	2/25/2017	Male	Adult	Non-reproducing	44.6	11.3	1.36	5.11	1	yes
Myotis velifer	2/25/2017	Female	Adult	Non-reproducing	46	11.6	1.22	5.38	1	
Myotis velifer	2/25/2017	Female	Adult	Non-reproducing	46.2	12.5	2.01	5.49	1	yes
Myotis velifer	2/25/2017	Female	Adult	Non-reproducing	45	12.1	1.58	5.41	2	yes
Myotis velifer	2/25/2017	Female	Adult	Non-reproducing	45.9	11.8	1.02	6.8	1	
Myotis velifer	2/25/2017	Female	Adult	Non-reproducing	46.2	12.8	1.45	5.95	3	yes
Myotis velifer	2/25/2017	Female	Adult	Non-reproducing	45.9	12.7	1.37	6.21	1	yes
Myotis velifer	2/25/2017	Male	Adult	Non-reproducing	45.6	12.5	1.51	5.23	1	yes
Myotis velifer	2/25/2017	Female	Adult	Non-reproducing	48.2	14.6	2.14	6.87	1	yes
Myotis velifer	2/25/2017	Female	Adult	Non-reproducing	46.3	11.3	1.01	4.31	1	
Myotis velifer	2/25/2017	Female	Adult	Non-reproducing	45.8	11.1	1.06	6.21	1	
Myotis velifer	2/25/2017	Female	Adult	Non-reproducing	47.5	12.9	1.81	5.46	1	yes
Myotis velifer	2/25/2017	Female	Adult	Non-reproducing	44.5	10.8	0.95	5.65	2	
Myotis velifer	2/25/2017	Male	Adult	Non-reproducing	43.5	11.9	1.27	5.9	1	
Myotis velifer	2/25/2017	Male	Adult	Non-reproducing	45.9	12.9	1.4	5.96	2	yes
Perimyotis subflavus	1/28/2017	Male	Adult	Non-reproducing	43.4	10.6	0.92	6.14	1	
Perimyotis subflavus	1/28/2017	Female	Adult	Non-reproducing	32.9	5.7	1.48	3.41	1	yes
Perimyotis subflavus	1/28/2017	Male	Adult	Non-reproducing	34.9	6.2	1.84	3.33	1	yes
Perimyotis subflavus	1/28/2017	Female	Adult	Non-reproducing	33.9	5.3	0.95	3.59	1	
Perimyotis subflavus	1/28/2017	Female	Adult	Non-reproducing	37.5	5.8	1.35	3.11	2	yes
Perimyotis subflavus	1/28/2017	Female	Adult	Non-reproducing	34	6.2	1.66	3.64	1	yes
Perimyotis subflavus	1/28/2017	Female	Adult	Non-reproducing	34.7	7	1.86	3.24	1	yes
Perimyotis subflavus	1/28/2017	Female	Adult	Non-reproducing	34.8	6	2.56	3.55	1	yes
Perimyotis subflavus	1/28/2017	Male	Adult	Non-reproducing	35.6	5.4	1.49	2.54	1	yes
Perimyotis subflavus	1/28/2017	Female	Adult	Non-reproducing	33.1	5.4	1.46	2.48	1	yes
Perimyotis subflavus	1/28/2017	Male	Adult	Non-reproducing	34.8	5.4	1.18	2.94	0	yes
Perimyotis subflavus	1/28/2017	Male	Adult	Non-reproducing	33.4	5.2	1.23	3.63	1	yes
Myotis velifer	2/25/2017	Female	Adult	Non-reproducing	45.9	12.9	1.4	5.96	2	yes
Corynorhinus townsendii	10/29/2017	Female	Adult	Non-reproducing	43	13		3.63	1	yes
Perimyotis subflavus	1/28/2017	Male	Adult	Non-reproducing	34.8	5.4	1.18	2.94	0	yes
Eptesicus fuscus	10/29/2017	Male	Adult	Scrotal	47.2	25.6		2.79	2	
Perimyotis subflavus	10/30/2017	Male	Adult	Non-reproducing	34.3	6.1	1.55	2.79	1	
Perimyotis subflavus	10/30/2017	Male	Adult	Non-reproducing	33.7	6.4	1.67	3.28	1	
Perimyotis subflavus	10/30/2017	Female	Adult	Non-reproducing	33.1	7.3	2.3	3.59	1	yes
Perimyotis subflavus	10/30/2017	Female	Adult	Non-reproducing	35.3	7.8	2.38	3.5	1	yes
Perimyotis subflavus	10/30/2017	Female	Adult	Non-reproducing	34.5	7.6	1.92	3.43	1	yes

Bat Species	Date	Sex	Age	Reproductive?	Forearm	Mass	Fat	Lean	Wing Score	Respirometry?
Perimyotis subflavus	10/30/2017	Male	Adult	Scrotal	34.3	7.1	1.89	3.41	0	
Perimyotis subflavus	10/30/2017	Male	Adult	Non-reproducing	34	6.9	1.88	3.64	2	
Perimyotis subflavus	10/30/2017	Male	Adult	Scrotal	34.3	6.3	1.76	3.35	0	
Perimyotis subflavus	10/30/2017	Male	Adult	Scrotal	33.3	7.3	2.11	3.51	0	yes
Perimyotis subflavus	10/30/2017	Female	Adult	Non-reproducing	35.3	7.8	2.43	3.23	1	yes
Perimyotis subflavus	10/30/2017	Female	Adult	Non-reproducing	33.4	7	2.09	3	1	
Perimyotis subflavus	10/30/2017	Male	Adult	Non-reproducing	34.6	6.8	1.79	3.54	1	
Perimyotis subflavus	10/30/2017	Male	Adult	Non-reproducing	33.5	6.4	1.85	2.85	2	
Perimyotis subflavus	10/30/2017	Male	Adult	Scrotal	35.1	7.2	2.06	3.51	2	
Perimyotis subflavus	10/30/2017	Female	Adult	Non-reproducing	33.2	6.5	1.58	3.21	1	
Perimyotis subflavus	10/30/2017	Male	Adult	Scrotal	33.2	6.5	1.57	3.05	2	
Perimyotis subflavus	10/30/2017	Male	Adult	Scrotal	34.3	7.7	2.63	3.23	1	yes
Perimyotis subflavus	10/30/2017	Female	Adult	Non-reproducing	34	7.4	2.14	3.68	1	
Perimyotis subflavus	10/30/2017	Female	Adult	Non-reproducing	32.8	7.2	2.14	3.57	0	yes
Perimyotis subflavus	10/30/2017	Female	Adult	Non-reproducing	34.9	7.4	1.5	0.93	1	
Perimyotis subflavus	10/30/2017	Female	Adult	Non-reproducing	34.5	7.2	2.25	3.36	1	
Perimyotis subflavus	10/30/2017	Female	Adult	Non-reproducing	35.1	7.5	2.31	2.96	1	yes
Perimyotis subflavus	10/30/2017	Male	Adult	Non-reproducing	33.5	7.1	2.19	3.53	1	yes
Myotis velifer	10/29/2017	Female	Adult	Non-reproducing	47.1	14.4	2.62	6.01	1	
Myotis velifer	10/29/2017	Female	Adult	Non-reproducing	44.2	13.5	2.41	6.04	1	
Myotis velifer	10/29/2017	Male	Adult	Scrotal	42.5	12.1	0.84	6.54	1	
Myotis velifer	10/29/2017	Male	Adult	Scrotal	42.6	11.9	0.74	5.88	1	
Myotis velifer	10/29/2017	Male	Adult	Scrotal	42.9	12.7	1.41	6.74	1	
Myotis velifer	10/29/2017	Male	Adult	Scrotal	41.2	12.2	0.86	5.88	1	
Myotis velifer	10/29/2017	Male	Adult	Scrotal	44.1	12.8	1.67	5.96	1	
Myotis velifer	10/29/2017	Male	Adult	Scrotal	46.2	12.8	1.37	6.31	1	
Myotis velifer	10/29/2017	Male	Adult	Scrotal	44.8	15.3	2.76	7.26	1	
Myotis velifer	10/29/2017	Male	Adult	Scrotal	44.5	14	2.76	5.88	3	
Myotis velifer	10/29/2017	Female	Adult	Non-reproducing	44.4	16.8	4.01	6.76	1	
Myotis velifer	10/29/2017	Male	Adult	Scrotal	45.3	13.9	2.03	6.61	2	
Myotis velifer	10/29/2017	Male	Adult	Scrotal	43.5	14	2.07	7.19	1	
Myotis velifer	10/29/2017	Male	Adult	Scrotal	42.6	13.6	2.66	6.7	1	
Myotis velifer	10/29/2017	Female	Adult	Non-reproducing	44.4	14.5	2.44	7.23	1	
Myotis velifer	10/29/2017	Female	Adult	Non-reproducing	44.8	16.2	3.1	6.48	1	
Myotis velifer	10/29/2017	Female	Adult	Non-reproducing	43.6	14.4	3.42	5.59	1	

Bat Species	Date	Sex	Age	Reproductive?	Forearm	Mass	Fat	Lean	Wing Score	Respirometry?
Myotis velifer	10/29/2017	Female	Adult	Non-reproducing	45.2	16.3	4.02	6.42	1	
Myotis velifer	10/29/2017	Male	Adult	Scrotal	43	15.6	2.69	7.27	1	
Myotis velifer	10/29/2017	Male	Adult	Scrotal	44.6	13.7	2.74	6.52	1	
Myotis velifer	10/29/2017	Male	Adult	Scrotal	45.8	15	3.21	6.79	1	
Myotis velifer	10/29/2017	Male	Adult	Scrotal	43.6	14.3	2.66	7.18	2	
Myotis velifer	10/29/2017	Female	Adult	Non-reproducing	45	14.8	2.95	7.21	1	
Myotis velifer	10/29/2017	Male	Adult	Scrotal	43.4	13.7	2.55	7.37	1	
Myotis velifer	10/29/2017	Male	Adult	Scrotal	45.2	13.8	2.35	6.76	1	
Myotis velifer	10/29/2017	Male	Adult	Scrotal	42.1	12.4	2.3	6.22	1	
Myotis velifer	10/29/2017	Female	Adult	Non-reproducing	43.4	15	2.34	7.1	1	
Myotis velifer	10/29/2017	Male	Adult	Scrotal	45.3	16.4	3.55	5.04	1	
Myotis velifer	10/29/2017	Male	Adult	Scrotal	42.5	13.8	2.42	6.97	1	
Myotis velifer	10/29/2017	Male	Adult	Scrotal	44.3	13.3	1.39	8.205	1	
Myotis velifer	10/29/2017	Male	Adult	Scrotal	44.2	13.5	2.93	7.23	1	
Myotis velifer	10/29/2017	Male	Adult	Scrotal	44.3	13.8	2.16	7.5	1	
Myotis velifer	10/29/2017	Female	Adult	Non-reproducing	46.6	17.2	3.94	7.13	1	
Myotis velifer	10/29/2017	Male	Adult	Scrotal	44.7	15.2	1.24	1.83	1	
Myotis velifer	10/29/2017	Female	Adult	Non-reproducing	45.8	16	3.07	5.25	1	
Myotis velifer	10/29/2017	Male	Adult	Scrotal	44.6	15	2.79	6.69	1	
Myotis velifer	10/29/2017	Female	Adult	Non-reproducing	44.9	15.3	2.4	4.09	1	
Myotis velifer	10/29/2017	Female	Adult	Non-reproducing	44.3	15.4	3.23	7.45	1	
Myotis velifer	10/29/2017	Male	Adult	Scrotal	42.5	16.5	2.06	1.8	1	
Myotis velifer	10/29/2017	Female	Adult	Non-reproducing	46.6	16.5	2.5	3.27	0	
Myotis velifer	10/29/2017	Female	Adult	Non-reproducing	46.3	16.1	2.94	7.17	1	
Myotis velifer	10/29/2017	Male	Adult	Scrotal	36.6	14.5	2.63	6.67	1	
Myotis velifer	10/29/2017	Female	Adult	Non-reproducing	44.4	16.9	3.58	6.7	1	
Myotis velifer	10/29/2017	Female	Adult	Non-reproducing	44.4	13.9	2.21	6.53	1	
Myotis velifer	10/29/2017	Female	Adult	Non-reproducing	43.8	15.9	3.34	7.33	1	
Myotis velifer	10/29/2017	Male	Adult	Scrotal	42.4	13.2	2.12	7.67	1	
Myotis velifer	10/29/2017	Male	Adult	Scrotal	43.4	17.2	4.1	7.63	1	
Myotis velifer	10/30/2017	Female	Adult	Non-reproducing	43.1	15.5	2.58	7.08	1	
Myotis velifer	10/30/2017	Female	Adult	Non-reproducing	45.3	15	2.81	7.5	2	
Myotis velifer	10/30/2017	Female	Adult	Non-reproducing	44	15.9	3.34	6.14	1	
Myotis velifer	10/30/2017	Female	Adult	Non-reproducing	43.5	15.3	3.23	6.28	1	
Myotis velifer	10/30/2017	Female	Adult	Non-reproducing	44.4	14.6	2.94	6.71	1	

Bat Species	Date	Sex	Age	Reproductive?	Forearm	Mass	Fat	Lean	Wing Score	Respirometry?
Myotis velifer	10/30/2017	Female	Adult	Non-reproducing	45	15	3.08	6.21	1	
Myotis velifer	10/30/2017	Female	Adult	Non-reproducing	46.2	16.6	4.26	7.16	1	
Myotis velifer	10/30/2017	Male	Adult	Scrotal	43.2	14.6	3.41	6.71	1	
Myotis velifer	10/30/2017	Female	Adult	Non-reproducing	44.5	14.3	2.96	6.63	1	
Myotis velifer	10/30/2017	Female	Adult	Non-reproducing	45.6	15.3	3.23	6.98	1	
Myotis velifer	10/30/2017	Male	Adult	Scrotal	43	13.4	2.91	7.06	1	
Myotis velifer	10/30/2017	Female	Adult	Non-reproducing	46.6	15.2	2.89	7.17	1	
Myotis velifer	10/30/2017	Female	Adult	Non-reproducing	44.2	13.8	2.41	6.17	1	
Myotis velifer	11/1/2017	Female	Adult	Non-reproducing	45.9	13.4	2.17	6.47	1	
Myotis velifer	11/1/2017	Female	Adult	Non-reproducing	43.8	14.9	2.71	6.5	1	
Myotis velifer	11/1/2017	Female	Adult	Non-reproducing	45.1	14.6	2.91	6.54	1	
Myotis velifer	11/1/2017	Male	Adult	Scrotal	45.5	13.8	2.66	5.78	1	
Myotis velifer	11/1/2017	Female	Adult	Non-reproducing	45.2	16.2	3.47	6.765	1	yes
Myotis velifer	11/1/2017	Male	Adult	Scrotal	45.3	12.3	1.12	7.19	1	
Myotis velifer	11/1/2017	Male	Adult	Scrotal	44.9	13.8	2.77	7.64	1	
Myotis velifer	11/1/2017	Male	Adult	Non-reproducing	45.9	15.6	3.1	7.275	1	yes
Myotis velifer	11/1/2017	Female	Adult	Non-reproducing	45.4	15.4	2.96	8.14	1	
Myotis velifer	11/1/2017	Female	Adult	Non-reproducing	47.2	16.5	3.52	7.12	1	yes
Myotis velifer	11/1/2017	Female	Adult	Non-reproducing	45.5	15.1	3.26	6.69	1	yes
Myotis velifer	11/1/2017	Female	Adult	Non-reproducing	45	15.8	3.37	7.89	1	
Myotis velifer	11/1/2017	Female	Adult	Non-reproducing	46.2	14.1	3.19	7.8	1	
Myotis velifer	11/1/2017	Male	Adult	Scrotal	44.8	15	2.94	7.6	3	
Myotis velifer	11/1/2017	Male	Adult	Scrotal	46.8	16	3.76	7.9	1	yes
Myotis velifer	11/1/2017	Female	Adult	Non-reproducing	43.4	15	3.22	6.48	1	
Myotis velifer	11/1/2017	Male	Adult	Scrotal	45.9	13.3	2	6.54	1	
Myotis velifer	11/1/2017	Female	Adult	Non-reproducing	45.3	15.6	3.06	5.99	1	
Myotis velifer	11/1/2017	Female	Adult	Non-reproducing	45.9	17.3	4.13	5.43	1	
Myotis velifer	11/1/2017	Female	Adult	Non-reproducing	44.5	14.6	3.1	6.38	1	
Myotis velifer	11/1/2017	Female	Adult	Non-reproducing	44.2	14.5	2.96	7.76	1	
Myotis velifer	11/1/2017	Male	Adult	Scrotal	43.9	14.2	2.44	8.36	1	
Myotis velifer	11/1/2017	Female	Adult	Non-reproducing	45.3	15.1	3.22	8.14	1	
Myotis velifer	11/1/2017	Male	Adult	Scrotal	36.4	15.4	3.08	6.57	1	yes
Myotis velifer	11/1/2017	Female	Adult	Non-reproducing	46	16.5	3.26	7.15	1	
Myotis velifer	11/1/2017	Male	Adult	Non-reproducing	46	17.6	4.35	8.22	2	yes
Myotis velifer	11/1/2017	Female	Adult	Non-reproducing	44.5	16.1	3.42	7.6	1	

Bat Species	Date	Sex	Age	Reproductive?	Forearm	Mass	Fat	Lean	Wing Score	Respirometry?
Myotis velifer	11/1/2017	Female	Adult	Non-reproducing	44	16.1	3.7	7.17	1	
Myotis velifer	11/1/2017	Female	Adult	Non-reproducing	44.6	14.4	3.07	6.72	2	
Myotis velifer	11/1/2017	Female	Adult	Non-reproducing	45.1	13.3	2.3	6.25	1	
Myotis velifer	11/1/2017	Female	Adult	Non-reproducing	45	15	2.87	7.5	1	
Myotis velifer	11/1/2017	Female	Adult	Non-reproducing	44.9	15.5	3.66	6.78	1	
Myotis velifer	11/1/2017	Female	Adult	Non-reproducing	48.6	13.3	2.46	6.86	1	
Myotis velifer	11/1/2017	Male	Adult	Scrotal	44.4	15.1	2.99	8.07	1	
Myotis velifer	11/1/2017	Male	Adult	Scrotal	44.5	12.2	1.86	6.61	1	
Myotis velifer	11/1/2017	Female	Adult	Non-reproducing	47	17.4	4.06	8.13	1	
Myotis velifer	11/1/2017	Male	Adult	Scrotal	44.5	13.5	2.73	7.15	2	yes
Myotis velifer	11/1/2017	Female	Adult	Non-reproducing	47.7	15.5	3.34	6.33	1	yes
Myotis velifer	11/1/2017	Female	Adult	Non-reproducing	44	14.5	2.85	6.58	1	yes
Myotis velifer	11/1/2017	Female	Adult	Non-reproducing	44.4	14.9	3.19	6.7	1	yes
Myotis velifer	11/1/2017	Male	Adult	Scrotal	43.7	14	2.09	7.15	2	
Myotis velifer	11/1/2017	Female	Adult	Non-reproducing	46.5	15.5	3.26	7.01	1	yes
Myotis velifer	11/1/2017	Male	Adult	Scrotal	45.2	14.3	2.62	6.63	1	
Myotis velifer	11/1/2017	Female	Adult	Non-reproducing	46.2	14.5	3.12	6.68	1	
Myotis velifer	11/1/2017	Female	Adult	Non-reproducing	47.1	16.4	3.96	7.64	1	yes
Myotis velifer	11/1/2017	Female	Adult	Non-reproducing	45.2	14.9	3.13	6.93	1	
Myotis velifer	11/1/2017	Female	Adult	Non-reproducing	46.2	16	3.3	7.37	1	
Myotis velifer	11/1/2017	Female	Adult	Non-reproducing	44.3	15.1			1	
Myotis velifer	11/1/2017	Female	Adult	Non-reproducing	46.1	14.3	3.45	7.16	1	
Myotis velifer	11/1/2017	Male	Adult	Scrotal	42.8	14.1	2.98	6.55	1	
Myotis velifer	11/1/2017	Female	Adult	Non-reproducing	46	14.6	3.06	6.81	1	
Myotis velifer	11/1/2017	Female	Adult	Non-reproducing	46	16.5	4.01	7.56	1	
Myotis velifer	11/1/2017	Male	Adult	Scrotal	46.9	15.5	2.73	7.85	1	
Myotis velifer	11/1/2017	Female	Adult	Non-reproducing	46.8	16	2.83	6.8	1	
Myotis velifer	11/1/2017	Female	Adult	Non-reproducing	46	16.5	4.02	7.54	1	
Myotis velifer	11/1/2017	Male	Adult	Scrotal	46.3	14.5	2.16	5.97	1	
Myotis velifer	11/1/2017	Female	Adult	Non-reproducing	47.3	17.1	3.75	4.24	1	
Myotis velifer	11/1/2017	Female	Adult	Non-reproducing	46.8	16.1	3.54	6.22	1	
Myotis velifer	11/1/2017	Female	Adult	Non-reproducing	44.5	14.7	2.48	3.25	2	
Myotis velifer	11/1/2017	Female	Adult	Non-reproducing	46.4	16.1	3.29	4.26	1	
Myotis velifer	11/1/2017	Female	Adult	Non-reproducing	44.6	14.5	2.88	4.02	1	
Myotis velifer	11/1/2017	Female	Adult	Non-reproducing	43.4	14	2.3	3.24	1	

Bat Species	Date	Sex	Age	Reproductive?	Forearm	Mass	Fat	Lean	Wing Score	Respirometry?
Myotis velifer	11/1/2017	Male	Adult	Scrotal	45.5	12.8	0.91	2.31	1	
Perimyotis subflavus	10/30/2017	Male	Adult	Non-reproducing	33.6	6.7	2	3.05	0	
Perimyotis subflavus	10/30/2017	Male	Adult	Non-reproducing	34.2	6.6	1.91	3.13	0	
Perimyotis subflavus	10/30/2017	Female	Adult	Non-reproducing	36.5	7.3	2.12	3.54	1	
Perimyotis subflavus	10/30/2017	Male	Adult	Scrotal	33.9	6	1.71	3.02	2	
Perimyotis subflavus	10/30/2017	Female	Adult	Non-reproducing	33.3	7.2	2.31	3.2	1	yes
Perimyotis subflavus	10/30/2017	Male	Adult	Scrotal	33.2	7.7	2.53	2.79	1	yes
Perimyotis subflavus	10/30/2017	Female	Adult	Non-reproducing	33.4	6.8	1.93	3.35	1	
Perimyotis subflavus	10/30/2017	Female	Adult	Non-reproducing	34.3	7.8	2.42	3.42	1	yes
Perimyotis subflavus	10/30/2017	Female	Adult	Non-reproducing	36.6	6.5	1.69	3.47	2	
Perimyotis subflavus	10/30/2017	Male	Adult	Non-reproducing	34.3	5.9	1.23	2.87	2	
Perimyotis subflavus	10/30/2017	Female	Adult	Non-reproducing	34.6	6	1.2	2.36	0	
Perimyotis subflavus	10/30/2017	Female	Adult	Non-reproducing	33.3	6.6	1.73	2.79	0	
Perimyotis subflavus	10/30/2017	Female	Adult	Non-reproducing	34.5	7.6	2.45	3.3	0	yes
Perimyotis subflavus	10/30/2017	Female	Adult	Non-reproducing	33.9	8.1	2.49	3.03	0	
Perimyotis subflavus	10/30/2017	Female	Adult	Non-reproducing	34.5	7.3	2.18	3.39	0	
Perimyotis subflavus	10/30/2017	Male	Adult	Scrotal	33.5	7.4	2.19	2.75	0	yes
Perimyotis subflavus	10/30/2017	Female	Adult	Non-reproducing	34	6.9	2.02	2.51	1	
Perimyotis subflavus	10/30/2017	Male	Adult	Scrotal	34	7	2.1	3.16	0	
Perimyotis subflavus	10/30/2017	Female	Adult	Non-reproducing	35.4	7.4	1.95	3.77	1	
Perimyotis subflavus	10/30/2017	Male	Adult	Scrotal	33.1	6.1	1.61	2.88	2	
Perimyotis subflavus	10/30/2017	Male	Adult	Scrotal	34.3	7.1	1.78	3	1	
Perimyotis subflavus	10/30/2017	Female	Adult	Non-reproducing	34.7	6.3	1.16	2.99	2	
Perimyotis subflavus	10/30/2017	Female	Adult	Non-reproducing	32.7	6.6	1.59	3.08	1	
Perimyotis subflavus	10/30/2017	Female	Adult	Non-reproducing	34.6	7.2	2.3	3.31	1	
Perimyotis subflavus	10/30/2017	Male	Adult	Non-reproducing	34	6.3	1.75	2.95	1	
Perimyotis subflavus	10/30/2017	Female	Adult	Non-reproducing	36.4	6.4	1.4	3.04	1	
Perimyotis subflavus	10/30/2017	Male	Adult	Non-reproducing	32.8	6.6	1.72	2.93	1	
Perimyotis subflavus	10/30/2017	Male	Adult	Non-reproducing	32.6	6.1	1.28	2.4	2	
Perimyotis subflavus	10/30/2017	Female	Adult	Non-reproducing	33.4	6.3	1.32	3.63	1	
Perimyotis subflavus	10/30/2017	Female	Adult	Non-reproducing	34.1	8.3	2.86	3.8	1	
Perimyotis subflavus	10/30/2017	Female	Adult	Non-reproducing	33.5	7	1.83	3.62	1	
Perimyotis subflavus	10/30/2017	Female	Adult	Non-reproducing	33.5	6.6	1.87	3.18	0	
Perimyotis subflavus	10/30/2017	Female	Adult	Non-reproducing	32.5	8.4	3.16	3.47	1	
Perimyotis subflavus	11/3/2017	Female	Adult	Non-reproducing	33.2	7.6	2.44	3.65	0	yes

Bat Species	Date	Sex	Age	Reproductive?	Forearm	Mass	Fat	Lean	Wing Score	Respirometry?
Perimyotis subflavus	11/3/2017	Male	Adult	Non-reproducing	35.4	6.3	1.32	3.04	1	
Perimyotis subflavus	11/3/2017	Female	Adult	Non-reproducing	33.3	6.8	1.72	3.91	0	
Perimyotis subflavus	11/3/2017	Male	Adult	Scrotal	34.4	6.3	1.8	3.1	1	yes
Perimyotis subflavus	11/3/2017	Male	Adult	Scrotal	34.5	7.2	2.21	3.56	0	yes
Perimyotis subflavus	11/3/2017	Male	Adult	Scrotal	35.4	7.1	2.3	3.5	1	yes
Perimyotis subflavus	11/3/2017	Male	Adult	Scrotal	39.8	5.7	1.77	2.97	1	
Perimyotis subflavus	11/3/2017	Female	Adult	Non-reproducing	35.7	6.8	2.14	3.4	1	yes
Perimyotis subflavus	11/3/2017	Female	Adult	Non-reproducing	34.2	8.4	2.99	3.63	0	yes
Perimyotis subflavus	11/3/2017	Male	Adult	Non-reproducing	33.1	6	1.5	3.56	1	
Perimyotis subflavus	11/3/2017	Female	Adult	Non-reproducing	34.6	8	2.32	3.74	1	yes
Perimyotis subflavus	11/3/2017	Female	Adult	Non-reproducing	34.2	7.3	2.26	3.2	1	
Perimyotis subflavus	11/3/2017	Male	Adult	Scrotal	34.7	6.7	1.99	3.42	1	
Perimyotis subflavus	11/3/2017	Female	Adult	Non-reproducing	34.3	7	1.98	3.4	0	
Perimyotis subflavus	11/3/2017	Male	Adult	Scrotal	32.4	6	1.65	2.7	1	
Perimyotis subflavus	11/3/2017	Male	Adult	Scrotal	33.6	7.1	1.65	3.24	1	
Perimyotis subflavus	11/3/2017	Female	Adult	Non-reproducing	33.8	5.7	1.17	3.03	1	
Myotis velifer	11/3/2017	Female	Adult	Non-reproducing	46.1	15.3	3.21	8.02	1	yes
Myotis velifer	11/3/2017	Female	Adult	Non-reproducing	47	15.1	2.95	7.48	1	yes
Myotis velifer	11/3/2017	Female	Adult	Non-reproducing	45.1	15.1	3.24	6.86	1	
Myotis velifer	11/3/2017	Female	Adult	Non-reproducing	44.8	15.8	3.36	7.79	1	
Myotis velifer	11/3/2017	Male	Adult	Scrotal	44.3	14.1	2.68	6.55	1	
Myotis velifer	11/3/2017	Male	Adult	Scrotal	44.3	14.2	2.62	6.16	1	yes
Myotis velifer	11/3/2017	Male	Adult	Scrotal	43.3	13.8	2.77	7.3	1	yes
Myotis velifer	11/3/2017	Male	Adult	Scrotal	44.1	14.5	2.6	7.44	3	yes
Myotis velifer	11/3/2017	Female	Adult	Non-reproducing	45.2	14.9	2.9	7.55	1	yes
Myotis velifer	11/3/2017	Female	Adult	Non-reproducing	45.3	14.6	3	5.75	1	yes
Myotis velifer	11/3/2017	Male	Adult	Scrotal	44.4	14.4	2.97	6.35	1	yes
Myotis velifer	11/3/2017	Female	Adult	Non-reproducing	43.7	13	2.26	7.37	1	
Myotis velifer	11/3/2017	Male	Adult	Scrotal	46.5	14.6	2.33	2.16	1	
Myotis velifer	11/3/2017	Female	Adult	Non-reproducing	46.5	15.3	2.74	4.06	3	
Myotis velifer	11/3/2017	Female	Adult	Non-reproducing	46.7	13.9	1.77	4.21	1	
Myotis velifer	11/3/2017	Male	Adult	Scrotal	45.9	14	1.19	1.07	1	
Myotis velifer	11/3/2017	Female	Adult	Non-reproducing	44.5	15	2.57	1.77	1	
Myotis velifer	11/3/2017	Female	Adult	Non-reproducing	47.3	17	2.95	3.95	1	
Myotis velifer	11/3/2017	Female	Adult	Non-reproducing	43.8	15.3	3.62	4.42	1	

Bat Species	Date	Sex	Age	Reproductive?	Forearm	Mass	Fat	Lean	Wing Score	Respirometry?
Myotis velifer	11/3/2017	Male	Adult	Scrotal	45.6	13.9	1.85	2.57	1	
Myotis velifer	11/3/2017	Female	Adult	Non-reproducing	44	14.2	2.45	5.3	1	
Myotis velifer	11/3/2017	Female	Adult	Non-reproducing	44.2	14.1	2.34	4.96	1	
Myotis velifer	11/3/2017	Male	Adult	Scrotal	46	18.6	3.14	5.83	1	
Myotis velifer	11/3/2017	Female	Adult	Non-reproducing	44.2	15.1	2.27	3.7	1	
Myotis velifer	11/3/2017	Male	Adult	Scrotal	43.6	13.5	2.33	4.35	1	
Myotis velifer	11/3/2017	Female	Adult	Non-reproducing	44.1	15.1	2.67	3.95	1	
Myotis velifer	11/3/2017	Male	Adult	Scrotal	44.5	15.5	2.97	4.14	1	
Myotis velifer	11/3/2017	Female	Adult	Non-reproducing	45.1	13	1.91	4.04	1	
Myotis velifer	11/3/2017	Female	Adult	Non-reproducing	45.1	16	3.23	6.33	1	
Myotis velifer	11/3/2017	Male	Adult	Scrotal	46.4	15.5	3.65	7.81	1	
Myotis velifer	11/3/2017	Female	Adult	Non-reproducing	44.8	15.2	3.78	6.95	1	
Myotis velifer	11/3/2017	Male	Adult	Scrotal	45.5	13.3	2.51	7.12	1	
Myotis velifer	11/3/2017	Female	Adult	Non-reproducing	45.3	14.5	3.32	7.14	1	
Myotis velifer	11/3/2017	Male	Adult	Scrotal	47	15	2.83	7.08	1	
Myotis velifer	11/3/2017	Female	Adult	Non-reproducing	46.5	15.8	3.01	7.88	1	
Myotis velifer	11/3/2017	Female	Adult	Non-reproducing	43.5	14.5	3.31	7.13	1	
Myotis velifer	11/3/2017	Female	Adult	Non-reproducing	43.2	14.9	3.46	7.43	1	
Myotis velifer	11/3/2017	Male	Adult	Scrotal	45.7	14.3	2.27	4.72	1	
Myotis velifer	11/3/2017	Female	Adult	Non-reproducing	45.7	16.5	3.04	5.61	1	
Myotis velifer	11/3/2017	Female	Adult	Non-reproducing	47	15.7	3.7	7.47	1	
Myotis velifer	11/3/2017	Male	Adult	Scrotal	44	14.8	3.38	6.91	1	
Myotis velifer	11/3/2017	Female	Adult	Non-reproducing	45.5	15.3	3.37	5.45	1	
Myotis velifer	11/3/2017	Male	Adult	Scrotal	45.9	15.1	2.91	7.47	1	
Myotis velifer	11/3/2017	Female	Adult	Non-reproducing	45.4	13.2	1.77	6.45	3	
Myotis velifer	11/3/2017	Female	Adult	Non-reproducing	44.9	15.5	2.94	6.02	1	
Myotis velifer	11/3/2017	Female	Adult	Non-reproducing	46.2	14.8	2.93	7.69	1	
Myotis velifer	11/3/2017	Female	Adult	Non-reproducing	44.3	12.8	2.26	7.05	1	
Myotis velifer	11/3/2017	Female	Adult	Non-reproducing	43.5	14.6	2.6	6.83	1	
Myotis velifer	11/3/2017	Male	Adult	Scrotal	47	14.8	2.82	7.28	1	
Myotis velifer	11/3/2017	Female	Adult	Non-reproducing	46.3	13.8	2.14	7.21	1	
Myotis velifer	11/3/2017	Male	Adult	Scrotal	43.2	12.5	2.21	5.65	1	
Myotis velifer	11/3/2017	Female	Adult	Non-reproducing	45.5	15.3	3.15	7.87	1	
Myotis velifer	11/3/2017	Female	Adult	Non-reproducing	44.5	13.9	2.6	7.62	1	
Myotis velifer	11/3/2017	Female	Adult	Non-reproducing	46.6	16.3	3.79	6.77	1	

Bat Species	Date	Sex	Age	Reproductive?	Forearm	Mass	Fat	Lean	Wing Score	Respirometry?
Myotis velifer	11/3/2017	Male	Adult	Non-reproducing	43.5	13.2	2.34	7.65	3	
Myotis velifer	11/3/2017	Female	Adult	Non-reproducing	45.6	13.2	2.04	7.54	1	
Myotis velifer	11/3/2017	Female	Adult	Non-reproducing	43.2	14.1	2.74	6.63	1	
Myotis velifer	11/3/2017	Female	Adult	Non-reproducing	46.4	15.9	3.83	7.35	1	
Myotis velifer	11/3/2017	Female	Adult	Non-reproducing	45.7	15.6	3.82	8.14	1	
Myotis velifer	11/3/2017	Male	Adult	Scrotal	44.4	13.3	2.53	6.83	1	
Myotis velifer	11/3/2017	Female	Adult	Non-reproducing	46	14.3	2.07	8.18	1	
Myotis velifer	11/3/2017	Female	Adult	Non-reproducing	44.4	14.5	2.88	6.8	1	
Myotis velifer	11/3/2017	Female	Adult	Non-reproducing	44.3	13.7	2.67	7.14	1	
Myotis velifer	11/3/2017	Female	Adult	Non-reproducing	47.3	15.2	3.37	7.715	0	
Myotis velifer	11/3/2017	Female	Adult	Non-reproducing	46.1	14.5	2.76	7.23	1	
Myotis velifer	11/3/2017	Female	Adult	Non-reproducing	44.9	15.3	3.37	7.06	1	
Myotis velifer	11/3/2017	Female	Adult	Non-reproducing	45.9	15.3			1	
Myotis velifer	11/3/2017	Female	Adult	Non-reproducing	43.9	14.2	2.97	6.47	1	
Myotis velifer	11/3/2017	Female	Adult	Non-reproducing	46.2	15.1	3.5	8.27	1	
Myotis velifer	11/3/2017	Female	Adult	Non-reproducing	47.4	15.2	3.37	7.89	1	
Perimyotis subflavus	1/13/2018	Male	Adult	Unknown	34.5	5.4	1.29	3.48	1	
Perimyotis subflavus	1/13/2018	Male	Adult	Unknown	32.4	5.2	0.76	3.76	2	yes
Perimyotis subflavus	1/13/2018	Female	Adult	Unknown	34.2	6.7	1.54	3.32	1	yes
Perimyotis subflavus	1/13/2018	Male	Adult	Unknown	35.5	6.2	1.28	4.03	1	yes
Perimyotis subflavus	1/13/2018	Female	Adult	Unknown	36	5.7	1.08	3.41	1	yes
Perimyotis subflavus	1/13/2018	Male	Adult	Unknown	34.3	5	0.77	2.56	1	
Perimyotis subflavus	1/13/2018	Female	Adult	Unknown	33.8	5.3	1.14	3.39	1	
Perimyotis subflavus	1/13/2018	Female	Adult	Unknown	35.1	6.1	1.13	4.06	1	yes
Perimyotis subflavus	1/13/2018	Male	Adult	Unknown	33.1	5.4	0.98	2.93	1	
Perimyotis subflavus	1/13/2018	Male	Adult	Unknown	33.3	5.1	0.91	2.55	1	
Perimyotis subflavus	1/13/2018	Male	Adult	Unknown	34.3	6.3	1.41	3.98	0	yes
Perimyotis subflavus	1/13/2018	Male	Adult	Unknown	35.3	5.6	0.81	3.2	1	yes
Perimyotis subflavus	1/13/2018	Female	Adult	Unknown	34.2	5.3	0.72	2.33	2	
Perimyotis subflavus	1/13/2018	Male	Adult	Unknown	35.1	5.4	1.09	3.46	0	
Perimyotis subflavus	1/13/2018	Male	Adult	Unknown	34.2	5.5	1.36	3.45	1	
Perimyotis subflavus	1/13/2018	Female	Adult	Unknown	33.8	5.3	0.82	2.98	1	
Perimyotis subflavus	1/13/2018	Male	Adult	Unknown	34.2	5.9	1.33	3.28	0	yes
Perimyotis subflavus	1/13/2018	Female	Adult	Unknown	34.2	6.4	1.14	3.77	1	
Perimyotis subflavus	1/13/2018	Male	Adult	Unknown	34.3	5.4	0.94	2.93	2	

Bat Species	Date	Sex	Age	Reproductive?	Forearm	Mass	Fat	Lean	Wing Score	Respirometry?
Perimyotis subflavus	1/13/2018	Female	Adult	Unknown	33.5	6.5	1.75	4	0	yes
Perimyotis subflavus	1/13/2018	Male	Adult	Unknown	33.5	5.1	0.94	3.36	1	
Perimyotis subflavus	1/13/2018	Male	Adult	Unknown	33.3	5.2	0.8	3.7	2	
Perimyotis subflavus	1/13/2018	Male	Adult	Unknown	33.8	6.5	1.62	3.63	1	yes
Perimyotis subflavus	1/13/2018	Female	Adult	Unknown	33.2	6	1.28	3.27	1	
Perimyotis subflavus	1/13/2018	Male	Adult	Unknown	34.2	6.1	1.53	3.81	1	yes
Perimyotis subflavus	1/13/2018	Male	Adult	Unknown	35.5	7.4	1.73	3.3	0	yes
Perimyotis subflavus	1/13/2018	Female	Adult	Unknown	34.1	6.5	1.76	3.88	0	yes
Perimyotis subflavus	1/13/2018	Female	Adult	Unknown	33.7	6	1.33	2.94	0	
Perimyotis subflavus	1/13/2018	Male	Adult	Unknown	35.3	5.5	1.24	3.35	0	yes
Perimyotis subflavus	1/13/2018	Female	Adult	Unknown	36.3	6	1.01	3.63	1	
Perimyotis subflavus	1/13/2018	Male	Adult	Unknown	34.1	5.7	0.67	3.42	0	
Corynorhinus townsendii	10/7/2016	Male	Adult	Scrotal	42.4	9.6	0.88	7.83	0	yes
Corynorhinus townsendii	10/7/2016	Male	Adult	Scrotal	43.6	10.7	1.35	8.53	0	
Myotis velifer	10/4/2016	Male	Adult	Scrotal	44.9	14			1	
Myotis velifer	10/4/2016	Female	Adult	Non-reproducing	46.7	16.4	5.63	9.98	3	
Myotis velifer	10/4/2016	Female	Adult	Non-reproducing	45.9	16.1	5.39	10.19	0	
Myotis velifer	10/4/2016	Female	Adult	Non-reproducing	46.6	15.7	4.21	10.8	1	
Myotis velifer	10/4/2016	Male	Adult	Scrotal	45.3	12.6	1.42	10.16	0	
Myotis velifer	10/4/2016	Female	Adult	Non-reproducing	45.6	16.1	5.93	9.49	0	
Myotis velifer	10/4/2016	Female	Adult	Non-reproducing	44.5	12.7	2.34	9.3	0	
Myotis velifer	10/4/2016	Male	Adult	Scrotal	47.2	13.9	1.99	10.41	1	
Myotis velifer	10/4/2016	Female	Adult	Non-reproducing	43.3	16.7	5.48	10.59	0	
Myotis velifer	10/4/2016	Female	Adult	Non-reproducing	43.3	14.2	4.28	9.34	0	
Myotis velifer	10/4/2016	Female	Adult	Non-reproducing	46.1	16	4.88	10.48	1	
Myotis velifer	10/4/2016	Female	Adult	Non-reproducing	45.1	14.2	3.75	9.65	0	
Myotis velifer	10/4/2016	Female	Adult	Non-reproducing	43.5	12			1	
Myotis velifer	10/4/2016	Female	Adult	Non-reproducing	47.1	15.6			1	
Myotis velifer	10/4/2016	Female	Adult	Non-reproducing	46	15.6			1	
Myotis velifer	10/4/2016	Female	Adult	Non-reproducing	43.4	12.6			1	
Myotis velifer	10/4/2016	Female	Adult	Non-reproducing	44.6	15.3			2	
Myotis velifer	10/4/2016	Male	Adult	Scrotal	43.8	16.1			1	
Myotis velifer	10/5/2016	Male	Adult	Scrotal	46.2	14.8	4.55	6.14	0	
Myotis velifer	10/5/2016	Male	Adult	Scrotal	46.2	13.7	2.91	10.39	0	
Myotis velifer	10/5/2016	Female	Adult	Non-reproducing	45.9	19.4	6.87	11.29	0	

Bat Species	Date	Sex	Age	Reproductive?	Forearm	Mass	Fat	Lean	Wing Score	Respirometry?
Myotis velifer	10/5/2016	Male	Adult	Scrotal	45.7	13.2	2.34	9.84	2	
Myotis velifer	10/5/2016	Male	Adult	Scrotal	43.7	15.6	4.54	10.26	1	
Myotis velifer	10/5/2016	Male	Adult	Scrotal	44.3	15.3	3.29	10.64	1	
Myotis velifer	10/5/2016	Male	Adult	Scrotal	46.2	14.8	2.59	11.05	0	
Myotis velifer	10/5/2016	Female	Adult	Non-reproducing	44.8	16.9	5.49	10.54	0	
Myotis velifer	10/5/2016	Male	Adult	Scrotal	44.5	12.7	2.03	9.1	1	
Myotis velifer	10/5/2016	Male	Adult	Scrotal	46.8	15.2	3.41	10.54	1	
Myotis velifer	10/5/2016	Male	Adult	Scrotal	45.8	15.6	4.17	10.04	0	
Myotis velifer	10/5/2016	Male	Adult	Scrotal	46.1	13.2	1.87	10.23	1	
Myotis velifer	10/5/2016	Male	Adult	Scrotal	46.5	15.7	3.39	10.6	0	
Myotis velifer	10/5/2016	Male	Adult	Scrotal	43.7	13.5	2.63	10.11	0	
Myotis velifer	10/5/2016	Male	Adult	Scrotal	44.3	13.3	2.59	9.87	0	
Myotis velifer	10/5/2016	Male	Adult	Scrotal	45.2	13.4	2.85	9.71	0	
Myotis velifer	10/5/2016	Male	Adult	Scrotal	46.4	13.5	2.92	9.63	0	
Myotis velifer	10/5/2016	Male	Adult	Scrotal	46.3	14	2.66	10.5	0	
Myotis velifer	10/5/2016	Male	Adult	Scrotal	46.3	12.5	1.87	9.41	0	
Myotis velifer	10/5/2016	Male	Adult	Scrotal	44.1	13.4	1.88	10.55	3	
Myotis velifer	10/5/2016	Male	Adult	Scrotal	43.8	17.4	6.33	10.16	0	
Myotis velifer	10/5/2016	Female	Adult	Non-reproducing	46	12.9	1.64	10.45	0	
Myotis velifer	10/5/2016	Female	Adult	Non-reproducing	44.9	13.1	2.7	9.46	1	
Myotis velifer	10/5/2016	Female	Adult	Non-reproducing	45.4	10.3	0.92	8.01	3	
Myotis velifer	10/5/2016	Female	Adult	Non-reproducing	45.9	15.1	3.34	10.52	0	
Myotis velifer	10/5/2016	Male	Adult	Scrotal	45.9	14.9	2.72	11.18	0	
Myotis velifer	10/5/2016	Male	Adult	Scrotal	44.4	12.9	1.86	10.18	0	
Myotis velifer	10/5/2016	Male	Adult	Scrotal	44.1	12.6	1.81	9.92	0	
Myotis velifer	10/5/2016	Female	Adult	Non-reproducing	45.4	15.8	5.35	9.54	0	
Myotis velifer	10/5/2016	Male	Adult	Scrotal	45.2	17.9	5.82	11.46	1	
Myotis velifer	10/5/2016	Female	Adult	Non-reproducing	44.8	14.8	3.47	10.76	0	
Myotis velifer	10/5/2016	Male	Adult	Scrotal	44.2	14.1	2.5	10.87	0	
Myotis velifer	10/5/2016	Female	Adult	Non-reproducing	44.1	13.5	3.03	9.29	0	
Myotis velifer	10/5/2016	Male	Adult	Scrotal	45	13.6	2.92	9.89	1	
Myotis velifer	10/5/2016	Male	Adult	Scrotal	44.5	14.5	2.24	10.69	0	
Myotis velifer	10/5/2016	Female	Adult	Non-reproducing	45.3	13.4	2.55	9.87	0	
Myotis velifer	10/5/2016	Male	Adult	Scrotal	44.1	14.5	2.7	10.84	0	
Myotis velifer	10/5/2016	Male	Adult	Scrotal	44.9	13.6	2.74	9.98	0	

Bat Species	Date	Sex	Age	Reproductive?	Forearm	Mass	Fat	Lean	Wing Score	Respirometry?
Myotis velifer	10/5/2016	Male	Adult	Scrotal	44.9	17	4.11	11.4	1	
Myotis velifer	10/5/2016	Male	Adult	Scrotal	44	14.8	2.69	11.05	1	
Myotis velifer	10/5/2016	Female	Adult	Non-reproducing	45.1	14	3.16	9.89	0	
Myotis velifer	10/5/2016	Female	Adult	Non-reproducing	45.6	14.7	3.09	10.74	0	
Myotis velifer	10/5/2016	Male	Adult	Scrotal	45	13.2	2.02	10.41	0	
Myotis velifer	10/5/2016	Female	Adult	Non-reproducing	44	17.4	6.19	10.46	0	
Myotis velifer	10/5/2016	Female	Adult	Non-reproducing	46	17.6	6.52	10.1	0	
Myotis velifer	10/5/2016	Male	Adult	Scrotal	44.1	13.5	2.79	9.9	0	
Myotis velifer	10/5/2016	Female	Adult	Non-reproducing	45	18.2	6.27	11.14	0	
Myotis velifer	10/5/2016	Female	Adult	Non-reproducing	48	19.5	6.72	11.75	1	
Myotis velifer	10/5/2016	Male	Adult	Scrotal	44.8	15.4	2.71	11.75	0	
Myotis velifer	10/5/2016	Male	Adult	Scrotal	45.2	13.6	2.72	10.08	0	
Myotis velifer	10/5/2016	Male	Adult	Scrotal	45.8	16.4	3.27	12.08	1	
Myotis velifer	10/5/2016	Male	Adult	Scrotal	46.8	17.6	3.81	12.28	0	
Myotis velifer	10/5/2016	Male	Adult	Scrotal	44.3	13.6	2.77	9.7	0	
Myotis velifer	10/5/2016	Male	Adult	Scrotal	44.6	13.2	2.01	10.26	2	
Myotis velifer	10/5/2016	Male	Adult	Scrotal	46.1	15.6	3.24	11.13	0	
Myotis velifer	10/5/2016	Male	Adult	Scrotal	44.2	15.5	3.16	11.27	1	
Myotis velifer	10/5/2016	Male	Adult	Scrotal	45	15.9	3.64	11.28	1	
Myotis velifer	10/5/2016	Male	Adult	Scrotal	43.9	14.9	2.9	10.82	1	
Myotis velifer	10/5/2016	Male	Adult	Scrotal	43	13.9	2.51	10.21	1	
Myotis velifer	10/5/2016	Female	Adult	Non-reproducing	43.5	18.1	6.71	10.44	0	
Myotis velifer	10/5/2016	Male	Adult	Scrotal	45.2	13.7	2.73	9.92	0	
Myotis velifer	10/5/2016	Male	Adult	Scrotal	46.3	16	2.93	11.6	0	
Myotis velifer	10/5/2016	Male	Adult	Scrotal	45.9	15.2	2.68	11.45	0	
Myotis velifer	10/5/2016	Male	Adult	Scrotal	45.7	14.1	3.22	9.73	2	
Myotis velifer	10/5/2016	Male	Adult	Scrotal	44	14.6	2.71	10.69	0	
Myotis velifer	10/5/2016	Female	Adult	Non-reproducing	45.3	13.4	2.69	9.48	0	
Myotis velifer	10/5/2016	Male	Adult	Scrotal	44.6	14.4	1.86	10.94	0	
Myotis velifer	10/5/2016	Male	Adult	Scrotal	45.6	15.3	3.34	10.62	1	
Myotis velifer	10/6/2016	Male	Adult	Scrotal	44.6	14.6	4.11	10.03	0	
Myotis velifer	10/6/2016	Female	Adult	Non-reproducing	45.3	17.1	5.32	10.89	0	
Myotis velifer	10/6/2016	Male	Adult	Non-reproducing	46.1	16.4	4.96	10.54	0	
Myotis velifer	10/6/2016	Female	Adult	Non-reproducing	48.3	17.3	5.74	10.76	0	

Bat Species	Date	Sex	Age	Reproductive?	Forearm	Mass	Fat	Lean	Wing Score	Respirometry?
Myotis velifer	10/6/2016	Male	Adult	Scrotal	44.6	12.9	1.63	10.43	0	
Myotis velifer	10/6/2016	Female	Adult	Non-reproducing	47	15.6	2.7	10.33	0	
Myotis velifer	10/6/2016	Male	Adult	Scrotal	42.8	12.2	1.36	9.98	1	
Myotis velifer	10/6/2016	Female	Adult	Non-reproducing	46.4	14.8	3.64	10.36	0	
Myotis velifer	10/6/2016	Female	Adult	Non-reproducing	43.5	18.2	7.12	10.14	0	
Myotis velifer	10/6/2016	Male	Adult	Scrotal	48	14.2	2.75	10.51	0	
Myotis velifer	10/6/2016	Male	Adult	Scrotal	47	14.2	2.31	10.9	0	
Myotis velifer	10/6/2016	Male	Adult	Scrotal	46.4	16	3.36	11.59	2	
Myotis velifer	10/6/2016	Male	Adult	Scrotal	46.1	14.5	3.16	10.59	0	
Myotis velifer	10/6/2016	Female	Adult	Non-reproducing	44.5	17.2	6.43	9.87	0	
Myotis velifer	10/6/2016	Male	Adult	Scrotal	45.2	13.9	2.73	10.1	1	
Myotis velifer	10/6/2016	Female	Adult	Non-reproducing	44.3	17.1	5.94	10.23	0	
Myotis velifer	10/6/2016	Male	Adult	Scrotal	41.8	12.4	1.53	10.03	1	
Myotis velifer	10/6/2016	Male	Adult	Scrotal	46.2	15.8	4.53	10.38	1	
Myotis velifer	10/6/2016	Female	Adult	Non-reproducing	45.1	14.3	3.18	10.38	0	
Myotis velifer	10/7/2016	Male	Adult	Scrotal	47.4	14.1	3.27	9.87	1	
Myotis velifer	10/7/2016	Male	Adult	Scrotal	43.5	12.4	2.74	8.77	0	
Myotis velifer	10/7/2016	Male	Adult	Non-reproducing	45.2	15.8	4.61	10.38	0	
Myotis velifer	10/7/2016	Male	Adult	Scrotal	45.2	12.1	1.76	9.5	0	
Myotis velifer	10/7/2016	Male	Adult	Scrotal	44.8	13.9	3.47	9.55	1	
Myotis velifer	10/7/2016	Male	Adult	Scrotal	43	12.6	2.26	9.33	0	
Myotis velifer	10/7/2016	Male	Adult	Scrotal	44.5	15.5	4.4	10.31	1	
Myotis velifer	10/7/2016	Female	Adult	Non-reproducing	45.1	14.7	4.09	9.66	1	
Myotis velifer	10/7/2016	Male	Adult	Scrotal	44.6	13.1	2.18	10.1	0	
Myotis velifer	10/7/2016	Male	Adult	Scrotal	44	13.7	2.81	9.82	1	
Myotis velifer	10/7/2016	Male	Adult	Scrotal	43.8	13	2.18	9.9	0	
Myotis velifer	10/7/2016	Male	Adult	Scrotal	44.4	11.7	1.31	9.45	0	
Myotis velifer	10/7/2016	Male	Adult	Scrotal	43.5	12.1	2.02	9.27	1	
Myotis velifer	10/7/2016	Male	Adult	Scrotal	44.5	13.7	2.34	10.4	0	
Myotis velifer	10/7/2016	Male	Adult	Scrotal	43.9	12.5	2.22	9.48	1	
Myotis velifer	10/7/2016	Female	Adult	Non-reproducing	45.3	15.1	4.47	9.7	0	
Myotis velifer	10/7/2016	Male	Adult	Scrotal	46.4	12.5	1.25	10.32	0	
Myotis velifer	10/7/2016	Male	Adult	Scrotal	45.1	12.6	1.79	9.8	1	
Myotis velifer	10/7/2016	Male	Adult	Scrotal	44.5	12.5	1.27	10.07	1	
Myotis velifer	10/7/2016	Male	Adult	Scrotal	44.4	11.4	0.61	9.94	1	

Bat Species	Date	Sex	Age	Reproductive?	Forearm	Mass	Fat	Lean	Wing Score	Respirometry?
Myotis velifer	10/7/2016	Male	Adult	Scrotal	43.1	15	3.02	10.99	1	
Myotis velifer	10/7/2016	Male	Adult	Scrotal	45.1	15.4	3.68	10.72	1	
Myotis velifer	10/7/2016	Male	Adult	Scrotal	43.4	12.1	2.08	9.1	0	
Myotis velifer	10/7/2016	Male	Adult	Scrotal	44.4	12.7	1.79	9.94	0	
Myotis velifer	10/7/2016	Male	Adult	Scrotal	45.2	13.6	1.88	10.54	1	
Myotis velifer	10/7/2016	Male	Adult	Scrotal	44.4	11.2	1.09	9.02	1	
Myotis velifer	10/7/2016	Male	Adult	Scrotal	44.2	12.1	1.55	9.53	1	
Myotis velifer	10/7/2016	Female	Adult	Non-reproducing	46.2	15.5	4.94	9.58	1	
Myotis velifer	10/7/2016	Male	Adult	Scrotal	45.7	10.8	0.74	9.45	0	
Myotis velifer	10/7/2016	Female	Adult	Non-reproducing	45.2	14.4	3.54	9.75	1	
Myotis velifer	10/7/2016	Male	Adult	Scrotal	46.4	14.9	3.93	9.9	1	
Myotis velifer	10/7/2016	Male	Adult	Scrotal	44.6	14.4	3.69	9.79	1	
Myotis velifer	10/7/2016	Female	Adult	Non-reproducing	46	14.9	3.01	10.79	1	
Myotis velifer	10/7/2016	Male	Adult	Scrotal	46	13.1	2.25	9.94	1	
Myotis velifer	10/7/2016	Female	Adult	Non-reproducing	43.2	13.9	3.21	9.71	0	
Myotis velifer	10/7/2016	Male	Adult	Scrotal	44.5	13.3	2.47	9.61	1	
Myotis velifer	10/7/2016	Female	Adult	Non-reproducing	46	16.5	5.05	10.37	1	
Myotis velifer	10/7/2016	Female	Adult	Non-reproducing	48.8	14.1	2.64	10.49	0	
Myotis velifer	10/7/2016	Male	Adult	Scrotal	44.2	13.6	2.46	10.14	1	
Myotis velifer	10/7/2016	Male	Adult	Scrotal	44.3	11.6	1.2	9.33	1	
Myotis velifer	10/7/2016	Male	Adult	Scrotal	42.2	13.6	2.87	9.7	1	
Myotis velifer	10/7/2016	Male	Adult	Scrotal	43.2	13.1	1.98	10.05	0	
Myotis velifer	10/7/2016	Male	Adult		45	12.3	1.55	9.49	1	
Myotis velifer	10/7/2016	Female	Adult	Non-reproducing	46.6	14.2	3.26	9.81	1	
Myotis velifer	10/7/2016	Female	Adult	Non-reproducing	46.1	14.4	4.09	9.37	1	
Myotis velifer	10/7/2016	Male	Adult	Scrotal	44.9	11.1	0.71	9.56	1	
Myotis velifer	10/7/2016	Male	Adult	Scrotal	45.2	16.7	3.66	12.03	0	
Myotis velifer	10/7/2016	Female	Adult	Non-reproducing	45.5	18.1	6.63	10.66	1	
Myotis velifer	10/7/2016	Male	Adult	Scrotal	44.1	13.9	1.88	10.91	2	
Myotis velifer	10/7/2016	Female	Adult	Non-reproducing	44.6	16.7	4.86	10.9	0	
Myotis velifer	10/7/2016	Male	Adult	Scrotal	43.8	12.9	1.31	10.53	0	
Myotis velifer	10/7/2016	Male	Adult	Scrotal	46	14.8	2.27	11.5	1	
Myotis velifer	10/7/2016	Male	Adult	Scrotal	45.2	15.4	3.38	11.08	1	
Myotis velifer	10/7/2016	Male	Adult	Scrotal	44.2	13.2	2.09	10.31	0	

Bat Species	Date	Sex	Age	Reproductive?	Forearm	Mass	Fat	Lean	Wing Score	Respirometry?
Myotis velifer	10/7/2016	Male	Adult	Scrotal	46.7	13.8	2.13	10.77	1	
Myotis velifer	10/7/2016	Male	Adult	Scrotal	45.6	17	3.83	11.98	1	
Myotis velifer	10/7/2016	Male	Adult	Scrotal	45.7	14.3	2.4	10.91	1	
Myotis velifer	10/7/2016	Male	Adult	Scrotal	44.4	14.8	3.6	10.47	1	
Myotis velifer	10/7/2016	Male	Adult	Scrotal	45	13.5	2.41	10.19	1	
Myotis velifer	10/7/2016	Male	Adult	Scrotal	43.9	15.4	4.18	10.45	1	
Myotis velifer	10/7/2016	Male	Adult		46	15.5	3.51	11.03	1	
Myotis velifer	10/7/2016	Male	Adult	Scrotal	46.5	14.2	2.53	10.43	1	
Myotis velifer	10/7/2016	Male	Adult	Scrotal	45.4	12.6	2.25	8.39	1	
Myotis velifer	10/7/2016	Male	Adult	Scrotal	42.1	14.8	2.73	10.87	1	
Myotis velifer	10/7/2016	Male	Adult	Scrotal	42.7	14.6	3.14	10.54	1	
Myotis velifer	10/7/2016	Male	Adult	Scrotal	45.3	13.2	2.17	9.99	1	
Myotis velifer	10/7/2016	Male	Adult	Scrotal	45.6	17.2	5.86	10.43	1	
Myotis velifer	10/7/2016	Male	Adult	Scrotal	46.1	14.7	2.93	10.67	1	
Perimyotis subflavus	10/4/2016	Male	Adult	Scrotal	34.2	5.6	2.11	2.59	2	
Perimyotis subflavus	10/5/2016	Male	Adult	Scrotal	34.2	6.1	1.53	3.92	3	
Perimyotis subflavus	10/5/2016	Male	Adult	Scrotal	33.7	6.3	1.84	4.28	0	
Perimyotis subflavus	10/5/2016	Male	Adult	Scrotal	33.8	6.7	1.71	4.67	0	
Perimyotis subflavus	10/6/2016	Female	Adult	Non-reproducing	37.1	8.6	3.51	4.71	2	
Perimyotis subflavus	10/6/2016	Male	Adult	Scrotal	34.6	8.5	3.82	4.46	1	
Myotis velifer	10/6/2016	Female	Adult	Non-reproducing	46.1	12.5	1.59	10.06	0	
Myotis velifer	10/6/2016	Male	Adult	Scrotal	44.6	12	1.76	9.39	1	
Myotis velifer	10/6/2016	Male	Adult	Scrotal	48.2	16.4	3.24	12.03	0	
Myotis velifer	10/6/2016	Male	Adult	Scrotal	46	14.1	3.26	9.81	2	
Myotis velifer	10/6/2016	Male	Adult	Scrotal	44.7	14.2	3.46	10.04	0	
Myotis velifer	10/6/2016	Female	Adult	Non-reproducing	43.5	12.6	2.88	8.93	0	
Myotis velifer	10/6/2016	Female	Adult	Non-reproducing	44.5	16.1	4.94	10.46	1	
Myotis velifer	10/6/2016	Female	Adult	Non-reproducing	45.4	15.6	4.99	9.81	0	
Myotis velifer	10/7/2016	Male	Adult	Scrotal	44.1	11.9	1.38	9.43	1	
Myotis velifer	10/7/2016	Male	Adult	Scrotal	42.9	11.6	1.69	8.77	2	
Myotis velifer	10/7/2016	Female	Adult	Non-reproducing	47	15.8	4.19	10.16	0	
Myotis velifer	10/7/2016	Female	Adult	Non-reproducing	45.8	11.9	1.45	9.23	0	
Myotis velifer	10/7/2016	Female	Adult	Non-reproducing	45.1	15.1	4.59	9.43	1	
Myotis velifer	10/7/2016	Male	Adult	Scrotal	44.9	12.9	2.3	9.43	0	
Myotis velifer	10/7/2016	Female	Adult	Non-reproducing	45.5	14.2	2.93	10.17	2	

Bat Species	Date	Sex	Age	Reproductive?	Forearm	Mass	Fat	Lean	Wing Score	Respirometry?
Myotis velifer	10/7/2016	Male	Adult	Scrotal	44.9	12.1	2.42	8.82	0	
Myotis velifer	10/7/2016	Male	Adult	Scrotal	43.6	12.2	2.04	9.26	0	
Myotis velifer	10/7/2016	Female	Adult	Non-reproducing	45.9	12	5.54	10.51	0	
Myotis velifer	10/7/2016	Male	Adult	Scrotal	45.2	13.8	2.21	10.38	0	
Myotis velifer	10/7/2016	Male	Adult	Scrotal	44.8	12.8	1.63	10.15	1	

Oregon Caves National Monument
Final Project Report 2018-2019
Under Permit ORCA-2018-SCI-0001

We caught a total of 57 bats: 32 *Corynorhinus townsendii*, 1 *Myotis californicus*, 8 *M. evotis*, 4 *M. thysanodes*, 3 *M. volans*, and 9 *M. yumanensis* (Table 1; Appendix) over the sampling period of fall 2018 to winter 2019. During the fall, bats were caught using mist nets and harp traps at the cave entrance. During the winter, bats were hand-captured from cave walls. We determined sex, age, reproductive condition, and wing score and measured forearm length and body mass of each bat. We used quantitative magnetic resonance (QMR; Echo-MRI-B, Echo Medical Systems, Houston, TX) to measure fat mass and lean mass. We measured metabolic rate (TMR) and evaporative water loss (EWL) during torpor using open-flow respirometry. We measured body fat from 43 individuals and processed 14 individuals through respirometry. Body mass and body fat were greater in females compared to males for the species we had both sexes (Figure 1). We only captured *C. townsendii* in both seasons; there was no difference in body mass nor fat mass between seasons (Figure 2). We only ran respirometry on *C. townsendii* during the winter months, so we could not compare metabolic rate or evaporative loss between seasons (Figure 3).

We predicted survival for *C. townsendii* (Figure 4) over the range of environmental conditions experienced in the cave. We also inferred the survival once affected with white-nose syndrome (Figure 4). The modified hibernation energetics model estimates the time until fat exhaustion during hibernation as a function of bat characteristics, hibernaculum microclimate, and fungal growth. Survival is determined by comparing model output time to winter duration – if time until fat exhaustion is greater than winter duration, survival occurs. We validated the model predictions with field and laboratory data and determined model sensitivity to bat characteristics.

For further information about our findings please visit www.science4bats.org/publications and review all project associated publications.

Table 1: The number of each species per year captured at Oregon Caves NM.

Species	Year	Count
Corynorhinus townsendii	2018	9
Corynorhinus townsendii	2019	23
Myotis californicus	2018	1
Myotis evotis	2018	8
Myotis thysanodes	2018	4
Myotis volans	2018	3
Myotis yumanensis	2018	9
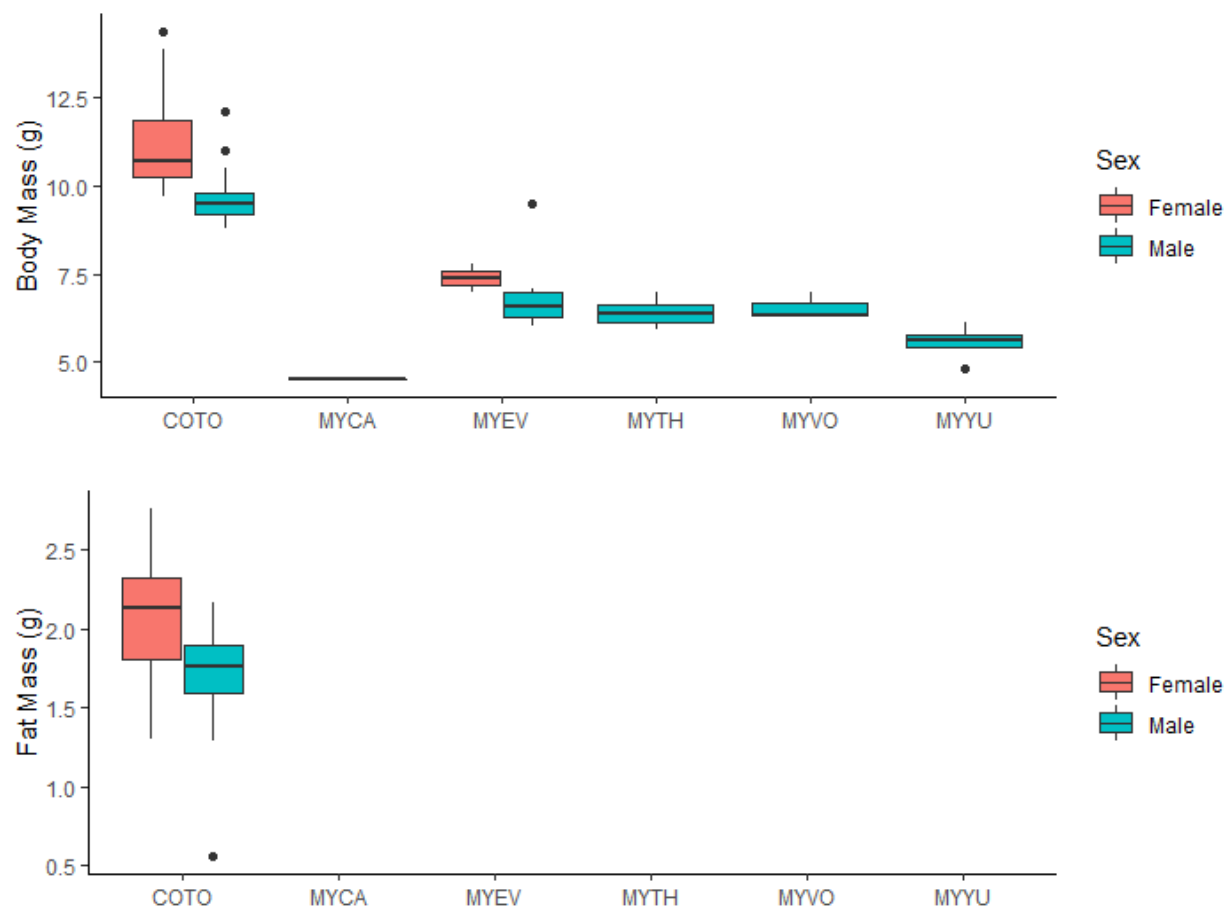
**Figure 1. Body mass (top) and fat mass (bottom) by sex for the six species captured at Oregon Caves NM.**
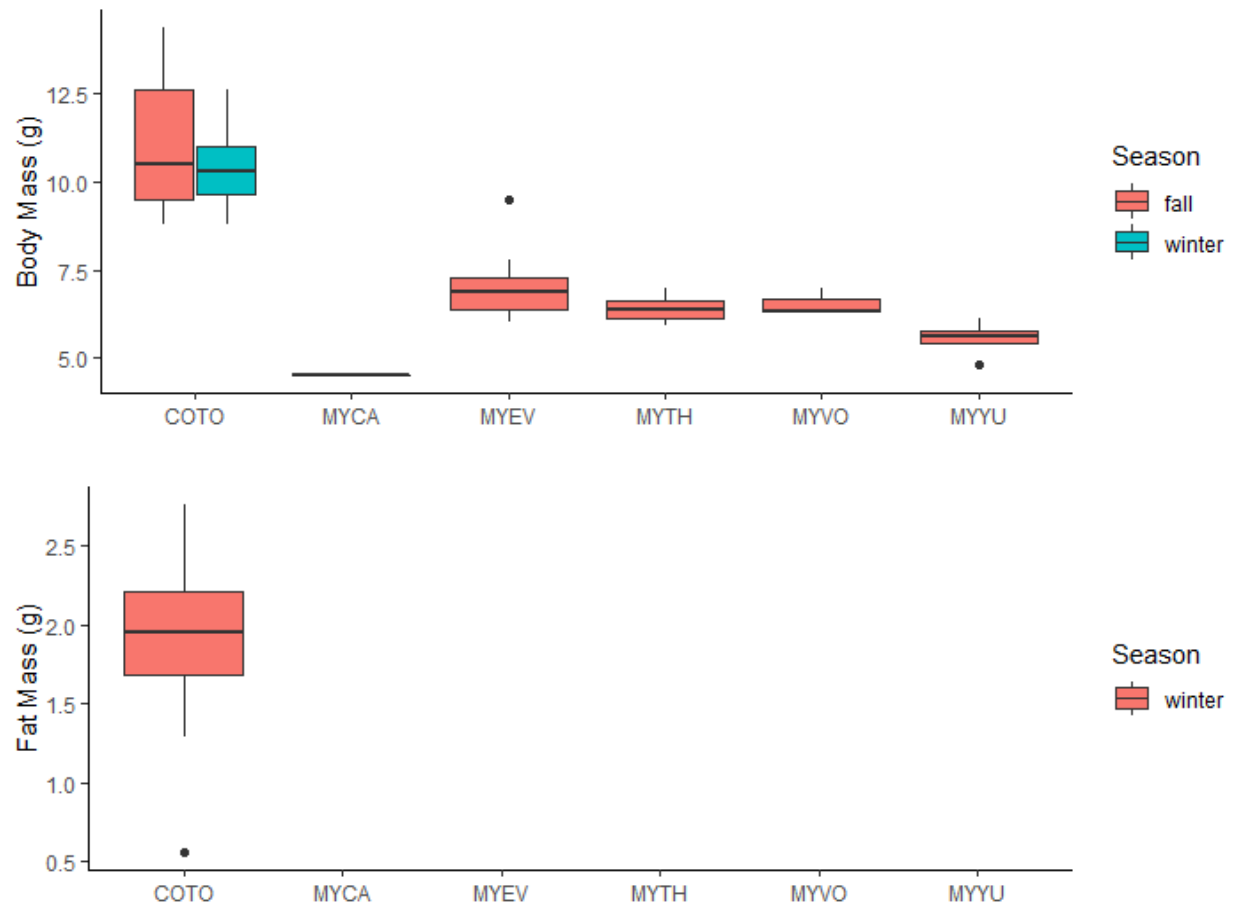
Figure 2. Body mass (top) and fat mass (bottom) by season for the six species captured at Oregon Caves NM. The single MYCA was captured in the fall.
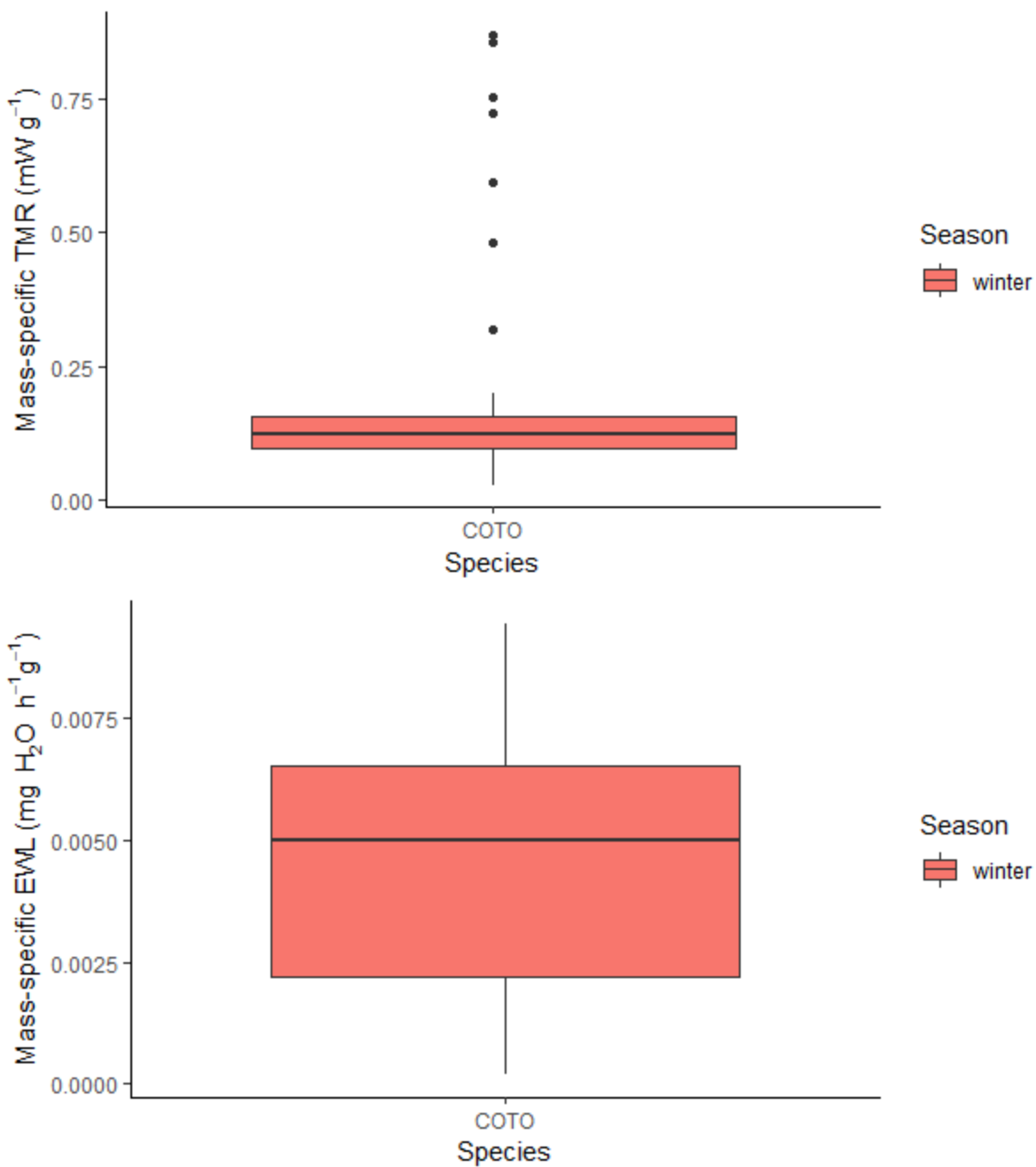
Figure 3. Mass-specific torpor metabolic rate (TMR; top) and mass-specific evaporative water loss (EWL; bottom) for COTO captured at Oregon Caves NM.
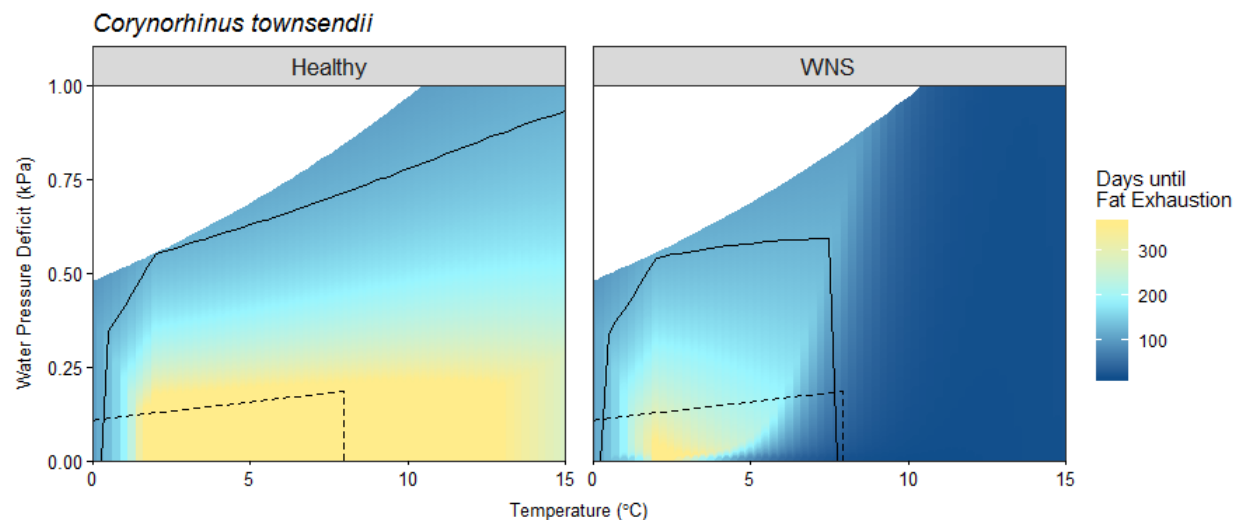
Figure 4: Predicted days until total fat exhaustion for *Corynorhinus townsendii* in Oregon Caves National Monument. Solid lines represent days of hibernation duration (125 days) predicted for Oregon Caves National Monument and the range of microclimate conditions that would allow survival in this area. Dashed lines represent microclimate conditions measured at the roosting location within the mine. The area where solid and dashed lines overlap is the microclimate conditions available that allow survival. White space represents impossible microclimate space based on the saturation potential for each temperature. Here, we predict that most microclimate space available in Oregon Caves National Monument would allow for survival from white-nose syndrome (WNS).

APPENDIX: Morphometric data from species captured at Oregon Caves NM. Forearm is in mm, mass, fat, and lean mass in g.

Species	Date	Sex	Age	Reproductive Condition	Forearm	Mass	Fat	Lean	Wing Score	Respirometry?
Corynorhinus townsendii	10/9/2018	Male	Adult	Scrotal	45.5	12.1			0	
Corynorhinus townsendii	10/9/2018	Female	Adult	Non-reproducing	35.3	13.9			0	
Corynorhinus townsendii	10/9/2018	Male	Adult	Scrotal	44.5	10.5			0	
Corynorhinus townsendii	10/9/2018	Female	Adult	Non-reproducing	45.3	12.6			0	
Corynorhinus townsendii	10/9/2018	Male	Adult	Scrotal	42.2	9.5			1	
Corynorhinus townsendii	10/12/2018	Female	Adult	Non-reproducing	44.3	14.4			0	
Corynorhinus townsendii	10/12/2018	Male	Adult	Non-reproducing	42.6	8.8			0	
Corynorhinus townsendii	10/12/2018	Female	Adult	Non-reproducing	44.2	9.9			0	
Corynorhinus townsendii	10/12/2018	Male	Adult	Scrotal	43	9.3			1	
Corynorhinus townsendii	2/7/2019	Male	Adult	Non-reproducing	44.7	9.2	1.76	7.15	1	
Corynorhinus townsendii	2/7/2019	Male	Adult	Non-reproducing	43.4	9.4	2.16	6.85	1	
Corynorhinus townsendii	2/7/2019	Female	Adult	Non-reproducing	45.6	10.6	2.19	7.98	1	yes
Corynorhinus townsendii	2/7/2019	Male	Adult	Scrotal	41.2	9.1	1.69	7.38	1	
Corynorhinus townsendii	2/7/2019	Female	Adult	Non-reproducing	43.7	9.6	1.76	7.56	0	yes
Corynorhinus townsendii	2/7/2019	Male	Adult	Scrotal	43.9	9.8	1.84	8.01	0	yes
Corynorhinus townsendii	2/7/2019	Male	Adult	Scrotal	43.9	10.7	2.23	8.54	0	yes
Corynorhinus townsendii	2/7/2019	Male	Adult	Non-reproducing	44.7	9.7	1.3	8.6	1	
Corynorhinus townsendii	2/7/2019	Female	Adult	Non-reproducing	43.1	11.4	2.76	8.18	1	yes
Corynorhinus townsendii	2/7/2019	Male	Adult	Scrotal	44.9	11	1.29	8.36	1	yes
Corynorhinus townsendii	2/7/2019	Female	Adult	Non-reproducing	43.4	10.2	1.49	8.7	0	yes
Corynorhinus townsendii	2/7/2019	Female	Adult	Non-reproducing	43.4	10.5	2.13	8.27	0	yes
Corynorhinus townsendii	2/7/2019	Female	Adult	Non-reproducing	45.3	12	2.51	8.07	0	yes
Corynorhinus townsendii	2/7/2019	Female	Adult	Non-reproducing	43.2	10	1.93	7.1	0	yes
Corynorhinus townsendii	2/7/2019	Female	Adult	Non-reproducing	45.2	10.6	1.68	8.8	1	yes
Corynorhinus townsendii	2/7/2019	Female	Adult	Non-reproducing	44.4	10.3	2.02	8.06	1	
Corynorhinus townsendii	2/7/2019	Female	Adult	Non-reproducing	45.4	11.4	2.37	8.87	1	yes
Corynorhinus townsendii	2/7/2019	Female	Adult	Non-reproducing	46.3	11	1.95	9.14	1	yes
Corynorhinus townsendii	2/7/2019	Female	Adult	Non-reproducing	43.1	9.5	2.05	7.36	1	yes
Corynorhinus townsendii	2/7/2019	Male	Adult	Scrotal	44.3	10.1	1.67	8.7	2	yes
Corynorhinus townsendii	2/7/2019	Male	Adult	Scrotal	43.7	8.8	0.56	8.5	0	
Corynorhinus townsendii	2/7/2019	Female	Adult	Non-reproducing	45.1	11.7	2.26	8.74	1	yes
Corynorhinus townsendii	2/7/2019	Female	Adult	Non-reproducing	46.1	12.6	2.62	10.58	1	yes
Myotis calfornicus	10/12/2018	Female	Adult	Non-reproducing	32.4	4.5			0	yes

Species	Date	Sex	Age	Reproductive Condition	Forearm	Mass	Fat	Lean	Wing Score	Respirometry?
Myotis evotis	10/9/2018	Male	Adult	Non-reproducing	36	6.7			1	
Myotis evotis	10/9/2018	Male	Adult	Non-reproducing	37.2	6			0	
Myotis evotis	10/12/2018	Male	Adult	Scrotal	38.9	7.1			0	
Myotis evotis	10/12/2018	Male	Adult	Scrotal	37.5	6.2			0	
Myotis evotis	10/12/2018	Female	Adult	Non-reproducing	37.4	7			0	
Myotis evotis	10/12/2018	Male	Adult	Scrotal	37.9	6.4			2	
Myotis evotis	10/12/2018	Male	Adult	Non-reproducing	36.4	9.5			0	
Myotis evotis	10/12/2018	Female	Adult	Non-reproducing	39.2	7.8			2	
Myotis thysanodes	10/9/2018	Male	Adult	Non-reproducing	41.1	6.5			1	
Myotis thysanodes	10/9/2018	Male	Adult	Non-reproducing	40.5	5.9			0	
Myotis thysanodes	10/12/2018	Male	Adult	Non-reproducing	39.5	7			0	
Myotis thysanodes	10/12/2018	Male	Adult	Scrotal	39.4	6.2			1	
Myotis volans	10/9/2018	Male	Adult	Scrotal	38.2	7			0	
Myotis volans	10/9/2018	Male	Adult	Non-reproducing	38.9	6.3			0	
Myotis volans	10/12/2018	Male	Adult	Scrotal	38.3	6.3			0	
Myotis yumanensis	10/9/2018	Male	Adult	Scrotal	33.5	5.4			0	
Myotis yumanensis	10/9/2018	Male	Adult	Scrotal	32.6	5.6			0	
Myotis yumanensis	10/9/2018	Male	Adult	Non-reproducing	34.8	5.4			0	
Myotis yumanensis	10/12/2018	Male	Adult	Scrotal	34.8	4.8			2	
Myotis yumanensis	10/12/2018	Male	Adult	Scrotal	35.2	5.7			0	
Myotis yumanensis	10/12/2018	Male	Adult	Scrotal	33.4	6			0	
Myotis yumanensis	10/12/2018	Male	Adult	Non-reproducing	33.3	6.1			0	
Myotis yumanensis	10/12/2018	Male	Adult	Scrotal	34.2	68			0	
Myotis yumanensis	10/12/2018	Male	Adult	Scrotal	34	5.6			0	

Utah Division of Wildlife
Final Project Report 2017-2018
Under permit 2COLL10094

We caught a total of 165 bats: 156 *Corynorhinus townsendii*, 1 *Eptesicus fuscus*, 1 *Myotis ciliolabrum*, 1 *M. evotis*, 5 *M. lucifugus*, and 1 *M. thysanodes* (Table 1; Appendix) over the sampling period of fall 2017 to winter 2018. During the fall, bats were caught using mist nets and harp traps at the cave entrance. During the winter, bats were hand-captured from cave walls. We determined sex, age, reproductive condition, and wing score and measured forearm length and body mass of each bat. We used quantitative magnetic resonance (QMR; Echo-MRI-B, Echo Medical Systems, Houston, TX) to measure fat mass and lean mass. We measured metabolic rate (TMR) and evaporative water loss (EWL) during torpor using open-flow respirometry. We measured body fat from 82 individuals and processed 27 individuals through respirometry. Body mass and body fat were greater in females compared to males for the species we had both sexes (Figure 1). We only captured *C. townsendii* in both seasons; there was no difference in body mass between seasons (Figure 2). There was also no difference between metabolic rate between seasons, but there was differences in evaporative water loss (Figure 3).

We measured hibernaculum temperature and relative humidity over each hibernation period using HOBO (Model U23-001, Onset Computer Corporation) and iButton (Model DS1921Z-F5, Maxim Integrated Products) microclimate data loggers. We placed four HOBO and ten iButton loggers throughout the hibernacula in the fall and recorded conditions at 3 h intervals. We collected loggers from the hibernacula in the spring (May) of each year. The mean temperature of the cave was 3.06 °C while the mean relative humidity was 75.80 % (Figure 4).

We predicted survival for *C. townsendii* (Figure 5) over the range of environmental conditions experienced in the cave. We also inferred the survival once affected with white-nose syndrome (Figure 5). The modified hibernation energetics model estimates the time until fat exhaustion during hibernation as a function of bat characteristics, hibernaculum microclimate, and fungal growth. Survival is determined by comparing model output time to winter duration – if time until fat exhaustion is greater than winter duration, survival occurs. We validated the model predictions with field and laboratory data and determined model sensitivity to bat characteristics.

For further information about our findings please visit www.science4bats.org/publications and review all project associated publications.

Table 1: The number of each species per year captured at Logan Cave.

| Species	Year	Count
Corynorhinus townsendii	2017	125
Corynorhinus townsendii	2018	31
Eptesicus fuscus	2017	1
Myotis ciliolabrum	2017	1
Myotis evotis	2017	1
Myotis lucifugus	2017	5
Myotis thysanodes	2017	1
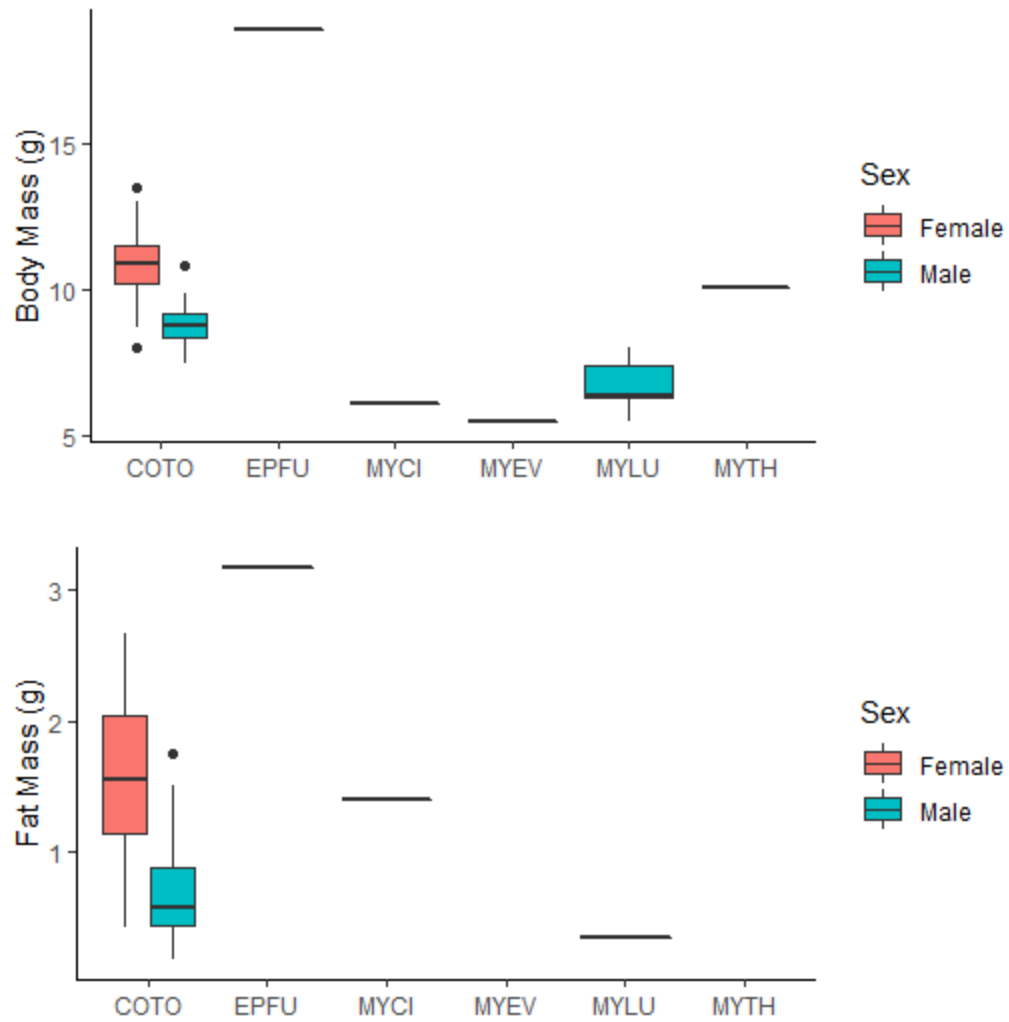
Figure 1. Body mass (top) and fat mass (bottom) by sex for the six species captured at Logan Cave. The single data points for MCI, MYEV, EPFU, and MYLU were all male.
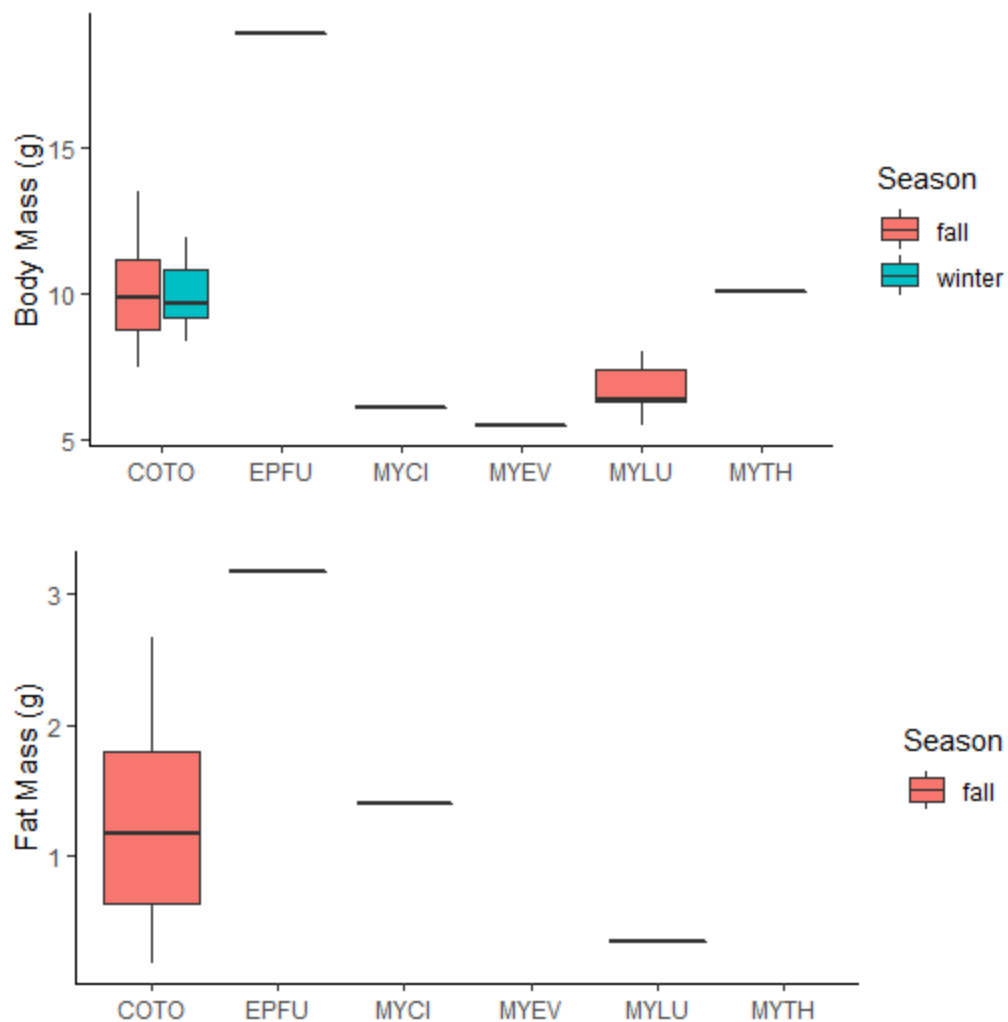
Figure 2. Body mass (top) and fat mass (bottom) by season for the six species captured at Logan Cave. The single data points for EPFU, MYCI, MYTH, and MYLU were all for fall.
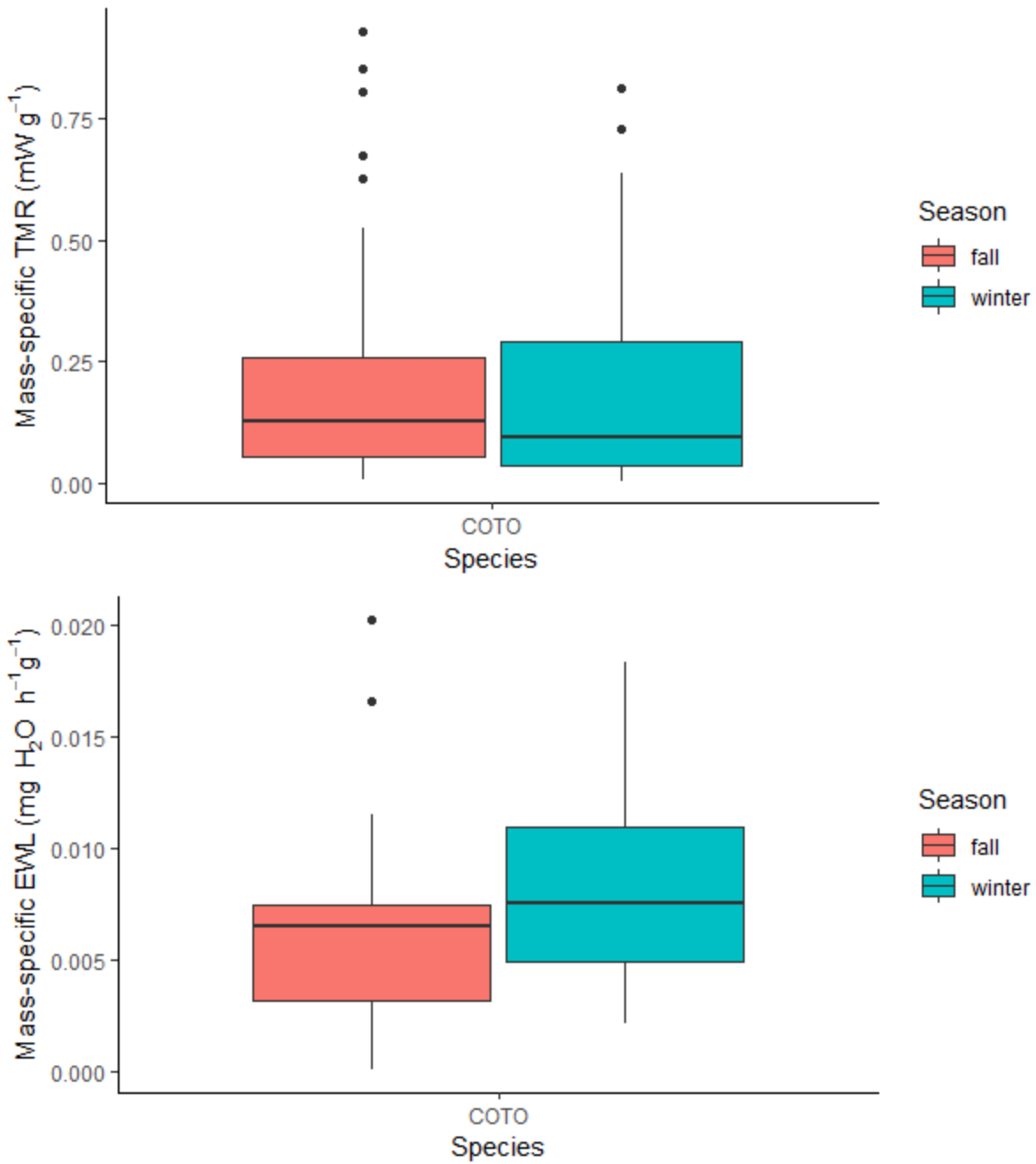
Figure 3. Mass-specific torpor metabolic rate (TMR; top) and mass-specific evaporative water loss (EWL; bottom) for COTO captured at Logan Cave.
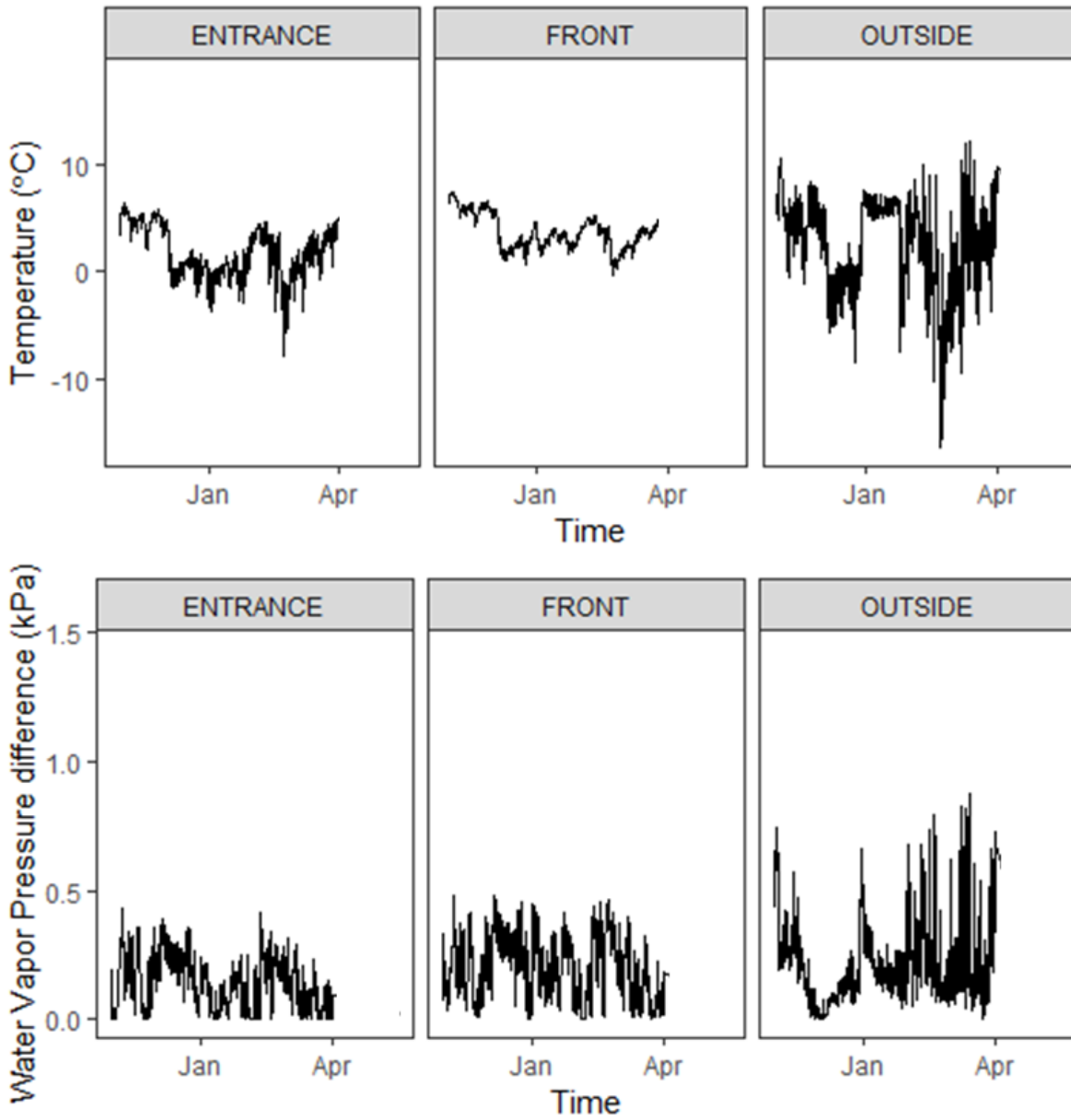
Figure 4: Microclimate (top: temperature, bottom: water vapor pressure difference) at different locations throughout Logan Cave cave.
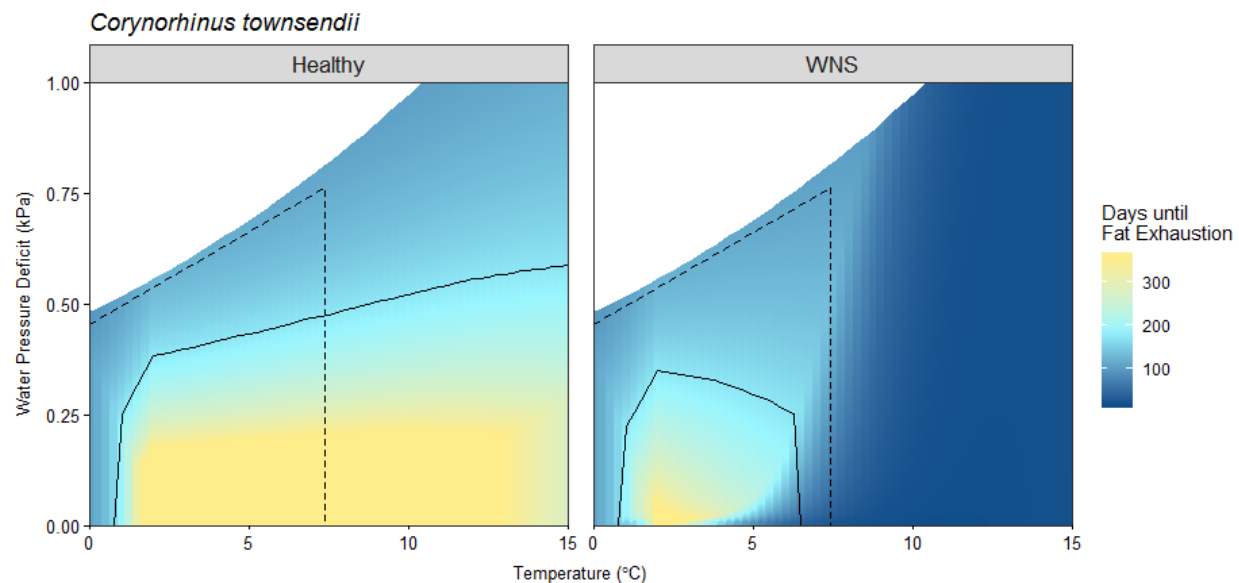
Figure 5: Predicted days until total fat exhaustion for *Corynorhinus townsendii* in Logan Cave. Solid lines represent days of hibernation duration (172 days) predicted for Logan Cave and the range of microclimate conditions that would allow survival in this area. Dashed lines represent microclimate conditions measured at the roosting location within the mine. The area where solid and dashed lines overlap is the microclimate conditions available that allow survival. White space represents impossible microclimate space based on the saturation potential for each temperature. Here, we predict that most microclimate space available in Logan Cave would allow for survival from white-nose syndrome (WNS).

APPENDIX: Morphometric data from species captured at Logan Cave. Forearm is in mm, mass, fat, and lean mass in g.

Species	Date	Sex	Age	Reproductive Condition	Forearm	Mass	Fat	Lean	Wing Score	Respirometry?
Corynorhinus townsendii	10/2/2017	Male	Adult	Scrotal	40.9	8.1	0.43	6.2	0	
Corynorhinus townsendii	10/2/2017	Female	Adult	Non-reproducing	44.7	13	2.53	6.37	1	
Corynorhinus townsendii	10/2/2017	Female	Adult	Non-reproducing	45.8	12	2.66	7.33	1	
Corynorhinus townsendii	10/2/2017	Female	Adult	Non-reproducing	44.8	9.9	0.84	3.87	1	
Corynorhinus townsendii	10/2/2017	Male	Adult	Non-reproducing	42.3	8.2	0.92	5.98	0	
Corynorhinus townsendii	10/2/2017	Male	Adult	Scrotal	44.3	9	0.48	5.04	1	
Corynorhinus townsendii	10/2/2017	Male	Adult	Non-reproducing	43.9	8.4	0.54	5.69	2	
Corynorhinus townsendii	10/2/2017	Male	Adult	Scrotal	41.1	8.1	0.17	6.9	0	
Corynorhinus townsendii	10/2/2017	Male	Adult	Scrotal	41.4	8.9	0.28	7.21	1	
Corynorhinus townsendii	10/2/2017	Female	Adult	Non-reproducing	44.7	12.3	2.4	8.37	1	
Corynorhinus townsendii	10/2/2017	Male	Adult	Non-reproducing	44.9	11.9	1.89	5.8	1	
Corynorhinus townsendii	10/2/2017	Male	Adult	Scrotal	42	8.5	0.47	4.8	1	
Corynorhinus townsendii	10/2/2017	Male	Adult	Non-reproducing	43.3	8.9	1.75	5.89	1	
Corynorhinus townsendii	10/2/2017	Male	Juvenile	Non-reproducing	42.8	7.5	0.46	5.87	0	
Corynorhinus townsendii	10/2/2017	Male	Adult	Non-reproducing	43.9	8.3	0.58	3.26	1	
Corynorhinus townsendii	10/2/2017	Female	Adult	Non-reproducing	43.3	11.4	1.83	5.26	1	
Corynorhinus townsendii	10/2/2017	Male	Adult	Scrotal	42.4	8.2	0.44	4.28	0	
Corynorhinus townsendii	10/2/2017	Female	Adult	Non-reproducing	43.4	11.1	1.84	7.86	1	
Corynorhinus townsendii	10/2/2017	Female	Adult	Non-reproducing	43	11.6	2.11	4.25	1	
Corynorhinus townsendii	10/2/2017	Female	Adult	Non-reproducing	45.4	9.7	1.12	6.93	0	
Corynorhinus townsendii	10/2/2017	Female	Adult	Non-reproducing	43.1	11	2.15	7.34	1	
Corynorhinus townsendii	10/2/2017	Female	Adult	Non-reproducing	43.3	11.8	2.57	7.5	1	
Corynorhinus townsendii	10/2/2017	Male	Juvenile	Non-reproducing	42.4	9.2	1.45	6.21	1	
Corynorhinus townsendii	10/2/2017	Female	Adult	Non-reproducing	44.4	10.2	1.21	3.71	1	
Corynorhinus townsendii	10/2/2017	Female	Adult	Non-reproducing	43.1	11.4	1.24	4.29	1	
Corynorhinus townsendii	10/2/2017	Female	Adult	Non-reproducing	45.4	11.5	2.41	7.97	1	
Corynorhinus townsendii	10/2/2017	Female	Adult	Non-reproducing	43.8	10.4	1.36	5.52	1	
Corynorhinus townsendii	10/2/2017	Female	Adult	Non-reproducing	42.9	10.9	1.86	7.95	1	
Corynorhinus townsendii	10/2/2017	Female	Adult	Non-reproducing	44.8	11	1.49	5.86	1	
Corynorhinus townsendii	10/2/2017	Female	Adult	Non-reproducing	44.2	10.9	1.78	7.58	1	
Corynorhinus townsendii	10/2/2017	Female	Adult	Non-reproducing	44	9.7	0.94	4.64	1	
Corynorhinus townsendii	10/2/2017	Female	Adult	Non-reproducing	45.9	11.2	1.82	7.88	1	
Corynorhinus townsendii	10/2/2017	Female	Adult	Non-reproducing	43.8	10.5	1.66	3.49	1	

Species	Date	Sex	Age	Reproductive Condition	Forearm	Mass	Fat	Lean	Wing Score	Respirometry?
Corynorhinus townsendii	10/2/2017	Female	Adult	Non-reproducing	43.9	10.8	2.04	4	1	
Corynorhinus townsendii	10/2/2017	Female	Adult	Non-reproducing	44.9	10.8	1.32	4.23	1	
Corynorhinus townsendii	10/2/2017	Male	Adult	Scrotal	43	8.5	0.53	6.65	0	
Corynorhinus townsendii	10/2/2017	Male	Adult	Scrotal	42.6	9.1	0.29	5.86	0	
Corynorhinus townsendii	10/2/2017	Male	Adult	Scrotal	44.3	8.6	0.48	6.76	1	
Corynorhinus townsendii	10/2/2017	Female	Adult	Non-reproducing	45.3	11.7	2.13	8.15	1	
Corynorhinus townsendii	10/2/2017	Male	Adult	Scrotal	42.3	8.8	0.30	4.81	0	
Corynorhinus townsendii	10/2/2017	Female	Adult	Non-reproducing	45.1	11	1.59	8.11	1	
Corynorhinus townsendii	10/2/2017	Female	Adult	Non-reproducing	45.2	10.6	1.5	7.59	1	
Corynorhinus townsendii	10/2/2017	Female	Adult	Non-reproducing	42.2	9.7	1.14	5.01	1	
Corynorhinus townsendii	10/2/2017	Female	Adult	Non-reproducing	45.2	11.5	2.11	6.39	1	
Corynorhinus townsendii	10/2/2017	Female	Adult	Non-reproducing	45.3	9.7	0.63	7.5	1	
Corynorhinus townsendii	10/2/2017	Female	Adult	Non-reproducing	46.4	10.9	1.12	6.15	1	
Corynorhinus townsendii	10/3/2017	Male	Adult	Scrotal	42.2	8.6			0	
Corynorhinus townsendii	10/3/2017	Female	Adult	Non-reproducing	44.4	12.5			0	yes
Corynorhinus townsendii	10/3/2017	Male	Juvenile	Non-reproducing	43.1	8.3			0	
Corynorhinus townsendii	10/3/2017	Male	Adult	Non-reproducing	42.3	8.7			1	yes
Corynorhinus townsendii	10/3/2017	Female	Adult	Non-reproducing	46.7	11.9			0	
Corynorhinus townsendii	10/3/2017	Female	Adult	Non-reproducing	46	11.7			0	
Corynorhinus townsendii	10/3/2017	Male	Adult	Non-reproducing	43.1	8.5			0	yes
Corynorhinus townsendii	10/3/2017	Female	Adult	Non-reproducing	45.3	11.5			0	yes
Corynorhinus townsendii	10/3/2017	Male	Adult	Scrotal	44.3	9.1			0	
Corynorhinus townsendii	10/3/2017	Male	Adult	Scrotal	44.5	9.5			0	yes
Corynorhinus townsendii	10/3/2017	Female	Adult	Non-reproducing	44.3	10.7			0	
Corynorhinus townsendii	10/3/2017	Female	Adult	Non-reproducing	46.2	13.5			0	yes
Corynorhinus townsendii	10/3/2017	Male	Adult	Non-reproducing	45.3	7.7			0	yes
Corynorhinus townsendii	10/3/2017	Female	Adult	Non-reproducing	45.9	9.1			0	
Corynorhinus townsendii	10/3/2017	Female	Adult	Non-reproducing	44.6	11.4			1	
Corynorhinus townsendii	10/3/2017	Female	Adult	Non-reproducing	42.9	9.3			0	
Corynorhinus townsendii	10/3/2017	Female	Adult	Non-reproducing	45.3	10.9			0	
Corynorhinus townsendii	10/3/2017	Male	Adult	Non-reproducing	45.3	12.6			0	yes
Corynorhinus townsendii	10/3/2017	Female	Adult	Non-reproducing	45.7	9			0	
Corynorhinus townsendii	10/3/2017	Female	Juvenile	Non-reproducing	40.2	9.5			0	
Corynorhinus townsendii	10/3/2017	Female	Adult	Non-reproducing	44.8	11.4			2	

Species	Date	Sex	Age	Reproductive Condition	Forearm	Mass	Fat	Lean	Wing Score	Respirometry?
Corynorhinus townsendii	10/3/2017	Male	Adult	Scrotal	43.4	8.1			0	
Corynorhinus townsendii	10/3/2017	Female	Adult	Non-reproducing	43	10.8			1	
Corynorhinus townsendii	10/3/2017	Female	Adult	Non-reproducing	45.3	11.8			1	
Corynorhinus townsendii	10/3/2017	Female	Adult	Non-reproducing	45.2	11.9			0	yes
Corynorhinus townsendii	10/3/2017	Female	Adult	Non-reproducing	44.1	10.1			1	
Corynorhinus townsendii	10/3/2017	Male	Adult	Scrotal	42.9	8.7			0	
Corynorhinus townsendii	10/3/2017	Female	Adult	Non-reproducing	44.2	10.9			0	
Corynorhinus townsendii	10/3/2017	Female	Adult	Non-reproducing	43	9			0	
Corynorhinus townsendii	10/3/2017	Female	Adult	Non-reproducing	45.1	11.2			0	
Corynorhinus townsendii	10/3/2017	Female	Adult	Non-reproducing	45.3	11.2			1	
Corynorhinus townsendii	10/3/2017	Female	Adult	Non-reproducing	44.6	11.7			1	
Corynorhinus townsendii	10/3/2017	Female	Adult	Non-reproducing	43.4	10.5			0	yes
Corynorhinus townsendii	10/3/2017	Female	Adult	Non-reproducing	45.7	11.3			1	
Corynorhinus townsendii	10/3/2017	Male	Adult	Non-reproducing	42.3	9.4			1	yes
Corynorhinus townsendii	10/3/2017	Male	Adult	Non-reproducing	41.5	8.7			0	yes
Corynorhinus townsendii	10/3/2017	Female	Adult	Non-reproducing	43.6	8			0	
Corynorhinus townsendii	10/3/2017	Female	Adult	Non-reproducing	42.3	11			1	
Corynorhinus townsendii	10/3/2017	Male	Adult	Scrotal	44	9.6			1	yes
Corynorhinus townsendii	10/3/2017	Female	Adult	Non-reproducing	44	10.5			1	
Corynorhinus townsendii	10/3/2017	Female	Adult	Non-reproducing	45.8	9.8			1	
Corynorhinus townsendii	10/3/2017	Female	Adult	Non-reproducing	45.5	12.5			1	yes
Corynorhinus townsendii	10/3/2017	Female	Adult	Non-reproducing	44.3	11.2			1	
Corynorhinus townsendii	10/3/2017	Female	Adult	Non-reproducing	44.5	10.7			0	
Corynorhinus townsendii	10/3/2017	Male	Adult	Non-reproducing	44.3	7.9			0	
Corynorhinus townsendii	10/3/2017	Female	Adult	Non-reproducing	44.2	11.5			0	
Corynorhinus townsendii	10/3/2017	Female	Adult	Non-reproducing	45.2	12.4			0	
Corynorhinus townsendii	1/23/2018	Female	Adult	Unknown	43.1	11.2			1	yes
Corynorhinus townsendii	1/23/2018	Female	Adult	Unknown	43.6	10.8			1	yes
Corynorhinus townsendii	1/23/2018	Male	Adult	Unknown	42.7	9.1			0	
Corynorhinus townsendii	1/23/2018	Female	Adult	Unknown	44.9	10.8			1	yes
Corynorhinus townsendii	1/23/2018	Female	Adult	Unknown	43.2	11.8			1	yes
Corynorhinus townsendii	1/23/2018	Male	Adult	Unknown	43.6	9.3			1	yes
Corynorhinus townsendii	1/23/2018	Male	Adult	Unknown	41.1	9			1	
Corynorhinus townsendii	1/23/2018	Male	Adult	Unknown	43.3	9.7			1	yes
Corynorhinus townsendii	1/23/2018	Female	Adult	Unknown	45	10.7			1	

Species	Date	Sex	Age	Reproductive Condition	Forearm	Mass	Fat	Lean	Wing Score	Respirometry?
Corynorhinus townsendii	1/23/2018	Male	Adult	Unknown	42.2	9			0	
Corynorhinus townsendii	1/23/2018	Male	Adult	Scrotal	41.6	9.1			1	
Corynorhinus townsendii	1/23/2018	Male	Adult	Unknown	43.1	9.3			0	
Corynorhinus townsendii	1/23/2018	Male	Adult	Unknown	44.9	11.1			1	
Corynorhinus townsendii	1/23/2018	Female	Adult	Unknown	47	10.9			1	
Corynorhinus townsendii	1/23/2018	Female	Adult	Unknown	44.5	11.9			1	yes
Corynorhinus townsendii	1/23/2018	Female	Adult	Unknown	44.1	9.2			0	yes
Corynorhinus townsendii	1/23/2018	Male	Adult	Unknown	43	9.7			0	
Corynorhinus townsendii	1/23/2018	Male	Adult	Unknown	42.1	9			1	yes
Corynorhinus townsendii	1/23/2018	Male	Adult	Unknown	44.8	9.5			1	
Corynorhinus townsendii	1/23/2018	Male	Adult	Unknown	44.1	9.1			1	yes
Corynorhinus townsendii	1/23/2018	Male	Adult	Unknown	43.9	9.3			1	
Corynorhinus townsendii	1/23/2018	Female	Adult	Unknown	46	10.8			2	yes
Corynorhinus townsendii	1/23/2018	Male	Adult	Unknown	42.3	8.4			1	
Corynorhinus townsendii	1/23/2018	Female	Adult	Unknown	46	11.8			1	yes
Corynorhinus townsendii	1/23/2018	Female	Adult	Unknown	43.6	9.2			1	
Corynorhinus townsendii	1/23/2018	Male	Adult	Unknown	41.7	9.7			0	yes
Corynorhinus townsendii	1/23/2018	Male	Adult	Unknown	44.8	10.8			1	yes
Corynorhinus townsendii	1/23/2018	Female	Adult	Unknown	44.1	10.5			1	
Corynorhinus townsendii	1/23/2018	Female	Adult	Unknown	4.1	10.2			1	
Corynorhinus townsendii	1/23/2018	Female	Adult	Unknown	45.5	9.5			1	
Eptesicus fuscus	10/11/2017	Male	Adult	Scrotal	47.9	18.9			1	
Myotis ciliolabrum	10/11/2017	Male	Adult	Non-reproducing	33.6	6.1			0	
Myotis evotis	10/3/2017	Male	Adult	Non-reproducing	37.3	5.5			0	
Myotis lucifugus	10/2/2017	Male	Adult	Scrotal	36.4	6.3			1	
Myotis lucifugus	10/3/2017	Male	Adult	Non-reproducing	37.2	8			0	
Myotis lucifugus	10/3/2017	Male	Adult	Scrotal	36.2	6.4			0	
Myotis lucifugus	10/3/2017	Male	Adult	Scrotal	38.7	7.4			1	
Myotis lucifugus	10/11/2017	Male	Adult	Scrotal	35.2	5.5			1	
Myotis thysanodes	10/3/2017	Male	Adult	Scrotal	42	10.1			1	